frontiers | Research Topics

External factors influencing stem cells' pluripotency, senescence, and differentiation

Edited by
Mustapha Najimi and Myon Hee Lee

Published in
Frontiers in Cell and Developmental Biology

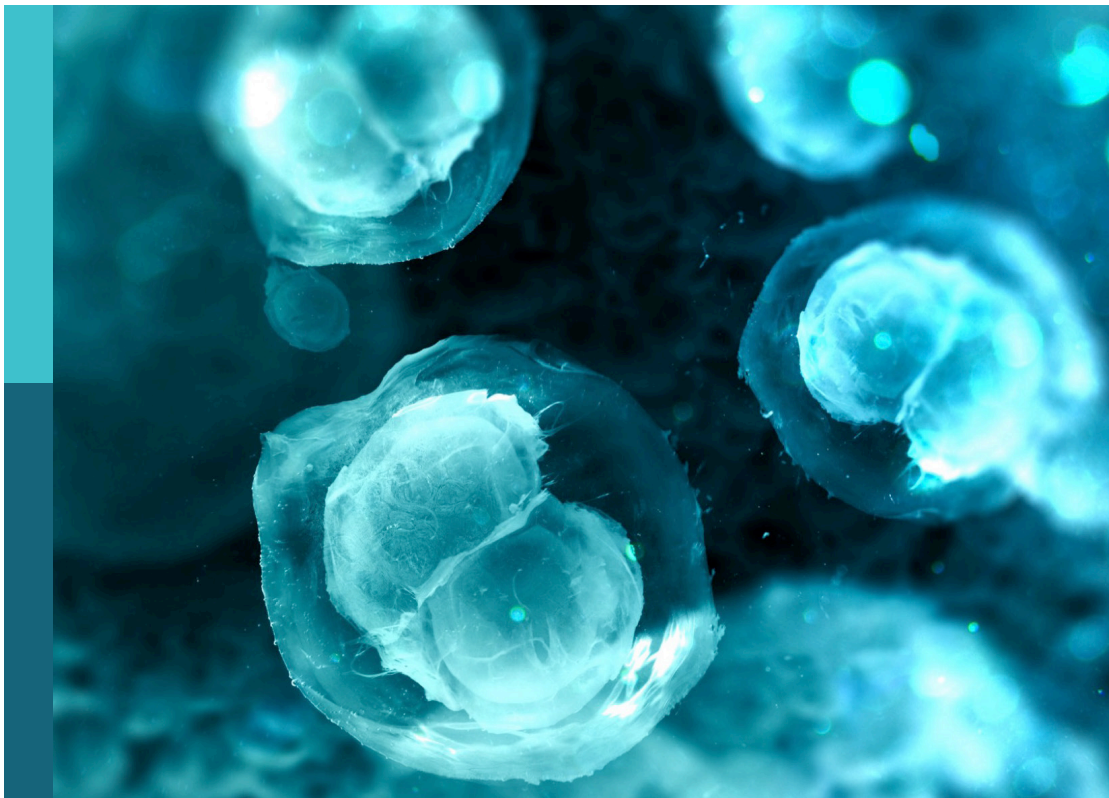

ISSN 1664-8714
ISBN 978-2-8325-7167-5
DOI 10.3389/978-2-8325-7167-5

Generative AI statement
Any alternative text (Alt text) provided alongside figures in the articles in this ebook has been generated by Frontiers with the support of artificial intelligence and reasonable efforts have been made to ensure accuracy, including review by the authors wherever possible. If you identify any issues, please contact us.

About Frontiers

Frontiers is more than just an open access publisher of scholarly articles: it is a pioneering approach to the world of academia, radically improving the way scholarly research is managed. The grand vision of Frontiers is a world where all people have an equal opportunity to seek, share and generate knowledge. Frontiers provides immediate and permanent online open access to all its publications, but this alone is not enough to realize our grand goals.

Frontiers journal series

The Frontiers journal series is a multi-tier and interdisciplinary set of open-access, online journals, promising a paradigm shift from the current review, selection and dissemination processes in academic publishing. All Frontiers journals are driven by researchers for researchers; therefore, they constitute a service to the scholarly community. At the same time, the *Frontiers journal series* operates on a revolutionary invention, the tiered publishing system, initially addressing specific communities of scholars, and gradually climbing up to broader public understanding, thus serving the interests of the lay society, too.

Dedication to quality

Each Frontiers article is a landmark of the highest quality, thanks to genuinely collaborative interactions between authors and review editors, who include some of the world's best academicians. Research must be certified by peers before entering a stream of knowledge that may eventually reach the public - and shape society; therefore, Frontiers only applies the most rigorous and unbiased reviews. Frontiers revolutionizes research publishing by freely delivering the most outstanding research, evaluated with no bias from both the academic and social point of view. By applying the most advanced information technologies, Frontiers is catapulting scholarly publishing into a new generation.

What are Frontiers Research Topics?

Frontiers Research Topics are very popular trademarks of the *Frontiers journals series*: they are collections of at least ten articles, all centered on a particular subject. With their unique mix of varied contributions from Original Research to Review Articles, Frontiers Research Topics unify the most influential researchers, the latest key findings and historical advances in a hot research area.

Find out more on how to host your own Frontiers Research Topic or contribute to one as an author by contacting the Frontiers editorial office: frontiersin.org/about/contact

External factors influencing stem cells' pluripotency, senescence, and differentiation

Topic editors

Mustapha Najimi — Institute of Experimental and Clinical Research- UCLouvain, Belgium

Myon Hee Lee — East Carolina University, United States

Citation

Najimi, M., Lee, M. H., eds. (2025). *External factors influencing stem cells' pluripotency, senescence, and differentiation*. Lausanne: Frontiers Media SA. doi: 10.3389/978-2-8325-7167-5

Table of contents

frontiers | Frontiers in Cell and Developmental Biology

TYPE Editorial
PUBLISHED 07 November 2025
DOI 10.3389/fcell.2025.1733564

OPEN ACCESS

EDITED AND REVIEWED BY
Valerie Kouskoff,
The University of Manchester,
United Kingdom

*CORRESPONDENCE
Mustapha Najimi,
mustapha.najimi@uclouvain.be
Myon Hee Lee,
leemy@ecu.edu

RECEIVED 27 October 2025
REVISED 27 October 2025
ACCEPTED 30 October 2025
PUBLISHED 07 November 2025

CITATION
Najimi M and Lee MH (2025) Editorial: External factors influencing stem cells' pluripotency, senescence, and differentiation. *Front. Cell Dev. Biol.* 13:1733564. doi: 10.3389/fcell.2025.1733564

Editorial: External factors influencing stem cells' pluripotency, senescence, and differentiation

Mustapha Najimi[1]* and Myon Hee Lee[2]*

[1]Laboratory of Pediatric Hepatology and Cell Therapy, Institute of Experimental and Clinical Research-UCLouvain, Brussels, Belgium, [2]Laboratory of Cell Fate Reprogramming, Hematology/Oncology Division, Department of Medicine, Brody School of Medicine at East Carolina University, Greenville, NC, United States

KEYWORDS

stem cells, pluripotency, senescence, differentiation, microenvironment, bioactivemolecules, reprogramming, regenerative medicine

Editorial on the Research Topic
External Factors Influencing Stem Cells' Pluripotency, Senescence, and Differentiation

Introduction

Stem cells have the unique capacities for self-renewal and differentiation into multiple types of functional cells, which are critical for regenerative medicine and tissue engineering (Ireland and Simmons, 2015). Their fate, such as whether they self-renew, differentiate, or enter senescence, is tightly regulated not only by intrinsic genetic and epigenetic factors but also by a complex array of extrinsic factors. In particular, external factors, including the microenvironment, receptor-ligand interactions, and mechanical forces, play critical roles in maintaining stem cell pluripotency, directing differentiation, and preventing or inducing senescence (Zhang et al., 2022; Sun et al.). Aberrant regulation of these extrinsic factors often leads to the loss of normal stem cells and other functional cells, or promotes the formation of unwanted cells, such as cancer stem cells or malignant cancer cells (Ponomarev et al., 2022).

This Research Topic compiles the latest research on external factors that regulate stem cell pluripotency, senescence, and differentiation. It emphasizes that understanding the complex regulation of these extrinsic factors is crucial for optimizing stem cell therapies and preventing abnormalities like cancer by integrating recent research, innovative methodologies, mechanistic insights, and future therapeutic strategies to improve outcomes.

Regulation of microenvironment, metabolism, and senescence by external factors

Several studies focus on how the cellular environment and metabolic factors govern stem cell senescence. Sun et al. emphasize the role of the external microenvironment cues,

such as extracellular matrix (ECM) components, mechanical stimuli, and oxidative stress, in regulating mesenchymal stem cell (MSC) senescence. They underscore that the aging process can be modulated by altering these external factors. Zheng et al. focus on how advanced glycation and products (AGEs), known to accumulate in diabetic and aged tissues, contribute to accelerated senescence and reduced differentiation potential through oxidative damage and inflammatory pathways. Using *Drosophila* as a model, Yan et al. demonstrate the potential of anti-diabetic drugs like dapagliflozin to mitigate intestinal stem cell aging through downregulation of MAPK signaling, suggesting pharmacological avenues for rejuvenating aged stem cells. Huang et al. explore the regenerative effects of MSC-conditioned medium (MSC-CM) in a diabetic wound model. They show that MSC-CM can promote tissue regeneration by influencing cytokine and chemokine signaling pathways, illustrating how paracrine signals serve as powerful external factors. All these findings underscore the intricate interplay between the metabolic conditions, pharmacological agents, and inflammatory signals in modulating stem cell longevity and functionality.

Differentiation pathways shaped by microenvironment and signaling

Another group of studies emphasizes how external cues direct stem cell differentiation toward specific lineages. Zhang et al. investigate the effect of the preconditioning p38 MAPK pathway on synovium-derived stem cells undergoing chondrogenesis. The study reveals that this preconditioning produces divergent outcomes depending on the ECM conditions, reflecting the context-dependent nature of signal interpretation. Nagalingam et al. reveal key pathways affected during the transition of human induced pluripotent stem cell (iPSC)-derived cardiac fibroblasts to myofibroblasts as demonstrated by using integrated transcriptomic and metabolomic profiling. Khaveh et al. identify key driver genes that mediate the phenotypic stability and differentiation of porcine MSCs, emphasizing the complex interplay between external signals, cell-matrix interactions, and lineage commitment. These studies collectively highlight the critical role of the external signals, in guiding stem cell differentiation.

Epigenetic and ligand-mediated modulation of stem cell fate

Recent work underscores the potential of small molecules, ligands, and epigenetic modifiers to influence stem cell fate and plasticity. Bae et al. provide an in-depth review of histone modification and its role in maintaining pluripotency and reprogramming in stem cells, with potential applications for cancer stem cell therapy. The authors propose that extrinsic signals can dynamically alter chromatin states, thereby modulating stem cell identity. Brown investigates retinoic acid receptor (RAR) signaling and its regulatory role in cell fate decision-making, suggesting that exogenous retinoic acid acts as a powerful switch in stem cell differentiation. Liu et al. expand their landscape by introducing ginsenosides, bioactive compounds from ginseng, as natural modulators capable of guiding stem cell behavior. These studies collectively point to the promising application of external small molecules and epigenetic modifiers to precisely reprogram stem cell identities.

Integrative perspective and clinical implications

Overall, the authors also emphasize the clinical challenges related to genetic instability, reprogramming fidelity, and safety in therapeutic applications. Collectively, this body of work reveals a complex but increasingly decipherable framework of how external signals integrate with intrinsic cellular networks to regulate stem cell behavior. Despite these hurdles, the growing understanding of this intricate framework offers promising avenues for advancing regenerative therapies and disease modeling by enabling precise modulation of stem cell functions.

Conclusion

This Research Topic collectively advances our understanding of how external factors shape stem cell identity and fate. From metabolic stressors and inflammatory cytokines to mechanical forces and small-molecule ligands, the external environment plays an indispensable role in directing stem cell responses. In conclusion, controlling stem cell fate is not solely an intrinsic endeavor and requires a deep understanding of how the external environment communicates with stem cells to modulate their identity, potential, and regenerative capabilities.

Author contributions

MN: Writing – review and editing, Writing – original draft. ML: Writing – original draft, Writing – review and editing.

Funding

The author(s) declare that financial support was received for the research and/or publication of this article. This work was supported by NSF (IOS 2132286) to MHL.

Acknowledgements

We thank all the contributing authors and reviewers for their support of the Research Topic.

Conflict of interest

The authors declare that the research was conducted in the absence of any commercial or financial relationships that could be construed as a potential conflict of interest.

The author(s) declared that they were an editorial board member of Frontiers, at the time of submission. This had no impact on the peer review process and the final decision.

Generative AI statement

The author(s) declare that no Generative AI was used in the creation of this manuscript.

Any alternative text (alt text) provided alongside figures in this article has been generated by Frontiers with the support of artificial intelligence and reasonable efforts have been made to ensure accuracy, including review by the authors wherever possible. If you identify any issues, please contact us.

Publisher's note

References

Ireland, R. G., and Simmons, C. A. (2015). Human pluripotent stem cell mechanobiology: manipulating the biophysical microenvironment for regenerative medicine and tissue engineering applications. *Stem Cells* 33, 3187–3196. doi:10.1002/stem.2105

Ponomarev, A., Gilazieva, Z., Solovyeva, V., Allegrucci, C., and Rizvanov, A. (2022). Intrinsic and extrinsic factors impacting cancer stemness and tumor progression. *Cancers (Basel)* 14. doi:10.3390/cancers14040970

Zhang, X., Zhang, S., and Wang, T. (2022). How the mechanical microenvironment of stem cell growth affects their differentiation: a review. *Stem Cell Res. Ther.* 13, 415. doi:10.1186/s13287-022-03070-0

frontiers | Frontiers in Cell and Developmental Biology

TYPE Review
PUBLISHED 04 April 2023
DOI 10.3389/fcell.2023.1182204

OPEN ACCESS

EDITED BY
Mustapha Najimi,
Université catholique de Louvain,
Belgium

REVIEWED BY
Istvan Szatmari,
University of Debrecen, Hungary
Gufa Lin,
Tongji University, China

*CORRESPONDENCE
Geoffrey Brown,
g.brown@bham.ac.uk

SPECIALTY SECTION
This article was submitted to Stem Cell Research,
a section of the journal
Frontiers in Cell and Developmental Biology

RECEIVED 08 March 2023
ACCEPTED 27 March 2023
PUBLISHED 04 April 2023

CITATION
Brown G (2023), Retinoic acid receptor regulation of decision-making for cell differentiation.
Front. Cell Dev. Biol. 11:1182204.
doi: 10.3389/fcell.2023.1182204

Retinoic acid receptor regulation of decision-making for cell differentiation

Geoffrey Brown*

School of Biomedical Sciences, Institute of Clinical Sciences, College of Medical and Dental Sciences, University of Birmingham, Birmingham, United Kingdom

All-*trans* retinoic acid (ATRA) activation of retinoic acid receptors (RARs) is crucial to an organism's proper development as established by findings for mouse foetuses from dams fed a vitamin A-deficient diet. ATRA influences decision-making by embryonic stem (ES) cells for differentiation including lineage fate. From studies of knockout mice, RARα and RARγ regulate haematopoiesis whereby active RARα modulates the frequency of decision-making for myeloid differentiation, but is not essential for myelopoiesis, and active RARγ supports stem cell self-renewal and maintenance. From studies of zebrafish embryo development, active RARγ plays a negative role in stem cell decision-making for differentiation whereby, in the absence of exogenous ATRA, selective agonism of RARγ disrupted stem cell decision-making for differentiation patterning for development. From transactivation studies, 0.24 nM ATRA transactivated RARγ and 19.3 nM (80-fold more) was needed to transactivate RARα. Therefore, the dose of ATRA that cells are exposed to *in vivo*, from gradients created by cells that synthesize and metabolize, is important to RARγ *versus* RARα and RARγ activation and balancing of the involvements in modulating stem cell maintenance *versus* decision-making for differentiation. RARγ activation favours stemness whereas concomitant or temporal activation of RARγ and RARα favours differentiation. Crosstalk with signalling events that are provoked by membrane receptors is also important.

KEYWORDS

retinoic acid receptors, vitamin A, stem cells, differentiation, haematopoiesis

Introduction

Vitamin A is required for the early development of many organs, including the eye, forelimbs, heart, hindbrain, posterior body axis, somites, and spinal cord (Clagett-Dame and Knutson, 2011; Berenger and Duester, 2022). ATRA, the most active metabolite of vitamin A, controls gene expression *via* the transcriptional activation of the three RAR types RARα, RARβ, and RARγ. They, as a heterodimer with retinoid X receptor, bind to target gene retinoic acid response elements (RAREs) to drive transcription when ATRA binds to RARs. When ATRA is absent, DNA-bound RAR/RXR heterodimers are associated with corepressors which with recruited histone deacetylases maintain a condensed chromatin and repress gene expression (Chambon, 1996).

A key question was does the transcription action of ATRA depends entirely on RARs? To answer, investigators developed RARα, RARβ, and RARγ triple knockout murine embryonic stem (ES) cell lines and examined genome-wide transcription following treatment with ATRA for 24 and 48 h (Laursen and Gudus, 2018). ATRA did not affect the genome-wide transcriptional profile of the triple knockout ES cells. By contrast to wild type cells,

proliferation was not affected by ATRA, the induction of differentiation markers (Cyp26a1, Hoxa1, Cdx1, Stra8, CoupTF1 and Meis1) was abrogated, and the repression of stem cell markers (Nanog, Oct4, Zfp42, Sox2, Klf4, and Sall4) was perturbed. *Cyp26a1* and *Hoxa1* are RARγ target genes (Kashyap et al., 2011; Kashyap et al., 2013) and ATRA failed to induce their expression within RARγ knockout and RARβ and RARγ double knockout cells (Laursen and Gudus, 2018). The transcriptional effects of ATRA and the capacity to decrease pluripotency markers, induce differentiation, and drive growth arrest are dependent on RARs. Even so, the biological functions of vitamin A and ATRA include non-genomic effects (Tanoury et al., 2013).

This review examines the roles of RARs in stem cell decision-making for cell differentiation from information gained from knockout mice and *in vitro* studies of ES cells and haematopoietic stem cells (HSCs). Regarding HSCs, various findings have challenged a longstanding model for how HSCs 'choose' to differentiate towards a mature cell type. Though new principles are still a matter of debate they are highly pertinent to consideration of how RARs influence HSC decision-making. In the conventional model of haematopoiesis, the progeny of HSCs undergoes a series of stepwise commitment decisions that eventually restrict intermediate progenitors to a single cell lineage. But HSCs can affiliate directly to a cell lineage as they are a heterogeneous population of cells as evidenced by the existence of megakaryocyte, erythroid, and macrophage lineage biased/affiliated HSCs [reviewed in Brown, 2020]. HSCs "choose" to develop along a pathway from a continuum of all options (Ceredig et al., 2009). Their differentiation is a continuous process that lacks a definite point of commitment (Velten et al., 2017) because trajectories are broad and flexible and HSCs and progenitors that have adopted a lineage fate can still veer towards an alternative fate (Nestorowa et al., 2016). Cytokines play a key role in orchestrating lineage affiliation because erythropoietin and macrophage colony stimulating factor instruct erythroid and myeloid fate within HSCs, respectively (Grover et al., 2014; Mossadegh-Keller et al., 2013). Granulocyte colony-stimulating factor and macrophage colony-stimulating factor instruct granulocyte and macrophage fate within bipotent progenitors, respectively (Rieger et al., 2009; Metcalf and Burgess, 1982). Crosstalk between ATRA- and membrane receptor-provoked events has been known for some time from the negative cross-modulation between RARs and the activator protein 1 (AP-1), which regulates gene expression in response to cytokines (Nicholson et al., 1990). AP-1 has been implicated in the regulation of the erythropoietin-driven survival/proliferation of erythroid cells (Jacobs-Helber et al., 1998).

Findings from studies of the development of embryonic cells

Findings for RAR null mutant mice confirmed the importance of vitamin A to embryonic development and addressed whether RARs are essential transducers of ATRA signalling *in vivo*. The defects seen for double null mutant mice recapitulated the congenital malformations seen in foetuses from dams fed a vitamin A-deficient diet, and these null mutant mice displayed additional abnormalities (Lohnes et al., 1994). Deletion of the whole RARα led to death of >90% of the homozygotes before the age of 2 months, but the mice failed to display any of the vitamin A deficiency-associated lesions other than testis degeneration. Mice null for the predominant RARα1 isoform appeared to be normal (Lufkin et al., 1993). Mice lacking all forms of RARβ developed normally (Luo et al., 1995), and mice lacking the most abundant RARβ2 isoform appeared to be normal (Mendelsohn et al., 1994). Mice null for all isoforms of RARγ exhibited deficient growth, early lethality, squamous metaplasia of the seminal vesicles and prostate, and male sterility, and RARγ2 null mice appeared to be normal (Lohnes et al., 1993). There is a degree of functional redundancy among the RARs. In keeping, RARγ null-cells failed to differentiate *in vitro* in response to ATRA and express several ATRA-induced genes and re-expression of RARγ or overexpression of RARα restored differentiation potential and target gene activation. RARβ restored target gene activation but poorly restored differentiation potential. ATRA-activation of *Cdx1*, *Gap43*, *Stra4*, and *Stra6* was specifically impaired within RARγ-null cells pointing to a distinct subset of target genes for RARγ and for other RARs (Taneja et al., 1995).

Embryonic stem (ES) cells are competent regarding the production of all the cell types and ATRA has been used to obtain different cell types from mouse ES cells grown as monolayers or as hanging drops to form embryoid bodies. Cells resembling male germ cells spontaneously arise from embryoid bodies and treatment with 2 μM ATRA, with or without testosterone, significantly increased the expression of male germ cell lineage-associated genes. (Silva et al., 2009). The findings for the generation of neuronal cells vary according to the cells and conditions used. ATRA activates transcription of the *Hoxa1* gene in ES cells and monolayer cultures of Hoxa1$^{-/-}$ ES cells treated with ATRA expressed genes that are associated with embryonic brain development at a lower level than wild type cells. The reintroduction of exogenous Hoxa1 was needed for 5 μM ATRA-induced ES cell neuronal differentiation (Martinez-Ceballos and Gudas, 2008). Other investigators reported that 1 μM ATRA enhanced the efficiency of differentiation of ES cells into neural precursor cells (Li et al., 2019) and that this conversion required both fibroblast growth factor and the elimination of signals for other fates (Ying et al., 2003). Neural precursor cells have been efficiently derived from ES cells without the addition of ATRA by using a three-dimensional culture system followed by two-dimensional derivation. The investigators used fibroblast growth factor and the B27 medium supplement containing retinyl acetate, which is a natural form of vitamin A (the acetate ester of retinol) and a precursor in ATRA metabolism (see below regarding the importance) (Yoon et al., 2021). A 100 nM concentration of ATRA has been used to induce the expression of mesodermal marker genes within mouse ES cells (Oeda et al., 2013).

The use of a pharmacological amount of ATRA (1—5 μM) to differentiate ES cells is a concern. The affinities of ATRA for RARα, RARβ, and RARγ are 9 nM, 3 nM, and 10 nM, respectively (Idres et al., 2002), and the physiological concentration of ATRA in tissues is ~1—10 nM (Czuba et al., 2020). ES cells are usually cultured in medium plus either foetal calf serum or the B27 supplement (Amit and Itskovitz-Elder, 2002; Sadhananthan and Touson, 2005) and they differentiate into cells that arise from the three germ cells layers. Medium with 10% foetal calf serum contains 50 nM all-*trans*-retinol

and the level of ATRA in the serum of humans and other mammalians is ~ 4–14 nM (Baltes et al., 2004). As mentioned above, the B27 supplement contains retinyl acetate and ES cells cultured in the B27 supplemented medium synthesized ATRA and their differentiation towards neural precursor cells (expressing *Sox1*) was reliant on ATRA produced endogenously (Engberg et al., 2010). ATRA was not measurable and to demonstrate the need for neuronal differentiation the investigators either removed retinyl acetate from the B27 supplemented medium, inhibited the enzymes that catalyse the synthesis of ATRA, or used the pan-RAR antagonist AGN193109 to block the activity of RARs and neural differentiation was prevented. For retinyl acetate deprived cells, neuronal differentiation was restored by the addition of 1 nM ATRA. When ATRA signalling was inhibited, there was change of fate from neuronal to mesoderm and Nodal signalling had repressed neuronal development in a Wnt-dependent manner. The investigators concluded that a neuronal to mesoderm fate switch depends on active Nodal-, Wnt-, and FGF signalling. It is well-documented that signalling *via* Nodal, a transforming growth factor β-related factor, and Wnt glycoproteins stimulation of complex intracellular signalling cascades play roles during organogenesis and ES cell differentiation (Schier and Shen, 2000; Takenaga et al., 2007; Koyima and Habas, 2008; Sokol, 2011).

The roles of individual RARs within mouse ES cells have been examined by homologous recombination disruption of the *Rara* and *Rarg* genes (Tanoury et al., 2014). ES cells were cultured as cellular aggregates and treated with 2 μM ATRA to generate neuronal cells. ES cells lacking RARα became neural progenitors, giving rise to neurons, cells lacking RARγ failed to do so, and RARγ2 rescued lines gave rise to neurons pointing to a role for RARγ2 in ES cell neuronal development. From comparison of ATRA-induced gene expression by wild type and the RARγ2 restored cells and RT-qPCR experiments, the investigators showed that RARγ2 regulates a small number of genes, exemplified by *meis homeobox 2 (Meis2)*, *left right determination factor 1* (*Lefty1*), *hepatocyte nuclear factor 1 homeobox B* (*Hnf1b*), *arginase 1*, and the homeobox (Hox) genes *Hoxa3*, and *Hoxa5*. RARs are phosphorylated in response to ATRA and the importance of phosphorylation of RARγ2 was investigated by expressing forms of RARγ2 that had been modulated in phospho-acceptor sites. For ATRA-mediated neuronal differentiation, gene expression that was controlled by phosphorylation of RARγ2 included that of *Meis2*, *Lefty1*, *Hnf1b*, and *gastrulation brain homeobox 2*. The genes targeted by phosphorylated RARγ2 depicted atypical DR7 retinoic acid response elements in addition to canonical DR2 and DR5 elements and the phosphorylated form of RARγ2 was recruited by DR7 and DR5 elements in response to ATRA. RARα1 was phosphorylated *in vitro* and *in vivo* by protein kinase A and phosphorylation at the site is involved in dibutyryl cAMP modulation of the differentiation of F9 embryonal carcinoma cells (Rochette-Egly et al., 1995).

Lessons from studies of ES cells are as follows. RARγ2 plays a role in ATRA-induced ES cell neuronal differentiation by either regulating the expression of specific genes or closing "unwanted" options regarding a proposed need. A physiological level (nM) of ATRA influences decision-making for differentiation including lineage fate. Endogenously produced ATRA plays a key role because vitamin A signalling is, in essence, driven by the intracellular ATRA concentration. In general, evaluation of the effect of treating cells with ATRA is confounded by all-*trans*-retinol or retinyl acetate in medium (Czuba et al., 2020) because of the need to take into consideration cryptic ATRA signalling from endogenous synthesis. Moreover, when epidermal keratinocytes were cultured in medium supplemented with 5% foetal calf serum, which contained 25 nM all-*trans* retinol and ATRA was undetectable, the level of all-*trans* retinol led to an intracellular level of ATRA of 25—50 nM (Randolph and Simon, 1997). This is well within the range of ATRA for activation of RARs. Growth factor-provoked signalling events are important to ES cell differentiation and RAR phosphorylation allows the relay of information from cell-surface receptor-provoked kinase cascades. Additionally, ATRA provoked non-transcription effects within differentiating mouse embryonic stem cells include the rapid and transient activation of kinase cascades [reviewed in Rochette-Egly, 2015].

Findings for RARα and haematopoietic cell differentiation

The RARα gene is expressed in almost all adult tissues, and expression of the major isoform RARa1 is also ubiquitous (Leroy et al., 1991). During haematopoiesis, RARα is expressed by HSCs and their differentiating offspring. Mouse lineage-negative, c-kit–positive, Sca-1–positive (LKS+) cells, that contain HSCs, and lineage-negative, c-kit–positive, Sca-1– negative (LKS–) cells, that lack HSCs, expressed RARα (Purton et al., 2006). RARα, particularly RARα2, expression increased dramatically during myeloid differentiation as seen for the induced differentiation of FDCP mixA4 mouse progenitor cells (Zhu et al., 2001). In addition to controlling homeostasis, RARs control the functional activity of some of the mature blood cells regarding the production of inflammatory cytokines [reviewed in Duong and Rochette-Egly, 2011]

A role for RARα in myeloid differentiation is well established (Collins, 2002). ATRA promotes the differentiation of promyeloid cell lines and normal myeloid progenitors and findings for the human promyeloid cell line HL-60 established a role for RARα in neutrophil differentiation. HL-60 cell differentiate towards neutrophils in response to treatment with ATRA (Breitman et al., 1980) and macrophages when treated with 1α,25-dihydroxyvitamin D3 (1,25D) to activate the vitamin D receptor (VDR) (Mangelsdorf et al., 1984). HL-60 cells undergo a low rate of spontaneous neutrophil differentiation because around 3%–10% of cells are more mature myelocytes, metamyelocytes, and banded and segmented neutrophils. A 1 μM concentration of ATRA promoted neutrophil differentiation with 90% of the cells terminally maturing, and 100 nM was effective. The identification of a PML-RARα fusion transcript in the cells from patients with acute promyelocytic leukaemia (de The et al., 1990) focused attention on RARα playing a key role during HL-60 neutrophil differentiation. Retroviral vector-mediated transduction of a single copy of RARα into an ATRA-resistant HL-60 subclone restored ATRA sensitivity for differentiation (Collins et al., 1990). Similarly, RARα agonism, by using AGN195183, was sufficient to promote HL-60 cell differentiation towards neutrophils (Brown et al., 2017). As mentioned above, G-CSF directs normal granulocyte/macrophage progenitors towards neutrophils (Rieger et al., 2009)

and co-operates with ATRA to promote HL-60 differentiation towards neutrophils. Treatment of HL-60 cells with 10 nM ATRA led to a low level of neutrophil differentiation, differentiation was rapid and effective when 10 nM ATRA was combined with 30 ng/ml G-SCF, and G-CSF alone had no effect. A low dose of ATRA had rendered HL-60 cells responsive to the action of G-CSF (Sakashita et al., 1991; Bunce et al., 1994).

The influence of ATRA on neutrophil differentiation is particularly well-documented. ATRA and RARα also promote monocyte differentiation as shown from studies of the promyelocytic cell line NB4 and myeloblast blast-like cell line KG-1 (Brown et al., 2017). These cells express RARα and do not express RARγ. For NB4cells, 100 nM of the RARα agonist promoted neutrophil differentiation (40% CD11b+/CD14-ve cells) and treatment with 10 nM 1,25D led to a low level of monocyte differentiation (CD11b+/CD14+ve and ~6%). The combined use of 100 nM of the RARα agonist and 10 nM 1,25D increased the level of monocyte differentiation (to ~50%). KG-1 cells differentiated towards neutrophils to a very small extent (~5%) in response to 100 nM of the RARα agonist and 10 nM 1,25D did not have a significant effect. Like NB4 cells, there was a significant level of monocyte differentiation (18%) when KG-1 cells were treated with the RARα agonist and 1,25D. RARs interact with several other nuclear receptors (Chambon, 1996) and the rationale to the interplay between the actions of the RARα agonist and 1,25D is that ATRA activation of RARα within NB4 and KG-1 cells upregulated the expression of a transcriptional variant of VDR that originates in exon 1a. KG-1 cells expressed RARα protein at a high level which in the absence of ATRA had repressed transcription of the VDR gene. The receptor interplay is complex and linked to cell status because ATRA downregulated VDR mRNA for HL-60 cells differentiating towards neutrophils in response to ATRA (Marchwicka et al., 2016).

For normal human bone marrow myeloid progenitor cells, ATRA supported their differentiation towards neutrophils but not towards erythrocytes (Gratas et al., 1993). Findings from *in vitro* cultures of cells from null mutant mice suggested roles for RARα1 and RARγ in neutrophil maturation (Labrecque et al., 1998). This was normal within myeloid colonies that were grown in methylcellulose from the bone marrow cells harvested from RARα1 and RARγ knockout mice. Neutrophil differentiation within myeloid colonies from cells harvested from the RARα1 and RARγ double knockout mouse was blocked at the myelocyte stage. The differentiation of cells within erythroid and macrophage colonies was not affected. The distribution of neutrophils, macrophage, and erythroid colonies was the same for cells from the wild type mice and the RARα1, RARγ, and compound null mutants, suggesting that lineage choice was not affected by a lack of RARα1 and/or RARγ. By contrast, various studies have reported that ATRA-mediated enhancement of myeloid-colony growth associates with a reduced production of colonies containing cells of other lineages, suggesting an influence of ATRA on multipotent cells [reviewed in Collins, 2002].

The influence of ATRA on primitive mouse haematopoietic cells was different to that seen for myeloid progenitor cells. Like ES cells, mouse LSK + cells, which are enriched for HSCs, differentiate spontaneously in liquid suspension culture and treatment with 1 μM ATRA delayed their differentiation. LSK + cells were allowed to differentiate for 7 days and then treated with 1 μM ATRA. The effect of ATRA on committed progenitor cells arising from the cultured LSK + cells was as seen for normal human bone marrow myeloid progenitor cells and HL-60 cells. There was a markedly decreased level of colony-forming cells and enhanced neutrophil differentiation which was attributed to enhanced maturation of committed granulocyte/monocyte progenitors (Purton et al., 1999).

Dormant mouse HSCs metabolize all-*trans* retinol to ATRA in a cell-autonomous manner (Cabezas-Wallscheid et al., 2017) and the aldehyde dehydrogenases (ALDHs), a family of oxidoreductases, convert retinaldehyde into ATRA. The importance of endogenous retinoid metabolism to cultured mouse HSCs ($CD34^-$ LSK+) was investigated by using diethylaminobenzaldehyde to inhibit ALDH activity. This impeded HSC differentiation leading to a ninefold expansion of HSCs, as measured by cells that were able to reconstitute lethally irradiated mice (Muramoto et al., 2010). Targeted siRNA of ALDH1a1 in HSCs revealed that this ALDH was the target of diethylaminobenzaldehyde inhibition. Similarly, inhibition of ALDH activity led to expansion of human HSCs that were able to repopulate NOD/SCID mice (Chute et al., 2006). From these studies, ALDH regulates HSC differentiation whereby the conversion of retinaldehyde into ATRA promotes HSC differentiation. Cyp26b1 is generally viewed as an enzyme that limits the effects of ATRA on cells by metabolising ATRA to 4-oxo-retinoic acid. A recent omics analysis revealed that the maintenance of mouse HSCs was reliant on the production of 4-oxo-retinoic acid and transmission of 4-oxo-retinoic acid-mediated signalling *via* RARβ (Schonberger et al., 2022). 4-oxo-retinoic acid activates the three RARs and the level required for activation of RARβ is lower than that for RARα and RARγ (EC_{50} values of 33 nM, 8 nM, and 89 nM, respectively) (Idres et al., 2002).

Purified human lineage-, CD133+, $CD34^+$ cells are enriched for HSCs and the role of RARα was investigated by treating these cells with antagonists. Cell production peaked at day 20 for control cultures and viable cells then declined rapidly. The pan-RAR antagonist AGN194310 treated cultures were maintained for up to 55 days, with 4-fold more cells by day 40. Both cultures produced mostly neutrophils and monocytes, in equal ratios, with the antagonist treated cultures generating more of the two mature cell types (as to the increased cumulative cell number) (Brown et al., 2017). AGN194310-provoked increased myeloid cell production by HSCs is in keeping with neutrophil numbers were strikingly increased in mice treated with AGN194310 (Walkley et al., 2002) and that vitamin A deficiency in mice caused a systemic expansion of myeloid cells (Kuwata et al., 2000). CD11b+ differentiated myeloid cells appeared and immature myeloid cells declined at the same rates in both control and AGN194310 treated cultures. Switching-off RARs had not slowed down myeloid cell differentiation and instead there was enhanced expansion of lineage-, CD133+, $CD34^+$ cells and colony-forming progenitors within the AGN194310 treated cultures. Antagonism of RARα, by AGN195183, was sufficient for the enhanced expansion of lineage-, CD133+, $CD34^+$ cells and antagonising RARγ did not lead to this enhancement. At first sight it seems paradoxical that antagonism of all RARs had delayed human HSCs differentiation and that agonism of all RARs (with ATRA) had delayed mouse LSK + cell differentiation (see above). The two cell populations are

different regarding their heterogeneity and the culture conditions used were different. Otherwise, the findings point to complex actions for RARα and RARγ. A lack of active RARα (RARα antagonism) had delayed the differentiation of human lineage-, CD133+, $CD34^+$ cells whereas the presence of activated RARγ (ATRA agonism) may have interfered with the differentiation of the mouse LSK + cells (see also later).

From studies of haematopoiesis, active RARα plays a role to enhance neutrophil differentiation of mouse progenitor cells and human HSCs and promyeloid cell lines. The role of RARα is to modulate/regulate rather than being essential for myelopoiesis (Kastner and Chan, 2001). For example, the terminal differentiation of cultures of human HSCs towards neutrophils and macrophages was unaffected when RARα was antagonised. For these cells, antagonism of RARα did not alter the relative proportions of neutrophils *versus* macrophages generated nor appeared to accelerate the terminal maturation of immature myeloid cells. Instead, active RARα positively modulated the frequency of decision-making for differentiation to favour differentiation. In other words, unliganded interferes with gene expression for differentiation which is promoted when ATRA or a specific RARα agonist is bound (Kastner and Chan, 2001; Collins, 2002). G-CSF is a key regulator of granulopoiesis and, like RARα, was dispensable. The combined action of these agents was investigated by conditional deletion of RARα on a G-CSF receptor-null background and treating G-CSF receptor null mice with the pan-RAR antagonist AGN194310 (referred to as NRX194310); granulopoiesis persisted in these mice (Chee et al., 2013). To differentiate or not is a multifactorial decision and the following section examines the extent to which RARγ plays a role in decision-making for cell differentiation.

Findings for RARγ and cell differentiation

Unlike RARα, the distribution of RARγ is very restricted and specific spatial and temporal distributions of RARγ during mouse embryogenesis led to the proposal that RARγ plays a role in early morphogenic events (Ruberte et al., 1990). During haematopoiesis, RARγ is selectively expressed by hematopoietic stem cells and primitive progenitors (Purton et al., 2006). In keeping with a restricted expression of RARγ within primitive cells, the binding sites for RAR/RXR dimers within undifferentiated F9 embryonal carcinoma cells coincided with loci that are targeted by transcription factors that are important to pluripotency (SOX2, NANOG, and POU5f1) (Chatagnon et al., 2015).

A special consideration to the role of RARγ *versus* that of RARα is the level of ATRA that cells are exposed to influences whether RARγ or RARγ together with RARα are transactivated within cells. The concentration of ATRA that is needed to activate RARγ is substantially lower than that required for activation RARα. A 0.24 nM level of ATRA transactivated RARγ whereas 19.3 nM (80-fold more) was needed to transactivate RARα (Brown et al., 2017). By contrast, the best ATRA induction of transcription was obtained for RARα which was 10-fold higher than that for RARγ, as seen from the fold-induction of luciferase activity from a RARE-tk-Luc reporter plasmid in the presence of each RAR (Idres et al., 2002). The increased fold induction by RARα suggests a greater efficiency to inducing transcription as governed by the interaction of the ligand-activated receptor complex with response elements.

The nature of the genes that are regulated by RARγ is germane to consideration of a role for RARγ. Comparison of ATRA-induced events within the wild type and RARγ null ES cells showed that RARγ is essential for ATRA-induced epigenetic marks at gene promoters, chromatin remodelling, and transcriptional activation. ATRA activation of RARγ greatly increased the transcript levels of genes that encode regulators of ATRA metabolism within cells. They were the genes encoding stimulated by retinoic acid 6 (Stra6), lecithin:retinol acyltransferase (LRAT), cellular retinoic acid binding protein 2 (CRABP2), and cytochrome p450 26A1 (CYP26A1) (Kashyap et al., 2013). Retinol-binding protein 4 (RBP4) transports all-*trans* retinol (vitamin A) in the blood for transfer into cells which is mediated by binding to Stra6. LRAT converts all-trans retinol into retinyl esters for storage, CRABP2 delivers ATRA to the nucleus and RARs, and CYP26A1 catabolises ATRA to polar metabolites for elimination. RARγ expression by stem cells might autoregulate a low ATRA content by virtue of ATRA activation leading to the diversion of "excess" all-*trans* retinol into retinyl esters for storage and elevated CYP26A1 expression increasing ATRA breakdown. These controls on ATRA-driven RAR events may be an important "housekeeping" function to stem cell stemness. From the studies of ATRA-regulated genes in the early zebrafish embryo, CYP26A1 was identified as one of the most robust genes regarding ATRA regulation, even when ATRA availability is drastically reduced (Samarut et al., 2014), and, as above, RARγ is transactivated by sub nM ATRA. A proposal from the zebrafish studies was also that RARγ subtypes appeared to play roles in the basal regulation of ATRA-responsive gene expression with RARα subtypes playing roles in the transcriptional response of cells to ATRA. (Samarut et al., 2014).

The above considerations point to active RARγ promoting stem cell maintenance and stemness. Indeed, RARγ plays a critical role in balancing HSC self-renewal/maintenance *versus* differentiation (Purton et al., 2006). The bone marrow of RARγ knockout mice had markedly reduced numbers of HSCs, measured as transplantable repopulating cells per femur, and the numbers of mature myeloid progenitors were increased. *Ex vivo* activation of RARγ, by ATRA, promoted the self-renewal of HSCs because loss of RARγ abrogated the capacity of ATRA to enhance the maintenance of HSCs in culture. Regarding stem cell stemness, a much more undifferentiated phenotype was seen for primitive haematopoietic precursors that were retroviral-mediated transduced to overexpress RARγ whereas primitive precursors that overexpressed RARα differentiated predominantly to granulocytes.

As considered above, RARγ2 has a role in specifying ES cell neuronal differentiation which might relate to either a positive influence or the proposed need for the elimination of other fates (Ying et al., 2003). Studies of zebrafish embryos revealed a negative role for active RARγ in cell differentiation. RARγ transcripts are restricted to primitive cells at the later stages of the zebrafish embryo. At 24 h post fertilisation they were restricted to mesodermal and neural crest stem and progenitor cells, in the head area, in the lateral plate mesoderm, and in the pre-somitic mesoderm of the tail bud. Transcripts were still visible in the tail bud at 48 h post fertilisation (Hale et al., 2006). Zebrafish embryos were

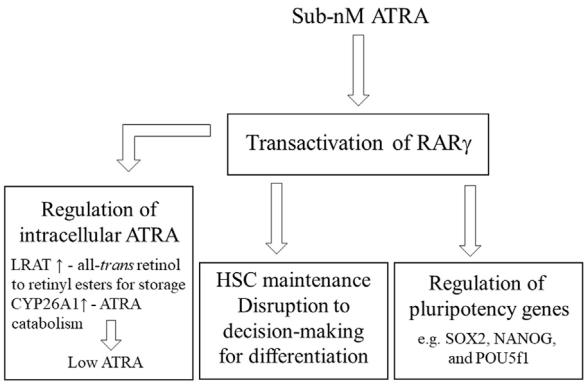

FIGURE 1
Controls on stem cell stemness Active RARγ is required for the maintenance of HSCs, for zebrafish embryos activation disrupted stem cell decision-making for differentiation for the patterning of development, and RARγ plays a role in regulating pluripotency genes. Genes that regulate the intracellular level of ATRA are expressed upon RARγ transactivation whereby lecithin:retinol acyltransferase (LRAT) converts all-*trans* retinol to retinyl esters for storage and cytochrome p450 26A1 (CYP26 A1) catabolizes ATRA. A sub nM intracellular level is sufficient to transactivate RARγ.

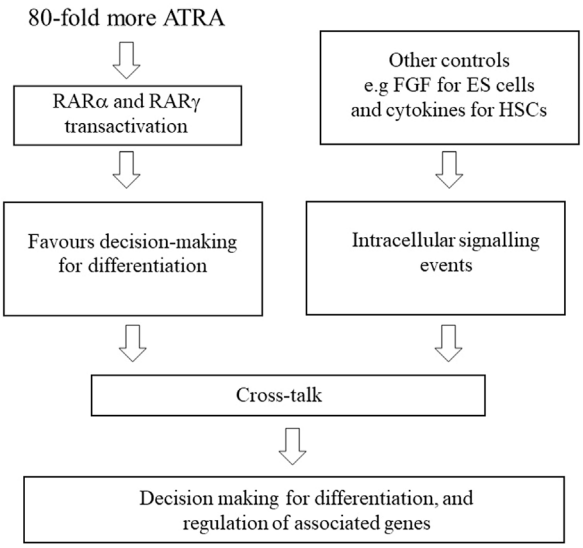

FIGURE 2
Controls on decision making for differentiation. For cell differentiation, ATRA is used at a dose that activates RARα and RARγ. As for ATRA, concomitant treatment of P19 and F9 embryonal carcinoma cells with RARα and RARγ agonists at receptor-selective concentrations favoured differentiation, whereas each agent when used alone failed to promote differentiation. Crosstalk with other signalling events is important, for example, fibroblast growth factor (FGF) for ES cells and the lineage instructive haematopoietic cytokines.

treated at 4 h post fertilisation (hpf) with 10 nM of the RARγ-selective agonist AGN205327. This dose of the agonist is close its binding affinity for RARγ (an ED_{50} of 32 nM). Treatment led to the development of viable fish that were substantially abnormal. There were substantial changes to head morphology, associated with loss of cranial bones and tissue, a reduced antero-posterior axis length, due to somite loss, and heart abnormalities that led to oedema. Regarding the loss of cranial bones and anterior line ganglia, the prevalence of Sox-9 neural crest cells was not affected other than a slight decrease in the head region. The agonist prevented caudal and pectoral fin formation and Tbx5a progenitors that form the pectoral fin were present in the bud region. The lack of pectoral outgrowth, provoked by the RARγ agonist at 4 hpf, was reversed by the addition, at 23 h post fertilization, of a RARγ antagonist, to reverse the action of the RARγ agonist, or wash out of the RARγ agonist at 23 h. The experiments were performed in E3 medium (for zebrafish embryos) which is a balanced salt solution. Therefore, and in the absence of exogenous ATRA, agonising RARγ had disrupted stem cell decision-making for differentiation for the patterning of zebrafish development. The option for fin development had been sustained within bud stem cells as to the reversibility of the action of the RARγ agonist (Wai et al., 2015). Regarding reversibility, it is noteworthy, as mentioned above, that RARγ regulates ATRA-induced chromatin epigenetic marks for gene expression within ES cells (Kashyap et al., 2013).

Controls on stem cell decision-making

The maintenance of stem cells is crucial to an organism to meet the need to replace any damaged and worn-out cells throughout life. The controls that ensure a pool of stem cells are likely to be multiple, and, therefore, rigorous. The presence of active RARγ regulates the maintenance of stem cell stemness because pluripotency genes are direct targets of RARγ. A sub-nM concentration of ATRA is sufficient for transactivation of RARγ. A higher level of ATRA is needed to transactivate RARα, to favour decision-making for differentiation. Stem cells may protect themselves from differentiation that is favoured by RARα activation, by a higher level of ATRA, by means of RARγ-mediated upregulation of the expression of LRAT, for the storage of all-*trans* retinol, and CYP26, for the degradation of ATRA (Figure 1). Regarding a low intracellular level of ATRA within stem cells, it has been proposed that ES cells do not have all the enzymes that are needed to metabolise all-*trans* retinol into ATRA (Chen and Khillan, 2010; Khillan, 2014). Instead, all-*trans* retinol has been proposed to play a role in promoting the self-renewal of ES cells by the direct activation of the phosphoinositide 3 kinase/Akt signalling pathway *via* insulin-like growth factor-1.

ATRA was used at a dose that activates RARα and RARγ for *in vitro* differentiation of the cells considered above. Studies have examined the effect of treating P19 and F9 embryonal carcinoma cells with a combination of the synthetic RARα- and RARγ-selective agonists Am80 and CD666, respectively (Roy et al., 1995). As seen for ATRA activation of RARα and RARγ, treatment of P19 cells with non-selective concentrations of AM80 and CD666, for activation of both RARα and RARγ, induced expression of the *Stra1*, *Stra2*, *CRABPII*, *RARβ* and *Hoxa-1* genes. *Stra1*, *Stra2*, and *CRABPII* were not induced when Am80 and CD666 were used separately at a receptor-selective concentration, and the induction of *RARβ* and *Hoxa-1* was substantially reduced. The combined use of receptor-selective concentrations of AM80 and CD666 led to inductions.

Similarly, P19 cells differentiated when treated with Am80 and CD666 when each agonist was used at a non-selective concentration, they failed to do so when each agonist was used at a receptor-selective concentration, and the combined use of receptor-selective concentrations of Am80 and CD666 led to differentiation The findings for F9 cells were similar other than the combinations of compounds appeared to be less efficient. The differentiation provoked by the combined use of agonists at receptor-selective concentrations was viewed as an additive/synergistic action and support to functional redundancy regarding RARα and RARγ. Alternatively, from these studies and the potent differentiating effects of ATRA the concomitant or temporal activation of both RARα and RARγ favours decision-making for differentiation in a more complex manner. Regarding complexity, RAR/RXR binding elements can distinguish pluripotency-from differentiation-associated genes which appears to be mediated by different sets of regulatory regions, with DR0-containing regions favoured in undifferentiated and DR5-enriched in differentiated cells (Chatagnon et al., 2015).

There are additional controls on decision-making for differentiation that include signalling events that are provoked by, for example, FGF for ES cells and the hematopoietic cytokines that instruct cell lineage (Figure 2). The importance of cytokines is emphasised by studies of HSCs derived from ES cells. Human HSCs ($CD34^+$) cells were efficiently derived from ES cells by coculture with OP9 bone marrow stromal cells. When isolated cells were cultured on MS-5 stromal cells with the addition of stem cell factor, Flt-3 ligand, interleukin 7 (IL-7), and IL-3 they generated granulocytes, macrophages, B-cell, and natural killer cells (Vodyanik et al., 2005). Similarly, the treatment of human ES cells with a combination of cytokines and bone morphogenic protein-4 promoted the differentiation of hematopoietic progenitors. The cells generated included colony-forming units for granulocytes, macrophages, and erythrocytes together with multipotent colony-forming units (Chadwick et al., 2003).

RARα and RARγ controls on decision making and cancer

Cancer is a decision-making process whereby cancer stem cells (CSCs) generate the hierarchy of developing cells to sustain a cancer (Dick, 2008). CSCs appear to arise largely from the malignant transformation of a tissue-specific stem cell and are, therefore, immortal [reviewed in Brown, 2022]. Often, the progeny of CSCs undergoes partial differentiation and belongs to a cell lineage; cancers are categorized according to the resemblance of the bulk cells to a cell type. Support to the lineage restriction of the progeny of CSCs has been provided by the findings from transgenic mice whereby restriction of an oncogenic insult to HSCs/haematopoietic progenitors led to restriction of the lineage options of CSCs or introduced a bias (Gonzales-Herrero et al., 2018).

A role for the fusion gene PML-RARα in the pathogenesis of acute promyelocytic leukaemia is well established (de The et al., 1990). For nine acute promyelocytic patients, fusions have been described between RARγ and the genes for PML, NUP98, CPSF6 and NPM1, and these patients failed to respond to ATRA except for the one patient with the PML-RARγ fusion (Conserva et al., 2019). A recent global study identified 34 patients with RARγ rearrangements, the partner genes were diverse, and the rearrangement conferred a poor prognosis (Zhu et al., 2023).

From the importance of RARγ to decision-making by stem cells, we might expect RARγ to be an oncogene. RARγ overexpression has been reported for good proportions of patients with cholangiocarcinoma, clear cell renal cell carcinoma, colorectal cancer, ovarian cancer, and pancreatic ductal adenocarcinoma. For cholangiocarcinoma, overexpression was associated with poor differentiation and metastasis to lymph nodes and contributed to multidrug resistance. Findings suggested that the role of RARγ is mediated *via* activation of the Akt/NFκB and Wnt/B-catenin pathways and upregulation of P glycoprotein (Huang et al., 2013). RARγ and RARβ were upregulated in clear renal cell carcinoma, as seen from a bioinformatics analysis and the use of quantitative PCR (Kudryavtseva et al., 2016). For colorectal cancer, RARγ overexpression was linked to multidrug resistance with knockdown leading to downregulation of multi-drug resistance 1 and suppression of the Wnt/β-catenin pathway (Huang et al., 2017). High expression on ovarian cancer was a predictor of poor overall survival outcomes and has been linked to accelerated disease progression *via* the regulation of cell proliferation (Xiu et al., 2022). Overexpression of RARγ in pancreatic ductal adenocarcinoma tissue and high-grade precancerous lesions was linked to a poor patient prognosis and blocking RARγ signalling supressed the proliferation of cancer cells (Yamakowa et al., 2022). For the above carcinomas, a common denominator was that a high level of expression of RARγ was linked to a poor prognosis. Targeting RARγ to treat disease is a promising prospect because for prostate cancer, agonism of RARγ stimulated the growth of and colony formation by prostate cancer cell line cells and antagonising led to necroptosis of the cell line colony forming CSC-like cells and patients' cells (Petrie et al., 2022). The pan-RAR antagonist AGN194310 was also effective in ablating the formation of neurosphere-like structures by the CSCs of two paediatric patients' primitive neuroectodermal tumours and a paediatric patient's astrocytoma and killed the progeny of CSCs (Brown and Petrie, 2012). The extent to which increased expression of RARγ and imbalance to the levels of expression of RARγ and RARα had led to the development of the above carcinomas by deregulating the behaviour of CSCs is still unclear. Overexpression of RARγ may play a role to maintain CSCs or to restrict these cells to a particular cell lineage. The latter is an intriguing consideration in view of the role of RARγ2 in ES neuronal differentiation and perhaps the need to eliminate other fates (Ying et al., 2003), agonising RARγ interfered with patterning for zebrafish development (Wai et al., 2015), and the need for RARγ for chromatin epigenetic marks (Kashyap et al., 2013). Regarding epigenetic marks, RARγ was identified as the predominant mediator of ATRA-mediated signalling within ES cells for activation of the *Hoxa* and *Hoxb* gene clusters. It was required for broad epigenomic organisation and necessary for the gene-specific removal of the polycomb repressive mark H3K27me3 during ES cell differentiation. *Hox* gene cluster reorganisation was triggered by RARγ located at the *Hoxa1* 3′-RARE and deletion of the RARγ binding site within the *Hoxa1* enhancer attenuated epigenomic activation of *Hoxa* and *Hoxb* gene structures (Kashyap et al., 2011).

Perspectives and conclusion

Distinct ATRA gradients and boundaries, from cells that synthesize and metabolize, are important to patterning embryogenesis, but there does not appear to be a linear relationship between dose and phenotype (Bernheim and Meilhac, 2020). Gradients and the dose of ATRA that stem cells and their progeny are exposed is relevant to decision-making because sub nM ATRA is sufficient to activate RARγ with RARα activation needing substantially more. Stem cells are equipped to store and degrade ATRA and seem unable to synthesize which may provide protection from ATRA-modulation of the frequency of decision-making for differentiation. RARγ activation is important to the maintenance of HSCs and their stemness and activation, in the absence of active RARα, interfered with decision-making by zebrafish embryonic stem cells for differentiation. The level of ATRA that is used routinely to drive the differentiation of ES cells and other cells, which express both RARγ and RARα, activates both RARα and RARγ and concomitant or temporal activation of these receptors favors differentiation. Stem cell differentiation is a continuous and progressive process which might favour a temporal interaction(s), but whether concomitant or temporal is yet unclear. Expression of RARγ decreases as stem cells differentiate leaving RARα to exert a sole influence on the progression of differentiation.

The roles of RARα and RARγ are modulatory, rather than obligatory, which raises the question what is nature of the events that are being modulated. Signalling *via* growth factors and hematopoietic cytokines provide a further input to ES cell and HSC decision-making for cell differentiation, respectively. That stem cell differentiation is a progressive and gradual process presumably requires learning and memory of the events that are provoked by growth factors/cytokines. There is evidence to support integration of ATRA signalling with how cells learn from the events that are provoked by growth factors because CRABP1 delivers ATRA to the CYP26 family members for degradation and such dampens the sensitivity of ES cells to growth factors to affect their learning and memory (Nagpal and Wei, 2019). An intriguing possibility is whether RARα and/or RARγ are modulatory by virtue of influencing the retention or loss of cell learning and memory for stemness and decision-making for differentiation. The epigenome has been proposed as the judge, jury, and executioner of stem cell fate (Tollervey and Lunyak, 2012). As above, RARγ is needed for ATRA-induced chromatin epigenetic marks [Kashyap et al., 2012], and memory/learning are written within the epigenome by marks.

Presently, we know how RARs work as heterodimers with RXRs, how they bind to response elements, that they repress gene expression in the absence of ligand and drive expression when ligand is bound, and that the RAR subtypes can regulate sub-sets of genes. However, the more complete picture regarding how all of this modulates the specification of cell lineage and/or the switch from stem cell maintenance to the onset of differentiation is still a complex and unresolved puzzle. Considerations include the extent to which ATRA is synthesized endogenously, which though cryptic is at a physiological level, the provision of ATRA by neighbouring cells including from gradients, which is again physiological, whether RARα and/or RARγ are activated, and crosstalk with other cytokine-provoked signalling cascades including phosphorylation of RARs.

Author contributions

GB wrote the manuscript.

Funding

This project received funding from the European Union's Seventh Framework Programme for research, technological development, and demonstration under grant agreement no 315902. GB was the lead within the Marie Curie Initial Training Network DECIDE.

Conflict of interest

The author declares that the research was conducted in the absence of any commercial or financial relationships that could be construed as a potential conflict of interest.

Publisher's note

References

Amit, M., and Itskovitz-Elder, J. (2002). Derivation and spontaneous differentiation of human embryonic stem cells. *J. Anat.* 200, 225–232. doi:10.1046/j.1469-7580.2002.00032.x

Baltes, S., Nau, H., and Lampen, A. (2004). All-trans retinoic acid enhances differentiation and influences permeability of intestinal Caco-2 cells under serum-free conditions. *Dev. Growth Differ.* 46, 503–514. doi:10.1111/j.1440-169x.2004.00765.x

Berenger, M., and Duester, G. (2022). Retinoic acid, RARs and early development. *J. Mol. Endocrinol.* 69, T59–T67. doi:10.1530/JME-22-0041

Bernheim, S., and Meilhac, S. M. (2020). Mesoderm patterning by a dynamic gradient of retinoic acid signalling. *Philos. Trans. R. Soc. Lond. B Boil. Sci.* 375, 20190556. doi:10.1098/rstb.2019.0556

Breitman, T. R., Selonick, S. E., and Collins, S. J. (1980). Induction of differentiation of the human promyelocytic leukemia cell line (HL-60) by retinoic acid. *Proc. Natl. Acad. Sci. U. S. A.* 77, 2936–2940. doi:10.1073/pnas.77.5.2936

Brown, G., and Petrie, K. (2012). The RARγ oncogene: An Achilles heel for some cancers. *Int. J. Mol. Sci.* 22, 3632. doi:10.3390/ijms22073632

Brown, G., Marchwicka, A., Cunningham, A., Toellner, K-M., and Marcinkowska, E. (2017). Antagonizing retinoic acid receptors increases myeloid cell production by cultured human hematopoietic stem cells. *Arch. Immunol. Ther. Exp.* 65, 69–81. doi:10.1007/s00005-016-0411-0

Brown, G. (2020). Towards a new understanding of decision-making by hematopoietic stem cells. *Int. J. Mol. Sci.* 21, 2362. doi:10.3390/ijms21072362

Brown, G. (2022). Hematopoietic and chronic myeloid leukemia stem cells: Multi-stability versus lineage restriction. *Int. J. Mol. Sci.* 23, 13570. doi:10.3390/ijms232113570

Bunce, C. M., French, P. J., Durham, J., Stockley, R. A., Michell, R. H., and Brown, G. (1994). Indomethacin potentiates the induction of HL60 differentiation to neutrophils, by retinoic acid and granulocyte colony-stimulating factor, and to monocytes, by vitamin D3. *Leukemia* 8, 595–604.

Cabezas-Wallscheid, N., Buettner, F., Sommerkamp, P., Klimmeck, D., Ladel, L., Thalheimer, F. B., et al. (2017). Vitamin A-retinoic acid signaling regulates hematopoietic stem cell dormancy. *Cell.* 169, 807–823.e19. doi:10.1016/j.cell.2017.04.018

Ceredig, R., Rolink, A. G., and Brown, G. (2009). Models of haematopoiesis: Seeing the wood for the trees. *Nat. Rev. Immunol.* 9, 293–300. doi:10.1038/nri2525

Chadwick, K., Wang, L., Li, L., Menendez, P., Murdock, B., Roulleau, A., et al. (2003). Cytokines and BMP-4 promote hematopoietic differentiation of human embryonic stem cells. *Blood* 102, 906–915. doi:10.1182/blood-2003-03-0832

Chambon, P. (1996). A decade of molecular biology of retinoic acid receptors. *FASEB J.* 10, 940–954. doi:10.1096/fasebj.10.9.8801176

Chatagnon, A., Veber, P., Marin, V., Bede, J., Triqueneaux, G., Semon, M., et al. (2015). RAR/RXR binding dynamics distinguish pluripotency from differentiation associated cis-regulatory elements. *Nucleic Acid. Res.* 43, 4833–4854. doi:10.1093/nar/gkv370

Chee, L. C., Hendy, J., Purton, L. E., and McArthur, G. A. (2013). The granulocyte-colony stimulating factor receptor (G-CSFR) interacts with retinoic acid receptors (RARs) in the regulation of myeloid differentiation. *J. Leukoc. Biol.* 93, 235–243. doi:10.1189/jlb.1211609

Chen, L., and Khillan, J. S. (2010). A novel signaling by vitamin A/retinol promotes self renewal of mouse embryonic stem cells by activating PI3K/Akt signaling pathway via insulin-like growth factor-1 receptor. *Stem Cells* 28, 57–63. doi:10.1002/stem.251

Chute, J. P., Muramoto, G. G., Whitesides, J., Calvin, M., Safi, R., Chao, N. J., et al. (2006). Inhibition of aldehyde dehydrogenase and retinoid signaling induces the expansion of human hematopoietic stem cells. *Proc. Natl. Acad. Sci. U. S. A.* 103, 11707–11712. doi:10.1073/pnas.0603806103

Clagett-Dame, M., and Knutson, D. (2011). Vitamin A in reproduction and development. *Nutrients* 3, 325–428. doi:10.3390/nu3040385

Collins, S. J., Robertson, K., and Mueller, L. (1990). Retinoic acid-induced granulocytic differentiation of HL-60 myeloid leukemia cells is mediated directly through the retinoic acid receptor (RAR-alpha). *Mol. Cell. Biol.* 10, 2154–2163. doi:10.1128/mcb.10.5.2154

Collins, S. J. (2002). The role of retinoids and retinoic acid receptors in normal hematopoiesis. *Leukemia* 16, 1896–1905. doi:10.1038/sj.leu.2402718

Conserva, M. R., Redavid, I., Anelli, L., Zagaria, A., Specchia, G., and Albano, F. (2019). RARG gene dysregulation in acute myeloid leukemia. *Front. Mol. Biosci.* 6, 114. doi:10.3389/fmolb.2019.00114

Czuba, L. C., Zhang, G., Yabat, K., and Isoherranen, N. (2020). Analysis of vitamin A and retinoids in biological matrices. *Methods Enzymol.* 637, 309–340. doi:10.1016/bs.mie.2020.02.010

de Thé, H., Chomienne, C., Lanotte, M., Degos, L., and Dejean, A. (1990). The t(15;17) translocation of acute promyelocytic leukaemia fuses the retinoic acid receptor alpha gene to a novel transcribed locus. *Nature* 347, 558–561. doi:10.1038/347558a0

Dick, J. E. (2008). Stem cell concepts renew cancer research. *Blood* 112, 4793–4807. doi:10.1182/blood-2008-08-077941

Duong, V., and Rochette-Egly, C. (2011). The molecular physiology of nuclear retinoic acid receptors. From health to disease. *Biochim. Biophys. Acta* 1812, 1023–1031. doi:10.1016/j.bbadis.2010.10.007

Engberg, N., Kahn, M., Peterson, D. R., Hanson, M., and Serup, P. (2010). Retinoic acid synthesis promotes development of neural progenitors from mouse embryonic stem cells by suppressing endogenous Wnt-dependent nodal signaling. *Stem Cells* 28, 1498–1509. doi:10.1002/stem.479

Gonzales-Herrero, I., Rodriguez-Hernandez, G., Luengas-Martinez, A., Isidro-Hernandez, M., Jimenez, R., Garcia-Cenader, M. B., et al. (2018). The making of leukemia. *Int. J. Mol. Sci.* 19, 1494. doi:10.3390/ijms19051494

Gratas, C., Menot, M. L., Dresch, C., and Chomienne, C. (1993). Retinoid acid supports granulocytic but not erythroid differentiation of myeloid progenitors in normal bone marrow cells. *Leukemia* 7, 1156–1162.

Grover, A., Mancini, E., Moore, S., Mead, A. J., Atkinson, D., Rasmussen, K. D., et al. (2014). Erythropoietin guides multipotent hematopoietic progenitor cells toward an erythroid fate. *J. Exp. Med.* 211, 181–188. doi:10.1084/jem.20131189

Hale, L. A., Tallafuss, A., Yan, Y.-L., Dudley, L., Eisen, J. S., and Postlethwait, J. H. (2006). Characterization of the retinoic acid receptor genes raraa, rarab and rarg during zebrafish development. *Gene Expr. Patterns* 6, 546–555. doi:10.1016/j.modgep.2005.10.007

Huang, G. L., Luo, Q., Rui, G., Zhang, W., Zhang, Q. Y., Chen, Q. X., et al. (2013). Oncogenic activity of retinoic acid receptor γ is exhibited through activation of the Akt/NF-κB and Wnt/β-catenin pathways in cholangiocarcinoma. *Mol. Cell. Biol.* 33, 3416–3425. doi:10.1128/MCB.00384-13

Huang, G. L., Song, W., Zhou, P., Fu, Q. R., Lin, C. L., Chen, Q. X., et al. (2017). Oncogenic retinoic acid receptor γ knockdown reverses multi-drug resistance of human colorectal cancer via Wnt/β-catenin pathway. *Cell. Cycle* 16, 685–692. doi:10.1080/15384101.2017.1295180

Idres, N., Marill, J., Flexer, M. A., and Chabot, G. G. (2002). Activation of retinoic acid receptor-dependent transcription by all-trans-retinoic acid metabolites and isomers. *J. Biol. Chem.* 277, 31491–31498. doi:10.1074/jbc.M205016200

Jacobs-Helber, S. M., Wickrema, A., Birrer, M. J., and Sawyers, S. T. (1998). AP1 regulation of proliferation and initiation of apoptosis in erythropoietin-dependent erythroid cells. *Mol. Cell. Biol.* 18, 3699–3707. doi:10.1128/MCB.18.7.3699

Kashyap, V., Gudas, L. J., Brenet, F., Funk, P., Viale, A., and Scandura, J. M. (2011). Epigenomic reorganization of the clustered Hox genes in embryonic stem cells induced by retinoic acid. *J. Biol. Chem.* 286, 3250–3260. doi:10.1074/jbc.M110.157545

Kashyap, V., Laursen, K. B., Brenet, F., Viale, A. J., Scandura, J. M., and Gudas, L. J. (2013). RAR is essential for retinoic acid induced chromatin remodeling and transcriptional activation in embryonic stem cells. *J. Cell. Sci.* 126, 999–1008. doi:10.1242/jcs.119701

Kastner, P., and Chan, S. (2001). Function of RARalpha during the maturation of neutrophils. *Oncogene* 20, 7178–7185. doi:10.1038/sj.onc.1204757

Khillan, J. S. (2014). Vitamin A/retinol and maintenance of pluripotency of stem cells. *Nutrients* 6, 1209–1222. doi:10.3390/nu6031209

Koyima, Y., and Habas, R. (2008). Wnt signal transduction pathways. *Organogenesis* 4, 68–75. doi:10.4161/org.4.2.5851

Kudryavtseva, A. V., Nyushko, K. M., Zaretsky, A. R., Shagin, D. A., Kaprin, A. D., and Yakovlevich Alekseev, B. (2016). Upregulation of rarb, rarg, and rorc genes in clear cell renal cell carcinoma. *Biomed. Pharmacol. J.* 9, 967–975. doi:10.13005/bpj/1036

Kuwata, T., Wang, I.-M., Tamara, T., Pannamperuma, R. H., Levine, R., Holmes, K. L., et al. (2000). Vitamin A deficiency in mice causes a systemic expansion of myeloid cells. *Blood* 95, 3349–3356. doi:10.1182/blood.v95.11.3349

Labrecque, J., Allan, D., Chambon, P., Iscove, N. N., Lohnes, D., and Hoang, T. (1998). Impaired granulocytic differentiation *in vitro* in hematopoietic cells lacking retinoic acid receptors α1 and γ. *Blood* 92, 607–615. doi:10.1182/blood.v92.2.607.414k06_607_615

Laursen, K. B., and Gudus, L. J. (2018). Combinatorial knockout of RARα, RARβ, and RARγ completely abrogates transcriptional responses to retinoic acid in murine embryonic stem cells. *J. Biol. Chem.* 293, 11891–11900. doi:10.1074/jbc.RA118.001951

Leroy, P., Krust, A., Zelent, A., Mendelsohn, C., Gamier, J. M., Kastner, P., et al. (1991). Multiple isoforms of the mouse retinoic acid receptor alpha are generated by alternative splicing and differential induction by retinoic acid. *EMBOJ* 10, 59–69. doi:10.1002/j.1460-2075.1991.tb07921.x

Li, Y., Mao, X., Zhao, X., Su, Y., Zhou, X., Shi, K., et al. (2019). An optimized method for neuronal differentiation of embryonic stem cells *in vitro*. *J. Neurosci. Methods* 330, 108486. doi:10.1016/j.jneumeth.2019.108486

Lohnes, D., Kastner, P., Dierich, A., Mark, M., LeMeur, M., and Chambon, P. (1993). Function of retinoic acid receptor gamma in the mouse. *Cell.* 73, 643–658. doi:10.1016/0092-8674(93)90246-m

Lohnes, D., Mark, M., Mendelsohn, C., Dolle, P., Dierich, A., Gorry, P., et al. (1994). Function of the retinoic acid receptors (RARs) during development (I). Craniofacial and skeletal abnormalities in RAR double mutants. *Development* 120, 2723–2748. doi:10.1242/dev.120.10.2723

Lufkin, T., Lohnes, D., Mark, M., Dierich, A., Gony, P., Gaub, M-P., et al. (1993). High postnatal lethality and testis degeneration in retinoic acid receptor α mutant mice. *Proc. Nat. Acad. Sci. U. S. A.* 90, 7225–7229. doi:10.1073/pnas.90.15.7225

Luo, T., Pasceri, P., Conlon, R. A., Rossant, J., and Giguere, V. (1995). Mice lacking all isoforms of retinoic acid receptor β develop normally and are susceptible to the teratogenic effects of retinoic acid. *Mech. Dev.* 53, 61–71. doi:10.1016/0925-4773(95)00424-6

Mangelsdorf, D. J., Koeffler, H. P., Donaldson, C. A., Pike, J. W., and Haussler, M. R. (1984). 1,25-Dihydroxyvitamin D3-induced differentiation in a human promyelocytic leukemia cell line (HL-60): Receptor-mediated maturation to macrophage like cells. *J. Cell. Biol.* 98, 391–398. doi:10.1083/jcb.98.2.391

Marchwicka, A., Cebrat, M., Lasziewicz, A., Sniezewski, L., Brown, G., and Marcinkowska, E. (2016). Regulation of vitamin D receptor expression by retinoic acid receptor alpha in acute myeloid leukemia cells. *J. Steroid Biochem. Mol. Biol.* 159, 121–130. doi:10.1016/j.jsbmb.2016.03.013

Martinez-Ceballos, E., and Gudas, L. J. (2008). Hoxa1 is required for the retinoic acid-induced differentiation of embryonic stem cells into neurons. *J. Neurosci. Res.* 86, 2809–2819. doi:10.1002/jnr.21729

Mendelsohn, C., Mark, M., Dolle, P., Dierich, A., Gaub, M. P., Krust, A., et al. (1994). Retinoic acid receptor beta 2 (RAR beta 2) null mutant mice appear normal. *Dev. Biol.* 166, 246–258. doi:10.1006/dbio.1994.1311

Metcalf, D., and Burgess, A. W. (1982). Clonal analysis of progenitor cell commitment of granulocyte or macrophage production. *J. Cell. Physiol.* 111, 275–283. doi:10.1002/jcp.1041110308

Mossadegh-Keller, N., Sarrazin, S., Kandalla, P. K., Espinosa, L., Stanley, E. R., Nutt, S. L., et al. (2013). M-CSF instructs myeloid lineage fate in single haematopoietic stem cells. *Nature* 497, 239–243. doi:10.1038/nature12026

Muramoto, G. G., Russell, J. L., Safi, R., Salter, A. B., Himberg, H. A., Dahler, P., et al. (2010). Inhibition of aldehyde dehydrogenase expands hematopoietic stem cells with radioprotective capacity. *Stem Cells* 28, 523–534. doi:10.1002/stem.299

Nagpal, I., and Wei, L-N. (2019). All-trans retinoic acid as a versatile cytosolic signal modulator mediated by CRABP1. *Int. J. Mol. Sci.* 20, 3610. doi:10.3390/ijms20153610

Nestorowa, S., Hamey, F. K., Pijuan Sala, B., Diamanti, F., Shepherd, M., Laurenti, E., et al. (2016). A single-cell resolution map of mouse hematopoietic stem and progenitor cell differentiation. *Blood* 128, e20–e31. –e31. doi:10.1182/blood-2016-05-716480

Nicholson, R. C., Maders, S., Nagpal, S., Leid, M., Rochette Egly, C., and Chambon, P. (1990). Negative regulation of the rat stromelysin gene promoter by retinoic acid is mediated by an AP1 binding site. *EMBO J.* 9, 4443–4454. doi:10.1002/j.1460-2075.1990.tb07895.x

Oeda, S., Hayashi, Y., Chan, T., Takasato, M., Aihara, Y., Obabayashima, K., et al. (2013). Induction of intermediate mesoderm by retinoic acid receptor signaling from differentiating mouse embryonic stem cells. *Int. J. Dev. Biol.* 57, 383–389. doi:10.1387/ijdb.130058ma

Petrie, K., Urban-Wojciuk, Z., Sbirkov, Y., Graham, A., Hamann, A., and Brown, G. (2022). Retinoic acid receptor γ is a therapeutically targetable driver of growth and survival in prostate cancer. *Cancer Rep.* 3, e1284. doi:10.1002/cnr2.1284

Purton, L. E., Bernstein, I. D., and Collins, S. J. (1999). All-trans retinoic acid delays the differentiation of primitive hematopoietic precursors (lin-c-kit+Sca-1(+)) while enhancing the terminal maturation of committed granulocyte/monocyte progenitors. *Blood* 94, 483–495. doi:10.1182/blood.v94.2.483.414k12_483_495

Purton, L. E., Dworkin, S., Olsen, G. H., Walkley, C. R., Fabb, S. A., Collins, S. J., et al. (2006). RARgamma is critical for maintaining a balance between hematopoietic stem cell self-renewal and differentiation. *J. Exp. Med.* 203, 1283–1293. doi:10.1084/jem.20052105

Randolph, R. K., and Simon, M. (1997). Metabolism of all-trans-retinoic acid by cultured human epidermal keratinocytes. *J. Lipid Res.* 3, 1374–1383. doi:10.1016/s0022-2275(20)37420-4

Rieger, M. A., Hoppe, P. S., Smejkal, B. M., Eitelhuber, A. C., and Schroeder, T. (2009). Hematopoietic cytokines can instruct lineage choice. *Science* 325, 217–218. doi:10.1126/science.1171461

Rochette-Egly, C., Quland-Abdelghani, M., Staub, A., Pfister, V., Chambon, P., Gaub, M-P., et al. (1995). Phosphorylation of the retinoic acid receptor-alpha by protein kinase A. *Mol. Endocrinol.* 9, 860–871. doi:10.1210/mend.9.7.7476969

Rochette-Egly, C. (2015). Retinoic acid signaling and mouse embryonic stem cell differentiation: Cross talk between genomic and non-genomic effects of RA. *Biochim. Biophys. Acta* 1851, 66–75. doi:10.1016/j.bbalip.2014.04.003

Roy, B., Taneja, R., and Chambon, P. (1995). Synergistic activation of retinoic acid (RA)-responsive genes and induction of embryonal carcinoma cell differentiation by an RA receptor α (RARα)-RARβ-or RARγ-selective ligand in combination with a retinoid X receptor-specific ligand. *Mol. Cell. Biol.* 15, 6481–6487. doi:10.1128/MCB.15.12.6481

Ruberte, E., Dolle, P., Krust, A., Zelent, A., Morris-Kay, G., and Chambon, P. (1990). Specific spatial and temporal distribution of retinoic acid receptor gamma transcripts during mouse embryogenesis. *Development* 108, 213–222. doi:10.1242/dev.108.2.213

Sadhananthan, A. H., and Touson, A. (2005). Human embryonic stem cells and spontaneous differentiation. *Ital. J. Anat. Embryol.* 110, 151–157.

Sakashita, A., Nakamaki, T., Tsuruoke, N., Honma, Y., and Hozumi, M. (1991). Granulocyte colony-stimulating factor, not granulocyte-macrophage colony-stimulating factor, co-operates with retinoic acid on the induction of functional N-formyl-methionyl-phenylalanine receptors in HL-60 cells. *Leukemia* 5, 26–31.

Samarut, E., Gaudin, C., Hughes, S., Gillet, B., de Bernard, S., Jouve, P-E., et al. (2014). Retinoic acid receptor subtype-specific transcriptomes in the early zebrafish embryo. *Mol. Endocrinol.* 28, 200–272.

Schier, A. F., and Shen, M. M. (2000). Nodal signalling in vertebrate development. *Nature* 403, 385–389. doi:10.1038/35000126

Schonberger, K., Obier, N., Romero-Mulero, M. C., Cauchy, P., Mess, J., Pavlovich, P. V., et al. (2022). Multilayer omics analysis reveals a nonclassical retinoic acid signaling axis that regulates hematopoietic stem cell identity. *Cell. Stem Cell.* 29, 131–148.e10. doi:10.1016/j.stem.2021.10.002

Silva, C., Wood, J. R., Salvador, L., Kostetskii, I., Williams, C. J., Strauss, J. F., III, et al. (2009). Expression profile of male germ cell-associated genes in mouse embryonic stem cell cultures treated with all-trans retinoic acid and testosterone. *Mol. Reprod. Dev.* 70, 11–21. doi:10.1002/mrd.20925

Sokol, S. Y. (2011). Maintaining embryonic stem cell pluripotency with Wnt signaling. *Development* 138, 4341–4350. doi:10.1242/dev.066209

Takenaga, M., Fukumoto, M., and Hari, Y. (2007). Regulated Nodal signaling promotes differentiation of the definitive endoderm and mesoderm from ES cells. *J. Cell. Sci.* 120, 2078–2090. doi:10.1242/jcs.004127

Taneja, R., Bouillet, P., Boylan, J. F., Gaub, M. P., Roy, B., Gudas, L. J., et al. (1995). Reexpression of retinoic acid receptor (RAR) gamma or overexpression of RAR alpha or RAR beta in RAR gamma-null F9 cells reveals a partial functional redundancy between the three RAR types. *Proc. Natl. Acad. Sci. U. S. A.* 92, 7854–7858. doi:10.1073/pnas.92.17.7854

Tanoury, Z. A., Gaouar, S., Piskunov, A., Tao, Y., Urban, S., Just, B., et al. (2014). Phosphorylation of RARγ2 is critical for the neuronal differentiation of mouse embryonic stem cells. *J. Cell. Sci.* 127, 2095–2105. doi:10.1242/jcs.145979

Tanoury, Z. A., Piskunov, A., and Rochette-Egly, C. (2013). Vitamin A and retinoid signaling: Genomic and nongenomic effects. *J. Lipid Res.* 54, 1761–1775. doi:10.1194/jlr.R030833

Tollervey, J. R., and Lunyak, V. V. (2012). Epigenetics: Judge, jury and executioner of stem cell fate. *Epigenetics* 7, 823–840. doi:10.4161/epi.21141

Velten, L., Haas, S. F., Raffel, S., Blaszkiecz, S., Islam, S., Hennig, B. P., et al. (2017). Human haematopoietic stem cell lineage commitment is a continuous process. *Nat. Cell. Biol.* 19, 271–281. doi:10.1038/ncb3493

Vodyanik, M. A., Bork, J. A., Thomson, J. A., and Slukin, I. I. (2005). Human embryonic stem cell-derived CD34$^+$ cells: Efficient production in the coculture with OP9 stromal cells and analysis of lymphohematopoietic potential. *Blood* 15, 617–626. doi:10.1182/blood-2004-04-1649

Wai, H. A., Kawakami, K., Wada, H., Muller, F., Vernalis, A. B., Brown, G., et al. (2015). The development and growth of tissues derived from cranial neural crest and primitive mesoderm is dependent on the ligation status of retinoic acid receptor γ: Evidence that retinoic acid receptor γ functions to maintain stem/progenitor cells in the absence of retinoic acid. *Stem Cells Dev.* 24, 507–519. doi:10.1089/scd.2014.0235

Walkley, C. R., Yuan, Y. D., Chandraratna, R. A., and McArthur, G. A. (2002). Retinoic acid receptor antagonism *in vivo* expands the numbers of pre-cursor cells during granulopoiesis. *Leukemia* 16, 1763–1772. doi:10.1038/sj.leu.2402625

Xiu, L., Zhao, Y., Li, N., Zeng, J., Liu, J., Fu, Y., et al. (2022). High expression of RARG accelerates ovarian cancer progression by regulating cell proliferation. *Front. Oncol.* 12, 1063031. doi:10.3389/fonc.2022.1063031

Yamakowa, K., Koyangi-Aoi, M., Machinaga, A., Kakiuchi, N., Hirano, T., Kodama, Y., et al. (2022). Blockage of retinoic acid signalling via RARg suppressed the proliferation of pancreatic cancer cells by arresting the cell cycle progression in G1-S phase. *Research Square*. doi:10.21203/rs.3.rs-2084078/v1

Ying, Q. L., Stavridis, M., Griffiths, P., Li, M., and Smith, A. (2003). Conversion of embryonic stem cells into neuroectodermal precursors in adherent monoculture. *Nat. Biotechnol.* 21, 183–186. doi:10.1038/nbt780

Yoon, S-H., Bae, M-R., La, H., Song, H., Hong, K., and Do, J-T. (2021). Efficient generation of neural stem cells from embryonic stem cells using a three-dimensional differentiation system. *Int. J. Mol. Sci.* 22, 8322. doi:10.3390/ijms22158322

Zhu, J., Heyworth, C. M., Glasow, A., Huang, Q-H., Petrie, K., Lanotte, M., et al. (2001). Lineage restriction of the RARalpha gene expression in myeloid differentiation. *Blood* 98, 2563–2567. doi:10.1182/blood.v98.8.2563

Zhu, H-H., Qin, Y-Z., Zhang, Z-L., Liu, Y-J., Wen, L-J., You, M. J., et al. (2023). A global study for acute myeloid leukemia with *RARG* rearrangement. *Blood Adv.*, 2022008364. Online ahead of print. doi:10.1182/bloodadvances.2022008364

frontiers | Frontiers in Cell and Developmental Biology

TYPE Review
PUBLISHED 05 July 2023
DOI 10.3389/fcell.2023.1190266

OPEN ACCESS

EDITED BY
Myon Hee Lee,
East Carolina University, United States

REVIEWED BY
Zhichao Xi,
Shanghai University of Traditional Chinese Medicine, China
Weinan Zhou,
University of Illinois at Urbana-Champaign, United States

*CORRESPONDENCE
Siming Wang,
lwsm126030@126.com
Meichen Liu,
liumc0367@163.com

RECEIVED 20 March 2023
ACCEPTED 22 June 2023
PUBLISHED 05 July 2023

CITATION
Liu Y, Jiang L, Song W, Wang C, Yu S, Qiao J, Wang X, Jin C, Zhao D, Bai X, Zhang P, Wang S and Liu M (2023), Ginsenosides on stem cells fate specification—a novel perspective. *Front. Cell Dev. Biol.* 11:1190266. doi: 10.3389/fcell.2023.1190266

Ginsenosides on stem cells fate specification—a novel perspective

Ying Liu[1], Leilei Jiang[1], Wenbo Song[1], Chenxi Wang[1], Shiting Yu[1], Juhui Qiao[1], Xinran Wang[1], Chenrong Jin[1], Daqing Zhao[1], Xueyuan Bai[1], Peiguang Zhang[2], Siming Wang[1]* and Meichen Liu[1]*

[1]Northeast Asia Research Institute of Traditional Chinese Medicine, Changchun University of Chinese Medicine, Changchun, China, [2]Changchun Institute of Optics, Fine Mechanics and Physics, Chinese Academy of Sciences Changchun, Changchun, Jilin, China

Recent studies have demonstrated that stem cells have attracted much attention due to their special abilities of proliferation, differentiation and self-renewal, and are of great significance in regenerative medicine and anti-aging research. Hence, finding natural medicines that intervene the fate specification of stem cells has become a priority. Ginsenosides, the key components of natural botanical ginseng, have been extensively studied for versatile effects, such as regulating stem cells function and resisting aging. This review aims to summarize recent progression regarding the impact of ginsenosides on the behavior of adult stem cells, particularly from the perspective of proliferation, differentiation and self-renewal.

KEYWORDS

ginsenosides, stem cells, proliferation, fate specification, differentiation, self-renewal

1 Introduction

Panax ginseng (*Panax ginseng* C. A. Mey.), is a perennial herb of the *Araliaceae* family (de Oliveira Zanuso et al., 2022). This plant is widely cultivated in East Asia, particularly in China, Japan, and South Korea, due to its characteristic of being both a food and a medicine (Ichim and de Boer, 2020). Ginseng contains ginsenosides, polysaccharides, proteins, polypeptides, amino acids and other chemical components, among which ginsenosides are the main medicinal components (Lee et al., 2019). Currently, around 200 types of ginsenosides have been reported (Ratan et al., 2021). Based on the classification of ginsenosides by glycoside type, ginsenosides generally be compartmentalized into two categories: dammarane-type tetracyclic triterpene and oleanane-type pentacyclic triterpene saponins (Hou et al., 2021). Dammarane-type ginsenosides are the primary types and biologically active components of ginsenosides, which are divided into protopanaxadiol (PPD) types (including ginsenosides Ra1, Ra2, Ra3, Rb1, Rb2, Rb3, Rc, Rd, Rg3, Rh2, F2, compound K, malonyl-Rb1, malonyl-Rb2, malonyl-Rc and malonyl-Rd, etc.) and protopanaxatriol (PPT) types (including ginsenosides Re, Rf, Rg1, Rg2, F1 and Rh1, etc.) (Pan et al., 2018). In contrast, oleanane-type ginsenosides (including Ro, Rh3, Ri, etc.) are rare in ginseng species (Zhang H. et al., 2022). The experimental pharmacological research of ginsenosides have shown that the number of sugar residues contained in the branched, the position of glycosides, and their stereoselectivity all affect the pharmacological activity of ginsenoside monomers (Piyasirananda et al., 2021; Yousof Ali et al., 2021; Ali et al., 2022). Oral administration of ginsenosides is the major approach, but they are not easily absorbed by themselves with low bioavailability (Won et al., 2019). On the contrary, a

TABLE 1 Clinical efficacy of ginsenosides.

Component	Application	Effect	Mechanism	References
Rd	AIS	neuroprotection	microglial proteasome activity and sequential inflammation↓	Zhang et al. (2016)
Rg3	AL	anti-angiogenic	PI3K/Akt and ERK1/2 pathways↓	Zeng et al. (2014)
Rb1	CKD	alleviate kidney dysfunction	oxidative stress and inflammation↓	Xu et al. (2017)
Rg1	sports challenge	reduce oxidative damage and inflammation	TBA activity↓ and TNF-α mRNA↓ and IL-10 mRNA↑	Hou et al. (2015)
Rg1	exercise resistance	induces immune stimulation and reduces skeletal muscle aging	$p16^{INK4a}$ and MPO mRNA levels↓	Lee et al. (2021)

AIS, acute ischemic stroke; AL, acute leukemia; CKD, chronic kidney disease.

large number of enzymes or gut microbiota can convert ginsenosides into deglycosylated products with a higher bioavailability and pharmacological activity that can be easily absorbed by human body (Yang L. et al., 2020). Ginsenosides have been found to possess a range of pharmacological effects, such as anti-aging (de Oliveira Zanuso et al., 2022), anti-tumor (Wong et al., 2015), hematopoietic recovery (He et al., 2021), promotion of osteogenesis (Wu et al., 2022), and neuroprotection (Rokot et al., 2016). In clinical trials, ginsenosides have been beneficial to the treatment of acute ischemic stroke, cancer, and chronic kidney disease, and can prompt oxidative stress or inflammation caused by exercise challenges (Table 1). Although ginsenosides exhibit various positive physiological activities, this review will focus on the relationship between ginsenosides and stem cells.

Stem cells, encompassing both adult stem cells and embryonic varieties, are essential for developing human tissues and maintaining homeostasis (Zakrzewski et al., 2019). Their unique properties of self-renewal, high proliferation, and differentiation into multiple lineages make them attractive for a variety of applications, such as cell replacement as well as tissue and organ renewal in regenerative medicine (Brassard and Lutolf, 2019), exploration of regulatory mechanisms during embryonic development (Weatherbee et al., 2021), therapy for various diseases (Sinenko et al., 2021), the establishment of disease models (Sterneckert et al., 2014) and drug screening and development (Kumar et al., 2021). Notably, the fate specification of stem cells (proliferation, differentiation and self-renewal) is involved in the regulation of the body's biological process. An imbalance in fate specification can lead to the emergence and progression of aging or even disease (Chandel et al., 2016). Excessive proliferation of stem cells can lead to the development of tumors and cancers (Najafi et al., 2019), while impaired self-renewal and differentiation of stem cells can limit the potential of tissue and organ regeneration and damage repair, such as in the case of aging and nervous system injury (De et al., 2021; Sivandzade and Cucullo, 2021). Consequently, understanding the regulation of stem cells fate is indispensable for the prevention of aging and many diseases. The stem cell niche refers to the microenvironment that maintains the proliferation, differentiation and self-renewal of stem cells (Hicks and Pyle, 2023). Stem cells can receive signals from the ecological niche and respond accordingly, which plays an important role in supporting and coordinating the activities of stem cells (Chacón-Martínez et al., 2018). Ginsenosides inhibit inflammatory responses and reduce oxidative stress to improve the stem cells niche (Hu et al., 2015; Wu et al., 2020). Also, ginsenosides can promote stem cell proliferation, differentiation into specific cell types, or self-renewal, thus regulating stem cell function (He et al., 2019; He and Yao, 2021). In this review, we summarize the effects of various ginsenosides on adult stem cells, especially mesenchymal stem cells (MSCs), hematopoietic stem cells (HSCs), neural stem cells (NSCs) and cancer stem cells (CSCs), thereby elucidating the underlying mechanisms of ginsenosides in regulating fate specification of stem cells.

2 Transport and metabolism in stem cell niche of ginsenosides

The stem cell niche refers to the microenvironment at a specific location in a tissue or organ, which provides the necessary support and regulation for stem cells to maintain their proliferation, differentiation and self-renewal capabilities (Chacón-Martínez et al., 2018). The niche consists of stromal cells and the factors they secrete, such as adhesion molecules, soluble factors (cytokines, growth factors, metabolites, and nutrients), and matrix proteins. In addition, physical factors such as calcium ions and oxygen concentration also influence the characteristics of the stem cell niche. Recently the transport and metabolism of prototypical ginsenosides or ginsenoside metabolites in various types of stem cell niches have received extensive attention. ATP-binding cassette (ABC) transporters (especially ABCB1 and ABCG2) are clinically important transporters and drug efflux pumps, and their expression affects the differentiation activities of NSC stem cells (Lin et al., 2006). Specifically, downregulation of ABCB1 (also known as P-glycoprotein, p-gp) or ABCG2 (BCRP) expression promotes the differentiation of NSCs into astrocytes or neurons (Lin et al., 2006). Ginsenosides and their metabolites (CK, PPD, and PPT) have been studied to be potential inhibitors of p-gp and BCRP (Jin et al., 2006; Li et al., 2014). Those findings suggest that ginsenoside metabolites may antagonize ABC transporter expression, thereby benefiting NSC differentiation. Furthermore, overexpression of ABC transporters in CSC supports drug resistance (Li et al., 2010). The inhibition of ginsenosides on the efflux effect of ABC transporters may be one of the means to promote the sensitivity of CSCs to chemotherapeutic drugs. In addition, the enzymes involved in drug metabolism are mainly cytochrome P450 (CYP450), including CYP2C9, CYP3A4, etc. The inhibition of CYP450 prolongs the metabolism time of the drug in the body

TABLE 2 Changes and effects of ginsenosides on the physiological behavior of various stem cells.

Cell type	Derive	Saponins	Effect	Targets/pathways	References
CSCs	colon	20(R)-Rg3	stemness and EMT↓	SNAIL signal axis↓	Phi et al. (2019b)
	colon	Rd	stemness and EMT↓	EGFR signal axis↓	Phi et al. (2019a)
	colon	CK	stemness and cancer metastasis↓	Nur77-Akt feedforward signaling↓	Zhang et al. (2022b)
	lung	Rk1/Rg5	EMT↓	Smad and NF-κB/ERK↓	Kim et al. (2021)
	breast	Rg3	stemness and self-renewal↓	Akt mediated self-renewal↓	Oh et al. (2019)
	skin/liver	Rh2	cell growth↓	Autophagy↑; β-catenin↓	Liu et al. (2015b), Yang et al. (2016)
	ovarian	Rb1	self-renewal↓	Wnt/β-catenin↓	Deng et al. (2017)
LSCs	CD34(+) CD38(−) LSCs	Rg1	proliferation↓ and cellular senescence↑	SIRT1/TSC2↑;p16INK4a↑ and hTERT↓	Tang et al. (2020a), Tang et al. (2021)
MSCs	human adipose	Rg1	proliferation↑ and adipogenic differentiation↑	Adipocytokine↑, IL-17↓	Xu et al. (2022)
	bone marrow	Rg1	aging↓	NRF2 and Akt↑; GSK-3β phosphorylation ↓ and Wnt↓	Wang et al. (2020b), Wang et al. (2021)
	bone marrow	Rg1	osteogenic differentiation↑	GR/BMP-2↑	Gu et al. (2016)
	bone marrow	Rg1	oxidative stress-induced apoptosis↓	PI3K/Akt↑	Hu et al. (2016)
	bone marrow	Rb1	migration↑	SDF-1/CXCR4 axis and PI3K/Akt↑	Liu et al. (2022b)
	bone marrow	20(S)-Rb2	Dex-induced apoptosis↓	GPR120↑, Ras-ERK1/2↑	Gao et al. (2015)
	human umbilical cord	Rg1	proliferation↑ and differentiation to NSCs↑	Wnt/β-catenin↓ and Notch↓	Xiao et al. (2022)
	muscle	Rb1	oxidative stress and mitochondrial dysfunction↓	NF-κB↓	Dong et al. (2022)
HSCs	Sca-1(+) HSC/HPCs	Rg1	HSCs aging↓	SIRT6↑, NF-κB↓; SIRT1-FOXO3 and SIRT3-SOD2↑; oxidative stress↓ and Wnt/β-catenin↑; p16(INK4a)-Rb and p19(Arf)-p53-p21(Cip/Waf1)↓; p53-p21-Rb signal↓	Chen et al. (2014), Yue et al. (2014), Tang et al. (2015), Li et al. (2016), Cai et al. (2018), Tang et al. (2020b), Zhou et al. (2020b), Wang et al. (2022a)
NSCs	-	Rg1	aging↓	Wnt/β-catenin↓; Akt/mTOR↓	Chen et al. (2018), Xiang et al. (2019)
	-	20(S)-PPD	proliferation↓ and differentiation↑	cell cycle↓, autophagy↑	Chen et al. (2020)
	endogenous	CK	neurogenesis↑	LXRα↑	Zhou et al. (2020a)

CK, Compound K.

and increases the blood drug concentration. CYP450 is highly expressed in the bone marrow niche (HSC living environment) (Zhang Y. et al., 2013). The competitive inhibition of ginsenoside metabolites (CK, PPD, and PPT) on the activity of liver drug enzymes (CYP2C9, CYP3A4) may be the reason why they reside in the bone marrow niche and exert their pharmacological effects, thereby regulating HSC function (Liu et al., 2006). Recently, the transport of ginsenosides in the NSC niche was found that the active transport of ginsenoside Rb1 to brain microvascular endothelial cells, the cellular component of the NSC niche, was dependent on the glucose transporter GLUT1 (Wang et al., 2018). This finding suggests that upregulation of GLUT1 can increase the bioavailability of ginsenosides in NSCs and their niche. In the future, more *in vivo* experiments are needed to screen and verify the key enzymes/proteins related to the transport and metabolism of ginsenosides in stem cells and niches, which will help the uptake of ginsenosides by stem cells.

3 Effects of ginseng on different types of stem cells

Stem cells are pluripotent cells with the capacity for self-renewal, self-replication, and differentiation into multiple cell types in a suitable microenvironment, which are divided into two forms according to developmental stages: embryonic stem cells and adult stem cells. Considering that embryonic stem cells are subject to ethical restrictions, are prone to self-differentiation, and may have abnormal karyotypes after many passages, the research on the effect of ginsenosides on stem cells mainly focuses on adult stem cells (Scott and Reijo Pera, 2008). Adult stem cells, including hematopoietic, neural, and mesenchymal stem cells, are slow-dividing and quiescent cells with low proliferative rates and are the source of adult tissue (Gurusamy et al., 2018). Additionally, adult tissue stem cells can turn into cancer stem cells (White and Lowry, 2015), in solid tumors, the acquisition of cancer

stem cells phenotype can be achieved through epithelial-mesenchymal transition (EMT) (Shibue and Weinberg, 2017). The wide application of stem cells in regenerative medicine has attracted much attention. At first, stem cells were transplanted into the human body to repair damaged tissues, utilizing their potential for self-replication and multi-directional differentiation (Giri et al., 2019). Furthermore, advancements in stem cells reprogramming technology have led to increased use of stem cells for the restoration of aging cells, that is, stem cells can restore proliferate, differentiate, and self-renewal ability to delay the aging process (Alle et al., 2021). Recently, stem cells were suggested as a promising therapeutic option for various diseases, including but not limited to neurodegenerative diseases, cancer, stroke, myocardial ischemia (Yamashita and Abe, 2016; Michler, 2018; Sivandzade and Cucullo, 2021; Yin et al., 2021). Meanwhile, ginsenosides have been proven to slow the pathological process of these diseases and improve the condition (Huang et al., 2019; Wang R. et al., 2020; Yang JE. et al., 2020; Yao and Guan, 2022). In recent times, research studies have demonstrated the significant regulatory impact of ginsenosides on the self-renewal, differentiation, and proliferation of stem cells, thereby highlighting their potential for clinical use in improving the field of stem cells research (Table 2).

3.1 Mesenchymal stem cells

Mesenchymal stem cells (MSCs) are the progenitors of numerous cell types and have the capacity to proliferate and differentiate into a variety of cell lineages such as osteoblasts, adipocytes, myoblasts, and others (Xie et al., 2020).

3.1.1 Effect on differentiation of MSCs

Ginsenosides have shown the potential to induce differentiation of MSCs *in vitro*, especially in inducing osteogenic differentiation, which is the consequence of expressing or activating genes/transcription factors and signaling pathways related to osteogenic differentiation (He et al., 2019). The role of BMP-2/Smad pathway in MSCs osteogenic differentiation has been fully confirmed (Aquino-Martínez et al., 2017). As an indispensable growth factor for driving osteogenic differentiation, BMP-2 can activate the intracellular Smad pathway to form Smad complexes that enter the nucleus and promote the expression of the osteogenic transcription factor RUNX2 (Wang et al., 2017). Such the BMP-2/Smad signaling pathway can be activated by ginsenoside Rg1 to promote osteogenic differentiation of bone marrow mesenchymal stem cells (BMSCs), which is mediated by glucocorticoid receptor (GR) nuclear translocation (Gu et al., 2016). In addition, the Wnt/β-catenin signaling pathway is a key pathway that regulates the osteogenic differentiation of MSCs by regulating the localization of β-catenin, thereby regulating the expression of downstream osteogenesis-related proteins and genes. GSK-3β is an intermediary of the Wnt/β-catenin signaling pathway, and its high activity negatively affects the stability and transcriptional activity of β-catenin, blocks the activation state of the signaling pathway, and thus regulates the function and fate of stem cells. Currently, researchers believe that ginsenosides regulate the osteogenic differentiation of MSCs by regulating the Wnt signaling pathway. For instance, ginsenoside Rg1 can regulate the differentiation capacity of MSCs, stimulate bone and cartilage formation, by inhibiting the phosphorylation of GSK-3β and reducing the excessive activation of the Wnt/β-catenin pathway in aging cells (Wang Z. et al., 2020). Conversely, ginsenoside compound K (CK) (the main metabolite of original propanediol ginsenoside in gut bacteria) activates the Wnt/β-catenin signaling pathway *in vitro* and promotes the expression of the downstream Wnt target gene Runx2 (osteogenic transcription factor), inducing the osteogenic differentiation of rat bone marrow-derived mesenchymal stem cells (rBMSCs) (Ding et al., 2022). In view of the fact that ginsenosides have two sides to the regulation of Wnt/β-catenin signaling pathway in promoting osteogenic differentiation of MSCs, that is, they show differences in different states (aging or normal) of MSCs. Future detailed functional exploration of individual members of the Wnt/β-catenin pathway will help to understand its regulatory mechanism.

Adipose tissue-derived MSCs (ADSCs) are also quite common in clinical practice. Ginsenoside Rg1-promoted cartilage gene expression in ADSCs *in vitro* induces cartilage phenotype differentiation (Xu et al., 2015; Guo et al., 2023). Co-administration of ginsenoside Rg1 and platelet-rich fibrin elevates cytokines (VEGF, HIF-1α) in human ADSCs niche and promotes soft tissue regeneration (Xu et al., 2016). Ginsenoside Rg1 can also improve the ADSC niche mediated by adipokine and IL-17 signaling pathways, and promote the adipogenic differentiation of human ADSCs (Xu et al., 2022). These results indicate that ginsenoside may expand MSCs by regulating MSC niche.

3.1.2 Effect on the proliferation and differentiation of MSCs in the aging process

Oxidative stress is the key contributor to the aging of stem cells (Chen et al., 2017). Ginsenoside Rg1 has been proven to promote superior antioxidant and anti-inflammatory capabilities, which can promote BMSC proliferation and improve the anti-aging hematopoietic microenvironment (Hu et al., 2015). Similarly, the senescence-associated secretory phenotype (SASP) resulting from DNA damage and oxidative damage associated with the aging of MSCs can be inhibited by ginsenoside Rg1, which promotes MSC proliferation by enhancing its antioxidant capacity, the activation of Nrf2 and PI3K/Akt is required for this process to occur (Wang et al., 2021). Ginsenoside Rg2 activates AMPK-mediated autophagy restores pig MSCs proliferation and inhibits oxidative stress-induced replicative senescence in pig MSCs (Che et al., 2023). Ginsenoside Rg3 mainly enhances the biogenesis ability of mitochondria and antioxidant function by promoting Ca^{2+} concentration properly, thus improving proliferation and differentiation potential and preventing human MSCs from aging (Hong et al., 2020). These results suggest that administration of ginsenosides may be a promising approach to counteract MSC aging by intervening in oxidative stress-related pathways (Figure 1).

3.2 Neutral stem cells

During central nervous system (CNS) development, neural stem cells (NSCs) are capable of generating neurons, astrocytes, and oligodendrocytes (Vieira et al., 2018). Recently, the use of neural stem cells therapy has emerged as a novel approach to treating

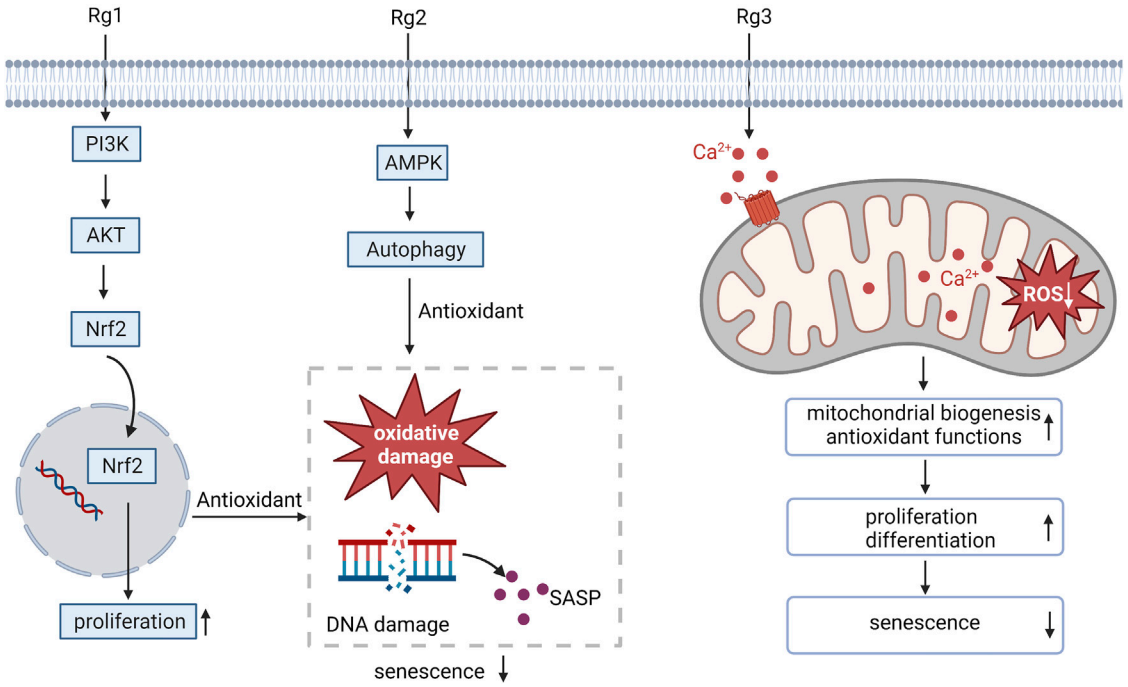

FIGURE 1
Ginsenosides resist oxidative stress, regulate MSC proliferation and differentiation, and alleviate MSC aging. SASP, senescence-associated secretory phenotype.

diverse neurological disorders and is an ideal approach for treating neurodegenerative diseases and CNS injuries (Liu Y et al., 2020).

3.2.1 Effect on proliferation and differentiation of NSCs

Ginsenoside Rg1 increases the activity of NSE, a neuron biomarker, in transplanted NSCs, implying neuron-like differentiation (Li et al., 2015). Similarly, the key to ginsenoside Rb1 regulating the progression of neurodegenerative diseases is to increase the levels of biomarkers such as Nestin (marking NSC), GFAP (marking astrocytes) and NSE in Alzheimer's disease (AD) rat models, and promote NSC proliferation and differentiation into astrocytes and neurons (Zhao et al., 2018). However, high levels of NSE have been shown to induce nerve injury and neuroblastoma, and the specific mechanism of how ginsenoside promotes NSE expression to exert neuroprotective effects needs to be further elucidated. Even though most ginsenosides are difficult to penetrate the blood-brain barrier due to their large molecular weight, their neuroprotective effects have been confirmed by a large number of experimental studies (Xie et al., 2018). The underlying mechanism may involve in improving the niche of NSCs. Nerve growth factor (NGF), a neurotrophic factor in the NSCs niche, can induce the differentiation of NSCs derived from the brain (Regalado-Santiago et al., 2016). Ginsenoside Rg1 precisely acts as an analog of NGF, attenuating oxygen and glucose deprivation-induced nerve injury and promoting proliferation and glial-like differentiation of cortical NSCs (Gao et al., 2017).

3.2.2 Effect on proliferation and differentiation of NSCs in the aging process

Recently, the function of WNT/β-catenin in the CNS has been studied and dysregulation of its signaling can lead to the production and aggregation of β-amyloid (Aβ) (Aghaizu et al., 2020). Ginseng total saponins extract and its intestinal metabolite 20(S)-protopanaxadiol (PPD) jointly induce the phosphorylation of GSK-3β (ser9), activate the Wnt/GSK-3β/β-catenin pathway to promote NSC proliferation and differentiation, thereby improving cognitive impairment in AD by replacing damaged neurons (Lin et al., 2020; Lin et al., 2022). However, in LiCl-induced NSC senescence, ginsenoside Rg1-dependent downregulation of phosphorylated GSK-3β expression interfered with the activation of the Wnt/β-catenin pathway, thereby promoting NSC proliferation and delaying senescence (Xiang et al., 2019). Screening potential Wnt/GSK-3β/β-catenin -targeted activators/inhibitors in ginsenosides will help ginsenosides promote the development of stem cell regenerative medicine and anti-aging drugs in nerves field.

Aging leads to a decline in the capacity of NSCs to enter the cell cycle efficiently (Audesse and Webb, 2020). Genes involved in cell cycle regulation play an essential role in the stability and activation of NSCs (Roccio et al., 2013). Ginsenoside Rg1 targets Akt/mTOR to downregulate the levels of cell cycle arrest-related proteins (p53, p16, p21, and Rb) in NSCs, promoting NSC proliferation and alleviating D-galactose-induced NSC aging (Chen et al., 2018). 20(S)-PPD induces autophagy and cell cycle arrest, and promote NSC from a proliferative state to a differentiated state and helps to repair neurons in age-related neurodegenerative AD (Chen et al., 2020).

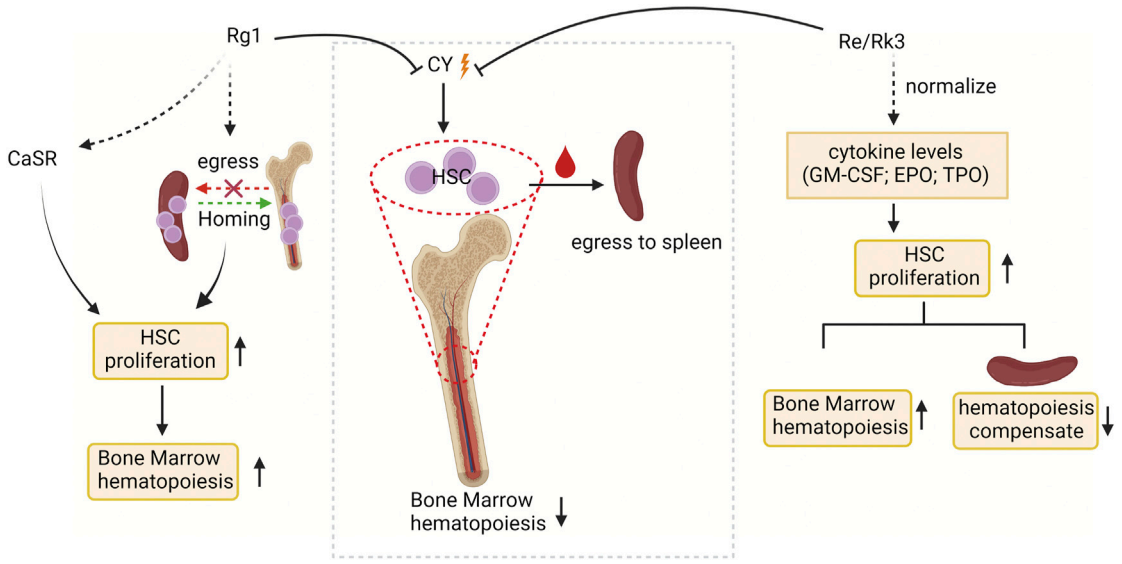

FIGURE 2
The targets of ginsenosides promoting HSC proliferation and stimulating bone marrow hematopoiesis at the molecular level. CY, cyclophosphamide; CaSR, Ca^{2+} sensitive receptor; GM-CSF, granulocyte-macrophage colony stimulatory factors; EPO, erythropoietin; and TPO, thrombopoietin.

This suggests that further understanding of the molecular mechanism by which ginsenosides alleviate NSC aging requires a deeper study of upstream signaling pathways and regulators that affect the cell cycle to maintain the continued health of NSCs.

3.2.3 Effect on transdifferentiation of NSCs

NSCs can also differentiate from other stem cells with transdifferentiation capability, such as MSCs (Feng et al., 2014). It was previously demonstrated that ginsenoside Rg1 promotes the differentiation of transplanted bone marrow mesenchymal stem cells (BMSCs) into neurons and glial cells (Bao et al., 2015). A recent report has shown that ginsenoside Rg1 regulates miRNA-124 expression *in vitro* to promote neural differentiation of mouse adipose stem cells (ADSCs) (Dong et al., 2017). Ginsenoside Rg1 promotes the neural phenotype differentiation of human ADSCs by activating the expression of NSC niche components including growth associated protein-43 (GAP-43), neural cell adhesion molecule (NCAM), and synapsin-1 (SYN-1) (Xu et al., 2014). In addition, ginsenoside Rg1 promotes the differentiation of human umbilical cord mesenchymal stem cells (hUCMSC) into NSCs by downregulating genes involved in the Wnt/β-catenin and Notch signaling pathways, including GSK3β, β-catenin, Notch1, and Hes1 (Xiao et al., 2022). However, the transdifferentiation capability of NSCs is still doubted since the possible contamination by other tissue stem cells or embryonic stem cells in those studies.

3.3 Hematopoietic stem cells

HSCs have self-renewal potential and can differentiate into various hematopoietic progenitor cells (HPC) and produce specific blood cell types to maintain the stability of the entire hematopoietic system (Zhao and Li, 2015).

3.3.1 Effect on proliferation of HSCs

External supplementation of HSCs is widely used to reconstruct damaged bone marrow (Ju et al., 2020). Bone marrow suppression and extramedullary hematopoiesis are often caused by the side effects of chemotherapy drugs (such as cyclophosphamide; CY) used by cancer patients, making stimulation of hematopoiesis, a critical issue in the context of cancer therapy in clinical practice (Wang et al., 2009; Ahlmann and Hempel, 2016; Hou et al., 2017). Ginsenosides relieve CY-induced myelosuppression by activating HSC proliferation (Figure 2). HSCs expansion in the bone marrow is strictly regulated by the HSCs niche (Pinho and Frenette, 2019). Multiple signal molecules are involved in HSCs-niche interactions, such as Ca^{2+} sensitive receptor (CaSR), and three cytokines, including granulocyte-macrophage colony stimulatory factors (GM-CSF), erythropoietin (EPO) and thrombopoietin (TPO), are essential for HSC proliferation (Szade et al., 2018). CaSR has been demonstrated that regulates calcium ion levels to maintain calcium homeostasis and plays critical regulatory roles in the retention and colonization of HSCs after transplantation (Cho et al., 2020; Uslu et al., 2020). Such the CaSR can be activated by ginsenoside Rg1 to relieve CY-induced inhibition of the proliferation of Lin-Sca-1+c-Kit + HSCs and $CD3^+$ in mouse bone marrow and peripheral blood, restoring bone marrow function (Xu et al., 2012). Another study found that ginsenosides Re and Rk3 compensated hematopoietic function by increasing the secretion of cytokines (GM-CSF, TPO, EPO) to restore HSC proliferation. (Han et al., 2019). In addition, the compensatory hematopoiesis of the spleen is the key means to restore the normal hematopoietic function of the bone marrow.

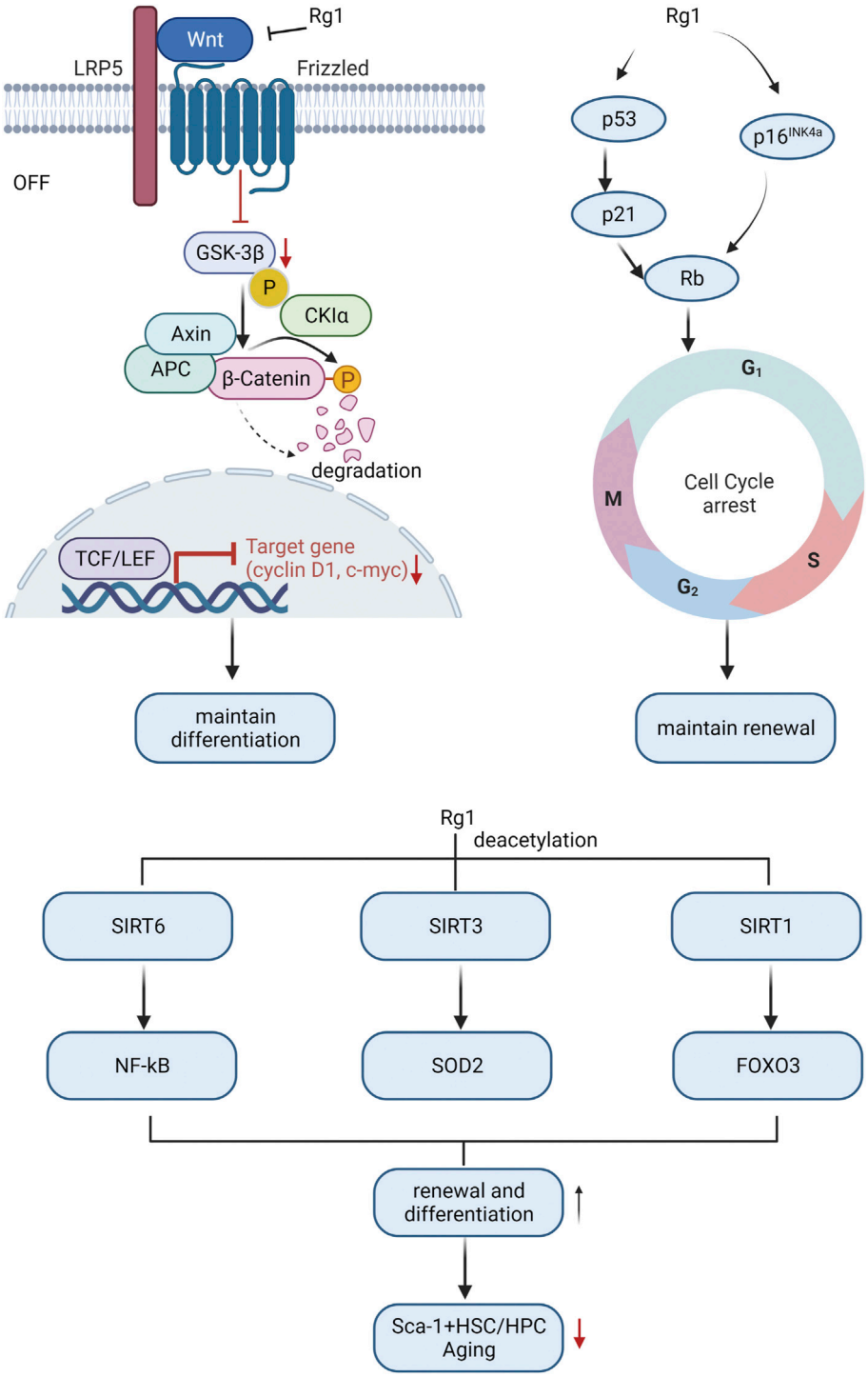

FIGURE 3
Molecular mechanism of ginsenosides affecting HSC differentiation and self-renewal ability to resist HSC aging.

Ginsenoside Rg1 treatment of CY-induced myelosuppressive mice can improve bone marrow hematopoietic activity by improving the spleen niche and promoting the proliferation and homing of c-Kit + HSCs in the spleen (Liu HH. et al., 2015). As mentioned above, the niche may be an important target for ginsenosides to regulate HSC proliferation and assist recovery from myelosuppression. It is necessary to focus on whether the effects of ginsenosides on other cellular components in the stem cell niche feed back to the stem cells so that we can more fully understand the regulatory mechanisms of ginsenosides on stem cell fate specification.

3.3.2 Effect on differentiation and self-renewal of HSCs in the aging process

Research indicates that HSC aging is linked to body aging since it impairs the self-renewal and differentiation ability of stem cells, resulting in decreased hematopoietic and immune function, and ultimately leading to tissue and organ structure and function deterioration throughout the body (Han et al., 2019). Therefore, it is meaningful to study the mechanism of HSC aging to elucidate the aging mechanism of the body. Ginsenoside Rg1 resisted HSC senescence to restore self-renewal and multi-differentiation abilities (Figure 3). Excessive ROS generated by oxidative stress may be the main mediator of stem cell senescence induced by excessive activation of Wnt/β-catenin signaling pathway (Zhang DY. et al., 2013). The proto-oncogene c-myc and cyclin D1 are target genes downstream of the Wnt pathway, and their overexpression may cause DNA damage and induce oxidative stress senescence (Shang et al., 2023). Ginsenoside Rg1 acts as a Wnt/β-catenin signal transduction inhibitor to inhibit Wnt target genes (such as cyclin D1 and c-myc) regulated by TCF/LEF transcription factors, thereby delaying LiCl and D-galactose-induced Sca-1 + HSC/HPC oxidative damage cascades restore their differentiation characteristics (Li et al., 2016; Wang et al., 2022a).

Cell cycle arrest is another main cause of HSC aging (Mohrin et al., 2015). Ginsenoside Rg1 antagonizes lead acetate, t-BHP, radiation, and d-galactose by repressing some key genes in the cell cycle regulator signaling pathway (p53-p21-Rb, $p16^{INK4a-Rb}$, and $p53-p21^{Cip/Waf1}$)-induced HSC senescence, improving HSC self-renewal capacity (Chen et al., 2014; Yue et al., 2014; Li et al., 2016; Cai et al., 2018).

Sirtuins alter protein activity and stability through lysine deacetylation is another important factor in regulating the cellular aging process (Lasiglié, 2021). The sirtuins SIRT1, SIRT3, and SIRT6 are key regulators of HSC lifespan (Wang et al., 2016; Fang et al., 2020; Wang et al., 2022b). Activation of SIRT6 by ginsenoside Rg1 inhibits NF-κB through H3K9 deacetylation, slows down t-BHP-induced Sca-1+HSC/HPC senescence, and enhances self-renewal and multi-differentiation abilities (Tang et al., 2015). Ginsenoside Rg1 activates SIRT3 to trigger deacetylation to enhance SOD2 activity and accelerate ROS clearance, slow down D-gal-induced $Sca-1^{+}$HSC/HPC senescence, and promote HSC self-renewal and multi-differentiation ability (Zhou Y. et al., 2020). Ginsenoside Rg1-mediated SIRT1-FOXO3 promotes $Sca-1^{+}$HSC/HPC multi-differentiation and self-renewal (Tang et al., 2020b), and inhibits gamma-ray-induced $Sca-1^{+}$HSC/HPC senescence, which is dependent on deactivation of SIRT1/SIRT3 Acetylation (Tang et al., 2020a).

Overall, the mechanisms of ginsenoside in reducing HSCs aging mainly involve Wnt/β-catenin, cell cycle, and sirtuins-mediated senescence signaling pathway.

3.4 Cancer stem cells

CSCs exhibit qualities of stem cells and cancer cells, contributing to tumor growth, metastasis formation, and recurrence (Tanabe, 2022). CSCs initiate and maintain cancer initiation and progression based on stemness characteristics, namely, self-renewal and abnormal proliferation/differentiation (Eun et al., 2017).

3.4.1 Effect on proliferation and self-renewal of CSCs

Wnt/β-catenin signaling is the main signaling pathway that promotes cancer cell stemness (Katoh and Katoh, 2022). Ginsenoside Rh2 inhibits cutaneous squamous cell carcinoma (SCC) proliferation by reducing the number of Wnt target gene Lgr5+ cells by inhibiting β-catenin signaling (Liu S. et al., 2015). Ginsenoside Rg3 and Rh2 reduced the self-renewal capacity of glioblastoma stem cells (GSC) by inhibiting the expression of transcription factor LCF1 and downstream Wnt target genes (c-myc, CCND1) of Wnt/β-catenin signaling (Ham et al., 2019). Notably, the anti-CSC capacity of Rh2 is better than that of ginsenoside Rg3, which supports that ginsenoside metabolites with fewer sugar groups have stronger anticancer activity.

Accumulating evidence indicates that EMT activation is abnormally high in CSCs, and there is a strong correlation between CSC stemness and EMT regulation (Tanabe et al., 2020). Recently, many studies have reported that ginsenosides exert anticancer effects by inhibiting EMT (Dai et al., 2019; Cai et al., 2021; Li et al., 2021). Ginsenoside Rg3R has been shown to reduce self-renewal in colorectal cancer cells (CRC) by targeting the SNAIL signaling pathway and modulating EMT features (Phi et al., 2019b). Ginsenoside Rk1/Rg5 inhibited EMT and self-renewal ability of A549 cells and reduced A549 stemness, which was dependent on the inhibition of TGF-b1-mediated downstream signaling pathways, including Smad2/3, NF-κB, ERK1/2, p38 MAPK and JNK (Kim et al., 2021). In addition, the hypoxic niche is the main place to maintain the stemness characteristics of CSCs. Nur77 is highly expressed in the hypoxic niche in a mouse model of colon cancer. Ginsenoside CK, as a Nur77 ligand target, prevents the Nur77-Akt activation circuit and inhibits CSCs proliferation and stemness (Zhang M. et al., 2022).

In summary, the regulation of ginsenosides on CSC stemness (especially self-renewal ability) involves a variety of signaling pathways. The key to solving the problem of targeted therapy is to further study whether these pathways exist independently or interact, which will be the key of tumor therapy in the context of ginsenoside.

3.4.2 Effect on proliferation and self-renewal of CSCs in the aging process

One subtype of CSC, leukemia stem cells (LSCs), is a crucial origin of leukemia due to its high proliferation and abnormal growth (Chavez-Gonzalez et al., 2017). Inducing LSCs aging can reduce the number of LSCs, thus reducing the incidence of leukemia (Liu W. et al., 2022). Ginsenosides mainly induce the aging of LSCs by the following signals, slowing down or inhibiting the development of leukemia.

One of the mechanisms by which ginsenosides induce senescence in LSCs is their inhibitory potential for proliferation and self-renewal, involving deacetylation mediated by SIRT1 (one of the sirtuins members). Ginsenoside Rg1 downregulates the expression of SIRT1/TSC2 in $CD34^{+}CD38-$LSCs, significantly increases the level of senescence marker SA-β-Gal, and reduces the unit of mixed colony-forming (a marker of proliferation ability), and reduces cell renewal and proliferation ability to induce LSCs senescence (Tang et al., 2020a).

Telomere is another pathway that ginsenosides participate in regulating the proliferation and self-renewal of LSCs to induce senescence. LSCs have relatively short telomeres, but they show higher levels of telomerase activity compared with normal cells. This enhanced telomerase activity may be an adaptive mechanism aimed at maintaining the continuous replication of LSCs and promoting leukemia development (Kuo and Bhatia, 2014). A recent study found that ginsenoside Rg1 inhibited $CD34^{+}CD38$-LSCs proliferative activity, increased expression of telomere damage effector $p16^{INK4a}$, and decreased human telomerase reverse transcriptase (hTERT, catalytic subunit of telomerase) to induce its replicative senescence for the treatment of leukemia (Tang et al., 2021). The above findings suggest that ginsenoside Rg1 inhibits the ability of LSCs to self-renewal and proliferation, and its targeted therapy based on the intervention of LSCs senescence is a valuable direction for healing leukemia in the future.

Noteworthy, we observed that the effects of ginsenosides on CSC and normal stem cell fate are asymmetric (inhibit CSC self-renewal, promote normal stem cell proliferation/differentiation), which may have multiple reasons. First, CSCs of various origins overexpress the glucose transporter GLUT1 (Maliekal et al., 2022). Due to their steroidal structure, ginsenosides have the property of recognizing GLUT carriers on tumor cell membranes (Chen et al., 2022). Ginsenoside Rh2 inhibits GLUT1-mediated aerobic glycolysis in tumor cells, and its role as a tumor energy blocker may be responsible for the inhibition of CSC self-renewal (Liu X Y et al., 2020). Second, ginsenoside Rb1 and its deglycosylated product compound K also decreased the expression of drug efflux pumps (ABCG2 and P-glycoprotein), inhibiting the resistance of CSCs to chemotherapeutic drugs (Deng et al., 2017). In addition, ginsenosides, as signal transduction regulators of the Wnt/β-catenin pathway, participate in the regulation of stem cell fate specification, with opposite effects on CSCs and normal stem cells. The regulation of ginsenosides on Wnt/β-catenin is mainly through regulating the activity of the intermediate GSK-3β to mediate the signal transmission triggered by β-catenin degradation/nuclear translocation, including the inhibition/activation of downstream transcription factors (TCF/LEF) and Wnt target genes (CCND1, c-myc, Lgr5), thereby affecting the function and fate of stem cells (Sferrazza et al., 2020). We speculate that ginsenosides inhibit CSC and stimulate normal stem cell proliferation/differentiation may be due to the different functions of Wnt target genes in CSC and normal stem cells. However, further verification *in vivo* or clinical experiments is needed to support this point of view. In conclusion, ginsenosides show potential as anticancer drugs, but further research and clinical trials are currently needed to determine their efficacy and safety.

3.5 Other kinds of adult stem cells

Although the effects of ginsenosides on other types of adult stem cells are not well understood, existing findings suggest a potential multifunctional regulatory capacity. For example, Ginsenoside Rd can stimulate the proliferation of intestinal stem cells (marked by Bmi and Msi-1) in rat inflammatory bowel disease model and promote the differentiation into intestinal epithelial cells expressing CDX-2, thereby restoring intestinal function (Yang et al., 2020). Ginsenoside Rg1 promotes the odontogenic differentiation of human dental pulp stem cells (hDPSCs) by upregulating osteogenesis-promoting factors, including bone morphogenetic protein-2 (BMP-2) and fibroblast growth factor 2 (FGF2) (Wang et al., 2014). In addition, PPT induced the proliferation and differentiation of sperm stem cells and resisted busulfan-induced reproductive toxicity in male mice (Ji et al., 2007). These findings suggest that ginsenosides have a wide range of effects, contributing to tissue repair and regeneration, and holding potential for the treatment of various diseases. Strengthening the study of the molecular mechanism of ginsenosides on other types of adult stem cells will help its clinical application.

4 Conclusion

This review gives an overview of the fate specification effects of ginsenosides on adult stem cells from the perspective of physiology (including aging states) and pathology. However, currently most of studies we reviewed are based on *in vitro* model and we still lack knowledge of how ginsenosides affect stem cell proliferation and differentiation or relieve dysfunctions in those processes *in vivo* and whether ginsenosides have considerable value in clinical practice. To figure out such limitations and the great potential of ginsenosides in tissue repair, cell replacement and disease treatment, more research (especially *in vivo* studies in distinct species) should be done to unravel the underlying mechanism of ginsenosides in proliferation, differentiation and self-renewal of different stem cell types. Considering the continuous proceeding of research on ginsenosides and proliferation as well as differentiation processes in various stem cells, we believe the promise of ginsenosides in regenerative medicine and healthy aging will be attested soon.

Author contributions

Information collection and interpretation: YL, LJ, WS, CW, SY, JQ, XW, XB, and CJ; critically revising the manuscript: YL, DZ, SW, PZ, XB, and ML. All authors contributed to the article and approved the submitted version.

Funding

This research was funded by the Scientific and Technological Development Planning Foundation of Jilin Province (YDZJ2022 01ZYTS683), the Scientific and Technological Developing Scheme of Ji Lin Province (20210204188YY), and the National Natural Science Foundation of China (U19A2013).

Acknowledgments

Images were created using BioRender.com.

Conflict of interest

The authors declare that the research was conducted in the absence of any commercial or financial relationships that could be construed as a potential conflict of interest.

Publisher's note

References

Aghaizu, N. D., Jin, H., and Whiting, P. J. (2020). Dysregulated Wnt signalling in the Alzheimer's brain. *Brain Sci.* 10 (12), 902. doi:10.3390/brainsci10120902

Ahlmann, M., and Hempel, G. (2016). The effect of cyclophosphamide on the immune system: Implications for clinical cancer therapy. *Cancer Chemother. Pharmacol.* 78 (4), 661–671. doi:10.1007/s00280-016-3152-1

Ali, M. Y., Zaib, S., Jannat, S., Khan, I., Rahman, M. M., Park, S. K., et al. (2022). Inhibition of aldose reductase by ginsenoside derivatives via a specific structure activity relationship with kinetics mechanism and molecular docking study. *Molecules* 27 (7), 2134. doi:10.3390/molecules27072134

Alle, Q., Le Borgne, E., Milhavet, O., and Lemaitre, J. M. (2021). Reprogramming: Emerging strategies to rejuvenate aging cells and tissues. *Int. J. Mol. Sci.* 22 (8), 3990. doi:10.3390/ijms22083990

Aquino-Martínez, R., Artigas, N., Gámez, B., Rosa, J. L., and Ventura, F. (2017). Extracellular calcium promotes bone formation from bone marrow mesenchymal stem cells by amplifying the effects of BMP-2 on SMAD signalling. *PLoS One* 12 (5), e0178158. doi:10.1371/journal.pone.0178158

Audesse, A. J., and Webb, A. E. (2020). Mechanisms of enhanced quiescence in neural stem cell aging. *Mech. Ageing Dev.* 191, 111323. doi:10.1016/j.mad.2020.111323

Bao, C., Wang, Y., Min, H., Zhang, M., Du, X., Han, R., et al. (2015). Combination of ginsenoside Rg1 and bone marrow mesenchymal stem cell transplantation in the treatment of cerebral ischemia reperfusion injury in rats. *Cell Physiol. Biochem.* 37 (3), 901–910. doi:10.1159/000430217

Brassard, J. A., and Lutolf, M. P. (2019). Engineering stem cell self-organization to build better organoids. *Cell Stem Cell* 24 (6), 860–876. doi:10.1016/j.stem.2019.05.005

Cai, N., Yang, Q., Che, D. B., and Jin, X. (2021). 20(S)-Ginsenoside Rg3 regulates the Hedgehog signaling pathway to inhibit proliferation and epithelial-mesenchymal transition of lung cancer cells. *Pharmazie* 76 (9), 431–436. doi:10.1691/ph.2021.1573

Cai, S. Z., Zhou, Y., Liu, J., Li, C. P., Jia, D. Y., Zhang, M. S., et al. (2018). Alleviation of ginsenoside Rg1 on hematopoietic homeostasis defects caused by lead-acetate. *Biomed. Pharmacother.* 97, 1204–1211. doi:10.1016/j.biopha.2017.10.148

Chacón-Martínez, C. A., Koester, J., and Wickström, S. A. (2018). Signaling in the stem cell niche: Regulating cell fate, function and plasticity. *Development* 145 (15), dev165399. doi:10.1242/dev.165399

Chandel, N. S., Jasper, H., Ho, T. T., and Passegué, E. (2016). Metabolic regulation of stem cell function in tissue homeostasis and organismal ageing. *Nat. Cell Biol.* 18 (8), 823–832. doi:10.1038/ncb3385

Chavez-Gonzalez, A., Bakhshinejad, B., Pakravan, K., Guzman, M. L., and Babashah, S. (2017). Novel strategies for targeting leukemia stem cells: Sounding the death knell for blood cancer. *Cell Oncol. (Dordr)* 40 (1), 1–20. doi:10.1007/s13402-016-0297-1

Che, L., Zhu, C., Huang, L., Xu, H., Ma, X., Luo, X., et al. (2023). Ginsenoside Rg2 promotes the proliferation and stemness maintenance of porcine mesenchymal stem cells through autophagy induction. *Foods* 12 (5), 1075. doi:10.3390/foods12051075

Chen, C., Mu, X. Y., Zhou, Y., Shun, K., Geng, S., Liu, J., et al. (2014). Ginsenoside Rg1 enhances the resistance of hematopoietic stem/progenitor cells to radiation-induced aging in mice. *Acta Pharmacol. Sin.* 35 (1), 143–150. doi:10.1038/aps.2013.136

Chen, C., Xia, J., Ren, H., Wang, A., Zhu, Y., Zhang, R., et al. (2022). Effect of the structure of ginsenosides on the *in vivo* fate of their liposomes. *Asian J. Pharm. Sci.* 17 (2), 219–229. doi:10.1016/j.ajps.2021.12.002

Chen, F., Liu, Y., Wong, N. K., Xiao, J., and So, K. F. (2017). Oxidative stress in stem cell aging. *Cell Transpl.* 26 (9), 1483–1495. doi:10.1177/0963689717735407

Chen, L., Yao, H., Chen, X., Wang, Z., Xiang, Y., Xia, J., et al. (2018). Ginsenoside Rg1 decreases oxidative stress and down-regulates akt/mTOR signalling to attenuate cognitive impairment in mice and senescence of neural stem cells induced by D-galactose. *Neurochem. Res.* 43 (2), 430–440. doi:10.1007/s11064-017-2438-y

Chen, S., He, J., Qin, X., Luo, T., Pandey, A., Li, J., et al. (2020). Ginsenoside metabolite 20(S)-protopanaxadiol promotes neural stem cell transition from a state of proliferation to differentiation by inducing autophagy and cell cycle arrest. *Mol. Med. Rep.* 22 (1), 353–361. doi:10.3892/mmr.2020.11081

Cho, H., Lee, J., Jang, S., Lee, J., Oh, T. I., Son, Y., et al. (2020). CaSR-mediated hBMSCs activity modulation: Additional coupling mechanism in bone remodeling compartment. *Int. J. Mol. Sci.* 22 (1), 325. doi:10.3390/ijms22010325

Dai, G., Sun, B., Gong, T., Pan, Z., Meng, Q., and Ju, W. (2019). Ginsenoside Rb2 inhibits epithelial-mesenchymal transition of colorectal cancer cells by suppressing TGF-β/Smad signaling. *Phytomedicine* 56, 126–135. doi:10.1016/j.phymed.2018.10.025

De, D., Karmakar, P., and Bhattacharya, D. (2021). Stem cell aging and regenerative medicine. *Adv. Exp. Med. Biol.* 1326, 11–37. doi:10.1007/5584_2020_577

De Oliveira Zanuso, B., De Oliveira Dos Santos, A. R., Miola, V. F. B., Guissoni Campos, L. M., Spilla, C. S. G., and Barbalho, S. M. (2022). Panax ginseng and aging related disorders: A systematic review. *Exp. Gerontol.* 161, 111731. doi:10.1016/j.exger.2022.111731

Deng, S., Wong, C. K. C., Lai, H. C., and Wong, A. S. T. (2017). Ginsenoside-Rb1 targets chemotherapy-resistant ovarian cancer stem cells via simultaneous inhibition of Wnt/β-catenin signaling and epithelial-to-mesenchymal transition. *Oncotarget* 8 (16), 25897–25914. doi:10.18632/oncotarget.13071

Ding, L., Gu, S., Zhou, B., Wang, M., Zhang, Y., Wu, S., et al. (2022). Ginsenoside compound K enhances fracture healing via promoting osteogenesis and angiogenesis. *Front. Pharmacol.* 13, 855393. doi:10.3389/fphar.2022.855393

Dong, J., Zhu, G., Wang, T. C., and Shi, F. S. (2017). Ginsenoside Rg1 promotes neural differentiation of mouse adipose-derived stem cells via the miRNA-124 signaling pathway. *J. Zhejiang Univ. Sci. B* 18 (5), 445–448. doi:10.1631/jzus.B1600355

Dong, W., Chen, W., Zou, H., Shen, Z., Yu, D., Chen, W., et al. (2022). Ginsenoside Rb1 prevents oxidative stress-induced apoptosis and mitochondrial dysfunction in muscle stem cells via NF-κB pathway. *Oxid. Med. Cell Longev.* 2022, 9159101. doi:10.1155/2022/9159101

Eun, K., Ham, S. W., and Kim, H. (2017). Cancer stem cell heterogeneity: Origin and new perspectives on CSC targeting. *BMB Rep.* 50 (3), 117–125. doi:10.5483/bmbrep.2017.50.3.222

Fang, Y., An, N., Zhu, L., Gu, Y., Qian, J., Jiang, G., et al. (2020). Autophagy-Sirt3 axis decelerates hematopoietic aging. *Aging Cell* 19 (10), e13232. doi:10.1111/acel.13232

Feng, N., Han, Q., Li, J., Wang, S., Li, H., Yao, X., et al. (2014). Generation of highly purified neural stem cells from human adipose-derived mesenchymal stem cells by Sox1 activation. *Stem Cells Dev.* 23 (5), 515–529. doi:10.1089/scd.2013.0263

Gao, B., Huang, Q., Jie, Q., Zhang, H. Y., Wang, L., Guo, Y. S., et al. (2015). Ginsenoside-Rb2 inhibits dexamethasone-induced apoptosis through promotion of GPR120 induction in bone marrow-derived mesenchymal stem cells. *Stem Cells Dev.* 24 (6), 781–790. doi:10.1089/scd.2014.0367

Gao, J., Wan, F., Tian, M., Li, Y., Li, Y., Li, Q., et al. (2017). Effects of ginsenoside-Rg1 on the proliferation and glial-like directed differentiation of embryonic rat cortical neural stem cells *in vitro*. *Mol. Med. Rep.* 16 (6), 8875–8881. doi:10.3892/mmr.2017.7737

Giri, T. K., Alexander, A., Agrawal, M., Saraf, S., Saraf, S., and Ajazuddin (2019). Current status of stem cell therapies in tissue repair and regeneration. *Curr. Stem Cell Res. Ther.* 14 (2), 117–126. doi:10.2174/1574888x13666180502103831

Gu, Y., Zhou, J., Wang, Q., Fan, W., and Yin, G. (2016). Ginsenoside Rg1 promotes osteogenic differentiation of rBMSCs and healing of rat tibial fractures through regulation of GR-dependent BMP-2/SMAD signaling. *Sci. Rep.* 6, 25282. doi:10.1038/srep25282

Guo, Y., Tian, T., Yang, S., and Cai, Y. (2023). Ginsenoside Rg1/ADSCs supplemented with hyaluronic acid as the matrix improves rabbit temporomandibular joint osteoarthrosis. *Biotechnol. Genet. Eng. Rev.* 9, 1–22. doi:10.1080/02648725.2023.2183575

Gurusamy, N., Alsayari, A., Rajasingh, S., and Rajasingh, J. (2018). Adult stem cells for regenerative therapy. *Prog. Mol. Biol. Transl. Sci.* 160, 1–22. doi:10.1016/bs.pmbts.2018.07.009

Ham, S. W., Kim, J. K., Jeon, H. Y., Kim, E. J., Jin, X., Eun, K., et al. (2019). Korean Red ginseng extract inhibits glioblastoma propagation by blocking the Wnt signaling pathway. *J. Ethnopharmacol.* 236, 393–400. doi:10.1016/j.jep.2019.03.031

Han, J., Xia, J., Zhang, L., Cai, E., Zhao, Y., Fei, X., et al. (2019). Studies of the effects and mechanisms of ginsenoside Re and Rk(3) on myelosuppression induced by cyclophosphamide. *J. Ginseng Res.* 43 (4), 618–624. doi:10.1016/j.jgr.2018.07.009

He, F., and Yao, G. (2021). Ginsenoside Rg1 as a potential regulator of hematopoietic stem/progenitor cells. *Stem Cells Int.* 2021, 4633270. doi:10.1155/2021/4633270

He, F., Yu, C., Liu, T., and Jia, H. (2019). Ginsenoside Rg1 as an effective regulator of mesenchymal stem cells. *Front. Pharmacol.* 10, 1565. doi:10.3389/fphar.2019.01565

He, M., Wang, N., Zheng, W., Cai, X., Qi, D., Zhang, Y., et al. (2021). Ameliorative effects of ginsenosides on myelosuppression induced by chemotherapy or radiotherapy. *J. Ethnopharmacol.* 268, 113581. doi:10.1016/j.jep.2020.113581

Hicks, M. R., and Pyle, A. D. (2023). The emergence of the stem cell niche. *Trends Cell Biol.* 33 (2), 112–123. doi:10.1016/j.tcb.2022.07.003

Hong, T., Kim, M. Y., Da Ly, D., Park, S. J., Eom, Y. W., Park, K. S., et al. (2020). Ca(2+)-activated mitochondrial biogenesis and functions improve stem cell fate in Rg3-treated human mesenchymal stem cells. *Stem Cell Res. Ther.* 11 (1), 467. doi:10.1186/s13287-020-01974-3

Hou, B., Liu, R., Qin, Z., Luo, D., Wang, Q., and Huang, S. (2017). Oral Chinese herbal medicine as an adjuvant treatment for chemotherapy, or radiotherapy, induced myelosuppression: A systematic review and meta-analysis of randomized controlled trials. *Evid. Based Complement. Altern. Med.* 2017, 3432750. doi:10.1155/2017/3432750

Hou, C. W., Lee, S. D., Kao, C. L., Cheng, I. S., Lin, Y. N., Chuang, S. J., et al. (2015). Improved inflammatory balance of human skeletal muscle during exercise after supplementations of the ginseng-based steroid Rg1. *PLoS One* 10 (1), e0116387. doi:10.1371/journal.pone.0116387

Hou, M., Wang, R., Zhao, S., and Wang, Z. (2021). Ginsenosides in Panax genus and their biosynthesis. *Acta Pharm. Sin. B* 11 (7), 1813–1834. doi:10.1016/j.apsb.2020.12.017

Hu, J., Gu, Y., and Fan, W. (2016). Rg1 protects rat bone marrow stem cells against hydrogen peroxide-induced cell apoptosis through the PI3K/Akt pathway. *Mol. Med. Rep.* 14 (1), 406–412. doi:10.3892/mmr.2016.5238

Hu, W., Jing, P., Wang, L., Zhang, Y., Yong, J., and Wang, Y. (2015). The positive effects of Ginsenoside Rg1 upon the hematopoietic microenvironment in a D-Galactose-induced aged rat model. *BMC Complement. Altern. Med.* 15, 119. doi:10.1186/s12906-015-0642-3

Huang, X., Li, N., Pu, Y., Zhang, T., and Wang, B. (2019). Neuroprotective effects of ginseng phytochemicals: Recent perspectives. *Molecules* 24 (16), 2939. doi:10.3390/molecules24162939

Ichim, M. C., and De Boer, H. J. (2020). A review of authenticity and authentication of commercial ginseng herbal medicines and food supplements. *Front. Pharmacol.* 11, 612071. doi:10.3389/fphar.2020.612071

Ji, M., Minami, N., Yamada, M., and Imai, H. (2007). Effect of protopanaxatriol saponin on spermatogenic stem cell survival in busulfan-treated male mice. *Reprod. Med. Biol.* 6 (2), 99–108. doi:10.1111/j.1447-0578.2007.00172.x

Jin, J., Shahi, S., Kang, H. K., Van Veen, H. W., and Fan, T. P. (2006). Metabolites of ginsenosides as novel BCRP inhibitors. *Biochem. Biophys. Res. Commun.* 345 (4), 1308–1314. doi:10.1016/j.bbrc.2006.04.152

Ju, W., Lu, W., Ding, L., Bao, Y., Hong, F., Chen, Y., et al. (2020). PEDF promotes the repair of bone marrow endothelial cell injury and accelerates hematopoietic reconstruction after bone marrow transplantation. *J. Biomed. Sci.* 27 (1), 91. doi:10.1186/s12929-020-00685-4

Katoh, M., and Katoh, M. (2022). WNT signaling and cancer stemness. *Essays Biochem.* 66 (4), 319–331. doi:10.1042/ebc20220016

Kim, H., Choi, P., Kim, T., Kim, Y., Song, B. G., Park, Y. T., et al. (2021). Ginsenosides Rk1 and Rg5 inhibit transforming growth factor-β1-induced epithelial-mesenchymal transition and suppress migration, invasion, anoikis resistance, and development of stem-like features in lung cancer. *J. Ginseng Res.* 45 (1), 134–148. doi:10.1016/j.jgr.2020.02.005

Kumar, D., Baligar, P., Srivastav, R., Narad, P., Raj, S., Tandon, C., et al. (2021). Stem cell based preclinical drug development and toxicity prediction. *Curr. Pharm. Des.* 27 (19), 2237–2251. doi:10.2174/1381612826666201019104712

Kuo, Y. H., and Bhatia, R. (2014). Pushing the limits: Defeating leukemia stem cells by depleting telomerase. *Cell Stem Cell* 15 (6), 673–675. doi:10.1016/j.stem.2014.11.014

Lasigliè, D. (2021). Sirtuins and the prevention of immunosenescence. *Vitam. Horm.* 115, 221–264. doi:10.1016/bs.vh.2020.12.011

Lee, I. S., Kang, K. S., and Kim, S. Y. (2019). Panax ginseng pharmacopuncture: Current status of the research and future challenges. *Biomolecules* 10 (1), 33. doi:10.3390/biom10010033

Lee, T. X. Y., Wu, J., Jean, W. H., Condello, G., Alkhatib, A., Hsieh, C. C., et al. (2021). Reduced stem cell aging in exercised human skeletal muscle is enhanced by ginsenoside Rg1. *Aging (Albany NY)* 13 (12), 16567–16576. doi:10.18632/aging.203176

Li, J., Cai, D., Yao, X., Zhang, Y., Chen, L., Jing, P., et al. (2016). Protective effect of ginsenoside Rg1 on hematopoietic stem/progenitor cells through attenuating oxidative stress and the wnt/β-catenin signaling pathway in a mouse model of d-Galactose-induced aging. *Int. J. Mol. Sci.* 17 (6), 849. doi:10.3390/ijms17060849

Li, N., Wang, D., Ge, G., Wang, X., Liu, Y., and Yang, L. (2014). Ginsenoside metabolites inhibit P-glycoprotein *in vitro* and *in situ* using three absorption models. *Planta Med.* 80 (4), 290–296. doi:10.1055/s-0033-1360334

Li, X., Liu, W., Geng, C., Li, T., Li, Y., Guo, Y., et al. (2021). Ginsenoside Rg3 suppresses epithelial-mesenchymal transition via downregulating notch-hes1 signaling in colon cancer cells. *Am. J. Chin. Med.* 49 (1), 217–235. doi:10.1142/s0192415x21500129

Li, Y. B., Wang, Y., Tang, J. P., Chen, D., and Wang, S. L. (2015). Neuroprotective effects of ginsenoside Rg1-induced neural stem cell transplantation on hypoxic-ischemic encephalopathy. *Neural Regen. Res.* 10 (5), 753–759. doi:10.4103/1673-5374.156971

Li, Y., Revalde, J. L., Reid, G., and Paxton, J. W. (2010). Interactions of dietary phytochemicals with ABC transporters: Possible implications for drug disposition and multidrug resistance in cancer. *Drug Metab. Rev.* 42 (4), 590–611. doi:10.3109/03602531003758690

Lin, K. L., Zhang, J., Chung, H. L., Wu, X. Y., Liu, B., Zhao, B. X., et al. (2022). Total ginsenoside extract from panax ginseng enhances neural stem cell proliferation and neuronal differentiation by inactivating GSK-3β. *Chin. J. Integr. Med.* 28 (3), 229–235. doi:10.1007/s11655-021-3508-1

Lin, K., Liu, B., Lim, S. L., Fu, X., Sze, S. C., Yung, K. K., et al. (2020). 20(S)-protopanaxadiol promotes the migration, proliferation, and differentiation of neural stem cells by targeting GSK-3β in the Wnt/GSK-3β/β-catenin pathway. *J. Ginseng Res.* 44 (3), 475–482. doi:10.1016/j.jgr.2019.03.001

Lin, T., Islam, O., and Heese, K. (2006). ABC transporters, neural stem cells and neurogenesis--a different perspective. *Cell Res.* 16 (11), 857–871. doi:10.1038/sj.cr.7310107

Liu, H. H., Chen, F. P., Liu, R. K., Lin, C. L., and Chang, K. T. (2015a). Ginsenoside Rg1 improves bone marrow haematopoietic activity via extramedullary haematopoiesis of the spleen. *J. Cell Mol. Med.* 19 (11), 2575–2586. doi:10.1111/jcmm.12643

Liu, S., Chen, M., Li, P., Wu, Y., Chang, C., Qiu, Y., et al. (2015b). Ginsenoside rh2 inhibits cancer stem-like cells in skin squamous cell carcinoma. *Cell Physiol. Biochem.* 36 (2), 499–508. doi:10.1159/000430115

Liu, W., Zhu, X., Tang, L., Shen, N., Cheng, F., Zou, P., et al. (2022a). ACSL1 promotes imatinib-induced chronic myeloid leukemia cell senescence by regulating SIRT1/p53/p21 pathway. *Sci. Rep.* 12 (1), 17990. doi:10.1038/s41598-022-21009-6

Liu, X. Y., Yang, L. P., and Zhao, L. (2020). Stem cell therapy for Alzheimer's disease. *World J. Stem Cells* 12 (8), 787–802. doi:10.4252/wjsc.v12.i8.787

Liu, Y., Liu, N., Li, X., Luo, Z., and Zhang, J. (2022b). Ginsenoside Rb1 modulates the migration of bone-derived mesenchymal stem cells through the SDF-1/CXCR4 Axis and PI3K/Akt pathway. *Dis. Markers* 2022, 5196682. doi:10.1155/2022/5196682

Liu, Y., Wang, J., Qiao, J., Liu, S., Wang, S., Zhao, D., et al. (2020). Ginsenoside Rh2 inhibits HeLa cell energy metabolism and induces apoptosis by upregulating voltage-dependent anion channel 1. *Int. J. Mol. Med.* 46 (5), 1695–1706. doi:10.3892/ijmm.2020.4725

Liu, Y., Zhang, J. W., Li, W., Ma, H., Sun, J., Deng, M. C., et al. (2006). Ginsenoside metabolites, rather than naturally occurring ginsenosides, lead to inhibition of human cytochrome P450 enzymes. *Toxicol. Sci.* 91 (2), 356–364. doi:10.1093/toxsci/kfj164

Maliekal, T. T., Dharmapal, D., and Sengupta, S. (2022). Tubulin isotypes: Emerging roles in defining cancer stem cell niche. *Front. Immunol.* 13, 876278. doi:10.3389/fimmu.2022.876278

Michler, R. E. (2018). The current status of stem cell therapy in ischemic heart disease. *J. Card. Surg.* 33 (9), 520–531. doi:10.1111/jocs.13789

Mohrin, M., Shin, J., Liu, Y., Brown, K., Luo, H., Xi, Y., et al. (2015). Stem cell aging. A mitochondrial UPR-mediated metabolic checkpoint regulates hematopoietic stem cell aging. *Science* 347 (6228), 1374–1377. doi:10.1126/science.aaa2361

Najafi, M., Mortezaee, K., and Majidpoor, J. (2019). Cancer stem cell (CSC) resistance drivers. *Life Sci.* 234, 116781. doi:10.1016/j.lfs.2019.116781

Oh, J., Yoon, H. J., Jang, J. H., Kim, D. H., and Surh, Y. J. (2019). The standardized Korean Red Ginseng extract and its ingredient ginsenoside Rg3 inhibit manifestation of breast cancer stem cell-like properties through modulation of self-renewal signaling. *J. Ginseng Res.* 43 (3), 421–430. doi:10.1016/j.jgr.2018.05.004

Pan, W., Xue, B., Yang, C., Miao, L., Zhou, L., Chen, Q., et al. (2018). Biopharmaceutical characters and bioavailability improving strategies of ginsenosides. *Fitoterapia* 129, 272–282. doi:10.1016/j.fitote.2018.06.001

Phi, L. T. H., Sari, I. N., Wijaya, Y. T., Kim, K. S., Park, K., Cho, A. E., et al. (2019a). Ginsenoside Rd inhibits the metastasis of colorectal cancer via epidermal growth factor receptor signaling Axis. *IUBMB Life* 71 (5), 601–610. doi:10.1002/iub.1984

Phi, L. T. H., Wijaya, Y. T., Sari, I. N., Kim, K. S., Yang, Y. G., Lee, M. W., et al. (2019b). 20(R)-Ginsenoside Rg3 influences cancer stem cell properties and the epithelial-mesenchymal transition in colorectal cancer via the SNAIL signaling Axis. *Onco Targets Ther.* 12, 10885–10895. doi:10.2147/OTT.S219063

Pinho, S., and Frenette, P. S. (2019). Haematopoietic stem cell activity and interactions with the niche. *Nat. Rev. Mol. Cell Biol.* 20 (5), 303–320. doi:10.1038/s41580-019-0103-9

Piyasirananda, W., Beekman, A., Ganesan, A., Bidula, S., and Stokes, L. (2021). Insights into the structure-activity relationship of glycosides as positive allosteric modulators acting on P2X7 receptors. *Mol. Pharmacol.* 99 (2), 163–174. doi:10.1124/molpharm.120.000129

Ratan, Z. A., Haidere, M. F., Hong, Y. H., Park, S. H., Lee, J. O., Lee, J., et al. (2021). Pharmacological potential of ginseng and its major component ginsenosides. *J. Ginseng Res.* 45 (2), 199–210. doi:10.1016/j.jgr.2020.02.004

Regalado-Santiago, C., Juárez-Aguilar, E., Olivares-Hernández, J. D., and Tamariz, E. (2016). Mimicking neural stem cell niche by biocompatible substrates. *Stem Cells Int.* 2016, 1513285. doi:10.1155/2016/1513285

Roccio, M., Schmitter, D., Knobloch, M., Okawa, Y., Sage, D., and Lutolf, M. P. (2013). Predicting stem cell fate changes by differential cell cycle progression patterns. *Development* 140 (2), 459–470. doi:10.1242/dev.086215

Rokot, N. T., Kairupan, T. S., Cheng, K. C., Runtuwene, J., Kapantow, N. H., Amitani, M., et al. (2016). A role of ginseng and its constituents in the treatment of central nervous system disorders. *Evid. Based Complement. Altern. Med.* 2016, 2614742. doi:10.1155/2016/2614742

Scott, C. T., and Reijo Pera, R. A. (2008). The road to pluripotence: The research response to the embryonic stem cell debate. *Hum. Mol. Genet.* 17 (R1), R3–R9. doi:10.1093/hmg/ddn074

Sferrazza, G., Corti, M., Brusotti, G., Pierimarchi, P., Temporini, C., Serafino, A., et al. (2020). Nature-derived compounds modulating Wnt/**β** -catenin pathway: A preventive and therapeutic opportunity in neoplastic diseases. *Acta Pharm. Sin. B* 10 (10), 1814–1834. doi:10.1016/j.apsb.2019.12.019

Shang, D., Li, Z., Tan, X., Liu, H., and Tu, Z. (2023). Inhibitory effects and molecular mechanisms of ginsenoside Rg1 on the senescence of hematopoietic stem cells. *Fundam. Clin. Pharmacol.* 37 (3), 509–517. doi:10.1111/fcp.12863

Shibue, T., and Weinberg, R. A. (2017). EMT, CSCs, and drug resistance: The mechanistic link and clinical implications. *Nat. Rev. Clin. Oncol.* 14 (10), 611–629. doi:10.1038/nrclinonc.2017.44

Sinenko, S. A., Ponomartsev, S. V., and Tomilin, A. N. (2021). Pluripotent stem cell-based gene therapy approach: Human de novo synthesized chromosomes. *Cell Mol. Life Sci.* 78 (4), 1207–1220. doi:10.1007/s00018-020-03653-1

Sivandzade, F., and Cucullo, L. (2021). Regenerative stem cell therapy for neurodegenerative diseases: An overview. *Int. J. Mol. Sci.* 22 (4), 2153. doi:10.3390/ijms22042153

Sterneckert, J. L., Reinhardt, P., and Schöler, H. R. (2014). Investigating human disease using stem cell models. *Nat. Rev. Genet.* 15 (9), 625–639. doi:10.1038/nrg3764

Szade, K., Gulati, G. S., Chan, C. K. F., Kao, K. S., Miyanishi, M., Marjon, K. D., et al. (2018). Where hematopoietic stem cells live: The bone marrow niche. *Antioxid. Redox Signal* 29 (2), 191–204. doi:10.1089/ars.2017.7419

Tanabe, S. (2022). Microenvironment of cancer stem cells. *Adv. Exp. Med. Biol.* 1393, 103–124. doi:10.1007/978-3-031-12974-2_5

Tanabe, S., Quader, S., Cabral, H., and Ono, R. (2020). Interplay of EMT and CSC in cancer and the potential therapeutic strategies. *Front. Pharmacol.* 11, 904. doi:10.3389/fphar.2020.00904

Tang, Y. L., Wang, X. B., Zhou, Y., Wang, Y. P., and Ding, J. C. (2021). Ginsenoside Rg1 induces senescence of leukemic stem cells by upregulating p16INK4a and downregulating hTERT expression. *Adv. Clin. Exp. Med.* 30 (6), 599–605. doi:10.17219/acem/133485

Tang, Y. L., Zhang, C. G., Liu, H., Zhou, Y., Wang, Y. P., Li, Y., et al. (2020a). Ginsenoside Rg1 inhibits cell proliferation and induces markers of cell senescence in CD34+CD38- leukemia stem cells derived from KG1α acute myeloid leukemia cells by activating the sirtuin 1 (SIRT1)/Tuberous sclerosis complex 2 (TSC2) signaling pathway. *Med. Sci. Monit.* 26, e918207. doi:10.12659/MSM.918207

Tang, Y. L., Zhou, Y., Wang, Y. P., He, Y. H., Ding, J. C., Li, Y., et al. (2020b). Ginsenoside Rg1 protects against Sca-1(+) HSC/HPC cell aging by regulating the SIRT1-FOXO3 and SIRT3-SOD2 signaling pathways in a gamma-ray irradiation-induced aging mice model. *Exp. Ther. Med.* 20 (2), 1245–1252. doi:10.3892/etm.2020.8810

Tang, Y. L., Zhou, Y., Wang, Y. P., Wang, J. W., and Ding, J. C. (2015). SIRT6/NF-κB signaling axis in ginsenoside Rg1-delayed hematopoietic stem/progenitor cell senescence. *Int. J. Clin. Exp. Pathol.* 8 (5), 5591–5596.

Uslu, M., Albayrak, E., and Kocabas, F. (2020). Temporal modulation of calcium sensing in hematopoietic stem cells is crucial for proper stem cell expansion and engraftment. *J. Cell Physiol.* 235 (12), 9644–9666. doi:10.1002/jcp.29777

Vieira, M. S., Santos, A. K., Vasconcellos, R., Goulart, V. a. M., Parreira, R. C., Kihara, A. H., et al. (2018). Neural stem cell differentiation into mature neurons: Mechanisms of regulation and biotechnological applications. *Biotechnol. Adv.* 36 (7), 1946–1970. doi:10.1016/j.biotechadv.2018.08.002

Wang, C. L., Xiao, F., Wang, C. D., Zhu, J. F., Shen, C., Zuo, B., et al. (2017). Gremlin2 suppression increases the BMP-2-induced osteogenesis of human bone marrow-derived mesenchymal stem cells via the BMP-2/smad/runx2 signaling pathway. *J. Cell Biochem.* 118 (2), 286–297. doi:10.1002/jcb.25635

Wang, H., Diao, D., Shi, Z., Zhu, X., Gao, Y., Gao, S., et al. (2016). SIRT6 controls hematopoietic stem cell homeostasis through epigenetic regulation of Wnt signaling. *Cell Stem Cell* 18 (4), 495–507. doi:10.1016/j.stem.2016.03.005

Wang, P., Wei, X., Zhang, F., Yang, K., Qu, C., Luo, H., et al. (2014). Ginsenoside Rg1 of Panax ginseng stimulates the proliferation, odontogenic/osteogenic differentiation and gene expression profiles of human dental pulp stem cells. *Phytomedicine* 21 (2), 177–183. doi:10.1016/j.phymed.2013.08.021

Wang, R., Wang, M., Zhou, J., Wu, D., Ye, J., Sun, G., et al. (2020a). Saponins in Chinese herbal medicine exerts protection in myocardial ischemia-reperfusion injury: Possible mechanism and target analysis. *Front. Pharmacol.* 11, 570867. doi:10.3389/fphar.2020.570867

Wang, Y., Meng, Q., Qiao, H., Jiang, H., and Sun, X. (2009). Role of the spleen in cyclophosphamide-induced hematosuppression and extramedullary hematopoiesis in mice. *Arch. Med. Res.* 40 (4), 249–255. doi:10.1016/j.arcmed.2009.04.003

Wang, Y. Z., Xu, Q., Wu, W., Liu, Y., Jiang, Y., Cai, Q. Q., et al. (2018). Brain transport profiles of ginsenoside Rb(1) by glucose transporter 1: *In vitro* and *in vivo*. *Front. Pharmacol.* 9, 398. doi:10.3389/fphar.2018.00398

Wang, Z., Jiang, R., Wang, L., Chen, X., Xiang, Y., Chen, L., et al. (2020b). Ginsenoside Rg1 improves differentiation by inhibiting senescence of human bone marrow mesenchymal stem cell via GSK-3β and β-catenin. *Stem Cells Int.* 2020, 2365814. doi:10.1155/2020/2365814

Wang, Z., Wang, L., Jiang, R., Li, C., Chen, X., Xiao, H., et al. (2021). Ginsenoside Rg1 prevents bone marrow mesenchymal stem cell senescence via NRF2 and PI3K/Akt signaling. *Free Radic. Biol. Med.* 174, 182–194. doi:10.1016/j.freeradbiomed.2021.08.007

Wang, Z., Xia, J., Li, J., Chen, L., Chen, X., Zhang, Y., et al. (2022a). Rg1 protects hematopoietic stem cells from LiCl-induced oxidative stress via Wnt signaling pathway. *Evid. Based Complement. Altern. Med.* 2022, 2875583. doi:10.1155/2022/2875583

Wang, Z., Zhang, C., Warden, C. D., Liu, Z., Yuan, Y. C., Guo, C., et al. (2022b). Loss of SIRT1 inhibits hematopoietic stem cell aging and age-dependent mixed phenotype acute leukemia. *Commun. Biol.* 5 (1), 396. doi:10.1038/s42003-022-03340-w

Weatherbee, B. a. T., Cui, T., and Zernicka-Goetz, M. (2021). Modeling human embryo development with embryonic and extra-embryonic stem cells. *Dev. Biol.* 474, 91–99. doi:10.1016/j.ydbio.2020.12.010

White, A. C., and Lowry, W. E. (2015). Refining the role for adult stem cells as cancer cells of origin. *Trends Cell Biol.* 25 (1), 11–20. doi:10.1016/j.tcb.2014.08.008

Won, H. J., Kim, H. I., Park, T., Kim, H., Jo, K., Jeon, H., et al. (2019). Non-clinical pharmacokinetic behavior of ginsenosides. *J. Ginseng Res.* 43 (3), 354–360. doi:10.1016/j.jgr.2018.06.001

Wong, A. S., Che, C. M., and Leung, K. W. (2015). Recent advances in ginseng as cancer therapeutics: A functional and mechanistic overview. *Nat. Prod. Rep.* 32 (2), 256–272. doi:10.1039/c4np00080c

Wu, T., Chen, Y., Liu, W., Tong, K. L., Suen, C. W., Huang, S., et al. (2020). Ginsenoside Rb1/TGF-β1 loaded biodegradable silk fibroin-gelatin porous scaffolds for inflammation inhibition and cartilage regeneration. *Mater Sci. Eng. C Mater Biol. Appl.* 111, 110757. doi:10.1016/j.msec.2020.110757

Wu, Y., Liu, Y., Xu, Y., Zheng, A., Du, J., Cao, L., et al. (2022). Bioactive natural compounds as potential medications for osteogenic effects in a molecular docking approach. *Front. Pharmacol.* 13, 955983. doi:10.3389/fphar.2022.955983

Xiang, Y., Wang, S. H., Wang, L., Wang, Z. L., Yao, H., Chen, L. B., et al. (2019). Effects of ginsenoside Rg1 regulating wnt/β-catenin signaling on neural stem cells to delay brain senescence. *Stem Cells Int.* 2019, 5010184. doi:10.1155/2019/5010184

Xiao, L., Wang, M., Zou, K., Li, Z., and Luo, J. (2022). Effects of ginsenoside Rg1 on proliferation and directed differentiation of human umbilical cord mesenchymal stem cells into neural stem cells. *Neuroreport* 33 (10), 413–421. doi:10.1097/wnr.0000000000001795

Xie, Q., Liu, R., Jiang, J., Peng, J., Yang, C., Zhang, W., et al. (2020). What is the impact of human umbilical cord mesenchymal stem cell transplantation on clinical treatment? *Stem Cell Res. Ther.* 11 (1), 519. doi:10.1186/s13287-020-02011-z

Xie, W., Zhou, P., Sun, Y., Meng, X., Dai, Z., Sun, G., et al. (2018). Protective effects and target network analysis of ginsenoside Rg1 in cerebral ischemia and reperfusion injury: A comprehensive overview of experimental studies. *Cells* 7 (12), 270. doi:10.3390/cells7120270

Xu, F. T., Li, H. M., Yin, Q. S., Cui, S. E., Liu, D. L., Nan, H., et al. (2014). Effect of ginsenoside Rg1 on proliferation and neural phenotype differentiation of human adipose-derived stem cells *in vitro*. *Can. J. Physiol. Pharmacol.* 92 (6), 467–475. doi:10.1139/cjpp-2013-0377

Xu, F. T., Li, H. M., Zhao, C. Y., Liang, Z. J., Huang, M. H., Li, Q., et al. (2015). Characterization of chondrogenic gene expression and cartilage phenotype differentiation in human breast adipose-derived stem cells promoted by ginsenoside Rg1 *in vitro*. *Cell Physiol. Biochem.* 37 (5), 1890–1902. doi:10.1159/000438550

Xu, F. T., Liang, Z. J., Li, H. M., Peng, Q. L., Huang, M. H., Li De, Q., et al. (2016). Ginsenoside Rg1 and platelet-rich fibrin enhance human breast adipose-derived stem cell function for soft tissue regeneration. *Oncotarget* 7 (23), 35390–35403. doi:10.18632/oncotarget.9360

Xu, F. T., Xu, Y. L., Rong, Y. X., Huang, D. L., Lai, Z. H., Liu, X. H., et al. (2022). Rg1 promotes the proliferation and adipogenic differentiation of human adipose-derived stem cells via FXR1/lnc-GAS5-AS1 pathway. *Curr. Stem Cell Res. Ther.* 17 (8), 815–824. doi:10.2174/1574888x16666211129121414

Xu, S. F., Yu, L. M., Fan, Z. H., Wu, Q., Yuan, Y., Wei, Y., et al. (2012). Improvement of ginsenoside Rg1 on hematopoietic function in cyclophosphamide-induced myelosuppression mice. *Eur. J. Pharmacol.* 695 (1-3), 7–12. doi:10.1016/j.ejphar.2012.07.050

Xu, X., Lu, Q., Wu, J., Li, Y., and Sun, J. (2017). Impact of extended ginsenoside Rb1 on early chronic kidney disease: A randomized, placebo-controlled study. *Inflammopharmacology* 25 (1), 33–40. doi:10.1007/s10787-016-0296-x

Yamashita, T., and Abe, K. (2016). Recent progress in therapeutic strategies for ischemic stroke. *Cell Transpl.* 25 (5), 893–898. doi:10.3727/096368916x690548

Yang, J. E., Jia, N., Wang, D., He, Y., Dong, L., and Yang, A. G. (2020a). Ginsenoside Rb1 regulates neuronal injury and Keap1-Nrf2/ARE signaling pathway in cerebral infarction rats. *J. Biol. Regul. Homeost. Agents* 34 (3), 1091–1095. doi:10.23812/20-143-l-7

Yang, L., Zou, H., Gao, Y., Luo, J., Xie, X., Meng, W., et al. (2020b). Insights into gastrointestinal microbiota-generated ginsenoside metabolites and their bioactivities. *Drug Metab. Rev.* 52 (1), 125–138. doi:10.1080/03602532.2020.1714645

Yang, N., Liang, G., Lin, J., Zhang, S., Lin, Q., Ji, X., et al. (2020). Ginsenoside Rd therapy improves histological and functional recovery in a rat model of inflammatory bowel disease. *Phytother. Res.* 34 (11), 3019–3028. doi:10.1002/ptr.6734

Yang, Z., Zhao, T., Liu, H., and Zhang, L. (2016). Ginsenoside Rh2 inhibits hepatocellular carcinoma through beta-catenin and autophagy. *Sci. Rep.* 6, 19383. doi:10.1038/srep19383

Yao, W., and Guan, Y. (2022). Ginsenosides in cancer: A focus on the regulation of cell metabolism. *Biomed. Pharmacother.* 156, 113756. doi:10.1016/j.biopha.2022.113756

Yin, W., Wang, J., Jiang, L., and James Kang, Y. (2021). Cancer and stem cells. *Exp. Biol. Med. (Maywood)* 246 (16), 1791–1801. doi:10.1177/15353702211005390

Yousof Ali, M., Jannat, S., and Mizanur Rahman, M. (2021). Ginsenoside derivatives inhibit advanced glycation end-product formation and glucose-fructose mediated protein glycation *in vitro* via a specific structure-activity relationship. *Bioorg Chem.* 111, 104844. doi:10.1016/j.bioorg.2021.104844

Yue, Z., Rong, J., Ping, W., Bing, Y., Xin, Y., Feng, L. D., et al. (2014). Gene expression of the p16(INK4a)-Rb and p19(Arf)-p53-p21(Cip/Waf1) signaling pathways in the regulation of hematopoietic stem cell aging by ginsenoside Rg1. *Genet. Mol. Res.* 13 (4), 10086–10096. doi:10.4238/2014.December.4.3

Zakrzewski, W., Dobrzyński, M., Szymonowicz, M., and Rybak, Z. (2019). Stem cells: Past, present, and future. *Stem Cell Res. Ther.* 10 (1), 68. doi:10.1186/s13287-019-1165-5

Zeng, D., Wang, J., Kong, P., Chang, C., Li, J., and Li, J. (2014). Ginsenoside Rg3 inhibits HIF-1α and VEGF expression in patient with acute leukemia via inhibiting the activation of PI3K/Akt and ERK1/2 pathways. *Int. J. Clin. Exp. Pathol.* 7 (5), 2172–2178.

Zhang, D. Y., Pan, Y., Zhang, C., Yan, B. X., Yu, S. S., Wu, D. L., et al. (2013a). Wnt/β-catenin signaling induces the aging of mesenchymal stem cells through promoting the ROS production. *Mol. Cell Biochem.* 374 (1-2), 13–20. doi:10.1007/s11010-012-1498-1

Zhang, G., Xia, F., Zhang, Y., Zhang, X., Cao, Y., Wang, L., et al. (2016). Ginsenoside Rd is efficacious against acute ischemic stroke by suppressing microglial proteasome-mediated inflammation. *Mol. Neurobiol.* 53 (4), 2529–2540. doi:10.1007/s12035-015-9261-8

Zhang, H., Hua, X., Zheng, D., Wu, H., Li, C., Rao, P., et al. (2022a). De novo biosynthesis of oleanane-type ginsenosides in *Saccharomyces cerevisiae* using two types of glycosyltransferases from panax ginseng. *J. Agric. Food Chem.* 70 (7), 2231–2240. doi:10.1021/acs.jafc.1c07526

Zhang, M., Shi, Z., Zhang, S., Li, X., To, S. K. Y., Peng, Y., et al. (2022b). The ginsenoside compound K suppresses stem-cell-like properties and colorectal cancer metastasis by targeting hypoxia-driven nur77-akt feed-forward signaling. *Cancers (Basel)* 15 (1), 24. doi:10.3390/cancers15010024

Zhang, Y., Dong, F., Zhang, N., Cheng, H., Pang, Y., Wang, X., et al. (2013b). Suppression of cytochrome p450 reductase enhances long-term hematopoietic stem cell repopulation efficiency in mice. *PLoS One* 8 (7), e69913. doi:10.1371/journal.pone.0069913

Zhao, J., Lu, S., Yu, H., Duan, S., and Zhao, J. (2018). Baicalin and ginsenoside Rb1 promote the proliferation and differentiation of neural stem cells in Alzheimer's disease model rats. *Brain Res.* 1678, 187–194. doi:10.1016/j.brainres.2017.10.003

Zhao, M., and Li, L. (2015). Regulation of hematopoietic stem cells in the niche. *Sci. China Life Sci.* 58 (12), 1209–1215. doi:10.1007/s11427-015-4960-y

Zhou, L., Yang, F., Yin, J. W., Gu, X., Xu, Y., and Liang, Y. Q. (2020a). Compound K induces neurogenesis of neural stem cells in thrombin induced nerve injury through LXRα signaling in mice. *Neurosci. Lett.* 729, 135007. doi:10.1016/j.neulet.2020.135007

Zhou, Y., Wang, Y. P., He, Y. H., and Ding, J. C. (2020b). Ginsenoside Rg1 performs anti-aging functions by suppressing mitochondrial pathway-mediated apoptosis and activating sirtuin 3 (SIRT3)/Superoxide dismutase 2 (SOD2) pathway in sca-1^{+} HSC/HPC cells of an aging rat model. *Med. Sci. Monit.* 26, e920666. doi:10.12659/MSM.920666

frontiers | Frontiers in Cell and Developmental Biology

TYPE Review
PUBLISHED 04 December 2023
DOI 10.3389/fcell.2023.1323678

OPEN ACCESS

EDITED BY
Konstantinos Chatzistergos,
Aristotle University of Thessaloniki, Greece

REVIEWED BY
Yuyao Tian,
Boston Children's Hospital and Harvard Medical School, United States
Dimitrios Kouroupis,
University of Miami, United States
Faizal Asumda,
Augusta University, United States
Maria Roubelakis,
National and Kapodistrian University of Athens, Greece

*CORRESPONDENCE
Shu Guo,
sguo@cmu.edu.cn
Mengzhu Lv,
mzlv@cmu.edu.cn

RECEIVED 18 October 2023
ACCEPTED 17 November 2023
PUBLISHED 04 December 2023

CITATION
Sun W, Lv J, Guo S and Lv M (2023), Cellular microenvironment: a key for tuning mesenchymal stem cell senescence.
Front. Cell Dev. Biol. 11:1323678.
doi: 10.3389/fcell.2023.1323678

Cellular microenvironment: a key for tuning mesenchymal stem cell senescence

Wenyang Sun, Jiacheng Lv, Shu Guo* and Mengzhu Lv*

Department of Plastic Surgery, The First Hospital of China Medical University, Shenyang, Liaoning, China

Mesenchymal stem cells (MSCs) possess the ability to self-renew and differentiate into multiple cell types, making them highly suitable for use as seed cells in tissue engineering. These can be derived from various sources and have been found to play crucial roles in several physiological processes, such as tissue repair, immune regulation, and intercellular communication. However, the limited capacity for cell proliferation and the secretion of senescence-associated secreted phenotypes (SASPs) pose challenges for the clinical application of MSCs. In this review, we provide a comprehensive summary of the senescence characteristics of MSCs and examine the different features of cellular microenvironments studied thus far. Additionally, we discuss the mechanisms by which cellular microenvironments regulate the senescence process of MSCs, offering insights into preserving their functionality and enhancing their effectiveness.

KEYWORDS

mesenchymal stem cells, tissue engineering, SASPs, cellular senescence, cellular microenvironment

1 Introduction

Over the past decade, there has been significant progress in the field of stem cell-based regenerative therapeutics and *ex vivo* disease models. This progress has been achieved by leveraging the pluripotent and immunological features of stem cells. Mesenchymal stem cells (MSCs), which are adult non-hematopoietic mesodermal stem cells, were first isolated from bone marrow in 1968. (Friedenstein et al., 1968). MSCs offer numerous advantages over other types of stem cells in terms of therapy and applications. These versatile cells can be derived from various sources such as bone marrow, umbilical cord, placenta, fat, cartilage, skin, lungs, and dental pulp. (Pittenger et al., 2019; Liu Yajun et al., 2022). Previous research has shown that genetic alteration of MSCs and gene delivery are both feasible and practical (Damasceno et al., 2020; Zhou et al., 2023). The immunological flexibility of MSCs makes them highly effective in regulating and improving the inflammatory microenvironment. (Zhuang et al., 2022). To date, treatments using MSCs and their extracellular vesicles (EVs) have demonstrated beneficial effects in a variety of diseases, such as osteoarthritis (OA) (Greif et al., 2020; Kim et al., 2020; Rizzo et al., 2023), diabetic mellitus (DM) (Sun F. et al., 2022; Yang et al., 2022), Crohn's disease (CD) (Garcia-Olmo et al., 2022; Huang et al., 2022), systemic lupus erythematosus (SLE) (Zhang Mingchao et al., 2022), myocardial infarction (MI) (Czosseck et al., 2022), acute respiratory distress disorder (ARD) (Jackson et al., 2016; Qiao et al., 2021) and graft-versus-host disease (GVHD) (Harrell et al., 2022). In 2006, the International Society for Cellular Therapy (ISCT) proposed minimal criteria to define MSCs. These criteria include: i. MSCs should adhere to plastic under standard culture conditions; ii. MSCs should express CD105, CD73, and CD90, while not expressing CD45, CD34, CD14 or

CD11b, CD79 or CD19, and HLA-DR surface markers; and iii. MSCs should demonstrate the ability to differentiate into three different lineages: osteogenic, lipogenic, and chondrogenic. (Dominici et al., 2006; Mareschi et al., 2006).

However, as MSCs undergo senescence, they also undergo a transition from an anti-inflammatory to a pro-inflammatory factor phenotype. This shift can reduce the immunomodulatory potential of MSCs and significantly limit the effectiveness of stem cell therapy. Moreover, senescent MSCs alter the cellular microenvironment surrounding them through the secretion of senescence-associated secreted phenotypes (SASPs), the generation of reactive oxygen species (ROS), and the remodeling of the extracellular matrix (Liu J. et al., 2022; Siraj et al., 2023). These changes induce senescence in non-senescent MSCs. As a result, stringent criteria may be necessary for creating high-quality MSCs for therapeutic applications and obtaining large quantities of high-purity MSCs from patients can be challenging. (Zhang Y. et al., 2021).

Efforts to enhance the efficiency of cell therapy must address the negative effects of senescence in MSCs. Multiple factors contribute to the senescence of MSCs, including cell-intrinsic regulatory mechanisms related to DNA damage, telomere shortening, and epigenetic modifications. Additionally, the cellular microenvironment in which MSCs reside plays a significant role in influencing their senescence-related behaviors. The cellular microenvironment refers to the local region consisting of neighboring cells and non-cellular components. It provides structural support and signaling that are crucial for maintaining the homeostasis and functionality of MSCs(Choi et al., 2014; Papait et al., 2020; Liu J. et al., 2022; Pei et al., 2023). Creating an appropriate cellular microenvironment is also essential for advancements in tissue engineering and regenerative medicine. The state and function of MSCs can be influenced by changes in the cellular microenvironment during various physiological and pathological conditions (Papait et al., 2020; Liu J. et al., 2022; Tan et al., 2022). The current body of literature does not provide a comprehensive overview of the impact of the cellular microenvironment on senescence in MSCs. As a result, the objective of this paper is to compile and summarize the effects and mechanisms of different cellular microenvironments on the senescence and behavior of MSCs. Additionally, this paper will explore potential avenues for future research in this field.

2 Characteristics of MSCs senescence

Cellular senescence is a physiological state that manifests as a stable cell cycle stagnation (Herranz and Gil, 2018). The discovery can be traced back to the 1960s, when Haflick and Moorhead experimentally cultured and observed human fibroblasts' inability to divide indefinitely. This phenomenon is known as the 'Hayflick limit'. (Hayflick and Moorhead, 1961). Senescent cells are characterized by heightened intracellular expression of senescence-related genes, such as p16 and p53 (Hernandez-Segura et al., 2018), as well as senescence-associated β-galactosidase (SA-β-gal). Additionally, they further induce the surrounding cells and microenvironment into senescence through paracrine effects. (Di Mitri and Alimonti, 2016).

Previous research has demonstrated that the presence and elimination of senescent cells have a beneficial effect on maintaining the microenvironment and organ function in the human body over a short period of time. However, the long-term accumulation of senescent cells can have the opposite effect and contribute to the development of age-related diseases (ARDs) (Yin Yujia et al., 2021). Cellular senescence is also a contributing factor to individual aging, a gradual decline in physiological function. Previous studies have demonstrated the effectiveness of Senolytics in eliminating senescent cells and addressing ARDs such as cardiovascular diseases, metabolic diseases, and frailty (Zhu et al., 2015; Chaib et al., 2022). For instance, the application of ABT-263 as a pretreatment for synovial MSCs has proven to be successful in eliminating senescent cells and enhancing the outcomes of patients with OA (Miura et al., 2022). Lopez-Otin et al. (Lopez-Otin et al., 2013) identified nine hallmarks of aging, including DNA damage, telomere attrition, epigenetic modification, loss of proteostasis, mitochondrial failure, cellular senescence, nutrition sensing, intracellular communication, and stem cell exhaustion. Cellular senescence and stem cell exhaustion are the main mechanisms of aging. In this section, we will focus on the characteristics of MSCs' senescence.

2.1 Cell cycle arrest

Unlike cells in a quiescent state, senescent cells are metabolically active but arrested in the G1/S phase of the cell cycle. This arrest is primarily caused by activation of the p53/p21CIP1 signaling pathway or the $p16^{INK4A/Rb}$ oncogenic pathway (Kamal et al., 2020; Engeland, 2022). p53, a tumor suppressor gene, promotes genomic stability by inducing cell cycle arrest and apoptosis (Chen, 2016). It also plays a significant role in cellular senescence and aging (Hafner et al., 2019). In p53-induced senescent MSCs, the expression of p53-regulated downstream miRNAs (such as miR-34a/b/c, miR-29, miR-145, and miR-192) increases, with miR-34a showing the strongest association with p53. Overexpression of miR-34a in MSCs inhibits osteogenic differentiation and accelerates senescence (Xia et al., 2021). Interestingly, the expression of $p16^{INK4A}$ is elevated in P3 MSCs overexpressing miR-34a, while the expression of p21WAF1/CIP remains largely unchanged, suggesting different mechanisms for replicative senescence (Pi et al., 2021). Apart from p53-dependent miRNAs, other miRNAs also play distinct roles in MSC senescence. For instance, miR-200c-3p inhibits the p53/p21 axis and enhances the transcription of stemness-related genes (Nanog, Oct4, and Sox2) (Anastasiadou et al., 2021).

2.2 Morphological and biological changes

There is a strong correlation between the morphology and function of MSCs. Previous studies have shown that larger MSCs have similar ATP levels and SA-β-gal activity as those obtained from older individuals (Liu J. et al., 2020). On the other hand, smaller MSCs resemble those obtained from younger individuals, suggesting that cell size could be used as a potential indicator to evaluate the level of senescence in MSCs (Block et al., 2017; Zhai et al., 2021). Senescent MSCs

undergo a transformation from their typical spindle shape to an enlarged, irregular, flattened form (Li et al., 2017). As the number of passages increases, the shape of human adipose-derived stem cells (ADSCs) changes, with the emergence of pseudopod structures in the 10th generation and a 'fried egg' morphology in the 15th generation. Additionally, prolonged culture significantly reduces cell density in the same magnification field, while the cell diameter gradually increases (Truong et al., 2019).

2.3 Senescence-associated-β-galactosidase

Senescence-associated-β-galactosidase (SA-β-gal) was initially discovered by Dimri et al., in 1995 (Dimri et al., 1995). Since then, it has emerged as the most extensively utilized biomarker for identifying senescent cells, both *in vitro* and *in vivo*. SA-β-gal activity is highly correlated with senescent cells and is not detectable in quiescent or differentiated cells. The level of SA-β-gal is associated with the amount of lysosomes inside cells (Lozono-Torres et al., 2019), and the increase in size and volume of lysosomes is primarily due to the presence of lipofuscin, a marker for senescent cells (Vida et al., 2017). Aspirin (2-Acetoxybenzoic acid) therapy was found to effectively reduce the number of SA-β-gal-positive cells in replicative senescent bone marrow stem cells (BMSCs). Additionally, there was a significant decrease in the expressions of p16, p53, and p21, and the blue staining of BMSCs nuclei was also reduced (Liu X. P. et al., 2022).

2.4 Colony-forming ability

The ability of a single cell to proliferate *ex vivo* for more than six generations and its progeny to form a population of cells is commonly referred to as a 'colony' or 'clone.' The colony formation rate serves as an indicator of the cell's ability to survive independently. Colony-forming ability is considered a significant characteristic of cell stemness, and MSCs tend to lose their colony-forming ability as their proliferation decreases and they enter senescence (Ridzuan et al., 2016). In a study conducted by Kapetanou et al., proteasomal changes associated with senescence were observed in late-passaged (p40) human mesenchymal stem cells (hMSCs). The researchers found a decrease in the expression of the β5 subunit, which was closely linked to the poor proliferative potential of hMSCs. However, when β5 was overexpressed in Wharton's jelly-derived mesenchymal stem cells (WJ-MSCs), the senescence-associated proteasomal alterations were rescued. This overexpression of β5 not only enhanced the stemness and proliferative capacity of late-passaged MSCs, but it also resulted in a decrease in proteasomal oxidative protein modifications and intracellular ROS levels (Kapetanou Marianna et al., 2017). Furthermore, it has been demonstrated that the ability of MSCs to form colonies is also influenced by telomere length (Guerrero et al., 2021) and the consistent expression of proto-oncogenes, such as B cell lymphoma 3 (Bcl-3) (Wang Fuxiao et al., 2022).

2.5 Differentiation bias

The ability of MSCs to differentiate into three lineages is a distinguishing characteristic, and an imbalance in the differentiation into osteogenic and lipogenic lineages is a problem associated with MSC senescence. MSCs in the bone marrow (BM) microenvironment show reduced proliferative capacity and increased SA-β-gal activity, which are linked to age-related osteoporosis and fractures. Additionally, there is a decrease in osteogenic differentiation and an increased tendency towards lipogenic differentiation (Yi et al., 2021). Bcl-3, an inhibitor of NF-κB that plays a role in maintaining Wnt/β-catenin signaling and promoting osteogenic differentiation while inhibiting lipogenic differentiation in BMSCs, is considered a crucial target for treating age-related osteoporosis (Chen Xi et al., 2020; Jing et al., 2022).

In recent years, researchers have postulated that several miRNAs affect biological characteristics in MSCs through various signaling pathways (Yang et al., 2021). One such miRNA, miR-204, has been found to be significantly increased in senescent cells and has regulatory effects on SASPs factors such as IL-6 and MMP-3 (Kang et al., 2019). Additionally, it has been observed to inhibit the osteogenic differentiation of BMSCs by regulating RUNX2 (Huang et al., 2010). Another important discovery is the role of the long noncoding RNA zinc finger antisense 1 (ZFAS1) in governing the osteogenic development of BMSCs through the ZFAS1-miR-499-EPHA5 axis. This finding suggests that targeting ZFAS1 could be crucial in the treatment of osteoporosis in the elderly, as BMSCs with ZFAS1 knockdown exhibit increased osteogenic differentiation and decreased lipogenic differentiation (Wu et al., 2022). Shen J. et al. (Shen et al., 2020)further discovered that miR-483-3p stimulates lipogenic differentiation in ADSCs and inhibits the IGF1 pathway, leading to senescence in ADSCs.

2.6 Metabolic alterations

Senescence is closely associated with disturbances in the maintenance of metabolism. As cells become senescent, several neutral amino acids such as valine, isoleucine, and glycine can be utilized as alternative energy sources to maintain energy homeostasis (Yi et al., 2020). Metabolomic analysis has revealed changes in glycerophospholipid metabolism, taurine and hypotaurine metabolism, glycerolipid metabolism, drug metabolism-cytochrome P450, and drug metabolism-other enzymes in senescent BMSCs(Chen et al., 2019; Yu X. et al., 2022). Lipid metabolism was found to be inhibited. Genes related to lipid metabolism, such as Scd, Scd2, Dgat2, Fads2, and Lpin1, were downregulated. Scd2, the most significant differentially expressed gene (DEG), may be involved in altering the biomembrane of senescent cells. In Scd2 overexpressing BMSCs, there was a significant reduction in SA-β-gal activity, and the expression of senescence-associated genes was suppressed. However, there have been limited reports on the roles and mechanisms related to Scd2 (Yu Xiao et al., 2022).

2.7 Phenotypic changes

During senescence, there are no significant differences in the expression of certain surface markers such as CD105, CD73, and CD90. However, other surface markers such as CD106, CD146, and STRO-1 are linked to senescence in MSCs and their expressions are downregulated during senescence. For example, MSCs derived from the BM of multiple sclerosis (MS) patients showed senescence-related characteristics such as reduced amplification capability and decreased STRO-1 expression (Redondo J. et al., 2018). The improved effectiveness of CD146+ MSCs in treating myocardial infarction (MI) may be attributed to lower levels of ROS(Zhang et al., 2019). On the other hand, replicative senescence enhances CD26 expression. MSCs with high CD26 levels have a decreased capacity for immunosuppression and proliferation compared to MSCs with low CD26 levels (Psaroudis et al., 2022).

SASPs were initially discovered and described by Coppe et al. in senescent fibroblasts and epithelial cells (Coppe et al., 2008). During senescence, cells produce unique secretions known as SASPs, which play a role in maintaining the senescent phenotype. SASPs consist of various components including inflammatory and immunomodulatory factors (e.g., IL-6, IL-7, and IL-8), chemokines (e.g., MCP-2 and MIP-3a), growth factors (e.g., GRO, HGF, and IGFBPs), cell surface receptors (e.g., ICAMs, uPAR, and TNF receptors), matrix metalloproteinases, and survival factors (Acosta et al., 2008; Acosta et al., 2013; Basisty et al., 2020). In replicative senescent MSCs, there is a significant increase in the levels of SASPs-associated proteins IL-6, IL-8, and MCP-1, with IL-6 showing the highest increase. The development of senescence in MSCs is attributed to enhanced autophagic activity (Bernard et al., 2020), which is closely linked to the upregulation of FOX3a levels and subsequent increase in IL-6 and IL-8 expression (Zheng et al., 2023). However, other SASPs-related proteins such as MIP-1α, MMP-2, MMP-3, IL-1α, and IL-1β were not found to be altered in association with senescence based on relevant studies (Marote et al., 2023).

Researchers have discovered that SASPs promote senescence in MSCs by suppressing B cell-specific Moloney murine leukemia virus Integration site 1 (Bmi-1). The expression of Bmi-1 was found to be downregulated in the senescence environment and reducing Bmi-1 levels decreased the proliferation rate of MSCs. Among the various standard components of SASPs that were tested and compared, IL-1α showed the highest impact on downregulating Bmi-1 (Zheng et al., 2021).

When investigating ways to mitigate senescence in MSCs caused by SASPs, researchers discovered that WNT/β-catenin signaling inhibits the paracrine effects of SASPs. Additionally, Wnt3a was found to have a positive effect on cell proliferation. Furthermore, it was observed that the combination of SASPs inhibitory factors FGF2 and Wnt3a may have a more significant anti-senescent effect (Lehmann et al., 2022). Moreover, in radiation-induced senescent cells, the levels of SASPs factors such as IL-1α, IL-6, MMP-3, resistin, lipocalin, and IGFBP-6 were significantly increased. These factors disrupted the colony-forming ability and multidirectional differentiation of BMSCs through paracrine effects. However, the adverse effects were alleviated when JAK1 inhibitors were used (Xu et al., 2021) (Figure 1).

3 Mechanisms of mesenchymal stem cell aging

According to Al-Azab M et al. (Al-Azab et al., 2022), the five main hallmarks of MSC senescence are damage to genetic material, non-coding RNA and exosomes, loss of protein homeostasis, intracellular signaling pathways, and mitochondrial dysfunction. In this section, we will summarize the relevant research progress.

3.1 Damage to genetic material

Damage to genetic material can occur through telomere shortening, DNA damage, and epigenetic alterations.

3.1.1 Shortened telomere

Telomeres, which are non-coding regions at the ends of chromosomes, consist of thousands of identical sequence repeats (Blackburn and Gail, 1978; Moyzis et al., 1988). During lagging strand synthesis, DNA polymerase is unable to fully replicate the 3′end of double-stranded DNA (Watson, 1972). Telomere depletion plays a role in regulating the senescence of MSCs through downstream signaling of the oncogene repressor protein p53 and inhibiting mitochondrial metabolic activity via the peroxisome proliferator-activated receptor gamma (PPARγ) coactivator 1α/β (PGC-1α/β) (Sui et al., 2016). MSCs obtained from telomerase knockout animals exhibit impaired replicative capacity and may even lose the ability to differentiate completely, even in early passages (Liu et al., 2004; Pignolo et al., 2008; Yang Y. K. et al., 2018). The average length of telomeres in MSCs is dependent on the age of the tissue donor in early-passage MSCs(Li et al., 2017). Previous research has indicated that the average length of telomeres in early cultures of MSCs ranges from 11–13 to 9–10 kb (Parsch et al., 2004; Bonab et al., 2006). Other studies have shown that during *in vitro* expansion, there is a rapid aging process, resulting in approximately 100 bp of telomere shortening every two passages. Senescence in MSCs is typically observed when the telomere length reaches 10 kb, although a different study reported a length of 6.8 ± 0.6 kb in senescent cells (Oja et al., 2018; Liu J. et al., 2020). The potential of using telomere length measurement as a biomarker in assessing the senescence of MSCs holds significant promise. Telomere shortening stands as one of the best-characterized mechanisms triggering cell senescence, and it can be expedited by the presence of oxidative stress (Jiang et al., 2023). The activation of the catalytic subunit of telomerase (known as hTERT) has been found to effectively impede the progression of senescence, resulting in a notable decrease in aneuploidy levels and the preservation of ploidy-controlling genes' regulation (Estrada et al., 2013). Hence, the close association between telomere length and MSC senescence implies that telomere-based examinations possess the potential to serve as valuable tools in diagnosing and managing cellular senescence (Bernadotte et al., 2016).

3.1.2 DNA damage

DNA damage can result in two outcomes. The first outcome involves the inaccurate repair of DNA damage, which can give rise to mutations or chromosomal aberrations, ultimately culminating in the development of cancer. The second outcome is persistent DNA damage that hinders replication and transcriptional processes, causing cellular dysfunction, cellular senescence, and apoptosis

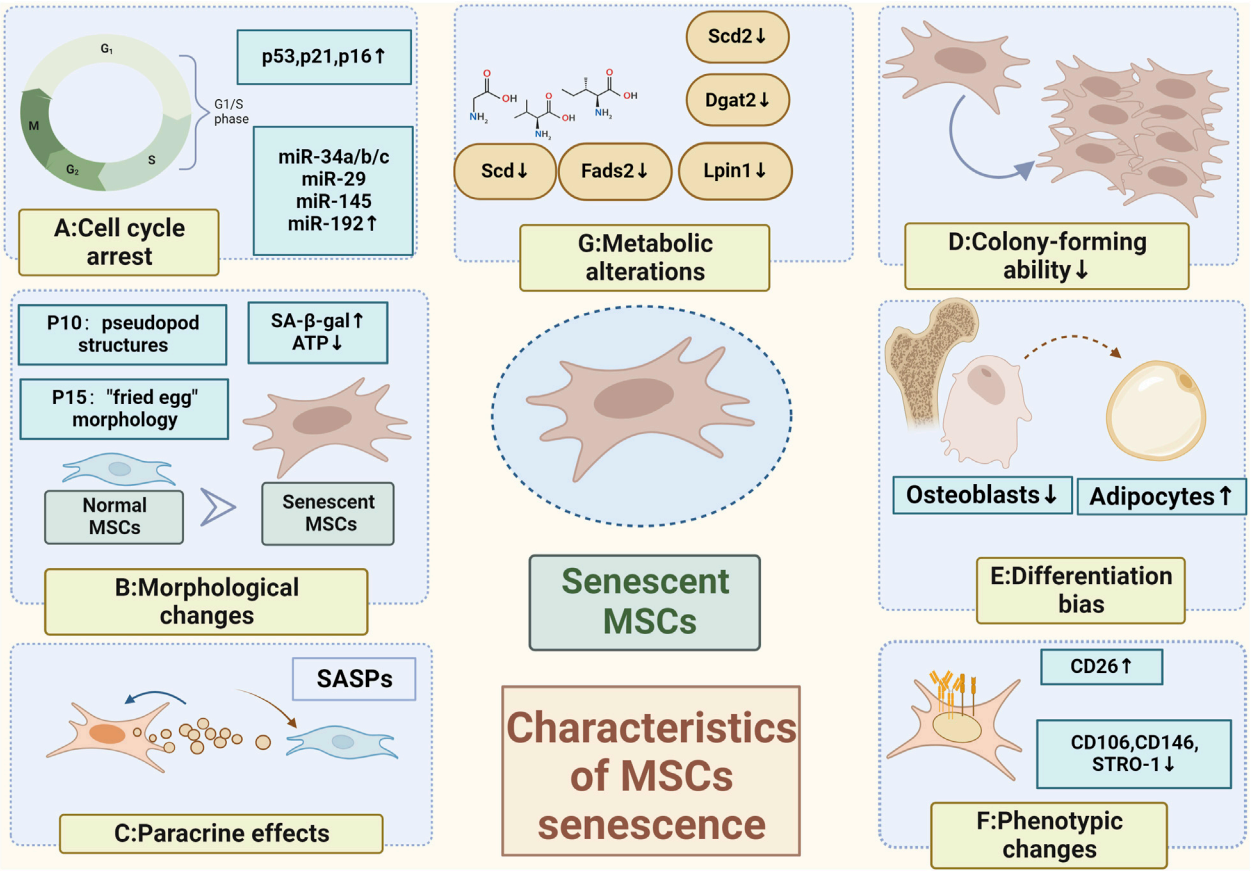

FIGURE 1
Characteristics of MSCs senescence **(A)** Cell cycle arrest caused by activation of the p53/p21CIP1 signaling pathway or the $p16^{INK4A/Rb}$ oncogenic pathway (Kamal et al., 2020); **(B)** Morphological changes with pseudopod structures appearing in the 10th generation and a "fried egg" morphology in the 15th generation (Truong et al., 2019); **(C)** Paracrine effects; **(D)** Loss of colony-forming abilities (Ridzuan et al., 2016); **(E)** Elevated osteogenic differentiation and a decreased lipogenic differentiation (Yi et al., 2021); **(F)** Phenotypic changes; **(G)** Metabolic alterations (Neutral amino acids such as valine, isoleucine, and glycine can be used as alternative energy sources to maintain energy homeostasis (Yi et al., 2020); Inhibited lipid metabolism (Yu Xiao et al., 2022)) (Created by Biorender. com).

(Ou and Schumacher, 2018; Banimohamad-Shotorbani et al., 2020). Among these outcomes, the accumulation of endogenous ROS plays a crucial role in DNA damage (Canli et al., 2017). As the number of passages increases, the accumulation of ROS and the aggravation of DNA damage can be observed in MSCs. Conversely, the expression of DNA repair-related proteins such as Ku70, Ku80, Rad 51, PAR, and 116 kDa PARP1 decreases with cell passages. The transcription factor PBX1 can mitigate ROS-mediated DNA damage and inhibit the senescence and apoptosis of MSCs(Wang Yuan et al., 2021). Consequently, comprehending the intricate molecular mechanisms driving MSC senescence is imperative to enhance the curative impact of MSCs and create viable approaches to impede or potentially revert the dysfunction of aged MSCs. This, in turn, holds promise for revitalizing individuals' holistic welfare and alleviating age-associated diseases (Weng et al., 2022).

3.1.3 Epigenetic alterations

The cellular senescence of MSCs is orchestrated by various epigenetic modifications, such as the organization of chromatin, posttranslational modifications of histones, DNA methylation, and the involvement of non-coding RNAs(Al Aboud et al., 2023; Sun et al., 2023). In a related study, it was discovered that 46 differentially regulated genes were identified in BMSCs from both young and senescent patients after undergoing *ex vivo* expansion. Out of these genes, 23 were found to be associated with selective shearing (Peffers et al., 2016). Other studies have also reported similar findings, indicating that selective shearing is a characteristic of aging in MSCs. Additionally, differences in methylation levels can influence selective shearing, as senescent MSCs exhibit high levels of hypomethylation or an overall loss of DNA methylation (Bork et al., 2010; Cakouros and Gronthos, 2020).

3.2 Non-coding RNA and exosomes

RNA serves as a transmitter of genetic information expression and plays a crucial role as a regulator. Small non-coding RNAs, which have diverse functions in cells, are involved in regulating important life processes such as growth and development, gene expression, genome stability, and cellular senescence. These small non-coding RNAs (SncRNAs) include various types, such as microRNAs (miRNAs), small nuclear RNAs (snRNAs), small nucleolar RNAs (snoRNAs),

P-element-induced wimpy testis (PIWI)-interacting RNAs (piRNAs), small interfering RNAs (siRNAs), transfer RNAs (tRNAs), and repeat-associated siRNAs (rasiRNAs). They function as epigenetic regulatory molecules in the regulation of cellular senescence in MSCs(Musavi et al., 2019; Wang S. et al., 2021).

BMSCs were amplified *ex vivo* and exhibited replicative senescence, as evidenced by increased SIRT1 mRNA expression and significantly increased SA-β-gal activity. Additionally, there were observed differences in gene expression of SncRNAs, including 203 miRNAs, 46 piRNAs, 63 snoRNAs, 12 snRNAs, and 7 rasiRNAs in p10 generation BMSCs compared to p1 generation BMSCs(Xiao et al., 2022).

miRNA is a crucial component of exosomes, which are a type of EVs that plays a dual role in anti-aging and senescence. It induces senescence when it is a part of SASPs, but resists senescence when secreted by young and healthy MSCs(Ahmadi and Rezaie, 2021). The imbalance between mitochondrial fusion and fission is closely related to cellular senescence. Liangge He et al. proposed that miR-311 derived from EVs could be an important indicator of senescence promotion for diagnosing inflammation and acute senescence in MSCs(He et al., 2023). Dynamin-related protein 1 (Drp1) mediates mitochondrial fission, resulting in the formation of small, round mitochondria. On the other hand, miR-155-5p derived from senescent MSCs induces mitochondrial fusion and drives normal MSCs into senescence by inhibiting the Cab39/AMPK signaling pathway. The senescence of MSCs can be alleviated by using miR-155-5p inhibitors, although this effect can be partially reversed by the Drp1 inhibitor Mdivi 1 (Hong et al., 2020). Furthermore, Nampt plays a key role in the regulation of natural and replicative senescence in MSCs through the inhibition of NAD-SIRT1 signaling (Ma et al., 2017). The expression of miR-34a increases in senescent MSCs and directly suppresses Nampt, thereby mediating the induction of MSC senescence (Pi et al., 2021).

3.3 Dysregulation of protein homeostasis

Protein homeostasis, the balance between protein synthesis and degradation, is regulated by a protein quality control system comprising molecular chaperones, ubiquitin proteasomes, and cellular autophagy. Additionally, the regulation of these signaling pathways involves mTOR pathways, Hippo signaling, and Rank signaling (Kapetanou Marianna et al., 2017). During aging, impairment of cellular function is closely associated with the imbalance of protein homeostasis, with the loss of proteasome function playing a central role in this process. Late-passing hMSCs exhibited senescence-associated proteasomal alterations, including reduced mRNA and protein expression of several characteristic proteasomal subunits (such as β1, β2, β5, α4, α7, and Rpt6), as well as decreased 26 S proteasome activity and increased 20 S proteasome activity (Chondrogianni et al., 2005; Kapetanou M. et al., 2017).

3.4 Mitochondrial dysfunction

Mitochondria in senescent cells undergo various changes, including altered metabolic function (Seok et al., 2020), increased production of ROS, higher mitochondrial mass, decreased membrane potential (Korolchuk et al., 2017), and subsequent acceleration of telomere shortening and DNA damage (Chapman et al., 2019).

Mitochondria function as the cell's energy factory, producing ATP and metabolic energy sources through oxidative phosphorylation (OXPHOS). However, the overproduction of ROS by complexes I and III of the respiratory chain can lead to cellular senescence in cases of mitochondrial failure (Ray et al., 2012). Mitochondrial autophagy plays a vital role in eliminating damaged or dysfunctional mitochondria. One example of its impact is the varying effect of H_2O_2 on mitochondrial autophagy, where prolonged exposure inhibits the process and leads to apoptosis in BMSCs. This inhibition is associated with the suppression of Jun N-terminal kinase (JNK), a member of the mitogen-activated protein kinase (MAPK) family (Fan et al., 2019). Another instance is the protective effect of curcumin (Cur) on cellular autophagy, which is essential for maintaining cellular homeostasis and controlling the senescence of MSCs (Deng et al., 2021).

3.5 Intracellular signaling pathways

3.5.1 IGF-1 pathway

Insulin-like growth factor 1 (IGF-1) plays a crucial role in processes such as growth and lipid metabolism. Previous research suggests that when IGF-1 binds to its receptor, it can alleviate senescence in MSCs. This effect is associated with the activation of the PI3K/Akt pathway (Tian et al., 2020). The phosphorylation of AKT and the high expression of SFRP2 further activate the Wnt/β-catenin pathway, which helps maintain the cellular proliferative capacity and metabolic functions of MSCs(Lin et al., 2020). Additionally, other studies have demonstrated that IGF-1 inhibits its downstream effector proteins (p70S6K and S6) through the Akt/mTOR pathway. This, in turn, increases cellular autophagy to prevent MSCs from undergoing apoptosis (Yang Ming et al., 2018).

3.5.2 mTOR pathway

Persistent activation of the growth-promoting mammalian target of rapamycin (mTOR) pathway has been shown to play a central role in cellular senescence and individual aging (Johnson et al., 2013). Inhibition of the mTOR pathway facilitates the delay of replicative senescence and the maintenance of cell stemness in MSCs(Antonioli et al., 2019). The protective mechanism mainly involves preventing the accumulation of intracellular ROS and DNA damage, as well as reducing the expression of senescence-associated inflammatory cytokines and genes (e.g., $p16^{INK4A}$). Increasing the level of cellular autophagy through selective inhibition of mTORC1 is an effective way to slow down MSC senescence. The combination of AMPK activator (5-aminoimidazole-4-carboxamide ribonucleotide, AICAR) and SIRT1 activator (nicotinamide, NAM) inhibits mTORC1 activity and delays MSC senescence. AICAR not only enhances the level of autophagy and maintains the morphological and proliferative capacity of MSCs but also preserves mitochondrial homeostasis through the activation of SIRT1 by AMPK, thereby reducing ROS and increasing the level of the anti-apoptotic gene Bcl-2 (Khorraminejad-Shirazi et al., 2020).

There are three Hedgehog proteins in mammals: sonic hedgehog (Shh), Indian hedgehog (Ihh), and desert hedgehog (Dhh). These proteins are highly conserved across evolution and species and have significant roles in the development of

skeletal tissue (Briscoe Therond, 2013). In a separate study investigating the impact on cell cycle pathways in MSCs, Al-Azab et al. (Al-Azab et al., 2020) discovered that the Ihh, hinders the progression of the ROS/PI3K/Akt/NF-B/mTOR/4EBP1-p70S6K pathway. Furthermore, the study revealed that when Ihh expression is suppressed, the cell cycle of MSCs is arrested and then enters a state of senescence.

3.5.3 AMPK pathway

AMP-activated protein kinase (AMPK) is a crucial regulator of cellular and organismal energy metabolism. Its activation depends on the energy status and the activity of upstream stimulatory and inhibitory signaling pathways. However, with aging, AMPK's reactivity declines, and its regulatory capacity diminishes (Salminen et al., 2016). FGF21, on the other hand, can regulate mitochondrial survival by modulating AMPK activation. This regulation involves increasing protein levels of p-AMPK and p-Drp1, reducing intracellular ROS levels, and delaying senescence in BMSCs (Li et al., 2019). Resveratrol also promotes osteogenic differentiation and delays aging in BMSCs through the AMPK/ROS signaling pathway (Zhou et al., 2019).

3.5.4 NF-κB pathway

The NF-kB family consists of five transcription factors (p50, p52, p65, c-REL, and ReIB) that are closely associated with immune and inflammatory responses (Kim et al., 2019). Numerous data indicate a strong correlation between p65, SASPs, and their paracrine effects. Similar levels of p65, IL-6, and IL-8 were observed in both DNA damage-induced MSCs senescence (DDIS) and treatment-induced senescence (TIS), as well as in a pro-inflammatory activation (PA) model in MSCs using TNF-α. This suggests that p65 pathway activation occurs during cellular senescence and pro-inflammatory activation in MSCs. Additionally, p65 can enhance the release of small extracellular vesicles (sEV) by MSCs, which in turn promotes peripheral cellular aging through a paracrine pathway (Banimohamad-Shotorbani et al., 2020; Mato-Basalo et al., 2021).

3.5.5 Sirtuins pathway

Sirtuins, a family of NAD-dependent deacetylases, consist of seven members known as SIRT1–7. These sirtuins have shown high conservation throughout evolution (Almeida and Porter, 2019). They play crucial roles in various cellular activities such as cellular autophagy, metabolism, DNA repair, apoptosis, and cellular senescence. Among them, SIRT1 is a significant target for extending lifespan and delaying senescence as it integrates multiple signaling and transcriptional pathways. Some of the known pathways involved in this process include the p65-NF-κB pathway, the p53-DNA damage pathway, the mTOR-cellular autophagy pathway, the AMPK pathway, the FOXO-DNA damage and oxidative stress pathway, and the PGC1α-mitochondrial autophagy pathway (Chen Cui et al., 2020). SIRT3, a mitochondrial sirtuin, is involved in various metabolic regulations. Studies have shown that SIRT3 upregulates the expression and activity of superoxide dismutase 2 (SOD2), which helps inhibit premature senescence in MSCs induced by natural and oxidative stress (Ma et al., 2020). On the other hand, senescent MSCs exhibit downregulation of the NAD/SIRT3 signaling pathway. To counteract this, supplementation with nicotinamide mononucleotide (NMN), a precursor of NAD, can upregulate the NAD/SIRT3 signaling pathway in replicative senescent MSCs. This supplementation improves mitochondrial function and rescues MSCs from senescence (Wang Huan et al., 2022).

4 Effects of different cellular microenvironments on MSCs' senescence and functions

4.1 Aging microenvironment

The senescent microenvironment is defined by several key features: impaired fibroblast function, an accumulation of senescent fibroblasts, disruption of the extracellular matrix's integrity, and the initiation of age-related chronic inflammation (Fane and Weeraratna, 2020; Wang X. et al., 2022; Ye et al., 2023).

The SASPs play a crucial role in the formation of the senescent microenvironment. While senescent cells and SASPs can have temporary beneficial effects, such as improving the regeneration and stemness of keratin-forming cells through brief exposure to SASPs, they can become problematic as the body ages. Senescent cells tend to accumulate in the body tissues and cause harm to the organism (Ritschka et al., 2017). Research has demonstrated that the existence of SASPs is linked to the emergence of degenerative diseases and cancer. Furthermore, SASPs contribute to chronic inflammation and hinder tissue repair functions. Another detrimental effect of SASPs is their paracrine influence, wherein neighboring cells are transformed into senescent cells through paracrine action (Xu et al., 2018; Al Suraih et al., 2020; Kowald et al., 2020). Eliminating senescent cells can decrease the production of SASPs, leading to a better prognosis for geriatric syndromes and aging-related diseases, as well as an enhanced organism repair capacity (Pignolo et al., 2020).

Extracellular vesicles (EVs) are significant components of the senescence microenvironment (Yin Y. et al., 2021). Mesenchymal stem cell-derived extracellular vesicles (MSC-EVs) are considered a promising therapeutic tool for immunomodulation and regeneration. These vesicles, which are nano-sized and enclosed by a membrane, contain important biomolecules such as mRNAs, microRNAs, bioactive lipids, and signaling proteins (Massa et al., 2020). The advantages of MSC-EVs over MSCs include a higher safety profile, lower immunogenicity, and the ability to traverse biological barriers (Varderidou-Minasian et al., 2020). Furthermore, the use of MSC-EVs helps avoid complications associated with stem cell-induced ectopic tumor formation, entrapment in lung microvasculature, and immune rejection. However, there are still challenges and barriers to the clinical translation of MSC-EVs, such as quality control and efficiency (Huang et al., 2019b; Weng et al., 2021). Additionally, as part of SASPs, MSC-EVs play a crucial role in promoting cellular senescence due to their paracrine effect and messaging function (Sun Zixuan et al., 2022). It is worth investigating further whether senescent MSC-EVs may have different effects depending on the tissue, age, or context (such as inflammation or disease). EVs derived from aged myoblasts have been discovered to induce senescence in primary BMSCs in an *ex vivo* setting (Jiang et al., 2023). Furthermore, studies have demonstrated that both circulating and tissue-derived aged EVs can induce senescence in MSCs cultured *ex vivo* (Weilner et al., 2016; Davis et al., 2017).

MSC therapies have shown promising prospects for applications in cellular and animal experiments. However, the current clinical outcomes are not satisfactory. Some scholars speculate that the age of the patient may contribute to this situation (Figure 2). This is

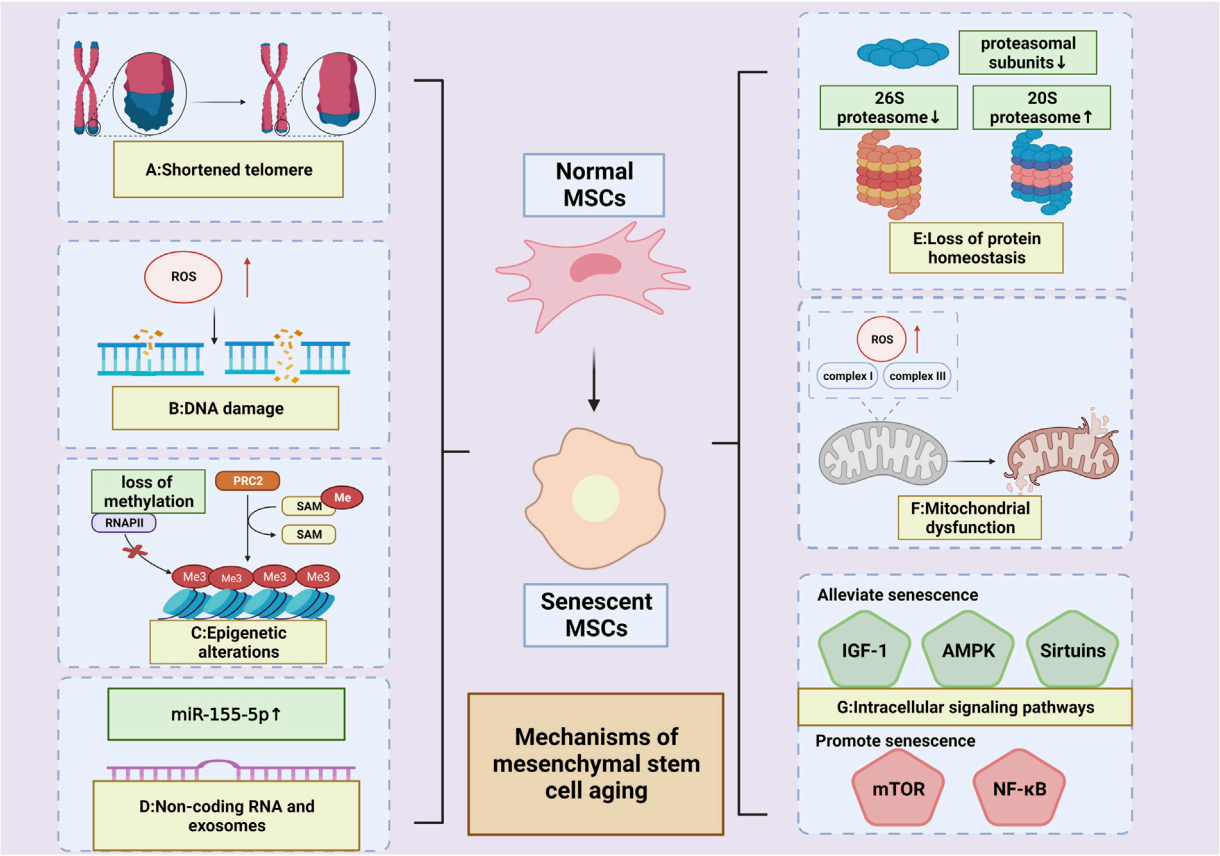

FIGURE 2
Mechanisms of MSCs' aging. **(A)** Shortened telomere; **(B)** DNA damage; **(C):** Epigenetic alterations (High levels of hypomethylation or an overall loss of DNA methylation (Cakouros et al., 2020; Bork et al., 2010)); **(D)**: Non-coding RNA and exosomes (Upregulated miR-155-5p (Hong et al., 2020)) **(E)** Loss of protein homeostasis (reduced proteasomal subunits; decreased 26 S proteasome activity; increased 20 S proteasome activity (Chondrogianni et al., 2005; Kapetanou M. et al., 2017)); **(F)**:Mitochondrial dysfunction (overproduction of ROS by complexes I and III of the respiratory chain (Ray et al., 2012));**(G)**: Intracellular signaling pathways (pathways alleviating senescence: IGF-1,AMPK&SIRT;pathways promoting senescence: mTOR&NF-κB). (Created by Biorender. com).

because, while most cell and animal experiments involve young individuals as donors and patients, in clinical practice, the elderly are the primary recipients of MSCs treatment. (Chen Huan et al., 2022).

With aging, elderly individuals often experience a chronic, low level of subclinical proinflammatory state (Chung et al., 2011; Lin et al., 2017). This is characterized by an increase in the expression of proinflammatory cytokines and chemokines in their serum. Specifically, the proinflammatory cytokine IL-6 shows a noticeable increase, while the anti-inflammatory cytokine IL-10 decreases significantly. The elevated levels of IL-6 trigger the activation of JAK/STAT and MAPK pathways, which further contribute to the aging of MSCs (Peng et al., 2022). Additionally, studies have shown that MSCs cultured in the extracellular matrices (ECM) of elderly individuals also exhibit reduced proliferation potential of BMSCs. This impairment is closely associated with a decrease in Cyr61/CCN1. However, the exogenous addition of Cyr61 has been found to help restore the ECM's response to IGF-1 signal (Marinkovic et al., 2022).

In addition to the aging of the treated patients themselves, the extraction of MSCs from aged individuals with premature aging properties significantly reduces the efficacy of the treatment. (Yamaguchi et al., 2018).

MSCs derived from aged individuals typically display the following characteristics: an elevated number of senescent cells, heightened expression of senescent genes and proteins (such as p21 and γH2AX), increased SA-β-gal activity, and reduced capacity for osteogenic, lipogenic, and angiogenic differentiation (Liu et al., 2017; Chen Xihang et al., 2021). The senescent microenvironment promotes premature aging and impairs the differentiation ability of MSCs through several mechanisms. These include upregulation of CD137 expression, inhibition of Bcl-3 expression (Wang F. X. et al., 2022), and disruption of Wnt/β-catenin signaling pathway transmission (Han et al., 2022).

BMSCs derived from aged individuals displayed impaired cell migration function and downregulation of genes involved in cell motility, such as DPP4, Egf, Actn3, Rho, Cav1, *etc.* Additionally, the reduced number of $CD90^{+}$ BMSCs was associated with impaired wound healing ability (Amini-Nik et al., 2022).

Metabolic dysfunction of BMSCs was found to be positively correlated with senescence. In BMSCs from senescent mice, the

expression levels of critical enzymes for mitochondrial genesis and glycolysis were reduced, resulting in impaired oxidative phosphorylation and glycolytic function. Consequently, this affected the stemness and differentiation potential of BMSCs(Li et al., 2022).

The adverse effects of MSCs from aged individuals during treatment are linked to their impaired macrophage recruitment. This impairment is attributed to altered expression of miRNAs that regulate this process. Specifically, miR-223-5p expression is downregulated, while miR-127-3p and miR-125b-5p expression are increased (Huang et al., 2019a).

The presence of a senescent microenvironment leads to chronic inflammation, which in turn significantly reduces the number and function of MSCs (Brunet et al., 2023). In the field of regenerative medicine, senotherapy research is currently focused on interventions that target the MSCs microenvironment and senescent stem cells during *in vitro* expansion. This research includes studying senolytics and senomorphic mechanisms and targets, exploring optimal therapeutic doses and routes of administration, as well as selecting and applying specific drugs (Wong et al., 2023) (Figure 3).

4.2 Hypoxic/ischemic microenvironment

In vivo, MSCs are commonly exposed to physiological conditions, encompassing oxygen concentrations that span from 2% to 8%.The oxygen levels typically observed in culture, around 18.4% O2, can be deemed as severely hyperoxia for MSCs when compared to their original niches (Phelps et al., 2023). Previous studies have examined the impact of hypoxic microenvironments on the senescence of MSCs, categorizing them into two groups: 'physiological hypoxia', which supports MSC survival (Buravkova et al., 2014), and 'pathological hypoxia', which accelerates senescence and apoptosis of MSCs. It is worth noting that the pathological hypoxic microenvironment is often accompanied by a lack of blood perfusion, further compromising cell survival.

Hypoxic preconditioning typically involves incubation at (1%–5%) O_2 for 48 h or 72 h, as compared to physiological conditions (21% O_2). Existing studies collectively indicate that hypoxic preconditioning effectively reverses the senescent state of MSCs primarily by modulating the cellular autophagy axis and enhancing intracellular ROS levels. Hypoxia preconditioning increased the expression level of HIF-1α in BMSCs, thereby enhancing cell viability and reducing the

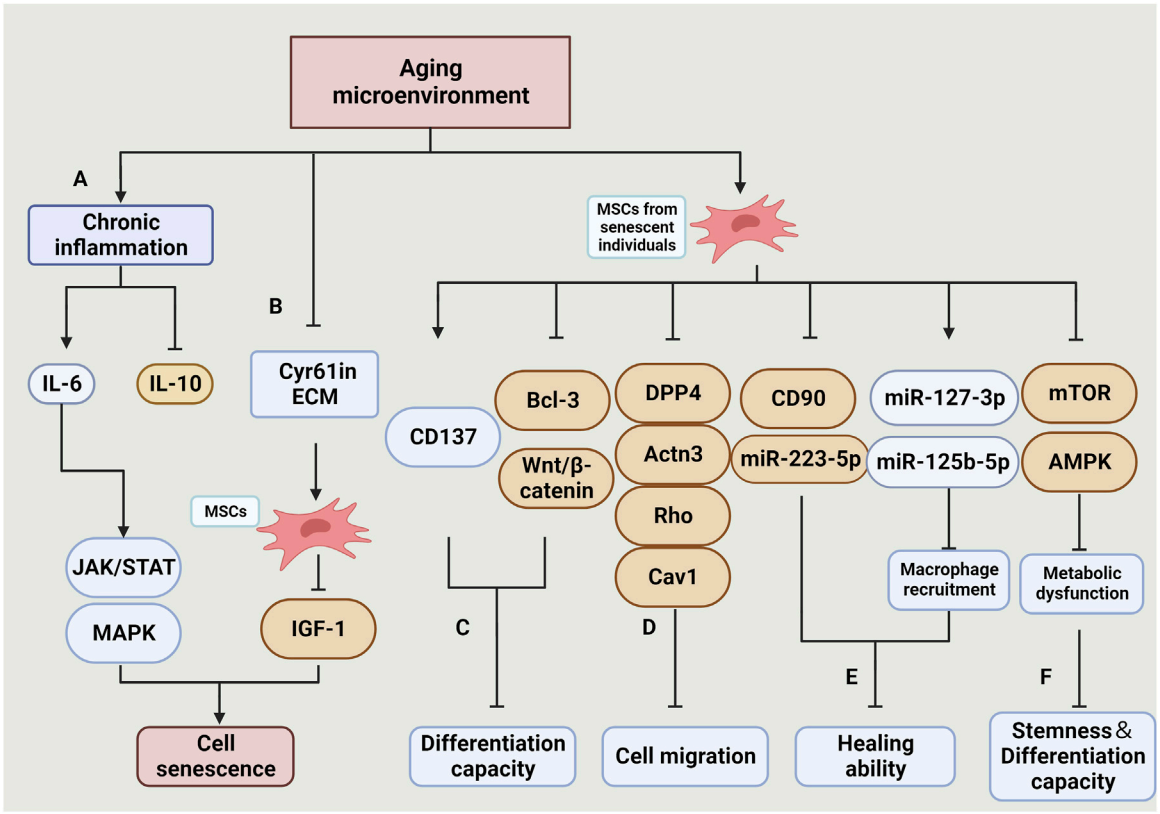

FIGURE 3
Effects and mechanisms of the aging microenvironment on MSCs. **(A)**: Chronic inflammation in the aging microenvironment results in an increase in pro-inflammatory factors, primarily IL-6, and a decrease in anti-inflammatory factors, primarily IL-10. The elevated IL-6 activates the JAK/STAT and MAPK signaling pathways, ultimately leading to the senescence of MSCs (Peng et al., 2022). **(B)**: Reduction of Cyr61 in ECM decreases the sensitivity of MSCs to IGF-1 signalling, thereby increasing their vulnerability to senescence (Marinkovic et al., 2022). **(C):**MSCs derived from senescent individuals exhibit impaired differentiation capacity in culture. This is primarily attributed to increased CD137 expression, decreased Bcl-3 expression, and inhibition of the Wnt/β-catenin pathway (Wang F. X. et al., 2022) (Han et al., 2022). **(D)**: The reduction in expression of DPP4, Actn3, Rho, Cav1, and other related genes is associated with impaired cell migration (Amini-Nik et al., 2022). **(E)**: The impaired therapeutic efficacy of MSCs is linked to the increased expression of CD90 and miR-223-5p, as well as the impaired recruitment of macrophages due to the decreased expression of miR-127-3p and miR-125b-5p (Huang et al., 2019a). **(F)**: Inhibition of the mTOR and AMPK signaling pathways results in impaired cellular metabolic function, ultimately leading to senescence in MSCs(Li et al., 2022). (Created by Biorender. com).

expression of the apoptotic protein caspase3, which leads to an increase in the transplantation viability of BMSCs under oxidative stress conditions (Luo et al., 2019). The improved survival rate of BMSCs after hypoxic pretreatment was attributed to the upregulation of survival-related genes LPL, PKM, and MAP3K13(Peck et al., 2021). According to Kim et al. (Kim et al., 2019) their study revealed that AIMP3 plays a crucial role in delaying the senescence of MSCs under hypoxic conditions. They also found that overexpression of AIMP3 inhibits cellular autophagy, which leads to senescence and dysfunction of MSCs. Additionally, the hypoxic microenvironment enhances the angiogenic capacity of BMSCs by increasing the expression of VEGF, a factor downstream of HIF-1α. Furthermore, BMSCs exhibit increased expression of osteogenic-related genes (RUNX2 and OCN) and enhanced potential for osteogenic differentiation (Zhang et al., 2018). Liu et al. (Liu Wei et al., 2020) discovered that culturing BMSCs under hypoxic conditions resulted in the increased release and secretion of exosomes and exosome-related proteins (TSG101, CD9, CD63, and CD81). Furthermore, they found that MSC-EVs under hypoxic conditions could effectively deliver miR-216a-5p to microglia. This delivery triggered a cascade reaction involving TLR4/NF-κB/PI3K/AKT, leading to the conversion of microglia from M1 to M2 type and subsequently reducing the associated inflammatory damage.

In contrast to the appropriate physiological hypoxic microenvironment described above, a pathological hypoxic (and ischaemic) microenvironment would undoubtedly lead to premature senescence and apoptosis of MSCs.

Systemic chronic hypoxia is a pathological state characterized by insufficient systemic oxygen supply. It is closely linked to conditions such as cyanotic congenital heart disease (CCHD), chronic obstructive pulmonary disease, chronic mountainous disease, and the development of pulmonary fibrosis. (Xing et al., 2018). Rehman SU et al. (Rehman et al., 2017) utilized patients with CCHD as a human disease model of chronic systemic hypoxia to investigate the conditions and the role of BM in association with gut microbes, and its effect on BMSCs aging. The study revealed an association between this phenomenon and an imbalance in intestinal ecology and the metabolism of d-galactose by the intestinal microbiota. Cellular senescence could be induced by d-galactose through the production of large amounts of ROS. Additionally, a negative correlation was observed between the concentration of d-galactose and the number of lactobacilli in the intestine. Upon administering appropriate amounts of *Lactobacillus*, the accumulation of d-galactose in rats was reduced, and the deficiency of BMSCs was significantly restored.

While stem cell transplantation has been shown to aid in cardiomyocyte repair following acute myocardial infarction (AMI) (Miao et al., 2017), it is important to note that the survival and differentiation of MSCs can be influenced by the local microenvironment. In particular, the ischemic and hypoxic microenvironment resulting from AMI can lead to a low survival rate of MSCs post-transplantation (Khodayari et al., 2019). Qi Y et al. (Qi et al., 2021) investigated the impact of hypoxic and serum deprivation (H/SD) conditions on the microenvironment of acute myocardial infarction (AMI). They observed that under H/SD conditions, the viability and migration of BMSCs were reduced compared to the normal control group. They also found an increase in apoptotic cells and the expression of apoptosis-related proteins Bax and cleaved-caspase3. This effect was attributed to the increased presence of M1-type macrophages and the upregulation of M1-type macrophage factors TNF-α and IL-1 in the H/SD condition. The secretion of TNF-α and IL-1 further increased, and M1-type macrophage exosomes inhibited the expression of Bcl-2 protein and induced apoptosis in BMSCs through miR-222. Moreover, BMSCs cultured in hypoxic ischemic (HI) environments exhibited reduced cell migration capacity compared to the normal controls. These cells also showed impaired cell proliferation, possibly due to the inhibition of the PI3K/AKT pathway (Chen Xuxiang et al., 2022).

Ischemia/reperfusion (I/R) injury is a significant contributor to tissue dysfunction, which often leads to organ transplant failure. When blood flow is interrupted, the kidney experiences hypoxia, increased oxidative stress, and microvascular dysfunction (Soares et al., 2019). Additionally, I/R kidney tissue shows elevated levels of ROS and reduced expression of VEGF in MSCs(Bai et al., 2018; Najafi et al., 2022).

In the context of the pathological hypoxic and/or ischaemic microenvironment, there are two primary mechanisms through which it negatively affects MSCs. Firstly, it regulates the cellular metabolic capacity. Secondly, it exposes the cells to pro-inflammatory factors such as TNF-α, IL-1β, and IL-6 for an extended period. This prolonged exposure to pro-inflammatory factors leads to apoptosis, necrosis, and autophagic cascades (Venkatachalam et al., 2009; Oka et al., 2012). Future research could focus on exploring the targets of hypoxic preconditioning to enhance the survival of MSCs. Additionally, investigating the effects of combining hypoxic preconditioning with other drugs could be a potential direction for further study (Figure 4).

4.3 Microenvironment of immune diseases

Due to their immunomodulatory and tissue repair effects, MSCs are considered valuable tools for treating immune diseases (Yang et al., 2023). However, various studies have revealed that MSCs in the microenvironment of immune diseases undergo senescence-related alterations. These alterations include reduced cell proliferation capacity, increased expression of p53 and p16, elevated levels of ROS and DNA-damage-response (DDR), and impaired differentiation capacity. These changes are likely associated with the persistent pro-inflammatory microenvironment created by immune diseases. In the subsequent discussion, we will explore the effects and underlying mechanisms of different immunological diseases on MSC senescence and function.

4.3.1 Systemic lupus erythematosus (SLE)

SLE is a chronic autoimmune disease characterized by an imbalance in T cell ratios (Wieliczko and Matuszkiewicz, 2017). The progression of SLE is exacerbated by an imbalance between Follicular helper T cells (Tfh) and regulatory T cells (Treg) (Lee, 2018). Additionally, the pathogenesis of SLE involves a deficiency of the cytokine IL-2, which is a crucial growth and survival factor for Treg cells that play a vital role in controlling autoimmunity in SLE (Humrich and Tiemekasten, 2016). Chen X et al. (Chen Xinpeng et al., 2021)discovered increased levels of LncRNA H19 in the serum and BMSCs of SLE patients. This increased level inhibited the proliferation and migration of BMSCs and promoted their apoptosis. Furthermore, lncRNA H19 impaired the immune properties of BMSCs by reducing the expression level of IL-2, thus inhibiting the differentiation of Treg cells, and disrupting the balance

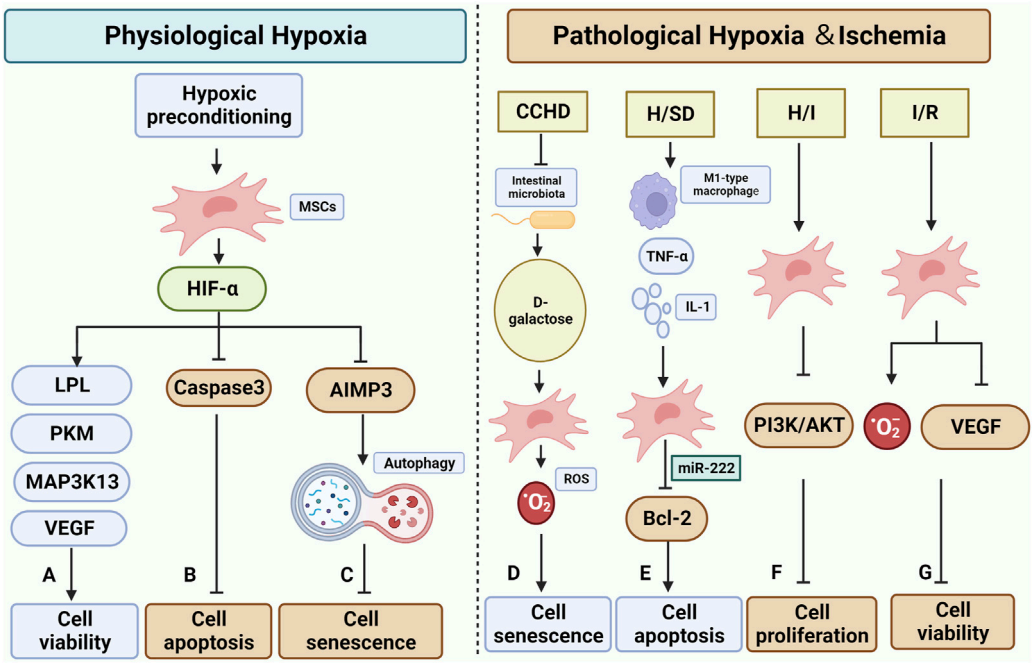

FIGURE 4
Effect and mechanisms of physiological and pathological hypoxic microenvironment on MSCs. **(A–C)** are the effects of normal physiological hypoxia on MSCs, mostly positive. Hypoxic preconditioning has been shown to impact the function of HIF-α in MSCs. **(A)** It increases cell survival by up-regulating the expression of LPL, PKM, MAP3K13, and VEGF(Peck et al., 2021) (Zhang et al., 2018). **(B)** It inhibits apoptosis by suppressing the expression of Caspase3(Luo et al., 2019). **(C)**: It inhibits the expression of AIMP3, which helps maintain cellular autophagy and consequently slows down cellular senescence (Zhang et al., 2018). D-G in the figure illustrate the impact of pathological hypoxic/ischemic microenvironment on MSCs. **(D)** Patients with CCHD undergo a reduction in Intestinal microbiota, leading to an increase in D-galactose. This increase in D-galactose can elevate the level of ROS in MSCs, contributing to cellular senescence (Rehman et al., 2017). **(E)** The H/SD microenvironment induces the increase of M1-type macrophage and the related regulatory factor TNF-α and IL-1, while decreasing the secretion of miR-222 from MSCs. This downregulates Bcl-2 and promotes apoptosis (Qi et al., 2021). **(F)** The H/I microenvironment hinders the PI3K/AKT pathway in MSCs, thereby suppressing cell proliferation (Chen Xuxiang et al., 2022). **(G)** MSCs in I/R encounter elevated ROS levels and downregulation of VEGF, resulting in decreased survival (Bai et al., 2018; Najafi et al., 2022) (Created by Biorender.com).

between Treg cells and Tfh cells. Immunomodulatory dysfunction in SLE-derived BMSCs is linked to the decrease in let-7f expressions. Research has shown that reduced expression of Let-7f leads to a decrease in the number of Th17 cells, an increase in the number of Treg cells, and an elevated rate of apoptosis in BMSCs. This effect is achieved through the activation of the STAT3 pathway by IL-6. (Geng et al., 2020).

In addition to altered immunomodulatory functions, hBMSCs derived from patients with SLE exhibited increased expression of genes related to SASP and pro-inflammatory cytokines. This upregulation was mediated by the MAVS-IFNβ axis and resulted in cellular senescence. The activation of the JAK-STAT signaling pathway in SLE-derived BMSCs was also found to be closely associated with premature cellular senescence (Gao and Bird, 2017; Ji et al., 2017). Furthermore, studies have demonstrated that the inflammatory factor HMGB1 in the SLE bone marrow microenvironment can induce senescence in MSCs through the TLR4/NF-κB signaling pathway. However, the HMGB1 inhibitor ethyl pyruvate (EP) can inhibit HMGB1 and improve lupus nephritis, leading to a reversal of senescence in MSCs (Ji et al., 2019).

4.3.2 Ankylosing spondylitis (AS)

AS is a common rheumatic disease that affects approximately 0.1%–0.5% of the global population (Ward et al., 2019). MSCs derived from AS patients exhibit an abnormally increased capacity for osteogenesis, leading to pathological osteogenesis and subsequent bone formation (Liu et al., 2019; Ye et al., 2019). The downregulation of Dickkopf-1 (DKK-1) expression, a crucial regulator of bone remodeling in spondyloarthropathies, is observed in MSCs from AS patients. This downregulation is believed to be caused by IL-17-mediated DKK-1 downregulation, resulting in the activation of the Wnt pathway and upregulation of osteogenesis-related genes (RUNX2, OSX, and ALP) (Daoussis et al., 2022).

The serum microenvironment of patients with AS exhibits abnormal levels of inflammatory factors (such as TNF-α and IL-17) and oxidative stress (Zeng et al., 2011). Among these factors, Advanced Oxidative Protein Products (AOPPs), which are markers of oxidative stress, are associated with disease activity and show a positive correlation. AOPPs can induce the production of ROS and lead to cell cycle arrest. Therefore, it is hypothesized that targeting AOPPs could be a key approach for treating AS-induced aging of MSCs(Karakoc et al., 2007; Sun et al., 2018; Ye et al., 2020).

4.3.3 Inflammatory bowel disease (IBD)

IBD is characterized by Crohn disease (CD) and ulcerative colitis (UC) (Chang, 2020). MSCs derived from CD are more

severely impaired in their ability to differentiate and cannot form cell colonies compared to MSCs derived from UC(Grim et al., 2021).

The senescence of MSCs is associated with the onset of inflammation in the lesion area. The presence of pro-inflammatory cytokines (such as INF-α, TNF-α, and IL-6) and paracrine effects lead to premature senescence of MSCs and hinder their differentiation into enterocytes. (Onyiah and Colgan, 2016; Wang et al., 2020). Currently, the low survival rate of stem cells is a pressing issue that needs to be addressed. Several approaches have shown promise in improving the success rate of treatment, including combining stem cell therapy with surgical treatment, orally delivering stem-cell-loaded hydrogel microcapsules (SC-HM), and utilizing EVs(Panés et al., 2018; Alpdundar Bulut et al., 2020; Kim et al., 2022).

4.3.4 Multiple sclerosis (MS)

MSCs derived from patients with multiple sclerosis (MS) exhibit impaired expansion in vitro culture, as well as accelerated rates of senescence and telomere loss. These changes are linked to a reduction in antioxidant capacity, as MS patient-derived MSCs demonstrate decreased secretion of the antioxidants superoxide dismutase 1 (SOD1) and glutathione S-transferase *p* (GSTP). Additionally, there is a decrease in the expression levels of Nrf2 and PGC1α, which regulate the secretion of SOD1 and GSTP. (Redondo et al., 2018b; Redondo et al., 2018c).

4.3.5 Neuromyelitis optica (NMO)

MSCs derived from NMO exhibit impaired proliferative capacity and increased susceptibility to senescence. This is accompanied by a significant upregulation of the pro-apoptosis-related gene Fas and a significant downregulation of the pro-survival gene Bcl-xl. Platelet-derived growth factor (PDGF) plays a crucial role in stimulating the proliferation of MSCs and has shown potential as a cytokine for treating demyelinating diseases. Specifically, PDGF-BB, the primary growth factor found in bone matrix (Chen et al., 2015), has been found to effectively enhance MSC proliferation and counteract premature senescence (Yang et al., 2019). Further research should investigate the specific target and conditions of PDGF-BB's action for potential therapeutic applications in MSC treatment.

4.3.6 Pulmonary fibrosis

BMSCs obtained from patients with idiopathic pulmonary fibrosis exhibit senescence characteristics, including reduced proliferation, trilineage differentiation, and migration capacity. These characteristics have been linked to the activation of the NADH-AMPK-p53 regulatory pathway, which results in mitochondrial dysfunction in BMSCs. Additionally, the paracrine effects of these cells induce premature senescence in lung fibroblasts. (Cardenes et al., 2018). The aforementioned study indicates that enhancing the secretory function of MSCs is a crucial aspect in the treatment of Pulmonary fibrosis conditions.

4.4 Hyperglycemic microenvironment

Hyperglycemia, oxidative stress, and altered immune responses are prominent features of the diabetic microenvironment. Previous studies have shown that these factors contribute to the senescence of MSCs. (Yin Min et al., 2021). hWJSCs obtained from pregnant women with gestational diabetes mellitus (GDM) exhibit impaired osteogenic and chondrogenic differentiation capacity. Additionally, these hWJSCs show downregulated levels of stemness markers, telomerase, antioxidant enzymes, and mitochondrial functional gene expression (ND2, TFAM, PGC1α, and NDUFB9). Moreover, there is an increase in cell cycle arrest-related factors (p16, p21, p27) and senescence-related gene p53 in these MSCs. It is worth noting that their lipogenic capacity remains unaffected (Kong et al., 2019).

The mechanism of hyperglycemia induced MSCs aging primarily involves a shift in the metabolic pattern of MSCs from glycolysis to oxidative phosphorylation. This shift leads to the excessive accumulation of ROS and DNA damage, activating the p53-p21-pRB axis (Wu, 2021). Consequently, telomerase is inactivated, and mitochondrial function is impaired. Additionally, the inhibition of mitochondrial biogenesis and related genes (PGC-1, SIRT-1, and NRF) occurs. Simultaneously, senescent MSCs in diabetic conditions can further enhance the senescence state by secreting SASPs, which convert normal cells in the surrounding environment into senescent cells. (Prattichizzo et al., 2018; Berlanga-Acosta et al., 2020).

Insulin application may contribute to the senescence of MSCs. Research has shown that insulin can induce senescence in BMSCs by inhibiting autophagy and upregulating the TGF-β1 pathway-related receptor II (TβRII). Furthermore, insulin also impairs the osteogenic differentiation capacity of BMSCs. (Zhang et al., 2020).

4.5 The obesity microenvironment

Obesity is a chronic, low-grade inflammatory state that contributes to bone loss and accelerates cellular aging. It is frequently linked to the onset of cardiovascular disease and other metabolic disorders (Li et al., 2020). In the obese microenvironment, MSCs exhibit various signs of early aging. The specific variations in aging-related manifestations of MSCs depend on intra-tissue signaling and the tissue source.

Alessio et al. conducted a study where they isolated MSCs from the body tissues of obese mice and compared them to MSCs derived from normal mice. The findings revealed several differences between the two groups. Firstly, the proliferation rate of MSCs from obese mice was reduced, as indicated by a lower percentage of S-phase cells. Additionally, there was an increased percentage of senescent cells in the obese mice. The expression of senescence-related genes RB21, p21, and p16 was found to be upregulated in MSCs from obese mice. Furthermore, the intracellular ROS levels were increased in these cells. Lastly, the DNA repair capacity of MSCs from obese mice was impaired (Alessio et al., 2020).

The senescence expression was more pronounced in white ADSCs than BMSCs, which could be attributed to the endocrine dysfunction associated with inflammation in white adipose tissue. Li Y et al. (Li et al., 2020) investigated the mechanism behind the altered senescence and differentiation ability of BMSCs caused by obesity. They discovered that by knocking down IL-6, the restoration of osteogenic function was facilitated, the lipogenic tendency of BMSCs was inhibited, and the senescence tendency caused by obesity was suppressed. These effects were potentially linked to the

TABLE 1 Effects of different microenvironments on the senescence of MSCs.

Microenvironment		Effect	Mechanism	Ref
Aging microenvironment		Cell senescence↑	JAK/STAT &MAPK↑	Peng et al. (2022)
		Cell senescence↑	SASPs; EVs	Ritschka et al., 2017; Sun et al., 2022b
			p21↑	Liu et al., 2017; Chen et al., 2021a
			γH2AX↑	
		Proliferative capacity↓	Cyr61in ECM↓	Marinkovic et al. (2022)
		Differentiation capacity↓	CD137↑	Han et al. (2022)
		Migration ability↓	DPP4, Egf, Actn3, Rho, Cav1↓	Amini-Nik et al. (2022)
Hypoxic/ischaemic microenvironment	Physiological hypoxic	Cell senescence↓	AIMP3↑	Buravkova et al., 2014; Kim et al., 2019
		Cell viability↑	HIF-1α↑	Luo et al. (2019)
			LPL, PKM, & MAP3K13↑	Peck et al. (2021)
		Angiogenic capacity↑	VEGF↑	Kim et al. (2019)
		Osteogenic differentiation↑	RUNX2 & OCN↑	Zhang et al. (2018)
	Pathological ischemic and hypoxic	Cell senescence↑	ROS↑	Rehman et al. (2017)
		Cell viability↓	Baxandcleaved-caspase3↑	Qi et al. (2021)
		Proliferative capacity↓	PI3K/AKT↓	Chen et al. (2022b)
Microenvironment of Immune diseases	SLE	Proliferative capacity↓	LncRNA H19↑	Chen et al. (2021b)
		Immunomodulatory dysfunction	let-7f↓	(Geng et al., 2020)
		Cell apoptosis↑	IL-6↑	
		Cell senescence↑	SASPs↑; JAK-STAT↑; HMGB1↑	Gao and Bird, 2017; Ji et al., 2017
	AS	Osteogenic differentiation↑	Dkk-1↓; RUNX2, OSX,& ALP↑	Daoussis et al. (2022)
		Cell senescence↑	AOPPs↑; ROS↑; p53, p21, & p16↑	Karakoc et al., 2007; Sun et al., 2018
	IBD	Cell senescence↑	p16↑; Paracrine effects	Onyiah and Colgan (2016), Wang et al., 2020
	MS	Cell senescence↑	Telomere loss; SOD1&GSTP↓	Redondo et al., 2018b; Redondo et al., 2018c
	NMO	Proliferative capacity↓ Cell senescence↑	Fas↑; Bcl-xl↓	Yang et al. (2019)
	Pulmonary fibrosis	Proliferative capacity↓ Differentiation capacity↓ Cell senescence↑	NADH-AMPK-p53↑	Cardenes et al. (2018)
Hyperglycemic microenvironment		Cell senescence↑	p16, p21, &p27↑; p53↑ Metabolic alteration (Oxidative phosphorylation↑; ROS↑; DNA damage↑	Kong et al., 2019; Yin et al., 2021a; Wu, 2021
		Osteogenic and chondrogenic differentiation ↓		Kong et al. (2019)
Obesity microenvironment		Proliferative capacity↓	RB21, p21, & p16↑; ROS↑; DNAdamage↑	Alessio et al. (2020)
		Cell senescence↑		
		Differentiation capacity↓	p53↑; Glucose metabolism↓	Chen et al. (2016)
		Lipogenic differentiation↑	PARG, FASN, IRS1↑	Tencerova et al. (2019)

(Continued on following page)

TABLE 1 (*Continued*) Effects of different microenvironments on the senescence of MSCs.

Microenvironment		Effect	Mechanism	Ref
Microenvironment of hematologic malignancies	AML&CML	Cell viability↓ Cell senescence↑	Oxidative Phosphorylation↑	Kim et al., 2015; Kumar et al., 2018
	LN	Cell senescence↑	p53↑; ROS↑; IL-6, IL-8, && CCL2↑	Vernot et al. (2017)
	MM	Osteogenic differentiation↓	DKK-1↑	Bereziat et al. (2019)
	tMN	Cell senescence↑ Lipogenic differentiation↓ Osteogenic differentiation↑ Metabolic alteration		Kutyna et al. (2022)
	MDS	Cell senescence↑ Proliferation capacity↓	S100A9↑; TLR4-NLRP3-IL-1β↑	Kim et al., 2012; Shi et al., 2019

inhibition of the IL-6/STAT3 pathway. In a separate study, Xiang QY's team (Xiang et al., 2020) explored the impact of postprandial triglyceride-rich lipoproteins (postprandial TRL) on the aging of ADSCs. They observed that the dose size and duration of application of postprandial TRL regulated the aging process of ADSCs. Furthermore, they identified the SIRT1/p53/Ac-p53/p21 pathway as the regulatory pathway for postprandial TRL-induced ADSCs.

However, the effects of obesity on MSCs metabolism and lipogenic differentiation have not been unanimously agreed upon by researchers. Differences in these results may be attributed to the origins of the MSCs. Chen JR et al. (Chen et al., 2016) isolated umbilical cord MSCs from obese pregnant women and found that these cells exhibited impaired lipogenic differentiation and osteogenesis, overexpression of p53, and lower levels of glucose metabolism (glycolysis and oxidative phosphorylation). Tencerova M et al. (Tencerova et al., 2019) discovered that BMSCs from obese patients showed increased expression of lipogenic differentiation genes (PPARG, FASN, IRS1). They also confirmed that activating insulin signaling reduced BMSCs' glycolytic efficiency, increased oxidative phosphorylation, and raised intracellular ROS levels, thus making the cells more prone to senescence.

4.6 Microenvironment of hematologic malignancies

The development of leukemic cells in the bone marrow (BM) can negatively impact the survival of MSCs in humans. Studies have shown that BMSCs derived from both acute myeloid leukemia (AML) and chronic myeloid leukemia (CML) sources exhibit senescence-related changes. (Kim et al., 2015; Kumar et al., 2018). Co-culturing MSCs with AML cells leads to a higher preference for oxidative phosphorylation over glycolysis in energy production. Additionally, the altered metabolic patterns observed in the leukemic disease are also linked to the worsening of the disease (Zhang Leisheng et al., 2021; Zhang Luwen et al., 2022). Bonilla X, Vanegas NP, et al. (Bonilla et al., 2019) developed an *in vitro* model called the leukemic ecotone (LN) model. They found that when induced with leukemic cells, MSCs exhibited senescence-related characteristics, such as increased SA-β-gal activity, elevated p53 expression, higher levels of intracellular ROS, and cell cycle arrest. Additionally, these MSCs showed increased secretion of pro-inflammatory factors IL-6, IL-8, and CCL2(Vernot et al., 2017). The researchers then compared LN-MSCs with MSCs derived from patients with B-lymphoblastic acute leukemia (B-ALL). They observed a similar tendency towards senescence, but these changes were reversible. Upon early removal of the leukemia cell effects, B-ALL-derived MSCs reversed senescence and re-entered the cell cycle (Vanegas et al., 2021). The differentiation ability of leukemic MSCs is still a subject of debate, with some researchers suggesting a tendency towards lipogenesis (Le et al., 2016; Azadniv et al., 2020). Furthermore, leukemic MSCs have been found to exhibit increased osteogenic capacity (Battula et al., 2017). The variations in these findings may be attributed to the specific type of leukemia and leukemic cell types involved.

Multiple myeloma (MM) is the second most common malignant hematological disorder, accounting for 13% of all malignant hematological disorders (Kumar et al., 2017). It is characterized by increased osteoclast activity and decreased osteoblast activity. The osteogenic differentiation capacity of bone BMSCs from MM patients is severely impaired in developing the lesion (Arnulf et al., 2007; Corre et al., 2007). The same is true for MM-derived ADSCs: while morphology, proliferation, and lipogenic differentiation capacity are similar to normal ADSCs, the osteogenic differentiation capacity is severely impaired, and SA-β-gal activity is increased. These functional changes may be related to DKK-1 expression (Bereziat et al., 2019).

Kutyna MM's team (Kutyna et al., 2022)investigated therapy-related myeloid neoplasm (tMN) patient-derived BMSCs and observed aging-related manifestations, including morphological changes, increased expression of aging genes, impaired DNA repair, and reduced lipogenic capacity. Interestingly, the osteogenic differentiation potential of these BMSCs was enhanced, and their energy metabolism tended to shift towards a glycolytic mode compared to normal BMSCs. In normal BMSCs, the mitochondrial OXPHOS: glycolytic ATP production rate was 64%:36%, whereas in tMN-derived BMSCs, it was only 31%:69%. Furthermore, tMN patient-derived BMSCs exhibited a more pronounced trend towards senescence compared to untreated myeloma patient-derived BMSCs, which could be attributed to DNA damage caused by cytotoxic treatment.

When MSCs derived from patients with myelodysplastic syndromes (MDS) are cultured in a laboratory setting, they show signs of senescence. This includes changes in cell shape, with cells becoming enlarged and flattened, as well as a decrease in their ability to divide. Additionally, there is an increase in the levels of a protein

TABLE 2 Typical clinical trials of MSCs.

Condition/Disease	NCT number	Study title	Phase	Sponsor
Healthy	NCT04313647	A Tolerance Clinical Study on Aerosol Inhalation of Mesenchymal Stem Cells Exosomes In Healthy Volunteers	Phase 1	Ruijin Hospital
	NCT01087996	The Percutaneous Stem Cell Injection Delivery Effects on Neomyogenesis Pilot Study (The POSEIDON-Pilot Study)	Phase1 Phase 2	University of Miami
Aging Frailty	NCT02065245	AllogeneiC Human Mesenchymal Stem Cells (hMSC) in Patients With Aging FRAilTy Via IntravenoUS Delivery	Phase1 Phase 2	Longeveron Inc
COVID-19	NCT04349631	A Clinical Trial to Determine the Safety and Efficacy of HB-adMSCs to Provide Protection Against COVID-19	Phase 2	Hope Biosciences Stem Cell Research Foundation
	NCT04362189	Efficacy and Safety Study of Allogeneic HB-adMSCs for the Treatment of COVID-19	Phase 2	Hope Biosciences Stem Cell Research Foundation
	NCT04348435	A Randomized, Double-Blind, Single Center, Efficacy and Safety Study of Allogeneic HB-adMSCs Against COVID-19	Phase 2	Hope Biosciences Stem Cell Research Foundation
	NCT04399889	hCT-MSCs for COVID-19 ARDS	Phase1 Phase 2	Joanne Kurtzberg, MD
	NCT04493242	Extracellular Vesicle Infusion Treatment for COVID-19 Associated ARDS	Phase 2	Direct Biologics, LLC
Acute Respiratory Distress Syndrome	NCT01775774	Human Mesenchymal Stem Cells For Acute Respiratory Distress Syndrome	Phase 1	Michael A. Matthay
	NCT04355728	Use of UC-MSCs for COVID-19 Patients	Phase1 Phase 2	Camillo Ricordi
Idiopathic Pulmonary Fibrosis	NCT01385644	A Study to Evaluate the Potential Role of Mesenchymal Stem Cells in the Treatment of Idiopathic Pulmonary Fibrosis	Phase 1	The Prince Charles Hospital
Bronchopulmonary Dysplasia	NCT03857841	A Safety Study of IV Stem Cell-derived Extracellular Vesicles (UNEX-42) in Preterm Neonates at High Risk for BPD	Phase 1	United Therapeutics
Ischemic Heart Failure	NCT02501811	Combination of Mesenchymal and C-kit + Cardiac Stem Cells as Regenerative Therapy for Heart Failure	Phase 2	The University of Texas Health Science Center, Houston
	NCT03925324	Serial Infusions of Allogeneic Mesenchymal Stem Cells in Cardiomyopathy Patients With Left Ventricular Assist Device	Phase 2	Medstar Health Research Institute
	NCT00768066	The Transendocardial Autologous Cells (hMSC or hBMC) in Ischemic Heart Failure Trial (TAC-HFT)	Phase1 Phase 2	University of Miami
	NCT00587990	Prospective Randomized Study of Mesenchymal Stem Cell Therapy in Patients Undergoing Cardiac Surgery (PROMETHEUS)	Phase1 Phase 2	Joshua M Hare
	NCT02013674	The Transendocardial Stem Cell Injection Delivery Effects on Neomyogenesis STudy (The TRIDENT Study)	Phase 2	Joshua M Hare
	NCT01781390	Safety Study of Allogeneic Mesenchymal Precursor Cell Infusion in Myocardial Infarction	Phase 2	Mesoblast, Inc
	NCT01270139	Plasmonic Nanophotothermal Therapy of Atherosclerosis	Not Applicable	Ural State Medical University
	NCT00927784	Effect of Intramyocardial Injection of Mesenchymal Precursor Cells on Heart Function in People Receiving an LVAD	Phase 2	Icahn School of Medicine at Mount Sinai

(Continued on following page)

TABLE 2 (*Continued*) Typical clinical trials of MSCs.

Condition/Disease	NCT number	Study title	Phase	Sponsor
Non-ischemic Heart Failure	NCT01392625	PercutaneOus StEm Cell Injection Delivery Effects On Neomyogenesis in Dilated CardioMyopathy (The POSEIDON-DCM Study)	Phase1 Phase 2	Joshua M Hare
	NCT02467387	A Study to Assess the Effect of Intravenous Dose of (aMBMC) to Subjects With Non-ischemic Heart Failure	Phase 2	CardioCell LLC
Cairdiomyopathy Due to Anthracyclines	NCT02509156	Stem Cell Injection in Cancer Survivors	Phase1	The University of Texas Health Science Center, Houston
Tendon Injury	NCT02298023	Treatment of Tendon Injury Using Allogenic Adipose-derived Mesenchymal Stem Cells (Rotator Cuff Tear)	Phase 2	Seoul National University Hospital
Focal articular cartilage lesions of the knee	NCT02037204	IMPACT: Safety and Feasibility of a Single-stage Procedure for Focal Cartilage Lesions of the Knee	Phase1 Phase 2	UMC Utrecht
Spinal Cord Injury	NCT02481440	Repeated Subarachnoid Administrations of hUC-MSCs in Treating SCI	Phase1 Phase 2	Limin Rong
	NCT01909154	Safety Study of Local Administration of Autologous Bone Marrow Stromal Cells in Chronic Paraplegia	Phase 1	Puerta de Hierro University Hospital
Osteoarthritis	NCT01586312	Treatment of Knee Osteoarthritis With Allogenic Mesenchymal Stem Cells	Phase1 Phase 2	Red de Terapia Celular
	NCT02958267	Investigation of Mesenchymal Stem Cell Therapy for the Treatment of Osteoarthritis of the Knee	Phase 2	OhioHealth
	NCT01183728	Treatment of Knee Osteoarthritis With Autologous Mesenchymal Stem Cells	Phase1 Phase 2	Red de Terapia Celular
	NCT02674399	A Phase 2 Study to Evaluate the Efficacy and Safety of JointStem in Treatment of Osteoarthritis	Phase 2	Nature Cell Co. Ltd
Rheumatoid Arthritis	NCT03691909	Phase 1/2a Clinical Trial to Assess the Safety of HB-adMSCs for the Treatment of Rheumatoid Arthritis	Phase1 Phase 2	Hope Biosciences
Degeneration Articular Cartilage Knee	NCT01733186	Evaluation of Safety and Exploratory Efficacy of CARTISTEM? a Cell Therapy Product for Articular Cartilage Defects	Phase1 Phase 2	Medipost Co. Ltd
Multiple Sclerosis, Chronic Progressive	NCT03799718	Safety and Efficacy of Repeated Administration of NurOwn (MSC-NTF Cells) in Participants With Progressive MS	Phase 2	Brainstorm-Cell Therapeutics
Xerostomia	NCT02513238	Mesenchymal Stemcells for Radiation Induced Xerostomia	Phase 2	Rigshospitalet, Denmark
Cystic Fibrosis	NCT02866721	Safety and Tolerability Study of Allogeneic Mesenchymal Stem Cell Infusion in Adults With Cystic Fibrosis	Phase1	University Hospitals Cleveland Medical Center
Acute Graft Versus Host Disease	NCT02379442	Early Treatment of Acute Graft Versus Host Disease With Bone Marrow-Derived Mesenchymal Stem Cells and Corticosteroids	Phase1 Phase 2	National Heart, Lung, and Blood Institute (NHLBI)
Diabetes Mellitus	NCT02886884	Allogeneic Mesenchymal Human Stem Cells Infusion Therapy for Endothelial DySfunctiOn in Diabetic Subjects	Phase1 Phase 2	Joshua M Hare
	NCT02387749	Effect Of Mesenchymal Stem Cells Transfusion on the Diabetic Peripheral Neuropathy Patients	Not Applicable	Cairo University

(Continued on following page)

TABLE 2 (*Continued*) Typical clinical trials of MSCs.

Condition/Disease	NCT number	Study title	Phase	Sponsor
Metabolic Syndrome	NCT03059355	Infusion of Umbilical Cord Versus Bone Marrow Derived Mesenchymal Stem Cells to Evaluate Cytokine Suppression	Phase1 Phase 2	Joshua M Hare
Breast Reconstruction	NCT01771913	Immunophenotyping of Fresh Stromal Vascular Fraction From Adipose Derived Stem Cells (ADSC) Enriched Fat Grafts	Phase 2	University of Sao Paulo
Alzheimer Disease	NCT03117738	A Study to Evaluate the Safety and Efficacy of AstroStem in Treatment of Alzheimer's Disease	Phase1 Phase 2	Nature Cell Co. Ltd
Cerebral Palsy	NCT03473301	A Study of UCB and MSCs in Children With CP: ACCeNT-CP	Phase1 Phase 2	Joanne Kurtzberg, MD
Cleft Lip and Palate	NCT01932164	Use of Mesenchymal Stem Cells for Alveolar Bone Tissue Engineering for Cleft Lip and Palate Patients	Not Applicable	Hospital Sirio-Libanes
Dental Pulp Regeneration	NCT03102879	Encapsulated Mesenchymal Stem Cells for Dental Pulp Regeneration	Not Applicable	Universidad de los Andes, Chile
Retinal Degeneration	NCT02330978	Intravitreal Mesenchymal Stem Cell Transplantation in Advanced Glaucoma	Phase 1	University of Sao Paulo
Malignant Melanoma	NCT02331134	Tissue and Hematopoietic/Mesenchymal Stem Cell for Humanized Xenograft Studies in Melanoma and Squamous Head and Neck Cancer	Not Applicable	University of Colorado, Denver

called SA-β-gal (Mattiucci et al., 2018), which is associated with high expression of S100A9 in MDS patients. This protein can induce senescence in MSCs through a signaling pathway involving TLR4, NLRP3, and IL-1β secretion (Kim et al., 2012; Shi et al., 2019).

4.7 Microenvironment of inborn errors of metabolism

Inborn errors of metabolism are caused by mutations in chromosomal genes, leading to the deletion or abnormality of enzymes. This disruption in the catalytic process of specific enzymes hinders normal metabolic processes. As a result, there is an accumulation of abnormal metabolic substrates and a deficiency of normal products, which affects the organism's normal development (Agana et al., 2018). Inborn metabolic disorders encompass various types with complex metabolic defects, and a perfect classification method has yet to be established. Previous research has primarily focused on experimental studies of stem cell therapy for inborn metabolic disorders related to the connective tissue, musculoskeletal, neurological, and hematopoietic systems (Ricci and Cacialli, 2021; Specchio et al., 2021). For instance, MSCs and their EVs have shown potential in treating corneal diseases caused by Mucopolysaccharidoses by delivering the enzyme N-acetylgalactosamine-6-sulfate sulfatase (GALNS) to defective cells (Flanagan et al., 2021). Moreover, MSCs and EVs can secrete endogenous coagulation factors FVIII and FIX, making them a promising therapeutic strategy for treating hemophilia (Sokal et al., 2015).

However, senescence-related changes in MSCs derived from the microenvironment of inborn errors of metabolism may have a detrimental impact on their efficacy. For instance, in glycogen storage disease type Ib (GSD-Ib), the ability of MSCs to differentiate into bone and fat cells is hindered due to the absence of glucose-6-phosphate transport protein (G6PT) and the suppression of the OHPOXS response (Sim et al., 2020). The differentially expressed genes (DEGs) in MSCs derived from premature aging syndromes (PAS) compared to MSCs derived from individuals without these syndromes primarily revolve around DNA double-strand damage, telomere damage, and DNA methylation. These genetic changes are associated with the impaired differentiation of MSCs(Trani et al., 2022). In response to these alterations in MSCs, the application of MSC-based cell therapies combined with genetic engineering can provide a safe and effective method for individuals to produce factors that are needed by cells in recipient organs with enzymatic or other defects (Meyerrose et al., 2010) (Tables 1 and 2).

5 Conclusion

MSCs have gained significant attention in the fields of organ repair, new drug development, anti-aging, and rare disease treatment due to their ability to differentiate in multiple directions and their immunological properties. However, along with these promising possibilities, there are also emerging challenges. These include establishing quality standards for MSCs, ensuring their activity during *in vitro* culture, guaranteeing the survival and functionality of MSCs at the site of the disease to achieve therapeutic effects,

understanding the potential negative effects of drugs used to treat the primary pathology on MSCs, and investigating the role of MSCs in tumorigenesis (Nowak et al., 2021). In this review, we provide a summary of the effects and mechanisms of different microenvironments on the senescence and function of MSCs. We also discuss possible ways to improve and explore further research directions. These include: 1. Pre-treating MSCs with specific media before transplantation or culture to enhance their survival rate post-transplantation. 2. Selecting the most suitable MSC donors to ensure efficient utilization of MSCs. 3. Exploring the combination of drugs, bioactive signals, natural and synthetic materials (such as Hydrogels and scaffolds) with MSCs. 4. Investigating the utilization of EVs as an alternative to MSCs and modifying them to address ethical concerns and potential carcinogenic effects. Understanding the interaction between MSCs and the cellular microenvironment is crucial for advancing MSC therapeutics and fostering realistic possibilities for their clinical application. Up to now, MSCs have been the subject of more than 1,599 clinical trials investigating their potential for treatment, with most of these trials still in the early stages. Although the preliminary data from these trials are promising, only two of them involve pretreatment (NCT03105284 and NCT01962233), indicating a lack of rigorous and uniform effective means of establishing a culture system related to pretreatment. Furthermore, MSC therapy still lacks long-term safety assessment, and large-scale and controlled trials are needed to make more conclusive judgments about MSC-based therapies, which are important for clinical translation. It is worth noting that clinical patients often suffer from multiple diseases, not a single disease, and most animal experiments with MSCs have focused on only a single disease model. Therefore, exploring the efficacy of MSCs under multiple diseases in future clinical translation is one of the future research priorities.

Author contributions

WS: Writing–original draft. JV: Writing–review and editing. SG: Conceptualization, Writing–review and editing. ML: Conceptualization, Supervision, Writing–review and editing.

Funding

The author(s) declare financial support was received for the research, authorship, and/or publication of this article. This research was funded by National Natural Science Foundation of China (No. 51872332); and funded by Project of Liaoning Xingliao Talents Plan (XLYC2002103); and funded by The Doctoral Research Initiation of Foundation of Liaoning Province (No. 2022-BS-132).

Conflict of interest

The authors declare that the research was conducted in the absence of any commercial or financial relationships that could be construed as a potential conflict of interest.

Publisher's note

References

Acosta, J. C., Banito, A., Wuestefeld, T., Georgilis, A., Janich, P., Morton, J. P., et al. (2013). A complex secretory program orchestrated by the inflammasome controls paracrine senescence. *Nat. Cell. Biol.* 15 (8), 978–990. doi:10.1038/ncb2784

Acosta, J. C., O'Loghlen, A., Banito, A., Guijarro, M. V., Augert, A., Raguz, S., et al. (2008). Chemokine signaling via the CXCR2 receptor reinforces senescence. *Cell.* 133 (6), 1006–1018. doi:10.1016/j.cell.2008.03.038

Agana, M., Frueh, J., Kamboj, M., Patel, D. R., and Kanungo, S. (2018). Common metabolic disorder (inborn errors of metabolism) concerns in primary care practice. *Ann. Transl. Med.* 6 (24), 469. doi:10.21037/atm.2018.12.34

Ahmadi, M., and Rezaie, J. (2021). Ageing and mesenchymal stem cells derived exosomes: molecular insight and challenges. *Cell. Biochem. Funct.* 39 (1), 60–66. doi:10.1002/cbf.3602

Al Aboud, N. M., Tupper, C., and Jialal, I. (2023). "Genetics, epigenetic mechanism," in StatPearls. *Treasure Island (FL) ineligible companies. Disclosure: connor Tupper declares no relevant financial relationships with ineligible companies. Disclosure: ishwarlal Jialal declares no relevant financial relationships with ineligible companies* (United States: StatPearls Publishing).

Al-Azab, M., Safi, M., Idiiatullina, E., Al-Shaebi, F., and MohamedZaky, Y. (2022). Aging of mesenchymal stem cell: machinery, markers, and strategies of fighting. *Cell. Mol. Biol. Lett.* 27 (1), 69. doi:10.1186/s11658-022-00366-0

Al-Azab, M., Wang, B., Elkhider, A., Williams, W., Li, W., Yuan, Bo, et al. (2020). Indian Hedgehog regulates senescence in bone marrow-derived mesenchymal stem cell through modulation of ROS/mTOR/4EBP1, p70S6K1/2 pathway. *Aging-Us* 12 (7), 5693–5715. doi:10.18632/aging.102958

Alessio, N., Acar, M. B., Demirsoy, I. H., Squillaro, T., Siniscalco, D., Di Bernardo, G., et al. (2020). Obesity is associated with senescence of mesenchymal stromal cells derived from bone marrow, subcutaneous and visceral fat of young mice. *Aging-Us* 12 (13), 12609–12621. doi:10.18632/aging.103606

Almeida, M., and Porter, R. M. (2019). Sirtuins and FoxOs in osteoporosis and osteoarthritis. *Bone* 121, 284–292. doi:10.1016/j.bone.2019.01.018

Alpdundar Bulut, E., Bayyurt Kocabas, B., Yazar, V., Aykut, G., Guler, U., Salih, B., et al. (2020). Human gut commensal membrane vesicles modulate inflammation by generating M2-like macrophages and myeloid-derived suppressor cells. *J. Immunol.* 205 (10), 2707–2718. doi:10.4049/jimmunol.2000731

Al Suraih, M. S., Trussoni, C. E., Splinter, P. L., LaRusso, N. F., and O'Hara, S. P. (2020). Senescent cholangiocytes release extracellular vesicles that alter target cell phenotype via the epidermal growth factor receptor. *Liver Int.* 40 (10), 2455–2468. doi:10.1111/liv.14569

Amini-Nik, S., Abdullahi, A., Vinaik, R., Ren, J., Yao, R., Yu, N., et al. (2022). Aging impairs the cellular interplay between myeloid cells and mesenchymal cells during skin healing in mice. *Aging Dis.* 13 (2), 540–551. doi:10.14336/ad.2021.1008

Anastasiadou, E., Ceccarelli, S., Messina, E., Gerini, G., Megiorni, F., Pontecorvi, P., et al. (2021). MiR-200c-3p maintains stemness and proliferative potential in adipose-derived stem cells by counteracting senescence mechanisms. *Plos One* 16 (9), e0257070. doi:10.1371/journal.pone.0257070

Antonioli, E., Torres, N., Ferretti, M., Piccinato, C. A., and Sertie, A. L. (2019). Individual response to mTOR inhibition in delaying replicative senescence of mesenchymal stromal cells. *PLoS One* 14 (1), e0204784. doi:10.1371/journal.pone.0204784

Arnulf, B., Lecourt, S., Soulier, J., Ternaux, B., Noelle Lacassagne, M., Crinquette, A., et al. (2007). Phenotypic and functional characterization of bone marrow mesenchymal stem cells derived from patients with multiple myeloma. *Leukemia* 21 (1), 158–163. doi:10.1038/sj.leu.2404466

Azadniv, M., Myers, J. R., McMurray, H. R., Guo, N., Rock, P., Coppage, M. L., et al. (2020). Bone marrow mesenchymal stromal cells from acute myelogenous leukemia patients demonstrate adipogenic differentiation propensity with implications for leukemia cell support. *Leukemia* 34 (2), 391–403. doi:10.1038/s41375-019-0568-8

Bai, M., Zhang, Li, Fu, Bo, Bai, J., Zhang, Y., Cai, G., et al. (2018). IL-17A improves the efficacy of mesenchymal stem cells in ischemic-reperfusion renal injury by increasing Treg percentages by the COX-2/PGE2 pathway. *Kidney Int.* 93 (4), 814–825. doi:10.1016/j.kint.2017.08.030

Banimohamad-Shotorbani, B., Kahroba, H., Sadeghzadeh, H., Wilson, D. M., 3rd, Maadi, H., Samadi, N., et al. (2020). DNA damage repair response in mesenchymal stromal cells: from cellular senescence and aging to apoptosis and differentiation ability. *Ageing Res. Rev.* 62, 101125. doi:10.1016/j.arr.2020.101125

Basisty, N., Kale, A., Jeon, O. H., Kuehnemann, C., Payne, T., Rao, C., et al. (2020). A proteomic atlas of senescence-associated secretomes for aging biomarker development. *PLoS Biol.* 18 (1), e3000599. doi:10.1371/journal.pbio.3000599

Battula, V. L., Le, P. M., Sun, J. C., Nguyen, K., Yuan, B., Zhou, X., et al. (2017). AML-induced osteogenic differentiation in mesenchymal stromal cells supports leukemia growth. *Jci Insight* 2 (13), e90036. doi:10.1172/jci.insight.90036

Bereziat, V., Mazurier, C., Auclair, M., Ferrand, N., Jolly, S., Marie, T., et al. (2019). Systemic dysfunction of osteoblast differentiation in adipose-derived stem cells from patients with multiple myeloma. *Cells* 8 (5), 441. doi:10.3390/cells8050441

Berlanga-Acosta, J. A., Guillen-Nieto, G. E., Rodriguez-Rodriguez, N., Mendoza-Mari, Y., Luisa Bringas-Vega, M., JorgeBerlanga-Saez, O., et al. (2020). Cellular senescence as the pathogenic hub of diabetes-related wound chronicity. *Front. Endocrinol.* 11, 573032. doi:10.3389/fendo.2020.573032

Bernadotte, A., Mikhelson, V. M., and Spivak, I. M. (2016). Markers of cellular senescence. Telomere shortening as a marker of cellular senescence. *Aging (Albany NY)* 8 (1), 3–11. doi:10.18632/aging.100871

Bernard, M., Yang, B., Migneault, F., Turgeon, J., Dieude, M., Olivier, M. A., et al. (2020). Autophagy drives fibroblast senescence through MTORC2 regulation. *Autophagy* 16 (11), 2004–2016. doi:10.1080/15548627.2020.1713640

Blackburn, E. H., and Gall, J. G. (1978). A tandemly repeated sequence at the termini of the extrachromosomal ribosomal RNA genes in Tetrahymena. *J. Mol. Biol.* 120 (1), 33–53. doi:10.1016/0022-2836(78)90294-2

Block, T. J., Marinkovic, M., Tran, O. N., Amanda Marshall, A. O. G., Dean, D. D., et al. (2017). Restoring the quantity and quality of elderly human mesenchymal stem cells for autologous cell-based therapies. *Stem Cell. Res. Ther.* 8, 239. doi:10.1186/s13287-017-0688-x

Bonab, M. M., Alimoghaddam, K., Talebian, F., Ghaffari, S. H., Ghavamzadeh, A., and Nikbin, B. (2006). Aging of mesenchymal stem cell *in vitro*. *BMC Cell. Biol.* 7, 14. doi:10.1186/1471-2121-7-14

Bonilla, X., Vanegas, N.-D. P., and Paul Vernot, J. (2019). Acute leukemia induces senescence and impaired osteogenic differentiation in mesenchymal stem cells endowing leukemic cells with functional advantages. *Stem Cells Int.* 2019, 3864948. doi:10.1155/2019/3864948

Bork, S., Pfister, S., Witt, H., Horn, P., Korn, B., Ho, A. D., et al. (2010). DNA methylation pattern changes upon long-term culture and aging of human mesenchymal stromal cells. *Aging Cell.* 9 (1), 54–63. doi:10.1111/j.1474-9726.2009.00535.x

Briscoe, J., and Thérond, P. P. (2013). The mechanisms of Hedgehog signalling and its roles in development and disease. *Nat. Rev. Mol. Cell. Biol.* 14 (7), 416–429. doi:10.1038/nrm3598

Brunet, A., Goodell, M. A., and Rando, T. A. (2023). Ageing and rejuvenation of tissue stem cells and their niches. *Nat. Rev. Mol. Cell. Biol.* 24 (1), 45–62. doi:10.1038/s41580-022-00510-w

Buravkova, L. B., Andreeva, E. R., Gogvadze, V., and Zhivotovsky, B. (2014). Mesenchymal stem cells and hypoxia: where are we? *Mitochondrion* 19, 105–112. doi:10.1016/j.mito.2014.07.005

Cakouros, D., and Gronthos, S. (2020). The changing epigenetic landscape of Mesenchymal Stem/Stromal Cells during aging. *Bone* 137, 115440. doi:10.1016/j.bone.2020.115440

Canli, O., Nicolas, A. M., Gupta, J., Finkelmeier, F., Goncharova, O., Pesic, M., et al. (2017). Myeloid cell-derived reactive oxygen species induce epithelial mutagenesis. *Cancer Cell.* 32 (6), 869–883. doi:10.1016/j.ccell.2017.11.004

Cardenes, N., Alvarez, D., Sellares, J., Peng, Y., Corey, C., Wecht, S., et al. (2018). Senescence of bone marrow-derived mesenchymal stem cells from patients with idiopathic pulmonary fibrosis. *Stem Cell. Res. Ther.* 9, 257. doi:10.1186/s13287-018-0970-6

Chaib, S., Tchkonia, T., and Kirkland, J. L. (2022). Cellular senescence and senolytics: the path to the clinic. *Nat. Med.* 28 (8), 1556–1568. doi:10.1038/s41591-022-01923-y

Chang, J. T. (2020). Pathophysiology of inflammatory bowel diseases. *N. Engl. J. Med.* 383 (27), 2652–2664. doi:10.1056/NEJMra2002697

Chapman, J., Fielder, E., and Passos, J. F. (2019). Mitochondrial dysfunction and cell senescence: deciphering a complex relationship. *Febs Lett.* 593 (13), 1566–1579. doi:10.1002/1873-3468.13498

Chen, C., Xia, S., He, J., Lu, G., Xie, Z., and Han, H. (2019). Roles of taurine in cognitive function of physiology, pathologies and toxication. *Life Sci.* 231, 116584. doi:10.1016/j.lfs.2019.116584

Chen, C., Zhou, M., Ge, Y., and Wang, X. (2020a). SIRT1 and aging related signaling pathways. *Mech. Ageing Dev.* 187, 111215. doi:10.1016/j.mad.2020.111215

Chen, H., Liu, O., Chen, S., and Zhou, Y. (2022a). Aging and mesenchymal stem cells: therapeutic opportunities and challenges in the older group. *Gerontology* 68 (3), 339–352. doi:10.1159/000516668

Chen, J. (2016). The cell-cycle arrest and apoptotic functions of p53 in tumor initiation and progression. *Cold Spring Harb. Perspect. Med.* 6 (3), a026104. doi:10.1101/cshperspect.a026104

Chen, J. R., Lazarenko, O. P., Blackburn, M. L., Rose, S., Frye, R. E., Badger, T. M., et al. (2016). Maternal obesity programs senescence signaling and glucose metabolism in osteo-progenitors from rat and human. *Endocrinology* 157 (11), 4172–4183. doi:10.1210/en.2016-1408

Chen, W., Baylink, D. J., Brier-Jones, J., Neises, A., Kiroyan, J. B., Rundle, C. H., et al. (2015). PDGFB-based stem cell gene therapy increases bone strength in the mouse. *Proc. Natl. Acad. Sci. U. S. A.* 112 (29), E3893–E3900. doi:10.1073/pnas.1501759112

Chen, X., Feng, J., Chang, Q., Lu, F., and Yuan, Yi (2021a). Senescence of donor cells impairs fat graft regeneration by suppressing adipogenesis and increasing expression of senescence-associated secretory phenotype factors. *Stem Cell. Res. Ther.* 12 (1), 311. doi:10.1186/s13287-021-02383-w

Chen, X., Luo, X., Wei, Y., Sun, H., Dai, L., Tangzhou, Y., et al. (2021b). LncRNA H19 induces immune dysregulation of BMMSCs, at least partly, by inhibiting IL-2 production. *Mol. Med.* 27 (1), 61. doi:10.1186/s10020-021-00326-y

Chen, Xi, Wang, C., Jiang, Y., Wang, Qi, Yu, T., Zhang, H., et al. (2020b). Bcl-3 promotes Wnt signaling by maintaining the acetylation of beta-catenin at lysine 49 in colorectal cancer. *Signal Transduct. Target. Ther.* 5 (1), 52. doi:10.1038/s41392-020-0138-6

Chen, X., Zhou, C., Xu, D., Liu, X., Li, S., Hou, J., et al. (2022b). Peptide hormone ELABELA promotes rat bone marrow-derived mesenchymal stem cell proliferation and migration by manipulating the cell cycle through the PI3K/AKT pathway under the hypoxia and ischemia microenvironment. *Stem Cell. Res. Ther.* 13 (1), 32. doi:10.1186/s13287-021-02691-1

Choi, J., Hwang, M. P., Lee, J. W., and Lee, K. H. (2014). A glimpse into the interactions of cells in a microenvironment: the modulation of T cells by mesenchymal stem cells. *Int. J. Nanomedicine* 9 (1), 127–139. doi:10.2147/ijn.S50767

Chondrogianni, N., Tzavelas, C., Pemberton, A. J., Nezis, I. P., Rivett, A. J., and Gonos, E. S. (2005). Overexpression of proteasome beta5 assembled subunit increases the amount of proteasome and confers ameliorated response to oxidative stress and higher survival rates. *J. Biol. Chem.* 280 (12), 11840–11850. doi:10.1074/jbc.M413007200

Chung, H. Y., Lee, E. K., Choi, Y. J., Kim, J. M., Kim, D. H., Zou, Y., et al. (2011). Molecular inflammation as an underlying mechanism of the aging process and age-related diseases. *J. Dent. Res.* 90 (7), 830–840. doi:10.1177/0022034510387794

Coppe, J.-P., Patil, C. K., Rodier, F., Sun, Yu, Munoz, D. P., Goldstein, J., et al. (2008). Senescence-associated secretory phenotypes reveal cell-nonautonomous functions of oncogenic RAS and the p53 tumor suppressor. *Plos Biol.* 6 (12), 2853–2868. doi:10.1371/journal.pbio.0060301

Corre, J., Mahtouk, K., Attal, M., Gadelorge, M., Huynh, A., Fleury-Cappellesso, S., et al. (2007). Bone marrow mesenchymal stem cells are abnormal in multiple myeloma. *Leukemia* 21 (5), 1079–1088. doi:10.1038/sj.leu.2404621

Czosseck, A., Chen, M. M., Nguyen, H., Meeson, A., Hsu, C.-C., Chen, C.-C., et al. (2022). Porous scaffold for mesenchymal cell encapsulation and exosome-based therapy of ischemic diseases. *J. Control. release official J. Control. Release Soc.* 352, 879–892. doi:10.1016/j.jconrel.2022.10.057

Damasceno, P. K. F., de Santana, T. A., Santos, G. C., Orge, I. D., Silva, D. N., Albuquerque, J. F., et al. (2020). Genetic engineering as a strategy to improve the therapeutic efficacy of mesenchymal stem/stromal cells in regenerative medicine. *Front. Cell. Dev. Biol.* 8, 737. doi:10.3389/fcell.2020.00737

Daoussis, D., Kanellou, A., Panagiotopoulos, E., and Papachristou, D. (2022). DKK-1 is underexpressed in mesenchymal stem cells from patients with ankylosing spondylitis and further downregulated by IL-17. *Int. J. Mol. Sci.* 23 (12), 6660. doi:10.3390/ijms23126660

Davis, C., Dukes, A., Drewry, M., Helwa, I., Johnson, M. H., Isales, C. M., et al. (2017). MicroRNA-183-5p increases with age in bone-derived extracellular vesicles, suppresses bone marrow stromal (stem) cell proliferation, and induces stem cell senescence. *Tissue Eng. Part A* 23 (21-22), 1231–1240. doi:10.1089/ten.TEA.2016.0525

Deng, J. Q., Ouyang, P., Li, W. Y., Zhong, L. J., Gu, C. W., Shen, L. H., et al. (2021). Curcumin alleviates the senescence of canine bone marrow mesenchymal stem cells during *in vitro* expansion by activating the autophagy pathway. *Int. J. Mol. Sci.* 22 (21), 11356. doi:10.3390/ijms222111356

Di Mitri, D., and Alimonti, A. (2016). Non-cell-autonomous regulation of cellular senescence in cancer. *Trends Cell. Biol.* 26 (3), 215–226. doi:10.1016/j.tcb.2015.10.005

Dimri, G. P., Lee, X., Basile, G., Acosta, M., Scott, G., Roskelley, C., et al. (1995). A biomarker that identifies senescent human cells in culture and in aging skin *in vivo*. *Proc. Natl. Acad. Sci. U. S. A.* 92 (20), 9363–9367. doi:10.1073/pnas.92.20.9363

Dominici, M., Le Blanc, K., Mueller, I., Slaper-Cortenbach, I., Marini, F. C., Krause, D. S., et al. (2006). Minimal criteria for defining multipotent mesenchymal stromal cells. The International Society for Cellular Therapy position statement. *Cytotherapy* 8 (4), 315–317. doi:10.1080/14653240600855905

Engeland, K. (2022). Cell cycle regulation: p53-p21-RB signaling. *Cell. Death Differ.* 29 (5), 946–960. doi:10.1038/s41418-022-00988-z

Estrada, J. C., Torres, Y., Benguría, A., Dopazo, A., Roche, E., Carrera-Quintanar, L., et al. (2013). Human mesenchymal stem cell-replicative senescence and oxidative stress are closely linked to aneuploidy. *Cell. Death Dis.* 4 (6), e691. doi:10.1038/cddis.2013.211

Fan, P., Xiao-Yu, Yu, Xie, X.-H., Chen, C.-H., Zhang, Po, Cheng, Y., et al. (2019). Mitophagy is a protective response against oxidative damage in bone marrow mesenchymal stem cells. *Life Sci.* 229, 36–45. doi:10.1016/j.lfs.2019.05.027

Fane, M., and Weeraratna, A. T. (2020). How the ageing microenvironment influences tumour progression. *Nat. Rev. Cancer* 20 (2), 89–106. doi:10.1038/s41568-019-0222-9

Flanagan, M., Pathak, I., Gan, Q., Winter, L., Emnet, R., Akel, S., et al. (2021). Umbilical mesenchymal stem cell-derived extracellular vesicles as enzyme delivery vehicle to treat Morquio A fibroblasts. *Stem Cell. Res. Ther.* 12 (1), 276. doi:10.1186/s13287-021-02355-0

Friedenstein, A. J., Petrakova, K. V., Kurolesova, A. I., and Frolova, G. P. (1968). *Heterotopic of bone marrow. Analysis of precursor cells for osteogenic and hematopoietic tissues.* United States: Transplantation.

Gao, L., Bird, A. K., Meednu, N., Dauenhauer, K., Liesveld, J., Anolik, J., et al. (2017). Bone marrow-derived mesenchymal stem cells from patients with systemic lupus erythematosus have a senescence-associated secretory phenotype mediated by a mitochondrial antiviral signaling protein-interferon-beta feedback loop. *Arthritis & Rheumatology* 69 (8), 1623–1635. doi:10.1002/art.40142

Garcia-Olmo, D., Gilaberte, I., Binek, M., Hoore Ajl, D., Lindner, D., Selvaggi, F., et al. (2022). Follow-up study to evaluate the long-term safety and efficacy of darvadstrocel (mesenchymal stem cell treatment) in patients with perianal fistulizing Crohn's disease: ADMIRE-CD phase 3 randomized controlled trial. *Dis. Colon Rectum* 65 (5), 713–720. doi:10.1097/dcr.0000000000002325

Geng, L., Tang, X., Wang, S., Sun, Y., Wang, D., Tsao, B. P., et al. (2020). Reduced let-7f in bone marrow-derived mesenchymal stem cells triggers Treg/Th17 imbalance in patients with systemic lupus erythematosus. *Front. Immunol.* 11, 233. doi:10.3389/fimmu.2020.00233

Greif, D. N., Kouroupis, D., Murdock, C. J., Griswold, A. J., Kaplan, L. D., Best, T. M., et al. (2020). Infrapatellar fat pad/synovium complex in early-stage knee osteoarthritis: potential new target and source of therapeutic mesenchymal stem/stromal cells. *Front. Bioeng. Biotechnol.* 8, 860. doi:10.3389/fbioe.2020.00860

Grim, C., Noble, R., Uribe, G., Khanipov, K., Johnson, P., Koltun, W. A., et al. (2021). Impairment of tissue-resident mesenchymal stem cells in chronic ulcerative colitis and Crohn's disease. *J. Crohns Colitis* 15 (8), 1362–1375. doi:10.1093/ecco-jcc/jjab001

Guerrero, E. N., Vega, S., Fu, C., De Leon, R., Beltran, D., and Solis, M. A. (2021). Increased proliferation and differentiation capacity of placenta-derived mesenchymal stem cells from women of median maternal age correlates with telomere shortening. *Aging-Us* 13 (22), 24542–24559. doi:10.18632/aging.203724

Hafner, A., Bulyk, M. L., Jambhekar, A., and Lahav, G. (2019). The multiple mechanisms that regulate p53 activity and cell fate. *Nat. Rev. Mol. Cell. Biol.* 20 (4), 199–210. doi:10.1038/s41580-019-0110-x

Han, J., Wang, Y., Zhou, H., Zhang, Y., and Wan, D. (2022). CD137 regulates bone loss *via* the p53 wnt/β-catenin signaling pathways in aged mice. *Front. Endocrinol.* 13, 922501. doi:10.3389/fendo.2022.922501

Harrell, C. R., Djonov, V., and Volarevic, V. (2022). Therapeutic potential of mesenchymal stem cells in the treatment of ocular graft-versus-host disease. *Int. J. Mol. Sci.* 23 (21), 13254. doi:10.3390/ijms232113254

Hayflick, L., and Moorhead, P. S. (1961). The serial cultivation of human diploid cell strains. *Exp. Cell. Res.* 25, 585–621. doi:10.1016/0014-4827(61)90192-6

He, L., Liao, J., Liu, Z., Wang, T., Zhou, Y., Wang, T., et al. (2023). Multi-omic analysis of mandibuloacral dysplasia type A patient iPSC-derived MSC senescence reveals miR-311 as a novel biomarker for MSC senescence. *Hum. Mol. Genet.* 32 (19), 2872–2886. doi:10.1093/hmg/ddad111

Hernandez-Segura, A., Nehme, J., and Demaria, M. (2018). Hallmarks of cellular senescence. *Trends Cell. Biol.* 28 (6), 436–453. doi:10.1016/j.tcb.2018.02.001

Herranz, N., and Gil, J. (2018). Mechanisms and functions of cellular senescence. *J. Clin. Investig.* 128 (4), 1238–1246. doi:10.1172/jci95148

Hong, Y., He, H., Jiang, G., Zhang, H., Tao, W., Ding, Y., et al. (2020). miR-155-5p inhibition rejuvenates aged mesenchymal stem cells and enhances cardioprotection following infarction. *Aging Cell.* 19 (4), e13128. doi:10.1111/acel.13128

Huang, J., Zhao, L., Xing, L., and Chen, Di (2010). MicroRNA-204 regulates Runx2 protein expression and mesenchymal progenitor cell differentiation. *Stem Cells* 28 (2), 357–364. doi:10.1002/stem.288

Huang, R., Qin, C., Wang, J., Hu, Y., Zheng, G., Qiu, G., et al. (2019a). Differential effects of extracellular vesicles from aging and young mesenchymal stem cells in acute lung injury. *Aging-Us* 11 (18), 7996–8014. doi:10.18632/aging.102314

Huang, Y., Wu, Q., and Paul Kwong Hang Tam (2022). Immunomodulatory mechanisms of mesenchymal stem cells and their potential clinical applications. *Int. J. Mol. Sci.* 23 (17), 10023. doi:10.3390/ijms231710023

Huang, Y. C., and Lai, L. C. (2019b). The potential roles of stem cell-derived extracellular vesicles as a therapeutic tool. *Ann. Transl. Med.* 7 (22), 693. doi:10.21037/atm.2019.11.66

Humrich, J. Y., and Riemekasten., G. (2016). Restoring regulation - IL-2 therapy in systemic lupus erythematosus. *Expert Rev. Clin. Immunol.* 12 (11), 1153–1160. doi:10.1080/1744666x.2016.1199957

Jackson, M. V., Morrison, T. J., Doherty, D. F., McAuley, D. F., Matthay, M. A., Kissenpfennig, A., et al. (2016). Mitochondrial transfer via tunneling nanotubes is an important mechanism by which mesenchymal stem cells enhance macrophage phagocytosis in the *in vitro* and *in vivo* models of ARDS. *Stem Cells* 34 (8), 2210–2223. doi:10.1002/stem.2372

Ji, J., Fu, T., Dong, C., Zhu, W., Yang, J., Kong, X., et al. (2019). Targeting HMGB1 by ethyl pyruvate ameliorates systemic lupus erythematosus and reverses the senescent phenotype of bone marrow-mesenchymal stem cells. *Aging-Us* 11 (13), 4338–4353. doi:10.18632/aging.102052

Ji, J., Wu, Y., Meng, Y., Zhang, L., Feng, G., Xia, Y., et al. (2017). JAK-STAT signaling mediates the senescence of bone marrow-mesenchymal stem cells from systemic lupus erythematosus patients. *Acta Biochimica Biophysica Sinica* 49 (3), 208–215. doi:10.1093/abbs/gmw134

Jiang, X., Li, W., Ge, L., and Lu, M. (2023). Mesenchymal stem cell senescence during aging:from mechanisms to rejuvenation strategies. *Aging Dis.* 14 (5), 1651–1676. doi:10.14336/ad.2023.0208

Jing, H., Su, X., Gao, Bo, Yi, S., Chen, Ji, Deng, Z., et al. (2022). Epigenetic inhibition of Wnt pathway suppresses osteogenic differentiation of BMSCs during osteoporosis. *Cell. Death Dis.* 13 (2). doi:10.1038/s41419-022-04616-z

Johnson, S. C., Rabinovitch, P. S., and Kaeberlein, M. (2013). mTOR is a key modulator of ageing and age-related disease. *Nature* 493 (7432), 338–345. doi:10.1038/nature11861

Kamal, N. S. M., Safuan, S., Shamsuddin, S., and Foroozandeh, P. (2020). Aging of the cells: insight into cellular senescence and detection Methods. *Eur. J. Cell. Biol.* 99 (6), 151108. doi:10.1016/j.ejcb.2020.151108

Kang, D., Shin, J., Cho, Y., Kim, H.-S., Gu, Y.-R., Kim, H., et al. (2019). Stress-activated miR-204 governs senescent phenotypes of chondrocytes to promote osteoarthritis development. *Sci. Transl. Med.* 11 (486), eaar6659. doi:10.1126/scitranslmed.aar6659

Kapetanou, M., Chondrogianni, N., Petrakis, S., George, K., and EfstathiosGonos, S. (2017b). Proteasome activation enhances stemness and lifespan of human mesenchymal stem cells. *Free Radic. Biol. Med.* 103, 226–235. doi:10.1016/j.freeradbiomed.2016.12.035

Kapetanou, M., Chondrogianni, N., Petrakis, S., Koliakos, G., and Gonos, E. S. (2017a). Proteasome activation enhances stemness and lifespan of human mesenchymal stem cells. *Free Radic. Biol. Med.* 103, 226–235. doi:10.1016/j.freeradbiomed.2016.12.035

Karakoc, M., Altindag, O., Keles, H., Soran, N., and Selek, S. (2007). Serum oxidative - antioxidative status in patients with ankylosing spondilitis. *Rheumatol. Int.* 27 (12), 1131–1134. doi:10.1007/s00296-007-0352-3

Khodayari, S., Hamid, K., Amiri, A. Z., Eslami, M., Farhud, D., Hescheler, J., et al. (2019). Inflammatory microenvironment of acute myocardial infarction prevents regeneration of heart with stem cells therapy. *Cell. physiology Biochem. Int. J. Exp. Cell. physiology, Biochem. Pharmacol.* 53 (5), 887–909. doi:10.33594/000000180

Khorraminejad-Shirazi, M., Sani, M., Talaei-Khozani, T., Dorvash, M., Mirzaei, M., Faghihi, M. A., et al. (2020). AICAR and nicotinamide treatment synergistically augment the proliferation and attenuate senescence-associated changes in mesenchymal stromal cells. *Stem Cell. Res. Ther.* 11 (1), 45. doi:10.1186/s13287-020-1565-6

Kim, C., Park, J.-M., Song, Y., Kim, S., and Moon, J. (2019). HIF1 alpha-mediated AIMP3 suppression delays stem cell aging via the induction of autophagy. *Aging Cell.* 18 (2), e12909. doi:10.1111/acel.12909

Kim, D. W., Jeong, H. S., Kim, E., Lee, H., Choi, C. H., and Lee, S. J. (2022). Oral delivery of stem-cell-loaded hydrogel microcapsules restores gut inflammation and microbiota. *J. Control Release* 347, 508–520. doi:10.1016/j.jconrel.2022.05.028

Kim, J.-A., Shim, J.-S., Lee, G.-Y., Yim, H. W., Kim, T.-M., Kim, M., et al. (2015). Microenvironmental remodeling as a parameter and prognostic factor of heterogeneous leukemogenesis in acute myelogenous leukemia. *Cancer Res.* 75 (11), 2222–2231. doi:10.1158/0008-5472.Can-14-3379

Kim, J. H., Oh, S.-H., Kim, E.-J., Park, S. J., Sung, P. H., Cheon, J. H., et al. (2012). The role of myofibroblasts in upregulation of S100A8 and S100A9 and the differentiation of myeloid cells in the colorectal cancer microenvironment. *Biochem. Biophysical Res. Commun.* 423 (1), 60–66. doi:10.1016/j.bbrc.2012.05.081

Kim, Y. G., Choi, J., and Kim, K. (2020). Mesenchymal stem cell-derived exosomes for effective cartilage tissue repair and treatment of osteoarthritis. *Biotechnol. J.* 15 (12), e2000082. doi:10.1002/biot.202000082

Kong, C.-M., Subramanian, A., Biswas, A., Walter, S., Chong, Y.-S., Bongso, A., et al. (2019). Changes in stemness properties, differentiation potential, oxidative stress, senescence and mitochondrial function in Wharton's jelly stem cells of umbilical

cords of mothers with gestational diabetes mellitus. *Stem Cell. Rev. Rep.* 15 (3), 415–426. doi:10.1007/s12015-019-9872-y

Korolchuk, V. I., Miwa, S., Carroll, B., and von Zglinicki, T. (2017). Mitochondria in cell senescence: is mitophagy the weakest link? *Ebiomedicine* 21, 7–13. doi:10.1016/j.ebiom.2017.03.020

Kowald, A., Passos, J. F., and Kirkwood, T. B. L. (2020). On the evolution of cellular senescence. *Aging Cell.* 19 (12), e13270. doi:10.1111/acel.13270

Kumar, A., Anand, T., Bhattacharyya, J., Sharma, A., and Grace Jaganathan, B. (2018). K562 chronic myeloid leukemia cells modify osteogenic differentiation and gene expression of bone marrow stromal cells. *J. Cell. Commun. Signal.* 12 (2), 441–450. doi:10.1007/s12079-017-0412-8

Kumar, S. K., Rajkumar, V., Kyle, R. A., van Duin, M., Sonneveld, P., Mateos, M. V., et al. (2017). Multiple myeloma. *Nat. Rev. Dis. Prim.* 3, 17046. doi:10.1038/nrdp.2017.46

Kutyna, M. M., Kok, C. H., Lim, Y., Ngoc Hoa Tran, E., Campbell, D., Paton, S., et al. (2022). A senescence stress secretome is a hallmark of therapy-related myeloid neoplasm stromal tissue occurring soon after cytotoxic exposure. *Leukemia* 36 (11), 2678–2689. doi:10.1038/s41375-022-01686-y

Le, Y., Fraineau, S., Priya, C., Mitchell, S., Brand, M., Lavoie, J. R., et al. (2016). Adipogenic mesenchymal stromal cells from bone marrow and their hematopoietic supportive role: towards understanding the permissive marrow microenvironment in acute myeloid leukemia. *Stem Cell. Rev. Rep.* 12 (2), 235–244. doi:10.1007/s12015-015-9639-z

Lee, G. R. (2018). The balance of Th17 versus Treg cells in autoimmunity. *Int. J. Mol. Sci.* 19 (3), 730. doi:10.3390/ijms19030730

Lehmann, J., Narcisi, R., Franceschini, N., Chatzivasileiou, D., Boer, C. G., Koevoet, W., et al. (2022). WNT/beta-catenin signalling interrupts a senescence-induction cascade in human mesenchymal stem cells that restricts their expansion. *Cell. Mol. Life Sci.* 79 (2), 82. doi:10.1007/s00018-021-04035-x

Li, X., Hong, Y., He, H., Jiang, G., You, W., Liang, X., et al. (2019). FGF21 mediates mesenchymal stem cell senescence via regulation of mitochondrial dynamics. *Oxidative Med. Cell. Longev.* 2019, 4915149. doi:10.1155/2019/4915149

Li, X., Wang, X., Zhang, C., Wang, J., Wang, S., and Hu, L. (2022). Dysfunction of metabolic activity of bone marrow mesenchymal stem cells in aged mice. *Cell. Prolif.* 55 (3), e13191. doi:10.1111/cpr.13191

Li, Y., Lu, L., Xie, Y., Chen, X., Tian, L., Liang, Y., et al. (2020). Interleukin-6 knockout inhibits senescence of bone mesenchymal stem cells in high-fat diet-induced bone loss. *Front. Endocrinol. (Lausanne)* 11, 622950. doi:10.3389/fendo.2020.622950

Li, Y., Wu, Q., Wang, Y., Li, L., Bu, H., and Bao, J. (2017). Senescence of mesenchymal stem cells (Review). *Int. J. Mol. Med.* 39 (4), 775–782. doi:10.3892/ijmm.2017.2912

Lin, H., Lunetta, K. L., Zhao, Q., Rong, J., Benjamin, E. J., Mendelson, M. M., et al. (2017). Transcriptome-wide association study of inflammatory biologic age. *Aging (Albany NY)* 9 (11), 2288–2301. doi:10.18632/aging.101321

Lin, M., Liu, X., Zheng, H., Huang, X., Wu, Yu, Huang, A., et al. (2020). IGF-1 enhances BMSC viability, migration, and anti-apoptosis in myocardial infarction via secreted frizzled-related protein 2 pathway. *Stem Cell. Res. Ther.* 11 (1), 22. doi:10.1186/s13287-019-1544-y

Liu, C.-H., Sengupta, R., Chen, C.-H., Hung, K.-H., Chou, C.-T., Chen, I.-Ho, et al. (2019). HLA-B27-mediated activation of TNAP phosphatase promotes pathogenic syndesmophyte formation in ankylosing spondylitis. *J. Clin. Investigation* 129 (12), 5357–5373. doi:10.1172/jci125212

Liu, J., Ding, Y., Liu, Z., and Liang, X. (2020a). Senescence in mesenchymal stem cells: functional alterations, molecular mechanisms, and rejuvenation strategies. *Front. Cell. Dev. Biol.* 8, 258. doi:10.3389/fcell.2020.00258

Liu, J., Gao, J., Liang, Z., Gao, C., Niu, Q., Wu, F., et al. (2022a). Mesenchymal stem cells and their microenvironment. *Stem Cell. Res. Ther.* 13 (1), 429. doi:10.1186/s13287-022-02985-y

Liu, L., DiGirolamo, C. M., Navarro, P., Blasco, M. A., and Keefe, D. L. (2004). Telomerase deficiency impairs differentiation of mesenchymal stem cells. *Exp. Cell. Res.* 294 (1), 1–8. doi:10.1016/j.yexcr.2003.10.031

Liu, M., Lei, H., Dong, P., Fu, X., Yang, Z., Yang, Y., et al. (2017). Adipose-derived mesenchymal stem cells from the elderly exhibit decreased migration and differentiation abilities with senescent properties. *Cell. Transplant.* 26 (9), 1505–1519. doi:10.1177/0963689717721221

Liu, W., Rong, Y., Wang, J., Zheng, Z., Ge, X., Ji, C., et al. (2020b). Exosome-shuttled miR-216a-5p from hypoxic preconditioned mesenchymal stem cells repair traumatic spinal cord injury by shifting microglial M1/M2 polarization. *J. Neuroinflammation* 17 (1), 47. doi:10.1186/s12974-020-1726-7

Liu, X. P., Zhan, Y. B., Xu, W. X., Liu, L. X., Liu, X. Y., Da, J. L., et al. (2022b). Characterization of transcriptional landscape in bone marrow-derived mesenchymal stromal cells treated with aspirin by RNA-seq. *Peerj* 10, e12819. doi:10.7717/peerj.12819

Liu, Y., Schwam, J., and Chen, Q. (2022c). Senescence-associated cell transition and interaction (sactai): a proposed mechanism for tissue aging, repair, and degeneration. *Cells* 11 (7), 1089. doi:10.3390/cells11071089

Lopez-Otin, C., Blasco, M. A., Partridge, L., Serrano, M., and Guido, K. (2013). The hallmarks of aging. *Cell.* 153 (6), 1194–1217. doi:10.1016/j.cell.2013.05.039

Lozono-Torres, B., Alejandro, E.-F., Rovira, M., Orzaez, M., Serrano, M., Martinez-Manez, R., et al. (2019). The chemistry of senescence. *Nat. Rev. Chem.* 3 (7), 426–441. doi:10.1038/s41570-019-0108-0

Luo, Z., Wu, F., Xue, E., Huang, L., Yan, P., Pan, X., et al. (2019). Hypoxia preconditioning promotes bone marrow mesenchymal stem cells survival by inducing HIF-1 alpha in injured neuronal cells derived exosomes culture system. *Cell. Death Dis.* 10, 134. doi:10.1038/s41419-019-1410-y

Ma, C., Pi, C., Yang, Y., Lin, L., Shi, Y., Li, Y., et al. (2017). Nampt expression decreases age-related senescence in rat bone marrow mesenchymal stem cells by targeting Sirt1. *PLoS One* 12 (1), e0170930. doi:10.1371/journal.pone.0170930

Ma, C., Sun, Y., Pi, C., Wang, H., Sun, H., Xiao, Yu, et al. (2020). Sirt3 attenuates oxidative stress damage and rescues cellular senescence in rat bone marrow mesenchymal stem cells by targeting superoxide dismutase 2. *Front. Cell. Dev. Biol.* 8, 599376. doi:10.3389/fcell.2020.599376

Mareschi, K., Ferrero, I., Rustichelli, D., Aschero, S., Gammaitoni, L., Aglietta, M., et al. (2006). Expansion of mesenchymal stem cells isolated from pediatric and adult donor bone marrow. *J. Cell. Biochem.* 97 (4), 744–754. doi:10.1002/jcb.20681

Marinkovic, M., Dai, Q., Gonzalez, A. O., Tran, O. N., Block, T. J., Harris, S. E., et al. (2022). Matrix-bound Cyr61/CCN1 is required to retain the properties of the bone marrow mesenchymal stem cell niche but is depleted with aging. *Matrix Biol.* 111, 108–132. doi:10.1016/j.matbio.2022.06.004

Marote, A., Santos, D., Mendes-Pinheiro, B., Serre-Miranda, C., Anjo, S. I., Vieira, J., et al. (2023). Cellular aging secretes: a comparison of bone-marrow-derived and induced mesenchymal stem cells and their secretome over long-term culture. *Stem Cell. Rev. Rep.* 19 (1), 248–263. doi:10.1007/s12015-022-10453-6

Massa, M., Croce, S., Campanelli, R., Abbà, C., Lenta, E., Valsecchi, C., et al. (2020). Clinical applications of mesenchymal stem/stromal cell derived extracellular vesicles: therapeutic potential of an acellular product. *Diagn. (Basel)* 10 (12), 999. doi:10.3390/diagnostics10120999

Mato-Basalo, R., Morente-Lopez, M., Arntz, O. J., van de Loo, F. A. J., Fafian-Labora, J., and Arufe, M. C. (2021). Therapeutic potential for regulation of the nuclear factor kappa-B transcription factor p65 to prevent cellular senescence and activation of pro-inflammatory in mesenchymal stem cells. *Int. J. Mol. Sci.* 22 (7), 3367. doi:10.3390/ijms22073367

Mattiucci, D., Maurizi, G., Leoni, P., and Poloni, A. (2018). Aging- and senescence-associated changes of mesenchymal stromal cells in myelodysplastic syndromes. *Cell. Transplant.* 27 (5), 754–764. doi:10.1177/0963689717745890

Meyerrose, T., Olson, S., Pontow, S., Kalomoiris, S., Jung, Y., Annett, G., et al. (2010). Mesenchymal stem cells for the sustained *in vivo* delivery of bioactive factors. *Adv. Drug Deliv. Rev.* 62 (12), 1167–1174. doi:10.1016/j.addr.2010.09.013

Miao, C., Lei, M., Hu, W., Han, S., and Wang, Qi (2017). A brief review: the therapeutic potential of bone marrow mesenchymal stem cells in myocardial infarction. *Stem Cell. Res. Ther.* 8, 242. doi:10.1186/s13287-017-0697-9

Miura, Y., Endo, K., Komori, K., and Sekiya, I. (2022). Clearance of senescent cells with ABT-263 improves biological functions of synovial mesenchymal stem cells from osteoarthritis patients. *Stem Cell. Res. Ther.* 13 (1), 222. doi:10.1186/s13287-022-02901-4

Moyzis, R. K., Buckingham, J. M., Cram, L. S., Dani, M., Deaven, L. L., Jones, M. D., et al. (1988). A highly conserved repetitive DNA sequence, (TTAGGG)n, present at the telomeres of human chromosomes. *Proc. Natl. Acad. Sci. U. S. A.* 85 (18), 6622–6626. doi:10.1073/pnas.85.18.6622

Musavi, M., Kohram, F., Abasi, M., Bolandi, Z., Ajoudanian, M., Mohammadi-Yeganeh, S., et al. (2019). Rn7SK small nuclear RNA is involved in cellular senescence. *J. Cell. Physiology* 234 (8), 14234–14245. doi:10.1002/jcp.28119

Najafi, H., Abolmaali, S. S., Heidari, R., Valizadeh, H., Tamaddon, A. M., and Azarpira, N. (2022). Integrin receptor-binding nanofibrous peptide hydrogel for combined mesenchymal stem cell therapy and nitric oxide delivery in renal ischemia/reperfusion injury. *Stem Cell. Res. Ther.* 13 (1), 344. doi:10.1186/s13287-022-03045-1

Nowak, B., Rogujski, P., Janowski, M., Lukomska, B., and Andrzejewska, A. (2021). Mesenchymal stem cells in glioblastoma therapy and progression: how one cell does it all. *Biochim. Biophys. Acta Rev. Cancer* 1876 (1), 188582. doi:10.1016/j.bbcan.2021.188582

Oja, S., Komulainen, P., Penttilä, A., Nystedt, J., and Korhonen, M. (2018). Automated image analysis detects aging in clinical-grade mesenchymal stromal cell cultures. *Stem Cell. Res. Ther.* 9 (1), 6. doi:10.1186/s13287-017-0740-x

Oka, T., Hikoso, S., Yamaguchi, O., Taneike, M., Takeda, T., Tamai, T., et al. (2012). Mitochondrial DNA that escapes from autophagy causes inflammation and heart failure. *Nature* 485 (7397), 251–255. doi:10.1038/nature10992

Onyiah, J. C., and Colgan, S. P. (2016). Cytokine responses and epithelial function in the intestinal mucosa. *Cell. Mol. Life Sci.* 73 (22), 4203–4212. doi:10.1007/s00018-016-2289-8

Ou, H.-L., and Schumacher, B. (2018). DNA damage responses and p53 in the aging process. *Blood* 131 (5), 488–495. doi:10.1182/blood-2017-07-746396

Panés, J., García-Olmo, D., Van Assche, G., Colombel, J. F., Reinisch, W., Baumgart, D. C., et al. (2018). Long-term efficacy and safety of stem cell therapy (Cx601) for complex perianal fistulas in patients with Crohn's disease. *Gastroenterology* 154 (5), 1334–1342.e4. doi:10.1053/j.gastro.2017.12.020

Papait, A., Stefani, F. R., Cargnoni, A., Magatti, M., Parolini, O., and Silini, A. R. (2020). The multifaceted roles of MSCs in the tumor microenvironment: interactions with immune cells and exploitation for therapy. *Front. Cell. Dev. Biol.* 8, 447. doi:10.3389/fcell.2020.00447

Parsch, D., Fellenberg, J., Brümmendorf, T. H., Eschlbeck, A. M., and Richter, W. (2004). Telomere length and telomerase activity during expansion and differentiation of human mesenchymal stem cells and chondrocytes. *J. Mol. Med. Berl.* 82 (1), 49–55. doi:10.1007/s00109-003-0506-z

Peck, S. H., Bendigo, J. R., Tobias, J. W., Dodge, G. R., Malhotra, N. R., Mauck, R. L., et al. (2021). Hypoxic preconditioning enhances bone marrow-derived mesenchymal stem cell survival in a low oxygen and nutrient-limited 3D microenvironment. *Cartilage* 12 (4), 512–525. doi:10.1177/1947603519841675

Peffers, M. J., Collins, J., Fang, Y., Goljanek-Whysall, K., Rushton, M., Loughlin, J., et al. (2016). Age-related changes in mesenchymal stem cells identified using a multi-omics approach. *Eur. Cell. Mater* 31, 136–159. doi:10.22203/ecm.v031a10

Pei, F., Ma, L., Jing, J., Feng, J., Yuan, Y., Guo, T., et al. (2023). Sensory nerve niche regulates mesenchymal stem cell homeostasis via FGF/mTOR/autophagy axis. *Nat. Commun.* 14 (1), 344. doi:10.1038/s41467-023-35977-4

Peng, X., Zhou, X., Yin, Y., Luo, B., Liu, Y., and Cheng, Y. (2022). Inflammatory microenvironment accelerates bone marrow mesenchymal stem cell aging. *Front. Bioeng. Biotechnol.* 10, 870324. doi:10.3389/fbioe.2022.870324

Phelps, J., Hart, D. A., Mitha, A. P., Duncan, N. A., and Sen, A. (2023). Physiological oxygen conditions enhance the angiogenic properties of extracellular vesicles from human mesenchymal stem cells. *Stem Cell. Res. Ther.* 14 (1), 218. doi:10.1186/s13287-023-03439-9

Pi, C., Cao, Ma, Wang, H., Sun, H., Xiao, Yu, Gao, X., et al. (2021). MiR-34a suppression targets Nampt to ameliorate bone marrow mesenchymal stem cell senescence by regulating NAD(+)-Sirt1 pathway. *Stem Cell. Res. Ther.* 12 (1), 271. doi:10.1186/s13287-021-02339-0

Pignolo, R. J., Passos, J. F., Khosla, S., Tchkonia, T., and Kirkland, J. L. (2020). Reducing senescent cell burden in aging and disease. *Trends Mol. Med.* 26 (7), 630–638. doi:10.1016/j.molmed.2020.03.005

Pignolo, R. J., Suda, R. K., McMillan, E. A., Shen, J., Lee, S.-H., Choi, Y., et al. (2008). Defects in telomere maintenance molecules impair osteoblast differentiation and promote osteoporosis. *Aging Cell.* 7 (1), 23–31. doi:10.1111/j.1474-9726.2007.00350.x

Pittenger, M. F., Discher, D. E., Péault, B. M., Phinney, D. G., Hare, J. M., and Caplan, A. I. (2019). Mesenchymal stem cell perspective: cell biology to clinical progress. *NPJ Regen. Med.* 4, 22. doi:10.1038/s41536-019-0083-6

Prattichizzo, F., De Nigris, V., Mancuso, E., Spiga, R., Giuliani, A., Matacchione, G., et al. (2018). Short-term sustained hyperglycaemia fosters an archetypal senescence-associated secretory phenotype in endothelial cells and macrophages. *Redox Biol.* 15, 170–181. doi:10.1016/j.redox.2017.12.001

Psaroudis, R. T., Singh, U., Lora, M., Jeon, P., Boursiquot, A., Stochaj, U., et al. (2022). CD26 is a senescence marker associated with reduced immunopotency of human adipose tissue-derived multipotent mesenchymal stromal cells. *Stem Cell. Res. Ther.* 13 (1), 358. doi:10.1186/s13287-022-03026-4

Qi, Y., Zhu, T., Zhang, T., Wang, Xi, Li, W., Chen, D., et al. (2021). M1 macrophage-derived exosomes transfer miR-222 to induce bone marrow mesenchymal stem cell apoptosis. *Lab. Investig.* 101 (10), 1318–1326. doi:10.1038/s41374-021-00622-5

Qiao, Q., Liu, X., Yang, T., Cui, K., Kong, L., Yang, C., et al. (2021). Nanomedicine for acute respiratory distress syndrome: the latest application, targeting strategy, and rational design. *Acta Pharm. Sin. B* 11 (10), 3060–3091. doi:10.1016/j.apsb.2021.04.023

Ray, P. D., Huang, B. W., and Tsuji, Y. (2012). Reactive oxygen species (ROS) homeostasis and redox regulation in cellular signaling. *Cell. Signal* 24 (5), 981–990. doi:10.1016/j.cellsig.2012.01.008

Redondo, J., Sarkar, P., Kemp, K., Heesom, K. J., Wilkins, A., Scolding, N. J., et al. (2018b). Dysregulation of mesenchymal stromal cell antioxidant responses in progressive multiple sclerosis. *Stem Cells Transl. Med.* 7 (10), 748–758. doi:10.1002/sctm.18-0045

Redondo, J., Sarkar, P., Kemp, K., Virgo, P. F., Pawade, J., Norton, A., et al. (2018a). Reduced cellularity of bone marrow in multiple sclerosis with decreased MSC expansion potential and premature ageing *in vitro*. *Mult. Scler.* 24 (7), 919–931. doi:10.1177/1352458517711276

Redondo, J., Sarkar, P., Kemp, K., Virgo, P. F., Pawade, J., Norton, A., et al. (2018c). Reduced cellularity of bone marrow in multiple sclerosis with decreased MSC expansion potential and premature ageing *in vitro*. *Multiple Scler. J.* 24 (7), 919–931. doi:10.1177/1352458517711276

Rehman, S.Ur, Shah, S. A., Ali, T., Chung, J.Il, and Kim, M.Ok (2017). Anthocyanins reversed D-galactose-induced oxidative stress and neuroinflammation mediated cognitive impairment in adult rats. *Mol. Neurobiol.* 54 (1), 255–271. doi:10.1007/s12035-015-9604-5

Ricci, S., and Cacialli, P. (2021). Stem cell research tools in human metabolic disorders: an overview. *Cells* 10 (10), 2681. doi:10.3390/cells10102681

Ridzuan, N., Al Abbar, A., Yip, W. K., Maqbool, M., and Ramasamy, R. (2016). Characterization and expression of senescence marker in prolonged passages of rat bone marrow-derived mesenchymal stem cells. *Stem Cells Int.* 2016, 8487264. doi:10.1155/2016/8487264

Ritschka, B., Storer, M., Mas, A., Heinzmann, F., Ortells, M. C., Morton, J. P., et al. (2017). The senescence-associated secretory phenotype induces cellular plasticity and tissue regeneration. *Genes. & Dev.* 31 (2), 172–183. doi:10.1101/gad.290635.116

Rizzo, M. G., Best, T. M., Huard, J., Philippon, M., Hornicek, F., Duan, Z., et al. (2023). Therapeutic perspectives for inflammation and senescence in osteoarthritis using mesenchymal stem cells, mesenchymal stem cell-derived extracellular vesicles and senolytic agents. *Cells* 12 (10), 1421. doi:10.3390/cells12101421

Salminen, A., Kaarniranta, K., and Kauppinen, A. (2016). Age-related changes in AMPK activation: role for AMPK phosphatases and inhibitory phosphorylation by upstream signaling pathways. *Ageing Res. Rev.* 28, 15–26. doi:10.1016/j.arr.2016.04.003

Seok, J., Jung, H. S., Park, S., Lee, J.Ok, Kim, C. J., and Kim, Gi J. (2020). Alteration of fatty acid oxidation by increased CPT1A on replicative senescence of placenta-derived mesenchymal stem cells. *Stem Cell. Res. Ther.* 11 (1), 1. doi:10.1186/s13287-019-1471-y

Shen, J., Zhu, X., and Liu, H. (2020). MiR-483 induces senescence of human adipose-derived mesenchymal stem cells through IGF1 inhibition. *Aging-Us* 12 (15), 15756–15770. doi:10.18632/aging.103818

Shi, L., Zhao, Y., Fei, C., Guo, J., Jia, Y., Wu, D., et al. (2019). Cellular senescence induced by S100A9 in mesenchymal stromal cells through NLRP3 inflammasome activation. *Aging-Us* 11 (21), 9626–9642. doi:10.18632/aging.102409

Sim, S. W., Weinstein, D. A., Lee, Y. M., and Jun, H. S. (2020). Glycogen storage disease type Ib: role of glucose-6-phosphate transporter in cell metabolism and function. *FEBS Lett.* 594 (1), 3–18. doi:10.1002/1873-3468.13666

Siraj, Y., Galderisi, U., and Alessio, N. (2023). Senescence induces fundamental changes in the secretome of mesenchymal stromal cells (MSCs): implications for the therapeutic use of MSCs and their derivates. *Front. Bioeng. Biotechnol.* 11, 1148761. doi:10.3389/fbioe.2023.1148761

Soares, R. O. S., Losada, D. M., Jordani, M. C., Evora, P., and Castro-e-Silva, O. (2019). Ischemia/reperfusion injury revisited: an overview of the latest pharmacological strategies. *Int. J. Mol. Sci.* 20 (20), 5034. doi:10.3390/ijms20205034

Sokal, E. M., Lombard, C., and Mazza, G. (2015). Mesenchymal stem cell treatment for hemophilia: a review of current knowledge. *J. Thromb. Haemost.* 13 (Suppl. 1), S161–S166. doi:10.1111/jth.12933

Specchio, N., Ferretti, A., Trivisano, M., Pietrafusa, N., Pepi, C., Calabrese, C., et al. (2021). Neuronal ceroid lipofuscinosis: potential for targeted therapy. *Drugs* 81 (1), 101–123. doi:10.1007/s40265-020-01440-7

Sui, B., Hu, C., and Jin, Y. (2016). Mitochondrial metabolic failure in telomere attrition-provoked aging of bone marrow mesenchymal stem cells. *Biogerontology* 17 (2), 267–279. doi:10.1007/s10522-015-9609-5

Sun, F., Sun, Y., Wu, F., Xu, W., and Qian, H. (2022a). Mesenchymal stem cell-derived extracellular vesicles: a potential therapy for diabetes mellitus and diabetic complications. *Pharmaceutics* 14 (10), 2208. doi:10.3390/pharmaceutics14102208

Sun, S., Xie, F., Xu, X., Cai, Q., Zhang, Q., Cui, Z., et al. (2018). Advanced oxidation protein products induce S-phase arrest of hepatocytes via the ROS-dependent, beta-catenin-CDK2-mediated pathway. *Redox Biol.* 14, 338–353. doi:10.1016/j.redox.2017.09.011

Sun, Y., Zhang, H., Qiu, T., Liao, L., and Su, X. (2023). Epigenetic regulation of mesenchymal stem cell aging through histone modifications. *Genes. Dis.* 10 (6), 2443–2456. doi:10.1016/j.gendis.2022.10.030

Sun, Z., Hou, X., Zhang, J., Li, J., Wu, P., Yan, L., et al. (2022b). Diagnostic and therapeutic roles of extracellular vesicles in aging-related diseases. *Oxidative Med. Cell. Longev.* 2022, 6742792. doi:10.1155/2022/6742792

Tan, L., Liu, X., Dou, H., and Hou, Y. (2022). Characteristics and regulation of mesenchymal stem cell plasticity by the microenvironment - specific factors involved in the regulation of MSC plasticity. *Genes. Dis.* 9 (2), 296–309. doi:10.1016/j.gendis.2020.10.006

Tencerova, M., Frost, M., Figeac, F., Nielsen, T. K., Ali, D., Lauterlein, J.-J. L., et al. 2019. "Obesity-associated hypermetabolism and accelerated senescence of bone marrow stromal stem cells suggest a potential mechanism for bone fragility." *Cell. Rep.* 27 (7): 2050–2062. doi:10.1016/j.celrep.2019.04.066

Tian, D., Liu, J., Chen, L., Zhu, B., and Jing, J. (2020). The protective effects of PI3K/Akt pathway on human nucleus pulposus mesenchymal stem cells against hypoxia and nutrition deficiency. *J. Orthop. Surg. Res.* 15 (1), 29. doi:10.1186/s13018-020-1551-9

Trani, J. P., Chevalier, R., Caron, L., El Yazidi, C., Broucqsault, N., Toury, L., et al. (2022). Mesenchymal stem cells derived from patients with premature aging syndromes display hallmarks of physiological aging. *Life Sci. Alliance* 5 (12), e202201501. doi:10.26508/lsa.202201501

Truong, N. C., Bui, K. H. T., and Pham, P. V. 2019. "Characterization of senescence of human adipose-derived stem cells after long-term expansion." In *Tissue engineering and regenerative medicine*, edited by P. VanPham, 109–128.

Vanegas, N.-D. P., Ruiz-Aparicio, P. F., Uribe, G. I., Adriana, L.-B., and Vernot, J.-P. (2021). Leukemia-induced cellular senescence and stemness alterations in mesenchymal

stem cells are reversible upon withdrawal of B-cell acute lymphoblastic leukemia cells. *Int. J. Mol. Sci.* 22 (15), 8166. doi:10.3390/ijms22158166

Varderidou-Minasian, S., and Lorenowicz, M. J. (2020). Mesenchymal stromal/stem cell-derived extracellular vesicles in tissue repair: challenges and opportunities. *Theranostics* 10 (13), 5979–5997. doi:10.7150/thno.40122

Venkatachalam, K., Venkatesan, B., Valente, A. J., Melby, P. C., Nandish, S., Reusch, J. E., et al. (2009). WISP1, a pro-mitogenic, pro-survival factor, mediates tumor necrosis factor-alpha (TNF-alpha)-stimulated cardiac fibroblast proliferation but inhibits TNF-alpha-induced cardiomyocyte death. *J. Biol. Chem.* 284 (21), 14414–14427. doi:10.1074/jbc.M809757200

Vernot, J.-P., Bonilla, X., Rodriguez-Pardo, V., and Vanegas, N.-D. P. (2017). Phenotypic and functional alterations of hematopoietic stem and progenitor cells in an *in vitro* leukemia-induced microenvironment. *Int. J. Mol. Sci.* 18 (2), 199. doi:10.3390/ijms18020199

Vida, C., Martinez de Toda, I., Cruces, J., Garrido, A., Gonzalez-Sanchez, M., and De la Fuente, M. (2017). Role of macrophages in age-related oxidative stress and lipofuscin accumulation in mice. *Redox Biol.* 12, 423–437. doi:10.1016/j.redox.2017.03.005

Wang, F., Guo, J., Wang, S., Wang, Y., Chen, J., Hu, Y., et al. (2022b). B-cell lymphoma-3 controls mesenchymal stem cell commitment and senescence during skeletal aging. *Clin. Transl. Med.* 12 (7), e955. doi:10.1002/ctm2.955

Wang, F. X., Guo, J. W., Wang, S. C., Wang, Y. L., Chen, J., Hu, Y., et al. (2022a). B-cell lymphoma-3 controls mesenchymal stem cell commitment and senescence during skeletal aging. *Clin. Transl. Med.* 12 (7), e955. doi:10.1002/ctm2.955

Wang, H., Sun, Y., Pi, C., Xiao, Yu, Gao, X., Zhang, C., et al. (2022c). Nicotinamide mononucleotide supplementation improves mitochondrial dysfunction and rescues cellular senescence by NAD+/Sirt3 pathway in mesenchymal stem cells. *Int. J. Mol. Sci.* 23 (23), 14739. doi:10.3390/ijms232314739

Wang, S., Wang, Z., Su, H., Chen, F., Ma, M., Yu, W., et al. (2021a). Effects of long-term culture on the biological characteristics and RNA profiles of human bone-marrow-derived mesenchymal stem cells. *Mol. Ther. Nucleic Acids* 26, 557–574. doi:10.1016/j.omtn.2021.08.013

Wang, X., Bootsma, H., Kroese, F., Dijkstra, G., and Pringle, S. (2020). Senescent stem and transient amplifying cells in Crohn's disease intestine. *Inflamm. Bowel Dis.* 26 (2), E8–E9. doi:10.1093/ibd/izz295

Wang, X., Ma, L., Pei, X., Wang, H., Tang, X., Pei, J. F., et al. (2022d). Comprehensive assessment of cellular senescence in the tumor microenvironment. *Brief. Bioinform* 23 (3), bbac118. doi:10.1093/bib/bbac118

Wang, Y., Sui, Y., Lian, A., Han, X., Liu, F., Zuo, K., et al. (2021b). PBX1 attenuates hair follicle-derived mesenchymal stem cell senescence and apoptosis by alleviating reactive oxygen species-mediated DNA damage instead of enhancing DNA damage repair. *Front. Cell. Dev. Biol.* 9, 739868. doi:10.3389/fcell.2021.739868

Ward, M. M., Deodhar, A., Gensler, L. S., Dubreuil, M., Yu, D., Khan, M. A., et al. (2019). 2019 update of the American College of rheumatology/spondylitis association of America/spondyloarthritis research and treatment network recommendations for the treatment of ankylosing spondylitis and nonradiographic axial spondyloarthritis. *Arthritis & Rheumatology* 71 (10), 1599–1613. doi:10.1002/art.41042

Watson, J. D. (1972). Origin of concatemeric T7 DNA. *Nat. New Biol.* 239 (94), 197–201. doi:10.1038/newbio239197a0

Weilner, S., Schraml, E., Wieser, M., Messner, P., Schneider, K., Wassermann, K., et al. (2016). Secreted microvesicular miR-31 inhibits osteogenic differentiation of mesenchymal stem cells. *Aging Cell.* 15 (4), 744–754. doi:10.1111/acel.12484

Weng, Z., Wang, Y., Ouchi, T., Liu, H., Qiao, X., Wu, C., et al. (2022). Mesenchymal stem/stromal cell senescence: hallmarks, mechanisms, and combating strategies. *Stem Cells Transl. Med.* 11 (4), 356–371. doi:10.1093/stcltm/szac004

Weng, Z., Zhang, B., Wu, C., Yu, F., Han, B., Li, B., et al. (2021). Therapeutic roles of mesenchymal stem cell-derived extracellular vesicles in cancer. *J. Hematol. Oncol.* 14 (1), 136. doi:10.1186/s13045-021-01141-y

Wieliczko, M., and Matuszkiewicz-Rowinska, J. (2017). Systemic lupus erythematosus - news 2017. *Wiadomosci Lek.* 70 (2), 1201–1204.

Wong, P. F., Dharmani, M., and Ramasamy, T. S. (2023). Senotherapeutics for mesenchymal stem cell senescence and rejuvenation. *Drug Discov. Today* 28 (1), 103424. doi:10.1016/j.drudis.2022.103424

Wu, J. H., Lin, T., Gao, Y., Li, X. M., Yang, C., Zhang, K., et al. (2022). Long noncoding RNA ZFAS1 suppresses osteogenic differentiation of bone marrow-derived mesenchymal stem cells by upregulating miR-499-EPHA5 axis. *Mol. Cell. Endocrinol.* 539, 111490. doi:10.1016/j.mce.2021.111490

Wu, K. K. (2021). Control of mesenchymal stromal cell senescence by tryptophan metabolites. *Int. J. Mol. Sci.* 22 (2), 697. doi:10.3390/ijms22020697

Xia, C., Jiang, T. Y., Wang, Y. H., Chen, X. T., Hu, Y., and Gao, Y. H. (2021). The p53/miR-145a Axis promotes cellular senescence and inhibits osteogenic differentiation by targeting cbfb in mesenchymal stem cells. *Front. Endocrinol.* 11, 609186. doi:10.3389/fendo.2020.609186

Xiang, Q.-yan, Tian, F., Du, X., Xu, J., Zhu, L.-yuan, Guo, L.-ling, et al. (2020). Postprandial triglyceride-rich lipoproteins-induced premature senescence of adipose-derived mesenchymal stem cells via the SIRT1/p53/Ac-p53/p21 axis through oxidative mechanism. *Aging-Us* 12 (24), 26080–26094. doi:10.18632/aging.202298

Xiao, F., Peng, J., Yang, Li, Zhou, X., Ding, Ma, Dai, L., et al. (2022). Small noncoding RNAome changes during human bone marrow mesenchymal stem cells senescence *in vitro*. *Front. Endocrinol.* 13, 808223. doi:10.3389/fendo.2022.808223

Xing, J., Ying, Y., Mao, C., Liu, Y., Wang, T., Zhao, Q., et al. (2018). Hypoxia induces senescence of bone marrow mesenchymal stem cells via altered gut microbiota. *Nat. Commun.* 9, 2020. doi:10.1038/s41467-018-04453-9

Xu, L., Wang, Y., Wang, J., Zhai, J., Ren, L., and Zhu, G. (2021). Radiation-induced osteocyte senescence alters bone marrow mesenchymal stem cell differentiation potential via paracrine signaling. *Int. J. Mol. Sci.* 22 (17), 9323. doi:10.3390/ijms22179323

Xu, M., Pirtskhalava, T., Farr, J. N., Weigand, B. M., Palmer, A. K., Weivoda, M. M., et al. 2018. "Senolytics improve physical function and increase lifespan in old age." *Nat. Med.* 24 (8):1246–1256. doi:10.1038/s41591-018-0092-9

Yamaguchi, S., Horie, N., Satoh, K., Ishikawa, T., Mori, T., Maeda, H., et al. (2018). Age of donor of human mesenchymal stem cells affects structural and functional recovery after cell therapy following ischaemic stroke. *J. Cereb. Blood Flow Metabolism* 38 (7), 1199–1212. doi:10.1177/0271678x17731964

Yang, C., Luo, M., Chen, Y., You, M., and Chen, Q. (2021). MicroRNAs as important regulators mediate the multiple differentiation of mesenchymal stromal cells. *Front. Cell. Dev. Biol.* 9, 619842. doi:10.3389/fcell.2021.619842

Yang, C., Yang, Y., Ma, Li, Zhang, G.-X., Shi, F.-D., Yan, Y., et al. (2019). Study of the cytological features of bone marrow mesenchymal stem cells from patients with neuromyelitis optica. *Int. J. Mol. Med.* 43 (3), 1395–1405. doi:10.3892/ijmm.2019.4056

Yang, G., Fan, X., Liu, Y., Jie, P., Mazhar, M., Liu, Y., et al. (2023). Immunomodulatory mechanisms and therapeutic potential of mesenchymal stem cells. *Stem Cell. Rev. Rep.* 19 (5), 1214–1231. doi:10.1007/s12015-023-10539-9

Yang, M., Chen, J., and Chen, Li (2022). The roles of mesenchymal stem cell-derived exosomes in diabetes mellitus and its related complications. *Front. Endocrinol.* 13, 1027686. doi:10.3389/fendo.2022.1027686

Yang, M., Tong, W., Chen, H., Deng, J., Yang, C., and Zhang, Z. (2018a). Knockdown of insulin-like growth factor 1 exerts a protective effect on hypoxic injury of aged BM-MSCs: role of autophagy. *Stem Cell. Res. Ther.* 9, 284. doi:10.1186/s13287-018-1028-5

Yang, Y. K., Ogando, C. R., Wang See, C., Chang, T. Y., and Barabino, G. A. (2018b). Changes in phenotype and differentiation potential of human mesenchymal stem cells aging *in vitro*. *Stem Cell. Res. Ther.* 9 (1), 131. doi:10.1186/s13287-018-0876-3

Ye, C., Zhang, W., Hang, K., Chen, Mo, Hou, W., Chen, J., et al. (2019). Extracellular IL-37 promotes osteogenic differentiation of human bone marrow mesenchymal stem cells via activation of the PI3K/AKT signaling pathway. *Cell. Death Dis.* 10, 753. doi:10.1038/s41419-019-1904-7

Ye, G., Xie, Z., Zeng, H., Wang, P., Li, J., Zheng, G., et al. (2020). Oxidative stress-mediated mitochondrial dysfunction facilitates mesenchymal stem cell senescence in ankylosing spondylitis. *Cell. Death Dis.* 11 (9), 775. doi:10.1038/s41419-020-02993-x

Ye, M., Huang, X., Wu, Q., and Liu, F. (2023). Senescent stromal cells in the tumor microenvironment: victims or accomplices? *Cancers (Basel)* 15 (7), 1927. doi:10.3390/cancers15071927

Yi, L., Ju, Y., He, Y., Yin, X., Xu, Ye, and Weng, T. (2021). Intraperitoneal injection of Desferal® alleviated the age-related bone loss and senescence of bone marrow stromal cells in rats. *Stem Cell. Res. Ther.* 12 (1), 45. doi:10.1186/s13287-020-02112-9

Yi, S., Lin, K., Jiang, T., Shao, W., Huang, C., Jiang, B., et al. (2020). NMR-based metabonomic analysis of HUVEC cells during replicative senescence. *Aging-Us* 12 (4), 3626–3646. doi:10.18632/aging.102834

Yin, M., Zhang, Y., Yu, H., and Xia, Li (2021a). Role of hyperglycemia in the senescence of mesenchymal stem cells. *Front. Cell. Dev. Biol.* 9, 665412. doi:10.3389/fcell.2021.665412

Yin, Y., Chen, H., Wang, Y., Zhang, L., and Wang, X. (2021b). Roles of extracellular vesicles in the aging microenvironment and age-related diseases. *J. Extracell. Vesicles* 10 (12), e12154. doi:10.1002/jev2.12154

Yin, Y., Chen, H., Wang, Y., Zhang, L., and Wang, X. (2021c). Roles of extracellular vesicles in the aging microenvironment and age-related diseases. *J. Extracell. Vesicles* 10 (12), e12154. doi:10.1002/jev2.12154

Yu, X., Sun, H., Gao, X., Zhang, C., Sun, Y., Wang, H., et al. (2022a). A comprehensive analysis of age-related metabolomics and transcriptomics reveals metabolic alterations in rat bone marrow mesenchymal stem cells. *Aging (Albany NY)* 14 (2), 1014–1032. doi:10.18632/aging.203857

Yu, X., Sun, H., Gao, X., Zhang, C., Sun, Y., Wang, H., et al. (2022b). A comprehensive analysis of age-related metabolomics and transcriptomics reveals metabolic alterations in rat bone marrow mesenchymal stem cells. *Aging-Us* 14 (2), 1014–1032. doi:10.18632/aging.203857

Zeng, L., Lindstrom, M. J., and Smith, J. A. (2011). Ankylosing spondylitis macrophage production of higher levels of interleukin-23 in response to lipopolysaccharide without induction of a significant unfolded protein response. *Arthritis Rheum.* 63 (12), 3807–3817. doi:10.1002/art.30593

Zhai, W., Tan, J., Russell, T., Chen, S., McGonagle, D., Win Naing, M., et al. (2021). Multi-pronged approach to human mesenchymal stromal cells senescence quantification with a focus on label-free methods. *Sci. Rep.* 11 (1), 1054. doi:10.1038/s41598-020-79831-9

Zhang, B., Zhang, J., Zhu, D., and Kong, Ye (2019). Mesenchymal stem cells rejuvenate cardiac muscle after ischemic injury. *Aging-Us* 11 (1), 63–72. doi:10.18632/aging.101718

Zhang, J., Feng, Z., Wei, J., Yu, Y., Luo, J., Zhou, J., et al. (2018). Repair of critical-sized mandible defects in aged rat using hypoxia preconditioned BMSCs with up-regulation of hif-1α. *Int. J. Biol. Sci.* 14 (4), 449–460. doi:10.7150/ijbs.24158

Zhang, L., Chi, Y., Wei, Y., Zhang, W., Wang, F., Zhang, L., et al. (2021a). Bone marrow-derived mesenchymal stem/stromal cells in patients with acute myeloid leukemia reveal transcriptome alterations and deficiency in cellular vitality. *Stem Cell. Res. Ther.* 12 (1), 365. doi:10.1186/s13287-021-02444-0

Zhang, L., Zhao, Q., Hui, C., Wang, Z., Hu, X., Pan, R., et al. (2022a). Acute myeloid leukemia cells educate mesenchymal stromal cells toward an adipogenic differentiation propensity with leukemia promotion capabilities. *Adv. Sci.* 9 (16), 2105811. doi:10.1002/advs.202105811

Zhang, M., Johnson-Stephenson, T. K., Wang, W., Wang, Y., Jing, Li, Li, L., et al. (2022b). Mesenchymal stem cell-derived exosome-educated macrophages alleviate systemic lupus erythematosus by promoting efferocytosis and recruitment of IL-17(+) regulatory T cell. *Stem Cell. Res. Ther.* 13 (1), 484. doi:10.1186/s13287-022-03174-7

Zhang, P., Zhang, H., Lin, J., Xiao, T., Xu, R., Fu, Yu, et al. (2020). Insulin impedes osteogenesis of BMSCs by inhibiting autophagy and promoting premature senescence via the TGF-beta 1 pathway. *Aging-Us* 12 (3), 2084–2100. doi:10.18632/aging.102723

Zhang, Y., Ravikumar, M., Ling, L., Nurcombe, V., and Cool, S. M. (2021b). Age-related changes in the inflammatory status of human mesenchymal stem cells: implications for cell therapy. *Stem Cell. Rep.* 16 (4), 694–707. doi:10.1016/j.stemcr.2021.01.021

Zheng, X., Wang, Q., Xie, Z., and Li, J. (2021). The elevated level of IL-1α in the bone marrow of aged mice leads to MSC senescence partly by down-regulating Bmi-1. *Exp. Gerontol.* 148, 111313. doi:10.1016/j.exger.2021.111313

Zheng, Y., Wu, S., Ke, H., Peng, S., and Hu, C. (2023). Secretion of IL-6 and IL-8 in the senescence of bone marrow mesenchymal stem cells is regulated by autophagy via FoxO3a. *Exp. Gerontol.* 172, 112062. doi:10.1016/j.exger.2022.112062

Zhou, H., He, Y., Xiong, W., Jing, S., Duan, X., Huang, Z., et al. (2023). MSC based gene delivery methods and strategies improve the therapeutic efficacy of neurological diseases. *Bioact. Mater* 23, 409–437. doi:10.1016/j.bioactmat.2022.11.007

Zhou, T., Yan, Y., Zhao, C., Xu, Y., Wang, Q., and Xu, Na (2019). Resveratrol improves osteogenic differentiation of senescent bone mesenchymal stem cells through inhibiting endogenous reactive oxygen species production via AMPK activation. *Redox Rep.* 24 (1), 62–69. doi:10.1080/13510002.2019.1658376

Zhu, Y., Tchkonia, T., Pirtskhalava, T., Gower, A. C., Ding, H., Giorgadze, N., et al. (2015). The Achilles' heel of senescent cells: from transcriptome to senolytic drugs. *Aging Cell.* 14 (4), 644–658. doi:10.1111/acel.12344

Zhuang, X., Hu, X., Zhang, S., Li, X., Yuan, X., and Wu, Y. (2022). Mesenchymal stem cell-based therapy as a new approach for the treatment of systemic sclerosis. *Clin. Rev. Allergy Immunol.* 64, 284–320. doi:10.1007/s12016-021-08892-z

frontiers | Frontiers in Cell and Developmental Biology

TYPE Original Research
PUBLISHED 06 November 2024
DOI 10.3389/fcell.2024.1478757

OPEN ACCESS

EDITED BY
Mustapha Najimi,
Institute of Experimental and Clinical Research-UCLouvain, Belgium

REVIEWED BY
Sebastien Sart,
Institut Pasteur, France
Jorge A. Piedrahita,
North Carolina State University, United States

*CORRESPONDENCE
Julia Metzger,
julia.metzger@tiho-hannover.de

RECEIVED 10 August 2024
ACCEPTED 28 October 2024
PUBLISHED 06 November 2024

CITATION
Khaveh N, Buschow R and Metzger J (2024) Deciphering transcriptome patterns in porcine mesenchymal stem cells promoting phenotypic maintenance and differentiation by key driver genes.
Front. Cell Dev. Biol. 12:1478757.
doi: 10.3389/fcell.2024.1478757

Deciphering transcriptome patterns in porcine mesenchymal stem cells promoting phenotypic maintenance and differentiation by key driver genes

Nadia Khaveh[1,2], René Buschow[3] and Julia Metzger[1,2]*

[1]Institute of Animal Genomics, University of Veterinary Medicine Hannover, Hannover, Germany, [2]Research Group Veterinary Functional Genomics, Max Planck Institute for Molecular Genetics, Berlin, Germany, [3]Microscopy and Cryo-Electron Microscopy Facility, Max Planck Institute for Molecular Genetics, Berlin, Germany

Mesenchymal stem cells (MSC) are fibroblast-like non-hematopoietic cells with self-renewal and differentiation capacity, and thereby great potential in regeneration and wound healing. MSC populations are heterogeneous not only inherently, but also among different model species. In particular, porcine MSC serve as a frequently used resource for translational research, due to pigs' distinctive closeness to human anatomy and physiology. However, information on gene expression profiles from porcine MSC and its dynamics during differentiation is sparse, especially with regard to cell surface and inner cell markers. In this study, we investigated the transcriptome of bone marrow-derived MSC and its differentiated cell types in a minipig breed for experimental research, known as Mini-LEWE, using bulk mRNA sequencing. Our data highlighted Rap1 signaling and downstream pathways PI3K-Akt and MAPK signaling as potential players for the maintenance of stemness of BM-MSC. In addition, we were able to link the process of differentiation to changes in the regulation of actin cytoskeleton. A total of 18 "BM-MSC differentiation driver markers" were identified, potentially promoting the process of differentiation into adipocytes, chondrocytes as well as osteocytes. Our results offer a new perspective on the molecular phenotype of porcine BM-MSC and the transcriptional responses in new differentiated progeny.

KEYWORDS

mesenchymal stem cells, bone marrow, transcriptome, RNA-seq, pig, Mini-Lewe, differentiation

1 Introduction

Mesenchymal stem cells (MSC) are adult stem cells with characteristic proliferative and differentiation capacities (Friedenstein et al., 1970; Tavassoli and Crosby, 1968; Caplan, 1991). Research goes back to a long history of studies on the multipotency and mesengenesis of these mesenchymal stromal cells and their potential use for wound healing, immunomodulation and regenerative medicine (Caplan, 1994; Caplan, 1995; Horwitz et al., 2005). One of the common sources of MSC is non-hematopoietic cell population of the bone marrow, contributing to tissue homeostasis, immune regulation and tissue

repair along with immune cells (Le Blanc and Ringden, 2007; Kfoury and Scadden, 2015; Sangiorgi and Panepucci, 2016).

MSC populations are known to be inherently heterogeneous and show different phenotypic and behavioural subtypes (Mets and Verdonk, 1981). In addition, subtle yet significant diversity is found in MSC from different tissue- and species sources, sampling procedures and culture conditions (Costa et al., 2021; Dominici et al., 2006). However, there are several MSC-specific characteristics common in all cultured MSC populations, namely their adherence to plastic surface, the ability to multilineage differentiate to adipocytes, osteocytes, chondrocytes *in vitro* as well as the expression of specific surface antigens (Dominici et al., 2006; Choudhery et al., 2022). In human, bone-marrow derived MSC (BM-MSC) were found to present the surface "cluster of differentiation" (CD) markers CD29, CD44, CD73, CD90 and CD105 in more than 95% of the cell population, and CD14 (CD11b), CD34, CD45, CD19 (or CD79α), and HLA-DR in less than 2% of cell population (Dominici et al., 2006; Choudhery et al., 2022). However, in animal models, the composition of cell surface markers is slightly different: For example, cultured BM-MSC from horses were shown to express CD29, CD44, CD90, CD105, CD166 and but lack CD34, CD45 and CD79α expression (Bundgaard et al., 2018). Similarly, in bovine BM-MSC, transcriptomic profiles suggested CD29, CD44 and CD73 to be highly expressed, whereas CD90 as one of the strongest MSC-indicators, held no and/or lower expression in comparison to human and horse MSC (Kato et al., 2004; Danev et al., 2024). It was demonstrated that bovine BM-MSCs share more common functionally relevant gene expression profiles with human BM-MSCs than compared to murine BM-MSCs and thus highlighted the particular potential of non-murine cells for translational studies (Danev et al., 2024). With regard to the surface marker CD105 in bovine BM-MSC, its role was controversially discussed as it was either found to be not highly expressed or missing (Kato et al., 2004; Danev et al., 2024). Similar findings were made for porcine BM-MSC, which were proposed to strongly express CD29, CD90, and CD44, but were found to have a lower CD105 expression compared to human BM-MSC, and no CD45 expression (Juhásova et al., 2011; Prinz, 2017). In contrast, in another study, the complete absence of CD73 and CD105 expression in porcine BM-MSC was highlighted and underlined the need for further investigations on the characteristics of these cells (Schweizer et al., 2020). Despite these studies reporting on selected markers, a full list of potential marker genes remains elusive. For successful detection, it was proposed that high throughput sequencing of RNA helps to improve stem cell characterization, which is otherwise limited due to the absence of appropriate antibodies against markers for various selected species (Dawson and Lunney, 2018). Subsequently, RNA sequencing was successfully applied for defining cell-specific mRNA expression to interrogate the spectrum of cell surface proteins, known as the surfaceome (Pais et al., 2019)

Pigs represent a particular valuable non-primate model for translational and clinical medicine to target disease, cell therapy, immunomodulation, regeneration and xenotransplantation, due to its similarities to human anatomy and physiology, and its relatively short as well as seasonal-independent gestation time (Lee et al., 2007; Krupa et al., 2007; Walters and Prather, 2013; Hatsushika et al., 2014; Khatri et al., 2015; Kawamura et al., 2015; Ock et al., 2016; Tseng et al., 2018; Fisher, 2021). Therefore, it is important to gain a comprehensible knowledge of the molecular phenotype of porcine MSC. So far, the majority of studies on the characterization of MSC relied on flow cytometry, Real-Time PCR (RT-qPCR) and microarrays. In addition, RNA sequencing approaches are used in human and few model species to not only characterize MSC, in particular BM-MSC, but also to unravel the underlying differentiation mechanisms and hierarchies (Danev et al., 2024; Roson-Burgo et al., 2014; Cho et al., 2017; Haga et al., 2024; Kanazawa et al., 2021; Zhan et al., 2019; Koch et al., 2022).

In pigs, RNA sequencing of MSC from subcutaneous adipose tissue and synovial joints was performed for different commercial large breeds in order to understand molecular mechanisms related to mesengenic formation and paracrine signaling in general, as well as to study diseases such as metabolic syndrome (Li et al., 2023; Ponsuksili et al., 2024; Conley et al., 2018; Eirin et al., 2017; Pawar et al., 2020). In a microarray analysis of MSC from Yorkshire crossbreed pigs, the transcriptome of adipose-derived and bone-marrow derived cells was compared and studied for its *in vitro* osteogenic and adipogenic differentiation (Monaco et al., 2012). It was highlighted that BM-MSC had larger angiogenic, osteogenic, migration and neurogenic capacities, presumably more suitable for specific therapeutic applications (Monaco et al., 2012). Moreover, expression profiling of porcine BM-MSC was done to study cryopreservation and treatment with histone deacetylase inhibitors to identify cellular responses related to cell stress, development and differentiation (Gurgul et al., 2017; Gurgul et al., 2018). These studies emphasized that BM-MSC represent the gold standard for its use in tissue regeneration and thereby require thorough molecular phenotyping and investigation of its differentiation processes (Monaco et al., 2012; Monaco et al., 2009).

In this research paper, our goal is to study the transcriptome profiles of BM-MSC and its differentiated cell lineages specifically in the miniature pig breed Mini-LEWE, using bulk mRNA sequencing. We aim to investigate the transcriptional expression of known or potential new candidate stem cell surface markers as well as potential intracellular markers in BM-MSC and its derivatives.

2 Material and methods

2.1 Sample collection

In this study, we obtained BM-MSC of the iliac crest of three 80-day-old Mini-LEWE piglets. The piglets underwent euthanasia in a two-step process using intramuscular injection of Azaperone (2 mg/kg) and Ketamine (20 mg/kg) and subsequent intracardial application of T61 (Tetracaine hydrochloride, Mebezonium iodine and Embutramide cocktail (6mL/50kg, MSD Tiergesundheit - Intervet Deutschland GmbH, Germany). This procedure was approved by the animal welfare officer of the University of Veterinary Medicine Hannover ("Tötungsanzeige", ID TIHO-T-2020-9), in accordance with national and international guidelines. After euthanasia, the laterofrontal of the ilium bone was exposed and a biopsy needle (Jamshidi with T-handle, Lehnecke, Germany) was used to aspirate bone marrow from the iliac crest. The aspirate was transferred to an EDTA-coated collection tube (BD vacutainer, New Jersey, United States), suspended in ice-cold CO_2-independent medium

(Gibco, New York, United States) with 2% Glutamax (Gibco), and transported to cell culture laboratory. In addition, Peripheral Blood Mononuclear Cells (PBMC), representing differentiated hematopoietic cells from bone-marrow, were used as the control samples to the non-hematopoietic undifferentiated BM-MSC. They were obtained from full progeny of the sampled pigs and proceeded into RNA isolation.

2.2 Cell isolation and culture

The acquired bone marrow samples were treated with Red Blood Cell Lysis Buffer (Roche, Basel, Switzerland) to remove the erythrocytes from the cell suspensions. Next, the samples were transferred to cell culture flask T-175 (Sarstedt, Nuembrecht, Germany) and incubated in DMEM (Gibco) with 10% Foetal Bovine Serum at 5% CO_2 and 37°C for 24 h. Then, the media were changed and cells were maintained initially in MesenPRO RS Medium (Gibco) and all further passages in Mesenchymal Stem Cell Growth Medium 2 (MSC-GM2, PromoCell, Heidelberg, Germany). Cells at passages four (P4) and five (P5) were used for differentiation and RNA isolation.

2.3 Directed differentiation of mesenchymal stem cells

BM-MSC-multipotency was tested by directed adipogenesis, chondrogenesis and osteogenesis during two consecutive passages P4 and P5. For this purpose, BM-MSCs were detached from their vessels with TrypLE Express Enzyme (1X) (Gibco), stained with Trypan Blue Solution, 0.4% (Gibco) and counted on Neubauer chamber (Roth, Karlsruhe, Germany). Next, 6×10^5 viable cells were seeded into three 10 cm^2 petri dishes (2,00,000/dish), one dish for each type of differentiation. Cells were maintained for 24 h at 5% CO_2 and 37°C in MSC-GM2 allowing them to recover and attach. Adipogenesis was induced using StemPro Adipogenesis Differentiation Kit (Gibco) for 10 days (media exchanged every second day). After differentiation, cells were maintained for another 7 days on Human Adipocyte Maintenance Media (Cell Application, San Diego, United States). Chondrogenesis was promoted using StemPro Chondrogenesis Differentiation Kit (Gibco) for 14 days and media was refreshed every second day. The differentiated chondrocytes were maintained for another 7 days on Chondrocyte Growth Medium (PromoCell). Osteogenesis was induced using Mesenchymal Stem Cell Osteogenic Differentiation Medium (PromoCell) for 24 days and the cells maintained for another 7 days in Minimum Essential Medium α, nucleosides (Gibco) containing 10% FBS and 2% Glutamax.

2.4 Staining and microscopy

After differentiation, cells from each cell type were transferred to μ-Slide 8 Well (ibidi GmbH, Graefelfing, Germany), maintained for 2 days, fixed with 4% ice-cold formaldehyde for exact 10 min at room temperature, and washed three times with distilled water. Transmitted light images of adipo-, chondro- and osteocytes were captured using the Celldiscoverer 7 (Zeiss, Oberkochen, Germany). Due to the lack of a condenser in the platform, the so-called phase gradient contrast (PGC) was utilized. The PGC images were automatically acquired with a self-adjusted aperture, so the cellular fine structures could be scanned throughout multiwall formats without edge or meniscus artefacts.

Next, the water was removed from the wells and each cell type was specifically stained. Fixed adipocytes were washed once with 60% isopropanol for 5 min, covered with filtered working Oil Red O solution (3 times stock Oil Red O (3 mg/ml) in 2 times distilled water) for 5 min at room temperature, and finally washed with distilled water until all excessive stain was removed. Fixed chondrocytes were washed once with PBS, then covered with 1% Alician blue in 0.1N HCl staining solution for 30 min at room temperature. Upon removal of the staining solution, the excess stain washed away with 0.1N HCl. Furthermore, fixed osteocytes were stained with 2% Alizarin Red solution (pH 4.2) for 3 min at room temperature, and washed with distilled water. All stained cells were maintained in 250 μL distilled water. RBG images were acquired using Axio Observer Z1 (Zeiss) equipped with RGB (red, green, and blue) camera.

2.5 RNA isolation and library preparation

In total, all three BM-MSC samples from three Mini-Lewe, six adipocyte, chondrocyte and osteocyte samples each underwent RNA isolation and library preparation (Supplementary Table S1). In addition, the RNA of three PBMC samples was isolated.

All cells were scraped from the plastic surface and resuspended in TRIzol, then transferred into innuSPEED Lysis Tubes X (Innuscreen GmbH, Berlin, Germany) for homogenization on a pre-cooled SpeedMill PLUS (Analytik Jena GmbH, Jena, Germany) for two interval steps. Subsequently, RNA isolation was performed based on TRIzol user guide provided by Invitrogen (Massachusetts, United States). The quality and integrity of the isolated RNA was controlled using a High Sensitivity RNA ScreenTape assay on 4200 TapeStation system (Agilent, Santa Clara, United States). Samples were selected for library preparation based on RNA integrity numbers (RIN) of >8 in BM-MSCs as well as >6 in PBMCs (due to a higher RNA-fragmentation rate of PBMCs in general).

2.6 RNA sequencing and data processing

RNA libraries of 24 samples (three BM-MSCs, six adipocytes, six chondrocytes, six osteocytes and three PBMCs) were prepared using NEBNext Ultra II Directional RNA Library Prep Kit for Illumina (NEB, Ipswich, United States) and Unique Dual Index Primer Pairs of NEBNext Multiplex Oligos for Illumina kit (NEB). Libraries were set in equal molarity and sequenced for 70 million reads 2 × 100 bp on an Illumina NextSeq200. The obtained data were quality controlled, pre-processed and mapped based on *Sus scrofa* 11.1 genome reference, as previously described (Khaveh et al., 2023).

2.7 Differential gene expression analysis

The raw counts of the mapped reads were extracted using the STAR *quatMode* (version 2.7.9a, (Dobin et al., 2013) and were

analysed using DESeq2 in R environment (version 1.44.0, (Love et al., 2014). Prior to differential expression analysis (DEA), preanalytical data quality control based on regularized logarithm (*rlog*) transformation and principal component analysis (PCA) was performed as recommended by Love et al. (2014). In addition, the Euclidian distance of all samples were calculated and clustered to observe their similarity and correlation. DEA was run to identify the unique transcriptome profile of Mini-Lewe BM-MSCs in contrast to PBMCs (control samples) and secondly to observe the differential transcriptomes of BM-MSCs and their differentiated cell types. Thus, six samples from each differentiated cell types (adipocytes, chondrocytes, and osteocytes) were contrasted separately with expression profile of BM-MSC as control. After the DEA for each aforementioned set, the genes with the absolute log2 fold change (|log2FC|)>2 and false discovery rate (padj) < 0.05 were considered as significantly differentially expressed. Finally, we identified and extracted gene expression patterns of cell surface markers and their differential expression information in our porcine BM-MSC and its differentiated cell lineages by comparing our dataset to a compiled list of all known CD markers (Engel et al., 2015) as well as notable MSC markers in human (Miller-Rhodes, 2023; Uder et al., 2018).

2.8 Enrichment analysis

First, the lists of differentially expressed genes (DEG) of each contrast, namely of BM-MSCs, adipocytes, chondrocytes and osteocytes, were overlapped with human orthologues acquired from Ensembl Biomart and submitted to enrichR tool (R package, version 3.2, (Chen et al., 2013; Kuleshov et al., 2016; Xie et al., 2021; Jawaid, 2023)) for enrichment with four gene-set databases "KEGG_Human_2021," "GO Biological Process 2023," "Reactome_2022" and "Jensen TISSUES." All term lists were filtered for *p*-value < 0.05. The notable pathway terms highlighted in "KEGG_Human_2021" were further investigated manually on KyotoEncyclopedia of Genes and Genomes website (KEGG: https://www.genome.jp/kegg/pathway.html) for pig (*sus scrofa*) specified pathways.

2.9 Differential exon usage

To observe the frequency of exon usage and therefore predict post-transcriptional changes BM-MSC and its derivative cell types, DEXSeq tool (version 1.50.0 (Anders et al., 2012; Reyes et al., 2013)) was used in R environment. First, the annotations of the pig reference genome from Ensembl Biomart were transformed into a TxD object using "makeTxDbFromBiomart" from GenomicFeatures package (Lawrence et al., 2013) and collapsed into counting bins. The counting bins were used to count the number of overlapping exons and read fragments from the aligned reads (Aligned.out.bam files by STAR) using "*summarizeOverlaps*" from GenomicAlignments package (Lawrence et al., 2013). At this stage, the data was split into two objects, one holding MSCs and PBMCs data and another containing MSCs and its derivative cell types. Next, the counted overlapped exons were fitted into a generalized linear model (GLM) with the formula "*~sample + exon + cell_type:exon*" normalized based on size factors estimation ("*estimateSizeFactors*") and dispersed ("*estimateDispersions*"). The interaction of condition (cell type) and exon (from aforementioned GLM) are compared on Chi squared distribution to establish a *p*-value. Finally, the data was tested for differential exon usage and exon fold changes were estimated based on samples' cell type. The result was summarised and filtered for significance threshold of |log2FC| > 2 and padj < 0.05.

2.10 Weighted gene co-expression network analysis (WGCNA)

We investigated the association of the expressed genes and their correlations with the cell type by modulating a hierarchical clustering and constructing gene networks with a high probability of co-expressing using the R package Weighted Gene Co-expression Network Analysis (WGCNA) (version 1.72-5. (Langfelder and Horvath, 2008; Langfelder and Horvath, 2012). For this purpose, the normalized and stabilized data matrix from DESeq2 analysis was used to build a topological overlapping matrix with soft-thresholding power value of three. The next step of network construction was performed following our previous suggestions (Khaveh et al., 2023). Furthermore, the correlations between each module and cell type were test using Fisher test. Genes from the significantly correlated modules were functionally enriched as described above for functional enrichment of DEGs.

2.11 Fluorescence staining and microscopy

For validation of the expression of cell surface markers and functional elements using fluorescent microscopy, we seeded 1,000 cells each cell lineage in dark-walled flat-bottomed 96 wells (Greiner Bio-One GmbH, Frickenhausen, Germany) and fixed as described above in Section 2.4. Next, the fixed cells were rinsed in PBS and permeabilized for 1 h blocked using Normal Donkey Serum Block (NDSB: 1% w/v BSA, 2% v/v Normal Donkey serum, 0.1% v/v Triton X, 0.05 v/v % Tween-20) for 30 min. Primary antibodies against CD105 (mouse anti-pig, Abcam Cat#ab53318, Cambridge, United Kingdom), CD29 (Mouse anti-pig, Cat#561496, BD Pharmingen, New Jersey, United States), CD90 (Mouse anti-pig, Cat#561972, BD Pharmingen) were diluted in 1:500 in the identical NDSB solution and incubated at 4°C overnight. Further primary antibody C7 (mouse anti-human, Proteintech Cat# 66908-1, Illinoise, United States) were diluted in 1:1,000 in NDSB, applied to the wells and incubated for 1 h at room temperature. The antibody solutions were washed out of the well by flushing the well with three times 1 × PBS. Secondary Antibodies as well as phalloidin (1 μg/mL) and Hoechst (0.5 μg/mL) were also diluted in the NDSB and incubated together in one well for 1 h at room temperature before a final flushing with three times PBS.

For evaluation of cellular protein contents (CD marker, or any endogenous content) we used Zeiss Celldiscoverer 7 running under Zen Blue 3.5. All experiment consisted several 1,000s of individual position per condition in large mosaics. The acquisitions were carried out fully automated using a surface detection strategy for stabilizing the focus position under controlled temperature. The

10.3389/fcell.2024.1478757

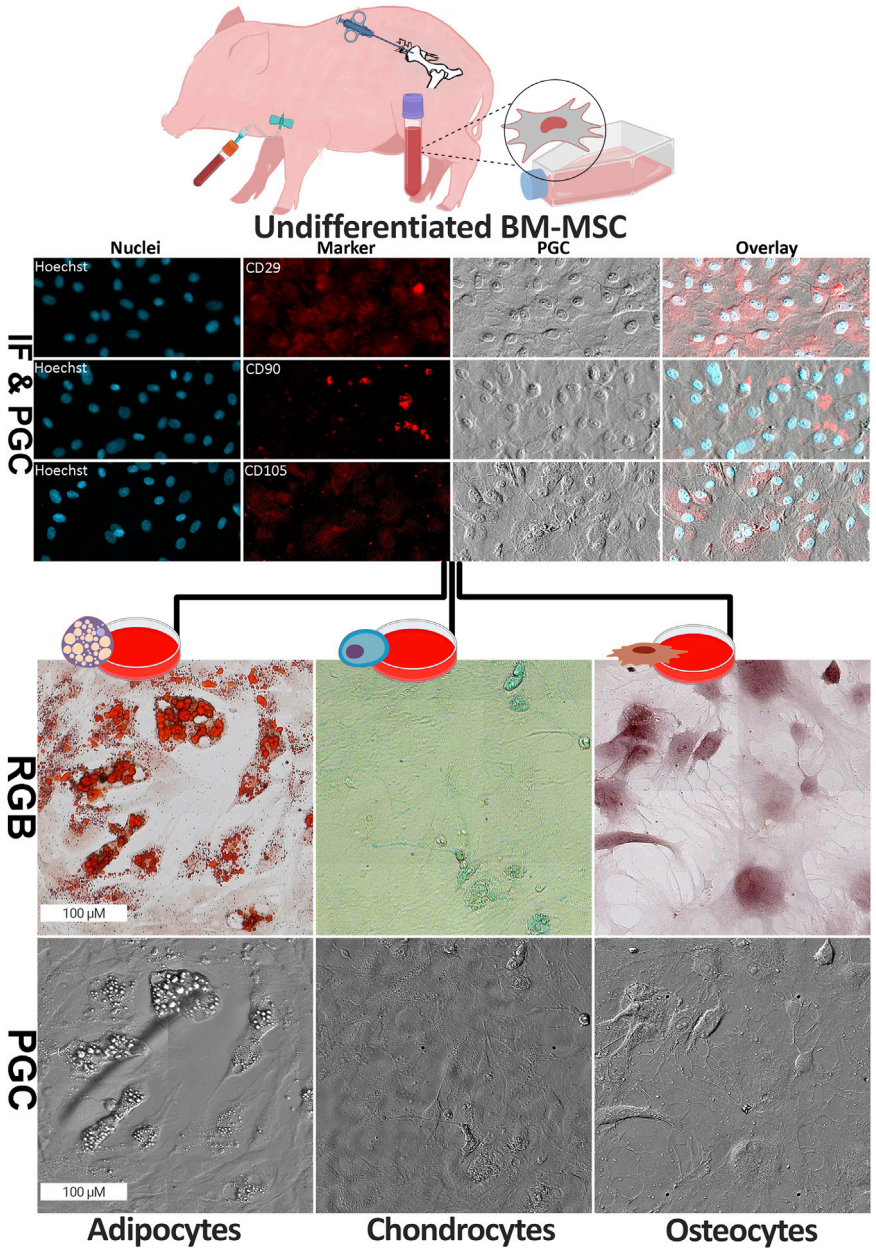

FIGURE 1
Morphology of undifferentiated and differentiated BM-MSC. (top) The formalin-fixed undifferentiated BM-MSC were investigated using phase gradient contrast (PGC) technique as well as immunofluorescence imaging (IF) for surface markers with anti-CD29, anti-CD90, anti-CD105 and counterstain (Hoechst). PGC capture of the cytoskeleton structure of these cells was done without any staining. (bottom) Successful differentiation of BM-MSC into three cell lineages, namely adipocyte, chondrocyte and osteocyte, was confirmed using cell type specific staining (Oil Red-O for adipocytes, Alician blue for chondrocytes and Alizarin Red for osteocytes; RGB = red, green and blue). In addition, changes in cell morphology were highlighted using PGC technique (Image partially created by BioRender, agreement number: VN275VWCHA).

acquisitions were carried out with a 20x, NA0.7 or 20x, NA0.95 objectives and a 1x or 2x post magnification the use camera chip was a 12 megapixel Axiocam 712. In Combination with Abbes resolution limit we had a typical lateral (XY) pixel size of 0.352 or 0.258 µm/pixel. The acquired images underwent a standard hierarchical image analysis strategy. Briefly nuclei were detected based on their fluorescence intensity, with fixed intensity thresholds, close by objects were separated by water shedding. The resulting masks were filtered towards an area in between 75 and 800 µm^2 and a circularity in between 0.6 and 1 (dimensionless). From this primary objects our routine automatically dilated 5 pixel before a secondary with a width around the nuclei of 100 pixel were drawn. Within this region the marker signals were quantified. Our fluorescence data is shown as total fluorescence intensity signal. Typically, we analyzed in between ~2,000 and 20,000 single cells per condition in more than 30 dimension. Finally, the obtained

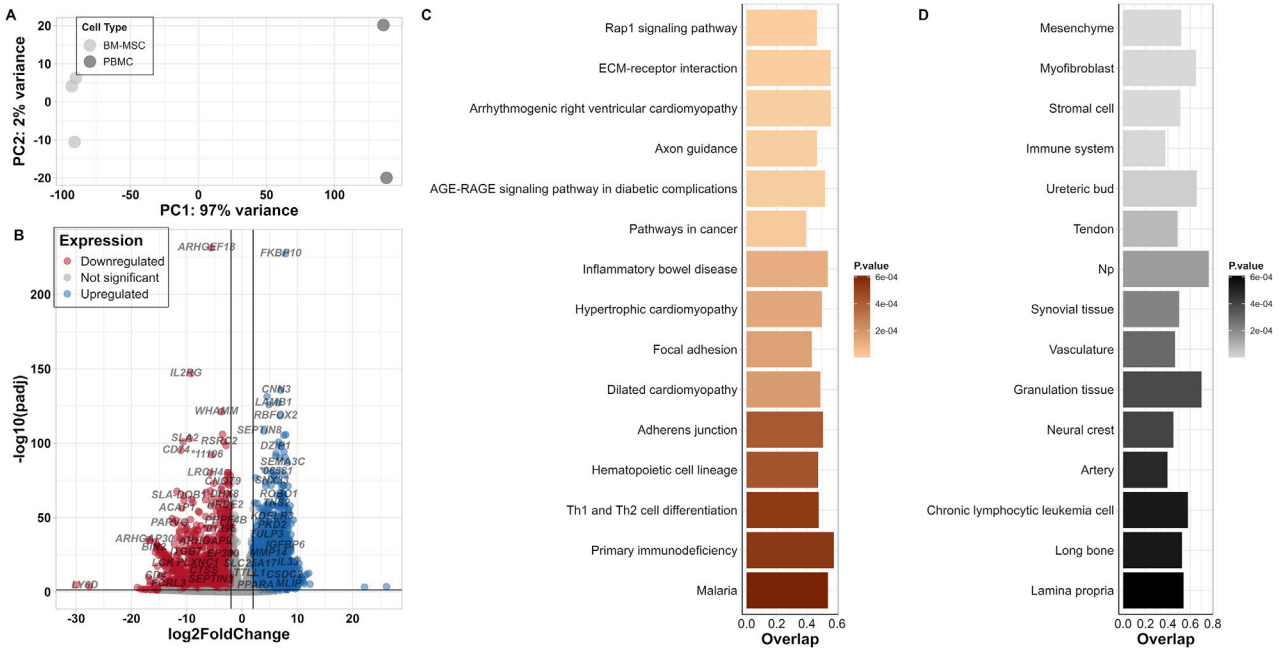

FIGURE 2
Differentially expressed genes in BM-MSC in contrast to PBMC. **(A)** PCA plot for BM-MSC and PBMC samples **(B)** Volcano plot of DEGs; log2FC is on the *x*-axis and padj on the *y*-axis (* = ENSSSCG000000). Thresholds of significance are shown on the left and right of the intersection lines. **(C)** Top 15 significant KEGG pathways (based on KEGG_Human_2021 database) and **(D)** Jensen TISSUEs displayed for their number of overlapped genes and *p*-value.

data for C7 and actin were analyzed using "ggbetweenstat" package (Patil, 2021) with parametric pairwise Welch's t-test and false discovery rate (FDR) < 0.05.

3 Results

3.1 Morphology of the undifferentiated and differentiated BM-MSC

First of all, we investigated the characteristics of the BM-MSC population using three cell surface markers, CD29, CD90 as well as CD105. The image analysis showed that all three CD markers were expressed strongly in the BM-MSC (Figure 1). Next, we aimed to validate the capacities of our approach to differentiate into osteo-, chondro- and adipocytes. Therefore, we used the well-established above described classical histological staining protocols on our differentiated cells and captured images with a contrast transmitted light strategy as well as RGB images of the identical cells in a second microscope. The undifferentiated BM-MSC were observed in small colonies and well as spread out as single cells. The cells in dense colonies had a spindle-like morphology, while the cells surrounding the colonies in less populated areas displayed a spread-out cytoplasm with a visible cytoskeleton organisation. In the adipocytes, Oil Red O stain highlighted lipid vacuoles distinctly in bright red (Figure 1). The chondrocytes' phenotype was observed with 1% Alician blue as the glycosaminoglycan became visible with fine blue signals within and surrounding the cells. In addition, osteocyte differentiation was confirmed by highlighting the calcium content of these cells stained in bright red by 2% Alizarin red stain.

3.2 Transcriptome profiles of undifferentiated BM-MSC

Cell type-specific expression profiles provide essential knowledge for cell identification and marker-based characterisation of cells *in vitro*. In our investigation of BM-MSC, we called 14,019 out of 35,670 annotated genes to be expressed based on normalised counts per million (cpm), of which 91.4% were protein-coding and 7.3% were long non-coding RNAs (lncRNA). Furthermore, the Euclidian distance test for BM-MSC showed a high dissimilarity to PBMC (Supplementary Figure S1). Each cell type displayed a clustering within its replicates. In comparison to PBMCs, BM-MSCs revealed a distinct separation on the first principal component (PC1) by 97% variance between the two groups, whereas the variance among the individual samples within each group (PC2) was less than 1% in PCA (Figure 2A). Within the transcriptome of porcine BM-MSC, we could identify 253 expressed genes out of 371 CD markers known in human.

In our DEA, we identified 6,285 DEGs within the significance threshold padj <0.05 and |log2FC| >2, of which 2,994 genes were upregulated and 3,291 were downregulated (Figure 2B; Supplementary Table S2). Furthermore, we could identify 146 DEGs from the list of human CD markers.

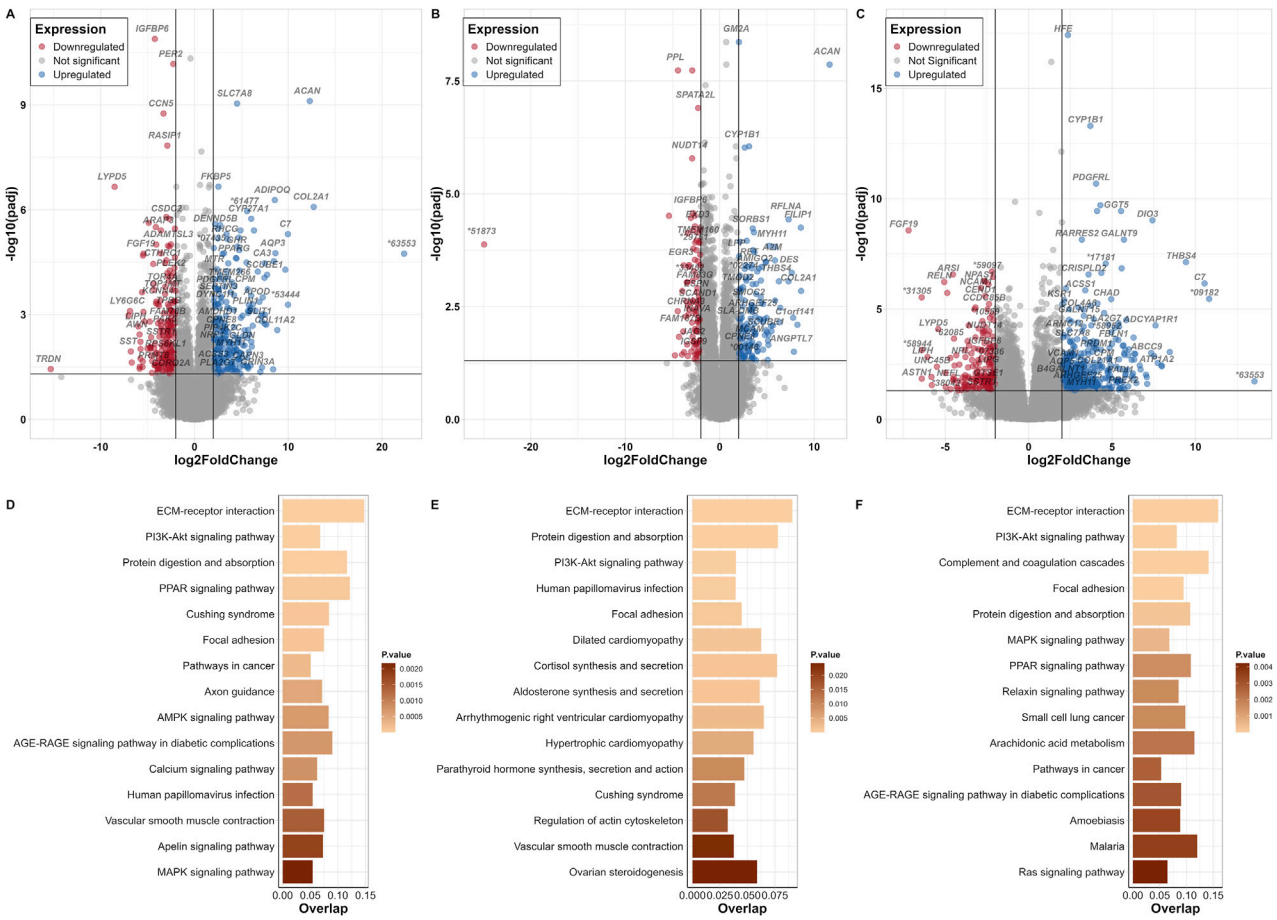

FIGURE 3
BM-MSC and its derivative cell-lineages. Volcano plots of DEGs from contrasts of **(A)** adipocyte versus BM-MSC (control), **(B)** chondrocyte versus BM-MSC (control), and **(C)** osteocyte versus BM-MSC (control) datasets; log2FC on the *x*-axis and padj on the *y*-axis (* = ENSSSCG000000). Thresholds of significance are shown on the left and right of the intersection lines. Top 15 significant KEGG pathways (based on KEGG_Human_2021 database) displayed for their number of overlapped genes and their *p*-value score for **(D)** adipocyte versus BM-MSC (control), **(E)** chondrocyte versus BM-MSC (control), and **(F)** osteocyte versus BM-MSC (control) datasets.

Enrichment analysis of DEGs for "KEGG_Human_2021" pathway revealed significantly enriched pathways such as Rap1 signalling pathway and ECM-receptor interactions (Figure 2C; Supplementary Table S3). In addition, "Jensen TISSUES" database highlighted the involvement of tissues and cells within the bone marrow referring to BM-MSCs in contrast to PBMCs such as "Mesenchyme," "Stromal cell," "Immune system" and "Chronic lymphocytic leukemia cell" (Figure 2D; Supplementary Table S3). From other two databases, "GO Biological Process 2023" and "Reactome_2022" enriched terms such as "Extracellular matrix organization (GO:0030198, R-HAS-1474244)," "Collagen fibril organization (GO:0030199)," "Collagen formation (R-HAS-1474290)," "External encapsulating structure organization (GO:0045229)," "Embryonic skeletal system development (GO:0048706)" and also immunomodulatory processes such as "Inflammatory Response (GO:0006954)," "B Cell Receptor Signaling Pathway (GO:0050853)," "Regulation Of T Cell Activation (GO:0050863)" were highlighted. In addition, gene families such as *COL*, *ADAM* and *HOX* genes were frequently observed in these clusters (Supplementary Table S3).

3.3 Mesengenic differentiation shifts transcriptome of BM-MSC

One of the widely known properties of BM-MSCs is the multipotency and the ability to differentiate into certain cell lineages, namely adipocyte, chondrocyte, and osteocyte (Caplan, 1991). In order to identify the transcriptome changes of BM-MSC after differentiation into new cell-phenotypes, we compared the different expression profiles. PCA revealed a 32% variance (PC1) among all four cell types, whereas on the PC2 dimension, the distinct separation among adipocytes, osteocytes and BM-MSC can be observed (Supplementary Figure S2).

About fifteen thousand genes were identified in adipocytes, chondrocytes and osteocytes, respectively. These included 88% protein coding genes and 10% lncRNAs in all three cell types. We identified 483 DEGs in adipocytes compared to BM-MSC, of which 259 were upregulated and 224 downregulated (Figure 3A; Supplementary Table S4). In chondrocytes, 246 DEGs (149 up- and 97 downregulated) were identified (Figure 3B; Supplementary Table S5). Furthermore, osteocytes revealed

10.3389/fcell.2024.1478757

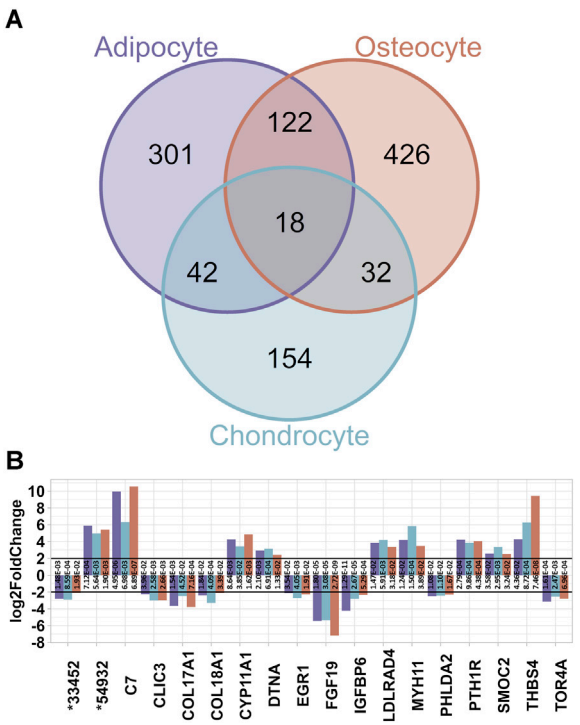

FIGURE 4
Common DEGs among the three differentiated lineages. **(A)** Venn diagram for the number of DEGs from each dataset. In total, 18 DEG are common. **(B)** Overview of the common 18 DEGs and their log2FC from all three datasets. The padj values of each test is displayed on each bar (* = ENSSSCG000000).

598 DEGs (387 up- and 211 downregulated) (Figure 3C; Supplementary Table S6).

Enrichment analysis based on "KEGG_Human_2021" pathway revealed significant common terms in all three DEG datasets such as "ECM-receptor interaction," "PI3K-Akt signalling pathway2" and "Focal adhesion" (Figures 3D–F). From other databases, terms such as such as "Mesenchyme" and "Abdominal adipose tissue," "Bone matrix" and "Adipocyte," "Fat cell differentiation (GO:0045444)," "Positive regulation of cell differentiation (GO:0045597)" and "Fatty acid transport (GO:0015908)" for adipocytes, "Long bone," "Epiphyseal growth plate" and" Chondrocyte cell line," "Skeletal system development (GO:0001501) for chondrocytes as well as "Long bone," "Mesenchyme," "Bone matrix," "Tibia," and "Osteoblast cell line" for osteocytes were highly significant (Supplementary Tables S7–S9).

Furthermore, comparisons of the three DEG lists of adipocytes, chondrocytes and osteocytes contrasted to BM-MSC revealed 301 DEGs unique for adipocytes, 426 for osteocytes and 154 for chondrocytes (Figure 4A). Additionally, 32 DEGs were detected both for chondrocytes and osteocytes, whereas 42 DEGs were called for adipocytes and chondrocytes as well, and 122 DEGs in adipocytes and osteocytes, respectively. Subsequently, 18 DEGs were common among all three datasets. These 18 DEGs showed similar pattern of up- or downregulation among all three DEG lists (Figure 4B). Interestingly, ten of these DEGs were also differentially expressed in BM-MSC compared to PBMCs. In contrast, genes such as *C7*, *MYH11*, *EGR1*, *CLIC3*, and *THBS4* were unique for the differentiated cell lineages. Among these, *C7*, *MYH11*, *THSB4* and *FGF19* were assigned to a common pathway "Regulation of actin cytoskeleton" in KEGG database (KEGG path ID: ssc04810). According to KEGG, this pathway was not only highlighted to influence PI3K-Akt and MAPK pathway, which contained several other DEGs (e.g. *FGFR2*, *PDGFRA*, and several *ITGA* genes) but was also shown to be affected by the upstream paths of "Focal adhesion signalling" (KEGG path ID: ssc04510, Figure 5).

Finally, 67 notable MSC marker genes according to our list of all known CD markers as well as notable MSC markers in human (Miller-Rhodes, 2023; Uder et al., 2018), which are not restricted to BM-MSC only, were investigated for the gene expression among our identified DEGs for their log2FCs of BM-MSC relative to PBMC as well as BM-MSC relative to adipocytes, chondrocytes or osteocytes (Figure 6). Among these markers, 21 of the analogous genes, such as *PTPRC* (CD45), *HLA-DRA* (MHC-II), *CD200* and *CD19* were downregulated in BM-MSC (in comparison with PBMCs). In contrast, 14 DEGs, including *ITGB1* (*CD29*), *Thy-1* (CD90, pig annotation: ENSSSCG00000032330), *FUT4* (CD15), *VCAM1* (CD106), *MME* (CD10), *CD70*, *NCAM1* (CD56), *NT5E* (CD73) were upregulated in BM-MSC (in comparison with PBMC). Additionally, 26 genes coding for MSC markers did not show significant differential gene expression in BM-MSC, however some markers such as *ENG* (CD105), *ITGA6* (CD49f) and *TFRC* (CD71) were close to the threshold of significance for upregulation (log2FC = 1.74 (*ENG*), 1.77 (*ITGA6*) 1.84 (*TFRC*) (Supplementary Figure S3). Furthermore, *MATN3* was upregulated in chondrocytes as well as *VCAM1* (*CD106*) in osteocytes. In contrast, we found a downregulation of *SOX11* and *MME* in osteocytes and *CD70* and *NT5E* in adipocytes.

3.4 Exon usage alterations in differentiating BM-MSC

Differential exon usage analysis was performed for the same contrasts as tested for DEGs: We called differences between BM-MSCs and PBMCs, as well as differences between BM-MSC and adipocytes, chondrocytes, or osteocytes. In total, 2,93,078 exons were aligned and counted. Among these exons, 20,507 (related to 7,126 genes) with padj < 0.05 differed in terms of exon usage in either PBMC or BM-MSCs, and 7,148 exons (related to 3,820 genes) with |l2FC|>2 were significantly differentially expressed (Supplementary Table S10).

Furthermore, exon usage analysis among adipocytes, chondrocytes, osteocytes and BM-MSCs (as control) revealed for all four groups 2,860 exons (related to 7,612 genes) with potential significant effects (padj < 0.05) on the phenotypes (Supplementary Table S11). Additionally, the exon expression was compared between each cell type to the control, resulting in 356 exons (related to 283 genes) in adipocytes, 3,346 exons (related to 2,177 genes) in chondrocytes and 2.735 exons (related to 1,810 genes) in osteocytes within the significance threshold |l2FC| >2 for differential expression of exons. Additionally, we found the three genes *C7*, *COL17A1* and *MYH11*, called as part of the group of the common 18 DEGs, in differentiated cell lineages to contain significantly differential exon usage in six (*C7*) or one (*COL17A1* and *MYH11*) exons, respectively (Figure 7).

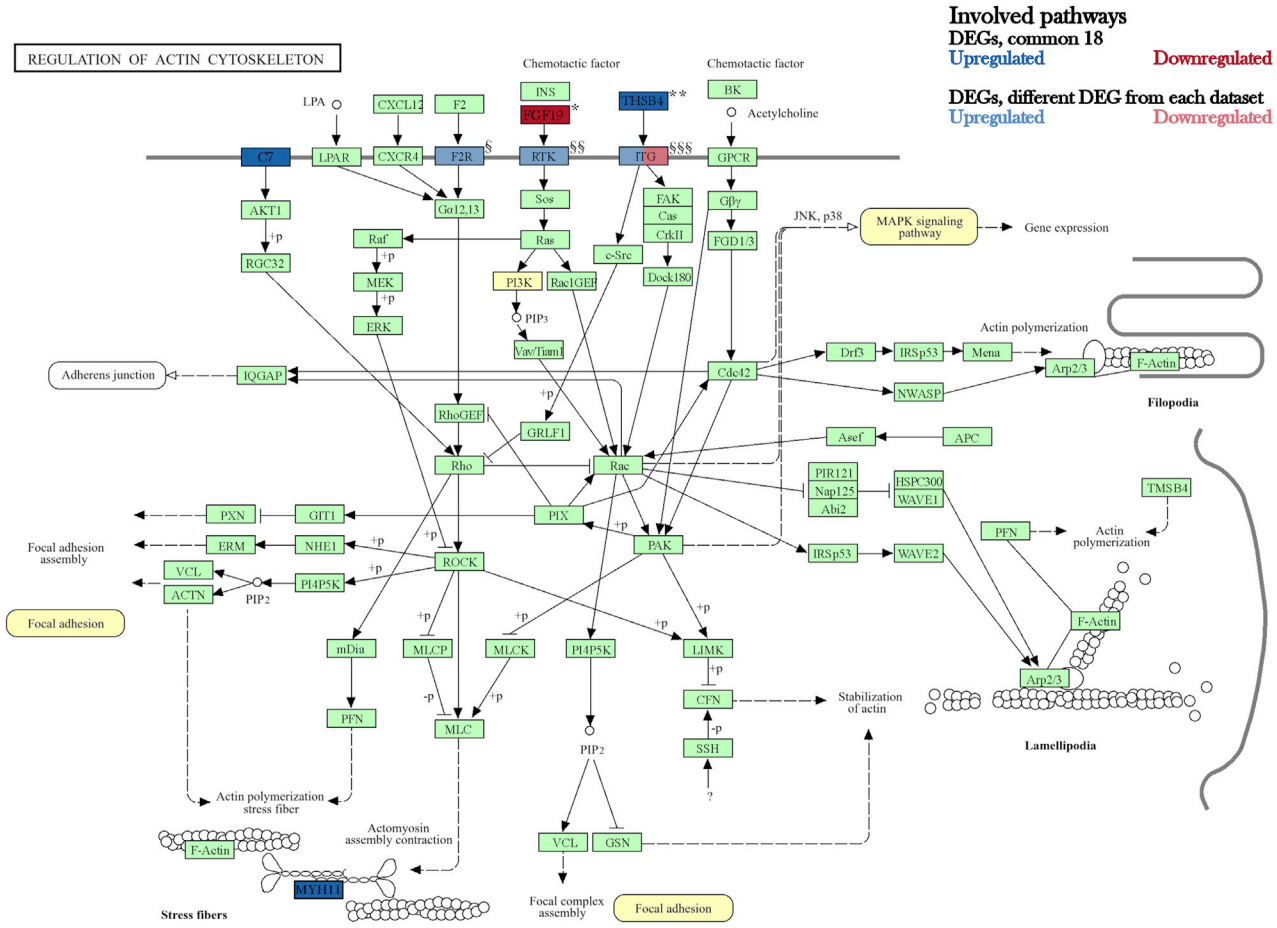

FIGURE 5
KEGG pathway "Regulation of actin cytoskeleton" (ssc04810). Modified figure according to KEGG database. The highlighted genes are DEGs observed in all three datasets. Individual gene names from gene clusters "Focal adhesion, ssc04510" and "PI3K/Akt signaling pathway, ssc04151" were added to the figure below (Copyright permission 240859 by Kanehisa labs).

3.5 WGCNA highlights clusters of co-expressed genes associated with BM-MSC lineage

The complete transcriptome of 25,484 expressed genes among all five groups of cells was fitted into 26 weighted co-expressed gene networks (Figure 8; Supplementary Table S12). Only one module was exclusively correlated to PBMCs (correlation = 1 and p-value < 2×10^{-50}), representing the largest module in terms of number of genes (19,976 genes, module "turquoise"). This module did not correlate with BM-MSC and its lineages. Therefore, the co-expressed genes within this module were specific to PBMC transcriptome. Furthermore, among the 26 clusters, the smallest module contained 55 co-expressed genes and held no significant correlation with any phenotype (module "darkorange"). The module with the highest correlation (correlation = 0.56 and p-value < 0.04) to BM-MSC phenotype was "lightcyan" with 140 co-expressed genes. However, no DEG related to BM-MSC could be identified within this module. The majority of DEGs in BM-MSC (versus PBMCs) were detected in module "turquoise" (6,162 out of 6,285 DEGs) and "yellow" (61 out of 6,285 DEGs). Adipocytes were correlated significantly with four different modules ("black," "darkred," "orange" and "yellow"). Chondrocytes showed a strong significant correlation with six different modules ("black" "blue" "brown" "lightgreen" "red" and "yellow") and osteocytes were correlated significantly with only two modules, "darkturquoise" and "green". In addition, all the significant clusters were investigated using enrichment analysis (Supplementary Table S13).

3.6 Fluorescence microscopy investigation of cell cycle stages as well as genes from "regulation of actin cytoskeleton" pathway on protein level

Active proliferation of all tested cell types was shown by DNA counter stain. The fluorescent intensity signals from DNA content in BM-MSC and differentiated lineages represented cell cycle stages G1 and G2 as indicators of actively mitotic cells. In our results, we found that osteocytes showed more cells in G1 cycle, whereas adipocytes had less cells in G1 stage. However, no significant changes were be observed in G2 stage among all cells (Figure 9).

Furthermore, fluorescent microscopy approach was used for validation of RNA-seq results on protein level regarding the

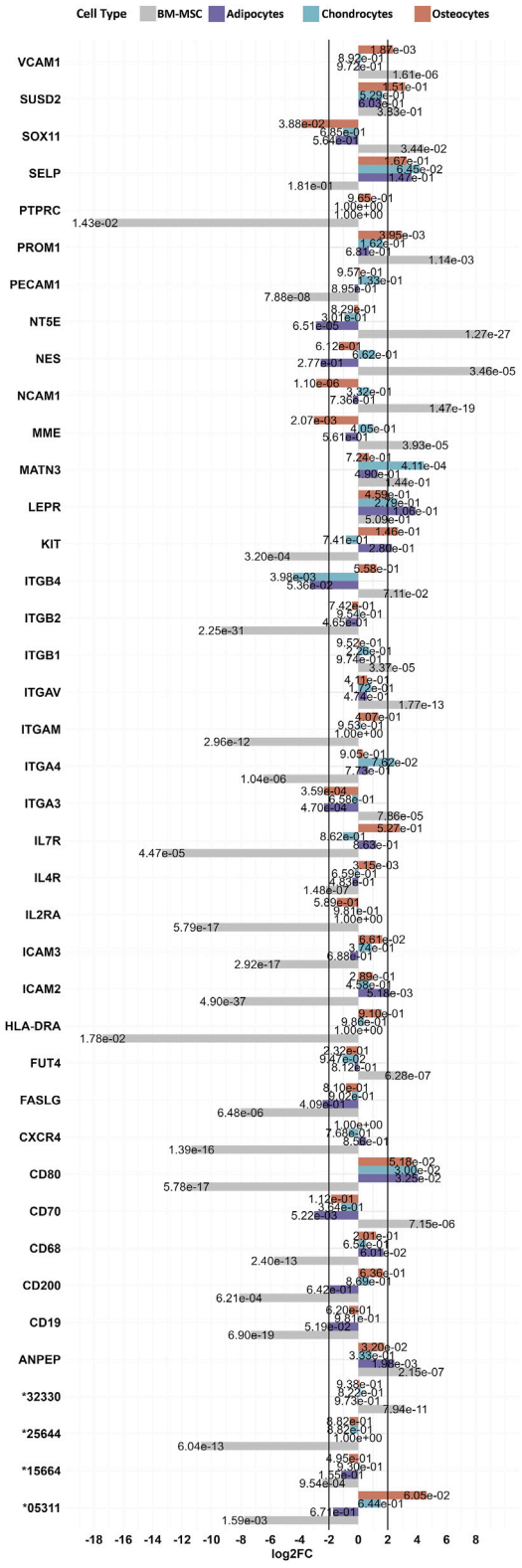

FIGURE 6
List of MSC markers with significant changes in porcine BM-MSC. The bar chart represents 40 significantly differentially expressed known cell surface markers in BM-MSC (vs. PBMC). Expression levels are compared to DEGs of adipocytes, chondrocytes and osteocytes (all vs. BM-MSC). Padj values for each dataset are presented on its related bars.

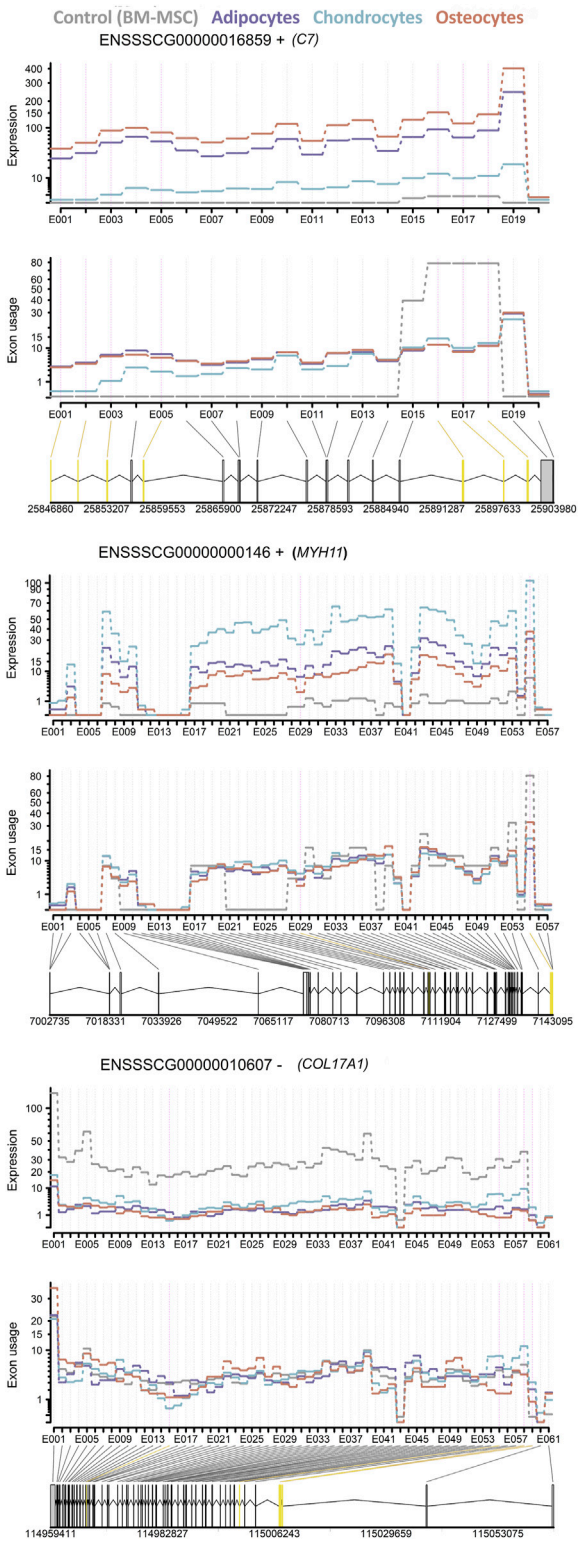

FIGURE 7
Differential exon usage of three DEGs *C7*, *MYH11* and *COL17A1*. The expression level and exon usage of each exon of (top) *C7*, (middle) *MYH11* and (bottom) *COL17A1* for all cell lineages are displayed. The differential exon usage for each cell lineage was tested against BM-MSC as control. Common significant differentially used exons in all three cell lineages are highlighted in yellow.

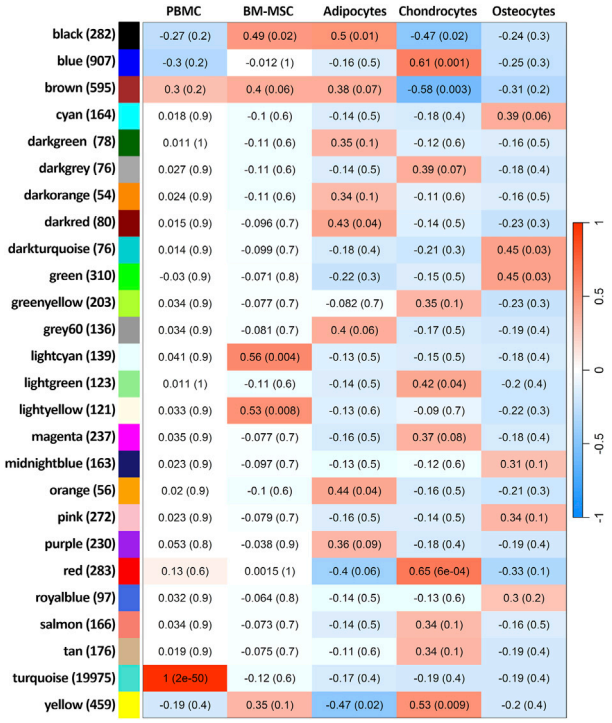

FIGURE 8
Weighted gene co-expression network analysis. The heat map presents the correlation between modules and cell types. The size of each module is mentioned in parenthesis next to the module's name. FDR of each correlation is present in parenthesis on its corresponding heat-cell.

"regulation of the actin cytoskeleton" in BM-MSC and differentiated cells. We targeted not only C7 as an upstream protein in the pathway but also actin filaments as the final product of the pathway (please refer to Figure 5). The fluorescent intensities of both C7 and actin in differentiated cells (adipocytes, chondrocytes, and osteocytes) showed a significant increase in comparison to BM-MSC (Figure 9). Alongside the detected fluorescent signal, the images displayed visually different patterns and rearrangements of the actin filaments, which indicated a more active pathway in the differentiated cells.

4 Discussion

In our work, we studied comprehensive transcriptome profiles linking BM-MSC gene expression patterns to cell-specific characteristics and highlighting transcriptome dynamics during targeted differentiation. To our knowledge, this is the first study in pigs, which investigates a profound list of genes coding for CD markers in BM-MSC to highlight expression patterns of these key stem cell surface markers as potential candidates for future improved cell-type characterization.

Our transcriptome data shed light to the debate regarding the expression of well-known markers such as CD73 (*NT5E*) and CD105 (*ENG*) in porcine BM-MSC. We observed the gene encoding the surface marker CD105 to be below the significance threshold but with an absolute log2 fold change approximating $|\log2FC|>2$ ($\log2FC = 1.74$ and $padj = 1.9 \times 10^{-6}$). This finding that CD105 is expressed in BM-MSC was also confirmed with our image analysis in which we used anti-CD105 anti-pig antibody. We assume, that this finding might explain the divergent results in previous studies, reporting on either no expression of CD105 or a "mild positivity" as suggested in flow cytometry data (Juhásova et al., 2011; Schweizer et al., 2020). Similarly, we found the gene encoding CD73 to be strongly upregulated in porcine BM-MSC, contradicting a previous study reporting on its absence (Schweizer et al., 2020). With regard to these discrepancies, we follow Prinz' (Prinz, 2017) reasoning, who suspects the low number of commercially available porcine antibodies and subsequent potential use of alternatives from human or mice to be the cause for differential results in different studies. Consequently, our list of expression patterns of genes encoding cell surface markers might be of help for future improved porcine stem cell characterization.

Furthermore, by using PBMCs as benchmark for our study, we found genes pointing to the immunomodulatory properties of BM-MSCs. We identified clusters of more than 800 genes involved in the regulation of the immune system. As demonstrated in previous studies (Khatri et al., 2015; Liu et al., 2012; Uccelli et al., 2007; Blanco et al., 2016), several of these genes belong to surface markers (such as CD4, CD8, CD19 and CD80), interleukin families and their receptors (IL1R, IL2R, IL4, IL10 and IL12 to name a few) and different growth factors (such as FGF2, FGF7 and FGF10) as well as interferons (IFNs) and tumor necrosis factors (TNFs). These results are in agreement with the findings of functional studies of MSCs, highlighting the inhibitory effect of BM-MSCs on the proliferation of T cells, B cells, dendritic cells and natural killer cells (Uccelli et al., 2007; Russell et al., 2016). It was suggested that this ability of MSCs could even be used to dampen immune-mediated diseases and transplant rejection (Uccelli et al., 2007).

In addition to these findings, we identified very interesting expression patterns in BM-MSC, which are obviously characteristic for this cell type with regard to its stemness properties; According to our analysis of DEGs for BM-MSC, we found a significant gene enrichment for "Rap1 signaling pathway" (KEGG pathway ssc04015) suggesting its activation, as well as interactions with "Extracellular matrix receptors" (KEGG pathway ssc04512). Interestingly, the components of Rap1 pathway have been shown to regulate paracrine MSC activities as well as promote cell survival by activating DNA double-strand break repair mechanisms (Ding et al., 2018; Khattar et al., 2019). In addition, Rap1/PI3K/Akt axis of this pathway was found to be involved in cell proliferation, migration and differentiation (Chen et al., 2022; Takahashi et al., 2013; Jiang et al., 2024; Jiang et al., 2019). Thus, these findings underline the differentiation capacity of BM-MSC (Chen et al., 2022).

This nature of BM-MSC was likewise highlighted by our findings of 18 common DEGs in all differentiated cell lineages. Collectively, these DEGs were apparently associated with either characteristic common molecular processes underlying the core stem cell properties of self-renewal or the generation of differentiated progeny, as referred to stemness (Douglas et al., 2014). Among these genes, we identified *FGF19*, downregulated in all three datasets, which is known to promote epithelial-mesenchymal transition (EMT) and self-renewal capacity of cancer stem cells, and to induce cell cycle arrest in differentiated

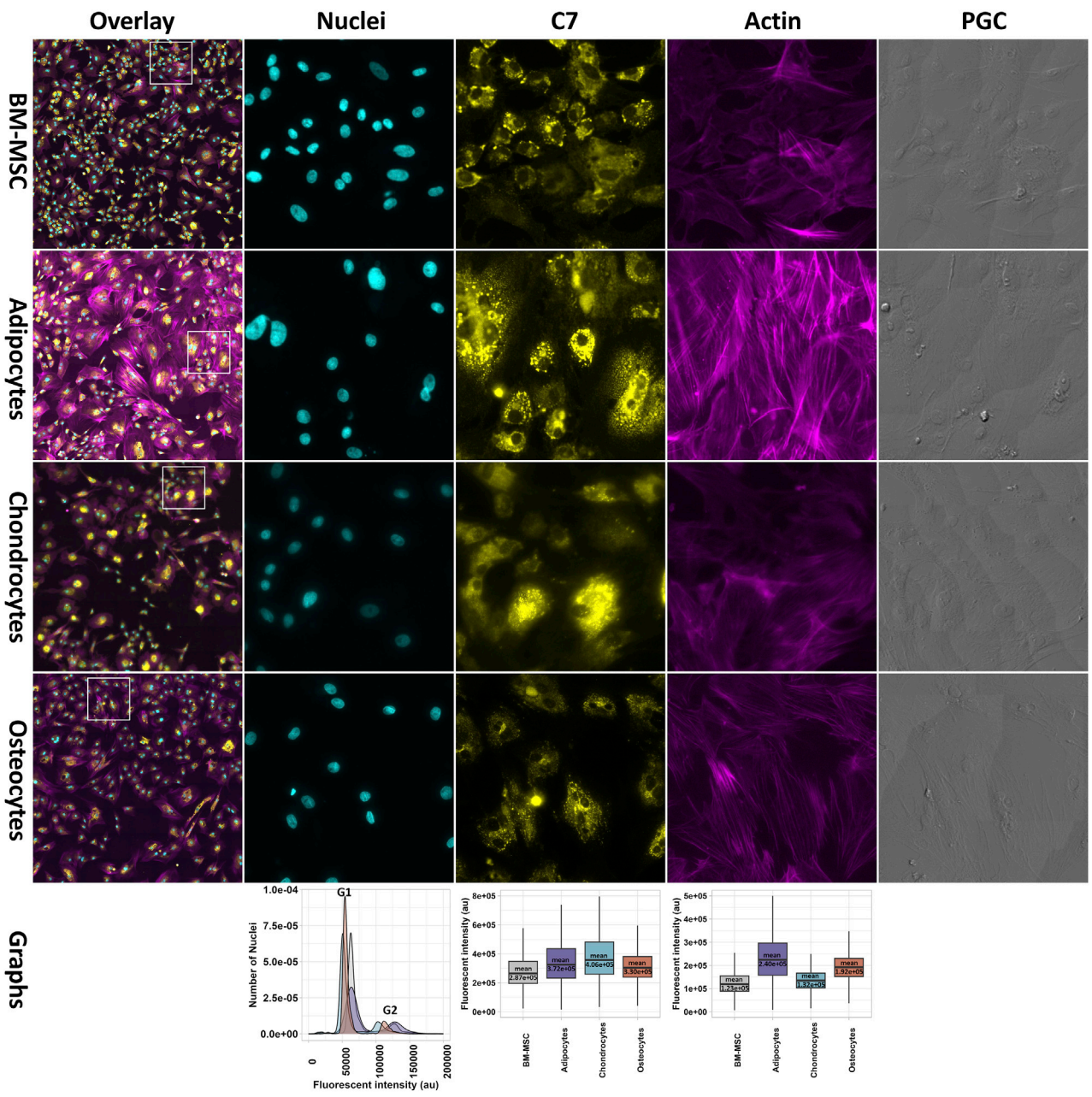

FIGURE 9
Fluorescence microscopy images of fixed BM-MSC and its differentiated cell lineages. The fixed cells were stained for nuclei (Hoechst, blue), C7 (anti-C7; yellow) and actin (Phalloidin, purple). The bottom panel, from left to right, shows the analytical graphs for fluorescent intensities for DNA content (left), anti-C7 (middle) and anti-actin (right). The histogram at the left shows the DNA content with fluorescent intensity on the *x* axis. The more intense signal is the indicator of G2 cycle due to DNA duplication. The boxplots display mean fluorescent intensity of C7 (middle) and actin (right). The plots show significant increase in C7 and actin in the differentiated cells in comparison to BM-MSC. The mean value of each intensity is written in each corresponding boxplot. All testes are significant with FDR <0.05 (the data is not shown).

chondrocytes (Wang et al., 2021; Zhao et al., 2016; Chen et al., 2023). Furthermore, our data also revealed a downregulation of *IGFBP6*, which is supposed to result in the inhibition of EMT and activation of differentiation (Cui et al., 2011; Nikulin et al., 2018) as well as *EGR1*, meditating actin assembly and mechanotransduction signaling in stem cells in response to cytoskeletal tension (Bleher et al., 2020; Baek et al., 2022). *PTH1R* is another example, which was upregulated in our datasets and subsequently might be involved in the initiation of bone formation and differentiation through activation of parathyroid hormone and Wnt signaling pathway (Yu et al., 2012). Furthermore, *SMOC2*, which was upregulated in all data-sets, could probably act as an enhancer in activating PI3K-Akt signaling pathway and subsequently promote differentiation as previously suggested (He et al., 2023). These findings suggest that these common DEGs might be key players represented as "BM-MSC differentiation driver markers.

Among these potential differentiation driver genes, ten DEGs were also found to be differential in BM-MSC vs. PBMC. This

strongly suggests that these genes might be of importance for the maintenance of the BM-MSC phenotype. For two out of the remaining eight genes, *C7* and *MYH11*, we found significant differential exon usage in addition to their upregulation in all differentiated cell-types. This finding follows previous assumption that the encoded proteins of these genes might play a significant role in the activation of stress fibers in the actin cytoskeleton (KEGG pathway ssc04810 (Kanehisa and Goto, 2000; Kanehisa, 2019; Kanehisa et al., 2023)) and therefore control cell proliferation, migration and lineage commitment (Muller et al., 2013; Burnette et al., 2011; Clarke and Martin, 2021). Notably, this pathway meditates PI3K signaling through growth factors such as *FGF19* (KEGG pathway ssc04810) as well as MAPK signaling pathway promoting the mechanically induced signal transduction and differentiation (Muller et al., 2013).

In summary, we presume that for porcine BM-MSC, Rap1 signaling and subsequently its downstream pathways PI3K-Akt as well as MAPK signaling are essential players for the cellular functionality and maintenance of its stemness. The increase in PI3K-Akt activity might lead the cell toward proliferation and differentiation. In addition, we assume that changes in the regulation of actin cytoskeleton during differentiation, might not only result in cell morphological changes but also facilitate the activity of PI3K and MAPK cascades. As potential key players in this differentiation process, our data highlight 18 candidate "BM-MSC differentiation driver markers." Subsequently, this study offers a comprehensive molecular phenotype of porcine BM-MSC and elucidates its potential underlying mechanisms *in vitro*.

Data availability statement

The datasets presented in this study can be found in online repositories. The names of the repository/repositories and accession number(s) can be found in the article/Supplementary Material.

Ethics statement

The animal study was approved by Animal welfare officer of the University of Veterinary Medicine Hannover. The study was conducted in accordance with the local legislation and institutional requirements.

Author contributions

NK: Conceptualization, Methodology, Writing–original draft, Writing–review and editing, Data curation, Formal Analysis, Investigation, Software, Validation, Visualization. RB: Formal Analysis, Methodology, Software, Validation, Visualization, Writing–original draft, Writing–review and editing. JM: Methodology, Writing–original draft, Writing–review and editing, Conceptualization, Funding acquisition, Project administration, Resources, Supervision.

Funding

The author(s) declare that financial support was received for the research, authorship, and/or publication of this article. This study was financially supported by the German Research Foundation (Deutsche Forschungsgemeinschaft), Heisenberg Grant (ME4517/3-1). In addition, the authors acknowledge financial support by the Open Access Publication Fund of the University of Veterinary Medicine Hannover, Foundation.

Acknowledgments

The authors would like to acknowledge Heike Klippert-Hasberg and Jörn Wrede for their contribution in RNA sequencing and data preparation. In addition, the authors are grateful for the support they received from MPI-MPG microscopy facility and the Institute for Anatomy at the University of Veterinary Medicine Hannover.

Conflict of interest

The authors declare that the research was conducted in the absence of any commercial or financial relationships that could be construed as a potential conflict of interest.

Publisher's note

Supplementary material

The Supplementary Material for this article can be found online at: https://www.frontiersin.org/articles/10.3389/fcell.2024.1478757/full#supplementary-material

SUPPLEMENTARY FIGURE S1
Heatmap of sample-sample distance and clustering. The heatmap visualizes the results of similarity and hierarchical clustering between each cell type and its replicates based on Euclidian distances. Distances are displayed on each cell of the heatmap.

SUPPLEMENTARY FIGURE S2
PCA plots from differential gene expression analysis. The PCA plot shows the variances among the BM-MSC, adipocytes, chondrocytes, and osteocytes datasets.

SUPPLEMENTARY FIGURE S3
Expression of not differentially expressed BM-MSC markers. The bar chart display the log2FC of known but not differentially expressed MSC markers in porcine BM-MSC, adipocytes, chondrocytes and osteocytes. Padj of each gens is displayed on its respective bar.

References

Anders, S., Reyes, A., and Huber, W. (2012). Detecting differential usage of exons from RNA-seq data. *Genome Res.* 22 (10), 2008–2017. doi:10.1101/gr.133744.111

Baek, J., Lopez, P. A., Lee, S., Kim, T. S., Kumar, S., and Schaffer, D. V. (2022). Egr1 is a 3D matrix-specific mediator of mechanosensitive stem cell lineage commitment. *Sci. Adv.* 8 (15), eabm4646. doi:10.1126/sciadv.abm4646

Blanco, B., Herrero-Sánchez, M. D., Rodríguez-Serrano, C., García-Martínez, M. L., Blanco, J. F., Muntión, S., et al. (2016). Immunomodulatory effects of bone marrow versus adipose tissue-derived mesenchymal stromal cells on NK cells: implications in the transplantation setting. *Eur. J. Haematol.* 97 (6), 528–537. doi:10.1111/ejh.12765

Bleher, M., Meshko, B., Cacciapuoti, I., Gergondey, R., Kovacs, Y., Duprez, D., et al. (2020). Egr1 loss-of-function promotes beige adipocyte differentiation and activation specifically in inguinal subcutaneous white adipose tissue. *Sci. Rep.* 10 (1), 15842. doi:10.1038/s41598-020-72698-w

Bundgaard, L., Stensballe, A., Elbaek, K. J., and Berg, L. C. (2018). Mapping of equine mesenchymal stromal cell surface proteomes for identification of specific markers using proteomics and gene expression analysis: an *in vitro* cross-sectional study. *Stem Cell Res. Ther.* 9 (1), 288. doi:10.1186/s13287-018-1041-8

Burnette, D. T., Manley, S., Sengupta, P., Sougrat, R., Davidson, M. W., Kachar, B., et al. (2011). A role for actin arcs in the leading-edge advance of migrating cells. *Nat. Cell Biol.* 13 (4), 371–381. doi:10.1038/ncb2205

Caplan, A. I. (1991). Mesenchymal stem cells. *J. Orthop. Res.* 9 (5), 641–650. doi:10.1002/jor.1100090504

Caplan, A. I. (1994). The mesengenic process. *Clin. Plast. Surg.* 21 (3), 429–435. doi:10.1016/s0094-1298(20)31020-8

Caplan, A. I. (1995). Osteogenesis imperfecta, rehabilitation medicine, fundamental research and mesenchymal stem cells. *Connect. Tissue Res.* 31 (4), S9–S14. doi:10.3109/03008209509116826

Chen, E. Y., Tan, C. M., Kou, Y., Duan, Q., Wang, Z., Meirelles, G. V., et al. (2013). Enrichr: interactive and collaborative HTML5 gene list enrichment analysis tool. *BMC Bioinforma.* 14, 128. doi:10.1186/1471-2105-14-128

Chen, H., Li, J., Pi, C., Guo, D., Zhang, D., Zhou, X., et al. (2023). FGF19 induces the cell cycle arrest at G2-phase in chondrocytes. *Cell Death Discov.* 9 (1), 250. doi:10.1038/s41420-023-01543-6

Chen, T., Peng, Y., Hu, W., Shi, H., Li, P., Que, Y., et al. (2022). Irisin enhances chondrogenic differentiation of human mesenchymal stem cells via Rap1/PI3K/AKT axis. *Stem Cell Res. Ther.* 13 (1), 392. doi:10.1186/s13287-022-03092-8

Cho, K. A., Park, M., Kim, Y. H., Woo, S. Y., and Ryu, K. H. (2017). RNA sequencing reveals a transcriptomic portrait of human mesenchymal stem cells from bone marrow, adipose tissue, and palatine tonsils. *Sci. Rep.* 7 (1), 17114. doi:10.1038/s41598-017-16788-2

Choudhery, M. S., Mahmood, R., Harris, D. T., and Ahmad, F. J. (2022). Minimum criteria for defining induced mesenchymal stem cells. *Cell Biol. Int.* 46 (6), 986–989. doi:10.1002/cbin.11790

Clarke, D. N., and Martin, A. C. (2021). Actin-based force generation and cell adhesion in tissue morphogenesis. *Curr. Biol.* 31 (10), R667–R680. doi:10.1016/j.cub.2021.03.031

Conley, S. M., Zhu, X. Y., Eirin, A., Tang, H., Lerman, A., van Wijnen, A. J., et al. (2018). Metabolic syndrome alters expression of insulin signaling-related genes in swine mesenchymal stem cells. *Gene* 644, 101–106. doi:10.1016/j.gene.2017.10.086

Costa, L. A., Eiro, N., Fraile, M., Gonzalez, L. O., Saa, J., Garcia-Portabella, P., et al. (2021). Functional heterogeneity of mesenchymal stem cells from natural niches to culture conditions: implications for further clinical uses. *Cell Mol. Life Sci.* 78 (2), 447–467. doi:10.1007/s00018-020-03600-0

Cui, J., Ma, C., Qiu, J., Ma, X., Wang, X., Chen, H., et al. (2011). A novel interaction between insulin-like growth factor binding protein-6 and the vitamin D receptor inhibits the role of vitamin D3 in osteoblast differentiation. *Mol. Cell Endocrinol.* 338 (1–2), 84–92. doi:10.1016/j.mce.2011.03.011

Danev, N., Li, G. S., Duan, J. Y., and van de Walle, G. R. (2024). Comparative transcriptomic analysis of bovine mesenchymal stromal cells reveals tissue-source and species-specific differences. *Iscience* 27 (2), 108886. doi:10.1016/j.isci.2024.108886

Dawson, H. D., and Lunney, J. K. (2018). Porcine cluster of differentiation (CD) markers 2018 update. *Res. Vet. Sci.* 118, 199–246. doi:10.1016/j.rvsc.2018.02.007

Ding, Y., Liang, X., Zhang, Y., Yi, L., Shum, H. C., Chen, Q., et al. (2018). Rap1 deficiency-provoked paracrine dysfunction impairs immunosuppressive potency of mesenchymal stem cells in allograft rejection of heart transplantation. *Cell Death Dis.* 9 (3), 386. doi:10.1038/s41419-018-0414-3

Dobin, A., Davis, C. A., Schlesinger, F., Drenkow, J., Zaleski, C., Jha, S., et al. (2013). STAR: ultrafast universal RNA-seq aligner. *Bioinformatics* 29 (1), 15–21. doi:10.1093/bioinformatics/bts635

Dominici, M., Le Blanc, K., Mueller, I., Slaper-Cortenbach, I., Marini, F., Krause, D., et al. (2006). Minimal criteria for defining multipotent mesenchymal stromal cells. The International Society for Cellular Therapy position statement. *Cytotherapy* 8 (4), 315–317. doi:10.1080/14653240600855905

Douglas, M. (2014). "Chapter 2 - "stemness": definitions, criteria, and standards," in *Essentials of stem cell biology*. 3rd Edn, Editors L. Robert and A. Anthony (Boston: Academic Press), 7–17.

Eirin, A., Zhu, X. Y., Puranik, A. S., Woollard, J. R., Tang, H., Dasari, S., et al. (2017). Integrated transcriptomic and proteomic analysis of the molecular cargo of extracellular vesicles derived from porcine adipose tissue-derived mesenchymal stem cells. *PLoS ONE* 12 (3), e0174303. doi:10.1371/journal.pone.0174303

Engel, P., Boumsell, L., Balderas, R., Bensussan, A., Gattei, V., Horejsi, V., et al. (2015). CD nomenclature 2015: human leukocyte differentiation antigen workshops as a driving force in immunology. *J. Immunol.* 195 (10), 4555–4563. doi:10.4049/jimmunol.1502033

Fisher, A. M. (2021). *Genetically engineered pigs for xenotransplantation: technischen universität münchen*.

Friedenstein, A. J., Chailakhjan, R. K., and Lalykina, K. S. (1970). The development of fibroblast colonies in monolayer cultures of Guinea-pig bone marrow and spleen cells. *Cell Tissue Kinet.* 3 (4), 393–403. doi:10.1111/j.1365-2184.1970.tb00347.x

Gurgul, A., Opiela, J., Pawlina, K., Szmatola, T., Bochenek, M., and Bugno-Poniewierska, M. (2017). The effect of histone deacetylase inhibitor trichostatin A on porcine mesenchymal stem cell transcriptome. *Biochimie* 139, 56–73. doi:10.1016/j.biochi.2017.05.015

Gurgul, A., Romanek, J., Pawlina-Tyszko, K., Szmatola, T., and Opiela, J. (2018). Evaluation of changes arising in the pig mesenchymal stromal cells transcriptome following cryopreservation and Trichostatin A treatment. *PLoS ONE* 13 (2), e0192147. doi:10.1371/journal.pone.0192147

Haga, C. L., Booker, C. N., Strivelli, J., Boregowda, S. V., and Phinney, D. G. (2024). Comparative transcriptome analysis of bone marrow resident versus culture-expanded mouse mesenchymal stem/stromal cells. *Cytotherapy* 26 (5), 498–505. doi:10.1016/j.jcyt.2024.01.008

Hatsushika, D., Muneta, T., Nakamura, T., Horie, M., Koga, H., Nakagawa, Y., et al. (2014). Repetitive allogeneic intraarticular injections of synovial mesenchymal stem cells promote meniscus regeneration in a porcine massive meniscus defect model. *Osteoarthr. Cartil.* 22 (7), 941–950. doi:10.1016/j.joca.2014.04.028

He, W. G., Deng, Y. X., Ke, K. X., Cao, X. L., Liu, S. Y., Yang, Y. Y., et al. (2023). Matricellular protein SMOC2 potentiates BMP9-induced osteogenic differentiation in mesenchymal stem cells through the enhancement of FAK/PI3K/AKT signaling. *Stem Cells Int.* 2023, 5915988. doi:10.1155/2023/5915988

Horwitz, E. M., Le Blanc, K., Dominici, M., Mueller, I., Slaper-Cortenbach, I., Marini, F. C., et al. (2005). Clarification of the nomenclature for MSC: the international society for cellular therapy position statement. *Cytotherapy* 7 (5), 393–395. doi:10.1080/14653240500319234

Jawaid, W. (2023). enrichR: provides an R interface to enrichr. Available at: https://CRAN.R-project.org/package=enrichR.

Jiang, N., Tian, X., Wang, Q., Hao, J., Jiang, J., and Wang, H. (2024). Regulation mechanisms and maintenance strategies of stemness in mesenchymal stem cells. *Stem Cell Rev. Rep.* 20 (2), 455–483. doi:10.1007/s12015-023-10658-3

Jiang, Y., Liu, F., Zou, F., Zhang, Y., Wang, B., Zhang, Y., et al. (2019). PBX homeobox 1 enhances hair follicle mesenchymal stem cell proliferation and reprogramming through activation of the AKT/glycogen synthase kinase signaling pathway and suppression of apoptosis. *Stem Cell Res. Ther.* 10 (1), 268. doi:10.1186/s13287-019-1382-y

Juhásova, J., Juhás, S., Klíma, J., Strnádel, J., Holubová, M., and Motlík, J. (2011). Osteogenic differentiation of miniature pig mesenchymal stem cells in 2D and 3D environment. *Physiol. Res.* 60 (3), 559–571. doi:10.33549/physiolres.932028

Kanazawa, S., Okada, H., Hojo, H., Ohba, S., Iwata, J., Komura, M., et al. (2021). Mesenchymal stromal cells in the bone marrow niche consist of multi-populations with distinct transcriptional and epigenetic properties. *Sci. Rep.* 11 (1), 15811. doi:10.1038/s41598-021-94186-5

Kanehisa, M. (2019). Toward understanding the origin and evolution of cellular organisms. *Protein Sci.* 28 (11), 1947–1951. doi:10.1002/pro.3715

Kanehisa, M., Furumichi, M., Sato, Y., Kawashima, M., and Ishiguro-Watanabe, M. (2023). KEGG for taxonomy-based analysis of pathways and genomes. *Nucleic Acids Res.* 51 (D1), D587–D592. doi:10.1093/nar/gkac963

Kanehisa, M., and Goto, S. (2000). KEGG: kyoto encyclopedia of genes and genomes. *Nucleic Acids Res.* 28 (1), 27–30. doi:10.1093/nar/28.1.27

Kato, Y., Imabayashi, H., Mori, T., Tani, T., Taniguchi, M., Higashi, M., et al. (2004). Nuclear transfer of adult bone marrow mesenchymal stem cells: developmental totipotency of tissue-specific stem cells from an adult mammal. *Biol. Reprod.* 70 (2), 415–418. doi:10.1095/biolreprod.103.020271

Kawamura, M., Miyagawa, S., Fukushima, S., Saito, A., Toda, K., Daimon, T., et al. (2015). Xenotransplantation of bone marrow-derived human mesenchymal stem cell sheets attenuates left ventricular remodeling in a porcine ischemic cardiomyopathy model. *Tissue Eng. Part A* 21 (15–16), 2272–2280. doi:10.1089/ten.TEA.2014.0036

Kfoury, Y., and Scadden, D. T. (2015). Mesenchymal cell contributions to the stem cell niche. *Cell Stem Cell* 16 (3), 239–253. doi:10.1016/j.stem.2015.02.019

Khatri, M., O'Brien, T. D., Chattha, K. S., and Saif, L. J. (2015). Porcine lung mesenchymal stromal cells possess differentiation and immunoregulatory properties. *Stem Cell Res. Ther.* 6, 222. doi:10.1186/s13287-015-0220-0

Khattar, E., Maung, K. Z. Y., Chew, C. L., Ghosh, A., Mok, M. M. H., Lee, P., et al. (2019). Rap1 regulates hematopoietic stem cell survival and affects oncogenesis and response to chemotherapy. *Nat. Commun.* 10 (1), 5349. doi:10.1038/s41467-019-13082-9

Khaveh, N., Schachler, K., Berghofer, J., Jung, K., and Metzger, J. (2023). Altered hair root gene expression profiles highlight calcium signaling and lipid metabolism pathways to be associated with curly hair initiation and maintenance in Mangalitza pigs. *Front. Genet.* 14, 1184015. doi:10.3389/fgene.2023.1184015

Koch, D. W., Schnabel, L. V., Ellis, I. M., Bates, R. E., and Berglund, A. K. (2022). TGF-β2 enhances expression of equine bone marrow-derived mesenchymal stem cell paracrine factors with known associations to tendon healing. *Stem Cell Res. Ther.* 13 (1), 477. doi:10.1186/s13287-022-03172-9

Krupa, P., Krsek, P., Javorník, M., Dostál, O., Spnec, R., Usvald, D., et al. (2007). Use of 3D geometry modeling of osteochondrosis-like iatrogenic lesions as a template for press-and-fit scaffold seeded with mesenchymal stem cells. *Physiol. Res.* 56, S107–S114. doi:10.33549/physiolres.931308

Kuleshov, M. V., Jones, M. R., Rouillard, A. D., Fernandez, N. F., Duan, Q., Wang, Z., et al. (2016). Enrichr: a comprehensive gene set enrichment analysis web server 2016 update. *Nucleic Acids Res.* 44 (W1), W90–W97. doi:10.1093/nar/gkw377

Langfelder, P., and Horvath, S. (2008). WGCNA: an R package for weighted correlation network analysis. *BMC Bioinforma.* 9, 559. doi:10.1186/1471-2105-9-559

Langfelder, P., and Horvath, S. (2012). Fast R functions for robust correlations and hierarchical clustering. *J. Stat. Softw.* 46 (11), i11. doi:10.18637/jss.v046.i11

Lawrence, M., Huber, W., Pages, H., Aboyoun, P., Carlson, M., Gentleman, R., et al. (2013). Software for computing and annotating genomic ranges. *PLoS Comput. Biol.* 9 (8), e1003118. doi:10.1371/journal.pcbi.1003118

Le Blanc, K., and Ringden, O. (2007). Immunomodulation by mesenchymal stem cells and clinical experience. *J. Intern Med.* 262 (5), 509–525. doi:10.1111/j.1365-2796.2007.01844.x

Lee, K. B., Hui, J. H., Song, I. C., Ardany, L., and Lee, E. H. (2007). Injectable mesenchymal stem cell therapy for large cartilage defects--a porcine model. *Stem Cells* 25 (11), 2964–2971. doi:10.1634/stemcells.2006-0311

Li, S., Siengdee, P., Oster, M., Reyer, H., Wimmers, K., and Ponsuksili, S. (2023). Transcriptome changes during osteogenesis of porcine mesenchymal stem cells derived from different types of synovial membranes and genetic background. *Sci. Rep.* 13 (1), 10048. doi:10.1038/s41598-023-37260-4

Liu, S., Yuan, M., Hou, K., Zhang, L., Zheng, X., Zhao, B., et al. (2012). Immune characterization of mesenchymal stem cells in human umbilical cord Wharton's jelly and derived cartilage cells. *Cell Immunol.* 278 (1-2), 35–44. doi:10.1016/j.cellimm.2012.06.010

Love, M. I., Huber, W., and Anders, S. (2014). Moderated estimation of fold change and dispersion for RNA-seq data with DESeq2. *Genome Biol.* 15 (12), 550. doi:10.1186/s13059-014-0550-8

Mets, T., and Verdonk, G. (1981). Variations in the stromal cell population of human bone marrow during aging. *Mech. Ageing Dev.* 15 (1), 41–49. doi:10.1016/0047-6374(81)90006-3

Miller-Rhodes, P. (2023). A guide to mesenchymal stem cell (MSC) markers. Available at: https://www.biocompare.com/Editorial-Articles/597087-A-Guide-to-Mesenchymal-Stem-Cell-MSC-Markers/.

Monaco, E., Bionaz, M., Rodriguez-Zas, S., Hurley, W. L., and Wheeler, M. B. (2012). Transcriptomics comparison between porcine adipose and bone marrow mesenchymal stem cells during *in vitro* osteogenic and adipogenic differentiation. *PLoS ONE* 7 (3), e32481. doi:10.1371/journal.pone.0032481

Monaco, E., Sobreira de Lima, A., Bionaz, M., Maki, A. J., Wilson, S. W., Hurley, W. L., et al. (2009). Morphological and transcriptomic comparison of adipose and bone marrow derived porcine stem cells. *Open Tissue Eng. & Regen. Med. J.* 6 (2), 14. doi:10.2174/1875043500902010020

Muller, P., Langenbach, A., Kaminski, A., and Rychly, J. (2013). Modulating the actin cytoskeleton affects mechanically induced signal transduction and differentiation in mesenchymal stem cells. *PLoS ONE* 8 (7), e71283. doi:10.1371/journal.pone.0071283

Nikulin, S. V., Raigorodskaya, M. P., Poloznikov, A. A., Zakharova, G. S., Schumacher, U., Wicklein, D., et al. (2018). Role of IGFBP6 protein in the regulation of epithelial-mesenchymal transition genes. *Bull. Exp. Biol. Med.* 164 (5), 650–654. doi:10.1007/s10517-018-4051-8

Ock, S. A., Baregundi, S. R., Lee, Y. M., Lee, J. H., Jeon, R. H., Lee, S. L., et al. (2016). Comparison of immunomodulation properties of porcine mesenchymal stromal/stem cells derived from the bone marrow, adipose tissue, and dermal skin tissue. *Stem Cells Int.* 2016, 9581350. doi:10.1155/2016/9581350

Pais, H., Ruggero, K., Zhang, J., Al-Assar, O., Bery, N., Bhuller, R., et al. (2019). Surfaceome interrogation using an RNA-seq approach highlights leukemia initiating cell biomarkers in an LMO2 T cell transgenic model. *Sci. Rep.* 9 (1), 5760. doi:10.1038/s41598-019-42214-w

Patil, I. (2021). Visualizations with statistical details: the "ggstatsplot" approach. *J. Open Source Softw.* 6 (61), 3167. doi:10.21105/joss.03167

Pawar, A. S., Eirin, A., Tang, H., Zhu, X. Y., Lerman, A., and Lerman, L. O. (2020). Upregulated tumor necrosis factor-α transcriptome and proteome in adipose tissue-derived mesenchymal stem cells from pigs with metabolic syndrome. *Cytokine* 130, 155080. doi:10.1016/j.cyto.2020.155080

Ponsuksili, S., Siengdee, P., Li, S., Kriangwanich, W., Oster, M., Reyer, H., et al. (2024). Effect of metabolically divergent pig breeds and tissues on mesenchymal stem cell expression patterns during adipogenesis. *BMC Genom* 25 (1), 407. doi:10.1186/s12864-024-10308-z

Prinz, C. (2017). *Biopharmaceutical characterization of porcine mesenchymal stromal cells as a model system for a human cell therapy product*. Munich, Germany: Ludwig-Maximilians-Universität München.

Reyes, A., Anders, S., Weatheritt, R. J., Gibson, T. J., Steinmetz, L. M., and Huber, W. (2013). Drift and conservation of differential exon usage across tissues in primate species. *Proc. Natl. Acad. Sci. U. S. A.* 110 (38), 15377–15382. doi:10.1073/pnas.1307202110

Roson-Burgo, B., Sanchez-Guijo, F., Del Canizo, C., and De Las Rivas, J. (2014). Transcriptomic portrait of human Mesenchymal Stromal/Stem Cells isolated from bone marrow and placenta. *BMC Genom* 15 (1), 910. doi:10.1186/1471-2164-15-910

Russell, K. A., Chow, N. H., Dukoff, D., Gibson, T. W., LaMarre, J., Betts, D. H., et al. (2016). Characterization and immunomodulatory effects of canine adipose tissue- and bone marrow-derived mesenchymal stromal cells. *PLoS ONE* 11 (12), e0167442. doi:10.1371/journal.pone.0167442

Sangiorgi, B., and Panepucci, R. A. (2016). Modulation of immunoregulatory properties of mesenchymal stromal cells by toll-like receptors: potential applications on GVHD. *Stem Cells Int.* 2016, 9434250. doi:10.1155/2016/9434250

Schweizer, R., Waldner, M., Oksuz, S., Zhang, W. S., Komatsu, C., Plock, J. A., et al. (2020). Evaluation of porcine versus human mesenchymal stromal cells from three distinct donor locations for cytotherapy. *Front. Immunol.* 11, 826. doi:10.3389/fimmu.2020.00826

Takahashi, M., Dillon, T. J., Liu, C., Kariya, Y., Wang, Z., and Stork, P. J. (2013). Protein kinase A-dependent phosphorylation of Rap1 regulates its membrane localization and cell migration. *J. Biol. Chem.* 288 (39), 27712–27723. doi:10.1074/jbc.M113.466904

Tavassoli, M., and Crosby, W. H. (1968). Transplantation of marrow to extramedullary sites. *Science* 161 (3836), 54–56. doi:10.1126/science.161.3836.54

Tseng, W. J., Huang, S. W., Fang, C. H., Hsu, L. T., Chen, C. Y., Shen, H. H., et al. (2018). Treatment of osteoarthritis with collagen-based scaffold: a porcine animal model with xenograft mesenchymal stem cells. *Histol. Histopathol.* 33 (12), 1271–1286. doi:10.14670/HH-18-013

Uccelli, A., Pistoia, V., and Moretta, L. (2007). Mesenchymal stem cells: a new strategy for immunosuppression?. *Trends Immunol.* 28 (5), 219–226. doi:10.1016/j.it.2007.03.001

Uder, C., Bruckner, S., Winkler, S., Tautenhahn, H. M., and Christ, B. (2018). Mammalian MSC from selected species: features and applications. *Cytom. A* 93 (1), 32–49. doi:10.1002/cyto.a.23239

Walters, E. M., and Prather, R. S. (2013). Advancing swine models for human health and diseases. *Mo Med.* 110 (3), 212–215.

Wang, J., Zhao, H., Zheng, L., Zhou, Y., Wu, L., Xu, Y., et al. (2021). FGF19/SOCE/NFATc2 signaling circuit facilitates the self-renewal of liver cancer stem cells. *Theranostics* 11 (10), 5045–5060. doi:10.7150/thno.56369

Xie, Z., Bailey, A., Kuleshov, M. V., Clarke, D. J. B., Evangelista, J. E., Jenkins, S. L., et al. (2021). Gene set knowledge discovery with enrichr. *Curr. Protoc.* 1 (3), e90. doi:10.1002/cpz1.90

Yu, B., Zhao, X., Yang, C., Crane, J., Xian, L., Lu, W., et al. (2012). Parathyroid hormone induces differentiation of mesenchymal stromal/stem cells by enhancing bone morphogenetic protein signaling. *J. Bone Min. Res.* 27 (9), 2001–2014. doi:10.1002/jbmr.1663

Zhan, X. S., El-Ashram, S., Luo, D. Z., Luo, H. N., Wang, B. Y., Chen, S. F., et al. (2019). A comparative study of biological characteristics and transcriptome profiles of mesenchymal stem cells from different canine tissues. *Int. J. Mol. Sci.* 20 (6), 1485. doi:10.3390/ijms20061485

Zhao, H., Lv, F., Liang, G., Huang, X., Wu, G., Zhang, W., et al. (2016). FGF19 promotes epithelial-mesenchymal transition in hepatocellular carcinoma cells by modulating the GSK3β/β-catenin signaling cascade via FGFR4 activation. *Oncotarget* 7 (12), 13575–13586. doi:10.18632/oncotarget.6185

frontiers | Frontiers in Cell and Developmental Biology

TYPE Original Research
PUBLISHED 04 December 2024
DOI 10.3389/fcell.2024.1496884

OPEN ACCESS

EDITED BY
Myon Hee Lee,
East Carolina University, United States

REVIEWED BY
Amelia Eva Aranega,
University of Jaén, Spain
Xiaolei Li,
University of Pennsylvania, United States

*CORRESPONDENCE
Glen Findlay Tibbits,
tibbits@sfu.ca

RECEIVED 15 September 2024
ACCEPTED 11 November 2024
PUBLISHED 04 December 2024

CITATION
Nagalingam RS, Jayousi F, Hamledari H, Dababneh S, Hosseini D, Lindsay C, Klein Geltink R, Lange PF, Dixon IM, Rose RA, Czubryt MP and Tibbits GF (2024) Molecular and metabolomic characterization of hiPSC-derived cardiac fibroblasts transitioning to myofibroblasts.
Front. Cell Dev. Biol. 12:1496884.
doi: 10.3389/fcell.2024.1496884

Molecular and metabolomic characterization of hiPSC-derived cardiac fibroblasts transitioning to myofibroblasts

Raghu Sundaresan Nagalingam[1,2], Farah Jayousi[1,2], Homa Hamledari[1,2], Saif Dababneh[1,3], Dina Hosseini[1,2], Chloe Lindsay[2], Ramon Klein Geltink[1,4,5], Philipp F. Lange[1,4,5], Ian Michael Dixon[6,7], Robert Alan Rose[8,9], Michael Paul Czubryt[6,7] and Glen Findlay Tibbits[1,2,10,11]*

[1]Cellular and Regenerative Medicine Centre, BC Children's Hospital Research Institute, Vancouver, BC, Canada, [2]Department of Biomedical Physiology and Kinesiology, Simon Fraser University, Burnaby, BC, Canada, [3]Department of Cellular and Physiological Sciences, Faculty of Medicine, University of British Columbia, Vancouver, BC, Canada, [4]Department of Pathology and Laboratory Medicine, University of British Colombia, Vancouver, BC, Canada, [5]BC Children's Hospital Research Institute, Vancouver, BC, Canada, [6]Institute of Cardiovascular Sciences, St. Boniface Hospital Albrechtsen Research Centre, Winnipeg, MB, Canada, [7]Department of Physiology and Pathophysiology, University of Manitoba, Winnipeg, MB, Canada, [8]Department of Cardiac Sciences, Cumming School of Medicine, Libin Cardiovascular Institute, University of Calgary, Calgary, AB, Canada, [9]Department of Physiology and Pharmacology, Cumming School of Medicine, Libin Cardiovascular Institute, University of Calgary, Calgary, AB, Canada, [10]Department of Molecular Biology and Biochemistry, Simon Fraser University, Burnaby, BC, Canada, [11]School of Biomedical Engineering, University of British Columbia, Vancouver, BC, Canada

Background: Mechanical stress and pathological signaling trigger the activation of fibroblasts to myofibroblasts, which impacts extracellular matrix composition, disrupts normal wound healing, and can generate deleterious fibrosis. Myocardial fibrosis independently promotes cardiac arrhythmias, sudden cardiac arrest, and contributes to the severity of heart failure. Fibrosis can also alter cell-to-cell communication and increase myocardial stiffness which eventually may lead to lusitropic and inotropic cardiac dysfunction. Human induced pluripotent stem cell derived cardiac fibroblasts (hiPSC-CFs) have the potential to enhance clinical relevance in precision disease modeling by facilitating the study of patient-specific phenotypes. However, it is unclear whether hiPSC-CFs can be activated to become myofibroblasts akin to primary cells, and the key signaling mechanisms in this process remain unidentified.

Objective: We aim to explore the notable changes in fibroblast phenotype upon passage-mediated activation of hiPSC-CFs with increased mitochondrial metabolism, like primary cardiac fibroblasts.

Methods: We activated the hiPSC-CFs with serial passaging from passage 0 to 3 (P0 to P3) and treatment of P0 with TGFβ1.

Results: Passage-mediated activation of hiPSC-CFs was associated with a gradual induction of genes to initiate the activation of these cells to myofibroblasts, including collagen, periostin, fibronectin, and collagen fiber processing enzymes with concomitant downregulation of cellular proliferation markers. Most importantly, canonical TGFβ1 and Hippo signaling component genes including TAZ were influenced by passaging hiPSC-CFs. Seahorse assay revealed that passaging and TGFβ1 treatment increased mitochondrial respiration, consistent with fibroblast activation requiring increased energy production, whereas treatment with the glutaminolysis inhibitor BPTES completely attenuated this process.

Conclusion: Our study highlights that the hiPSC-CF passaging enhanced fibroblast activation, activated fibrotic signaling pathways, and enhanced mitochondrial metabolism approximating what has been reported in primary cardiac fibroblasts. Thus, hiPSC-CFs may provide an accurate *in vitro* preclinical model for the cardiac fibrotic condition, which may facilitate the identification of putative anti-fibrotic therapies, including patient-specific approaches.

KEYWORDS

fibroblast, myofibroblast, induced pluripotent stem cells, arrhythmia, cardiac fibrosis, cardiac remodeling, cardiac ECM

Highlights

- Passaging promotes the activation of fibroblasts to myofibroblasts.
- TGFβ1 treatment activates the fibroblasts, but their expression profile was uniquely different from passaged myofibroblasts.
- High energy requiring fibroblast activation is dependent on glutaminase-based mitochondrial metabolism.
- Passaging induces TGFβ1 and Hippo signaling pathways in activated fibroblasts and myofibroblasts.

Introduction

Extracellular matrix (ECM) remodeling in the heart is crucial to forming a stable scar after myocardial infarction (MI) and contributes to replacement fibrosis after a significant loss of cardiomyocytes upon injury (Bohl et al., 2008; Sutton and Sharpe, 2000). In hypertensive and diabetic myocardia, uncontrolled ECM alteration can lead to reactive fibrosis upon activation of renin-angiotensin and β-adrenergic signalling (Tanaka et al., 1986; Weber and Brilla, 1991; Weber et al., 1988). ECM remodeling is tightly coordinated, and several trophic factors

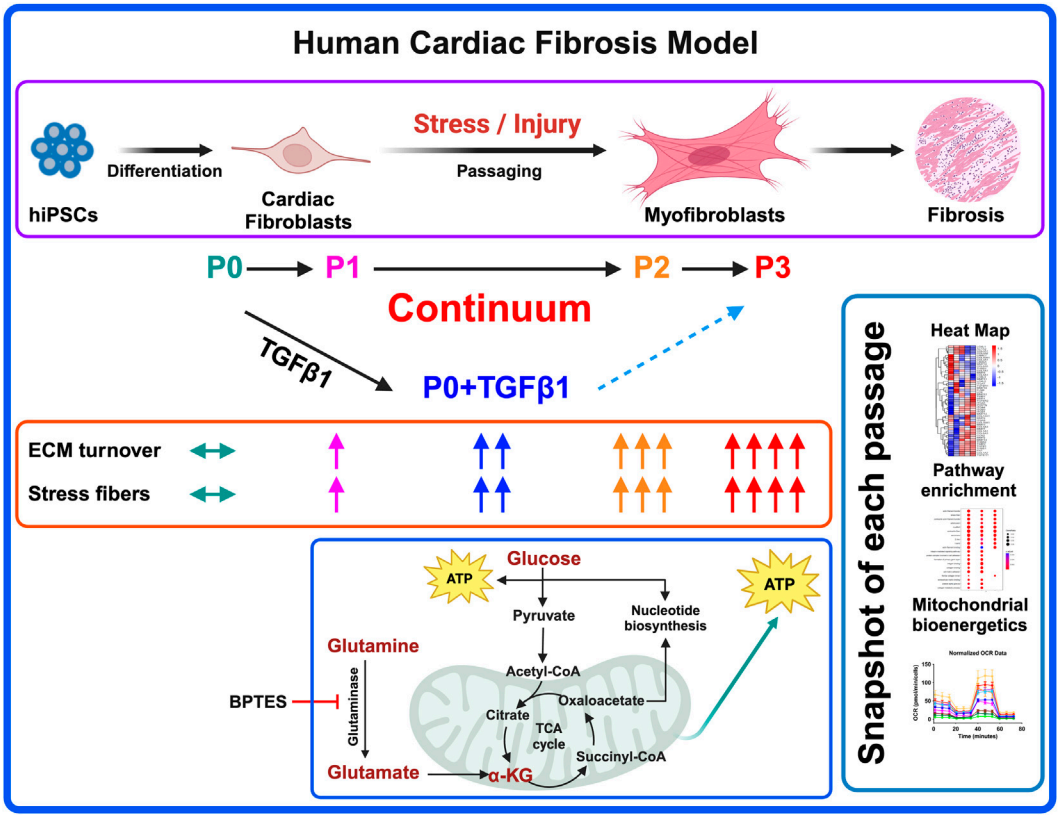

GRAPHICAL ABSTRACT
Probing the activation of fibroblasts to myofibroblasts is key in ECM remodeling processes to avoid fibrosis-related adverse complications, and to better understand disease pathology. Here we report that passaging of hiPSC-derived cardiac fibroblasts promotes fibroblast activation along with a gradual shift in gene expression and metabolic changes towards myofibroblasts. TGFβ1 treatment activates non-passaged fibroblasts, but they are dissimilar to myofibroblasts. The energy-intensive fibroblast to myofibroblast activation process is dependent on glutaminase-mediated mitochondrial metabolism and is prevented by treatment with GLS-1 inhibitor BPTES. Our work demonstrates that hiPSC-CFs can offer a preclinical model analogous to primary cardiac fibroblasts that is comparable with passage-mediated myofibroblast activation and increased mitochondrial metabolism. hiPSC-CFs may also facilitate patient-specific novel anti-fibrosis drug screening and disease management.

are known to stimulate cardiac fibroblast activation. Wound healing, in the absence of fibrosis, is marked by fibroblast activation to myofibroblasts (Frangogiannis, 2021) and rapid scar formation followed by a period of myofibroblast apoptosis which results in healed tissue characterized by continuous and relatively slow matrix turn-over. Conversely wound healing after myocardial infarction, or in response to prolonged stress in the heart such as in pressure overload, is typified by the relative persistence of myofibroblasts with attendant excessive synthesis and deposition of ECM and matrix-associated proteins (Hinz and Lagares, 2020; Nagalingam et al., 2022). This excessive deposition includes structural collagens as well as periostin (Shimazaki et al., 2008) and the fibronectin ED-A splice variant. As our understanding of the pathophysiology and signaling mechanisms of cardiac fibroblast activation and the genes that are associated with this activation remains incomplete, its investigation is warranted. Several groups have investigated the signaling mechanisms governing fibroblast activation using primary murine cardiac fibroblasts (Klingberg et al., 2018). The expression of α-smooth muscle actin (α-SMA) by myofibroblasts is often cited as a standard marker protein of fibroblast activation and after acute MI, increased numbers of α-SMA-positive myofibroblasts are found within the infarct region (Virag and Murry, 2003). Lineage tracing of cardiac myofibroblasts in a murine MI model revealed that after scar formation, some myofibroblasts transition towards quiescent matrifibrocytes, and that in the human myocardial scar, similar matrifibrocytes with unique gene expression and secretome exist and are separate from myofibroblasts (Fu et al., 2018). Whether the persistence of myofibroblasts and appearance of matrifibrocytes occurs in hearts of various etiologies of disease and in non-murine preclinical models remains an open question. In a left ventricular pressure overload model, α-SMA expressing myofibroblasts were found to be elevated at 2 weeks and then declined after 4 weeks, and *in vitro* cultured fibroblasts revealed that α-SMA expression peaked at 9 days and declined by 12 days, indicating that fibroblast activation may present as a dynamic transition (Gilles et al., 2020). Removal of periostin-positive myofibroblasts results in less severity of the disease phenotype by limiting collagen synthesis and scar formation after MI (Kanisicak et al., 2016). TGFβ1 (Algeciras et al., 2021; Dobaczewski et al., 2010; Saadat et al., 2020; Villalobos et al., 2019; Zeglinski et al., 2016), and hippo signaling (Landry et al., 2021) is also elevated when fibroblasts are activated to become myofibroblasts. Fibroblast activation to myofibroblasts utilizes energy via mitochondrial metabolism (Negmadjanov et al., 2015) and is highly dependent on glutaminolysis and its rate-limiting enzyme GLS1 (Chattopadhyaya et al., 2022; Gibb et al., 2022). Most fibroblast activation studies to date were performed either in stable cell lines or murine primary cells due to the scarcity of human tissues to prepare primary cells, and commercially available cardiac fibroblasts are often passaged multiple times prior to sale.

There are multiple protocols published so far to differentiate cardiac fibroblasts from iPSCs; however, most of them share a similar path with various small molecules to initiate the cardiac mesoderm formation followed by epicardial cell conversion to cardiac fibroblasts. To generate the cardiac mesoderm and cardiac progenitors from iPSCs, most protocols used a GSK3 inhibitor (CHIR99021) and a WNT signaling inhibitor (IWR1 or XAV939); after cardiac mesoderm formation, a TGFβ-inhibitor (SB431542) and retinoic acid (RA) promoted conversion to epicardial lineage cells, followed by FGF-2 treatment to generate hiPSC-CFs (Beauchamp et al., 2020; Campostrini et al., 2021; Cumberland et al., 2023; Giacomelli et al., 2020; Hall et al., 2023; Soussi et al., 2023; Whitehead et al., 2022; Yu et al., 2022; Zhang et al., 2022; Zhang H. et al., 2019). The differentiation protocols for iPSC-derived lung and dermal fibroblasts differ in the growth factors and chemical signals used on specific lineages to become tissue-specific fibroblasts (Alvarez-Palomo et al., 2020; Itoh et al., 2013; Kim et al., 2018; Mitchell et al., 2023; Tamai et al., 2022; Wong et al., 2015). Most notably, NKX2.5 defines the cardiac-specific lineage from cardiac mesoderm (Zhang et al., 2022; Zhang H. et al., 2019), whereas NKX2.1 directs lung-specific lineage (Mitchell et al., 2023; Wong et al., 2012). iPSC-CFs express cardiac-specific genes like GATA4, BMP4, TCF21, DDR2, TE-7, HAND2, HEY1, ISL1 and α-SMA and are influenced by their epicardial lineage (Campostrini et al., 2021; Giacomelli et al., 2020; Zhang et al., 2022; Zhang H. et al., 2019; Zhang J. et al., 2019). iPSC-derived lung fibroblasts express different sets of genes like NKX2.1, GATA6, DNP63a, FOXA1, ACE1, AQP5, T1α, SPA, SPB, SPC FOXF1, and FOXA2 (Alvarez-Palomo et al., 2020; Mitchell et al., 2023; Tamai et al., 2022; Wong et al., 2015); whereas iPSC-derived dermal fibroblasts and keratinocytes presented with not only KRT14, but also ΔNp63, DSG3, ITGB4, laminin 5, KRT5, KRT1 and loricrin (Itoh et al., 2013; Kim et al., 2018).

Current advancements and optimization in protocols that are more efficient in generating hiPSC-derived cardiac fibroblasts provide a compelling model to mimic myofibroblast activation to study fibrosis. A recent study reported the use of TGFβ1 inhibitors to maintain the fibroblasts as quiescent for up to five passages (Zhang H. et al., 2019). Fibroblasts locally generate TGFβ1 during mechanical stretch upon interacting with integrins (Munger et al., 1999; Sarrazy et al., 2014) and TGFβ1 is a critical player in activating the fibroblasts and fibrosis-associated ECM gene expression in cultured fibroblasts (Dobaczewski et al., 2010; Eghbali et al., 1991; Heimer et al., 1995; Sarrazy et al., 2014; Villarreal et al., 1996; Yi et al., 2014). Several studies used passaging and TGFβ1 to induce fibroblast activation and the myofibroblast phenotype in primary cardiac fibroblasts. It is unclear whether TGFβ1-induced fibroblast activation is similar to the myofibroblastic phenotype produced by passaging. In this study, our goal was to capture a snapshot of passage-mediated cardiac fibroblast to myofibroblast transition and TGFβ1-induced fibroblast activation in hiPSC-derived cardiac fibroblasts using transcriptomic, proteomic, and metabolomic profiling and signaling mechanisms involved to provide a better understanding of the fibrosis-associated disease phenotype; also using hiPSC-CFs as a better alternate model than murine and human cardiac fibroblasts.

Materials and methods

Human induced pluripotent stem cell maintenance and fibroblast differentiation

We used two hiPSC lines (iPS IMR90-1 and STAN248i-617C1), obtained from the WiCell Research Institute, for fibroblast

differentiation, which was accomplished using a few modifications of previously published protocols (Zhang et al., 2022; Zhang H. et al., 2019). The hiPSCs were maintained on Corning Matrigel-coated 6-well tissue culture plates with mTeSR-Plus medium (STEMCELL Technologies). Cells were passaged every 4 days using ReLeSR media (StemCell Technologies) and were then seeded on a six-well Matrigel-coated plate at a density of 175,000 cells cm^{-2} in mTeSR-Plus medium. For fibroblast differentiation, on day-0 >90% confluent hiPSC monolayers were treated with 6 μM CHIR99021 containing RPMI-1640 + B27- insulin media for 48 h. On day-2 the media was replaced with RPMI-1640 + B27-insulin media for 24 h; on day-3, cells were treated with 5 μM of the WNT signaling inhibitor IWR1 (I0161, Sigma) containing RPMI-1640 + B27-insulin media for 48 h; On day-5, the media was replaced with RPMI-1640 + B27-insulin media for 24 h. On day-6, hiPSC-derived progenitor cells (hiPSC-PCs) were passaged and replated at a density of 200,000 cells cm^{-2} in advanced DMEM medium (12634028, Gibco) consisting of 1% FBS and glutaMax along with 5 μM CHIR99021 and 2 μM retinoic acid (R2625, Sigma-Aldrich) for 72 h. On day-9, cells were maintained in advanced DMEM consisting of 1% FBS and glutaMax for 48 h. On day-11, hiPSC-PCs were passaged and replated at a density of 100,000 cells cm^{-2} then treated with 10 μM SB431542 (S1067, Selleck chemicals) in fibroblast growth medium-3 (FGM-3) (PromoCell) for another 72 h. On day-14, hiPSC-derived epicardial cells (hiPSC-EPCs) were passaged and replated at a density of 100,000 cells cm^{-2} then treated with 20 ng/mL FGF2 (100–18B, PeproTech) and 10 μM SB431542 (S1067, Selleck chemicals) in fibroblast growth medium-3 (FGM-3) (PromoCell) for another 6 days, with the media changed every 48 h. On day-20, hiPSC derived fibroblasts (hiPSC-CFs) (P0) were ready to be passaged and replated at a density of 75,000 cells cm^{-2} with FGM-3 media. Then after every 96 h hiPSC-CFs were passaged until passage-3 (P3). We considered each differentiation into a replicate and multiple differentiations were carried out with two different hiPSC lines. For the TGFβ1 treatment, hiPSC-CFs were serum starved for 6 h without serum supplement in FGM-3 media, prior to the treatment with 10 ng/mL of TGFβ1 for 48 h.

The critical part in biological/technical replicates in these experiments has to do with the manual differentiation of hiPSCs and the subsequent passaging of hiPSC-CFs. Both protocols can cause significant variations in gene expression and proteomic profiles. For these experiments, at least four separate differentiations/passages were performed by the same highly experienced scientist and the variance was very limited.

Protein isolation and purification

The hiPSC-CF proteins were isolated from cell pellets using TrypLE dissociation reagent, which was added to each well and incubated for ~5–6 min. This was followed by media neutralization and the collection of detached cells. The homogenous cell suspension was centrifuged to obtain the cell pellet. The pellet was then resuspended in an aliquot of lysis buffer in which the volume was proportional to the number of cells. The cells were counted using the CellDrop automated cell counter. The lysis buffer contained 100 mM HEPES (pH = 8–8.5) + 20% SDS. Cell lysates were then placed for 5 min in 95°C water bath, followed by 3 min on ice. To complete the lysis, the samples were sonicated twice for 30 s, and placed on ice between rounds. This was followed by treatment with benzonase (EMD Millipore-Sigma) at 37°C for 30 min to fragment the chromatin.

After obtaining the lysates, each sample was reduced with 10 mM dithiothreitol (DTT) at 37°C for 30 min, followed by alkylation with 50 mM chloroacetamide (CAA) for 30 min in the dark. The alkylation was quenched in 50 mM DTT for 10 min at room temperature. To each sample, hydrophilic and hydrophobic Sera-Mag Speed Beads (GE Life Sciences, Washington, US) were added in 1:1 ratio. Proteins were then bound to the beads with 100% ethanol (80% v/v) and washed twice with 90% ethanol.

After binding of the proteins to the beads, the samples underwent an overnight enzymatic digestion with trypsin (1: 50 w/w), followed by C18 matrix midi-column clean up and elution. The BioPure midi columns (Nest Group Inc.) were conditioned with 200 μL methanol, 200 μL 0.1% formic acid (FA), 60% acetonitrile (ACN), and 200 μL 0.1% trifluoroacetic acid (TFA). The sample pH was adjusted to pH = 3 – 4 using 10% TFA prior to loading the columns. Samples were sequentially eluted 3 times with 70 μL, 70 μL, and 50 μL 0.1% FA, 60% ACN. The eluate was collected into LoBind tubes and placed into a SpeedVac to remove the organic ACN. Lastly, the samples were resuspended in 0.1% FA (ready for MS injection).

Protein detection and quantification using LC/MS

The total protein concentration for each of the purified samples was determined using Nanodrop. Mass spectrometric analyses were performed on Q Exactive HF Orbitrap mass spectrometer coupled with an Easy-nLC liquid chromatography system (Thermo Scientific). The time of flight was calculated as the period between injection to detection. In the MS sample chamber (96-well plate), the samples were completely randomized across all conditions and biological replicates. A total of 1 μg peptides per sample was injected for analysis. The peptides were separated over a 3-h gradient consisting of Buffer A (0.1% FA in 2% ACN) and 2%–80% Buffer B (0.1% FA in 95% ACN) at a set flow rate of 300 nL/min. The raw mass-to-charge (M/Z) data acquired from the Q Exactive HF were searched with MaxQuant (MQ)-version 2.0.0.0 (Max Planck Institute, Germany), and Proteome discoverer software (Thermo Fisher Scientific, CA, United States), using the built-in search engine, and embedded standard DDA settings. The false discovery rate for protein and peptide searches was set at 1%. Digestion settings were set to trypsin. Oxidation (M) and Acetyl (N-term) were set as dynamic modifications. Carbamidomethyl (C) was set as fixed modification, and Phosphorylation (STY) was set as a variable modification. For the main comparative protein search, the human proteome database (FASTA) was downloaded from Uniprot (2022_06; 20,365 sequences) and used as the reference file. Common contaminants were embedded from MaxQuant. Peptide sequences that were labeled as "Potential contaminant/REV" were excluded from the final analysis.

Seahorse assay

hiPSCs were differentiated 4 days apart to attain all the passages (P0, P1, P2 and P3) on the same day to perform Seahorse assay. hiPSC-derived fibroblasts were dissociated using TrypLE and replated at a density of 15,000 cells/well on Matrigel-coated Seahorse Xfe96 well cell culture plates. Cells were serum starved for 6 h without serum supplement in FGM-3 media, after 24 h of initial plating, followed by treatment with 10 ng/mL TGFβ1 for 48 h or 10 μM BPTES treated after 24 h of TGFβ1 treatment for 24 h. On the day of the experiment, the cell medium was changed to Seahorse media containing RPMI1640 medium without glucose and sodium bicarbonate (R1383, Sigma) supplemented with glucose (10 mM, Sigma), glutamine (2 mM, Sigma), and sodium pyruvate (1 mM, Sigma) and cells were incubated in a non-CO_2 incubator for a maximum of 45 min. Subsequently, the Seahorse Mito Stress test was performed using Agilent Seahorse XFe96 Analyzer by sequential injection of ATP synthase inhibitor oligomycin (1 μM, Sigma), mitochondrial uncoupler FCCP (1.5 μM, Sigma), and mitochondrial complex I and III inhibitors rotenone (100 nM, Sigma)/antimycin A (1 μM, Sigma). The raw oxygen consumption rate (OCR) and extracellular acidification rate (ECAR) values were normalized based on cell numbers per each well using Wave software (Agilent Technologies, Inc.). Data analysis and visualization were performed using GraphPad Prism [Version 9.5.1 (528)].

Immunofluorescence staining

hiPSC-derived fibroblasts were cultured on a cover glass coated with Matrigel with appropriate seeding density. Cells were washed thrice with PBS followed by 4% PFA for 10 min at room temperature (RT). Fixed cells were quenched with 100 mM glycine for 5 min at RT, then washed with PBS thrice. Cells were permeabilized using 0.1%–0.3% triton X-100 in PBS for 3 mins, followed by washing with PBS thrice. Permeabilized cells were then blocked with 5% BSA for 45 mins, followed by overnight incubation with 1:500 dilution of DDR-2 antibody (ab63337, Abcam). The cover glass with the cells was then washed with PBS 3 times for 5 min in an orbital motion shaker at 50–60 rpm. The cells were incubated with phalloidin (A34055, ThermoFisher) and 1:500 dilution of goat anti-rabbit secondary antibody in 1% BSA for an hour at RT in the dark. The cells were washed with PBS for 5 min three times in an orbital motion shaker, then mounted on a glass slide using ProLong Glass Antifade Mountant (P36980, ThermoFisher) and dried for 2 h, then imaged under a Nikon Ti microscope.

Quantitative real-time PCR

hiPSC-derived fibroblasts were dissociated using TrypLE, and the cells were pelleted by centrifugation and flash-frozen prior to RNA isolation. Total RNA from flash-frozen cells was processed using NucleoMag (744350.1, Takara) Magnetic bead-based RNA isolation following the manufacturer's instructions. cDNA was generated from 1 μg RNA samples using the iScript cDNA Synthesis kit (Bio-Rad, United States). qPCR reactions were prepared using 5 mL SsoAdvanced Universal SYBR Green Supermix (Bio-Rad, United States) and 4 mL 1:6 diluted cDNA template along with 200 nM forward and reverse primers in a total volume of 10 mL per reaction. PCR amplification was performed in duplicate for each reaction on a CFX384 Touch Real-Time PCR (Bio-Rad, United States). The cycling conditions were 95°C (3 min), followed by 40 cycles of denaturation at 95°C (15 s) and extension at 62°C (30 s). After amplification, a continuous melt curve was generated from 60°C to 95°C to confirm the amplification of single amplicons. Relative gene expression was calculated using the $2^{-\Delta\Delta CT}$ method with normalization to GAPDH (primer sequences are in Supplementary Table S1).

NanoString analysis for mRNA expression profile

Total RNA from flash-frozen cells was processed using NucleoMag (744350.1, Takara) Magnetic bead-based RNA isolation, according to the manufacturer's instructions. The concentration and purity of the RNA were determined using a NanoDrop ND-1000 spectrophotometer (Thermo Fisher Scientific). Multiplexed mRNA profiling was conducted using a human fibrosis V2 panel codeset containing 762 fibrosis-specific gene probes synthesized by NanoString Technologies Inc. and read on the NanoString nCounter® SPRINT Profiler. A total of 50 ng purified RNA per sample was hybridized overnight (16 h) to the custom capture and reporter probes. Hybridized samples were loaded into each channel of the nCounter® SPRINT cartridge. Raw mRNA counts were collected, and the results were normalized to ten housekeeping genes (ACAD9, ARMH3, CNOT10, GUSB, MTMR14, NOL7, NUBP1, PGK1, PPIA, RPLP0). Analysis was performed on the nSolver analysis software and the Advanced Analysis module (NanoString Technologies Inc.).

Statistical analysis

Data are reported as mean ± standard deviation of a minimum of three independent biological replicates. To reduce variability, all cells, including control and treatment groups, were isolated and cultured on the same day. For data analysis, different treatments and samples between groups were kept blinded. Violin plots from NanoString and mass spectrometry data sets were generated and analyzed using GraphPad prism (9.5.1) software with one-way analysis of variance with Tukey's post-hoc analysis as appropriate, with $p < 0.05$ considered to be statistically significant. Principal component analysis (PCA) was performed based on the Benjamini–Hochberg method false discovery rate (FDR) adjusted to p-value <0.05. Group correlation heatmap was based on Pearson correlation and FDR adjusted to p-value <0.05. Volcano plots were prepared based on Welch's t-test and adjusted $p < 0.05$ using Perseus v2.0.10.0 software. Heatmap for selected genes was generated with the pheatmap package (clustering_distance_rows = "euclidean") and with a p-value of <0.05 considered statistically significant. The compareCluster function was used to compare the top 10 gene ontology (GO) terms between each group (pAdjustMethod = "BH", pvalueCutoff = 0.05,

qvalueCutoff = 0.2). Gene set enrichment analysis was performed using the gseGO function (pvalueCutoff = 0.05). Dot s were generated using ggplot2 dotplot (Wickham, 2016).

Results

Passaging promotes fibroblast activation to myofibroblasts

In our hiPSC-derived cardiac fibroblasts, upon passaging towards the myofibroblast (P3) phenotype or treatment with TGFβ1 to become activated fibroblasts (P0+TGFβ1), both phenotypes display a reduction in the expression of the proliferation markers CDK-4 at the mRNA level (Supplementary Figure S1A) and CDK-1, MCM3, and PCNA at the protein level (Supplementary Figures S1B–D) compared to the non-passaged fibroblasts (P0). The characteristic hallmark of fibroblast to myofibroblast activation is α-SMA positive stress fiber incorporation inside the myofibroblasts (Hinz, 2007). Phalloidin staining and DDR immunofluorescence revealed that hiPSC-derived cardiac fibroblasts that underwent three passages (P1 to P3) or P0+TGFβ1 showed gradual expression of stress fibers in higher passaged cells compared to non-passaged cells (P0) (Figure 1B). Most importantly, after passaging hiPSC-CFs displayed a reduction in TCF21 gene expression from P0 to P3 and in P0+TGFβ1, whereas myofibroblast marker genes (e.g., periostin (POSTN) and ED-A-fibronectin [ED-A-Fn)] showed an incremental expression pattern in P0 to P3 and in P0+TGFβ1 compared to P0 cells at the mRNA level using qPCR analysis (Figures 1C–E). These results clearly indicate that hiPSC-derived fibroblasts, upon passaging TGFβ, gradually become myofibroblasts.

Passaging elevates fibrosis-associated genes while transitioning to the myofibroblast phenotype

We compared the different passages of hiPSC-CFs with the NanoString codeset using a PCA plot displaying unique clusters of various passages of hiPSC-CFs (P0, P1, P2, P3) and TGFβ1 treated non-passaged cells (P0+TGFβ1). The differences are 55.6% and 14.6% in component-1 (*X*-axis) and component-2 (*Y*-axis), respectively. The P0 and P3 clusters showed the greatest differences between each other, while other clusters (P1, P2, P0+TGFβ1) fell between P0 and P3 (Figure 2A). The group correlation of gene expression between various passages of hiPSC-CFs were plotted based on Pearson correlation, and the higher intensity of red corresponds to high correlation, and higher green corresponds less correlation between groups (Figure 2B). Volcano plots were generated based on fold change between P0+TGFβ1 vs. P0 (Figure 2C), P1 vs. P0 (Figure 2D), P2 vs. P0 (Figure 2E), P3 vs. P0 (Figure 2F), P3 vs. P0+TGFβ1 (Figure 2G), in which upregulated genes are depicted on the left side and downregulated genes are on the right side of the panel. Volcano plot analysis revealed that each passage of hiPSC-CFs (P1, P2, P3) and P0+TGFβ1 gene expression pattern is distinct when compared to P0; also, P3 displayed significantly different gene expression compared to P0+TGFβ1. The P3 group showed significant upregulation in profibrotic and myofibroblast-related genes, whereas P1, P2, and P0+TGFβ1 showed a steady shift towards myofibroblast-related profibrotic genes such as POSTN, ED-A-Fn and key fibrillar collagens (Col1α1 and Col1α2), whereas α-smooth muscle actin (ACTA2) expression was higher in the P1 and P0+TGFβ1 compared to P0 but not in P2 and P3. We tested the differential expression of selective ECM-related genes comparing various passages of hiPSC-CFs (P0, P1, P2, P3) and P0+TGFβ1 using heatmap analysis (Figure 2H). The heatmap data revealed that the expression profile of different passages of hiPSC-CFs (P1, P2, P3) and P0+TGFβ1 caused a significant shifting towards the myofibroblast phenotype upon passage-mediated fibroblast activation. Activated fibroblasts and myofibroblasts are responsible for the increased ECM turnover in reparative and reactive fibrosis, increasing collagen, fibronectin, and other secretory proteins. Passaging of hiPSC-CFs revealed that gene expression of major fibrotic fibrillar collagens, Col1α1 and Col1α2, was significantly higher in both P0+TGFβ1and P3 compared to P0, whereas Col3α1 showed a reduction in P0+TGFβ1 and P3 compared to P0 (Supplementary Figures S3A–C). Similarly, gene expression of structural and secretory proteins like α-smooth muscle actin (ACTA2), periostin (POSTN), fibronectin (FN1), vimentin (VIM), integrin beta-1 (ITGB1), and integrin alpha-4 (ITGA4) were significantly elevated in P0+TGFβ1 and P3 compared to P0 (Supplementary Figures S3D–I). ECM remodeling enzymes play a crucial role in the formation and maturation of stable scars, and their expression was elevated in parallel with a significant accumulation of mature collagen fibers in the failing myocardium. Lysyl oxidase (LOX) acts as a catalyst in linking collagen fibers to become mature collagen, and along with other matrix remodeling enzymes such as MMP2 and MMP1 was upregulated in both P3 and P0+TGFβ1 compared to P0 (Supplementary Figures S2A–C). Comparative cluster enrichment analysis revealed the top 10 upregulated pathways when comparing P3 vs. P0, P0+TGFβ1 vs. P0, or P3 vs. P0+TGFβ1 (Figure 2H); similar analysis provided the top 10 downregulated pathways in these comparisons (Figure 2I). Passage mediated activation of fibroblasts results in alterations in gene expression in the transcripts shown in Figure 3 relative to P0 with each passage (P1, P2 and P3), significant upregulation (Figure 3A) and downregulation (Figure 3B) observed with each consecutive passage.

Passaging alters the proteomic profile of hiPSC-derived cardiac fibroblasts

To understand the passage-mediated proteome profile changes, we performed PCA to see the clustering differences between non-passaged fibroblasts (P0), myofibroblasts (P3), and growth factor activated fibroblasts (P0+TGFβ1) using the Benjamini–Hochberg method (Figure 4A). The cluster differences are 46.3% in component-1 (*X*-axis) and 16.9% in component-2 (*Y*-axis). The P0 and P3 clusters are notably far apart from each other, with P0+TGFβ1 falling in the middle. Group correlation analysis of proteomic expression in P0, P3, and P0+TGFβ1 based on Pearson correlation revealed intensity gradient differences between groups, in which higher intensity of brown corresponds to high correlation and higher blue corresponds minimal correlation (Figure 4B). Proteome profiles of different passages of hiPSC-CFs

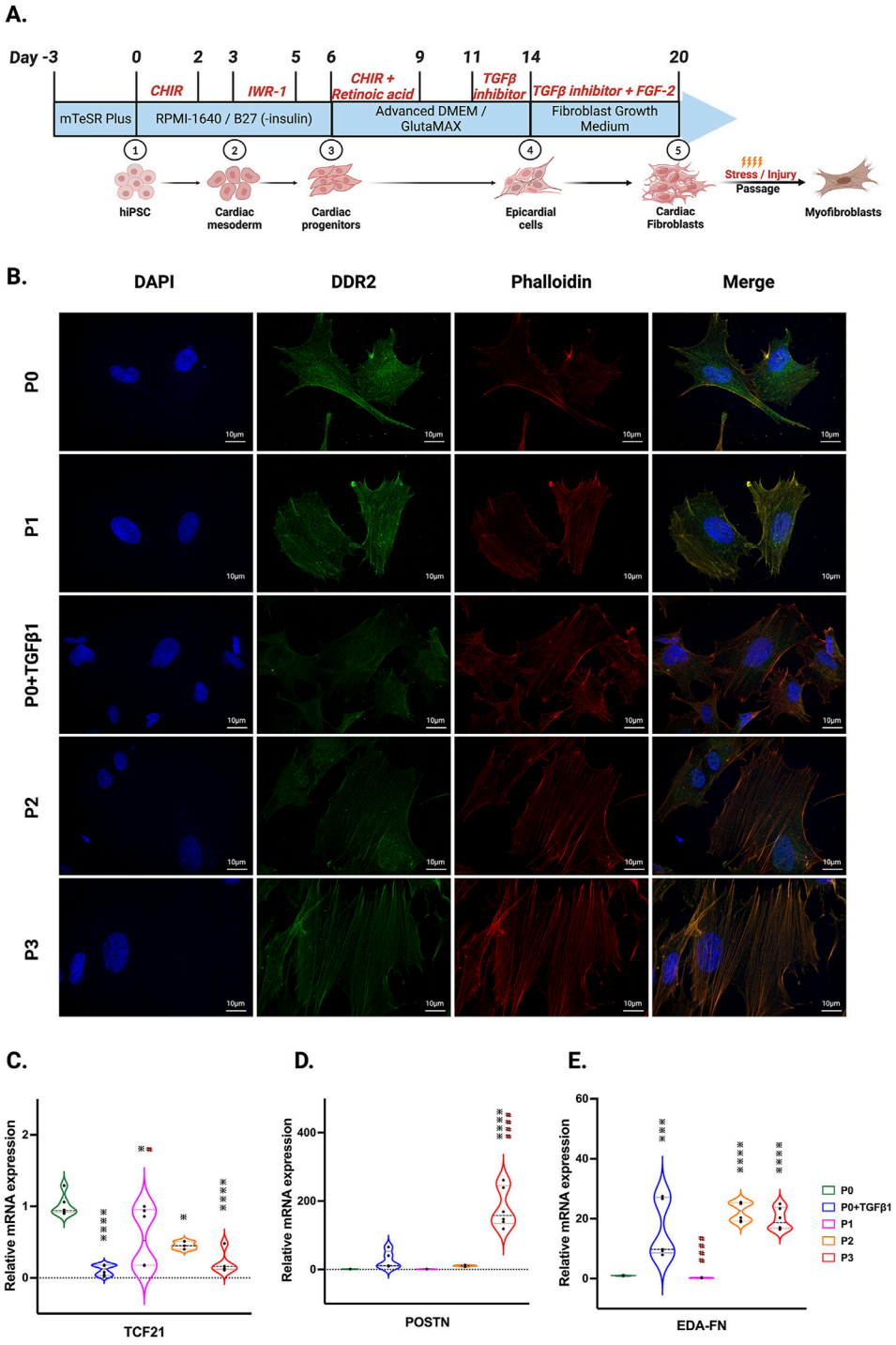

FIGURE 1
hiPSC-derived fibroblast transition to the myofibroblast phenotype after passaging. Timeline and differentiation of fibroblasts from hiPSCs **(A)**. Images represent stress fibers stained with phalloidin (red), DDR-2 (green) and DAPI (blue) in hiPSC-derived non-passaged fibroblasts (P0), non-passaged fibroblasts treated with TGFβ (P0+TGFβ1) and different passages of fibroblasts (P1, P2, P3) **(B)**. Passaging of fibroblasts initiates myofibroblast activation, altering the mRNA expression of TCF21 **(C)**, POSTN **(D)**, and EDA-Fn **(E)** as assessed by qPCR. Statistical significance was determined by one-way ANOVA with Tukey's *post hoc* test (n = 3–4). *$p < 0.05$, **$p < 0.01$, ***$p < 0.001$, ****$p < 0.0001$ vs. P0 and #$p \leq 0.05$, ####$p \leq 0.0001$ vs. P0+TGFβ1. The STAN248i-617C1 hiPSC line was used to generate the data for **(B)** and the iPS IMR90-1 line was used to generate the data for **(**C–E**)**.

(P0, P1, P2, P3) and P0+TGFβ1 were plotted based on fold change between P0+ TGFβ1 vs. P0 (Figure 4C), P3 vs. P0 (Figure 4D), P3 vs. P0+ TGFβ1 (Figure 4E) using volcano plot analysis; these plots indicated that passaging promoted the myofibroblast phenotype in hiPSC-CFs, whereas TGFβ1-treated non-passaged fibroblasts also exhibited distinct proteomic expression compared to either P0 or P3. Differential expression of selected ECM-related proteins compared between P0, P3, and P0+TGFβ1 was examined using heatmap

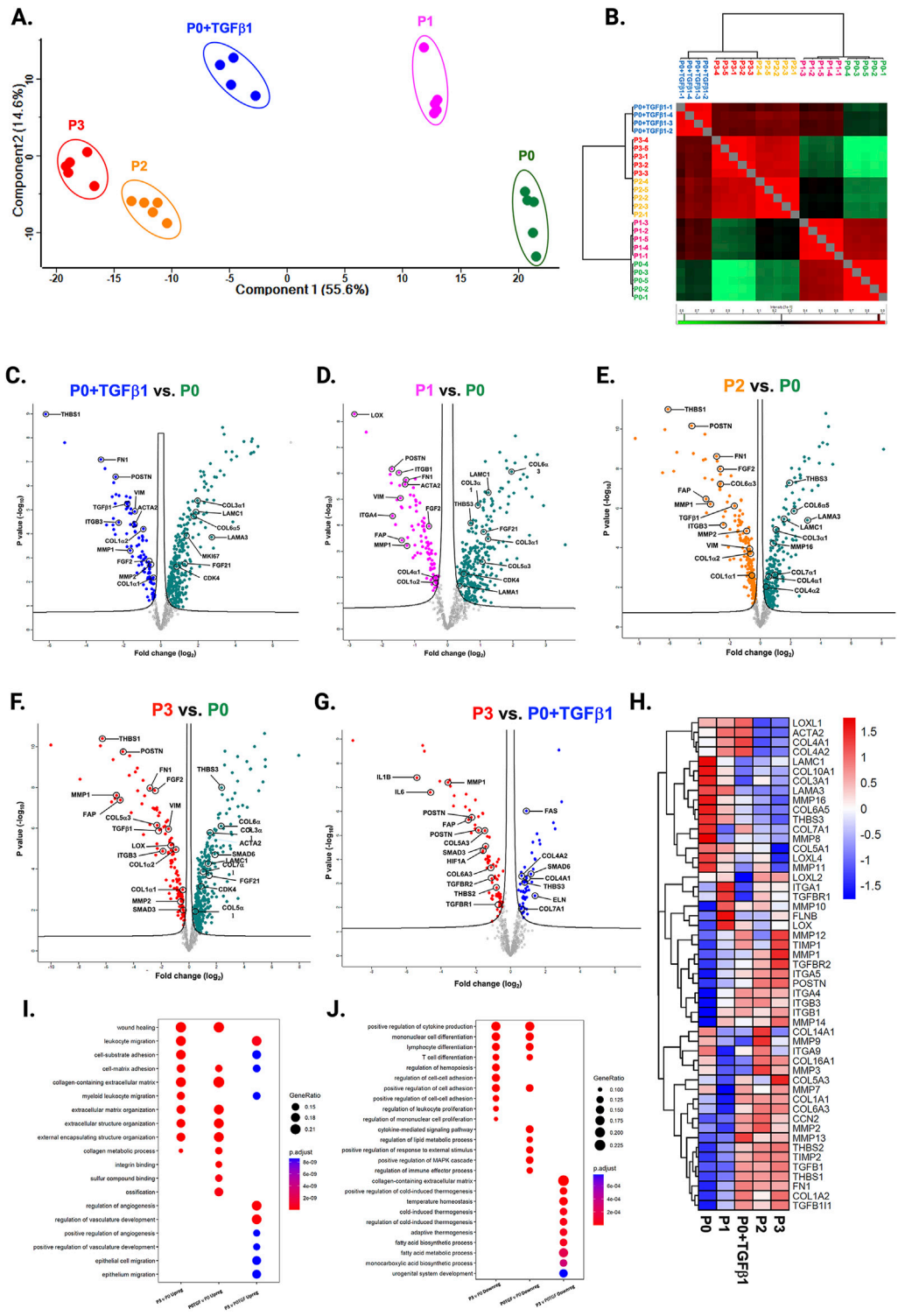

FIGURE 2
Passaging promotes fibrosis-responsive gene expression. PCA of NanoString data **(A)**, based on Benjamini–Hochberg method FDR adjusted to *p*-value <0.05. Group correlation of different passages of fibroblasts based on Pearson correlation method **(B)**, and the gene expression values were scaled from 86.5 to 98.5. Volcano plot of fibrosis gene expression profile in hiPSC-derived fibroblasts P0+TGFβ1 vs. P0 **(C)**, P1 vs. P0 **(D)**, P2 vs. P0 **(E)**, P3 vs. P0 **(F)**, P3 vs. P0+TGFβ1 **(G)**, (adjusted $p < 0.05$), upregulated genes on the left side of the panel and downregulated on the right side (n = 4–5), per group and the fold-change was compared using Welch's *t*-test. Heatmap of differential expression of selected genes comparing various passages of hiPSC-derived fibroblasts **(H)** and the expression values were scaled from −1.5 to 1.5, similarity was calculated using a heatmap package (clustering_distance_rows = "euclidean"). Compare cluster analysis of enrichment of the top 10 upregulated pathways **(I)** and downregulated pathways **(J)** between P3 vs. P0, P0+TGFβ1 vs. P0, and P3 vs. P0+TGFβ1, based on adjusted *p*-value <0.05.The iPS IMR90-1and STAN248i-617C1 lines were used to generate the data for (A–J).

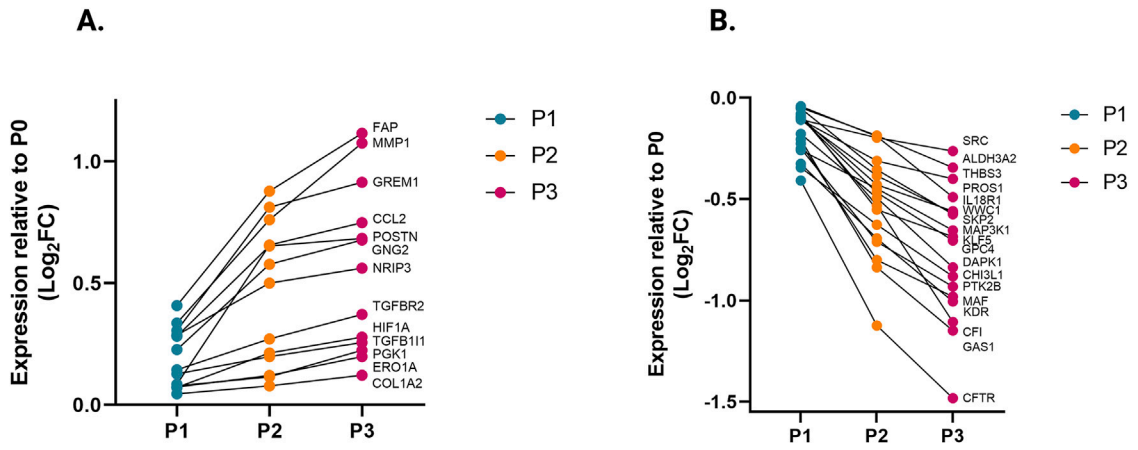

FIGURE 3
Transcriptomic profile transition of hiPSC-CFs with each passage. Plot demonstrates the change in gene expression relative to P0 with each passage, showing genes that are significantly **(A)** upregulated and **(B)** downregulated with each consecutive passage. Statistical significance between each passage (P1 vs. P0, P2 vs. P1, P3 vs. P2) was determined by Student's t-test, with a *p*-value <0.05 cut-off. Only genes that significantly differed between each passage were included. The iPS IMR90-1and STAN248i-617C1 lines were used to generate the data for **(A, B)**.

analysis (Figure 4F), and the data revealed that each group is unique, with expression profiles that differ from one another. Passage-mediated myofibroblasts and TGFβ1-treated hiPSC-CFs revealed that profibrotic proteins such as fibrillar collagens (Col1α1 and Col1α2) and non-fibrillar collagens (Col4α1) were significantly higher in P3 compared to P0, whereas Col3α1 showed a reduction in P0+TGFβ1 and P3 compared to P0 (Figures 5A–D). Structural proteins like ACTA2, FN1, integrin α-1 (ITGA1), and integrin β-3 (ITGB3) were significantly elevated in P0+TGFβ1 and P3 compared to P0; however, vimentin (VIM) protein expression went down in P3 compared to P0 (Figures 5E–I). Additionally, ECM remodeling enzymes such as lysyl oxidase and lysyl hydroxylase-2 (PLOD2) protein expression was upregulated in both P3 and P0+TGFβ1 compared to P0, an indication of elevated collagen processing (Supplementary Figures S2D, E). Comparative cluster enrichment analysis of proteomic expression profiles revealed the top 10 upregulated (Figure 4G) and downregulated (Figure 4H) signaling pathways between (P3 vs. P0), (P0+TGFβ1 vs. P0), and (P3 vs. P0+ TGFβ1); these results indicate that both P3 and P0+TGFβ1 exhibit distinct profibrotic gene expression profiles and signaling when compared to P0.

Metabolic profiling of hiPSC-derived cardiac fibroblasts transitioning to myofibroblasts

To understand the potential metabolic changes involved in hiPSC-derived cardiac fibroblast to myofibroblast conversion, Seahorse assays for mitochondrial respiration were performed at different passages with/without TGFβ1 treatment. Interestingly, the results of our study showed a significant concomitant increase in both mitochondrial oxygen consumption rate (OCR) (Figure 6A) and extracellular acidification rate (ECAR) which is a proxy for glycolysis (Figure 6B) with increased passage number, with the highest values observed in P3 compared to non-passaged fibroblasts (P0). To further understand the role of glutamine metabolism in passage-mediated cardiac myofibroblast phenotype switching in hiPSC-CFs, we treated the various passages of hiPSC-CFs with glutaminase (GLS1) inhibitor BPTES, which limits the conversion of glutamine to glutamate, decreasing energy production via the TCA cycle. We noted a significant attenuation of OCR and ECAR by BPTES, indicating that passage-mediated metabolic changes depended on glutaminolysis, which appears to play an essential role in cardiac fibroblast to myofibroblast transition.

The OCR/ECAR ratio reveals a more pronounced shift toward mitochondrial respiration than glycolysis for energy metabolism in higher passages with or without TGFβ1, which was inhibited by BPTES treatment (Figure 6C). The significant boost in spare respiratory capacity in higher passages corresponds to the metabolic adaptability of cells in responding to the increased energy demand during the transition to the myofibroblast stage; however, these responses were reduced with BPTES treatment (Figure 6D). Similarly, basal and maximal respiration also showed an increased trend toward higher passages with TGFβ1 treatment. ATP production, proton leak, and non-mitochondrial OCR were significantly increased in higher passages and following TGFβ1 treatment compared to P0 (Figures 6E–H; Supplementary Figure S4A) and these effects were abolished with BPTES treatment. Additionally, we did not observe any differences in coupling efficiency with passage or TGFβ1-mediated fibroblast activation or treatment with glutaminolysis inhibitor BPTES treatment (Supplementary Figure S4B).

Signaling mechanisms involved in passage-mediated myofibroblast transition in hiPSC-derived cardiac fibroblasts

In our hiPSC-derived cardiac fibroblasts, upon passage, there was a significant increase in TGFβ1 mRNA and protein expression in both P3 and P0+TGFβ1 (Figure 7A,C). TGFβ1-induced transcript-1 (TGFβ1I1) also known as Hic-5, involved in

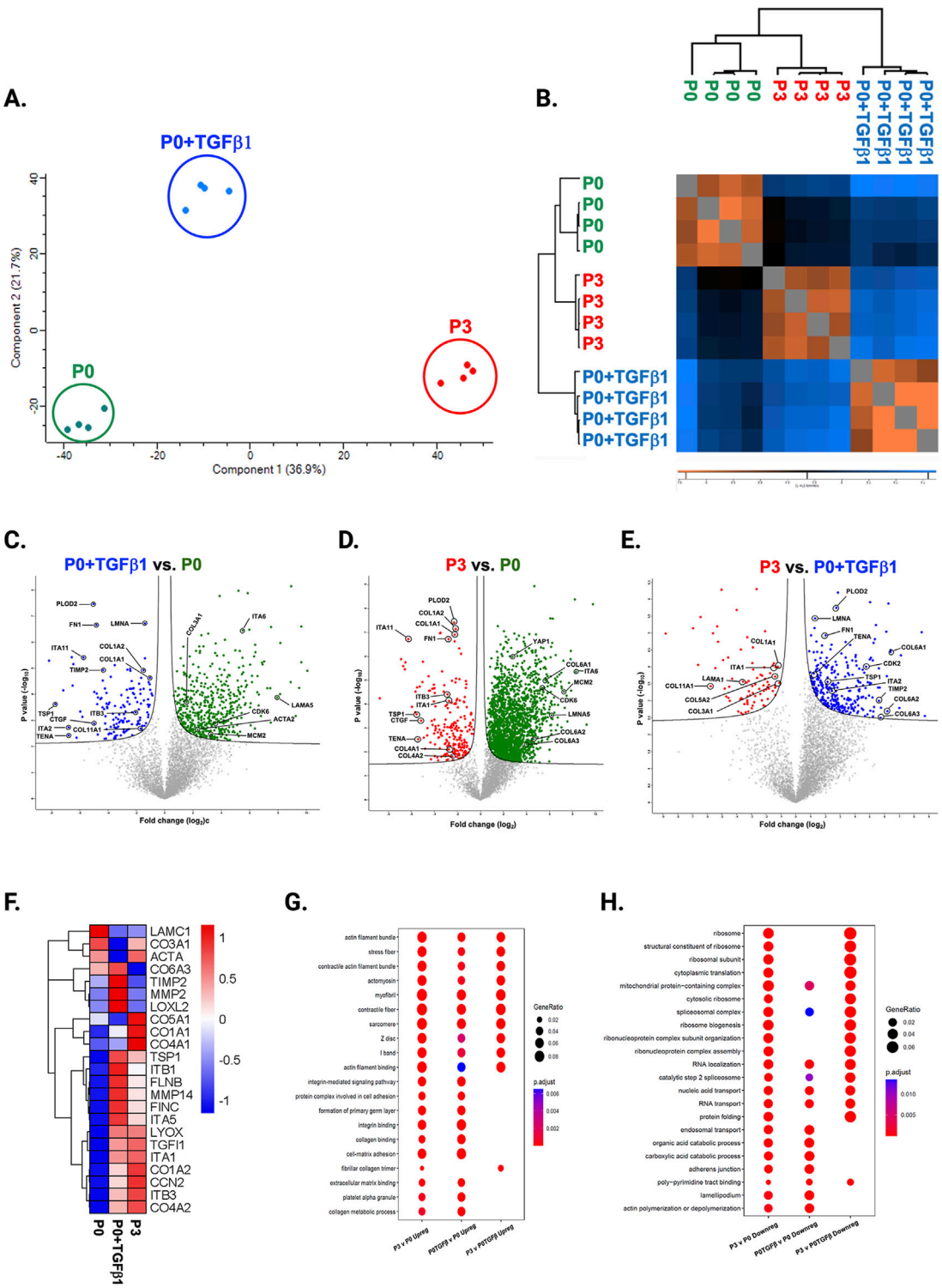

FIGURE 4
Passaging alters the proteomic expression profile of fibroblasts, activated fibroblasts and myofibroblasts. PCA analysis of proteomic gene expression data by mass spectrometry **(A)**, FDR adjusted to *p*-value <0.01. Pearson group correlation of different passages of fibroblasts and their gene expression **(B)**. Volcano plot of proteomic gene expression profile in P3 vs. P0 **(C)**, P0+TGFβ1 vs. P0 **(D)**, P3 vs. P0+TGFβ1 **(E)**, *p*-value adjusted to <0.05; (n = 3–4), per group and the fold-change was measured using Welch's *t*-test. Heatmap of differential expression of selective ECM-related genes comparing hiPSC derived P0, P0+TGFβ and P3 **(F)**, expression values were scaled from −1.0 to +1.0. Comparative cluster analysis of enrichment of top 10 upregulated pathways **(G)** and downregulated pathways **(H)** between P3 vs. P0, P0+TGFβ1 vs. P0, and P3 vs. P0+TGFβ1, based on adjusted *p*-value <0.05. The iPS IMR90-1 line was used to generate the data for **(A–H)**.

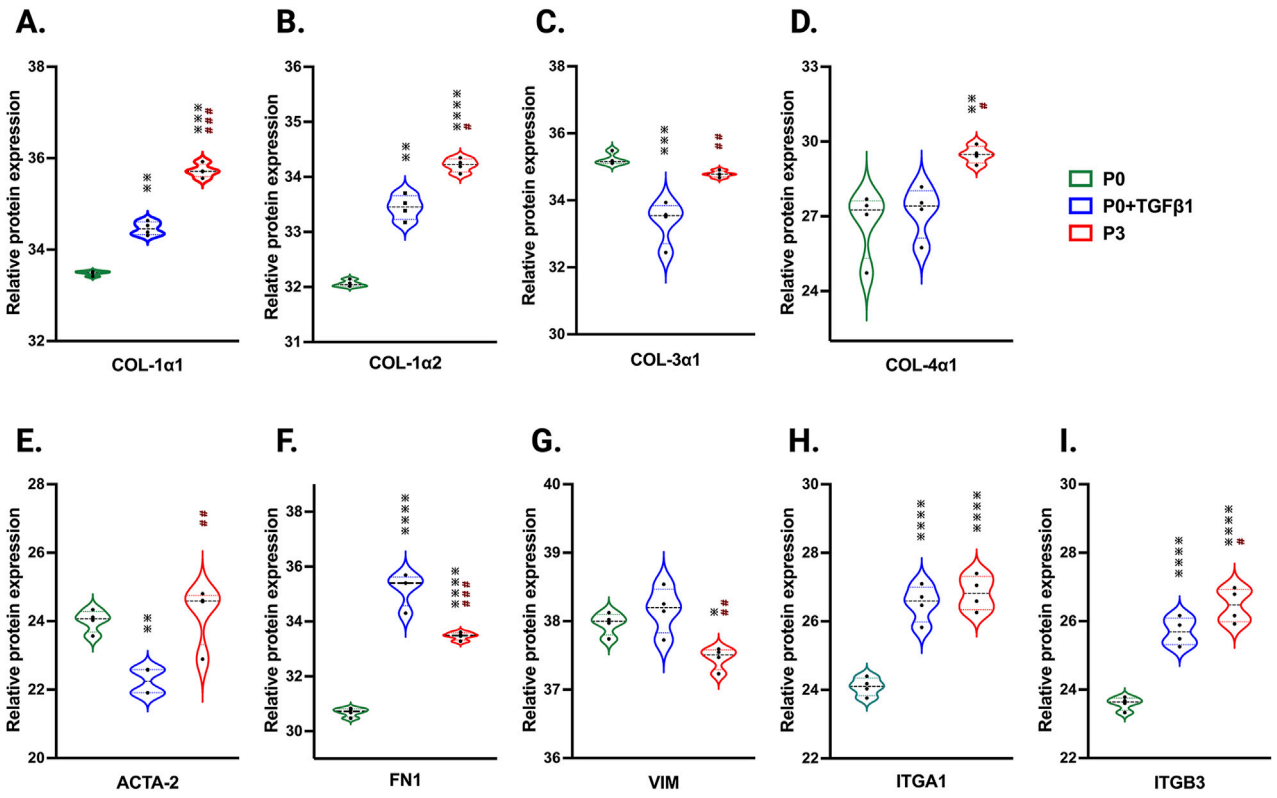

FIGURE 5
Passaging accelerates the turnover of profibrotic extracellular matrix genes during phenotype. Violin plots of profibrotic ECM protein expression in P0+TGFβ1 and P3 compared to P0, **(A–I)**. Statistical significance was determined by one-way ANOVA with Tukey's *post hoc* test (n = 4); *$p < 0.05$, **$p < 0.01$, ***$p < 0.001$, ***$p < 0.0001$ vs. fibroblasts (P0) and #$p \leq 0.05$, ##$p \leq 0.01$, ###$p \leq 0.001$, vs. P0+TGFβ1. The iPS IMR90-1 line was used to generate the data for **(A–I)**.

activation, stress fiber growth and assembly of myofibroblasts, was highly upregulated in both P3 and P0+TGFβ1 compared to P0 (Figure 7B). Our hiPSC-derived CFs P0+TGFβ1 and P3 showed a significant reduction in YAP protein expression compared to P0, whereas TAZ expression was upregulated in both P3 and P0+TGFβ1 (Figures 7D,E). We observed that YAP1 is phosphorylated at S127 site (Figure 7F), and we also noted no change in the total YAP1 vs. YAP1 phosphorylation ratio in P3 and P0+TGFβ1 compared to P0 (Figure 7G). Phosphorylation of YAP1 promotes the degradation or retains the YAP1/TAZ complex in the cytoplasm to limit the profibrotic signaling. Our activated hiPSC-CFs displayed an increase in the active form of YAP1 than P0; however, we did not observe any change in total YAP1 vs. phosphorylated YAP1.

Discussion

Our passaged hiPSC-CFs phenotypically resemble human or murine cardiac fibroblasts upon activation, which was evident in their key marker protein expression, such as TCF21, POSTN, and ED-A-Fn. Several studies have reported that primary human and murine cardiac fibroblasts attain a myofibroblast phenotype upon serial passaging, with reduced motility, incorporation of α-SMA into stress fibers, and formation of focal adhesions (Roche et al., 2016; Rohr, 2011; Rupert et al., 2020; Santiago et al., 2010). This is the first study to show that passaging hiPSC-derived cardiac fibroblasts similarly promotes the activation of fibroblasts and transition to a myofibroblast phenotype. We systematically captured snapshots of transcriptomic, proteomic, and metabolomic changes over three passages to understand the plasticity of hiPSC-CFs. This approach has provided insight into hiPSC-CFs and their use as *ex vivo* human models to study cardiac fibrosis and injury-related mechanistic aspects.

Cardiac fibroblasts undergo a surge in proliferation rate within 2–4 days of activation upon myocardial infarction or pressure overload injury, followed by a reduction in proliferation when they become myofibroblasts (Ali et al., 2014; Farbehi et al., 2019; Fu et al., 2018; Ivey et al., 2018; Ma et al., 2017; Moore-Morris et al., 2014). Several *in vitro* studies reported that while passaging murine primary adult cardiac fibroblasts, upon activation they undergo a proliferative burst followed by a significant reduction in the rate of proliferation when they attain the myofibroblast phenotype (Roche et al., 2016; Santiago et al., 2010). Similarly, in our hiPSC-CFs, we observed that proliferation indicators such as PCNA, MCM3, CDK1, and CDK4 were downregulated when passaged three times (P3), whereas TGFβ1-treated P0 fibroblasts displayed no significant difference in PCNA expression compared to P0. Our results suggest that passaging of hiPSC-CFs reduces their proliferative potential as they become more secretory and nonmotile myofibroblasts.

In the healthy myocardium, the ECM framework protects fibroblasts from stress. Injury or stress-related changes affect the

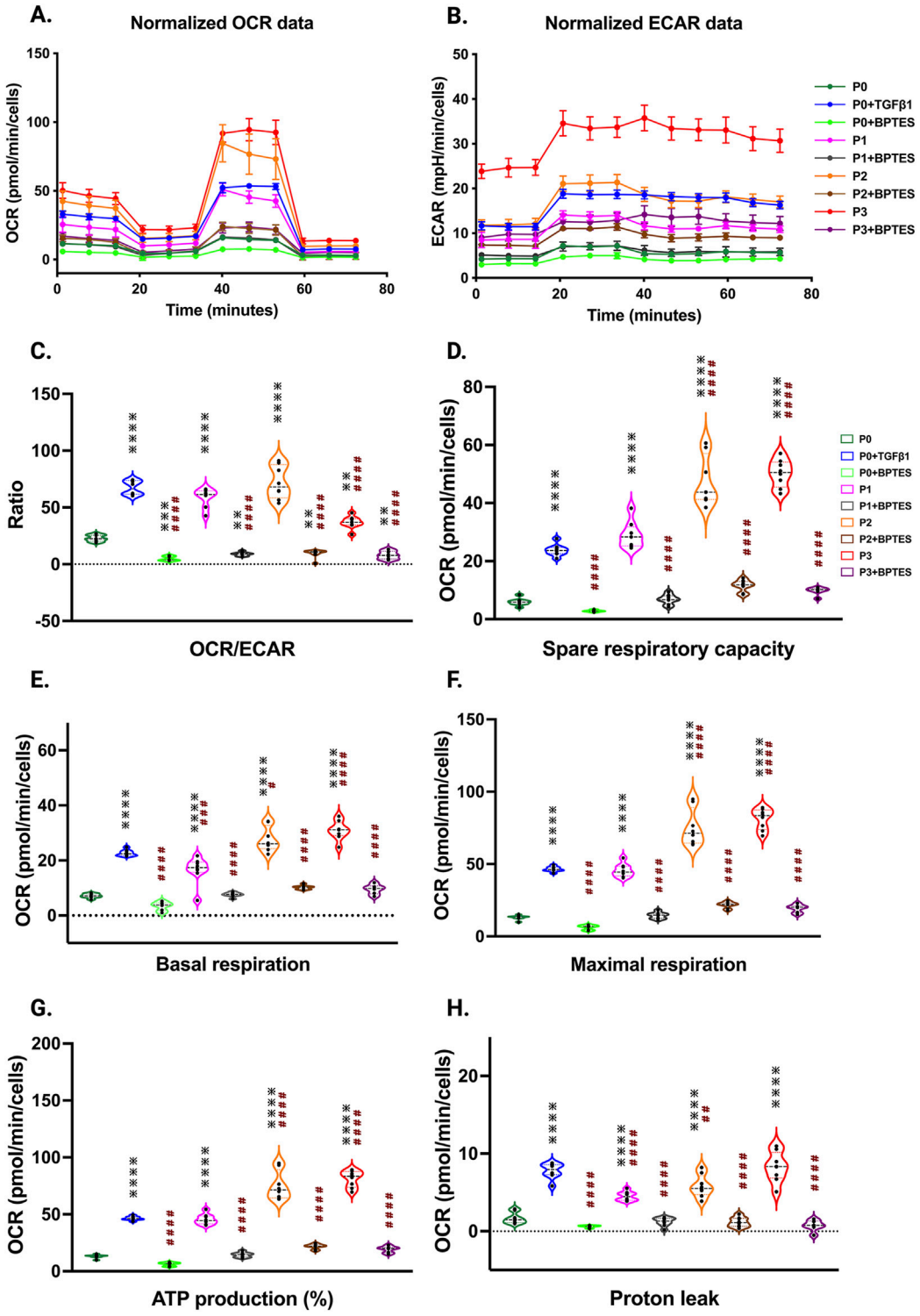

FIGURE 6
Passage-mediated myofibroblast activation depended on mitochondrial metabolism. Oxygen consumption rate is elevated in higher passage of fibroblasts and in TGFβ1 treatment than no passage fibroblasts Seahorse assay reveals that increased OCR rate upon passage (P3) and/or TGFβ1 treatment, whereas the glutaminase inhibitor BPTES limits this process when compared to non-passaged fibroblasts (P0) **(A–H)**, indicating that activation of myofibroblasts primarily depended on the α-keto-glutarate (α-KG) mediated glutaminolysis pathway. Statistical significance for the violin plots was determined by one-way ANOVA with Tukey's *post hoc* test (n = 3–8); *$p \leq 0.05$, **$p \leq 0.01$, ***$p \leq 0.001$, ****$p \leq 0.0001$, vs. fibroblasts (P0) and #$p \leq 0.05$, ##$p \leq 0.01$, ###$p \leq 0.001$, ####$p \leq 0.0001$ vs. P0+TGFβ1. The iPS IMR90-1and STAN248i-617C1 lines were used to generate the data for **(A–H)**.

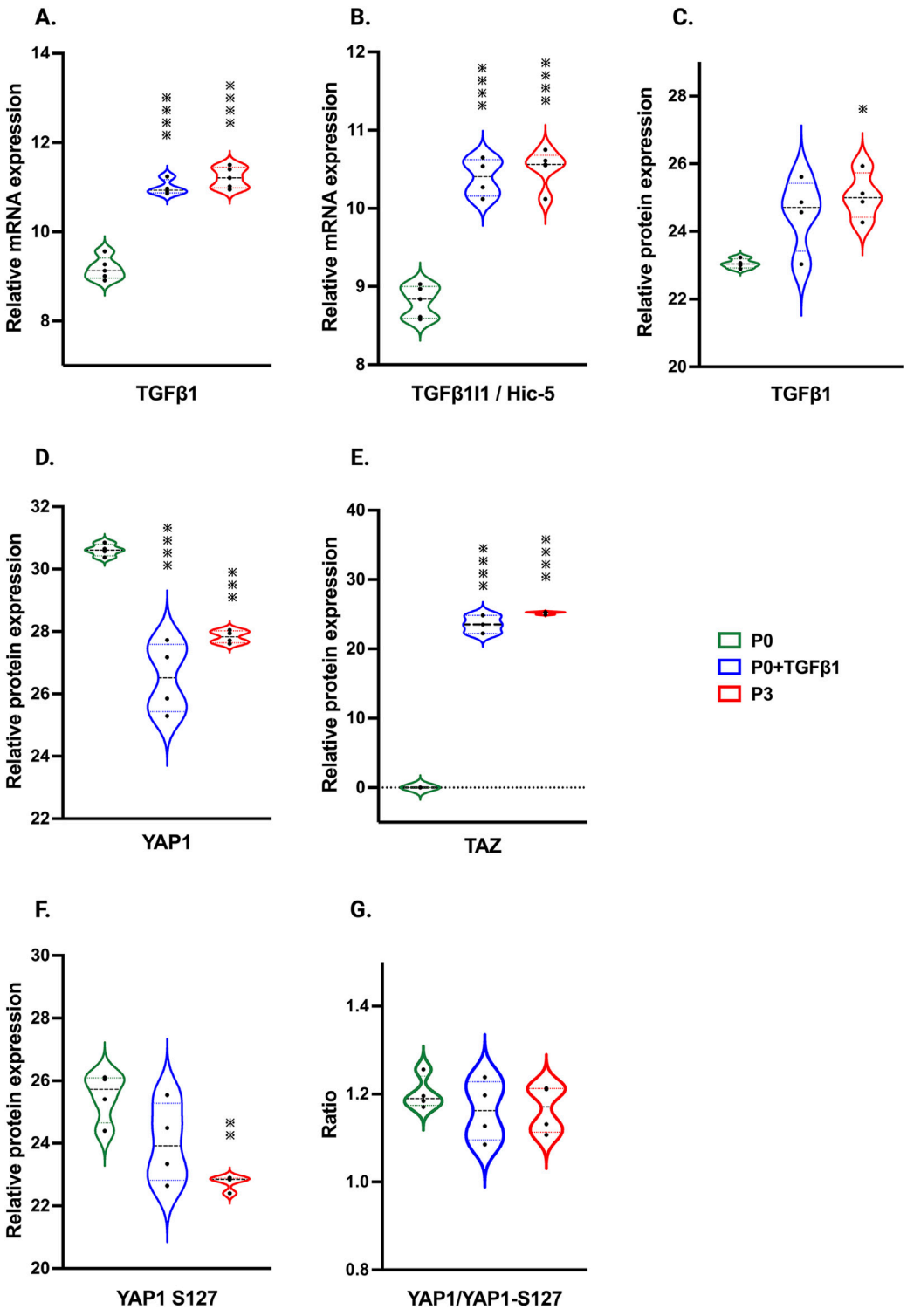

FIGURE 7
Passaging influences TGFβ1 and Hippo signaling pathway. Violin plots represent mRNA expression of TGFβ1 **(A)**, TGFβ1I1 **(B)** and proteomic expression of TGFβ1 **(C)**, showing upregulation in the TGFβ1-mediated canonical signaling pathway in P3 and P0+TGFβ1compared to fibroblasts (P0). Proteomic expression of hippo signaling mediators YAP **(D)**, TAZ **(E)** and phosphorylated sites of YAP on S127 **(F)**, was observed in P3 and P0+TGFβ1. Ratio of total YAP1 vs. YAP1 phosphorylation plotted between YAP1/YAP1-S127 **(G)** showed no differences between groups upon fibroblast activation. Statistical significance was determined by one-way ANOVA with Tukey's *post hoc* test (n = 3–4) *$p \leq 0.05$, **$p \leq 0.01$, ***$p \leq 0.001$, ****$p \leq 0.0001$, vs. fibroblasts (P0). The iPS IMR90-1 line was used to generate the data for **(A–G)**.

ECM microenvironment and architectural integrity, and these changes promote fibroblast activation to become myofibroblasts (Burgess et al., 2002; Hinz and Gabbiani, 2003; Kural and Billiar, 2016; Snider et al., 2009; Wang et al., 2003). Fibroblast activation comes with notable changes in the secretion of ECM proteins compared to quiescent fibroblasts, which is reflected in altered gene expression of ED-A-Fn, Postn, Colα1, Colα3, integrins, and α-SMA in myofibroblasts (Davis and Molkentin, 2014; Ignotz and Massagué, 1986; Ivey and Tallquist, 2016; Serini et al., 1998; Snider et al., 2009; Tomasek et al., 2002). Lysyl oxidase and its family members are involved in the crosslinking of collagen and significantly contributes to cardiac remodeling (González-Santamaría et al., 2016). MMPs are also known to contribute to cardiac remodeling and the degradation of collagen during wound healing (DeLeon-Pennell et al., 2017; Visse and Nagase, 2003). In our hiPSC-CFs, similar changes were observed with passage-mediated fibroblast activation in Col1α1, Col1α2, Col4α1, ED-A-Fn, Postn, ITGA1, ITGB3, Lox, PLOD2, MMP-1, and MMP-2 expression, whereas Col3α1 and Vim expression were downregulated. Surprisingly, in our hiPSC-CFs, α-SMA mRNA expression was increased in P1 and P0+TGFβ1, but not in P2 or P3, whereas α-SMA protein expression was elevated in P3, but not in P0+ TGFβ1; indicating that α-SMA/ACTA2 showed a biphasic wave/effect in our mRNA and protein expression profiles at the time of sampling. However, recent studies on matrifibrocytes indicate that ACTA2 elevation may be transient; 2–4 days after MI injury, activated CFs begin to express αSMA, followed by 4–7 days after injury, activated CFs become myofibroblasts and display high levels of αSMA, eventually by day 10, these CFs further differentiate into matrifibrocytes resulting in loss of αSMA expression and halted the proliferation (Fu et al., 2018). Similar findings, like reduction in proliferation and transient αSMA expression, were observed in our hiPSC-CFs. Li et al. reported that cardiac-specific loss of ACTA2 expression in CFs and lineage tracing showed no change in proliferation, migration, contractility, or survival rate after MI compared to the WT animals. Most importantly, loss of ACTA2 does not reduce stress fiber incorporation in their myofibroblasts. In contrast, increase in other actin filaments like skeletal muscle alpha-actin (Acta1), cytoplasmic beta-actin (Actb), cardiac muscle alpha-actin (Actc1), cytoplasmic gamma-actin (Actg1), and smooth muscle gamma-actin (Actg2) to compensate the loss of ACTA2, indicating that ACTA2 loss does not alter the myofibroblast phenotype or total stress fiber incorporation (Li et al., 2022). We observed similar effects in increased stress fiber incorporation using phalloidin staining in our passage-mediated activated fibroblasts. These results closely resemble the *in vivo* gene expression changes observed upon fibroblast activation to become myofibroblasts in the fibrotic myocardium.

Mitochondrial and metabolomic changes are crucial in determining the nature of fibroblast activation, persistence, and function in failing human hearts (Gibb et al., 2022). Fibrosis-associated myofibroblast transition is highly dependent on oxidative phosphorylation and increased mitochondrial content for energy production (Gibb et al., 2020; Negmadjanov et al., 2015). Glutaminolysis ensures the bioavailability of α-keto-glutarate (α-KG) to feed into the TCA cycle to increase collagen synthesis required for the ECM remodeling (Gibb et al., 2020; Lombardi et al., 2019). Myofibroblasts exhibit increased aerobic glycolysis and lactate production (Lombardi et al., 2019). During idiopathic pulmonary fibrosis, lung myofibroblasts enhance the glutaminolysis-mediated α-KG pathway for energy production that ensures the stability of collagen when remodeling occurs (Ge et al., 2018). Glutaminolysis inhibitors (e.g., CB-839 and BPTES, which inhibit GLS1) attenuate this process and collagen synthesis (Ge et al., 2018; Gibb et al., 2022). Our results provide evidence of similar metabolic changes during passage-mediated hiPSC-CFs activation to myofibroblasts, and notably, these changes were fully reversible by the GLS1 inhibitor BPTES.

Recent studies showed that in a murine MI model, increased collagen synthesis is correlated with higher glycolytic protein synthesis; this process is attenuated with the glycolysis inhibitor 2-deoxy-D-glucose (2-DG) which limited the activation of cardiac fibroblasts (Chen et al., 2021). In primary adult rat cardiac fibroblasts, passaging or TGFβ1 treatment promoted fibroblast activation and GLS1 expression; this process is limited by treatment with CB-839 (Chattopadhyaya et al., 2022). In our hiPSC-CFs upon passaging (P0 to P3) or TGFβ1 treatment, a gradual increase in mitochondrial oxygen consumption rate and ECAR (glycolysis) were observed, indicating that quiescent cardiac fibroblasts are activated and utilizing high energy while they become myofibroblasts. However, BPTES, a glutaminolysis inhibitor, limited passage-mediated increases in OCR. Thus, activated hiPSC-CFs phenotypically resemble cardiac fibrosis-associated human or murine myofibroblasts.

TGFβ1 is a potent inducer of cardiac fibroblast to myofibroblast phenotype switching during pathological remodeling via canonical (Algeciras et al., 2021; Dobaczewski et al., 2010; Saadat et al., 2020; Villalobos et al., 2019) and non-canonical signaling (Zeglinski et al., 2016). Cardiac fibroblasts secrete the active form of TGFβ1 to promote myofibroblast activation (Sarrazy et al., 2014). TGFβ1I1 is also known as hydrogen peroxide inducible clone-5 (Hic-5), which was colocalized with α-SMA in human hypertrophic scars. In human dermal fibroblasts, mechanosensitive Hic-5 expression is dependent on TGFβ1 signaling and it was mediated by canonical Smad-3 and non-canonical MRTF-A and SRF pathways. Hic-5 plays a crucial role in the activation of myofibroblasts, stress fiber growth and assembly, and also nuclear translocation of MRTF-A (Dabiri et al., 2008; Varney et al., 2016). In our hiPSC-CFs, upon passaging, there was an induction of TGFβ1 and TGFb1I1/Hic-5 expression in myofibroblasts compared to non-passaged fibroblasts. These results are congruent with activation of the canonical TGFβ1-Smad signaling pathway, which potently promotes activation of fibroblasts and stress fiber assembly in cardiac myofibroblasts upon stress or injury.

Hippo signaling is also an important mechanism that activates fibroblasts to become myofibroblasts (Landry et al., 2021). YAP and TAZ bind together to translocate into the nucleus to activate the profibrotic signaling pathway, and phosphorylation of YAP hinders nuclear translocation in fibroblasts and myofibroblasts. We found that passage-mediated fibroblast activation in hiPSC-CFs resulted in increased TAZ expression and dephosphorylation of YAP1 at S127, which may induce YAP1 nuclear translocation along with TAZ to promote profibrotic gene expression.

To mimic fibrosis-associated fibroblast activation and other cellular changes in cardiac fibroblasts, *in vitro* experiments have been largely focused on murine primary fibroblasts (Gilles et al., 2020). Most commercially available human primary cardiac fibroblasts (HCFs) are very limited in cell numbers and are

passaged more than once prior to freezing. Frozen cells need to be further expanded to increase the cell numbers before initiating the experiments. Fibroblasts are highly mechano-sensitive in nature, and upon passaging are activated and transition towards the myofibroblast phenotype which was clearly evident in our hiPSC-CFs. The main advantages over murine fibroblasts are avoidance of batch-to-batch variability and low passage number, whereas hiPSC-CFs can be maintained up to five passages quiescently using the TGFβ1inhibitor SB431542 (Zhang H. et al., 2019). In our hands, hiPSC-CFs can be obtained in larger quantities, which helps with conducting multiple experiments and with reproducibility of results, as our cells exhibited relatively low variability across experiments. hiPSC-CFs can be cryopreserved at the P0 stage, which will help avoid batch variations. Mimicking the profibrotic condition with proper controls in HCFs is very unlikely due to limited cell numbers as well as nature of the cells after passaging.

A major advantage of hiPSC-derived cells is that they can be bioprinted as three-dimensional cardiac tissue-like structures, consisting of cardiomyocytes, fibroblasts, and endothelial cells together from the same patient-specific hiPSC cells, and can mimic the cardiac fibrotic condition inside the myocardium. These patient-specific hiPSC-derived cells will help to better understand gene related abnormalities and the severity of disease phenotypes. In hiPSC-CFs, gene-specific alterations like knock-in or knock-out variants can be easily achieved; this will greatly facilitate mimicking and delineating the detailed human profibrotic signaling mechanisms and targeted drug screening for cardiac fibrosis. Most Importantly, understating the changes in the fibroblast to myofibroblast phenotype transition will help unlock the true potential in identifying novel therapeutic druggable targets for cardiac fibrosis and heart failure. Thus hiPSC-CFs offer distinct advantages over murine or human cardiac fibroblasts.

The present study shows that passage-mediated hiPSC-CFs activation aligns well with the *in vivo* physiology of fibrotic myocardium, as shown by transcriptomic, proteomic and metabolomic analysis. Mimicking profibrotic conditions in hiPSC-CFs is highly feasible as shown by our analyses, and more physiologically relevant to humans than murine primary fibroblasts. Most importantly, in our hiPSC-CFs, in P0+TGFβ1, TGFβ1 activates the fibroblasts and their transcriptomic, proteomic and metabolomic profile shows that they are in the continuum phase to become myofibroblasts but are not identical to P3 fibroblasts. Our study results will help clarify the misrepresentations of phenotype and disparity in previous studies.

Study limitations

- We used passage and TGFβ1 to activate the fibroblasts. It is important to mention that inflammation/inflammatory modulators also can promote the fibroblast activation after myocardial infarction.
- We have cultured hiPSC-CFs in tissue culture dishes not on the soft hydrogel matrices, which tend to promote the activation of fibroblasts.
- We have used BPTES as a glutaminolysis inhibitor, but we have not elucidated the mechanistic role of BPTES mediated inhibition in cardiac myofibroblasts.

Data availability statement

The original contributions presented in the study are publicly available. This data can be found here: https://www.dropbox.com/scl/fo/wnrsoztbgh3limnuxta20/AMsh_HQTg4v2e36INN2mLUo?rlkey=9y3l3yns171z7tooupb3ptp70&st=09jw7ngc&dl=0.

Ethics statement

The ethics protocol for using human induced pluripotent stem cells was approved by the Harmonized Minimal Risk Clinical Study Board at the University of British Columbia and Simon Fraser University.

Author contributions

RN: Conceptualization, Data curation, Methodology, Project administration, Supervision, Writing–original draft, Writing–review and editing, Formal Analysis, Investigation. FJ: Data curation, Formal Analysis, Writing–review and editing. HH: Data curation, Writing–review and editing, Methodology. SD: Writing–review and editing, Data curation. DH: Writing–review and editing, Data curation, Investigation. CL: Writing–review and editing, Data curation. RKG: Supervision, Writing–review and editing, Methodology. PL: Supervision, Writing–review and editing, Validation. ID: Conceptualization, Supervision, Writing–review and editing. RR: Writing–review and editing, Formal Analysis, Supervision. MC: Writing–review and editing, Formal Analysis, Supervision. GT: Data curation, Writing–review and editing, Conceptualization, Funding acquisition, Methodology, Project administration, Supervision, Visualization, Writing–original draft.

Funding

The author(s) declare that financial support was received for the research, authorship, and/or publication of this article. GFT research is supported by grants from the Canadian Institutes of Health Research (CIHR PJT488595) and the Stem Cell Network (FY21/ACCT2-13). The RAR research program is supported by The Heart and Stroke Foundation of Canada (G-22-0032033) and CIHR grants (PJT166105 and PJT180474). RN is supported by postdoctoral research fellowships from CIHR and Michael Smith Health Research BC. MPC is supported by a grant from CIHR (PJT162422).

Acknowledgments

Most importantly, we appreciate the incredible infrastructural support from BC Children's Hospital Foundation and the Mining for Miracles (MoM) for the creation of the Cellular and Regenerative Medicine Centre (CRMC) at the BC Children's Hospital Research Institute.

Conflict of interest

The authors declare that the research was conducted in the absence of any commercial or financial relationships that could be construed as a potential conflict of interest.

The author(s) declared that they were an editorial board member of Frontiers, at the time of submission. This had no impact on the peer review process and the final decision.

Publisher's note

All claims expressed in this article are solely those of the authors and do not necessarily represent those of their affiliated organizations, or those of the publisher, the editors and the reviewers. Any product that may be evaluated in this article, or claim that may be made by its manufacturer, is not guaranteed or endorsed by the publisher.

Supplementary material

The Supplementary Material for this article can be found online at: https://www.frontiersin.org/articles/10.3389/fcell.2024.1496884/full#supplementary-material

References

Algeciras, L., Palanca, A., Maestro, D., RuizdelRio, J., and Villar, A. V. (2021). Epigenetic alterations of TGFβ and its main canonical signaling mediators in the context of cardiac fibrosis. *J. Mol. Cell. Cardiol.* 159, 38–47. doi:10.1016/j.yjmcc.2021.06.003

Ali, S. R., Ranjbarvaziri, S., Talkhabi, M., Zhao, P., Subat, A., Hojjat, A., et al. (2014). Developmental heterogeneity of cardiac fibroblasts does not predict pathological proliferation and activation. *Circ. Res.* 115, 625–635. doi:10.1161/circresaha.115.303794

Alvarez-Palomo, B., Sanchez-Lopez, L. I., Moodley, Y., Edel, M. J., and Serrano-Mollar, A. (2020). Induced pluripotent stem cell-derived lung alveolar epithelial type II cells reduce damage in bleomycin-induced lung fibrosis. *Stem Cell. Res. Ther.* 11, 213. doi:10.1186/s13287-020-01726-3

Beauchamp, P., Jackson, C. B., Ozhathil, L. C., Agarkova, I., Galindo, C. L., Sawyer, D. B., et al. (2020). 3D Co-culture of hiPSC-derived cardiomyocytes with cardiac fibroblasts improves tissue-like features of cardiac spheroids. *Front. Mol. Biosci.* 7, 14. doi:10.3389/fmolb.2020.00014

Bohl, S., Wassmuth, R., Abdel-Aty, H., Rudolph, A., Messroghli, D., Dietz, R., et al. (2008). Delayed enhancement cardiac magnetic resonance imaging reveals typical patterns of myocardial injury in patients with various forms of non-ischemic heart disease. *Int. J. Cardiovasc Imaging* 24, 597–607. doi:10.1007/s10554-008-9300-x

Burgess, M. L., Terracio, L., Hirozane, T., and Borg, T. K. (2002). Differential integrin expression by cardiac fibroblasts from hypertensive and exercise-trained rat hearts. *Cardiovasc Pathol.* 11, 78–87. doi:10.1016/s1054-8807(01)00104-1

Campostrini, G., Meraviglia, V., Giacomelli, E., van Helden, R. W. J., Yiangou, L., Davis, R. P., et al. (2021). Generation, functional analysis and applications of isogenic three-dimensional self-aggregating cardiac microtissues from human pluripotent stem cells. *Nat. Protoc.* 16, 2213–2256. doi:10.1038/s41596-021-00497-2

Chattopadhyaya, S., Nagalingam, R. S., Ledingham, D. A., Moffatt, T. L., Al-Hattab, D. S., Narhan, P., et al. (2022). Regulation of cardiac fibroblast GLS1 expression by scleraxis. *Cells* 11, 1471. doi:10.3390/cells11091471

Chen, Z. T., Gao, Q. Y., Wu, M. X., Wang, M., Sun, R. L., Jiang, Y., et al. (2021). Glycolysis inhibition alleviates cardiac fibrosis after myocardial infarction by suppressing cardiac fibroblast activation. *Front. Cardiovasc Med.* 8, 701745. doi:10.3389/fcvm.2021.701745

Cumberland, M. J., Euchner, J., Azad, A. J., N, T. N. V., Kirchhof, P., Holmes, A. P., et al. (2023). Generation of a human iPSC-derived cardiomyocyte/fibroblast engineered heart tissue model. *F1000Res* 12, 1224. doi:10.12688/f1000research.139482.1

Dabiri, G., Tumbarello, D. A., Turner, C. E., and Van de Water, L. (2008). Hic-5 promotes the hypertrophic scar myofibroblast phenotype by regulating the TGF-beta1 autocrine loop. *J. Investig. Dermatol* 128, 2518–2525. doi:10.1038/jid.2008.90

Davis, J., and Molkentin, J. D. (2014). Myofibroblasts: trust your heart and let fate decide. *J. Mol. Cell. Cardiol.* 70, 9–18. doi:10.1016/j.yjmcc.2013.10.019

DeLeon-Pennell, K. Y., Meschiari, C. A., Jung, M., and Lindsey, M. L. (2017). Matrix metalloproteinases in myocardial infarction and heart failure. *Prog. Mol. Biol. Transl. Sci.* 147, 75–100. doi:10.1016/bs.pmbts.2017.02.001

Dobaczewski, M., Bujak, M., Li, N., Gonzalez-Quesada, C., Mendoza, L. H., Wang, X. F., et al. (2010). Smad3 signaling critically regulates fibroblast phenotype and function in healing myocardial infarction. *Circ. Res.* 107, 418–428. doi:10.1161/circresaha.109.216101

Eghbali, M., Tomek, R., Sukhatme, V. P., Woods, C., and Bhambi, B. (1991). Differential effects of transforming growth factor-beta 1 and phorbol myristate acetate on cardiac fibroblasts. Regulation of fibrillar collagen mRNAs and expression of early transcription factors. *Circ. Res.* 69, 483–490. doi:10.1161/01.res.69.2.483

Farbehi, N., Patrick, R., Dorison, A., Xaymardan, M., Janbandhu, V., Wystub-Lis, K., et al. (2019). Single-cell expression profiling reveals dynamic flux of cardiac stromal, vascular and immune cells in health and injury. *Elife* 8, e43882. doi:10.7554/eLife.43882

Frangogiannis, N. G. (2021). Cardiac fibrosis. *Cardiovasc Res.* 117, 1450–1488. doi:10.1093/cvr/cvaa324

Fu, X., Khalil, H., Kanisicak, O., Boyer, J. G., Vagnozzi, R. J., Maliken, B. D., et al. (2018). Specialized fibroblast differentiated states underlie scar formation in the infarcted mouse heart. *J. Clin. Investig.* 128, 2127–2143. doi:10.1172/jci98215

Ge, J., Cui, H., Xie, N., Banerjee, S., Guo, S., Dubey, S., et al. (2018). Glutaminolysis promotes collagen translation and stability via α-Ketoglutarate-mediated mTOR activation and proline hydroxylation. *Am. J. Respir. Cell. Mol. Biol.* 58, 378–390. doi:10.1165/rcmb.2017-0238OC

Giacomelli, E., Meraviglia, V., Campostrini, G., Cochrane, A., Cao, X., van Helden, R. W. J., et al. (2020). Human-iPSC-Derived cardiac stromal cells enhance maturation in 3D cardiac microtissues and reveal non-cardiomyocyte contributions to heart disease. *Cell. Stem Cell.* 26, 862–879. doi:10.1016/j.stem.2020.05.004

Gibb, A. A., Huynh, A. T., Gaspar, R. B., Ploesch, T. L., Lombardi, A. A., Lorkiewicz, P. K., et al. (2022). Glutamine uptake and catabolism is required for myofibroblast formation and persistence. *J. Mol. Cell. Cardiol.* 172, 78–89. doi:10.1016/j.yjmcc.2022.08.002

Gibb, A. A., Lazaropoulos, M. P., and Elrod, J. W. (2020). Myofibroblasts and fibrosis: mitochondrial and metabolic control of cellular differentiation. *Circ. Res.* 127, 427–447. doi:10.1161/circresaha.120.316958

Gilles, G., McCulloch, A. D., Brakebusch, C. H., and Herum, K. M. (2020). Maintaining resting cardiac fibroblasts *in vitro* by disrupting mechanotransduction. *PLoS One* 15, e0241390. doi:10.1371/journal.pone.0241390

González-Santamaría, J., Villalba, M., Busnadiego, O., López-Olañeta, M. M., Sandoval, P., Snabel, J., et al. (2016). Matrix cross-linking lysyl oxidases are induced in response to myocardial infarction and promote cardiac dysfunction. *Cardiovasc Res.* 109, 67–78. doi:10.1093/cvr/cvv214

Hall, C., Law, J. P., Reyat, J. S., Cumberland, M. J., Hang, S., Vo, N. T. N., et al. (2023). Chronic activation of human cardiac fibroblasts *in vitro* attenuates the reversibility of the myofibroblast phenotype. *Sci. Rep.* 13, 12137. doi:10.1038/s41598-023-39369-y

Heimer, R., Bashey, R. I., Kyle, J., and Jimenez, S. A. (1995). TGF-beta modulates the synthesis of proteoglycans by myocardial fibroblasts in culture. *J. Mol. Cell. Cardiol.* 27, 2191–2198. doi:10.1016/s0022-2828(95)91479-x

Hinz, B. (2007). Formation and function of the myofibroblast during tissue repair. *J. Investig. Dermatol* 127, 526–537. doi:10.1038/sj.jid.5700613

Hinz, B., and Gabbiani, G. (2003). Mechanisms of force generation and transmission by myofibroblasts. *Curr. Opin. Biotechnol.* 14, 538–546. doi:10.1016/j.copbio.2003.08.006

Hinz, B., and Lagares, D. (2020). Evasion of apoptosis by myofibroblasts: a hallmark of fibrotic diseases. *Nat. Rev. Rheumatol.* 16, 11–31. doi:10.1038/s41584-019-0324-5

Ignotz, R. A., and Massagué, J. (1986). Transforming growth factor-beta stimulates the expression of fibronectin and collagen and their incorporation into the extracellular matrix. *J. Biol. Chem.* 261, 4337–4345. doi:10.1016/s0021-9258(17)35666-1

Itoh, M., Umegaki-Arao, N., Guo, Z., Liu, L., Higgins, C. A., and Christiano, A. M. (2013). Generation of 3D skin equivalents fully reconstituted from human induced pluripotent stem cells (iPSCs). *PLoS One* 8, e77673. doi:10.1371/journal.pone.0077673

Ivey, M. J., Kuwabara, J. T., Pai, J. T., Moore, R. E., Sun, Z., and Tallquist, M. D. (2018). Resident fibroblast expansion during cardiac growth and remodeling. *J. Mol. Cell. Cardiol.* 114, 161–174. doi:10.1016/j.yjmcc.2017.11.012

Ivey, M. J., and Tallquist, M. D. (2016). Defining the cardiac fibroblast. *Circ. J.* 80, 2269–2276. doi:10.1253/circj.CJ-16-1003

Kanisicak, O., Khalil, H., Ivey, M. J., Karch, J., Maliken, B. D., Correll, R. N., et al. (2016). Genetic lineage tracing defines myofibroblast origin and function in the injured heart. *Nat. Commun.* 7, 12260. doi:10.1038/ncomms12260

Kim, Y., Park, N., Rim, Y. A., Nam, Y., Jung, H., Lee, K., et al. (2018). Establishment of a complex skin structure via layered co-culture of keratinocytes and fibroblasts derived from induced pluripotent stem cells. *Stem Cell. Res. Ther.* 9, 217. doi:10.1186/s13287-018-0958-2

Klingberg, F., Chau, G., Walraven, M., Boo, S., Koehler, A., Chow, M. L., et al. (2018). The fibronectin ED-A domain enhances recruitment of latent TGF-β-binding protein-1 to the fibroblast matrix. *J. Cell. Sci.* 131, jcs201293. doi:10.1242/jcs.201293

Kural, M. H., and Billiar, K. L. (2016). Myofibroblast persistence with real-time changes in boundary stiffness. *Acta Biomater.* 32, 223–230. doi:10.1016/j.actbio.2015.12.031

Landry, N. M., Rattan, S. G., Filomeno, K. L., Meier, T. W., Meier, S. C., Foran, S. J., et al. (2021). SKI activates the Hippo pathway via LIMD1 to inhibit cardiac fibroblast activation. *Basic Res. Cardiol.* 116, 25. doi:10.1007/s00395-021-00865-9

Li, Y., Li, C., Liu, Q., Wang, L., Bao, A. X., Jung, J. P., et al. (2022). Loss of Acta2 in cardiac fibroblasts does not prevent the myofibroblast differentiation or affect the cardiac repair after myocardial infarction. *J. Mol. Cell. Cardiol.* 171, 117–132. doi:10.1016/j.yjmcc.2022.08.003

Lombardi, A. A., Gibb, A. A., Arif, E., Kolmetzky, D. W., Tomar, D., Luongo, T. S., et al. (2019). Mitochondrial calcium exchange links metabolism with the epigenome to control cellular differentiation. *Nat. Commun.* 10, 4509. doi:10.1038/s41467-019-12103-x

Ma, Y., Iyer, R. P., Jung, M., Czubryt, M. P., and Lindsey, M. L. (2017). Cardiac fibroblast activation post-myocardial infarction: current knowledge gaps. *Trends Pharmacol. Sci.* 38, 448–458. doi:10.1016/j.tips.2017.03.001

Mitchell, A., Yu, C., Zhao, X., Pearmain, L., Shah, R., Hanley, K. P., et al. (2023). Rapid generation of pulmonary organoids from induced pluripotent stem cells by Co-culturing endodermal and mesodermal progenitors for pulmonary disease modelling. *Biomedicines* 11, 1476. doi:10.3390/biomedicines11051476

Moore-Morris, T., Guimarães-Camboa, N., Banerjee, I., Zambon, A. C., Kisseleva, T., Velayoudon, A., et al. (2014). Resident fibroblast lineages mediate pressure overload-induced cardiac fibrosis. *J. Clin. Investig.* 124, 2921–2934. doi:10.1172/jci74783

Munger, J. S., Huang, X., Kawakatsu, H., Griffiths, M. J., Dalton, S. L., Wu, J., et al. (1999). The integrin alpha v beta 6 binds and activates latent TGF beta 1: a mechanism for regulating pulmonary inflammation and fibrosis. *Cell.* 96, 319–328. doi:10.1016/s0092-8674(00)80545-0

Nagalingam, R. S., Chattopadhyaya, S., Al-Hattab, D. S., Cheung, D. Y. C., Schwartz, L. Y., Jana, S., et al. (2022). Scleraxis and fibrosis in the pressure-overloaded heart. *Eur. Heart J.* 43, 4739–4750. doi:10.1093/eurheartj/ehac362

Negmadjanov, U., Godic, Z., Rizvi, F., Emelyanova, L., Ross, G., Richards, J., et al. (2015). TGF-β1-mediated differentiation of fibroblasts is associated with increased mitochondrial content and cellular respiration. *PLoS One* 10, e0123046. doi:10.1371/journal.pone.0123046

Roche, P. L., Nagalingam, R. S., Bagchi, R. A., Aroutiounova, N., Belisle, B. M., Wigle, J. T., et al. (2016). Role of scleraxis in mechanical stretch-mediated regulation of cardiac myofibroblast phenotype. *Am. J. Physiol. Cell. Physiol.* 311, C297–C307. doi:10.1152/ajpcell.00333.2015

Rohr, S. (2011). Cardiac fibroblasts in cell culture systems: myofibroblasts all along? *J. Cardiovasc Pharmacol.* 57, 389–399. doi:10.1097/FJC.0b013e3182137e17

Rupert, C. E., Kim, T. Y., Choi, B. R., and Coulombe, K. L. K. (2020). Human cardiac fibroblast number and activation state modulate electromechanical function of hiPSC-cardiomyocytes in engineered myocardium. *Stem Cells Int.* 2020, 9363809. doi:10.1155/2020/9363809

Saadat, S., Noureddini, M., Mahjoubin-Tehran, M., Nazemi, S., Shojaie, L., Aschner, M., et al. (2020). Pivotal role of TGF-β/smad signaling in cardiac fibrosis: non-coding RNAs as effectual players. *Front. Cardiovasc Med.* 7, 588347. doi:10.3389/fcvm.2020.588347

Santiago, J. J., Dangerfield, A. L., Rattan, S. G., Bathe, K. L., Cunnington, R. H., Raizman, J. E., et al. (2010). Cardiac fibroblast to myofibroblast differentiation *in vivo* and *in vitro*: expression of focal adhesion components in neonatal and adult rat ventricular myofibroblasts. *Dev. Dyn.* 239, 1573–1584. doi:10.1002/dvdy.22280

Sarrazy, V., Koehler, A., Chow, M. L., Zimina, E., Li, C. X., Kato, H., et al. (2014). Integrins αvβ5 and αvβ3 promote latent TGF-β1 activation by human cardiac fibroblast contraction. *Cardiovasc Res.* 102, 407–417. doi:10.1093/cvr/cvu053

Serini, G., Bochaton-Piallat, M. L., Ropraz, P., Geinoz, A., Borsi, L., Zardi, L., et al. (1998). The fibronectin domain ED-A is crucial for myofibroblastic phenotype induction by transforming growth factor-beta1. *J. Cell. Biol.* 142, 873–881. doi:10.1083/jcb.142.3.873

Shimazaki, M., Nakamura, K., Kii, I., Kashima, T., Amizuka, N., Li, M., et al. (2008). Periostin is essential for cardiac healing after acute myocardial infarction. *J. Exp. Med.* 205, 295–303. doi:10.1084/jem.20071297

Snider, P., Standley, K. N., Wang, J., Azhar, M., Doetschman, T., and Conway, S. J. (2009). Origin of cardiac fibroblasts and the role of periostin. *Circ. Res.* 105, 934–947. doi:10.1161/circresaha.109.201400

Soussi, S., Savchenko, L., Rovina, D., Iacovoni, J. S., Gottinger, A., Vialettes, M., et al. (2023). IPSC derived cardiac fibroblasts of DMD patients show compromised actin microfilaments, metabolic shift and pro-fibrotic phenotype. *Biol. Direct* 18, 41. doi:10.1186/s13062-023-00398-2

Sutton, M. G., and Sharpe, N. (2000). Left ventricular remodeling after myocardial infarction: pathophysiology and therapy. *Circulation* 101, 2981–2988. doi:10.1161/01.cir.101.25.2981

Tamai, K., Sakai, K., Yamaki, H., Moriguchi, K., Igura, K., Maehana, S., et al. (2022). iPSC-derived mesenchymal cells that support alveolar organoid development. *Cell. Rep. Methods* 2, 100314. doi:10.1016/j.crmeth.2022.100314

Tanaka, M., Fujiwara, H., Onodera, T., Wu, D. J., Hamashima, Y., and Kawai, C. (1986). Quantitative analysis of myocardial fibrosis in normals, hypertensive hearts, and hypertrophic cardiomyopathy. *Br. Heart J.* 55, 575–581. doi:10.1136/hrt.55.6.575

Tomasek, J. J., Gabbiani, G., Hinz, B., Chaponnier, C., and Brown, R. A. (2002). Myofibroblasts and mechano-regulation of connective tissue remodelling. *Nat. Rev. Mol. Cell. Biol.* 3, 349–363. doi:10.1038/nrm809

Varney, S. D., Betts, C. B., Zheng, R., Wu, L., Hinz, B., Zhou, J., et al. (2016). Hic-5 is required for myofibroblast differentiation by regulating mechanically dependent MRTF-A nuclear accumulation. *J. Cell. Sci.* 129, 774–787. doi:10.1242/jcs.170589

Villalobos, E., Criollo, A., Schiattarella, G. G., Altamirano, F., French, K. M., May, H. I., et al. (2019). Fibroblast primary cilia are required for cardiac fibrosis. *Circulation* 139, 2342–2357. doi:10.1161/circulationaha.117.028752

Villarreal, F. J., Lee, A. A., Dillmann, W. H., and Giordano, F. J. (1996). Adenovirus-mediated overexpression of human transforming growth factor-beta 1 in rat cardiac fibroblasts, myocytes and smooth muscle cells. *J. Mol. Cell. Cardiol.* 28, 735–742. doi:10.1006/jmcc.1996.0068

Virag, J. I., and Murry, C. E. (2003). Myofibroblast and endothelial cell proliferation during murine myocardial infarct repair. *Am. J. Pathol.* 163, 2433–2440. doi:10.1016/s0002-9440(10)63598-5

Visse, R., and Nagase, H. (2003). Matrix metalloproteinases and tissue inhibitors of metalloproteinases: structure, function, and biochemistry. *Circ. Res.* 92, 827–839. doi:10.1161/01.Res.0000070112.80711.3d

Wang, J., Chen, H., Seth, A., and McCulloch, C. A. (2003). Mechanical force regulation of myofibroblast differentiation in cardiac fibroblasts. *Am. J. Physiol. Heart Circ. Physiol.* 285, H1871–H1881. doi:10.1152/ajpheart.00387.2003

Weber, K. T., and Brilla, C. G. (1991). Pathological hypertrophy and cardiac interstitium. Fibrosis and renin-angiotensin-aldosterone system. *Circulation* 83, 1849–1865. doi:10.1161/01.cir.83.6.1849

Weber, K. T., Janicki, J. S., Shroff, S. G., Pick, R., Chen, R. M., and Bashey, R. I. (1988). Collagen remodeling of the pressure-overloaded, hypertrophied nonhuman primate myocardium. *Circ. Res.* 62, 757–765. doi:10.1161/01.res.62.4.757

Whitehead, A. J., Hocker, J. D., Ren, B., and Engler, A. J. (2022). Improved epicardial cardiac fibroblast generation from iPSCs. *J. Mol. Cell. Cardiol.* 164, 58–68. doi:10.1016/j.yjmcc.2021.11.011

Wickham, H. (2016). *ggplot2: elegant graphics for data analysis*. 2nd Edition Edition. Springer Cham. doi:10.1007/978-3-319-24277-4

Wong, A. P., Bear, C. E., Chin, S., Pasceri, P., Thompson, T. O., Huan, L. J., et al. (2012). Directed differentiation of human pluripotent stem cells into mature airway epithelia expressing functional CFTR protein. *Nat. Biotechnol.* 30, 876–882. doi:10.1038/nbt.2328

Wong, A. P., Chin, S., Xia, S., Garner, J., Bear, C. E., and Rossant, J. (2015). Efficient generation of functional CFTR-expressing airway epithelial cells from human pluripotent stem cells. *Nat. Protoc.* 10, 363–381. doi:10.1038/nprot.2015.021

Yi, X., Li, X., Zhou, Y., Ren, S., Wan, W., Feng, G., et al. (2014). Hepatocyte growth factor regulates the TGF-β1-induced proliferation, differentiation and secretory function of cardiac fibroblasts. *Int. J. Mol. Med.* 34, 381–390. doi:10.3892/ijmm.2014.1782

Yu, B., Zhao, S. R., Yan, C. D., Zhang, M., and Wu, J. C. (2022). Deconvoluting the cells of the human heart with iPSC technology: cell types, protocols, and uses. *Curr. Cardiol. Rep.* 24, 487–496. doi:10.1007/s11886-022-01670-z

Zeglinski, M. R., Roche, P., Hnatowich, M., Jassal, D. S., Wigle, J. T., Czubryt, M. P., et al. (2016). TGFβ1 regulates Scleraxis expression in primary cardiac myofibroblasts by a Smad-independent mechanism. *Am. J. Physiol. Heart Circ. Physiol.* 310, H239–H249. doi:10.1152/ajpheart.00584.2015

Zhang, H., Shen, M., and Wu, J. C. (2022). Generation of quiescent cardiac fibroblasts derived from human induced pluripotent stem cells. *Methods Mol. Biol.* 2454, 109–115. doi:10.1007/7651_2020_300

Zhang, H., Tian, L., Shen, M., Tu, C., Wu, H., Gu, M., et al. (2019a). Generation of quiescent cardiac fibroblasts from human induced pluripotent stem cells for *in vitro* modeling of cardiac fibrosis. *Circ. Res.* 125, 552–566. doi:10.1161/circresaha.119.315491

Zhang, J., Tao, R., Campbell, K. F., Carvalho, J. L., Ruiz, E. C., Kim, G. C., et al. (2019b). Functional cardiac fibroblasts derived from human pluripotent stem cells via second heart field progenitors. *Nat. Commun.* 10, 2238. doi:10.1038/s41467-019-09831-5

frontiers | Frontiers in Cell and Developmental Biology

TYPE Review
PUBLISHED 24 December 2024
DOI 10.3389/fcell.2024.1532614

OPEN ACCESS

EDITED BY
Mustapha Najimi,
Institute of Experimental and Clinical Research-UCLouvain, Belgium

REVIEWED BY
Armel Hervé Nwabo Kamdje,
Université de Garou, Cameroon
Xiaolei Li,
University of Pennsylvania, United States

*CORRESPONDENCE
Yanfang Zhou,
yfzhou@gdmu.edu.cn
Xinsheng Peng,
xspeng@gdmu.edu.cn

†These authors have contributed equally to this work

RECEIVED 22 November 2024
ACCEPTED 09 December 2024
PUBLISHED 24 December 2024

CITATION
Zheng Z, Zhou H, Zhang W, Wang T, Swamiappan S, Peng X and Zhou Y (2024) Effects of advanced glycation end products on stem cell.
Front. Cell Dev. Biol. 12:1532614.
doi: 10.3389/fcell.2024.1532614

Effects of advanced glycation end products on stem cell

Zetai Zheng[1], Hui Zhou[2], Wenwen Zhang[1], Tingyu Wang[1], Sathiskumar Swamiappan[2], Xinsheng Peng[2*†] and Yanfang Zhou[1*†]

[1]Department of Pathophysiology, Guangdong Medical University, Dongguan, China, [2]School of Pharmaceutical Sciences, Guangdong Medical University, Dongguan, China

In recent years, stem cell therapy has become a pivotal component of regenerative medicine. Stem cells, characterized by their self-renewal capacity and multidirectional differentiation potential, can be isolated from a variety of biological tissues, including adipose tissue, bone marrow, the umbilical cord, and the placenta. The classic applications of stem cells include human pluripotent stem cells (hPSCs) and mesenchymal stem cells (MSCs). However, numerous factors can influence the normal physiological function of stem cells. For instance, in diabetes mellitus, advanced glycation end products (AGEs) accumulate in the extracellular matrix (ECM), impairing the physiological function of stem cells. These substances are closely associated with aging and the progression of numerous degenerative diseases. AGEs can create an environment that is detrimental to the normal physiological functions of stem cells. By binding to the primary cellular receptor for advanced glycation end products (RAGE), AGEs disrupt the physiological activities of stem cells. The binding of RAGE to various ligands triggers the activation of downstream signaling pathways, contributing to the pathophysiological development of diabetes, aging, neurodegenerative diseases, and cancer. Therefore, there is an urgent need for comprehensive research on the impact of AGEs on stem cells, which could provide new insights into the therapeutic application of stem cells in regenerative medicine.

KEYWORDS

stem cell, cell functions, advanced glycation end products, rage, glycation

Abbreviations: AGEs, Advanced Glycation End Products; SCs, stem cells; MSCs, mesenchymal stem cells; hPSCs, human pluripotent stem cells; BMSCs, bone marrow mesenchymal stem cells; ECM, extracellular matrix; ERK, extracellular signal-regulated kinases; CML, N-ε-carboxymethyl-lysine; GOLD, glyoxal-lysine dimer; MOLD, methylglyoxal-lysine dimer; HMGB1, high-mobility histone B1; FZD, Frizzled; GSK-3, glycogen synthase kinase 3; Dvl, Dishevelled proteins; NF-κB, Nuclear Factor Kappa B; COMP-Ang1, cartilage oligomeric matrix protein-angiopoietin-1; PKC, Protein Kinase C; PCP, planar cell polarity; p38/MAPK, p38 mitogen-activated protein kinase; LRP5/6, Low-density lipoprotein receptor associated protein 5/6; RORs, receptor tyrosine kinase-like orphan receptors; ROS, reactive oxygen species; OSX, osterix; TLR2/4, Toll-like receptors 2 and 4; BMPs, bone morphogenetic proteins; PI3K/AKT, phosphatidylinositol 3-kinase/protein kinase B; RAGE, Receptor for advanced glycation end products; sRAGE, soluble RAGE.

1 Introduction

Stem cells (SCs) possess unique self-renewal capacity and multidirectional differentiation potential. They can be derived from various biological tissues, including bone marrow, adipose tissue, the umbilical cord, and the placenta. Additionally, SCs exhibit multiple functions, including nutritional support, migration ability, and immunosuppression, and hold broad potential for research and application in regenerative medicine (Naji et al., 2019). In regenerative medicine, treatment strategies focus on tissue repair and cell replacement. The self-renewal capacity and multidirectional differentiation potential of SCs offer extensive applications in treating various diseases (Hoang et al., 2022). Numerous studies focus on exploring the effects of SCs on various diseases. Currently, SCs are utilized directly as therapeutic agents, as exosomes, or synergistically with other drugs. For instance, bone marrow mesenchymal stem cells (BMSCs), a type of biomaterial, have shown promising results in cell therapy, demonstrating high safety and low immunogenicity, and can be rapidly applied to treat diseases (Hoang et al., 2022; Lotfy et al., 2023). Stem cell therapy now spans various fields, including cardiovascular diseases (Zhang et al., 2021a), digestive system diseases (Wang et al., 2021), and cancer-related treatments (Barisic and Childs, 2022). However, available data on the safety of autologous or allogeneic mesenchymal stem cells (MSCs) therapy are often preliminary, thus, precise control over SC characterization, production and delivery methods, and therapeutic regimens is still required (Naji et al., 2017).

In recent years, significant advancements in stem cell therapy have led to a clearer understanding of its functions and mechanisms, highlighting its immense therapeutic potential. Moreover, various factors influencing the physiological function of SCs have garnered widespread attention and research. Numerous studies have shown that under pathological conditions, the accumulation of Advanced Glycation End Products (AGEs) within the extracellular matrix (ECM) significantly threatens the normal physiological function of SCs (Mouw et al., 2014). This nonenzymatic glycosylation process differs from enzyme-directed glycosylation (Figure 1). It occurs spontaneously between carbohydrates and molecules containing free amino groups, including proteins (Fournet et al., 2018a). AGEs, as nonenzymatic glycation end products, are composed of macromolecules such as proteins, lipids, or nucleic acids and can be classified into two categories: exogenous and endogenous (Singh et al., 2001). AGEs can trigger various pathological mechanisms in the body, including cross-linking with proteins to alter their properties and functions, and activating intracellular signals through receptor and nonreceptor-mediated mechanisms, which increase reactive oxygen species (ROS) and inflammation-related factors (Uribarri et al., 2015). AGEs can accumulate in cells, tissues, and organs throughout the body, leading to oxidative stress and inflammatory responses, and causing detrimental effects on human health. Under the influence of AGEs, the activation of downstream signaling pathways triggers the release of various inflammatory cytokines, which may contribute to the development of diabetes, kidney disease, rheumatoid arthritis, neurodegeneration, cancer and other diseases (Ahmad et al., 2018).

Overall, the cytotoxic effects of AGEs are primarily reflected in irreversible damage to protein structure and functional integrity, resulting from both intermolecular and intramolecular cross-linking. AGEs can cross-link with each other and bind to specific proteins, thereby altering their structure and disrupting their functional properties (Uribarri et al., 2015). This covalent cross-linking leads to the inactivation of biologically active proteins and enzymes, resulting in protein hydrolysis and resistance to digestion. It also creates catalytic sites for ROS formation, thereby exacerbating inflammation and oxidative stress (Wan et al., 2022). Furthermore, AGEs induce various metabolic and biochemical disorders by interfering with intracellular signal transduction processes, and their interactions with different cell surface receptors trigger various cell-mediated pathophysiological responses. For instance, when AGEs bind to the homologous receptor RAGE, they activate multiple downstream signaling pathways, directly affecting the physiological function of SCs (Kume et al., 2005; Uribarri et al., 2015; Ahmad et al., 2018).

This article aims to provide a comprehensive review of how AGEs exert multifaceted effects on the physiological functions of SCs, including their survival, proliferation, differentiation potential, with the goal of exploring the underlying mechanisms in detail. To elucidate the correlation between the physiological function of SCs and the accumulation of AGEs in the ECM, focusing on how AGEs affect the physiological function of SCs. Additionally, we summarize the current methods for addressing the effects of cytotoxic AGEs on SCs. By answering and discussing these questions, we will advance our understanding of the physiological mechanisms and influencing factors of SCs.

2 Sources of AGEs

The accumulation of AGEs primarily occurs through two pathways: endogenous and exogenous pathways. Exogenous AGEs are widely present in various foods. The formation of exogenous AGEs is, in fact, closely associated with cooking methods employed in the food industry. Specifically, during food heat treatment, the application of dry heat technologies, such as deep frying, barbecuing, and baking, significantly promotes AGE production. These exogenous AGEs contribute significantly to the total AGEs in the human body (Kellow and Coughlan, 2015). When these AGEs are ingested into the human body through the daily diet, approximately 10%–30% are absorbed and enter the systemic circulation, while the rest are excreted through metabolic pathways (Garay-Sevilla et al., 2021; Khalid et al., 2022). More than 20 AGEs have been identified, with the most common ones being N-ε-carboxymethyl-lysine (CML), N-ε-carboxyethyl-lysine (CEL), pentosidine, pyrraline, glyoxal-lysine dimer (GOLD), methylglyoxal-lysine dimer (MOLD), among others (Figure 2) (Singh et al., 2001).

The formation of endogenous AGEs predominantly occurs via a complex, multistage glycosylation process known as the Maillard reaction. The synthesis of endogenous AGEs involves three steps: 1. The aldehyde group of reducing sugars undergoes nonenzymatic glycation with proteins to form Schiff bases, resulting from the condensation of electrophilic carbonyl groups of reducing sugars with free amino groups; 2. Schiff bases undergo structural rearrangement to produce more stable Amadori products; 3. Amadori products dehydrate and degrade to form AGEs (Xu

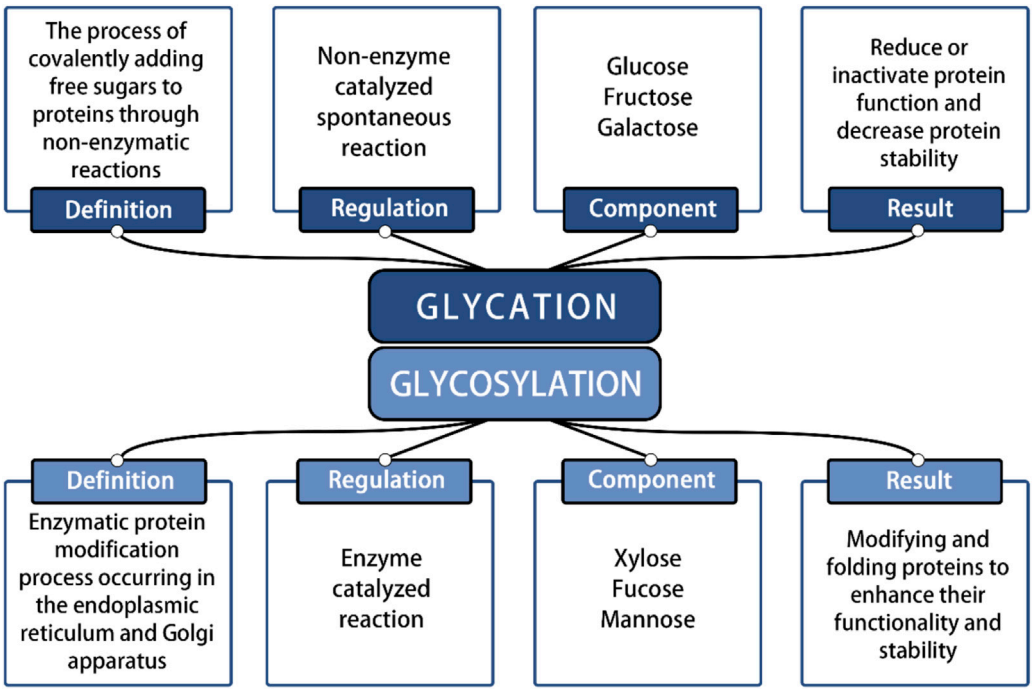

FIGURE 1
Identification of glycation reaction and glycosylation reaction.

et al., 2023) (Figure 3). Within an organization, glycation results in protein aggregates forming through three different mechanisms: 1. covalent bonds are formed between AGEs; 2. Oxidation of thiol groups into disulfide bridges; 3. New reactive groups are formed inside proteins. The chemical cross-links created by AGEs contribute to protein network formation and ECM cross-linking, thereby significantly increasing structural rigidity (Fournet et al., 2018b). This nonenzymatic glycosylation process accelerates under hyperglycemic conditions, as commonly seen in diabetes (Stratmann, 2022). The Maillard reaction generates numerous highly reactive carbonyl AGE precursors. Among these precursors, dicarbonyl compounds serve as critical intermediates in carbonyl AGE formation due to their unique chemical properties, playing an indispensable role in the generating endogenous AGEs. In addition, dicarbonyl compounds can be generated through various other reaction pathways and ultimately converted into AGEs. For example, Schiff bases follow the Namiki pathway during oxidation and can be converted into dicarbonyl compounds; Glucose undergoes automatic oxidation through the Wolff pathway under metal catalysis, generating dicarbonyl compounds. Under the oxidation of the acetone pathway, fats also create a series of highly active dicarbonyl compounds. The endogenous production pathways of these dicarbonyl compounds, also known as α-Acetaldehyde, include glucose autooxidation, the polyol pathway, and lipid oxidation. Imbalances in ketone metabolism, especially under hyperglycemic conditions, lead to dicarbonyl stress, a phenomenon particularly common in diabetic patients (Kellow and Coughlan, 2015; Uribarri et al., 2015; Kuzan, 2021) (Figure 3).

3 Effects of AGEs on SCs survival and proliferation

AGEs significantly impact the survival and proliferation of SCs, with numerous studies demonstrating their inhibitory effect on SCs proliferation across various sources (Kroemer et al., 2010; Zhang et al., 2021b; Liang et al., 2022; Dobrucki et al., 2024). This effect is closely linked to the impact of AGEs on the ECM. The ECM offers localization and structural support for cells, influencing tissue and organ formation, differentiation, and maintenance by modulating growth factor and receptor levels and regulating the cellular environment's pH. (Mouw et al., 2014). Blackburn et al. (2017) demonstrated that AGEs significantly impair cell adhesion within the ECM. Specifically, the adhesion ability of BMSCs is significantly diminished when interacting with AGE-modified collagen. This interaction heightens cellular sensitivity to apoptosis, diminishes the progenitor cell population, and impairs SCs differentiation into vascular tissue.

AGEs contribute to apoptosis and senescence in SCs. One of the primary mechanisms of apoptosis involves initiating a cascade of reactions via the activation of cysteine-containing caspases (Cavalcante et al., 2019). In addition to AGEs, RAGE recognizes various ligands, including pro-inflammatory cytokine mediators of the S100/calcogranulin family, high-mobility histone B1 (HMGB1), and the mucopolysaccharide β-amyloid. This nuclear protein is released upon cell necrosis and functions in the extracellular environment. As a pattern recognition receptor, RAGE shares ligands and signaling pathways with many members of the receptor family (Uribarri et al., 2015; Dobrucki et al., 2024).

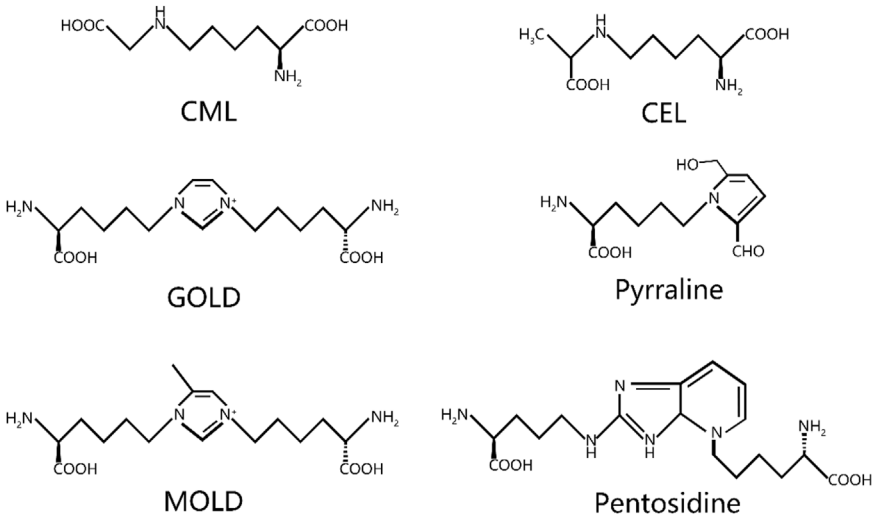

FIGURE 2
Chemical structure of common AGEs. CML, N-ε-carboxymethyl-lysine; CEL, N-ε-carboxyethyl-lysine; GOLD, glyoxal-lysine dimer; MOLD, methylglyoxal-lysine dimer.

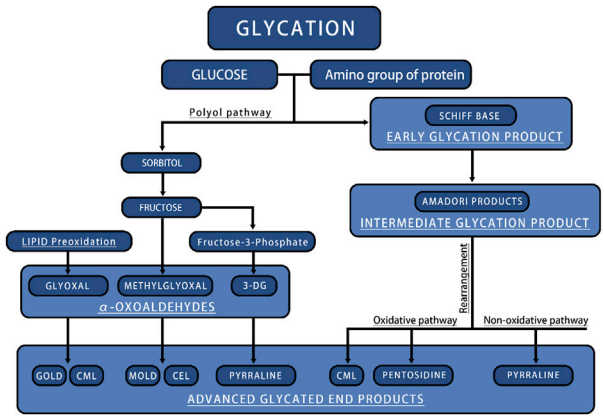

FIGURE 3
The main process of endogenous AGEs production. CML, N-ε-carboxymethyl-lysine; CEL, N-ε-carboxyethyl-lysine; GOLD, glyoxal-lysine dimer; MOLD, methylglyoxal-lysine dimer.

AGE-RAGE binding induces oxidative stress and activates the mitogen-activated protein kinase (MAPK) pathway. MAPK belong to the serine/threonine kinase family, which is not only involved in apoptotic signaling, but also accelerates the process of stem cell apoptosis (Ahmad et al., 2018).

In addition to influencing apoptosis, AGEs also regulate another form of cell death—autophagy. Apoptosis involves the orderly fragmentation of cells into apoptotic bodies, which are swiftly recognized and removed via phagocytosis. Autophagy is an intracellular degradative process in which endogenous or exogenous cytoplasmic components are delivered to lysosomes for degradation. Its primary function is to maintain cell survival and homeostasis by recycling and reusing essential components under stress or nutrient limitation (Kroemer et al., 2010). While autophagy is crucial for cellular homeostasis, excessive autophagy can have harmful effects In Zhang et al. study (Zhang et al., 2021b), it was found that knocking out RAGE can inhibit cell autophagy, indicating that AGEs/RAGE promote autophagy. In Liang et al. (2022) study, it was also found that receptors for AGEs and RAGE are associated with fibrosis and autophagy. Furthermore, inhibiting RAGE provides cardiac protection by reducing hypertrophy and fibrosis in mice. Similarly, Zhang et al. (2023) observed that AGE/RAGE interactions stimulate autophagy.

4 Impact of AGEs on the differentiation potential of SCs

The regeneration of tissues is intricately linked to the differentiation of SCs. For instance, during bone development, MSCs migrate to the target site of bone formation, thereby initiating the first stage of bone development. The mechanism of osteogenesis in the human body involves two main pathways: 1. The direct differentiation of cells into osteoblasts, a process known as intramembranous osteogenesis; 2. The indirect pathway, endochondral osteogenesis, involves the differentiation of chondrocytes and their eventual transformation into bone tissue. This osteogenic process ensures normal bone development and formation. Currently, most osteogenic studies focus on osteogenic differentiation as the primary strategy for osteogenic differentiation (Ding et al., 2022). Various mechanisms affect the differentiation process of MSCs, including the AGE/RAGE pathway (Wang et al., 2022), Wnt/β-catenin pathway (Zhang et al., 2018), Notch-Hes1 pathway (Islam and Aboussekhra, 2019), TGFβ pathway (Notsu et al., 2014). The osteogenic differentiation potential of SCs has remarkable plasticity and can be regulated and transformed through a variety of mechanisms. For instance, specific growth factors or pharmacological agents can effectively direct SC differentiation into osteoblasts. These growth factors or drugs direct the transformation of SCs into osteoblasts by interacting with intracellular signaling

pathways that regulate gene expression and cellular function (Fu et al., 2021).

4.1 AGE/RAGE pathway

Sun et al. (2020) proposed that the AGE/RAGE axis can inhibit the osteogenic differentiation of BMSCs. Their study employed inhibition of the AGE/RAGE axis to mitigate dysfunction in SCs differentiation. Okazaki et al. found that AGEs constrained the osteogenic differentiation of mouse stromal ST2 cells by inhibiting Osterix (OSX) expression and partially increasing RAGE expression. Furthermore, AGEs interfere with the process of SCs differentiation into bone cells by potentially reducing osteocalcin production while increasing RAGE expression (Okazaki et al., 2012). AGEs exert a more pronounced impact during the immature stage of osteoblasts compared to the differentiation stage, inhibiting differentiation and reducing the number of mature osteoblasts (Ogawa et al., 2007). Stolzing et al. (2010) added different doses of AGEs to cultured MSCs and found that the self-renewal and osteogenic differentiation of MSCs were significantly reduced. Under osteogenic differentiation conditions, the extent of this effect depended on the concentration of AGEs in the culture medium. Furthermore, the proliferation of MSCs significantly increased in the low-concentration group, while normal proliferation and osteogenic differentiation of MSCs were impaired in the high-concentration group. They also observed that AGEs suppressed osteocalcin mRNA expression in rat MSCs, thereby hindering their differentiation. Lin et al. (2016) reported that HMGB1 facilitate the osteogenic differentiation of BMSCs while also increasing the expression of RAGE and Toll-like receptors 2 and 4 (TLR2/4) bound to HMGB1. RAGE, a high-affinity receptor for HMGB1, can activate the p38/MAPK and NF-κB pathways upon binding to HMGB1, thereby promoting the osteogenic differentiation of BMSCs (Park et al., 2004). The p38/MAPK pathway plays a crucial role in cell cycle regulation (Barnum and O'Connell, 2014); Kim et al. reported (Kim and Kwon, 2013) that COMP-Ang1 induces the upregulation of the PI3K/AKT and p38/MAPK pathways, thereby facilitating the attenuation of osteogenic differentiation of MSCs by AGEs via the Ang1/Tie2 pathway.

4.2 TGF-β pathway

TGF-β is a crucial factor in regulating the differentiation of MSCs and plays a vital role in stem cell differentiation (Li et al., 2024). Notsu et al. considered that AGEs increase TGF-β by binding to RAGE, and the AGE-TGF-β pathway has a negative effect on the differentiation of MSCs into osteoblasts, impairing their differentiation. This indicates that TGF-β is one of the factors influencing the differentiation potential of SCs (Notsu et al., 2014). In recent years, joint cartilage regeneration technology has advanced significantly, driven by continuous improvements in biological scaffold materials. TGF-β3, as an important isoform of the TGF-β family, plays a pivotal role in mesenchymal stem cell differentiation through both Smad-dependent and non-Smad pathways. Its active involvement and tightly regulated role in the bone healing process have been widely recognized. In recent years, there has been increasing interest in the potential of TGF-β3 to promote and induce the proliferation, osteogenesis, and chondrogenic differentiation of adult SCs in biological scaffold materials. In particular, the induction of TGF-β3 is particularly significant in the early stages of the osteogenic process, providing new therapeutic strategies and research ideas for bone tissue regeneration. These studies not only help us to understand the mechanism of cartilage repair and regeneration deeply, but also provide a solid theoretical basis and experimental foundation for future clinical applications (Li et al., 2018; Roth et al., 2019; Martin et al., 2021).

In general, the role of TGF-β3 in cartilage formation is cell-type specific. Jin et al.'s reported that the inhibitory effect of TGF-β3 on chondrocytes is achieved through the activation of Notch signaling, which inhibits the proliferation of mesenchymal cells and pre-cartilage condensation (Jin et al., 2007). In another study, they also reported a similar finding regarding the inhibitory effect of TGF-β3 on the differentiation of MSCs, which is that TGF-β3 downregulates Protein Kinase C-α (PKC-α) mediated activation of connexin 43, integrin β4, and ERK, inhibiting chondrogenic differentiation of mesenchymal cells (Jin et al., 2008). In contrast to the inhibitory effect of TGF-β3 on MSC differentiation mentioned above, Zheng et al. found that knocking out the TβRIII gene can promote TGF-β3-induced MSCs cartilage differentiation, demonstrating the positive induction effect of TGF-β3 on mesenchymal stem cell differentiation (Zheng et al., 2018). Similarly, Jin et al. found that TGF-β3 stimulates the differentiation of MSCs into chondrocytes and inhibits the differentiation of chondrocytes. This is because TGF-β3 promotes chondrogenic differentiation of mesenchymal cells by activating the PKC-α and p38 MAPK pathways (Jin et al., 2006). Based on the multiple studies on TGF-β3 specified above, it can be concluded that the differences in TGF-β3 are due to its various functions, manifested as a mixed effect of induction and inhibition on the differentiation process of MSCs.

Overall, it is crucial to investigate the complex signaling pathways and mechanisms by which AGEs affect the differentiation process of SCs. This will not only aid in revealing the mechanisms by which AGEs influence SC differentiation, but also provide insight into potential strategies to reverse the toxic effects of AGEs.

4.3 Wnt/β-catenin pathway

The Wnt/β-catenin pathway, a central signaling pathway, precisely regulates cell polarity, determines the differentiation fate of cells, guides the migration process of cells, and has a profound impact on spindle formation, organ development, and stem cell renewal (Nayak et al., 2016). Currently, 19 Wnt ligands have been identified, and all of these ligands specifically bind to a seven-transmembrane Wnt receptor named Frizzled (FZD) (Houschyar et al., 2019). The Wnt pathway, a well-established osteogenic differentiation pathway, is a complex system comprising three distinct pathways, which are believed to be activated upon Wnt receptor activation: the canonical Wnt/β-catenin cascade, the noncanonical planar cell polarity (PCP) pathway, and the Wnt/Ca2+ pathway.

In the canonical Wnt/β-catenin cascade, the central event is the nuclear translocation of the β-catenin protein and its regulation of target genes. In the absence of Wnt ligands, β-catenin is degraded by intracellular complexes-primarily composed of glycogen synthase kinase 3 (GSK-3). However, once the canonical Wnt/β-catenin cascade is activated, Dishevelled proteins (Dvl) are triggered, which in turn inhibit GSK-3, thereby stabilizing β-catenin and promoting its nuclear translocation and target gene expression. Atypical Wnt signaling also plays a crucial role in the differentiation of bone tissue. Unlike the canonical Wnt/β-catenin cascade, the atypical $Ca2^{+}$ dependent Wnt pathway uniquely promotes osteogenesis in MSCs. When the Wnt ligand binds to the FZD receptor, it activates G proteins, triggering the release of $Ca2^{+}$ ions from the endoplasmic reticulum. This process initiates the Protein Kinase C (PKC) pathway and continue signaling to promote osteogenesis (Ahmadi et al., 2022). The Wnt pathway is initiated when Wnt ligands bind to FZD receptors, activating G proteins that subsequently trigger the release of $Ca2^{+}$ ions from the endoplasmic reticulum, which then initiates the PKC pathway. Low-density lipoprotein receptor associated protein 5/6 (LRP5/6) or receptor tyrosine kinase-like orphan receptors (RORs) function as common receptors alongside FZD, facilitating the binding of Wnt proteins to their receptors. The involvement of these co-receptors dictates the downstream effects following successful ligand binding, initiating either the canonical Wnt/β-catenin cascade or the noncanonical planar cell polarity (PCP) pathway (Houschyar et al., 2019; Ahmadi et al., 2022) (Figure 4). Zhou et al. (2023) found that AGEs can impair the osteogenic differentiation process of BMSCs by upregulating the expression of fat and obesity-related gene FTO. This process is regulated by FTO to modify the SOST transcript with m6A, increase the mRNA stability recognized by YTHDF2, inhibit the Wnt signaling pathway, and ultimately disrupt the differentiation of BMSCs into bone. Minear et al. (2010) amplified the cell Wnt response by removing the Axin 2 gene in a mouse model and found that delivering liposome vesicles containing purified Wnt-3a protein can promote the Wnt pathway, leading to increased proliferation and early differentiation of BMSCs, thereby accelerating fracture healing.

Growth factors activate aspects of the Wnt pathway. The TGF-β pathway is a membrane-to-nucleus signaling cascade activated by receptor-mediated transcription factors. Due to structural and functional considerations, the 32 family members are classified into TGF-β and bone morphogenetic proteins (BMPs) subfamilies, along with other variations (David and Massagué, 2018). BMPs have been extensively studied, with BMPs 2, 6, and 9 being the primary isoforms. As potent growth factor, BMPs stimulate MSCs to differentiate into osteoblasts (Carreira et al., 2014). The functional Wnt signaling pathway constitutes the core mechanism of BMP-induced osteogenic differentiation of MSCs. There is a significant interaction between the Wnt and the TGF-β pathways, as they share some key regulatory targets, thus forming a complex signaling network. Among them, β-catenin, a key node in this network, plays a crucial role in regulation (Case and Rubin, 2010). β-catenin plays various roles during different phases of bone repair. In the initial stages following injury, it modulates the osteoblast-to-chondrocyte ratio within the callus tissue induced by MSCs, ensuring a balanced and coordinated repair process (Bao et al., 2017). In the later stages of bone healing, β-catenin induces osteoblasts to differentiate and produce an osteogenic matrix, promoting bone reconstruction and regeneration (Wang et al., 2017). Zhang et al. (2009) suggest that BMP2 regulates β-catenin by stimulating the expression of Lrp5 in osteoblasts and inhibiting the expression of β-Trcp. Chen et al. (2019) also found that the key growth factor BMP2 stimulates the Wnt/β-catenin pathway to promote the osteogenic differentiation of BMSCs. The addition of Wnt-3a enhances the osteogenic effect of BMP9. However, it is counteracted by the downregulation of β-catenin or the increased expression of FrzB, which acts as an antagonist of the FZD receptor (Boland et al., 2004).

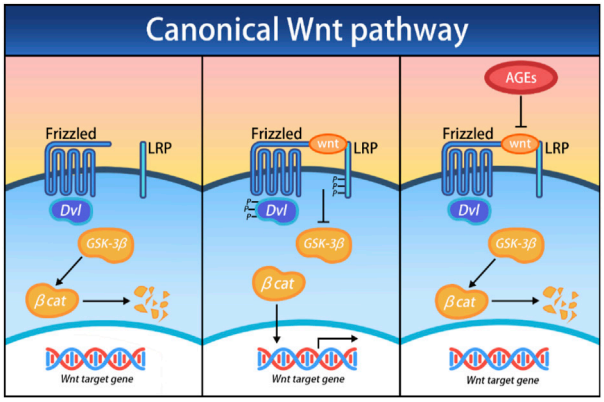

FIGURE 4
Effects of AGEs on the canonical Wnt/β-catenin cascade; Dvl, Dishevelled; GSK-3β, glycogen synthase kinase 3 beta; βcat, β-catenin.

5 Strategies for dealing with the toxic effects of AGEs on SCs

Effective intervention in AGEs-induced damage is critical for promoting the normal physiological activity of SCs. Given the central role of AGEs in stimulating tissue fibrosis and mediating matrix cross-linking, strategies such as reducing AGEs formation, enhancing AGEs degradation, and blocking AGEs cross-linking show promise as therapeutic approaches. Currently, interventions targeting AGEs focus on blocking the pathways through which they exert their effects, thereby mitigating the deleterious impact of AGEs on SCs' physiological functions. In this process, AGE/RAGE and Wnt/β-catenin signaling pathways have become the focus of our attention, and they provide important clues for us to understand the mechanism of AGEs and develop effective interventions.

5.1 Targeting the AGE/RAGE pathway

The glyoxalase system is integral, serving as a key enzyme system present in all mammalian cells. This system consists of two enzymes that act in concern: glyoxalase 1 (Glo1) and glyoxalase 2 (Glo2). The AGE/RAGE pathway alleviate differentiation dysfunction of BMSCs by enhancing the activity of Glo1. AGEs activate complex signaling pathways by binding to RAGE, thereby triggering various toxic effects in the organism. These enzymes catalyze sequential reactions,

with reduced glutathione (GSH) serving as a catalytically active and essential component. The Glo1 enzyme plays a crucial role in the metabolic process by catalyzing the nonenzymatic isomerization of the active dicarbonyl metabolite methylglyoxal (MG) with glutathione to produce dithiol acetaldehyde. Additionally, Glo2 catalyzes the hydrolysis of S-D-lactoylglutathione to generate D-lactic acid, thereby efficiently supplementing the glutathione consumed in the Glo1-catalyzed process. Due to this synergistic action, the glyoxalase system is able to efficiently process dicarbonyl compounds *in vivo* and maintain normal metabolic functions of cells (Rabbani and Thornalley, 2019). Wang et al. (2019) used glycine to inhibit the formation of AGEs, and the study described that Glo1 also mediates this effect. In Jandial et al. mouse model (Jandial et al., 2018), blocking Glo1 resulted in increased AGE production and upregulation of RAGE expression. Consequently, Glo1 inhibition caused cellular accumulation of MG, triggering rapid modifications of proteins, lipids, and DNA, ultimately inducing apoptosis. To counteract the adverse effects of AGEs on primary SCs, an effective strategy involves blocking the interaction between AGE and RAGE. The discovery of Zhang et al. can be utilized with the RAGE inhibitor FPS-ZM1, which can attenuate the adverse effects of AGEs on the osteogenic potential of SCs (Zhang et al., 2018). Rasheed et al. (2011) found that knocking down RAGE by pre-treating soluble RAGE (sRAGE) or using siRNAs effectively reduced the cytotoxicity of AGEs. Based on the above research, activating Glo1 or directly inhibiting the binding of AGEs to RAGE is a highly feasible strategy to mitigate the toxic effects of AGEs.

5.2 Promoting DNA demethylation

Alterations in the Wnt/β-catenin pathway significantly influence bone metabolism. Notably, elevated concentrations of Wnt3a can inhibit the osteogenic differentiation of BMSCs, indicating that regulating the Wnt/β-catenin pathway needs to be fully balanced to avoid adverse effects on stem cell differentiation. Therefore, comprehensive research on the Wnt/β-catenin pathway and its interaction with DNA methylation processes is highly important for optimizing the physiological functions of SCs in AGEs -induced environments (Boland et al., 2004). In Liang et al.'s study, DNA methylation was found to have a substantial impact on the expression of Wnt/β-catenin signaling pathway genes, which also proves that the impact of DNA methylation on the physiological function of MSCs is achieved through the Wnt/β-catenin pathway (Liang et al., 2015). DNA methylation is a molecular modification that determines cell identity and lineages by regulating gene expression and maintaining genomic stability. Under the action of DNA methyltransferase, the covalent bond at the cytosine 5 carbon position of the CpG dinucleotide in the genome binds to a methyl group. DNA methylation induces changes in chromatin structure, DNA conformation, stability, and the dynamics of DNA-protein interactions, thus exerting control over gene expression (Nishiyama and Nakanishi, 2021). DNMT1, DNMT3a and DNMT3b play indispensable roles in DNA methylation. Recent research by Zhang et al. (2018) demonstrated that the expression of DNMT1 and DNMT3a was upregulated, indicating that AGEs increased the level of DNA methylation in ADSCs. To reverse this effect, the investigators used FPS-ZM1, which successfully rescued the loss of osteogenic differentiation in ADSCs by inhibiting AGEs induced DNA methylation. In a study by Li et al. (2020), when ADSCs were cultured in a medium containing AGEs, they exhibited high levels of 5-mC and DNMTs, accompanied by a significant reduction in osteogenic differentiation capacity *in vitro*. However, by applying DNMT inhibitors (5-aza-dC), investigators found that the osteogenic differentiation potential of ADSCs was improved. The promotion of DNA demethylation enhanced the osteogenic differentiation of ADSCs, highlighting the critical role of DNA methylation levels in regulating this process.

6 Conclusion

Both endogenous and exogenous AGEs negatively affect the physiological function of SCs. These strong oxidants continuously weaken the cell's natural defense mechanisms, leading to abnormal oxidative stress and inflammatory responses. However, this unfavorable situation is not irreversible and stem cell therapy is a potential coping strategy to curb the damage caused by AGEs effectively. Elucidating the underlying mechanisms of the impact of AGEs on stem cell toxicity and devising pertinent solutions are vital for advancing stem cell therapy technology.

Author contributions

ZZ: Data curation, Investigation, Writing–original draft. HZ: Funding acquisition, Supervision, Writing–review and editing. WZ: Software, Validation, Writing–original draft. TW: Investigation, Software, Writing–original draft. SS: Supervision, Writing–review and editing. XP: Funding acquisition, Project administration, Writing–review and editing. YZ: Funding acquisition, Supervision, Writing–review and editing.

Funding

The author(s) declare that financial support was received for the research, authorship, and/or publication of this article. Our work described in the present manuscript is supported by research grants from Guangdong Provincial Natural Science Foundation, Guangdong, China, No. 2021A1515012437 and Guangdong Provincial Scientific Research Project, Guangdong Provincial Department of Education, No. 2021KTSCX040, Guangdong, China.

Conflict of interest

The authors declare that the research was conducted in the absence of any commercial or financial relationships that could be construed as a potential conflict of interest.

Generative AI statement

The author(s) declare that no Generative AI was used in the creation of this manuscript.

Publisher's note

References

Ahmad, S., Khan, H., Siddiqui, Z., Khan, M. Y., Rehman, S., Shahab, U., et al. (2018). AGEs, RAGEs and s-RAGE; friend or foe for cancer. *Seminars Cancer Biol.* 49, 44–55. doi:10.1016/j.semcancer.2017.07.001

Ahmadi, A., Mazloomnejad, R., Kasravi, M., Gholamine, B., Bahrami, S., Sarzaeem, M. M., et al. (2022). Recent advances on small molecules in osteogenic differentiation of stem cells and the underlying signaling pathways. *Stem Cell. Res. Ther.* 13, 518. doi:10.1186/s13287-022-03204-4

Bao, Q., Chen, S., Qin, H., Feng, J., Liu, H., Liu, D., et al. (2017). An appropriate Wnt/β-catenin expression level during the remodeling phase is required for improved bone fracture healing in mice. *Sci. Rep.* 7, 2695. doi:10.1038/s41598-017-02705-0

Barisic, S., and Childs, R. W. (2022). Graft-versus-solid-tumor effect: from hematopoietic stem cell transplantation to adoptive cell therapies. *Stem Cells* 40, 556–563. doi:10.1093/stmcls/sxac021

Barnum, K. J., and O'Connell, M. J. (2014). Cell cycle regulation by checkpoints. *Methods Mol. Biol.* 1170, 29–40. doi:10.1007/978-1-4939-0888-2_2

Blackburn, N. J. R., Vulesevic, B., McNeill, B., Cimenci, C. E., Ahmadi, A., Gonzalez-Gomez, M., et al. (2017). Methylglyoxal-derived advanced glycation end products contribute to negative cardiac remodeling and dysfunction post-myocardial infarction. *Basic Res. Cardiol.* 112, 57. doi:10.1007/s00395-017-0646-x

Boland, G. M., Perkins, G., Hall, D. J., and Tuan, R. S. (2004). Wnt 3a promotes proliferation and suppresses osteogenic differentiation of adult human mesenchymal stem cells. *J. Cell. Biochem.* 93, 1210–1230. doi:10.1002/jcb.20284

Carreira, A. C., Lojudice, F. H., Halcsik, E., Navarro, R. D., Sogayar, M. C., and Granjeiro, J. M. (2014). Bone morphogenetic proteins: facts, challenges, and future perspectives. *J. Dent. Res.* 93, 335–345. doi:10.1177/0022034513518561

Case, N., and Rubin, J. (2010). Beta-catenin--a supporting role in the skeleton. *J. Cell. Biochem.* 110, 545–553. doi:10.1002/jcb.22574

Cavalcante, G. C., Schaan, A. P., Cabral, G. F., Santana-da-Silva, M. N., Pinto, P., Vidal, A. F., et al. (2019). A cell's fate: an overview of the molecular biology and genetics of apoptosis. *Int. J. Mol. Sci.* 20, 4133. doi:10.3390/ijms20174133

Chen, X.-J., Shen, Y.-S., He, M.-C., Yang, F., Yang, P., Pang, F.-X., et al. (2019). Polydatin promotes the osteogenic differentiation of human bone mesenchymal stem cells by activating the BMP2-Wnt/β-catenin signaling pathway. *Biomed. and Pharmacother.* 112, 108746. doi:10.1016/j.biopha.2019.108746

David, C. J., and Massagué, J. (2018). Contextual determinants of TGFβ action in development, immunity and cancer. *Nat. Rev. Mol. Cell. Biol.* 19, 419–435. doi:10.1038/s41580-018-0007-0

Ding, P., Gao, C., Gao, Y., Liu, D., Li, H., Xu, J., et al. (2022). Osteocytes regulate senescence of bone and bone marrow. *Elife* 11, e81480. doi:10.7554/eLife.81480

Dobrucki, I. T., Miskalis, A., Nelappana, M., Applegate, C., Wozniak, M., Czerwinski, A., et al. (2024). Receptor for advanced glycation end-products: biological significance and imaging applications. *WIREs Nanomed Nanobiotechnol* 16, e1935. doi:10.1002/wnan.1935

Fournet, M., Bonté, F., and Desmoulière, A. (2018a). Glycation damage: a possible hub for major pathophysiological disorders and aging. *Aging Dis.* 9, 880–900. doi:10.14336/AD.2017.1121

Fournet, M., Bonté, F., and Desmoulière, A. (2018b). Glycation damage: a possible hub for major pathophysiological disorders and aging. *Aging Dis.* 9, 880–900. doi:10.14336/AD.2017.1121

Fu, R., Liu, C., Yan, Y., Li, Q., and Huang, R.-L. (2021). Bone defect reconstruction via endochondral ossification: a developmental engineering strategy. *J. Tissue Eng.* 12, 20417314211004211. doi:10.1177/20417314211004211

Garay-Sevilla, M. E., Rojas, A., Portero-Otin, M., and Uribarri, J. (2021). Dietary AGEs as exogenous boosters of inflammation. *Nutrients* 13, 2802. doi:10.3390/nu13082802

Hoang, D. M., Pham, P. T., Bach, T. Q., Ngo, A. T. L., Nguyen, Q. T., Phan, T. T. K., et al. (2022). Stem cell-based therapy for human diseases. *Sig Transduct. Target Ther.* 7, 272. doi:10.1038/s41392-022-01134-4

Houschyar, K. S., Tapking, C., Borrelli, M. R., Popp, D., Duscher, D., Maan, Z. N., et al. (2019). Wnt pathway in bone repair and regeneration – what do we know so far. *Front. Cell. Dev. Biol.* 6, 170. doi:10.3389/fcell.2018.00170

Islam, S. S., and Aboussekhra, A. (2019). Sequential combination of cisplatin with eugenol targets ovarian cancer stem cells through the Notch-Hes1 signalling pathway. *J. Exp. Clin. Cancer Res.* 38, 382. doi:10.1186/s13046-019-1360-3

Jandial, R., Neman, J., Lim, P., Tamae, D., Kowolik, C., Wuenschell, G., et al. (2018). Inhibition of GLO1 in glioblastoma multiforme increases DNA-AGEs, stimulates RAGE expression, and inhibits brain tumor growth in orthotopic mouse models. *IJMS* 19, 406. doi:10.3390/ijms19020406

Jin, E.-J., Choi, Y.-A., Sonn, J.-K., and Kang, S.-S. (2007). Suppression of ADAM 10-induced delta-1 shedding inhibits cell proliferation during the chondro-inhibitory action of TGF-β3. *Mol. Cells* 24, 139–147. doi:10.1016/s1016-8478(23)10766-7

Jin, E.-J., Lee, S.-Y., Jung, J.-C., Bang, O.-S., and Kang, S.-S. (2008). TGF-beta3 inhibits chondrogenesis of cultured chick leg bud mesenchymal cells via downregulation of connexin 43 and integrin beta4. *J. Cell. Physiol.* 214, 345–353. doi:10.1002/jcp.21202

Jin, E.-J., Park, J.-H., Lee, S.-Y., Chun, J.-S., Bang, O.-S., and Kang, S.-S. (2006). Wnt-5a is involved in TGF-beta3-stimulated chondrogenic differentiation of chick wing bud mesenchymal cells. *Int. J. Biochem. Cell. Biol.* 38, 183–195. doi:10.1016/j.biocel.2005.08.013

Kellow, N. J., and Coughlan, M. T. (2015). Effect of diet-derived advanced glycation end products on inflammation. *Nutr. Rev.* 73, 737–759. doi:10.1093/nutrit/nuv030

Khalid, M., Petroianu, G., and Adem, A. (2022). Advanced glycation end products and diabetes mellitus: mechanisms and perspectives. *Biomolecules* 12, 542. doi:10.3390/biom12040542

Kim, S., and Kwon, J. (2013). COMP-Ang1 inhibits apoptosis as well as improves the attenuated osteogenic differentiation of mesenchymal stem cells induced by advanced glycation end products. *Biochimica Biophysica Acta (BBA) - General Subj.* 1830, 4928–4934. doi:10.1016/j.bbagen.2013.06.035

Kroemer, G., Mariño, G., and Levine, B. (2010). Autophagy and the integrated stress response. *Mol. Cell.* 40, 280–293. doi:10.1016/j.molcel.2010.09.023

Kume, S., Kato, S., Yamagishi, S., Inagaki, Y., Ueda, S., Arima, N., et al. (2005). Advanced glycation end-products attenuate human mesenchymal stem cells and prevent cognate differentiation into adipose tissue, cartilage, and bone. *J. Bone Mineral Res.* 20, 1647–1658. doi:10.1359/JBMR.050514

Kuzan, A. (2021). Toxicity of advanced glycation end products (Review). *Biomed. Rep.* 14, 46. doi:10.3892/br.2021.1422

Li, M., Qiu, L., Hu, W., Deng, X., Xu, H., Cao, Y., et al. (2018). Genetically-modified bone mesenchymal stem cells with TGF-β3 improve wound healing and reduce scar tissue formation in a rabbit model. *Exp. Cell. Res.* 367, 24–29. doi:10.1016/j.yexcr.2018.02.006

Li, X., Lin, H., Yu, Y., Lu, Y., He, B., Liu, M., et al. (2024). *In situ* rapid-formation sprayable hydrogels for challenging tissue injury management. *Adv. Mater.* 36, 2400310. doi:10.1002/adma.202400310

Li, Y., Wang, L., Zhang, M., Huang, K., Yao, Z., Rao, P., et al. (2020). Advanced glycation end products inhibit the osteogenic differentiation potential of adipose-derived stem cells by modulating Wnt/β-catenin signalling pathway via DNA methylation. *Cell. Prolif.* 53, e12834. doi:10.1111/cpr.12834

Liang, B., Zhou, Z., Yang, Z., Liu, J., Zhang, L., He, J., et al. (2022). AGEs-RAGE axis mediates myocardial fibrosis via activation of cardiac fibroblasts induced by autophagy in heart failure. *Exp. Physiol.* 107, 879–891. doi:10.1113/EP090042

Liang, L., He, H., Lv, R., Zhang, M., Huang, H., An, Z., et al. (2015). Preliminary mechanism on the methylation modification of Dkk-1 and Dkk-3 in hepatocellular carcinoma. *Tumour Biol.* 36, 1245–1250. doi:10.1007/s13277-014-2750-y

Lin, F., Zhang, W., Xue, D., Zhu, T., Li, J., Chen, E., et al. (2016). Signaling pathways involved in the effects of HMGB1 on mesenchymal stem cell migration and osteoblastic differentiation. *Int. J. Mol. Med.* 37, 789–797. doi:10.3892/ijmm.2016.2479

Lotfy, A., AboQuella, N. M., and Wang, H. (2023). Mesenchymal stromal/stem cell (MSC)-derived exosomes in clinical trials. *Stem Cell. Res. Ther.* 14, 66. doi:10.1186/s13287-023-03287-7

Martin, A. R., Patel, J. M., Locke, R. C., Eby, M. R., Saleh, K. S., Davidson, M. D., et al. (2021). Nanofibrous hyaluronic acid scaffolds delivering TGF-β3 and SDF-1α for articular cartilage repair in a large animal model. *Acta Biomater.* 126, 170–182. doi:10.1016/j.actbio.2021.03.013

Minear, S., Leucht, P., Jiang, J., Liu, B., Zeng, A., Fuerer, C., et al. (2010). Wnt proteins promote bone regeneration. *Sci. Transl. Med.* 2, 29ra30. doi:10.1126/scitranslmed.3000231

Mouw, J. K., Ou, G., and Weaver, V. M. (2014). Extracellular matrix assembly: a multiscale deconstruction. *Nat. Rev. Mol. Cell. Biol.* 15, 771–785. doi:10.1038/nrm3902

Naji, A., Eitoku, M., Favier, B., Deschaseaux, F., Rouas-Freiss, N., and Suganuma, N. (2019). Biological functions of mesenchymal stem cells and clinical implications. *Cell. Mol. Life Sci.* 76, 3323–3348. doi:10.1007/s00018-019-03125-1

Naji, A., Suganuma, N., Espagnolle, N., Yagyu, K.-I., Baba, N., Sensebé, L., et al. (2017). Rationale for determining the functional potency of mesenchymal stem cells in preventing regulated cell death for therapeutic use. *Stem Cells Transl. Med.* 6, 713–719. doi:10.5966/sctm.2016-0289

Nayak, L., Bhattacharyya, N. P., and De, R. K. (2016). Wnt signal transduction pathways: modules, development and evolution. *BMC Syst. Biol.* 10 (Suppl. 2), 44. doi:10.1186/s12918-016-0299-7

Nishiyama, A., and Nakanishi, M. (2021). Navigating the DNA methylation landscape of cancer. *Trends Genet.* 37, 1012–1027. doi:10.1016/j.tig.2021.05.002

Notsu, M., Yamaguchi, T., Okazaki, K., Tanaka, K., Ogawa, N., Kanazawa, I., et al. (2014). Advanced glycation end product 3 (AGE3) suppresses the mineralization of mouse stromal ST2 cells and human mesenchymal stem cells by increasing TGF-β expression and secretion. *Endocrinology* 155, 2402–2410. doi:10.1210/en.2013-1818

Ogawa, N., Yamaguchi, T., Yano, S., Yamauchi, M., Yamamoto, M., and Sugimoto, T. (2007). The combination of high glucose and advanced glycation end-products (AGEs) inhibits the mineralization of osteoblastic MC3T3-E1 cells through glucose-induced increase in the receptor for AGEs. *Horm. Metab. Res.* 39, 871–875. doi:10.1055/s-2007-991157

Okazaki, K., Yamaguchi, T., Tanaka, K., Notsu, M., Ogawa, N., Yano, S., et al. (2012). Advanced glycation end products (AGEs), but not high glucose, inhibit the osteoblastic differentiation of mouse stromal ST2 cells through the suppression of osterix expression, and inhibit cell growth and increasing cell apoptosis. *Calcif. Tissue Int.* 91, 286–296. doi:10.1007/s00223-012-9641-2

Park, J. S., Svetkauskaite, D., He, Q., Kim, J.-Y., Strassheim, D., Ishizaka, A., et al. (2004). Involvement of toll-like receptors 2 and 4 in cellular activation by high mobility group box 1 protein. *J. Biol. Chem.* 279, 7370–7377. doi:10.1074/jbc.M306793200

Rabbani, N., and Thornalley, P. J. (2019). Glyoxalase 1 modulation in obesity and diabetes. *Antioxidants and Redox Signal.* 30, 354–374. doi:10.1089/ars.2017.7424

Rasheed, Z., Akhtar, N., and Haqqi, T. M. (2011). Advanced glycation end products induce the expression of interleukin-6 and interleukin-8 by receptor for advanced glycation end product-mediated activation of mitogen-activated protein kinases and nuclear factor- B in human osteoarthritis chondrocytes. *Rheumatology* 50, 838–851. doi:10.1093/rheumatology/keq380

Roth, S. P., Brehm, W., Groß, C., Scheibe, P., Schubert, S., and Burk, J. (2019). Transforming growth factor beta 3-loaded decellularized equine tendon matrix for orthopedic tissue engineering. *IJMS* 20, 5474. doi:10.3390/ijms20215474

Singh, R., Barden, A., Mori, T., and Beilin, L. (2001). Advanced glycation end-products: a review. *Diabetologia* 44, 129–146. doi:10.1007/s001250051591

Stolzing, A., Sellers, D., Llewelyn, O., and Scutt, A. (2010). Diabetes induced changes in rat mesenchymal stem cells. *Cells Tissues Organs* 191, 453–465. doi:10.1159/000281826

Stratmann, B. (2022). Dicarbonyl stress in diabetic vascular disease. *Int. J. Mol. Sci.* 23, 6186. doi:10.3390/ijms23116186

Sun, Y., Zhu, Y., Liu, X., Chai, Y., and Xu, J. (2020). Morroniside attenuates high glucose–induced BMSC dysfunction by regulating the Glo1/AGE/RAGE axis. *Cell. Prolif.* 53, e12866. doi:10.1111/cpr.12866

Uribarri, J., Del Castillo, M. D., De La Maza, M. P., Filip, R., Gugliucci, A., Luevano-Contreras, C., et al. (2015). Dietary advanced glycation end products and their role in health and disease. *Adv. Nutr.* 6, 461–473. doi:10.3945/an.115.008433

Wan, L., Bai, X., Zhou, Q., Chen, C., Wang, H., Liu, T., et al. (2022). The advanced glycation end-products (AGEs)/ROS/NLRP3 inflammasome axis contributes to delayed diabetic corneal wound healing and nerve regeneration. *Int. J. Biol. Sci.* 18, 809–825. doi:10.7150/ijbs.63219

Wang, Q.-N., Yan, Y.-Z., Zhang, X.-Z., Lv, J.-X., Nie, H.-P., Wu, J., et al. (2022). Rescuing effects of periostin in advanced glycation end-products (AGEs) caused osteogenic and oxidative damage through AGE receptor mediation and DNA methylation of the CALCA promoter. *Chem. Biol. Interact.* 354, 109835. doi:10.1016/j.cbi.2022.109835

Wang, R., Yao, Q., Chen, W., Gao, F., Li, P., Wu, J., et al. (2021). Stem cell therapy for Crohn's disease: systematic review and meta-analysis of preclinical and clinical studies. *Stem Cell. Res. Ther.* 12, 463. doi:10.1186/s13287-021-02533-0

Wang, T., Zhang, X., and Bikle, D. D. (2017). Osteogenic differentiation of periosteal cells during fracture healing. *J. Cell. Physiol.* 232, 913–921. doi:10.1002/jcp.25641

Wang, Z., Zhang, J., Chen, L., Li, J., Zhang, H., and Guo, X. (2019). Glycine suppresses AGE/RAGE signaling pathway and subsequent oxidative stress by restoring Glo1 function in the aorta of diabetic rats and in HUVECs. *Oxidative Med. Cell. Longev.* 2019, 4628962–4629014. doi:10.1155/2019/4628962

Xu, K., Zhang, L., Yu, N., Ren, Z., Wang, T., Zhang, Y., et al. (2023). Effects of advanced glycation end products (AGEs) on the differentiation potential of primary stem cells: a systematic review. *Stem Cell. Res. Ther.* 14, 74. doi:10.1186/s13287-023-03324-5

Zhang, J., Bolli, R., Garry, D. J., Marbán, E., Menasché, P., Zimmermann, W.-H., et al. (2021a). Basic and translational research in cardiac repair and regeneration: JACC state-of-the-art review. *J. Am. Coll. Cardiol.* 78, 2092–2105. doi:10.1016/j.jacc.2021.09.019

Zhang, L., Guo, Y.-N., Liu, J., Wang, L.-H., Wu, H.-Q., Wang, T., et al. (2023). Plantamajoside attenuates cardiac fibrosis via inhibiting AGEs activated-RAGE/autophagy/EndMT pathway. *Phytother. Res.* 37, 834–847. doi:10.1002/ptr.7663

Zhang, L., He, J., Wang, J., Liu, J., Chen, Z., Deng, B., et al. (2021b). Knockout RAGE alleviates cardiac fibrosis through repressing endothelial-to-mesenchymal transition (EndMT) mediated by autophagy. *Cell. Death Dis.* 12, 470. doi:10.1038/s41419-021-03750-4

Zhang, M., Li, Y., Rao, P., Huang, K., Luo, D., Cai, X., et al. (2018). Blockade of receptors of advanced glycation end products ameliorates diabetic osteogenesis of adipose-derived stem cells through DNA methylation and Wnt signalling pathway. *Cell. Prolif.* 51, e12471. doi:10.1111/cpr.12471

Zhang, M., Yan, Y., Lim, Y.-B., Tang, D., Xie, R., Chen, A., et al. (2009). BMP-2 modulates beta-catenin signaling through stimulation of Lrp5 expression and inhibition of beta-TrCP expression in osteoblasts. *J. Cell. Biochem.* 108, 896–905. doi:10.1002/jcb.22319

Zheng, S., Zhou, H., Chen, Z., Li, Y., Zhou, T., Lian, C., et al. (2018). Type III transforming growth factor- β receptor RNA interference enhances transforming growth factor β 3-induced chondrogenesis signaling in human mesenchymal stem cells. *Stem Cells Int.* 2018, 4180857–4180911. doi:10.1155/2018/4180857

Zhou, J., Zhu, Y., Ai, D., Zhou, M., Li, H., Li, G., et al. (2023). Advanced glycation end products impair bone marrow mesenchymal stem cells osteogenesis in periodontitis with diabetes via FTO-mediated N6-methyladenosine modification of sclerostin. *J. Transl. Med.* 21, 781. doi:10.1186/s12967-023-04630-5

frontiers | Frontiers in Cell and Developmental Biology

TYPE Mini Review
PUBLISHED 03 March 2025
DOI 10.3389/fcell.2025.1559183

OPEN ACCESS

EDITED BY
Christoph Schaniel,
Icahn School of Medicine at Mount Sinai, United States

REVIEWED BY
Hongbing Liu,
Tulane University, United States

*CORRESPONDENCE
Woori Bae,
woori.bae@nyulangone.org
Eun A. Ra,
eunra@jhmi.edu
Myon Hee Lee,
leemy@ecu.edu

†These authors have contributed equally to this work

RECEIVED 12 January 2025
ACCEPTED 13 February 2025
PUBLISHED 03 March 2025

CITATION
Bae W, Ra EA and Lee MH (2025) Epigenetic regulation of reprogramming and pluripotency: insights from histone modifications and their implications for cancer stem cell therapies.
Front. Cell Dev. Biol. 13:1559183.
doi: 10.3389/fcell.2025.1559183

Epigenetic regulation of reprogramming and pluripotency: insights from histone modifications and their implications for cancer stem cell therapies

Woori Bae[1*†], Eun A. Ra[2,3*†] and Myon Hee Lee[4*]

[1]Department of Biochemistry and Molecular Pharmacology, New York University School of Medicine, New York, NY, United States, [2]Institute for Cell Engineering, Johns Hopkins University School of Medicine, Baltimore, MD, United States, [3]Department of Neurology, Johns Hopkins University School of Medicine, Baltimore, MD, United States, [4]Department of Medicine, Hematology/Oncology Division, Brody School of Medicine at East Carolina University, Greenville, NC, United States

Pluripotent stem cells (PSCs) possess the extraordinary capability to differentiate into a variety of cell types. This capability is tightly regulated by epigenetic mechanisms, particularly histone modifications. Moreover, the reprogramming of somatic or fate-committed cells into induced pluripotent stem cells (iPSCs) largely relies on these modifications, such as histone methylation and acetylation of histones. While extensive research has been conducted utilizing mouse models, the significance of histone modifications in human iPSCs is gaining increasing recognition. Recent studies underscore the importance of epigenetic regulators in both the reprogramming process and the regulation of cancer stem cells (CSCs), which are pivotal in tumor initiation and the development of treatment resistance. This review elucidates the dynamic alterations in histone modifications that impact reprogramming and emphasizes the necessity for a balance between activating and repressive marks. These epigenetic marks are influenced by enzymes such as DNA methyltransferases (DNMTs) and histone deacetylases (HDACs). Furthermore, this review explores therapeutic strategies aimed at targeting these epigenetic modifications to enhance treatment efficacy in cancer while advancing the understanding of pluripotency and reprogramming. Despite promising developments in the creation of inhibitors for histone-modifying enzymes, challenges such as selectivity and therapy resistance continue to pose significant hurdles. Therefore, future endeavors must prioritize biomarker-driven approaches and gene-editing technologies to optimize the efficacy of epigenetic therapies.

KEYWORDS

pluripotent stem cells (PSCs), histone modifications, epigenetic regulations, cancer stem cells, reprogramming

1 Introduction

The discovery of PSCs and their ability to differentiate into various cell types has significantly advanced regenerative medicine. PSCs, including embryonic stem cells (ESCs) and iPSCs, have tremendous therapeutic potential due to their pluripotency and self-renewal capabilities.

Maintaining pluripotency and reprogramming somatic cells into iPSCs relies on key transcription factors such as OCT4, SOX2, and NANOG, as well as critical signaling pathways, including Wnt, TGF-beta, and FGF (Marson et al., 2008; Maherali and Hochedlinger, 2009; Mossahebi-Mohammadi et al., 2020). Additionally, many studies have demonstrated that epigenetic factors play a crucial role in sustaining pluripotency and facilitating the reprogramming of somatic cells into iPSCs. Specifically, histone modifications can alter chromatin structure and influence gene expression.

Notably, PSCs and CSCs share many similarities. Therefore, understanding how histone modifications regulate PSCs could open up new avenues for therapeutic interventions in cancer.

2 Histone modifications in PSCs and CSCs

Histone modifications, which include methylation, acetylation, and phosphorylation, play a vital role in regulating chromatin dynamics and gene expression in PSCs (Guenther et al., 2010; Delgado-Olguin and Recillas-Targa, 2011). These modifications primarily occur on the N-terminal tails of histones H3 and H4, impacting the structural configuration of chromatin and controlling the accessibility of transcriptional machinery to DNA (Kouzarides, 2007) (Table 1). Among these modifications, histone methylation and acetylation are particularly important for regulating the pluripotency and differentiation potential of PSCs.

For instance, trimethylation at lysine four on histone H3 (H3K4me3) serves as a marker commonly found at the promoters of actively transcribed genes, such as OCT4 and SOX2. These genes are critical for maintaining pluripotency and fostering an open chromatin state that facilitates gene expression (Benayoun et al., 2014). In contrast, trimethylation at lysine 27 on histone H3 (H3K27me3), mediated by the Polycomb Repressive Complex 2 (PRC2), marks silent genes like cyclin-dependent kinase inhibitor 2A (CDKN2A) and compacts chromatin into a repressive state, which inhibits transcription (Guo et al., 2021) (Table 1).

The interaction between these two marks is essential for maintaining the "bivalent" chromatin state characteristic of PSCs, where both activating (H3K4me3) and repressive (H3K27me3) marks coexist at important developmental gene promoters. This bivalency allows PSCs to remain in a poised state, ready for rapid activation or repression in response to differentiation signals (Bernstein et al., 2006).

Histone acetylation marks, particularly H3K9ac and H3K27ac, are essential for the differentiation of stem cells into specialized cell types (Creyghton et al., 2010). These acetylation marks are linked with active transcription, allowing the chromatin structure to become more open and accessible to transcription factors (McCool et al., 2007) (Table 1).

During differentiation, histone acetyltransferases (HATs) play a crucial role by adding acetyl groups to specific lysine residues on histones. This process facilitates the activation of genes necessary for lineage commitment and functional specialization. On the other hand, HDACs remove these acetyl groups, resulting in a more compact chromatin structure that represses stem cell-associated genes.

The balance between HAT and HDAC activity is vital for directing stem cells through the differentiation process, as it determines which genes are expressed and when. This dynamic regulation of histone acetylation marks influences the transcriptional landscape, guiding stem cells to assume specific fates while preventing premature differentiation (McCool et al., 2007).

During the reprogramming of somatic cells into iPSCs, significant changes occur in histone modifications, which help reset the epigenetic landscape from a differentiated state to a pluripotent one (Liang and Zhang, 2013). Repressive marks such as H3K9me3 and H3K27me3, which are abundant in differentiated cells and indicate regions of heterochromatin, must be actively removed or modified to activate pluripotency genes (Chandra et al., 2012). For example, the removal of H3K9me3 from the NANOG promoter by the lysine demethylase 4B (KDM4B) is essential for initiating reprogramming and maintaining pluripotency (Wei et al., 2017) (Table 1). Additionally, the H3K27me3 demethylase UTX plays a crucial role during the early stages of reprogramming (Mansour et al., 2012). These enzymes work together to erase differentiation-specific epigenetic memory, thus improving both the efficiency and fidelity of the reprogramming process (Dimitrova et al., 2015).

Furthermore, histone acetylation marks play a crucial role in the reprogramming process by enhancing chromatin accessibility. Studies have demonstrated that using HDAC inhibitors, such as valproic acid (VPA), increases reprogramming efficiency (Huangfu et al., 2008; Zhai et al., 2015). These inhibitors work by preventing the removal of acetyl groups, which helps maintain an open chromatin state that is favorable for activating pluripotency-associated genes (Zhai et al., 2015; Duan et al., 2019).

For example, HDAC inhibitors enhance acetylation at the promoter regions of key genes like MYC, thereby promoting the activation of essential pluripotency pathways (Kretsovali et al., 2012) (Table 1). Additionally, the balance of histone modifications is dynamically regulated by histone-modifying enzymes, which are closely controlled during the reprogramming process (Huang et al., 2015; Yang et al., 2022; Kelly et al., 2024).

One specific example is the histone methyltransferase Set1/COMPASS complex, which is responsible for the trimethylation of H3K4. This complex is upregulated during the establishment of pluripotency, facilitating the activation of genes essential for maintaining the pluripotent state (Sze et al., 2017).

CSCs are small populations of tumor cells with the unique ability to self-renew, differentiate, and drive tumor development (Batlle and Clevers, 2017). These cells are believed to contribute significantly to tumor heterogeneity, resistance to therapies, and metastasis, making them critical targets for cancer treatment (Yu et al., 2012; Rich, 2016). Similar to PSCs, the stemness potential of CSCs is heavily influenced by epigenetic modifications, particularly histone modifications, which play a key role in regulating gene expression programs necessary for maintaining their stem-like properties.

TABLE 1 The roles of epigenetic modifications in stem cells and CSCs.

Epigenetic marker	Role in stem cells	Role in CSCs	References
DNA Methylation	Controls pluripotency and differentiation by silencing lineage-specific genes	Aberrant DNA methylation leads to self-renewal, tumorigenesis, and therapy resistance in CSCs	Smith and Meissner (2013), Baylin and Jones (2016), Li and Sun (2019)
Histone Modifications	Regulates gene expression through histone acetylation, methylation, phosphorylation, etc	Alterations in histone marks control CSC plasticity, growth, and therapeutic resistance	Kouzarides (2007), Berdasco and Esteller (2010), Kumar et al. (2022)
Chromatin Remodeling	Modulates chromatin accessibility to transcription factors, regulating self-renewal and differentiation	Aberrant remodeling sustains stem-like properties, enabling CSC survival and metastasis	Wilson and Roberts (2011), Trevino et al. (2021), Chu et al. (2024)
Non-Coding RNAs (miRNAs, lncRNAs)	MicroRNAs and long non-coding RNAs regulate stem cell fate and self-renewal	Dysregulated miRNAs/lncRNAs contribute to CSC maintenance, metastasis, and drug resistance	Wang et al. (2010), Iorio and Croce (2012), Khan et al. (2019)
Polycomb Repressive Complex (PRC)	Maintains stem cell identity by silencing differentiation-associated genes	PRC components such as EZH2 are highly expressed in CSCs, promoting an undifferentiated state	Wen et al. (2017), Guo et al. (2021), Parreno et al. (2022)
Histone Demethylases (KDMs)	Histone demethylases regulate the balance between pluripotency and differentiation by removing methyl groups	Dysregulated KDMs promote stem-like features and survival in CSCs	Mosammaparast and Shi (2010), Wei et al. (2017), Wang et al. (2021)
Histone Deacetylases (HDACs)	Deacetylation of histones keeps chromatin in a condensed, inactive state, regulating gene expression	Overactive HDACs in CSCs suppress tumor suppressor genes, enhancing self-renewal and survival	McCool et al. (2007), Jiang et al. (2024)
CpG Island Methylator Phenotype (CIMP)	Methylation at CpG islands in promoter regions affects gene silencing and differentiation	CIMP in CSCs leads to the silencing of key tumor suppressors, promoting aggressive tumor phenotypes	Barzily-Rokni et al. (2011)
RNA Methylation (m6A)	Modifies mRNA stability, affecting stem cell pluripotency and lineage commitment	Dysregulation of m6A promotes CSC formation, drug resistance, and tumor growth	Zhang et al. (2017), Chen et al. (2021), Wang et al. (2023)

In CSCs, specific histone modifications are crucial for promoting tumor aggressiveness by preserving a gene expression profile that enhances cell survival, proliferation, and resistance to programmed cell death. These epigenetic changes enable CSCs to maintain their tumor-initiating capacity and contribute to their resistance to conventional cancer treatments (French and Pauklin, 2021; Keyvani-Ghamsari et al., 2021; Zhou et al., 2021; Chehelgerdi et al., 2023) (Table 1).

Several histone marks play a crucial role in regulating the identity of CSCs. One significant mark is H3K27me3, a repressive modification added by EZH2, which is a component of the PRC2 (Margueron and Reinberg, 2011). This mark is often overexpressed in CSCs (Wen et al., 2017; Parreno et al., 2022) (Table 1). The H3K27me3 modification silences tumor suppressor genes, such as CDKN2A, as well as differentiation-related genes, like bone morphogenetic protein 2 (BMP2). This silencing helps maintain the cells in a more stem-like, undifferentiated state (Gosselet et al., 2007; Shi et al., 2022).

In breast cancer, elevated levels of EZH2 correlate with an increased population of CSCs and a poorer prognosis, highlighting its role in promoting tumorigenesis and metastasis (Wen et al., 2017; Verma et al., 2022) (Table 1). Similarly, H3K9me3, which is catalyzed by the histone-lysine N-methyltransferase SUV39H1 (also known as KMT1A), has been associated with the repression of differentiation pathways in glioblastoma CSCs. This repression supports their self-renewal and tumor-initiating capabilities (Saha and Muntean, 2021; Li et al., 2024).

Conversely, the activation of specific histone marks, such as H3K4me3 and H3K27ac, plays a significant role in regulating CSCs. These marks are associated with the expression of genes that provide CSCs with stemness and survival advantages. For instance, H3K4me3 is enriched at the promoters of genes crucial for stem cell maintenance and cell cycle regulation, including NANOG and OCT4, in various types of cancer, such as leukemia and colorectal cancer (Deb et al., 2014; Liu et al., 2023). Additionally, acetylation of histone H3 at lysine 27 (H3K27ac) by HATs promotes an open chromatin structure at oncogene enhancers, which contributes to the aggressive characteristics of CSCs in tumors like pancreatic and ovarian cancers (Li et al., 2021; Parreno et al., 2022; Yang et al., 2022) (Table 1). The dynamic regulation of these histone modifications enables CSCs to respond to environmental cues, including stress from chemotherapy and radiation (Li et al., 2023).

3 Epigenetic barriers to reprogramming

Despite significant advances in reprogramming technologies, achieving high efficiency in converting somatic cells to iPSCs remains a challenge due to various epigenetic barriers. Histone modifications, which are often irregularly distributed in differentiated cells, can create a chromatin environment that resists reprogramming (Papp and Plath, 2013; Chehelgerdi et al., 2023; Costa et al., 2023). For instance, repressive histone marks such as H3K9me3 at LINE-1 retrotransposons and H3K27me3 at the promoters of key pluripotency genes, including OCT4 and SOX2, lead to a tightly packed chromatin structure that is inaccessible to the transcription factors required to initiate reprogramming (Sun et al., 2021). The persistence of these repressive marks hinders the activation of pluripotency-associated genes, ultimately reducing both the efficiency and fidelity of the reprogramming process.

Furthermore, DNA methylation at CpG islands and the presence of histone variants, such as macroH2A, contribute to the maintenance of a differentiated state, making reprogramming more challenging. For example, DNA methylation at the GATA4 promoter can inhibit its expression, which is crucial for initiating mesendoderm differentiation during reprogramming (Barzily-Rokni et al., 2011; Hatziapostolou and Iliopoulos, 2011) (Table 1). While it is important to remove or modify these repressive marks, this process is often incomplete because the activity of the involved enzymes depends on the context and cellular environment. Enzymes such as histone demethylases (like KDM4A and KDM4B, which target H3K9me3) and HATs must be precisely directed to specific genomic regions to effectively alter chromatin states (Pack et al., 2016; Young and Dere, 2021). However, this precise targeting is frequently ineffective due to the existing chromatin structure, which is influenced by the cell's previous transcriptional history and current epigenetic landscape.

Moreover, to successfully reprogram cells into a pluripotent state, significant changes in the cell's gene activity, or transcriptome, are required. This process involves two key steps: removing repressive marks that silence genes and adding active marks, such as H3K4me3 and H3K27ac, at the segments that control pluripotency genes (Papp and Plath, 2011; 2013). For instance, restoring H3K4me3 to the SOX2 enhancer is critical for achieving complete reprogramming (Koche et al., 2011).

However, this process is complicated by the interactions between different histone modifications. One type of modification can influence the presence or absence of another, resulting in a complex and resilient network of epigenetic changes. To address these challenges, researchers employ various strategies. These include HDAC inhibitors to enhance chromatin accessibility, DNA methyltransferase inhibitors to reduce DNA methylation, and chromatin remodelers to physically alter chromatin structure (Li and Sun, 2019) (Table 1).

Nonetheless, determining the optimal combination of these approaches can be challenging, as the epigenetic landscape varies significantly from 1 cell type to another. These variations can lead to unintended consequences, such as genomic instability or incomplete reprogramming, ultimately resulting in a mix of different cell types. This limitation can restrict the potential applications of iPSCs in medical treatments. The roles of epigenetic mechanisms in stem cells and CSCs are summarized in Table 1.

4 Targeting histone modifications in CSCs for therapy

Histone modifications play a crucial role in maintaining the characteristics of CSCs and promoting tumor progression. As a result, disrupting these epigenetic markers has become a promising strategy for cancer treatment. Recent advancements have led to the development of novel small-molecule inhibitors that specifically target key histone-modifying enzymes, including histone methyltransferases and HDACs (Kumar et al., 2023) (Table 1). These inhibitors work by dismantling the epigenetic frameworks that underpin CSC maintenance, reducing stem-like properties, promoting differentiation, and enhancing sensitivity to traditional therapies such as chemotherapy and radiation (Figure 1).

One notable advancement in cancer treatment is the development of EZH2 inhibitors, with tazemetostat being a key example that has received FDA approval for patients with both hematologic and solid tumors (Straining and Eighmy, 2022) (Figure 1). EZH2 is a component of the PRC2, which is responsible for the H3K27me3 (Figure 1). This modification is linked to gene silencing and inhibits the differentiation of mesenchymal stem cells and potential CSCs (Momparler and Côté, 2015; Straining and Eighmy, 2022) (Figure 1). High levels of EZH2 activity can repress genes associated with cell cycle arrest, promoting self-renewal in stem or progenitor cells (Kim and Roberts, 2016).

In cancer therapy, treating doxorubicin-resistant high-grade complex karyotype soft tissue sarcoma (STS) cell lines with tazemetostat has shown a reduction in the STS-CSC population. Furthermore, when tazemetostat is combined with doxorubicin, it has been found to restore chemosensitivity (O'Donnell et al., 2024). Promising results from early-phase clinical trials in cancers such as epithelioid sarcoma and follicular lymphoma highlight the potential of EZH2 inhibitors in targeting CSC populations through epigenetic reprogramming (Italiano et al., 2018).

In parallel, HDAC inhibitors like vorinostat and romidepsin have garnered attention for their ability to enhance histone acetylation, particularly at positions H3K27ac and H3K9ac, which are associated with active gene transcription (Gallinari et al., 2007) (Figure 1). By inhibiting HDAC, these compounds create a more accessible chromatin structure, allowing for the expression of genes that promote differentiation, such as p21 (CDKN1A) and BAX (Johnstone, 2002). Moreover, HDAC inhibitors increase the sensitivity of breast CSCs to treatments like cisplatin and doxorubicin across various breast cancer subtypes (Hii et al., 2020).

Vorinostat is the first FDA-approved HDAC inhibitor, specifically approved for the treatment of refractory cutaneous T Cell lymphoma (CTCL). It has been shown to reduce the expression of CSC markers and promote differentiation in glioma stem cell-like populations (GSCs) (Duvic et al., 2007; Booth et al., 2014). Additionally, Sirtuin 1 (SIRT1), the first identified member of the

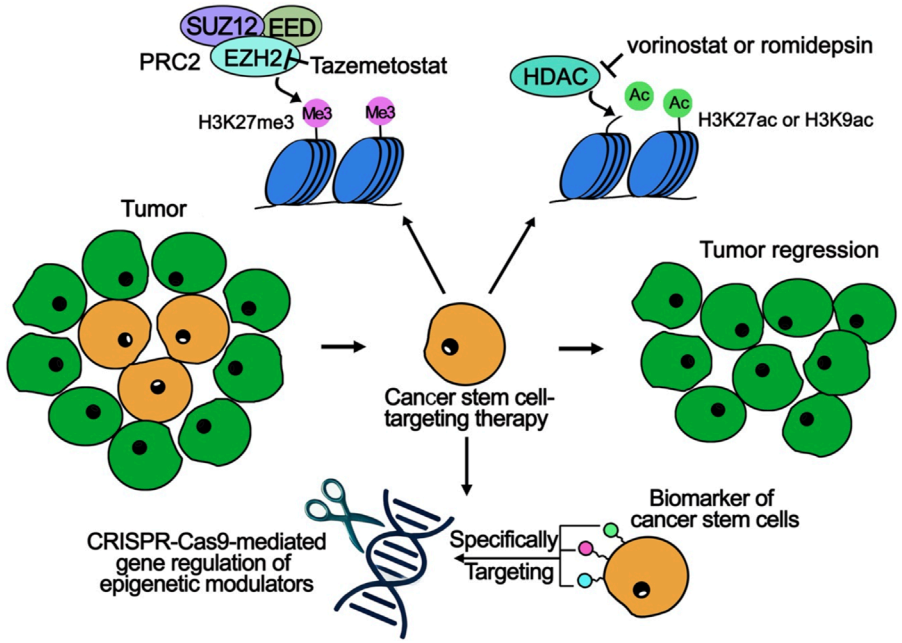

FIGURE 1
Epigenetic Modulation and Targeting Strategies for CSCs in Cancer Therapies. The upper part demonstrates two key epigenetic modifications: (1) Tazemetostat, an EZH2 inhibitor, targets the PRC2 complex (comprising SUZ12, EED, and EZH2) to reduce H3K27me3 levels and increase gene expression. (2) Vorinostat and Romidepsin are HDAC inhibitors that upregulate H3K27ac or H3K9ac levels, promoting chromatin accessibility and active transcription. The lower section highlights CSC-targeting strategies: (1) CSC biomarkers are identified and targeted to achieve selective elimination of CSC populations. (2) Epigenetic modulators are regulated using CRISPR-Cas9 to precisely modify CSC-specific pathways. The central route shows how CSC-specific therapies cause tumor regression by targeting the CSC population (orange cells), while sparing normal tumor cells (green cells).

class III HDACs, requires NAD^+ to catalyze the deacetylation of both histone and non-histone proteins (Liu et al., 2009). The SIRT1 inhibitor Tenovin-6 (TV-6) has demonstrated the ability to disrupt the dependence of lung adenocarcinoma CSCs on mitochondrial oxidative phosphorylation (mtOXPHOS), thereby enhancing and prolonging the therapeutic effectiveness of tyrosine kinase inhibitors (TKIs) like gefitinib (Sun et al., 2020).

Research into the potential of combining HDAC inhibitors with other therapies to overcome resistance mechanisms is ongoing. Such combinations have shown promise in increasing CSC sensitivity to radiation and chemotherapy.

Recent advances in gene therapy and single-cell epigenomic techniques are enhancing epigenetic therapies by providing detailed insights into CSC heterogeneity. Single-cell analysis allows for precise targeting of epigenetic vulnerabilities, while CRISPR-Cas9 technology is being employed to modify key epigenetic regulators involved in CSC-driven tumor growth (Xing and Meng, 2020) (Figure 1). A recent study emphasizes that the overexpression of Achaete-scute homolog 1 (ASCL1), ASCL2, and Transcription Factor AP-4 (TFAP4) significantly contributes to the regulation of CSC-like cell populations, influencing their differentiation potential based on the cellular environment through epigenetic mechanisms (Chen et al., 2023). Furthermore, haploinsufficiency of DNA methyltransferase 1 (Dnmt1) has been shown to effectively impair the self-renewal capabilities of leukemia stem cells while largely leaving normal hematopoiesis unaffected (Trowbridge et al., 2012). In the future, targeting epigenetic regulators specifically in CSCs using CRISPR-Cas9 presents a promising strategy for cancer therapies, as manipulating key factors like ASCL1, TFAP4, and Dnmt1 could disrupt CSC plasticity and differentiation, thus reducing tumorigenicity and improving treatment outcomes (Figure 1).

Despite these advancements, there are several challenges to the development of epigenetic therapies. A primary concern is the lack of selectivity—many histone-modifying enzymes, such as EZH2, are crucial not only for regulating CSCs but also for normal stem cell function. For example, studies have demonstrated that loss of EZH2 function in hematopoietic stem cells increases the likelihood of mice developing various hematologic malignancies (Mochizuki-Kashio et al., 2015). Additionally, CSCs exhibit epigenetic plasticity, allowing them to evade therapeutic interventions by activating compensatory pathways or upregulating alternative histone-modifying enzymes (Cabrera et al., 2015). This adaptability poses a significant barrier to long-term treatment success, often resulting in therapy resistance.

To address these challenges, biomarker-driven patient stratification is emerging as a promising approach that enables more personalized methods for epigenetic therapies. By identifying specific CSC markers such as CD44, CD133, ALDH, and EpCAM, clinicians can categorize patients based on the epigenetic profiles of their tumors, allowing them to select individuals who are more likely to benefit from targeted treatments (Chu et al., 2024) (Table 1). An optimal future strategy could involve the use of specific antibodies recognizing these CSC markers in combination with epigenetic-targeting agents such as tazemetostat (an EZH2 inhibitor) or vorinostat (HDAC inhibitor). This combinatorial

approach may enhance therapeutic precision by selectively targeting CSC populations while minimizing off-target effects.

Furthermore, an effective strategy may involve knocking out epigenetic regulators essential for CSC self-renewal and proliferation. Advances in single-cell technologies, such as single-cell RNA sequencing and single-cell ATAC-seq, offer a valuable solution by enabling the identification of CSC-specific epigenetic signatures. Integrating this information with CRISPR-based gene editing—where Cas9 expression is regulated by CSC-specific promoters like CD133 and EpCAM—could enhance precision in modulating CSC-associated regulators while preserving normal cellular function. This strategy may contribute to the development of highly selective and efficient epigenetic therapies tailored to CSCs and their regulatory mechanisms.

Additionally, combination therapies are showing significant potential. Pairing HDAC inhibitors with other agents that target multiple epigenetic pathways has demonstrated synergistic effects in preclinical models. This combination effectively inhibits CSC functions, such as self-renewal and resistance to apoptosis (Kumar et al., 2022) (Table 1).

The next-generation of epigenetic inhibitors aims to enhance selectivity, minimize off-target effects, and improve the durability of therapeutic responses. Furthermore, gene-editing technologies like CRISPR-Cas9 are being investigated to precisely target epigenetic regulators, offering a more permanent solution for disrupting CSC plasticity.

5 Concluding remarks

Epigenetic therapies targeting CSCs hold significant potential for overcoming tumor growth and resistance to treatment. Advanced technologies such as single-cell epigenomic analysis and CRISPR-Cas9 gene editing allow for precise targeting of critical epigenetic regulators that support CSC adaptability and survival. Despite this progress, challenges still remain, including the non-specificity of current epigenetic drugs and the ability of CSCs to adapt and resist therapy. Utilizing biomarker-based patient stratification combined with treatment strategies may enhance therapeutic precision and minimize off-target effects. Moving forward, advancing selective epigenetic inhibitors and integrating gene-editing tools could offer more effective approaches to eliminate CSCs and improve clinical outcomes.

Author contributions

WB: Writing–original draft, Writing–review and editing. ER: Writing–original draft, Writing–review and editing. ML: Conceptualization, Funding acquisition, Writing–review and editing, Writing–original draft.

Funding

The author(s) declare that financial support was received for the research, authorship, and/or publication of this article. Funding for this work is supported by research grants from the National Science Foundation (IOS 2132286) to ML.

Conflict of interest

The authors declare that the research was conducted in the absence of any commercial or financial relationships that could be construed as a potential conflict of interest.

The author(s) declared that they were an editorial board member of Frontiers, at the time of submission. This had no impact on the peer review process and the final decision.

Generative AI statement

The author(s) declare that no Generative AI was used in the creation of this manuscript.

Publisher's note

References

Barzily-Rokni, M., Friedman, N., Ron-Bigger, S., Isaac, S., Michlin, D., and Eden, A. (2011). Synergism between DNA methylation and macroH2A1 occupancy in epigenetic silencing of the tumor suppressor gene p16(CDKN2A). *Nucleic Acids Res.* 39, 1326–1335. doi:10.1093/nar/gkq994

Batlle, E., and Clevers, H. (2017). Cancer stem cells revisited. *Nat. Med.* 23, 1124–1134. doi:10.1038/nm.4409

Baylin, S. B., and Jones, P. A. (2016). Epigenetic determinants of cancer. *Cold Spring Harb. Perspect. Biol.* 8, a019505. doi:10.1101/cshperspect.a019505

Benayoun, B. A., Pollina, E. A., Ucar, D., Mahmoudi, S., Karra, K., Wong, E. D., et al. (2014). H3K4me3 breadth is linked to cell identity and transcriptional consistency. *Cell* 158, 673–688. doi:10.1016/j.cell.2014.06.027

Berdasco, M., and Esteller, M. (2010). Aberrant epigenetic landscape in cancer: how cellular identity goes awry. *Dev. Cell* 19, 698–711. doi:10.1016/j.devcel.2010.10.005

Bernstein, B. E., Mikkelsen, T. S., Xie, X., Kamal, M., Huebert, D. J., Cuff, J., et al. (2006). A bivalent chromatin structure marks key developmental genes in embryonic stem cells. *Cell* 125, 315–326. doi:10.1016/j.cell.2006.02.041

Booth, L., Roberts, J. L., Conley, A., Cruickshanks, N., Ridder, T., Grant, S., et al. (2014). HDAC inhibitors enhance the lethality of low dose salinomycin in parental and stem-like GBM cells. *Cancer Biol. Ther.* 15, 305–316. doi:10.4161/cbt.27309

Cabrera, M. C., Hollingsworth, R. E., and Hurt, E. M. (2015). Cancer stem cell plasticity and tumor hierarchy. *World J. Stem Cells* 7, 27–36. doi:10.4252/wjsc.v7.i1.27

Chandra, T., Kirschner, K., Thuret, J. Y., Pope, B. D., Ryba, T., Newman, S., et al. (2012). Independence of repressive histone marks and chromatin compaction during senescent heterochromatic layer formation. *Mol. Cell* 47, 203–214. doi:10.1016/j.molcel.2012.06.010

Chehelgerdi, M., Behdarvand Dehkordi, F., Kabiri, H., Salehian-Dehkordi, H., Abdolvand, M., Salmanizadeh, S., et al. (2023). Exploring the promising potential of

induced pluripotent stem cells in cancer research and therapy. *Mol. Cancer* 22, 189. doi:10.1186/s12943-023-01873-0

Chen, C., Guo, Y., Wu, X., Si, C., Xu, Y., Kang, Q., et al. (2021). m6A modification in non-coding RNA: the role in cancer drug resistance. *Front. Oncol.* 11, 746789. doi:10.3389/fonc.2021.746789

Chen, C. C., Tran, W., Song, K., Sugimoto, T., Obusan, M. B., Wang, L., et al. (2023). Temporal evolution reveals bifurcated lineages in aggressive neuroendocrine small cell prostate cancer trans-differentiation. *Cancer Cell* 41, 2066–2082.e9. doi:10.1016/j.ccell.2023.10.009

Chu, X., Tian, W., Ning, J., Xiao, G., Zhou, Y., Wang, Z., et al. (2024). Cancer stem cells: advances in knowledge and implications for cancer therapy. *Signal Transduct. Target Ther.* 9, 170. doi:10.1038/s41392-024-01851-y

Costa, P., Sales, S. L. A., Pinheiro, D. P., Pontes, L. Q., Maranhao, S. S., Pessoa, C. D. O., et al. (2023). Epigenetic reprogramming in cancer: from diagnosis to treatment. *Front. Cell Dev. Biol.* 11, 1116805. doi:10.3389/fcell.2023.1116805

Creyghton, M. P., Cheng, A. W., Welstead, G. G., Kooistra, T., Carey, B. W., Steine, E. J., et al. (2010). Histone H3K27ac separates active from poised enhancers and predicts developmental state. *Proc. Natl. Acad. Sci. U. S. A.* 107, 21931–21936. doi:10.1073/pnas.1016071107

Deb, M., Kar, S., Sengupta, D., Shilpi, A., Parbin, S., Rath, S. K., et al. (2014). Chromatin dynamics: H3K4 methylation and H3 variant replacement during development and in cancer. *Cell Mol. Life Sci.* 71, 3439–3463. doi:10.1007/s00018-014-1605-4

Delgado-Olguin, P., and Recillas-Targa, F. (2011). Chromatin structure of pluripotent stem cells and induced pluripotent stem cells. *Brief. Funct. Genomics* 10, 37–49. doi:10.1093/bfgp/elq038

Dimitrova, E., Turberfield, A. H., and Klose, R. J. (2015). Histone demethylases in chromatin biology and beyond. *EMBO Rep.* 16, 1620–1639. doi:10.15252/embr.201541113

Duan, Q., Li, S., Wen, X., Sunnassee, G., Chen, J., Tan, S., et al. (2019). Valproic acid enhances reprogramming efficiency and neuronal differentiation on small molecules staged-induction neural stem cells: suggested role of mTOR signaling. *Front. Neurosci.* 13, 867. doi:10.3389/fnins.2019.00867

Duvic, M., Talpur, R., Ni, X., Zhang, C., Hazarika, P., Kelly, C., et al. (2007). Phase 2 trial of oral vorinostat (suberoylanilide hydroxamic acid, SAHA) for refractory cutaneous T-cell lymphoma (CTCL). *Blood* 109, 31–39. doi:10.1182/blood-2006-06-025999

French, R., and Pauklin, S. (2021). Epigenetic regulation of cancer stem cell formation and maintenance. *Int. J. Cancer* 148, 2884–2897. doi:10.1002/ijc.33398

Gallinari, P., Di Marco, S., Jones, P., Pallaoro, M., and Steinkühler, C. (2007). HDACs, histone deacetylation and gene transcription: from molecular biology to cancer therapeutics. *Cell Res.* 17, 195–211. doi:10.1038/sj.cr.7310149

Gosselet, F. P., Magnaldo, T., Culerrier, R. M., Sarasin, A., and Ehrhart, J. C. (2007). BMP2 and BMP6 control p57(Kip2) expression and cell growth arrest/terminal differentiation in normal primary human epidermal keratinocytes. *Cell Signal* 19, 731–739. doi:10.1016/j.cellsig.2006.09.006

Guenther, M. G., Frampton, G. M., Soldner, F., Hockemeyer, D., Mitalipova, M., Jaenisch, R., et al. (2010). Chromatin structure and gene expression programs of human embryonic and induced pluripotent stem cells. *Cell Stem Cell* 7, 249–257. doi:10.1016/j.stem.2010.06.015

Guo, Y., Zhao, S., and Wang, G. G. (2021). Polycomb gene silencing mechanisms: PRC2 chromatin targeting, H3K27me3 'readout', and phase separation-based compaction. *Trends Genet.* 37, 547–565. doi:10.1016/j.tig.2020.12.006

Hatziapostolou, M., and Iliopoulos, D. (2011). Epigenetic aberrations during oncogenesis. *Cell Mol. Life Sci.* 68, 1681–1702. doi:10.1007/s00018-010-0624-z

Hii, L. W., Chung, F. F., Soo, J. S., Tan, B. S., Mai, C. W., and Leong, C. O. (2020). Histone deacetylase (HDAC) inhibitors and doxorubicin combinations target both breast cancer stem cells and non-stem breast cancer cells simultaneously. *Breast Cancer Res. Treat.* 179, 615–629. doi:10.1007/s10549-019-05504-5

Huang, K., Zhang, X., Shi, J., Yao, M., Lin, J., Li, J., et al. (2015). Dynamically reorganized chromatin is the key for the reprogramming of somatic cells to pluripotent cells. *Sci. Rep.* 5, 17691. doi:10.1038/srep17691

Huangfu, D., Maehr, R., Guo, W., Eijkelenboom, A., Snitow, M., Chen, A. E., et al. (2008). Induction of pluripotent stem cells by defined factors is greatly improved by small-molecule compounds. *Nat. Biotechnol.* 26, 795–797. doi:10.1038/nbt1418

Iorio, M. V., and Croce, C. M. (2012). MicroRNA dysregulation in cancer: diagnostics, monitoring and therapeutics. A comprehensive review. *EMBO Mol. Med.* 4, 143–159. doi:10.1002/emmm.201100209

Italiano, A., Soria, J. C., Toulmonde, M., Michot, J. M., Lucchesi, C., Varga, A., et al. (2018). Tazemetostat, an EZH2 inhibitor, in relapsed or refractory B-cell non-Hodgkin lymphoma and advanced solid tumours: a first-in-human, open-label, phase 1 study. *Lancet Oncol.* 19, 649–659. doi:10.1016/S1470-2045(18)30145-1

Jiang, L., Huang, L., and Jiang, W. (2024). H3K27me3-mediated epigenetic regulation in pluripotency maintenance and lineage differentiation. *Cell Insight* 3, 100180. doi:10.1016/j.cellin.2024.100180

Johnstone, R. W. (2002). Histone-deacetylase inhibitors: novel drugs for the treatment of cancer. *Nat. Rev. Drug Discov.* 1, 287–299. doi:10.1038/nrd772

Kelly, R. D. W., Stengel, K. R., Chandru, A., Johnson, L. C., Hiebert, S. W., and Cowley, S. M. (2024). Histone deacetylases maintain expression of the pluripotent gene network via recruitment of RNA polymerase II to coding and noncoding loci. *Genome Res.* 34, 34–46. doi:10.1101/gr.278050.123

Keyvani-Ghamsari, S., Khorsandi, K., Rasul, A., and Zaman, M. K. (2021). Current understanding of epigenetics mechanism as a novel target in reducing cancer stem cells resistance. *Clin. Epigenetics* 13, 120. doi:10.1186/s13148-021-01107-4

Khan, A. Q., Ahmed, E. I., Elareer, N. R., Junejo, K., Steinhoff, M., and Uddin, S. (2019). Role of miRNA-regulated cancer stem cells in the pathogenesis of human malignancies. *Cells* 8, 840. doi:10.3390/cells8080840

Kim, K. H., and Roberts, C. W. (2016). Targeting EZH2 in cancer. *Nat. Med.* 22, 128–134. doi:10.1038/nm.4036

Koche, R. P., Smith, Z. D., Adli, M., Gu, H., Ku, M., Gnirke, A., et al. (2011). Reprogramming factor expression initiates widespread targeted chromatin remodeling. *Cell Stem Cell* 8, 96–105. doi:10.1016/j.stem.2010.12.001

Kouzarides, T. (2007). Chromatin modifications and their function. *Cell* 128, 693–705. doi:10.1016/j.cell.2007.02.005

Kretsovali, A., Hadjimichael, C., and Charmpilas, N. (2012). Histone deacetylase inhibitors in cell pluripotency, differentiation, and reprogramming. *Stem Cells Int.* 2012, 184154. doi:10.1155/2012/184154

Kumar, A., Emdad, L., Fisher, P. B., and Das, S. K. (2023). Targeting epigenetic regulation for cancer therapy using small molecule inhibitors. *Adv. Cancer Res.* 158, 73–161. doi:10.1016/bs.acr.2023.01.001

Kumar, V. E., Nambiar, R., De Souza, C., Nguyen, A., Chien, J., and Lam, K. S. (2022). Targeting epigenetic modifiers of tumor plasticity and cancer stem cell behavior. *Cells* 11, 1403. doi:10.3390/cells11091403

Li, C., Xie, Q., Ghosh, S., Cao, B., Du, Y., Vo, G. V., et al. (2024). SUV39H1 preserves cancer stem cell chromatin state and properties in glioblastoma. *bioRxiv*, 2024.08.15.607856. doi:10.1101/2024.08.15.607856

Li, W., and Sun, Z. (2019). Mechanism of action for HDAC inhibitors-insights from omics approaches. *Int. J. Mol. Sci.* 20, 1616. doi:10.3390/ijms20071616

Li, W., Wu, H., Sui, S., Wang, Q., Xu, S., and Pang, D. (2021). Targeting histone modifications in breast cancer: a precise weapon on the way. *Front. Cell Dev. Biol.* 9, 736935. doi:10.3389/fcell.2021.736935

Li, Y. R., Fang, Y., Lyu, Z., Zhu, Y., and Yang, L. (2023). Exploring the dynamic interplay between cancer stem cells and the tumor microenvironment: implications for novel therapeutic strategies. *J. Transl. Med.* 21, 686. doi:10.1186/s12967-023-04575-9

Liang, G., and Zhang, Y. (2013). Embryonic stem cell and induced pluripotent stem cell: an epigenetic perspective. *Cell Res.* 23, 49–69. doi:10.1038/cr.2012.175

Liu, R., Zhao, E., Yu, H., Yuan, C., Abbas, M. N., and Cui, H. (2023). Methylation across the central dogma in health and diseases: new therapeutic strategies. *Signal Transduct. Target Ther.* 8, 310. doi:10.1038/s41392-023-01528-y

Liu, T., Liu, P. Y., and Marshall, G. M. (2009). The critical role of the class III histone deacetylase SIRT1 in cancer. *Cancer Res.* 69, 1702–1705. doi:10.1158/0008-5472.CAN-08-3365

Maherali, N., and Hochedlinger, K. (2009). Tgfbeta signal inhibition cooperates in the induction of iPSCs and replaces Sox2 and cMyc. *Curr. Biol.* 19, 1718–1723. doi:10.1016/j.cub.2009.08.025

Mansour, A. A., Gafni, O., Weinberger, L., Zviran, A., Ayyash, M., Rais, Y., et al. (2012). The H3K27 demethylase Utx regulates somatic and germ cell epigenetic reprogramming. *Nature* 488, 409–413. doi:10.1038/nature11272

Margueron, R., and Reinberg, D. (2011). The Polycomb complex PRC2 and its mark in life. *Nature* 469, 343–349. doi:10.1038/nature09784

Marson, A., Foreman, R., Chevalier, B., Bilodeau, S., Kahn, M., Young, R. A., et al. (2008). Wnt signaling promotes reprogramming of somatic cells to pluripotency. *Cell Stem Cell* 3, 132–135. doi:10.1016/j.stem.2008.06.019

Mccool, K. W., Xu, X., Singer, D. B., Murdoch, F. E., and Fritsch, M. K. (2007). The role of histone acetylation in regulating early gene expression patterns during early embryonic stem cell differentiation. *J. Biol. Chem.* 282, 6696–6706. doi:10.1074/jbc.M609519200

Mochizuki-Kashio, M., Aoyama, K., Sashida, G., Oshima, M., Tomioka, T., Muto, T., et al. (2015). Ezh2 loss in hematopoietic stem cells predisposes mice to develop heterogeneous malignancies in an Ezh1-dependent manner. *Blood* 126, 1172–1183. doi:10.1182/blood-2015-03-634428

Momparler, R. L., and Côté, S. (2015). Targeting of cancer stem cells by inhibitors of DNA and histone methylation. *Expert Opin. Investig. Drugs* 24, 1031–1043. doi:10.1517/13543784.2015.1051220

Mosammaparast, N., and Shi, Y. (2010). Reversal of histone methylation: biochemical and molecular mechanisms of histone demethylases. *Annu. Rev. Biochem.* 79, 155–179. doi:10.1146/annurev.biochem.78.070907.103946

Mossahebi-Mohammadi, M., Quan, M., Zhang, J. S., and Li, X. (2020). FGF signaling pathway: a key regulator of stem cell pluripotency. *Front. Cell Dev. Biol.* 8, 79. doi:10.3389/fcell.2020.00079

O'donnell, E., Muñoz, M., Davis, R., Bergonio, J., Randall, R. L., Tepper, C., et al. (2025). *Genetic and epigenetic characterization of sarcoma stem cells across subtypes identifies EZH2 as a therapeutic target*. NPJ Precis. Oncol. 9 (1), 7. doi:10.1038/s41698-024-00776-7

Pack, L. R., Yamamoto, K. R., and Fujimori, D. G. (2016). Opposing chromatin signals direct and regulate the activity of lysine demethylase 4C (KDM4C). *J. Biol. Chem.* 291, 6060–6070. doi:10.1074/jbc.M115.696864

Papp, B., and Plath, K. (2011). Reprogramming to pluripotency: stepwise resetting of the epigenetic landscape. *Cell Res.* 21, 486–501. doi:10.1038/cr.2011.28

Papp, B., and Plath, K. (2013). Epigenetics of reprogramming to induced pluripotency. *Cell* 152, 1324–1343. doi:10.1016/j.cell.2013.02.043

Parreno, V., Martinez, A. M., and Cavalli, G. (2022). Mechanisms of Polycomb group protein function in cancer. *Cell Res.* 32, 231–253. doi:10.1038/s41422-021-00606-6

Rich, J. N. (2016). Cancer stem cells: understanding tumor hierarchy and heterogeneity. *Med. Baltim.* 95, S2–S7. doi:10.1097/MD.0000000000004764

Saha, N., and Muntean, A. G. (2021). Insight into the multi-faceted role of the SUV family of H3K9 methyltransferases in carcinogenesis and cancer progression. *Biochim. Biophys. Acta Rev. Cancer* 1875, 188498. doi:10.1016/j.bbcan.2020.188498

Shi, W. K., Li, Y. H., Bai, X. S., and Lin, G. L. (2022). The cell cycle-associated protein CDKN2A may promotes colorectal cancer cell metastasis by inducing epithelial-mesenchymal transition. *Front. Oncol.* 12, 834235. doi:10.3389/fonc.2022.834235

Smith, Z. D., and Meissner, A. (2013). DNA methylation: roles in mammalian development. *Nat. Rev. Genet.* 14, 204–220. doi:10.1038/nrg3354

Straining, R., and Eighmy, W. (2022). Tazemetostat: EZH2 inhibitor. *J. Adv. Pract. Oncol.* 13, 158–163. doi:10.6004/jadpro.2022.13.2.7

Sun, J., Li, G., Liu, Y., Ma, M., Song, K., Li, H., et al. (2020). Targeting histone deacetylase SIRT1 selectively eradicates EGFR TKI-resistant cancer stem cells via regulation of mitochondrial oxidative phosphorylation in lung adenocarcinoma. *Neoplasia* 22, 33–46. doi:10.1016/j.neo.2019.10.006

Sun, L., Fu, X., Ma, G., and Hutchins, A. P. (2021). Chromatin and epigenetic rearrangements in embryonic stem cell fate transitions. *Front. Cell Dev. Biol.* 9, 637309. doi:10.3389/fcell.2021.637309

Sze, C. C., Cao, K., Collings, C. K., Marshall, S. A., Rendleman, E. J., Ozark, P. A., et al. (2017). Histone H3K4 methylation-dependent and -independent functions of Set1A/COMPASS in embryonic stem cell self-renewal and differentiation. *Genes Dev.* 31, 1732–1737. doi:10.1101/gad.303768.117

Trevino, A. E., Muller, F., Andersen, J., Sundaram, L., Kathiria, A., Shcherbina, A., et al. (2021). Chromatin and gene-regulatory dynamics of the developing human cerebral cortex at single-cell resolution. *Cell* 184, 5053–5069.e23. doi:10.1016/j.cell.2021.07.039

Trowbridge, J. J., Sinha, A. U., Zhu, N., Li, M., Armstrong, S. A., and Orkin, S. H. (2012). Haploinsufficiency of Dnmt1 impairs leukemia stem cell function through derepression of bivalent chromatin domains. *Genes Dev.* 26, 344–349. doi:10.1101/gad.184341.111

Verma, A., Singh, A., Singh, M. P., Nengroo, M. A., Saini, K. K., Satrusal, S. R., et al. (2022). EZH2-H3K27me3 mediated KRT14 upregulation promotes TNBC peritoneal metastasis. *Nat. Commun.* 13, 7344. doi:10.1038/s41467-022-35059-x

Wang, C., Danli, M., Yu, H., Zhuo, Z., and Ye, Z. (2023). N6-methyladenosine (m6A) as a regulator of carcinogenesis and drug resistance by targeting epithelial-mesenchymal transition and cancer stem cells. *Heliyon* 9, e14001. doi:10.1016/j.heliyon.2023.e14001

Wang, Z., Cai, H., Zhao, E., and Cui, H. (2021). The diverse roles of histone demethylase KDM4B in normal and cancer development and progression. *Front. Cell Dev. Biol.* 9, 790129. doi:10.3389/fcell.2021.790129

Wang, Z., Li, Y., Ahmad, A., Azmi, A. S., Kong, D., Banerjee, S., et al. (2010). Targeting miRNAs involved in cancer stem cell and EMT regulation: an emerging concept in overcoming drug resistance. *Drug Resist Updat* 13, 109–118. doi:10.1016/j.drup.2010.07.001

Wei, J., Antony, J., Meng, F., Maclean, P., Rhind, R., Laible, G., et al. (2017). KDM4B-mediated reduction of H3K9me3 and H3K36me3 levels improves somatic cell reprogramming into pluripotency. *Sci. Rep.* 7, 7514. doi:10.1038/s41598-017-06569-2

Wen, Y., Cai, J., Hou, Y., Huang, Z., and Wang, Z. (2017). Role of EZH2 in cancer stem cells: from biological insight to a therapeutic target. *Oncotarget* 8, 37974–37990. doi:10.18632/oncotarget.16467

Wilson, B. G., and Roberts, C. W. (2011). SWI/SNF nucleosome remodellers and cancer. *Nat. Rev. Cancer* 11, 481–492. doi:10.1038/nrc3068

Xing, H., and Meng, L. H. (2020). CRISPR-cas9: a powerful tool towards precision medicine in cancer treatment. *Acta Pharmacol. Sin.* 41, 583–587. doi:10.1038/s41401-019-0322-9

Yang, Y., Zhang, M., and Wang, Y. (2022). The roles of histone modifications in tumorigenesis and associated inhibitors in cancer therapy. *J. Natl. Cancer Cent.* 2, 277–290. doi:10.1016/j.jncc.2022.09.002

Young, N. L., and Dere, R. (2021). Mechanistic insights into KDM4A driven genomic instability. *Biochem. Soc. Trans.* 49, 93–105. doi:10.1042/BST20191219

Yu, Z., Pestell, T. G., Lisanti, M. P., and Pestell, R. G. (2012). Cancer stem cells. *Int. J. Biochem. Cell Biol.* 44, 2144–2151. doi:10.1016/j.biocel.2012.08.022

Zhai, Y., Chen, X., Yu, D., Li, T., Cui, J., Wang, G., et al. (2015). Histone deacetylase inhibitor valproic acid promotes the induction of pluripotency in mouse fibroblasts by suppressing reprogramming-induced senescence stress. *Exp. Cell Res.* 337, 61–67. doi:10.1016/j.yexcr.2015.06.003

Zhang, C., Chen, Y., Sun, B., Wang, L., Yang, Y., Ma, D., et al. (2017). m(6)A modulates haematopoietic stem and progenitor cell specification. *Nature* 549, 273–276. doi:10.1038/nature23883

Zhou, H. M., Zhang, J. G., Zhang, X., and Li, Q. (2021). Targeting cancer stem cells for reversing therapy resistance: mechanism, signaling, and prospective agents. *Signal Transduct. Target Ther.* 6, 62. doi:10.1038/s41392-020-00430-1

frontiers | Frontiers in Cell and Developmental Biology

TYPE Original Research
PUBLISHED 23 April 2025
DOI 10.3389/fcell.2025.1576258

OPEN ACCESS

EDITED BY
Myon Hee Lee,
East Carolina University, United States

REVIEWED BY
Tzu-Yang Lin,
Academia Sinica, Taiwan
Kan Xie,
Helmholtz Association of German Research Centers (HZ), Germany

*CORRESPONDENCE
Haiou Chen,
chenhaiou@wchscu.cn
Jinhua Yan,
dryanhuahua666@163.com

†These authors have contributed equally to this work

RECEIVED 13 February 2025
ACCEPTED 07 April 2025
PUBLISHED 23 April 2025

CITATION
Yan J, Feng C, Zhang H, Luo T, Chen H and Chen H (2025) Dapagliflozin ameliorates intestinal stem cell aging by regulating the MAPK signaling pathway in *Drosophila*. *Front. Cell Dev. Biol.* 13:1576258. doi: 10.3389/fcell.2025.1576258

Dapagliflozin ameliorates intestinal stem cell aging by regulating the MAPK signaling pathway in *Drosophila*

Jinhua Yan[1,2*†], Chenxi Feng[2†], Hanmei Zhang[2†], Ting Luo[1,2], Haiyang Chen[1] and Haiou Chen[1*]

[1]Center of Gerontology and Geriatrics and Laboratory of Metabolism and Aging Frontiers Science Center for Disease-Related Molecular Network, State Key Laboratory of Respiratory Health and Multimorbidity and National Clinical Research Center for Geriatrics, West China Hospital, Sichuan University, Chengdu, China, [2]West China School of Medicine, Sichuan University, Chengdu, Sichuan, China

Introduction: Intestinal stem cells (ISCs) possess the ability to self-renew and differentiate, which is essential for maintaining intestinal tissue homeostasis. However, their functionality significantly declines with age, leading to diminished tissue regeneration and an increased risk of age-associated diseases.

Methods: This study investigates the effects of Dapagliflozin (DAPA), a novel insulin sensitizer and SGLT2 inhibitor, on aging ISCs using the *Drosophila melanogaster* model. Our findings demonstrate that DAPA can inhibit the MAPK signaling pathway, as confirmed by network pharmacology analysis and molecular docking experiments.

Results: DAPA ameliorates ISC aging, improves intestinal function (including enhanced fecal excretion, restored intestinal barrier integrity and acid-base balance), and enhances healthspan. These results highlight the potential of DAPA as an anti-aging therapeutic agent.

Discussion: This study provides new evidence for the application of DAPA as an anti-aging treatment.

KEYWORDS

dapagliflozin, intestinal stem cell, aging, MAPK signaling, *Drosophila*

1 Introduction

Aging is a complex biological process characterized by multidimensional and multilevel functional decline across cells, tissues, and organs, thereby increasing the risk of diseases (López-Otín et al., 2013, López-Otín et al., 2023). Normal intestinal stem cells (ISCs) possess the dual abilities of self-renewal and differentiation, which are essential for maintaining tissue and organ homeostasis (Ohlstein and Spradling, 2006). However, their functionality significantly declines with age, resulting in diminished tissue regeneration capacity and an elevated risk of age-related diseases (Brunet, Goodell, and Rando, 2023; Ermolaeva et al., 2018). Consequently, combating ISC aging represents a promising yet challenging field (Du et al., 2021; Yan et al., 2022). Investigating small molecule drugs to mitigate age-related impairments in ISC function can promote healthy aging and complement the mechanisms of age-related decline.

Dapagliflozin (DAPA), a novel insulin sensitizer and SGLT2 inhibitor, exerts direct, sugar-independent effects by reducing oxidative stress and endoplasmic reticulum stress (Shibusawa et al., 2019), restoring mitochondrial health, stimulating mitochondrial biogenesis (Lee et al., 2019), and decreasing pro-inflammatory and profibrotic pathways (Kounatidis et al., 2023). These effects rejuvenate aging cells, tissues, and organs (O'Keefe et al., 2023), and are associated with a reduced risk of various common age-related diseases, including heart failure (Butt et al., 2022), chronic kidney disease (Jhund et al., 2021), atrial fibrillation (Butt et al., 2022), cancer (Basak et al., 2023), gout (Lai et al., 2023), neurodegenerative diseases (Wu et al., 2023), and atherosclerosis (Ortega et al., 2019). Recent Studies have shown that DAPA can reduce the accumulation of reactive oxygen species (ROS) in cells and improve age-related endothelial dysfunction (Tai et al., 2023). Moreover, recent studies have shown that the SGLT2 inhibitors canagliflozin enhances the clearance of senescent cells, thereby improving age-related phenotypic changes and extending lifespan (Katsuumi et al., 2024). We hypothesize that DAPA can modulate ISC function and delay aging, which needs further validation.

Drosophila melanogaster, a model organism renowned for aging research, serves as an ideal model for studying ISC aging (Promislow et al., 2022). During homeostasis, the midgut of fly is composed of ISCs and various differentiated cell types, closely resembling the complexity of the mammalian gut (Jasper, 2020). Fly ISCs are characterized by their expression of Delta (Dl, a Notch ligand) and Escargot (Esg, a transcription factor). ISCs divide and differentiate into enteroblasts (EBs) and enteroendocrine progenitor cells (EEPs), which further differentiate into enterocytes (ECs) and enteroendocrine cells (EEs), thereby maintaining the self-renewal of the intestinal epithelium (Biteau et al., 2008; Ayyaz and Jasper, 2013; Biteau et al., 2011). In the aging fly intestine, aberrant ISCs function leads to hyper-proliferation,thereby disrupting intestinal homeostasis and impairing intestinal function. Extensive research has demonstrated that alleviating ISC hyperplasia, which is caused by dysplasia (Rodriguez-Fernandez et al., 2020), plays a crucial role in extending lifespan (Biteau et al., 2010; Du et al., 2020). Thus, the fly intestine is a valuable model for studying the impact and mechanism of DAPA on stem cell aging.

Research has shown that the MAPK signaling pathway exerts regulatory influence over ISC aging in *Drosophila* (He et al., 2020), and modulating MAPK activity can contribute to maintaining normal function (Ureña et al., 2024; Zhang et al., 2019; Park et al., 2009). In our study, using the *Drosophila* gut as a model system, we found that DAPA alleviates hyper-proliferation of ISCs, maintains gut homeostasis, improves age-related declines in intestinal function, and prolongs the lifespan of *Drosophila*. Additionally, our findings indicate that these effects of DAPA are mediated through the inhibition of the MAPK signaling pathway. Therefore, our study not only highlights DAPA's potential as a novel anti-aging drug but also underscores the importance of the MAPK pathway in stem cell aging and longevity. In conclusion, the study demonstrates that DAPA can serve as an effective and safe anti-aging drug to promote healthy aging.

2 Results

2.1 Dapagliflozin prevents gut hyperplasia of ISCs in aged *Drosophila melanogaster*

In the *Drosophila* midgut, intestinal stem cells (ISCs) maintain intestinal cell homeostasis through proliferation and differentiation (Figure 1A). However, in aging *Drosophila*, the regulation of stem cell proliferation is dysregulated, leading to abnormal accumulation of Esg + cells (including ISCs, EBs, and pre-EE), while the number of fully differentiated intestinal cells decreases, thereby impairing normal intestinal function (Choi et al., 2008).

To investigate whether certain small molecule compounds can prevent age-related ISC dysfunction, we utilized the; esg-Gal4, UAS-GFP, tub-Gal80TS/Cyo; system (hereafter referred to as esgts) to express green fluorescent protein (GFP) under the control of the esg gene at 29°C. This system allowed us to monitor and quantify changes in esg-GFP + cells in real-time, enabling us to screen for small molecule drugs that can alleviate age-related ISC dysfunction. The esgts system is based on the TARGET system, which is a powerful tool for spatiotemporal gene expression targeting in *Drosophila* (McGuire et al., 2004). The TARGET system utilizes a temperature-sensitive GAL80 protein (GAL80ts) to control the activity of GAL4. At the permissive temperature (e.g., 18°C), GAL80ts binds to and inhibits GAL4, preventing it from activating downstream UAS-driven gene expression. When the temperature is shifted to the restrictive temperature (e.g., 29°C), GAL80ts loses its binding affinity for GAL4, allowing GAL4 to activate the expression of genes under the control of UAS elements. This temperature-dependent regulation enables precise temporal control of gene expression, making it an ideal system for studying the effects of small molecule compounds on ISC function over time.

At 30 days old, flies are in the middle and old age stages, and they begin to show physiological changes associated with aging, such as decreased intestinal cell homeostasis, abnormal accumulation of Esg + cells, and a reduction in the number of fully differentiated intestinal cells. We supplemented the diet of 30-day-old flies with Dapagliflozin (DAPA) and maintained them at 29°C for 10 days (Figure 1B). we used the entire gut for the pH3+ cell (phosphorylated histone H3, which specifically stains dividing ISCs) count, which is a common approach in the field to provide a comprehensive assessment of cell proliferation across the entire organ. This method allows us to capture the overall proliferative activity within the gut, which is essential for understanding the biological processes we are investigating. Among the three tested concentrations of DAPA (1 μM, 10 μM, and 100 μM), the 100 μM concentration exhibited the most pronounced effect on pH3+, significantly mitigating intestinal hyperplasia caused by dysplasia in aged flies (Figure 1C). Compared to aged flies without DAPA supplementation, those supplemented with DAPA for 10 days showed a significant reduction in the number of esg + cells (Figures 1D–G). Further quantification of Dl + cells (ISC markers) demonstrated that the number of Dl + cells (Figures 1D–H) in aged flies *a* supplemented with 100 μM DAPA was significantly lower than in the control group. These findings suggest that DAPA supplementation prevents excessive ISC proliferation and subsequent intestinal hyperplasia in aged flies.

10.3389/fcell.2025.1576258

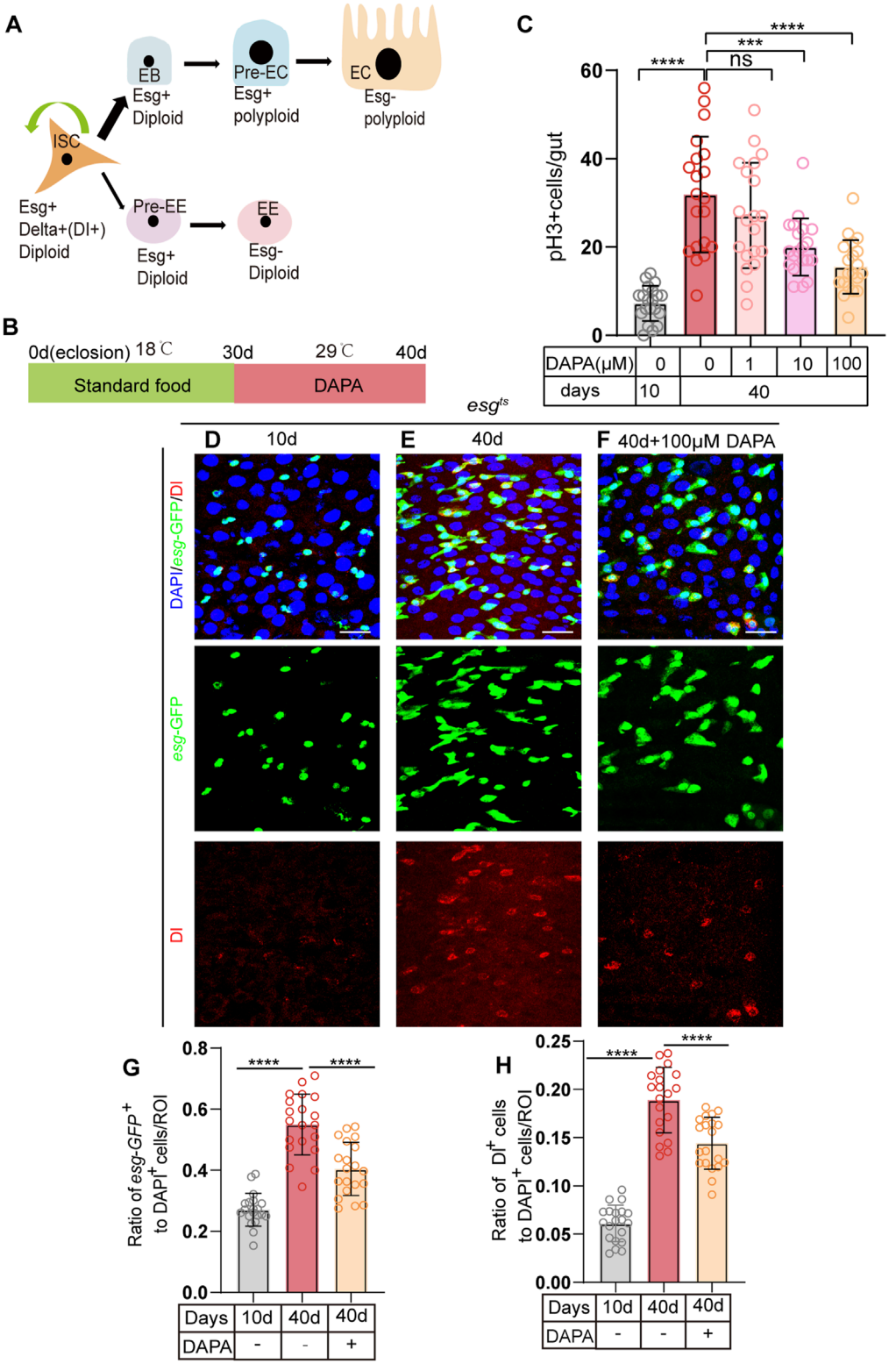

FIGURE 1
Dapagliflozin Prevents gut hyperplasia of ISCs in Aged *Drosophila melanogaster*. **(A)** The lineages of *Drosophila* intestinal stem cells (ISCs). ISCs (identified by Esg$^+$,delta$^+$) undergo asymmetric division to self-renew and give rise to enteroblasts (EBs) or enteroendocrine progenitor cells (EEPs/Pre-EE). EBs differentiate to form enterocytes (ECs), while EEPs differentiate to form enteroendocrine cells (EEs). **(B)** Schematic diagram depicting the process of oral DAPA in *Drosophila*. **(C)** The number of pH3+ cells (a marker of mitotic activity) was assessed in the whole guts of 10-day-old and 40-day-old female flies (esg^{ts}) without DAPA supplementation and with three concentrations of DAPA (1 μM, 10 μM, and 100 μM). **(D–F)** Immunofluorescence images of posterior midguts of 10- **(D)** and 40-day-old **(E)** female flies without DAPA supplementation and 40-day-old male flies with 100 μM DAPA supplementation **(F)** stained with DAPI (blue; nuclei), GFP (green; ISCs and progenitor cells marker), and Dl (red; ISCs marker). The top panels represent the merged images, the middle panels represent *esg*-GFP, and the bottom panels represent Dl. Scale bars represent

(*Continued*)

FIGURE 1 (Continued)
20 μm. **(G)** The ratio of *esg*-GFP$^+$ cells to DAPI$^+$ cells per ROI (region of interest) in posterior midguts of 10- and 40-day-old female flies without DAPA supplementation and 40-day-old female flies with 100 μM DAPA supplementation. **(H)** The ratio of Dl$^+$ cells to DAPI$^+$ cells per ROI (region of interest) in female flies experiments. The numbers of counted guts are 20. Data are represented as means ± SD. ANOVA or unpaired Kruskal Wallis test be used, *p < 0.05, **p < 0.01, ***p < 0.001, and ****p < 0.0001, and ns indicates p > 0.05.

2.2 Dapagliflozin prevents age-related gut dysfunction in aged *Drosophila melanogaster*

To further explore the potential effects of DAPA supplementation on intestinal function, we investigated its impact on the gut of aged flies. Previous studies have demonstrated that age-related dysfunction of ISCs leads to a significant deterioration of intestinal function in flies, including disruption of gastrointestinal acid-base homeostasis, reduced fecal excretion, and compromised intestinal barrier integrity (Lemaitre and Miguel-Aliaga, 2013; Kühn et al., 2020). To address this issue, flies were fed a diet with or without DAPA supplementation and subsequently treated with bromophenol blue (BPB) or non-absorbable blue dye (Figure 2A). BPB is a pH indicator. Following BPB feeding, wild-type fly midguts were examined for acidification. A yellow copper cell region (CCR) revealed acidification (pH < 2.3), while the blue anterior and posterior midgut indicated a neutral to basic pH (pH > 4). Our results demonstrated that DAPA supplementation significantly enhanced fecal excretion in aged flies (Figures 2B, C). In flies, the size and function of the CCR decline with age, resulting in disrupted acid-base balance in the gut (Dubreuil, 2004). We observed that DAPA supplementation significantly restored acid-base balance in the gut of aged flies (Figures 2D, E). The integrity of the intestinal barrier is essential for maintaining epithelial homeostasis, defending against pathogens, and promoting immune tolerance to commensal bacteria (Martel et al., 2022). Furthermore, to assess the impact of DAPA on intestinal barrier function, we conducted the blue dye assay. Smurf (+) indicates that the flies exhibit compromised intestinal barrier function, with visible blue dye staining on the body surface due to leakage. Smurf (−) indicates that the intestinal barrier function is intact, with no visible blue dye staining (Figure 2F). Our study demonstrates that supplementation with DAPA significantly enhances intestinal barrier function in aged flies (Figure 2G). In conclusion, these findings demonstrate that DAPA ameliorates age-related intestinal dysfunction in aged flies.

2.3 Dapagliflozin extends lifespan under both natural and stress-induced conditions in *Drosophila melanogaster*

Intestinal health is closely related to lifespan extension. Accumulating evidence has demonstrated that maintaining intestinal homeostasis can contribute to longevity (Jing et al., 2025; Choi and Augenlicht, 2024). we observed that DAPA alleviates age-related ISC hyperplasia and prevents age-related gut dysfunction in aged flies, which prompted us to further investigate the effects of DAPA supplementation on the lifespan of flies. Initially, DAPA was supplemented into the diet of the experimental group, and the results demonstrated that DAPA supplementation significantly extended the lifespan of flies compared to the control group (Figures 3A, B).

Subsequently, we sought to explore whether DAPA could extend lifespan under various environmental stress conditions. Flies were exposed to various environmental stress models, including dextran sulfate sodium (DSS)-induced ulcerative colitis (Yan et al., 2023), paraquat (PQ)-induced oxidative damage (Lyles et al., 2021), and bleomycin (BLM)-induced DNA damage (Du et al., 2020). Under DSS-induced stress, we observed that DAPA mitigated the damage to the tight junctions between intestinal cells. Specifically, the damage to the tight junctions, as marked by Armadillo (Arm), was less severe in the DAPA-treated group compared to the control group (Supplementary Figure S1A). In the PQ-induced oxidative stress model, the transcriptional levels of ROS-related genes were downregulated in the DAPA-supplemented group, suggesting that DAPA may enhance antioxidant capacity (Supplementary Figure S1B). Furthermore, in the BLM-induced DNA damage model, the transcriptional levels of DNA damage-related genes were significantly reduced in the DAPA-treated group, indicating that DAPA could mitigate DNA damage (Supplementary Figure S1C). The scavenging effects of DAPA supplementation on oxidative and DNA damage likely involve multiple mechanisms, including direct antioxidant actions, regulation of DNA repair mechanisms, and inhibition of inflammatory responses (Arow et al., 2020; Alsereidi et al., 2024). The synergistic action of these mechanisms may contribute to the extended lifespan of fruit flies under various stress conditions.

Under DSS-induced stress, DAPA significantly extended the lifespan of flies (Figures 3C, D). In the PQ-induced acute aging model, DAPA supplementation significantly extended the lifespan of flies and effectively mitigated acute oxidative stress (Figures 3E, F). Additionally, in the BLM exposure model, DAPA significantly prolonged the lifespan of flies (Figures 3G, H). In summary, our findings demonstrate that DAPA supplementation not only extends the normal lifespan of flies but also significantly prolongs lifespan under various stress-induced model.

2.4 Dapagliflozin alleviates aging-induced gut hyperplasia of ISCs primarily through repressing the MAPK signaling pathway

Based on prior studies demonstrating that DAPA may regulate the MAPK signaling pathway (Wang et al., 2022; Phongphithakchai et al., 2025) and our PPI network/pathway enrichment analysis (Supplementary Figure S2), we further explored the potential molecular mechanisms using both PPI network analysis and pathway enrichment analysis (Supplementary

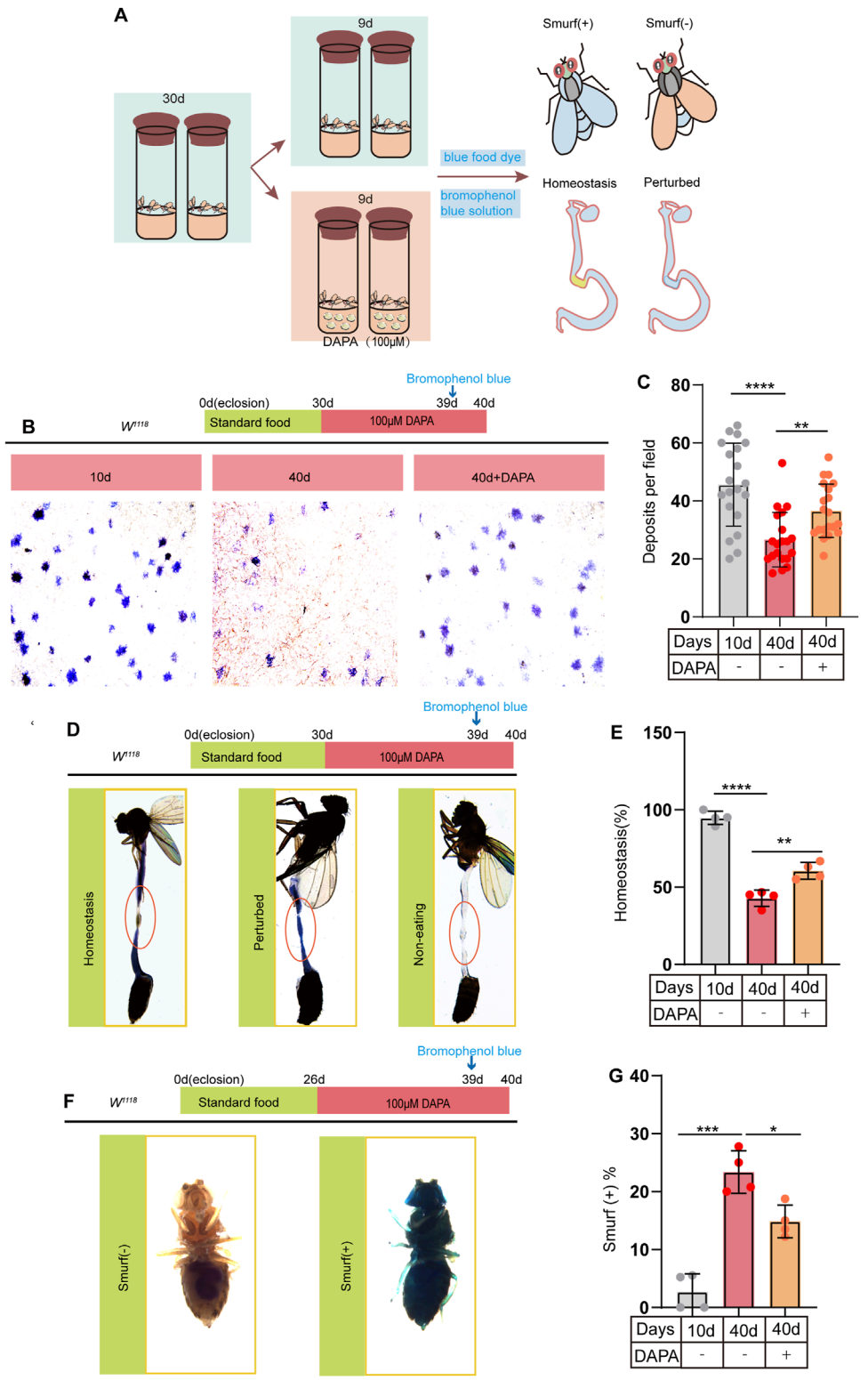

FIGURE 2
Dapagliflozin Prevents Age-Related Gut Dysfunction in Aged *Drosophila melanogaster* **(A)** Schematic diagram depicting the procedure of DAPA administration in *Drosophila*: *Drosophila* were cultured at 26°C until reaching 30 days of age, following which they were randomly divided into two groups: a control group and a group supplemented with DAPA. After a feeding period of 9 days, flies were selected for "Smurf," deposits and intestinal "Homeostasis," respectively. **(B)** Representative images of excretion deposits from female flies at 10 and 40 days old without DAPA supplementation, and 40 days old with 100 μM DAPA supplementation. **(C)** Quantification of excretion deposits from female at 10 and 40 days old without DAPA supplementation, and 40 days old with 100 μM DAPA supplementation. Excretions are quantified for 6 fields in each group of 20 flies. **(D)** Representative images of the intestinal acid-base homeostasis and the non-eating intestine: "Homeostasis" corresponds to CCR as yellow; "Perturbed" corresponds to CCR as blue; "Non-eating" indicates that the flies did not ingest food, and the guts are not stained with bromophenol blue

(*Continued*)

FIGURE 2 (Continued)
(E). The percentage of "Homeostasis" female in experiment. Each group included 20 flies. **(F)** Representative images of the gut leakage:Smurf (+) corresponds to the leakage of blue dye from the gut into surrounding tissues. **(G)** The ratio of the female flies of smurf (+) in experiment. Each group included 20 flies. Three independent experiments were conducted more than three times. Data are represented as means ± SD. ANOVA or unpaired Kruskal Wallis test be used. *p < 0.05, **p < 0.01, ***p < 0.001, and ****p < 0.0001, and ns indicates p > 0.05.

Figure S2). These analyses collectively suggest that DAPA may exert its protective effects via the EGFR/MAPK signaling pathway in ISC aging. To test this hypothesis, we conducted the following experiments.

The Epidermal Growth Factor Receptor (EGFR) is a well-known regulator of ISC activity. Activation of EGFR leads to the phosphorylation and activation of ERK, which in turn promotes ISC proliferation and maintains intestinal homeostasis. This pathway directly feeds into the MAPK cascade, making it a primary upstream regulator (Zhang et al., 2022; Li et al., 2015). To further explore the potential of DAPA in regulating the EGFR signaling pathway, we first measured the transcriptional level of EGFR in ISCs and found that DAPA supplementation significantly reduced EGFR transcription in intestinal ISCs (Figure 4A). Subsequently, we observed that the fluoreoxidative stress and endoplasmicscence intensity of phosphorylated Extracellular Signal-Regulated Kinase (pERK), a marker of MAPK activation, was also significantly reduced in the DAPA supplementation group, indicating that DAPA alleviated intestinal hyperplasia by inhibiting pERK expression (Figure 4B; Supplementary Figure S3A).

To further confirm the role of DAPA in regulating the EGFR signaling pathway, we first induced overexpression of the dominant-negative form of EGFR ($EGFR^{DN}$) in *Drosophila*. We hypothesized that DAPA slows the aging of *Drosophila* ISCs by inhibiting the EGFR pathway and predicted that no synergistic effect would be observed in *Drosophila* expressing $EGFR^{DN}$ (driven by esgts-gal4) upon DAPA administration. Compared to normal aged *Drosophila*, the number of esg-GFP + cells was significantly suppressed in aged *Drosophila* with esgts-gal4-driven $EGFR^{DN}$. Consistent with our expectations, DAPA supplementation did not lead to a further reduction in esg-GFP + cells (Figures 4C, D), and statistical analysis demonstrated similar effects in Dl+ and pH3+ cell counts (Figures 4E, F; Supplementary Figure S3B).

In addition, we conducted experiments with the constitutively active form of EGFR ($EGFR^{CA}$). We hypothesized that overexpression of $EGFR^{CA}$ would counteract the protective effects of DAPA on ISC dysfunction. The results showed that, compared to normal aged *Drosophila*, the number of esg-GFP + cells was significantly increased in *Drosophila* expressing $EGFR^{CA}$ (Figures 4C, D), indicating that $EGFR^{CA}$ overexpression induces ISC hyperproliferation. Notably, DAPA treatment failed to significantly reduce the number of esg-GFP + cells in *Drosophila* expressing $EGFR^{CA}$ (Figures 4C, D), with parallel resistance observed in Dl+ and pH3+ cell counts (Figures 4E, F; Supplementary Figure S3B). This further substantiates that $EGFR^{CA}$ overexpression counteracted the protective effects of DAPA (Figures 4C–F). These findings suggest that DAPA-induced mitigation of age-related ISC hyperproliferation in *Drosophila* is associated with inhibition of the MAPK/EGFR signaling pathway (Figure 4G).

3 Discussion

Researchers in the field of aging have long been dedicated to understanding the mechanisms of aging and identifying precise therapeutic strategies to delay aging and alleviate age-related diseases. A critical frontier in biomedical science is the pursuit of interventions that can mitigate the adverse effects of aging on stem cell function. This study demonstrates for the first time that Dapagliflozin (DAPA) ameliorates intestinal stem cell (ISC) aging in *Drosophila melanogaster* by repressing the MAPK signaling pathway. Our findings reveal that DAPA supplementation reduces age-related ISC hyperplasia (evidenced by decreased pH3+ and Dl + cells), restores intestinal barrier integrity, acid-base homeostasis, and excretory function, while extending lifespan under both natural and stress-induced conditions. Network pharmacology and molecular docking analyses further validate that DAPA suppresses ERK phosphorylation by targeting EGFR/MAPK3, thereby maintaining ISC homeostasis. These results provide direct evidence for DAPA as a potential anti-aging therapeutic agent.

The extracellular-signal-regulated kinases (ERK) signaling pathway, a classic pathway of mitogen-activated protein kinases (MAPK), plays a crucial role in regulating cell growth, differentiation, survival, inflammation (Fang and Richardson, 2005; Chen et al., 2020; Schafer et al., 2017). Numerous studies have demonstrated a negative correlation between ERK and healthy lifespan, and a decrease in ERK is able to inhibit age-related degenerative diseases (Tarragó et al., 2018; Sun et al., 2020). Additionally, as one of the most important pathways regulating cell proliferation, the overactivation of the ERK pathway can autonomously stimulate the proliferation of intestinal stem cells (Zhang et al., 2019). Live-cell imaging of colon monolayers reveals that ERK is localized in the stem cell niche to maintain epithelial homeostasis (Pond et al., 2022). Furthermore, in *Drosophila* intestine, ERK regulates the homeostasis and regeneration of intestinal stem cells (Jiang et al., 2011).

Beyond its glucose-lowering effects, DAPA has been shown to exert a range of beneficial effects unrelated to blood glucose control. Consistent with previous studies, SGLT2 inhibitors (including DAPA) exert anti-aging effects through multiple pathways, such as mitigating oxidative stress and mitochondrial dysfunction (Tai et al., 2023; Jiang et al., 2023; Katsuumi et al., 2024). However, their role in intestinal stem cell aging remains underexplored. Our work bridges this gap by uncovering DAPA's unique mechanism via MAPK pathway inhibition. Notably, hyperactivation of MAPK signaling is a key driver of age-related ISC dysfunction, and DAPA's suppression of this pathway aligns with the pro-aging role of ERK signaling in mammals (Ureña et al., 2024; Nászai et al., 2021; Kabiri et al., 2018).

The anti-aging effects of Dapagliflozin (DAPA) on intestinal stem cell (ISC) dysfunction may involve both SGLT2-dependent and -independent mechanisms. While DAPA is primarily known

10.3389/fcell.2025.1576258

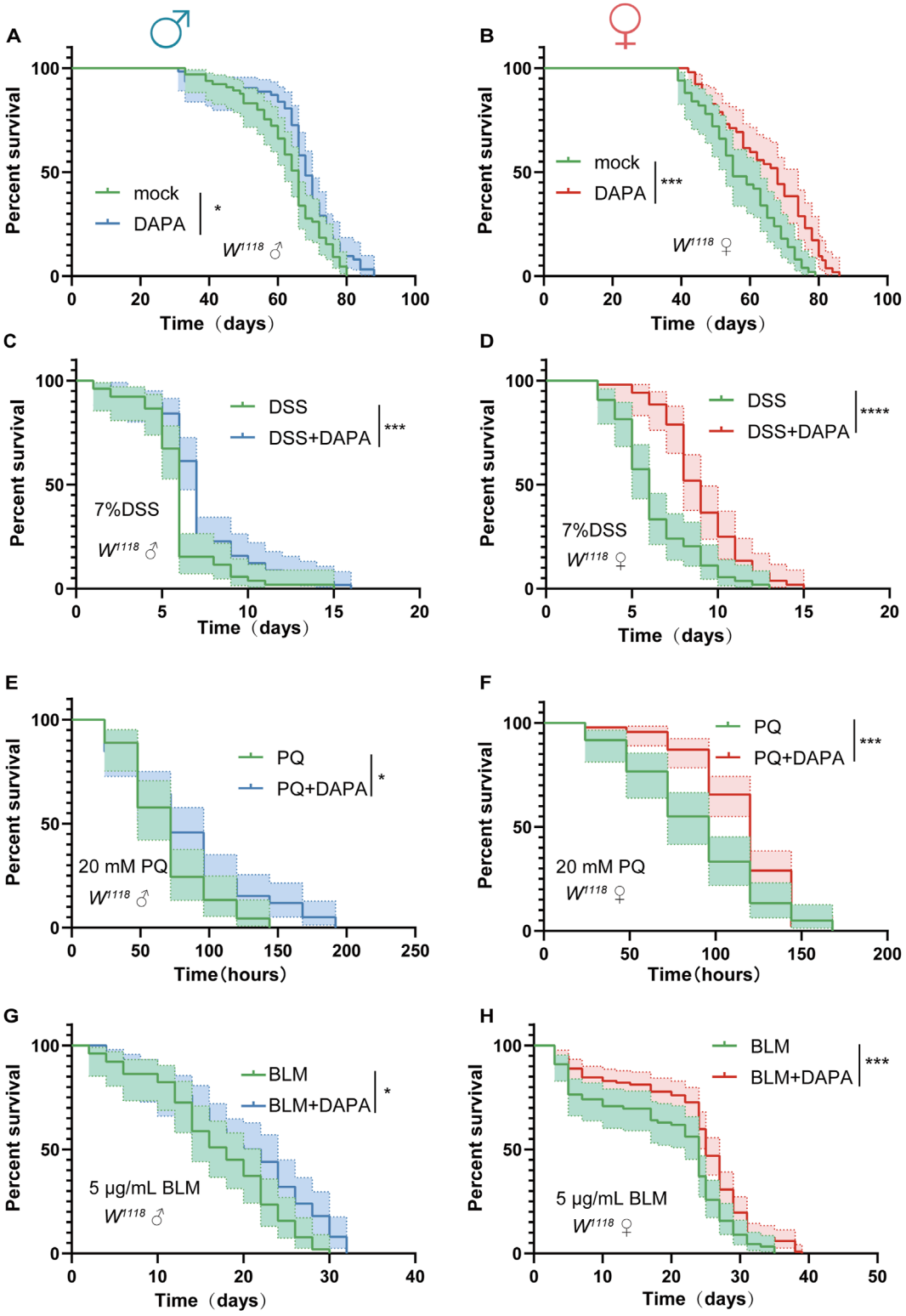

FIGURE 3
Dapagliflozin Extends Lifespan Under Both Natural and Stress-Induced Conditions in *Drosophila* **(A, B)** Survival percentage of male flies (W^{1118}, control: n = 65, DAPA: n = 65) **(A)** and female flies (W^{1118}, control: n = 50, DAPA: n = 50) **(B)** with or without DAPA supplementation. **(C, D)** Survival percentage of male flies (W^{1118}, control: n = 52, DAPA: n = 57) **(C)** and female flies (W^{1118}, control: n = 54, DAPA: n = 51) **(D)** with or without DAPA supplementation during 7% dextran sulfate sodium (DSS) treatment. **(E, F)** Survival percentage of male flies (W^{1118}, control: n = 45, DAPA: n = 57) **(E)** and female flies (W^{1118}, control: n = 60, DAPA: n = 90). **(F)** with or without DAPA supplementation during 20 mM paraquat (PQ) treatment. **(G, H)** Survival percentage of male flies (W^{1118}, control: n = 48, DAPA: n = 47) **(G)** and female flies (W^{1118}, control: n = 89, DAPA: n = 117) **(H)** with or without DAPA supplementation during 5 μg/mL bleomycin (BLM) treatment. Three independent experiments were conducted. Lifespan analysis was performed using the log-rank test, *p < 0.05, **p < 0.01, ***p < 0.001, and ****p < 0.0001, and ns indicates p > 0.05.

10.3389/fcell.2025.1576258

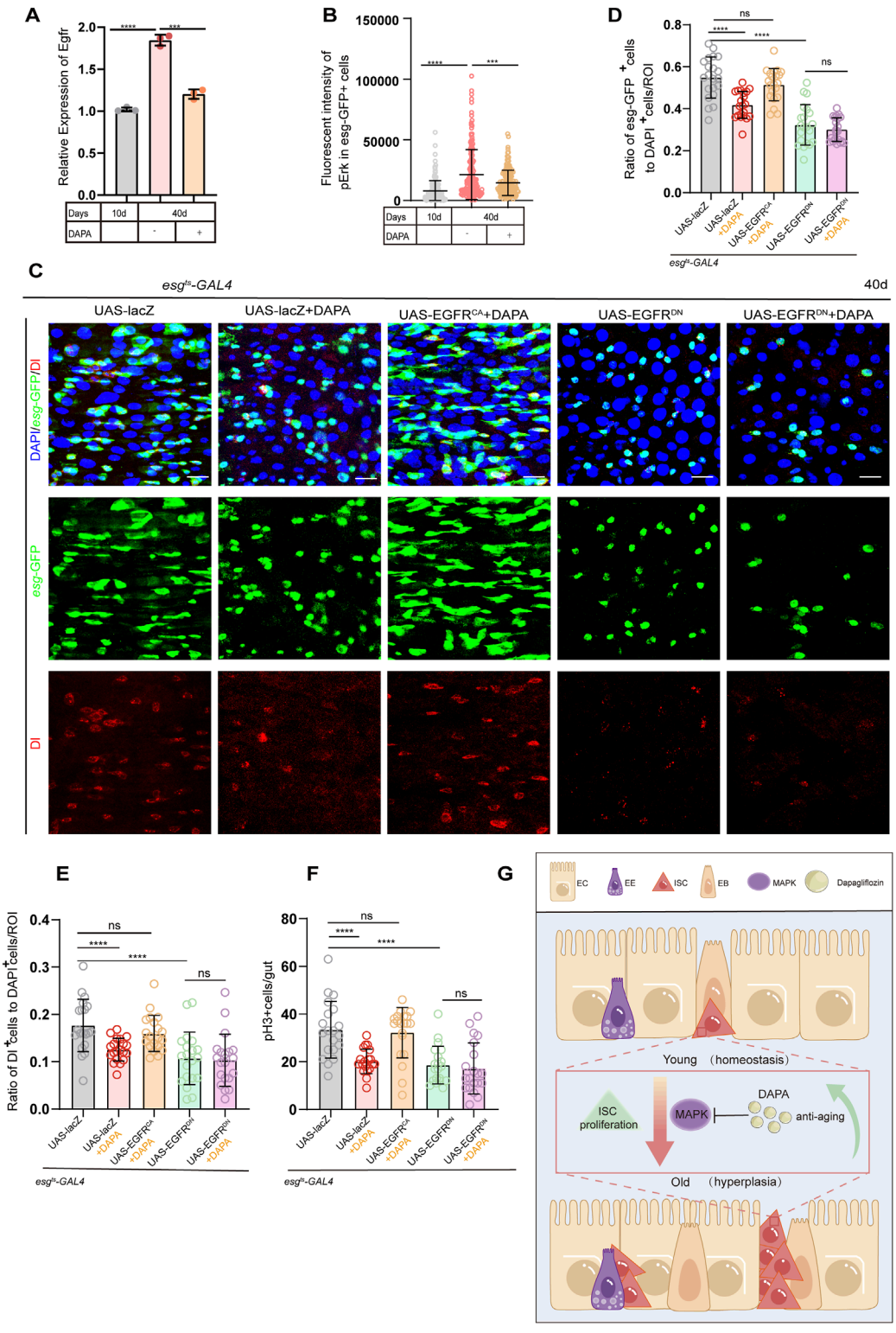

FIGURE 4
Dapagliflozin alleviates aging-induced gut hyperplasia of ISCs primarily through repressing the MAPK signaling pathway **(A)** RT-qPCR was used to measure the mRNA levels of Egfr gene in esg + ISCs isolated from the midguts of esg-GFP *Drosophila* at three different time points: 10 days, 40 days, and 40 days + DAPA **(B)** Quantification of fluorescent intensity of pErk in *esg*-GFP^{+} cells from 40-day-old female flies (*esg^{ts}-Gal4 > UAS-lacZ*) at three different time points: 10 days, 40 days, and 40 days + DAPA. Cells were stained with pErk antibody. Each dot represents one esg-GFP + cell. n = 165 per group, with each n representing one esg-GFP + cell, and the n values for each group were derived from 30 flies.**(C)** Immunofluorescence images of posterior midguts of female flies carrying *esg^{ts}-Gal4*-driven *UAS-lacZ*, *UAS-lacZ* + DAPA, *UAS-EGFR^{CA}* + DAPA, *UAS-EGFR^{DN}*, and *UAS-EGFR^{DN}* + DAPA stained with Dl,DAPI and GFP. The top panels represent the merged images, the middle panels represent esg-GFP, and the bottom panels represent Delta (Dl). Scale bars represent 20 μm. **(D)** The ratio of *esg*-GFP^{+} cells to DAPI^{+} cells per ROI (region of interest) in posterior midguts of female flies in experiment. **(E)** The ratio of Dl^{+} cells to DAPI^{+} cells per ROI (region of interest) in posterior midguts of female flies. **(F)** The number of pH3^{+} cells in the

(*Continued*)

FIGURE 4 (Continued)
whole guts of female flies carrying. **(G)** Model of mechanism: how DAPA modulates ISC aging. In *Drosophila melanogaster*, DAPA inhibits the MAPK signaling pathway, thereby suppressing intestinal hyperplasia during aging. Data are represented as means ± SD. ANOVA or unpaired Kruskal Wallis test be used, *p < 0.05, **p < 0.01, ***p < 0.001, and ****p < 0.0001, and ns indicates p > 0.05.

for its glycemic control through SGLT2 inhibition, recent studies suggest that its benefits on ISC function could be mediated by non-glycemic actions. These include anti-inflammatory and antioxidant effects, which reduce oxidative stress and inflammation via pathways such as NOX4/p38MAPK inhibition (Dihoum et al., 2024; Alsereidi et al., 2024); autophagy regulation, which supports cellular homeostasis by clearing damaged organelles and proteins n (Jaikumkao et al., 2021; Arab et al., 2021); and cardiovascular protection through pathways like ALDH2 and SK2 modulation (James et al., 2024; Madero et al., 2024; Panico et al., 2024). DAPA is known to inhibit the ERK signaling pathway, thereby mitigating age-related dysfunction of ISC. However, DAPA may also exert its effects by modulating other MAPK pathways, such as JNK and p38 MAPK (Sun et al., 2019). For instance, in models of diabetic cardiomyopathy, DAPA has been shown to provide direct cardioprotection by modulating the NHE1/MAPK signaling pathway (Lin et al., 2022). Moreover, DAPA has been reported to attenuate cellular stress and inflammation through the modulation of the PI3K/AKT pathway (Alsereidi et al., 2024). Although there is currently no direct evidence demonstrating DAPA's effects on JNK and p38 MAPK signaling pathways in our *Drosophila* models, considering DAPA's regulatory actions on these pathways in other systems, we cannot rule out the possibility that it may also act through these pathways in *Drosophila*. Although these multifaceted actions highlight the potential for non-glycemic mechanisms in DAPA's anti-aging effects, further research is needed to elucidate the precise contributions of SGLT2-dependent and -independent pathways using *Drosophila* diabetes models (Miao et al., 2022). This will contribute to a more comprehensive understanding of DAPA's anti-aging potential and provide a theoretical basis for the development of novel anti-aging therapeutics.

While this study establishes DAPA's efficacy in flies, further validation in mammalian models is essential. Additionally, whether DAPA's inhibition of MAPK synergizes with other aging-related pathways (e.g., AMPK or mTOR) warrants investigation (Sung et al., 2024). Future research should also address dose-response relationships and long-term safety to facilitate clinical translation. In conclusion, our findings position DAPA as a promising anti-aging compound and underscore the therapeutic potential of targeting MAPK signaling to combat stem cell aging.

4 Materials and methods

4.1 *Drosophila* strains and culture

The following *Drosophila* strains were used in this study: w^{1118} line (BDSC# 3605), *UAS-lacZ* line (from Allan Spradling), esg^{ts}*-Gal4* line (from Benjamin Ohlstein), *UAS-EGFR*^{CA} line (BDSC# 9533) and *UAS-EGFR*^{DN} line (BDSC #5364).

Flies were maintained on standard cornmeal-agar medium (80 g sucrose, 50 g cornmeal, 20 g glucose, 18.75 g yeast, 5 g agar, and 30 mL propionic acid per 1 L of water) and kept at standard conditions (25°C, 60% relative humidity, and 12 h light/dark cycle). Unless indicated otherwise, only mated females were used in this study (due to the higher incidence of age-related intestinal dysfunction observed in female fruit flies). The gene overexpression or knockdown mediated by the esgts-Gal4 *Drosophila* line was repressed at 18°C and activated at 29°C.

4.2 Drugs treatment

4.2.1 Dapagliflozin treatment

Dapagliflozin (Macklin, Shanghai, China, #D830111) was first dissolved in deionized water, then added to standard food to obtain different concentrations. Flies were collected randomly and maintained in the medium with different concentrations of Dapagliflozin (DAPA).

4.2.2 Bleomycin and paraquat treatment

A chromatography paper was cut into 3.7 × 5.8 cm strips and soaked in 25 μg/mL BLM (Aladdin, B107423), or 20 mM PQ (Aladdin, M106761) dissolved in 5% (wt/vol) sucrose. After being starved for 1 h, flies were transferred into vials with the BLM or PQ solution–saturated chromatography paper with 5% sucrose.

4.3 Immunofluorescence

Drosophila intestines were dissected in cold phosphate-buffered saline (PBS), fixed at room temperature for 30 min with 4% paraformaldehyde (PFA) (for anti-dpErk immunostaining, guts were fixed in 8% paraformaldehyde for 50 min), and then washed three times (10 min each) in PBS containing 0.1% Tween-20 (PBST). Tissues were immersed in the primary antibodies diluted in PBST and incubated overnight at 4°C.

The following primary antibodies were used: chicken anti-GFP, Abcam, 1:1,000; mouse anti-Delta, DSHB, 1:50; rabbit anti phospho-Histone H3 (Ser10), Millipore, 1:1,000; rabbit anti-dpERK, Cell Signaling, 1:500; Mouse anti-Armadillo 1:100, DSHB, #AB_528089,1:100. After washing, guts were incubated with secondary antibodies (Alexa 488, 568 or 647, Invitrogen, 1:2000) and DAPI (Sigma, 1 μg/mL) for more than 2 h at room temperature with shaking. Finally, seal and preserve the intestines by soaking them with the anti-fluorescence quenching agent and placing them on slides.

Immunofluorescence images were captured with a Leica TCS-SP8 confocal microscope and assembled with Application Suite X, Adobe Illustrator, and ImageJ software.

4.4 Smurf assay

To test the integrity of the *Drosophila* intestinal barrier (Rera et al., 2011), *Drosophila* treated with different drugs (fed with or without DAPA) were starved for 1 h and then cultured in the medium with added 2.5% (wt/vol) blue food dye (Spectrum Chemical Manufacturing Corp, Shanghai, China, #FD110) for 12 h. Flies leaking blue dye outside the intestine were considered as "Smurf (+)" flies. Smurf (+) indicates that the flies exhibit compromised intestinal barrier function, with visible blue dye staining on the body surface due to leakage. Smurf (−) indicates that the intestinal barrier function is intact, with no visible blue dye staining.

4.5 Bromophenol blue assay

To determine the pH of *Drosophila* midguts, the bromophenol blue assay was performed in the following steps (Li et al., 2016): add 200 μL of 2% bromophenol blue solution (Sigma, #B5525, dissolved in 5% sucrose) to the surface of the standard medium, followed by punching several holes with a pipet tip to allow the solution to be fully absorbed. The flies were starved for 1 h and cultured in the above food for 24 h. Then dissect the intestines and capture the images immediately to prevent carbon dioxide from affecting the rendering results.

To ensure accurate assessment of intestinal function, only flies that had consumed food, as indicated by blue staining in their guts (due to bromophenol blue), were included in the analysis. Flies that did not consume food, evidenced by the absence of blue staining, were excluded. The percentage of flies with blue-stained guts, representing those with functional food intake, was then calculated. We refer to flies whose guts were all dyed blue after ingesting food containing bromophenol blue as "perturbed" flies, while whose CCR areas retained yellow were described as "homeostasis."

4.6 *Drosophila* excretion assay

To measure the excretory function of the *Drosophila* intestinal tract [3](Cognigni et al., 2011), *Drosophila* treated with different drugs (fed with or without DAPA) were starved for 1 h and cultured in the bromophenol blue food vial (whose wall was surrounded by chromatography paper) for 24 h. Finally, image the deposits on the paper with a Leica M205 FA stereomicroscope and quantify the number of deposits.

4.7 Lifespan assay

To determine the effect of DAPA on the lifespan, 50–100 female or male flies hatched within 48 h were collected and divided equally into five vials, in which the food was mixed with or without DAPA.

To determine the lifespan under stressful conditions, the flies were randomized into the following groups: DSS (7%) + water, DSS (7%) + DAPA (100 μM). PQ (20 mM) + water, PQ (20 mM) + DAPA (100 μM), BLM (5 μg/mL) +water, and BLM (5 μg/mL) + DAPA (100 μM) group. For each group, 50–100 female or male flies hatched within 48 h were collected and divided equally into five vials.

In addition, the female flies used in the experiments are virgins [to avoid confounding factors introduced by mating and to focus on the intrinsic aging processes (Liu et al., 2024)]. The number of dead flies was recorded every 2 days, and the experiments were repeated at least three times.

4.8 Network pharmacology

The targets corresponding to DAPA (https://pubchem.ncbi.nlm.nih.gov/) were obtained from the PharmMapper database and filtered the targets with Norm Fit >0.5 (http://www.lilab-ecust.cn/pharmmapper/). The targets of aging were searched by the OMIM (https://omim.org/), TTD (http://db.idrblab.net/ttd/), DrugBank (https://go.drugbank.com/), GeneCards (http://www.genecards.org/), and DisGeNET (https://www.disgenet.org/) databases using "Intestinal stem cells aging" as the keyword. The gene names of these targets were obtained from the Uniprot database after removing the duplicates (http://www.uniprot.org).

The common targets of DAPA and aging were analyzed by the Venny 2.1.0 database to predict the potential targets of DAPA against aging. These common targets were imported into the STRING database (https://cn.string-db.org/), the minimum required interaction score was set to 0.7 and the isolated targets were removed to obtain the protein-protein interaction (PPI) network. Kyoto Encyclopedia of Genes and Genomes (KEGG, https://www.kegg.jp/kegg/pathway.html) enrichment analysis of the common targets was performed using the Metascape database (https://metascape.org/). The enrichment results of KEGG pathways were visualized by the Bioinformatics platform (https://www.bioinformatics.com.cn/).

4.9 Molecular docking

The 3D structure of DAPA in the SDF file was obtained from the PubChem database (https://pubchem.ncbi.nlm.nih.gov/), converted to a PDB file via Open Babel 2.4.1 software, used AutoDockTools-1.5.6 to add hydrogen bonds, detect the root, and set rotatable bonds, then saved as PDBQT format. The conformation of proteins obtained from the PDB database were exported to the PDB file, then charged into AutoDockTools-1.5.6 software to remove the water molecules and excess inactive ligands, get hydrogenated and exported to PDBQT format. The molecular docking was performed using AutoDockTools-1.5.6 software and the results were visualized by PyMol (DeLano Scientific, United States) and proteins. plus website (https://proteins.plus/).

4.10 Flow cytometry-based isolation of esg$^+$ cells from *Drosophila* midguts

A total of 200 female *Drosophila* midgut were dissected under ice-cold PBS (pH 7.4) supplemented with 1% penicillin-streptomycin. The midguts (R1–R5 regions) were carefully excised and immersed in PBS containing diethylpyrocarbonate (DEPC) to

inactivate ribonucleases. Tissues were then treated with 1 mg/mL Elastase solution (Sigma, cat. no. E0258) at 25°C for 30 min with periodic gentle mechanical disruption every 10 min to ensure complete dissociation. The resulting cell suspension was passed through a 40 μm cell strainer (Biologix) to generate a single-cell population, which was subsequently sorted using a BD FACS AriaTM III sorter (BD Biosciences) equipped with a 488 nm laser and a 530/30 nm emission filter. Sorting gates were set based on GFP fluorescence intensity and forward/side scatter profiles to exclude esg-cells. Sorted cells were pelleted by centrifugation at 400 × g for 20 min at 4°C, resuspended in 0.2 mL ice-cold PBS/DEPC, and stored at −80°C until further analysis. For each of three biological replicates, approximately 1×10^5–1×10^6 GFP-positive cells were obtained.

4.11 RNA isolation and RT-qPCR for *Drosophila*

40 adult midguts or 1×10^5–1×10^6 esg^+ cells collected into 4°C diethylpyrocarbonate (DEPC)-treated water-PBS solution. Samples were homogenized in RNA-easy Isolation Reagent (Vazyme, R701) for total RNA isolation and cDNA synthesis. RT-qPCRwas performedon aCFX96TouchDeepWell (Bio Rad) usingChamQUniversal SYBRqPCRMasterMix (Vazyme, Q711). The reference standardgroup was Rp49. The expression levels were counted by the$2^{-\triangle\triangle CT}$method.The primers used were listed as below:

Rp49-F:GCCCAAGGGTATCGACAACA.
Rp49-R:GCGCTTGTTCGATCCGTAAC.
Egfr-F: CGACCGTACTACGACGACAGTA.
Egfr-R:TGATCTTGGTGAGGACGATGA.
dmp53-F:CGTGATTGCTGTGGTTACGTGTACT.
dmp53-R:GCTGCAGAATGCGTTGCTGAAATGTG.
chk2-F:ATGGTGCCGTTGTTGATGTGCAGAT.
chk2-R:TGCAGATGTGCGTTGATGTGGTGCCAT.
sod-F: CAAGGGCACGGTTTTCTTC.
sod-R: CCTCACCGGAGACCTTCAC.
cat-F:TTCCTGTGGGCAAAATGGTG.
cat-R:ATCTTCACCTTGTACGGGCA.

4.12 Statistical analyses

For all the experiments, the data were processed using GraphPad Prism version 8.0 and presented as average ±SD from at least three independent experiments. Statistical significance was determined using the two-tailed Student's t-test unless otherwise specified in the figure legends. For all the tests, $p < 0.05$ was considered to indicate statistical significance.

Data availability statement

The original contributions presented in the study are included in the article/Supplementary Material, further inquiries can be directed to the corresponding authors.

Ethics statement

The animal study was approved by the Ethics Committee of West China Hospital, Sichuan University (Ethics Approval Number: 20231027008. The study was conducted in accordance with the local legislation and institutional requirements.

Author contributions

JY: Conceptualization, Data curation, Formal Analysis, Resources, Software, Supervision, Writing – original draft. CF: Investigation, Methodology, Project administration, Resources, Software, Supervision, Validation, Visualization, Writing – original draft. HZ: Conceptualization, Investigation, Methodology, Project administration, Resources, Visualization, Writing – original draft. TL: Methodology, Project administration, Resources, Software, Writing – original draft. HyC: Supervision, Writing – review and editing. HoC: Funding acquisition, Software, Supervision, Validation, Visualization, Writing – review and editing.

Funding

The author(s) declare that financial support was received for the research and/or publication of this article. This work was supported by the National Key R&D Program of China (2020YFA0803602), the National Natural Science Foundation of China (32470879 and 92157109) (HyC), Sichuan Science and Technology Program, Sichuan Provincial Natural Science Foundation (Grant No. 2025ZNSFSC0720 (HyC) the 1.3.5 project for disciplines of excellence, West China Hospital, Sichuan University (ZYYC20024) (HyC) and 1·3·5 projects for Artificial Intelligence (ZYAI24024), West China Hospital, Sichuan University. The funders had no role in the study design, data collection, and analysis, decision to publish, or manuscript preparation.

Acknowledgments

We thank BDSC, VDRC, and THFC for providing fly strains, and DSHB for providing the antibodies. We also would like to thank Dr. Allan Spradling for providing fly strains. We thank the central microscopy facility at the Department of Laboratory of Metabolism and Aging Research Biology at Sichuan University for support with confocal microscopy. We would like to thank Professor Haiyang Chen for his valuable insights and guidance on this project.

Conflict of interest

The authors declare that the research was conducted in the absence of any commercial or financial relationships that could be construed as a potential conflict of interest.

Generative AI statement

The author(s) declare that no Generative AI was used in the creation of this manuscript.

Publisher's note

Supplementary material

The Supplementary Material for this article can be found online at: https://www.frontiersin.org/articles/10.3389/fcell.2025.1576258/full#supplementary-material

SUPPLEMENTARY FIGURE S1
DAPA mitigates oxidative stress and DNA damage in *Drosophila* midgut under different stress conditions **(A)** Reduced Armadillo (Arm) fluorescence intensity in DAPA-treated flies under 7% DSS-mediated intestinal injury.(scale bar = 20 μm). **(B)** Downregulation of ROS-related genes (*sod* and *cat*) in DAPA-treated flies exposed to paraquat (PQ). Gene expression was analyzed by qRT-PCR using RNA extracted from whole midgut tissues (n = 40 guts per group). **(C)** Downregulation of DNA damage-related genes (*chk2* and *dmp53*) in DAPA-treated flies receiving bleomycin (BLM). Data are represented as means ± SD. ANOVA or unpaired Kruskal Wallis test be used,$^{*}p < 0.05$,$^{**}p < 0.01$,$^{***}p < 0.001$, and$^{****}p < 0.0001$, and ns indicates $p > 0.05$.

SUPPLEMENTARY FIGURE S2
Network pharmacology analysis and molecular docking of Dapagliflozin. **(A)** The structure of DAPA. **(B)** Venn diagram illustrating the intersection between DAPA and Aging. **(C)** PPI network of DAPA and aging intersection targets. **(D)** Kyoto Encyclopedia of Genes and Genomes (KEGG) pathways bubble diagram. **(E)** The gene ontology (GO) functional enrichment analysis revealed a significant enrichment of MAPK-related proteins in biological processes and molecular functions. **(F, G)** Diagram of the molecular docking of DAPA with EGFR or MAPK3, the binding energies for the targets docked into the DAPA are EGFR (−5.44 kcal/mol), MAPK3/ERK (−4.92 kcal/mol).

SUPPLEMENTARY FIGURE S3
Representative images of pErk and pH3 staining in gut of ISCs **(A)** Representative immunofluorescence images of pErk in esg-GFP+ cells from female flies (esgts-Gal4 > UAS-lacZ) at three different time points: 10 days old (10d), 40 days old (40d), and 40 days old with DAPA treatment (40d + DAPA). Cells were stained with pErk antibody. Scale bar represents 20 μm. **(B)** Representative immunofluorescence images of pH3 in the posterior midguts from female flies carrying esg^{ts}-*Gal4*-driven *UAS-lacZ*, *UAS-lacZ* +DAPA, $UAS\text{-}EGFR^{CA}$ + DAPA, $UAS\text{-}EGFR^{DN}$, and $UAS\text{-}EGFR^{DN}$ + DAPA stained with pH3 (red), DAPI (blue). Scale bar represents 20 μm.

References

Alsereidi, F. R., Khashim, Z., Marzook, H., Al-Rawi, A. M., Salomon, T., Almansoori, M. K., et al. (2024). Dapagliflozin mitigates cellular stress and inflammation through PI3K/AKT pathway modulation in cardiomyocytes, aortic endothelial cells, and stem cell-derived β cells. *Cardiovasc Diabetol.* 23 (1), 388. doi:10.1186/s12933-024-02481-y

Arab, H. H., Al-Shorbagy, M. Y., and Saad, M. A. (2021). Activation of autophagy and suppression of apoptosis by dapagliflozin attenuates experimental inflammatory bowel disease in rats: targeting AMPK/mTOR, HMGB1/RAGE and Nrf2/HO-1 pathways. *Chem. Biol. Interact.* 335, 109368. doi:10.1016/j.cbi.2021.109368

Arow, M., Waldman, M., Yadin, D., Nudelman, V., Shainberg, A., Abraham, N. G., et al. (2020). Sodium-glucose cotransporter 2 inhibitor Dapagliflozin attenuates diabetic cardiomyopathy. *Cardiovasc Diabetol.* 19 (1), 7. doi:10.1186/s12933-019-0980-4

Ayyaz, A., and Jasper, H. (2013). Intestinal inflammation and stem cell homeostasis in aging *Drosophila melanogaster*. *Front. Cell Infect. Microbiol.* 3, 98. doi:10.3389/fcimb.2013.00098

Basak, D., Gamez, D., and Deb, S. (2023). SGLT2 inhibitors as potential anticancer agents. *Biomedicines* 11 (7), 1867. doi:10.3390/biomedicines11071867

Biteau, B., Hochmuth, C. E., and Jasper, H. (2008). JNK activity in somatic stem cells causes loss of tissue homeostasis in the aging Drosophila gut. *Cell Stem Cell* 3 (4), 442–455. doi:10.1016/j.stem.2008.07.024

Biteau, B., Hochmuth, C. E., and Jasper, H. (2011). Maintaining tissue homeostasis: dynamic control of somatic stem cell activity. *Cell Stem Cell* 9 (5), 402–411. doi:10.1016/j.stem.2011.10.004

Biteau, B., Karpac, J., Supoyo, S., Degennaro, M., Lehmann, R., and Jasper, H. (2010). Lifespan extension by preserving proliferative homeostasis in Drosophila. *PLoS Genet.* 6 (10), e1001159. doi:10.1371/journal.pgen.1001159

Brunet, A., Goodell, M. A., and Rando, T. A. (2023). Ageing and rejuvenation of tissue stem cells and their niches. *Nat. Rev. Mol. Cell Biol.* 24 (1), 45–62. doi:10.1038/s41580-022-00510-w

Butt, J. H., Dewan, P., Merkely, B., Belohlávek, J., Drożdż, J., Kitakaze, M., et al. (2022). Efficacy and safety of dapagliflozin according to frailty in heart failure with reduced ejection fraction: a *post hoc* analysis of the DAPA-HF trial. *Ann. Intern Med.* 175 (6), 820–830. doi:10.7326/m21-4776

Chen, H., Chen, H., Liang, J., Gu, X., Zhou, J., Xie, C., et al. (2020). TGF-β1/IL-11/MEK/ERK signaling mediates senescence-associated pulmonary fibrosis in a stress-induced premature senescence model of Bmi-1 deficiency. *Exp. Mol. Med.* 52 (1), 130–151. doi:10.1038/s12276-019-0371-7

Choi, J., and Augenlicht, L. H. (2024). Intestinal stem cells: guardians of homeostasis in health and aging amid environmental challenges. *Exp. Mol. Med.* 56 (3), 495–500. doi:10.1038/s12276-024-01179-1

Choi, N. H., Kim, J. G., Yang, D. J., Kim, Y. S., and Yoo, M. A. (2008). Age-related changes in Drosophila midgut are associated with PVF2, a PDGF/VEGF-like growth factor. *Aging Cell* 7 (3), 318–334. doi:10.1111/j.1474-9726.2008.00380.x

Cognigni, P., Bailey, A. P., and Miguel-Aliaga, I. (2011). Enteric neurons and systemic signals couple nutritional and reproductive status with intestinal homeostasis. *Cell Metab.* 13 (1), 92–104. doi:10.1016/j.cmet.2010.12.010

Dihoum, A., Brown, A. J., McCrimmon, R. J., Lang, C. C., and Mordi, I. R. (2024). Dapagliflozin, inflammation and left ventricular remodelling in patients with type 2 diabetes and left ventricular hypertrophy. *BMC Cardiovasc Disord.* 24 (1), 356. doi:10.1186/s12872-024-04022-7

Du, G., Liu, Z., Yu, Z., Zhuo, Z., Zhu, Y., Zhou, J., et al. (2021). Taurine represses age-associated gut hyperplasia in Drosophila via counteracting endoplasmic reticulum stress. *Aging Cell* 20 (3), e13319. doi:10.1111/acel.13319

Du, G., Xiong, L., Li, X., Zhuo, Z., Zhuang, X., Yu, Z., et al. (2020). Peroxisome elevation induces stem cell differentiation and intestinal epithelial repair. *Dev. Cell* 53 (2), 169–184. doi:10.1016/j.devcel.2020.03.002

Dubreuil, R. R. (2004). Copper cells and stomach acid secretion in the Drosophila midgut. *Int. J. Biochem. Cell Biol.* 36 (5), 745–752. doi:10.1016/j.biocel.2003.07.004

Ermolaeva, M., Neri, F., Ori, A., and Rudolph, K. L. (2018). Cellular and epigenetic drivers of stem cell ageing. *Nat. Rev. Mol. Cell Biol.* 19 (9), 594–610. doi:10.1038/s41580-018-0020-3

Fang, J. Y., and Richardson, B. C. (2005). The MAPK signalling pathways and colorectal cancer. *Lancet Oncol.* 6 (5), 322–327. doi:10.1016/s1470-2045(05)70168-6

He, D., Wu, H., Xiang, J., Ruan, X., Peng, P., Ruan, Y., et al. (2020). Gut stem cell aging is driven by mTORC1 via a p38 MAPK-p53 pathway. *Nat. Commun.* 11 (1), 37. doi:10.1038/s41467-019-13911-x

Jaikumkao, K., Promsan, S., Thongnak, L., Swe, M. T., Tapanya, M., Htun, K. T., et al. (2021). Dapagliflozin ameliorates pancreatic injury and activates kidney autophagy by modulating the AMPK/mTOR signaling pathway in obese rats. *J. Cell Physiol.* 236 (9), 6424–6440. doi:10.1002/jcp.30316

James, S., Erlinge, D., Storey, R. F., McGuire, D. K., de Belder, M., Eriksson, N., et al. (2024). Dapagliflozin in myocardial infarction without diabetes or heart failure. *NEJM Evid.* 3 (2), EVIDoa2300286. doi:10.1056/EVIDoa2300286

Jasper, H. (2020). Intestinal stem cell aging: origins and interventions. *Annu. Rev. Physiol.* 82, 203–226. doi:10.1146/annurev-physiol-021119-034359

Jhund, P. S., Solomon, S. D., Docherty, K. F., Heerspink, H. J. L., Anand, I. S., Böhm, M., et al. (2021). Efficacy of dapagliflozin on renal function and outcomes in patients with heart failure with reduced ejection fraction: results of DAPA-HF. *Circulation* 143 (4), 298–309. doi:10.1161/circulationaha.120.050391

Jiang, E., Dinesh, A., Jadhav, S., Miller, R. A., and Garcia, G. G. (2023). Canagliflozin shares common mTOR and MAPK signaling mechanisms with other lifespan extension treatments. *Life Sci.* 328, 121904. doi:10.1016/j.lfs.2023.121904

Jiang, H., Grenley, M. O., Bravo, M. J., Blumhagen, R. Z., and Edgar, B. A. (2011). EGFR/Ras/MAPK signaling mediates adult midgut epithelial homeostasis and regeneration in Drosophila. *Cell Stem Cell* 8 (1), 84–95. doi:10.1016/j.stem.2010.11.026

Jing, Y., Wang, Q., Bai, F., Li, Z., Li, Y., Liu, W., et al. (2025). Age-related alterations in gut homeostasis are microbiota dependent. *NPJ Biofilms Microbiomes* 11 (1), 51. doi:10.1038/s41522-025-00677-y

Kabiri, Z., Greicius, G., Zaribafzadeh, H., Hemmerich, A., Counter, C. M., and Virshup, D. M. (2018). Wnt signaling suppresses MAPK-driven proliferation of intestinal stem cells. *J. Clin. Invest* 128 (9), 3806–3812. doi:10.1172/jci99325

Katsuumi, G., Shimizu, I., Suda, M., Yoshida, Y., Furihata, T., Joki, Y., et al. (2024). SGLT2 inhibition eliminates senescent cells and alleviates pathological aging. *Nat. Aging* 4 (7), 926–938. doi:10.1038/s43587-024-00642-y

Kounatidis, D., Vallianou, N., Evangelopoulos, A., Vlahodimitris, I., Grivakou, E., Kotsi, E., et al. (2023). SGLT-2 inhibitors and the inflammasome: what's next in the 21st century? *Nutrients* 15 (10), 2294. doi:10.3390/nu15102294

Kühn, F., Adiliaghdam, F., Cavallaro, P. M., Hamarneh, S. R., Tsurumi, A., Hoda, R. S., et al. (2020). Intestinal alkaline phosphatase targets the gut barrier to prevent aging. *JCI Insight* 5 (6), e134049. doi:10.1172/jci.insight.134049

Lai, S. W., Hwang, B. F., Kuo, Y. H., Liu, C. S., and Liao, K. F. (2023). Sodium-glucose cotransporter-2 inhibitors use and the risk of gout: a systematic review and meta-analysis. *Front. Endocrinol. (Lausanne)* 14, 1158153. doi:10.3389/fendo.2023.1158153

Lee, Y. H., Kim, S. H., Kang, J. M., Heo, J. H., Kim, D. J., Park, S. H., et al. (2019). Empagliflozin attenuates diabetic tubulopathy by improving mitochondrial fragmentation and autophagy. *Am. J. Physiol. Ren. Physiol.* 317 (4), F767-F780–f780. doi:10.1152/ajprenal.00565.2018

Lemaitre, B., and Miguel-Aliaga, I. (2013). The digestive tract of *Drosophila melanogaster*. *Annu. Rev. Genet.* 47, 377–404. doi:10.1146/annurev-genet-111212-133343

Li, H., Qi, Y., and Jasper, H. (2016). Preventing age-related decline of gut compartmentalization limits microbiota dysbiosis and extends lifespan. *Cell Host Microbe* 19 (2), 240–253. doi:10.1016/j.chom.2016.01.008

Li, Z., Liu, S., and Cai, Y. (2015). EGFR/MAPK signaling regulates the proliferation of Drosophila renal and nephric stem cells. *J. Genet. Genomics* 42 (1), 9–20. doi:10.1016/j.jgg.2014.11.007

Lin, K., Yang, N., Luo, W., Qian, J. F., Zhu, W. W., Ye, S. J., et al. (2022). Direct cardio-protection of Dapagliflozin against obesity-related cardiomyopathy via NHE1/MAPK signaling. *Acta Pharmacol. Sin.* 43 (10), 2624–2635. doi:10.1038/s41401-022-00885-8

Liu, C., Tian, N., Chang, P., and Zhang, W. (2024). Mating reconciles fitness and fecundity by switching diet preference in flies. *Nat. Commun.* 15 (1), 9912. doi:10.1038/s41467-024-54369-w

López-Otín, C., Blasco, M. A., Partridge, L., Serrano, M., and Kroemer, G. (2013). The hallmarks of aging. *Cell* 153 (6), 1194–1217. doi:10.1016/j.cell.2013.05.039

López-Otín, C., Blasco, M. A., Partridge, L., Serrano, M., and Kroemer, G. (2023). Hallmarks of aging: an expanding universe. *Cell* 186 (2), 243–278. doi:10.1016/j.cell.2022.11.001

Lyles, J. T., Luo, L., Liu, K., Jones, D. P., Jones, R. M., and Quave, C. L. (2021). Cruciferous vegetables (*Brassica oleracea*) confer cytoprotective effects in Drosophila intestines. *Gut Microbes* 13 (1), 1–6. doi:10.1080/19490976.2021.1921926

Madero, M., Chertow, G. M., and Mark, P. B. (2024). SGLT2 inhibitor use in chronic kidney disease: supporting cardiovascular, kidney, and metabolic health. *Kidney Med.* 6 (8), 100851. doi:10.1016/j.xkme.2024.100851

Martel, J., Chang, S. H., Ko, Y. F., Hwang, T. L., Young, J. D., and Ojcius, D. M. (2022). Gut barrier disruption and chronic disease. *Trends Endocrinol. Metab.* 33 (4), 247–265. doi:10.1016/j.tem.2022.01.002

McGuire, S. E., Mao, Z., and Davis, R. L. (2004). Spatiotemporal gene expression targeting with the TARGET and gene-switch systems in Drosophila. *Sci. STKE* 2004 (220), pl6. doi:10.1126/stke.2202004pl6

Miao, Y., Chen, R., Wang, X., Zhang, J., Tang, W., Zhang, Z., et al. (2022). *Drosophila melanogaster* diabetes models and its usage in the research of anti-diabetes management with traditional Chinese medicines. *Front. Med. (Lausanne)* 9, 953490. doi:10.3389/fmed.2022.953490

Nászai, M., Bellec, K., Yu, Y., Román-Fernández, A., Sandilands, E., Johansson, J., et al. (2021). RAL GTPases mediate EGFR-driven intestinal stem cell proliferation and tumourigenesis. *Elife* 10, e63807. doi:10.7554/eLife.63807

Ohlstein, B., and Spradling, A. (2006). The adult Drosophila posterior midgut is maintained by pluripotent stem cells. *Nature* 439 (7075), 470–474. doi:10.1038/nature04333

O'Keefe, J. H., Weidling, R., O'Keefe, E. L., and Franco, W. G. (2023). SGLT inhibitors for improving Healthspan and lifespan. *Prog. Cardiovasc Dis.* 81, 2–9. doi:10.1016/j.pcad.2023.10.003

Ortega, R., Collado, A., Selles, F., Gonzalez-Navarro, H., Sanz, M. J., Real, J. T., et al. (2019). SGLT-2 (Sodium-Glucose cotransporter 2) inhibition reduces ang II (angiotensin II)-Induced dissecting abdominal aortic aneurysm in ApoE (apolipoprotein E) knockout mice. *Arterioscler. Thromb. Vasc. Biol.* 39 (8), 1614–1628. doi:10.1161/atvbaha.119.312659

Panico, C., Felicetta, A., Kunderfranco, P., Cremonesi, M., Salvarani, N., Carullo, P., et al. (2024). Single-cell RNA sequencing reveals metabolic stress-dependent activation of cardiac macrophages in a model of dyslipidemia-induced diastolic dysfunction. *Circulation* 150 (19), 1517–1532. doi:10.1161/circulationaha.122.062984

Park, J. S., Kim, Y. S., and Yoo, M. A. (2009). The role of p38b MAPK in age-related modulation of intestinal stem cell proliferation and differentiation in Drosophila. *Aging (Albany NY)* 1 (7), 637–651. doi:10.18632/aging.100054

Phongphithakchai, A., Tedasen, A., Netphakdee, R., Leelawattana, R., Srithongkul, T., Raksasuk, S., et al. (2025). Dapagliflozin in chronic kidney disease: insights from network pharmacology and molecular docking simulation. *Life (Basel)* 15 (3), 437. doi:10.3390/life15030437

Pond, K. W., Morris, J. M., Alkhimenok, O., Varghese, R. P., Cabel, C. R., Ellis, N. A., et al. (2022). Live-cell imaging in human colonic monolayers reveals ERK waves limit the stem cell compartment to maintain epithelial homeostasis. *Elife* 11, e78837. doi:10.7554/eLife.78837

Promislow, D. E. L., Flatt, T., and Bonduriansky, R. (2022). The Biology of aging in insects: from Drosophila to other insects and back. *Annu. Rev. Entomol.* 67, 83–103. doi:10.1146/annurev-ento-061621-064341

Rera, M., Bahadorani, S., Cho, J., Koehler, C. L., Ulgherait, M., Hur, J. H., et al. (2011). Modulation of longevity and tissue homeostasis by the Drosophila PGC-1 homolog. *Cell Metab.* 14 (5), 623–634. doi:10.1016/j.cmet.2011.09.013

Rodriguez-Fernandez, I. A., Tauc, H. M., and Jasper, H. (2020). Hallmarks of aging Drosophila intestinal stem cells. *Mech. Ageing Dev.* 190, 111285. doi:10.1016/j.mad.2020.111285

Schafer, M. J., White, T. A., Iijima, K., Haak, A. J., Ligresti, G., Atkinson, E. J., et al. (2017). Cellular senescence mediates fibrotic pulmonary disease. *Nat. Commun.* 8, 14532. doi:10.1038/ncomms14532

Shibusawa, R., Yamada, E., Okada, S., Nakajima, Y., Bastie, C. C., Maeshima, A., et al. (2019). Dapagliflozin rescues endoplasmic reticulum stress-mediated cell death. *Sci. Rep.* 9 (1), 9887. doi:10.1038/s41598-019-46402-6

Sun, L., Zhang, J., Chen, W., Chen, Y., Zhang, X., Yang, M., et al. (2020). Attenuation of epigenetic regulator SMARCA4 and ERK-ETS signaling suppresses aging-related dopaminergic degeneration. *Aging Cell* 19 (9), e13210. doi:10.1111/acel.13210

Sun, Y., Zhang, D., Guo, X., Li, W., Li, C., Luo, J., et al. (2019). MKK3 modulates JNK-dependent cell migration and invasion. *Cell Death Dis.* 10 (3), 149. doi:10.1038/s41419-019-1350-6

Sung, P. H., Yue, Y., Chen, Y. L., Chiang, J. Y., Cheng, B. C., Yang, C. C., et al. (2024). Combined dapagliflozin and roxadustat effectively protected heart and kidney against cardiorenal syndrome-induced damage in rodent through activation of cell stress-Nfr2/ARE signalings and stabilizing HIF-1α. *Biomed. Pharmacother.* 180, 117567. doi:10.1016/j.biopha.2024.117567

Tai, S., Zhou, Y., Fu, L., Ding, H., Zhou, Y., Yin, Z., et al. (2023). Dapagliflozin impedes endothelial cell senescence by activating the SIRT1 signaling pathway in type 2 diabetes. *Heliyon* 9 (8), e19152. doi:10.1016/j.heliyon.2023.e19152

Tarragó, M. G., Chini, C. C. S., Kanamori, K. S., Warner, G. M., Caride, A., de Oliveira, G. C., et al. (2018). A potent and specific CD38 inhibitor ameliorates age-related metabolic dysfunction by reversing tissue NAD(+) decline. *Cell Metab.* 27 (5), 1081–1095.e10. doi:10.1016/j.cmet.2018.03.016

Ureña, E., Xu, B., Regan, J. C., Atilano, M. L., Minkley, L. J., Filer, D., et al. (2024). Trametinib ameliorates aging-associated gut pathology in Drosophila females by reducing Pol III activity in intestinal stem cells. *Proc. Natl. Acad. Sci. U. S. A.* 121 (4), e2311313121. doi:10.1073/pnas.2311313121

Wang, A., Li, Z., Zhuo, S., Gao, F., Zhang, H., Zhang, Z., et al. (2022). Mechanisms of cardiorenal protection with SGLT2 inhibitors in patients with T2DM based on network pharmacology. *Front. Cardiovasc Med.* 9, 857952. doi:10.3389/fcvm.2022.857952

Wu, C. Y., Iskander, C., Wang, C., Xiong, L. Y., Shah, B. R., Edwards, J. D., et al. (2023). Association of sodium-glucose cotransporter 2 inhibitors with time to dementia: a population-based cohort study. *Diabetes Care* 46 (2), 297–304. doi:10.2337/dc22-1705

Yan, L., Guo, X., Zhou, J., Zhu, Y., Zhang, Z., and Chen, H. (2022). Quercetin prevents intestinal stem cell aging via scavenging ROS and inhibiting insulin signaling in Drosophila. *Antioxidants (Basel)* 12 (1), 59. doi:10.3390/antiox12010059

Yan, L., Zhou, J., Yuan, L., Ye, J., Zhao, X., Ren, G., et al. (2023). Silibinin alleviates intestinal inflammation via inhibiting JNK signaling in Drosophila. *Front. Pharmacol.* 14, 1246960. doi:10.3389/fphar.2023.1246960

Zhang, C., Jin, Y., Marchetti, M., Lewis, M. R., Hammouda, O. T., and Edgar, B. A. (2022). EGFR signaling activates intestinal stem cells by promoting mitochondrial biogenesis and β-oxidation. *Curr. Biol.* 32 (17), 3704–3719.e7. doi:10.1016/j.cub.2022.07.003

Zhang, P., Holowatyj, A. N., Roy, T., Pronovost, S. M., Marchetti, M., Liu, H., et al. (2019). An SH3PX1-dependent endocytosis-autophagy network restrains intestinal stem cell proliferation by counteracting EGFR-ERK signaling. *Dev. Cell* 49 (4), 574–589. doi:10.1016/j.devcel.2019.03.029

frontiers | Frontiers in Cell and Developmental Biology

TYPE Original Research
PUBLISHED 24 September 2025
DOI 10.3389/fcell.2025.1659444

OPEN ACCESS

EDITED BY
Mustapha Najimi,
Institute of Experimental and Clinical Research- UCLouvain, Belgium

REVIEWED BY
Giacomina Brunetti,
University of Bari Aldo Moro, Italy
Ahmet Emin Topal,
Bahçeşehir University, Türkiye

*CORRESPONDENCE
Naishun Liao,
liaons046@163.com
Xiaodan Wu,
wxiaodan@sina.com

†These authors have contributed equally to this work

RECEIVED 07 July 2025
ACCEPTED 02 September 2025
PUBLISHED 24 September 2025

CITATION
Huang L, Lin Z, Liu H, Lin X, Liao N and Wu X (2025) Mesenchymal stem cell-conditioned medium accelerates type 2 diabetic wound healing by targeting TNF and chemokine signaling.
Front. Cell Dev. Biol. 13:1659444.
doi: 10.3389/fcell.2025.1659444

Mesenchymal stem cell-conditioned medium accelerates type 2 diabetic wound healing by targeting TNF and chemokine signaling

Long Huang[1†], Zhongbao Lin[2†], Haiyun Liu[3], Xiankun Lin[2], Naishun Liao[4*] and Xiaodan Wu[5*]

[1]Department of Respiratory and Critical Care Medicine, Fuzhou University Affiliated Provincial Hospital, Fujian Provincial Hospital, Shengli Clinical Medical College of Fujian Medical University, Fuzhou, China, [2]Department of Critical Care Medicine, Fuzhou University Affiliated Provincial Hospital, Fujian Provincial Hospital, Shengli Clinical Medical College of Fujian Medical University, Fuzhou, China, [3]Shengli Clinical Medical College of Fujian Medical University; Department of Emergency, Fujian Provincial Hospital; Fuzhou University Affiliated Provincial Hospital; Fujian Provincial Key Laboratory of Emergency Medicine, Fuzhou, China, [4]The United Innovation of Mengchao Hepatobiliary Technology Key Laboratory of Fujian Province, Mengchao Hepatobiliary Hospital of Fujian Medical University, Fuzhou, China, [5]Department of Anesthesiology, Shengli Clinical Medical College of Fujian Fuzhou University Affiliated Provincial Hospital, Fuzhou, China

Introduction: Given the crucial role of paracrine signaling in the therapeutic function of adipose tissue-derived mesenchymal stem cells (ADSCs) for skin wound repair, this study aimed to evaluate the efficacy of ADSC-conditioned medium (ACM) in enhancing type 2 diabetic (T2D) wound healing.
Methods: The effect of ACM on the viability and angiogenesis of human umbilical vein endothelial cells (HUVECs) was first evaluated using the CCK-8 assay and q-PCR analysis, respectively. Next, a T2D rat model was established through the combination of a high-fat diet and streptozotocin (STZ). Following the establishment of full-thickness skin defects in T2D rats, ACM or serum-free cultured medium was daily injected around the wound edges for 7 days. Afterward, the skin wound healing rate was analyzed, and the skin tissues were assessed by histopathological examination. The mRNA levels of TNF-α, IL-1β, IL-6, COX-2, IL-12, and IFN-γ were evaluated by q-PCR analysis. Additionally, transcriptome sequencing and immunohistochemistry were performed to reveal the potential mechanisms of ACM in T2D skin wound healing.
Results: ACM significantly enhanced HUVEC proliferation and angiogenesis while upregulating the expression of EGF, bFGF, VEGF, and KDR. In T2D rats, ACM accelerated wound closure and suppressed pro-inflammatory mediators (TNF-α, IL-1β, IL-6, COX-2, IL-12, and IFN-γ). Notably, transcriptome analysis revealed ACM-mediated downregulation of TNF and chemokine signaling pathways.
Discussion: ACM promotes diabetic wound healing through dual mechanisms: (1) stimulating vascularization by inducing growth factor expression and (2) modulating the inflammatory microenvironment by inhibiting TNF/chemokine

cascades. These findings position ACM as a promising cell-free therapy for impaired wound healing in diabetes.

KEYWORDS

adipose tissue-derived mesenchymal stem cells, conditioned medium, type 2 diabetes, skin wound, regeneration

1 Introduction

Skin wound healing is a complex process involving multiple stages, such as hemostasis, inflammation, angiogenesis, and remodeling, which requires the coordinated effort of various cell types and signaling pathways (Freedman et al., 2023; Martin and Nunan, 2015). There are several factors, such as ischemia, diabetes, age, nutrition, hormones, obesity, infection, smoking, alcoholism, and radiation and chemotherapy, which can influence one or more stages of this process, resulting in improper or impaired wound healing (Roux et al., 2025). In particular, delayed wound healing in diabetic patients is increasing globally due to the lack of effective intervention strategies and the widespread prevalence of diabetes (De Souza et al., 2023).

Given their excellent immunoregulation, multidirectional differentiation ability, and paracrine function, adipose-derived mesenchymal stem cells (ADSCs) have emerged as a novel and promising strategy for treating diabetic wounds in both preclinical and clinical studies (Yan et al., 2024; Carstens et al., 2021; Huerta et al., 2023). However, the effectiveness of ADSCs in repairing diabetic wounds is limited by their low engraftment efficiency, which could be partially attributed to the stark contrast between optimized *in vitro* culture conditions and the harsh pathological microenvironment of chronic wound sites (Yu et al., 2023). Therefore, further research is needed to improve the efficacy of ADSC therapy for diabetic wound healing. Recently, increasing evidence has suggested that the paracrine function of ADSCs plays a leading role in skin wound regeneration (Ma et al., 2023; Ren et al., 2024; Wei et al., 2024; Wang et al., 2024). In particular, instead of mesenchymal stem cells (MSCs), using MSC-conditioned medium or secretome also provides a therapeutic potential for reducing irradiated skin injuries (Lin et al., 2023) and scar fibrosis (Zhang et al., 2021; Wang et al., 2024). More importantly, this cell-free strategy effectively avoids the potential limitation of low cell engraftment of MSCs for wound healing.

In this study, we investigated whether ADSC-conditioned medium (ACM) can be used for accelerating diabetic wound healing in rats. To achieve this purpose, we evaluated the therapeutic effect of ACM on skin wounds both *in vitro* and *in vivo* and the potential mechanism of ACM in diabetic wound healing. The results suggest that ACM may offer a promising strategy to promote diabetic wound recovery.

2 Materials and methods

2.1 Animals

Twenty adult male Sprague–Dawley (SD) rats (weighing 180 g–200 g) were obtained from the Shanghai Slack Laboratory Animal Center (license number: SCXK hu 2022-0004). All rats were housed in a standard specific pathogen-free (SPF) barrier environment at 20 °C–26 °C and 40%–70% humidity under a 12 h/12 h light–dark cycle. All animal experiments were approved by the Experimental Animal Ethics Center of Mengchao Hepatobiliary Hospital of Fujian Medical University (MCHH-AEC-2022-08). All experiments were designed and reported in accordance with the Animal Research: Reporting of *In Vivo* Experiments (ARRIVE) guidelines 2.0.

2.2 Preparation of ADSC-conditioned medium

The ADSCs were isolated and cultured according to previously published methods (Liao et al., 2017). In brief, adipose tissues were obtained from the inguinal region of male SD rats (n = 5) and washed with PBS solution. The tissues were then cut into small fragments and digested with 0.1% type I collagenase, followed by neutralization with α-MEM containing 10% FBS. Subsequently, the cells were cultured at a density of 1×10^6 cells/mL in T-75 plates. ADSCs at passage 3 were collected and cultured at a density of 2×10^6 cells per 10 cm plate. After overnight cell adhesion, the cultured ADSCs were washed with PBS solution to remove residual serum and then replaced with serum-free medium (YOCON, China) for 48 h. After incubation, the conditioned medium (10 mL/2×10^6 ADSCs) was collected and centrifuged at 3,000 *g* for 5 min to remove any cell debris. Furthermore, the ADSC-conditioned medium was concentrated using ultrafiltration with a tangential flow filtration capsule (Pall, United States) containing a 3-kDa molecular weight cut-off membrane, following the manufacturer's instructions. Finally, the concentration of the ADSC-conditioned medium was analyzed using a BCA assay kit (TransGen Biotech, China) and stored at −80 °C. A concentration of 100 ng/mL ADSC-conditioned medium was used in the present study.

2.3 HUVEC culture

The human umbilical vein endothelial cell (HUVEC) line was obtained from the National Institutes for Food and Drug Control (Beijing, China) and cultured with RPMI 1640 containing 10% FBS supplemented with 2% FBS, VEGF, IGF-1, and EGF at 37 °C/5% CO_2. For the tubule formation assay, 96-well plates were pre-coated with Matrigel (Corning, 10 mg/mL, 1:50 dilution in EGM-2) for 1 h at 37 °C to simulate the basement membrane matrix, as standardized in angiogenesis assays.

TABLE 1 Primer sequences.

Gene	Forward primer	Reverse primer
TNF-α	CAGAGGGAAGAGTTCCCCAG	CCTTGGTCTGGTAGGAGACG
IL-1β	CACCTCTCAAGCAGAGCACAG	GGGTTCCATGGTGAAGTCAAC
IL-6	CACTGGTCTTTTGGAGTTTGAG	GGACTTTTGTACTCATCTGCAC
COX-2	CGGAGGAGAAGTGGGGTTTAGGAT	TGGGAGGCACTTGCGTTGATGG
IL-12	AGTTCTTCGTCCGCATCCAG	CTTGCACGCAGAT ATTCGCC
IFN-γ	CAACCCACAGATCCAGCACA	TCAGCACCGACTCCTTTTCC
VEGF	CCCAGAAGTTGGACGAAAA	TGAGTTGGGAGGAGGATG
EGF	ACACGGAGGGAGGCTACA	GTAGCCTCCCTCCGTGTT
bFGF	CGCACCCTATCCCTTCACA	CAACGACCAGCCTTCCAC
KDR	ACTCCTCCTCATTCAGCG	GGGTCCCACAACTTCTCA
β-actin	GTGGACA TCCGCAA AGAC	AAAGGGTGTAACGC AACTA

2.4 Cell viability assay

HUVECs were cultured at a density of 1×10^4 cells per well in 96-well plates. After overnight cell adhesion, the cell supernatants were removed and replaced with 100 μL ADSC-conditioned medium, while the cells treated with serum-free medium were used as the negative control. After incubation for 24 h or 48 h, cell viability was evaluated using a CCK-8 assay kit (TransGen Biotech, China), according to the manufacturer's instructions.

2.5 Quantitative real-time PCR analysis

Total RNA was collected using a TRIzol reagent kit (TransGen Biotech, China) following the manufacturer's instructions. Afterward, mRNA was reverse-transcribed into cDNA using a cDNA synthesis kit (Roche, Germany). The quantitative real-time PCR analysis was performed in an ABI StepOnePlus Real-time PCR System (Carlsbad, United States), and the PCR conditions were as follows: 95 °C for 15 s, 60 °C for 30 s, and 70 °C for 30 s, for a total of 40 cycles. The primer sequences are listed in Table 1. The $2^{-\triangle\triangle Ct}$ formula was used to analyze the relative gene expression.

2.6 Diabetic skin-injured model and ACM treatment

The type 2 diabetic (T2D) model was established using a previously described method (Liao et al., 2017). In brief, the SD rats (n = 10) were fed with a high-fat diet (HFD) containing 66.5% normal chow, 20% sucrose, 10% lard, 2% cholesterol, and 1.5% cholate. After being fed with the HFD for 4 weeks, all rats were administered 25 mg/kg of streptozotocin (STZ) by intraperitoneal injection twice/week for 2 weeks. Rats treated with STZ and exhibiting a non-fasting blood glucose level ≥11.1 mmol/L were considered successful in establishing the T2D model. Next, the T2D rats were anesthetized with 40 mg/kg of pentobarbital sodium, and a full-thickness skin defect of 1 cm in diameter was created using a previously described method (Hur et al., 2017). Subsequently, the rats were randomly (random table method) divided into T2D skin-injured model and ACM groups (n = 5/group) and housed separately. Rats in the ACM group were treated daily with 100 μL ACM administered intradermally around the wound edges for 7 days, while model rats received an equal volume of serum-free medium. Normal rats (n = 5) were used as the negative control. On the 5th day after the last ACM treatment (the 12th day in total), all rats were euthanized with 100 mg/kg of pentobarbital sodium, and the wounds were harvested for further evaluation. All animals were selected at random for outcome assessment.

2.7 Histological examination

Tissues were collected and fixed in 4% paraformaldehyde for 24 h and then paraffin-embedded and sectioned into slices. Tissue sections were evaluated with hematoxylin and eosin (HE) staining and Masson staining, respectively. Finally, a double-blind histological examination was performed using an ortho-microscope (Zeiss, Germany) by two expert pathologists.

2.8 RNA sequencing

Total RNA from skin tissues was subjected to polyA-selected RNA-sequencing on the Illumina HiSeq X10 platform in a blinded manner. Using the DESeq2 package, RNA-seq analysis was carried out to determine the different gene expression (DEG) among three

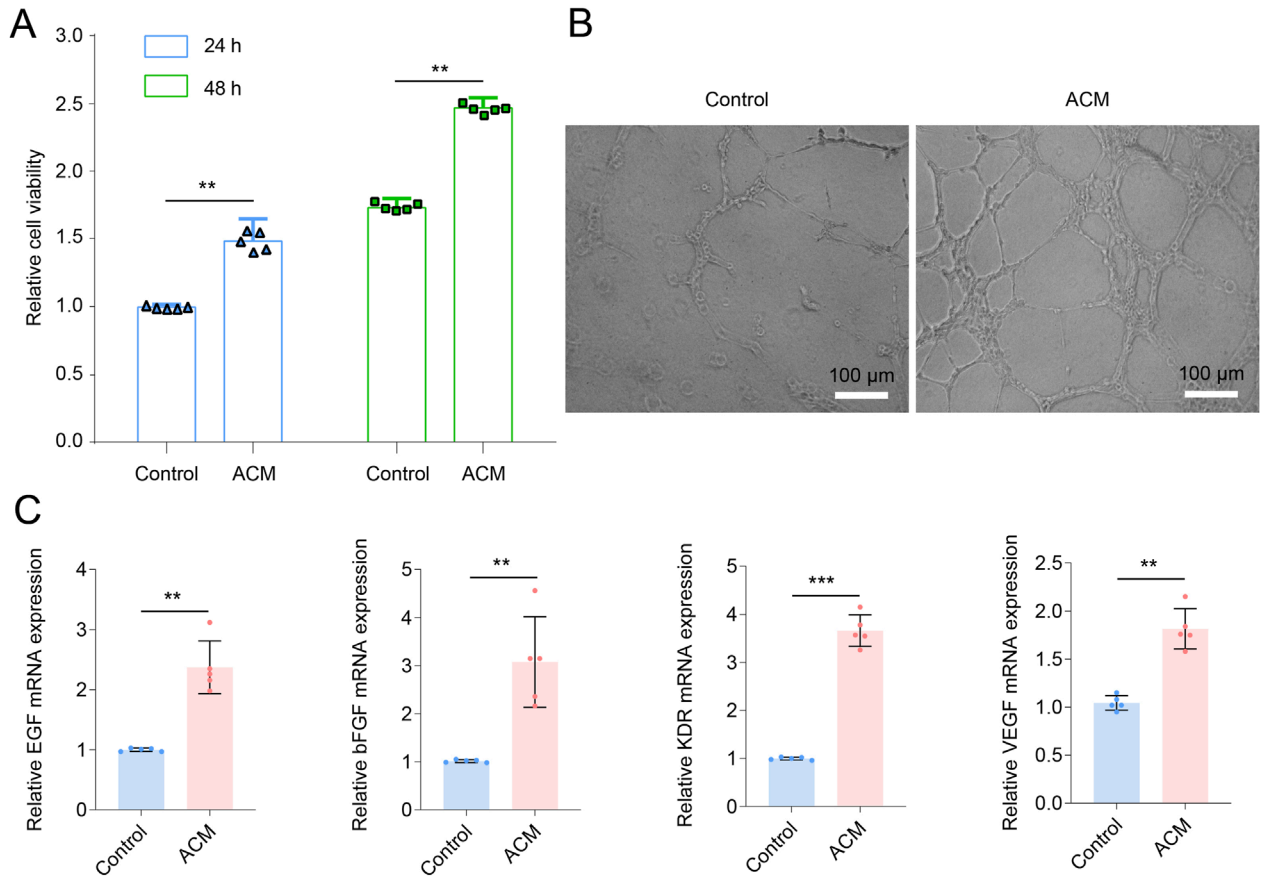

FIGURE 1
ACM promotes vascular cell proliferation and angiogenesis. **(A)** ACM promotes HUVEC proliferation. **(B)** Representative images of HUVECs after ACM treatment (scale bar, 100 μm). **(C)** Relative mRNA expression of EGF, bFGF, VEGF, and KDR in HUVECs after ACM treatment.

groups: normal vs. model and ACM vs. model. False discovery rate (FDR) of < 0.05 and fold change of ≥ 2 or ≤ 2 were the principles for DEG screening. Gene Ontology (GO) analysis was used to analyze the gene functions of the DEGs, and the Kyoto Encyclopedia of Genes and Genomes (KEGG) analysis was used to target the DEGs' enrichment pathway.

2.9 Immunohistochemistry

The skin wound sections were drenched in a citrate antigen retrieval solution (Beyotime Institute of Biotechnology, China) and heat-treated in a pressure cooker for 2 min, naturally cooled to RT, and washed with PBS buffer three times. Following incubation with 3% H_2O_2 for 10 min, the sections were blocked with 5% BSA for 30 min. The sections were then incubated overnight at 4 °C with primary antibodies against TNF-α, NF-κB, p-NF-κB, MAPK, p-MAPK, CXCL1, CXCL2, and CXCL8 at a dilution ratio of 1:200 . After washing three times with PBS, the sections were incubated with the secondary antibody at RT for another 2 h, followed by staining with DAB. The samples were observed using an ortho-microscope (Zeiss, Germany) in a blinded manner by the assessors.

2.10 Statistical analysis

All quantitative data were expressed as the mean ± standard deviation. GraphPad Prism version 9.0 (GraphPad Software, United States) was used for statistical analysis. The ANOVA was used to evaluate the significant differences among three independent groups, while the two-tailed paired sample Student's t-tests were used to evaluate the significant differences between two groups. $p < 0.05$ was considered a statistically significant difference.

3 Results

3.1 ACM promotes HUVEC angiogenesis and proliferation *in vitro*

Flow cytometry analysis showed that ADSCs typically expressed CD73 and CD90 while lacking expression of CD45, CD19, and CD34 (Supplementary Figure S1), suggesting the successful isolation and culture of ADSCs in this study. The impaired skin wound healing in diabetic individuals is largely attributed to diabetic angiopathy, which is characterized by the dysfunction and impairment of the arteries throughout the body (Jin et al., 2022). We, therefore, investigated

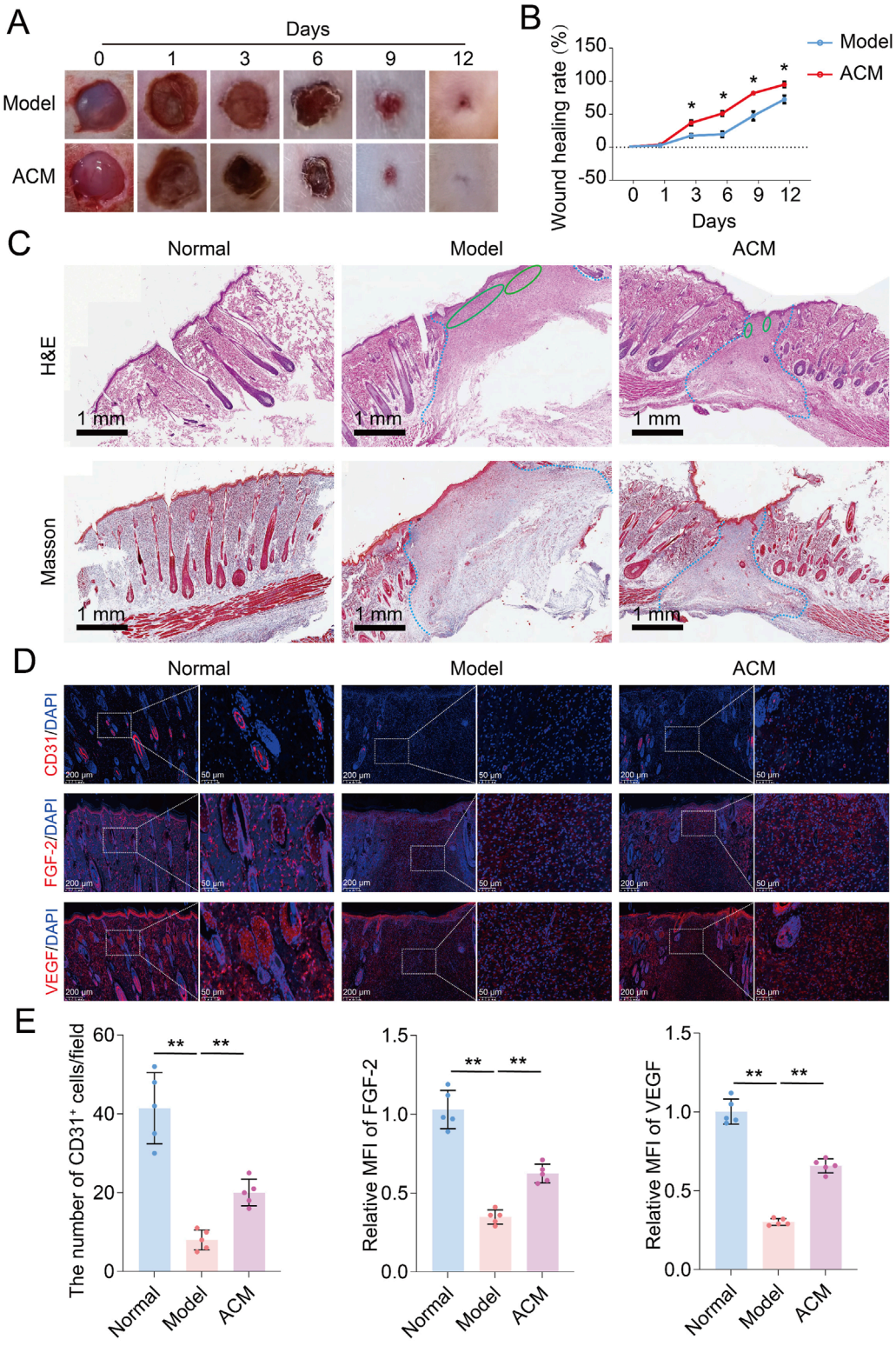

FIGURE 2
ACM accelerates T2D skin wound healing in rats. **(A)** General observation of skin wounds after ACM treatment. **(B)** Skin wound healing rate after ACM treatment. **(C)** Histopathological changes in skin wounds after ACM treatment by HE and Masson staining, respectively (scale bar, 1 mm). The area within the blue dotted line represents the damaged region. The green oval shape represents the area of inflammation. **(D)** Immunofluorescence expression of CD31, FGF-2, and VEGF in skin wounds after ACM treatment. Scale bar = 200 μm and 50 μm, respectively. **(E)** Number of $CD31^+$ cells and the relative MFI of FGF-2 and VEGF expression in skin wounds after ACM treatment.

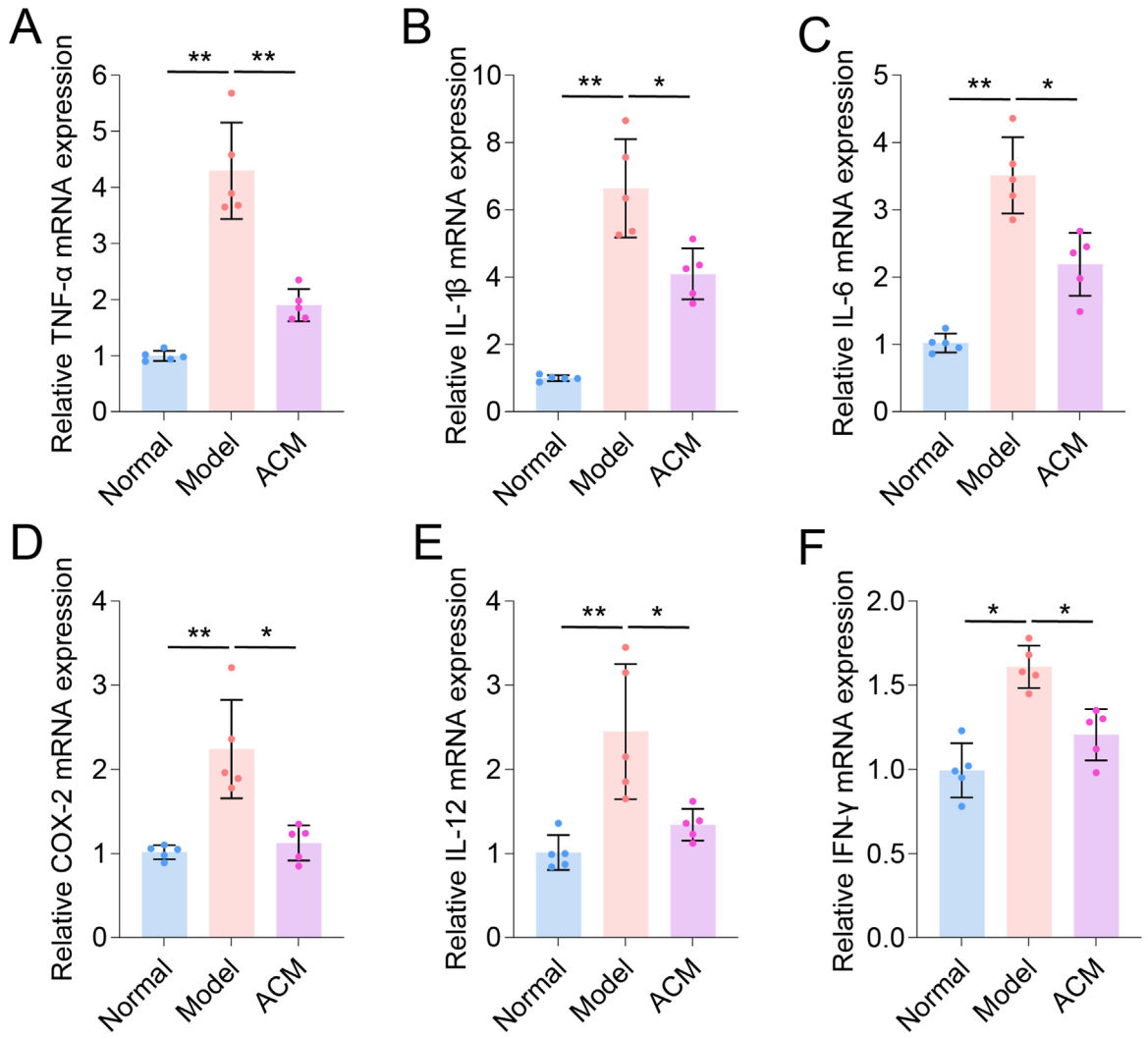

FIGURE 3
ACM inhibits the mRNA level of inflammatory factors in T2D skin wounds. The relative mRNA expression of TNF-α **(A)**, IL-1β **(B)**, IL-6 **(C)**, COX-2 **(D)**, IL-12 **(E)**, and IFN-γ **(F)** in skin wounds.

the effect of ACM on the angiogenesis and proliferation of vascular cells *in vitro*. After incubation with ACM for 24 or 48 h, the viability of HUVECs was significantly increased (Figure 1A), suggesting that ACM promoted HUVEC proliferation. After 2 days of continuous ACM incubation, HUVECs showed vascular-like morphological changes (Figure 1B), and the expression of genes associated with angiogenesis, including EGF, bFGF, VEGF, and KDR, was significantly upregulated after ACM treatment (Figure 1C), implying that ACM promotes HUVEC angiogenesis *in vitro*.

3.2 ACM accelerates T2D skin wound healing

Based on the pro-angiogenic potential of ACM in vascular cells, we established a T2D skin wound model to further evaluate its therapeutic effects. As shown in Figures 2A, B, the skin wound healing rate of T2D rats was significantly improved by the continuous ACM treatment for 7 days compared to that of the model group. Moreover, increased tissue regeneration and decreased inflammatory infiltration were also observed in the ACM group compared to those in the model group (Figure 2C). Given the excellent performance of ACM on angiogenesis *in vitro*, we also investigated the beneficial effect of ACM on angiopathy *in vivo*. We found that the number of $CD31^+$ cells and the expression of FGF-2 and VEGF were markedly increased in the ACM group compared to those in the model group (Figures 2D, E), suggesting that ACM could also improve angiopathy *in vivo*. Therefore, these data suggest that ACM accelerates T2D skin wound healing.

3.3 ACM inhibits T2D skin wound inflammation

Given that excessive inflammation is a typical characteristic of skin wounds (Huang et al., 2022), we further analyzed the inflammatory

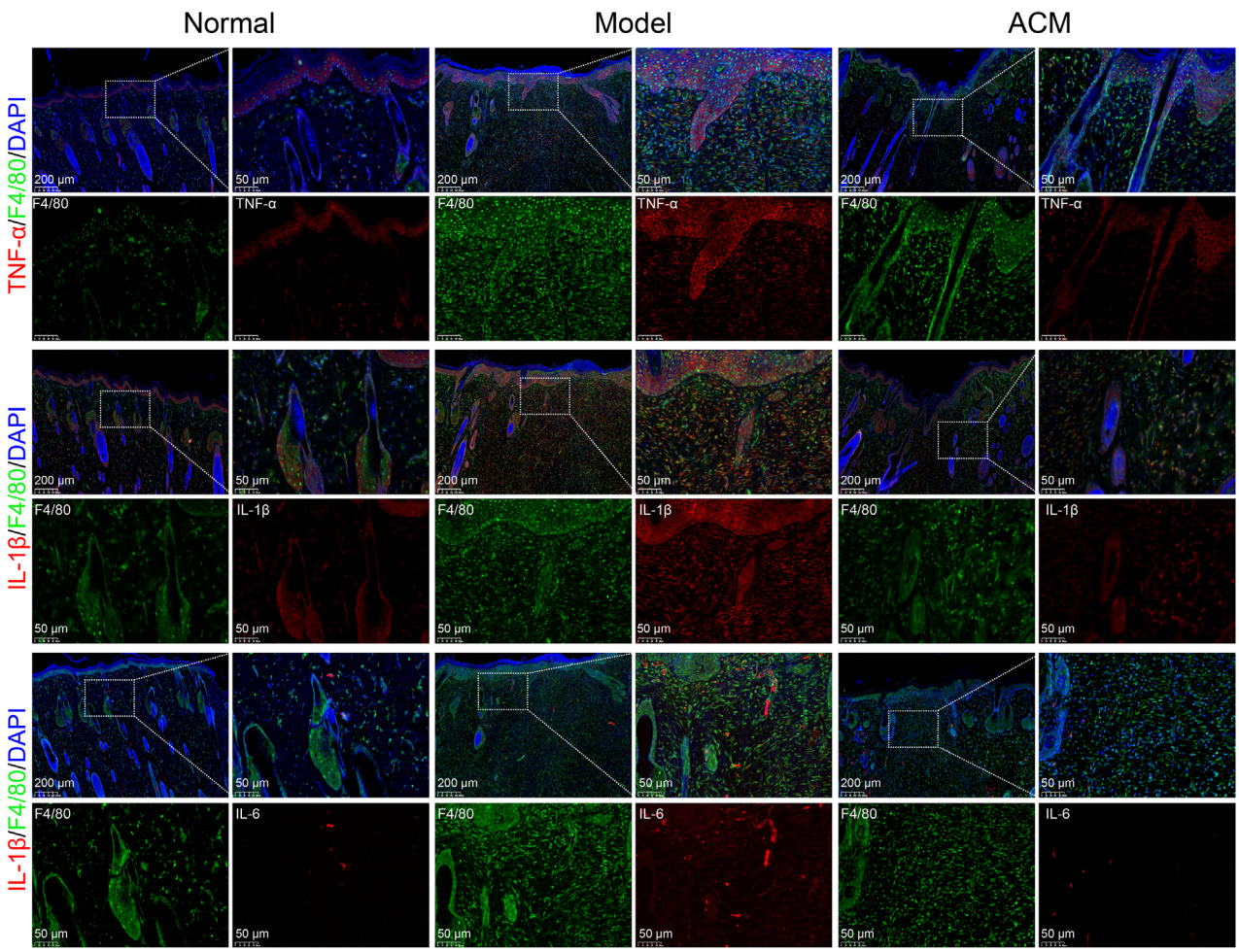

FIGURE 4
ACM inhibits the expression of inflammatory factors in macrophages. The immunofluorescence expression of TNF-α, IL-1β, and IL-6 in F4/80$^+$ macrophages in skin wounds after ACM treatment. Scale bar = 200 μm and 50 μm, respectively.

genes in T2D skin wound tissues. As shown in Figure 3, the mRNA expression levels of TNF-α, IL-1β, IL-6, COX-2, IL-12, and IFN-γ were significantly increased in T2D skin wounds compared to those in normal skin tissues, indicating excessive inflammation. However, these levels were effectively decreased after ACM treatment compared to those in the model groups, suggesting that ACM could inhibit this excessive inflammation. Moreover, we found that ACM treatment reduced inflammatory cell infiltration. This included a reduction in both the CD3$^+$ T cells and F4/80$^+$ macrophages (Supplementary Figure S3). Furthermore, the expression of TNF-α, IL-1β, and IL-6 was significantly decreased in the ACM-treated groups (Figure 4). Taken together, these data suggest that ACM mitigates the inflammatory response in skin wounds of diabetic rats.

3.4 ACM promotes T2D skin wound healing by targeting the TNF and chemokine signaling pathway

The potential molecular mechanism of ACM in accelerating T2D skin wound healing was further explored by RNA sequencing. Volcano plot analysis revealed differential expression of 10,655 genes was different between the normal and model groups (normal vs. model) and 5,287 genes between the ACM and model groups (ACM vs. model); a total of 4,269 genes were common to both comparisons (Figures 5A–C). GO annotation and pathway enrichment analysis showed that the upregulation of TNF and chemokine signaling was observed in the model group (compared with the normal group), while downregulation of TNF and chemokine signaling was clearly observed in the ACM group compared with the model groups (Figures 5D, E), suggesting that the potential molecular mechanism of ACM in T2D skin wound healing is by targeting the TNF and chemokine signaling pathway.

To confirm the RNA sequencing results, we further evaluated the protein expression of the main regulators in TNF and chemokine signaling. As shown in Figure 6, the TNF signaling-related proteins, including TNF-α, NF-κB, p-NF-κB, MAPK, and p-MAPK, and the chemokine signaling-related proteins, including CXCL1, CXCL2, and CXCL8, were all downregulated by ACM treatment in T2D skin wounds, suggesting that ACM accelerated T2D skin wound healing via the downregulation of TNF and chemokine signaling.

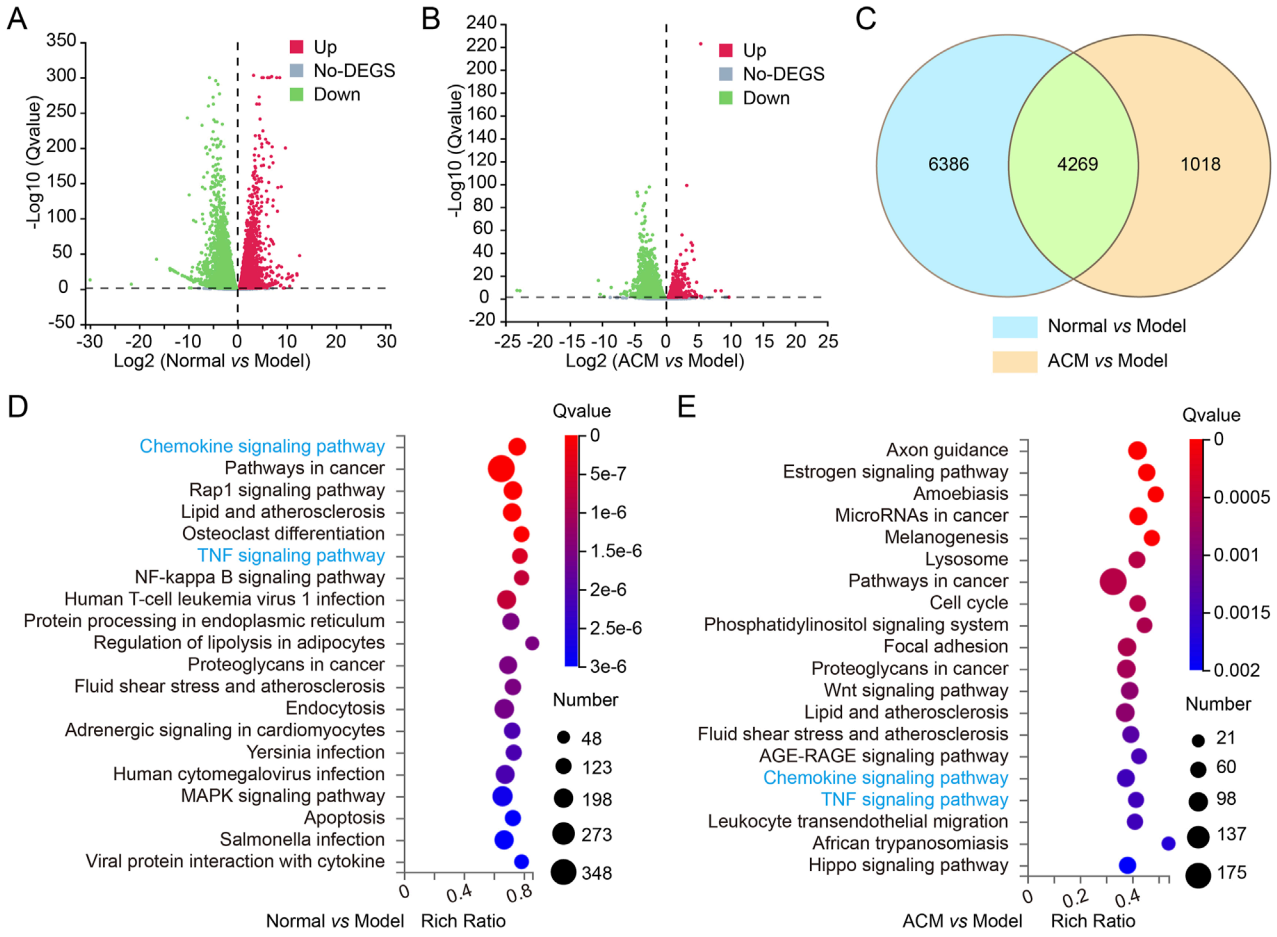

FIGURE 5
Transcriptome sequencing analysis of T2D skin wound tissues in rats. The volcano plot for differential gene expression of normal vs. model groups **(A)** and ADSC vs. model **(B)** groups. The gray pixel represents a gene where the difference in expression is not significant, while red and green pixels represent those that are significant. **(C)** Venn diagrams exhibiting the number of identified genes and the overlay of these identified genes. GO annotation and pathway enrichment analysis in normal vs. model groups **(D)** and ADSC vs. model **(E)** groups.

4 Discussion

Angiogenesis is an essential part of skin wound regeneration, and it is also prone to being impaired by the diabetes status (Fan et al., 2024), excessive inflammation (Guo et al., 2023), oxidative stress, and other chronic wound conditions (De Wolde et al., 2021). Given the excellent performance of MSCs in promoting vasculogenesis through paracrine factors (e.g., VEGF, EGF, and bFGF) (Guillamat-Prats, 2021), MSC secretome or conditioned medium provides a new strategy for accelerating angiogenesis of skin wounds (Hade et al., 2022). Adipose tissue-derived ACM was assessed in this study to confirm its beneficial effects on angiogenesis, owing to the abundant availability and easy accessibility of adipose tissues (Bunnell, 2021). As expected, ACM effectively promoted HUVEC proliferation and angiogenesis. In particular, ACM also upregulated the expression of VEGF, EGF, bFGF, and KDR in HUVECs. Therefore, these data suggest that ACM contributes to cutaneous wound regeneration.

Considering that T2D accounts for more than 90% of diabetes cases (Edlitz and Segal, 2022), a T2D skin wound injury rat model was used to assess the therapeutic effect of ACM on skin wounds. Significantly, we found that ACM could promote the skin wound healing rate. It is well-known that excessive inflammation is caused by the crosstalk of various immune cells, including neutrophils (Zhu et al., 2021), macrophages (Lv et al., 2023), and lymphocytes (Baltzis et al., 2014), which is also characterized by the high expression of various pro-inflammatory factors, including TNF-α, IL-1β, IL-6, COX-2, IL-12, and IFN-γ (Quagliariello et al., 2021; Acosta et al., 2008; Schürmann et al., 2014). In this study, we proved that these pro-inflammatory factors were highly expressed in skin wounds, which means that excessive inflammation occurred in T2D rats. More importantly, we found that ACM could reduce the excessive inflammation. In particular, the transcriptome sequencing data further confirmed that ACM-accelerated T2D skin wound healing is closely related to the downregulation of TNF and the chemokine signaling pathway. Taken together, ACM provides a new

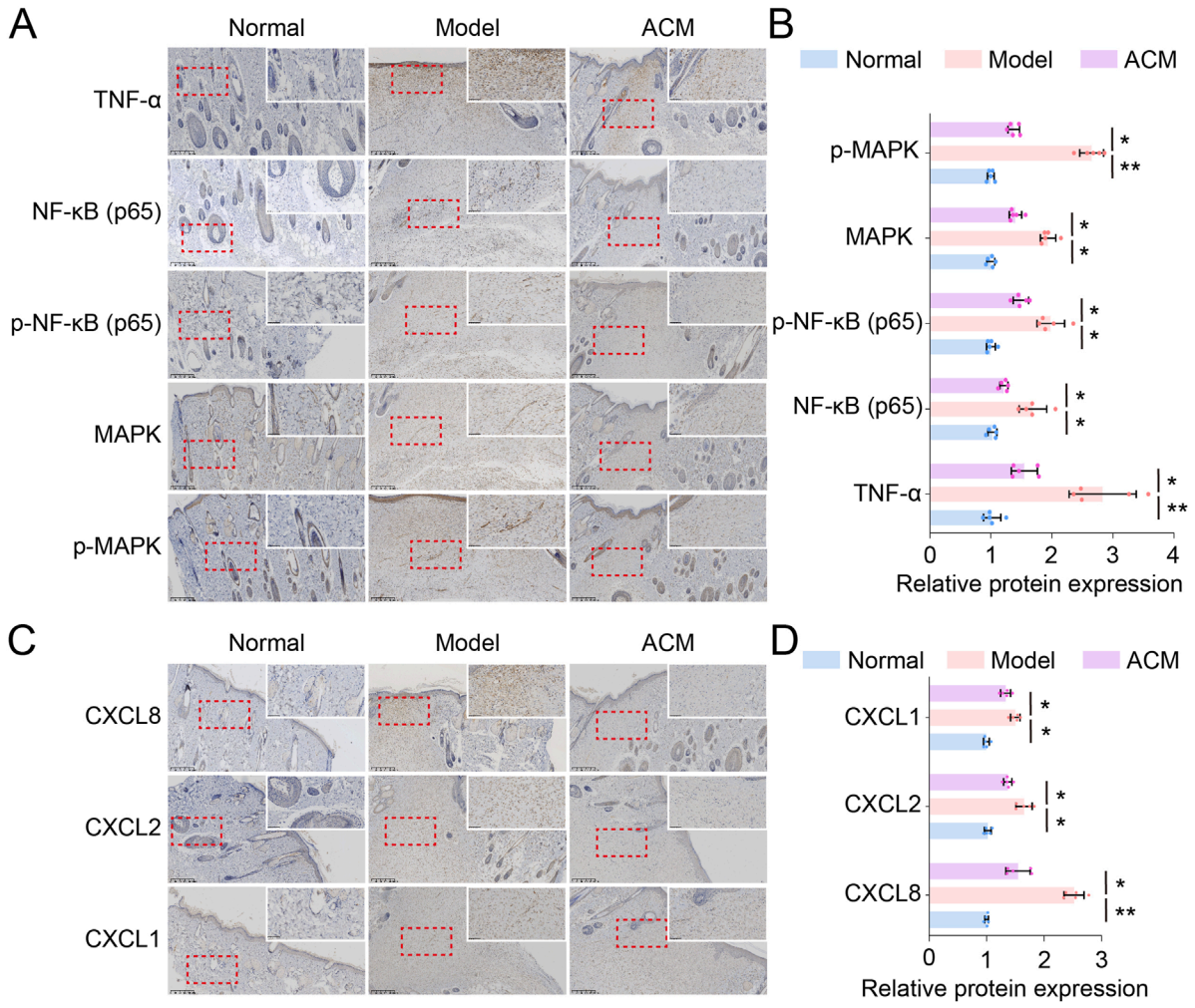

FIGURE 6
ACM downregulates TNF and chemokine signaling in T2D skin wound tissues. **(A)** Representative images of TNF-α, NF-κB, p-NF-κB, MAPK, and p-MAPK expression in skin tissues. Scale bars = 200 μm. **(B)** Relative expressions of TNF-α, NF-κB, p-NF-κB, MAPK, and p-MAP . **(C)** Representative images of CXCL1, CXCL2, and CXCL8 expression in skin tissues. Scale bars = 200 μm. **(D)** Relative expressions of CXCL1, CXCL2, and CXCL8.

promising strategy for accelerating T2D skin wound healing, which is partly through the TNF and chemokine signaling pathway.

It was previously shown that ADSC secretome reduces scar formation in skin wound healing (An et al., 2021) by inhibiting TGF-β1 and collagen expression (Wang et al., 2024). Paracrine cytokines and extracellular vesicles (e.g., exosomes) have been reported to be the major factors in the biological effects of ADSCs on wound healing (Wang et al., 2024). In this study, we further demonstrated that ACM accelerated diabetic skin wound healing through its anti-inflammatory functions. Given that MSC-conditioned medium or secretome has a complex composition, including extracellular vesicles (containing various types of lipids, proteins, and nucleic acids) and effector molecules (e.g., PGE2 and IDO) (Kota et al., 2017; Maughon et al., 2022; Zhao et al., 2023), the enhancement of ACM in skin wound regeneration may involve multiple targets and pathways. Further studies should focus on the different components and targets of ACM in the therapeutic role in T2D skin wound repair to verify more detailed mechanisms. Recently, Yin et al. reported that ADSC exosomes promote diabetic wound healing by regulating macrophage polarization (Yin and Shen, 2024) and epidermal autophagy (Ren et al., 2024). Therefore, exosomes of ACM would play a key role in accelerating diabetic wound healing. Furthermore, before proceeding with further clinical trials or applications, it is crucial to ensure strict control over the large-scale production, stability, and quality considerations related to ACM production.

In this study, we showed that ACM could enhance vascular proliferation and angiogenesis, promote skin wound healing in type 2 diabetes, and inhibit the inflammatory response. The mechanism may involve the downregulation of the TNF and chemokine pathways.

5 Conclusion

In conclusion, our study demonstrates that ACM can significantly accelerate the healing of diabetic skin wounds by

promoting vascular remodeling and suppressing inflammation through the TNF and chemokine pathways.

Data availability statement

The datasets presented in this study can be found in online repositories. The names of the repository/repositories and accession number(s) can be found in the article/Supplementary Material.

Ethics statement

The animal study was approved by the Animal Ethics Committee of Mengchao Hepatobiliary Hospital of Fujian Medical University. The study was conducted in accordance with the local legislation and institutional requirements.

Author contributions

LH: Funding acquisition, Investigation, Methodology, Validation, Visualization, Writing – original draft, Writing – review and editing. ZL: Investigation, Methodology, Visualization, Writing – review and editing. HL: Formal analysis, Resources, Writing – review and editing. XL: Methodology, Writing – review and editing. NL: Methodology, Supervision, Writing – review and editing. XW: Funding acquisition, Supervision, Writing – review and editing.

Funding

The author(s) declare that financial support was received for the research and/or publication of this article. This study was supported by the Scientific Foundation of Fujian Health Department (grant no. 2020QNB006), the Startup Fund for Scientific Research, Fujian Medical University (grant no. 2020QH1139), the Natural Science Foundation of Fujian Province (grant nos. 2024J011028 and 2024J011219), and the Natural Science Foundation of China (grant no. 82271238).

Conflict of interest

The authors declare that the research was conducted in the absence of any commercial or financial relationships that could be construed as a potential conflict of interest.

Generative AI statement

The author(s) declare that no Generative AI was used in the creation of this manuscript.

Any alternative text (alt text) provided alongside figures in this article has been generated by Frontiers with the support of artificial intelligence and reasonable efforts have been made to ensure accuracy, including review by the authors wherever possible. If you identify any issues, please contact us.

Publisher's note

Supplementary material

The Supplementary Material for this article can be found online at: https://www.frontiersin.org/articles/10.3389/fcell.2025.1659444/full#supplementary-material

References

Acosta, J. B., del Barco, D. G., Vera, D. C., Savigne, W., Lopez-Saura, P., Guillen Nieto, G., et al. (2008). The pro-inflammatory environment in recalcitrant diabetic foot wounds. *Int. Wound. J.* 5, 530–539. doi:10.1111/j.1742-481X.2008.00457.x

An, Y. H., Kim, D. H., Lee, E. J., Lee, D., Park, M. J., Ko, J., et al. (2021). High-efficient production of adipose-derived stem cell (ADSC) secretome through maturation process and its non-scarring wound healing applications. *Front. Bioeng. Biotechnol.* 9, 681501. doi:10.3389/fbioe.2021.681501

Baltzis, D., Eleftheriadou, I., and Veves, A. (2014). Pathogenesis and treatment of impaired wound healing in diabetes mellitus: new insights. *Adv. Ther.* 31, 817–836. doi:10.1007/s12325-014-0140-x

Bunnell, B. A. (2021). Adipose tissue-derived mesenchymal stem cells. *stem cells* 10, 3433. doi:10.3390/cells10123433

Carstens, M. H., Quintana, F. J., Calderwood, S. T., Sevilla, J. P., Ríos, A. B., Rivera, C. M., et al. (2021). Treatment of chronic diabetic foot ulcers with adipose-derived stromal vascular fraction cell injections: safety and evidence of efficacy at 1 year. *Stem Cells Transl. Med.* 10, 1138–1147. doi:10.1002/sctm.20-0497

De Souza, A., Santo, G. E., Amaral, G. O., Sousa, K. S. J., Parisi, J. R., Achilles, R. B., et al. (2023). Electrospun skin dressings for diabetic wound treatment: a systematic review. *J. Diabetes Metab. Disord.* 23, 49–71. doi:10.1007/s40200-023-01324-z

De Wolde, S. D., Hulskes, R. H., Weenink, R. P., Hollmann, M. W., and Van Hulst, R. A. (2021). The effects of hyperbaric oxygenation on oxidative stress, inflammation and angiogenesis. *Biomolecules* 11, 1210. doi:10.3390/biom11081210

Edlitz, Y., and Segal, E. (2022). Prediction of type 2 diabetes mellitus onset using logistic regression-based scorecards. *Elife* 11, e71862. doi:10.7554/eLife.71862

Fan, R., Zhao, J., Yi, L., Yuan, J., McCarthy, A., Li, B., et al. (2024). Anti-inflammatory peptide-conjugated silk fibroin/cryogel hybrid dual fiber scaffold with hierarchical structure promotes healing of chronic wounds. *Adv. Mat.* 36, e2307328. doi:10.1002/adma.202307328

Freedman, B. R., Hwang, C., Talbot, S., Hibler, B., Matoori, S., and Mooney, D. J. (2023). Breakthrough treatments for accelerated wound healing. *Sci. Adv.* 9, eade7007. doi:10.1126/sciadv.ade7007

Guillamat-Prats, R. (2021). The role of MSC in wound healing, scarring and regeneration. *Cells* 10, 1729. doi:10.3390/cells10071729

Guo, Y., Ma, M., Liu, Z., Lv, L., Pan, X., Liu, Q., et al. (2023). Chronic poor healing wounds of post cesarean scar diverticulum: altered angiogenesis and immunobiology. *J. Reprod. Immunol.* 157, 103929. doi:10.1016/j.jri.2023.103929

Hade, M. D., Suire, C. N., Mossell, J., and Suo, Z. (2022). Extracellular vesicles: emerging frontiers in wound healing. *Med. Res. Rev.* 42, 2102–2125. doi:10.1002/med.21918

Huang, C., Dong, L., Zhao, B., Lu, Y., Huang, S., Yuan, Z., et al. (2022). Anti-inflammatory hydrogel dressings and skin wound healing. *Clin. Transl. Med.* 12, e1094. doi:10.1002/ctm2.1094

Huerta, C. T., Voza, F. A., Ortiz, Y. Y., Liu, Z. J., and Velazquez, O. C. (2023). Mesenchymal stem cell-based therapy for non-healing wounds due to chronic limb-threatening ischemia: a review of preclinical and clinical studies. *Front. Cardiovasc. Med.* 10, 1113982. doi:10.3389/fcvm.2023.1113982

Hur, W., Lee, H. Y., Min, H. S., Wufuer, M., Lee, C. W., Hur, J. A., et al. (2017). Regeneration of full-thickness skin defects by differentiated adipose-derived stem cells into fibroblast-like cells by fibroblast-conditioned medium. *Stem Cell Res. Ther.* 8, 92. doi:10.1186/s13287-017-0520-7

Jin, W., Chen, X., Kong, L., and Huang, C. (2022). Gene therapy targeting inflammatory pericytes corrects angiopathy during diabetic wound healing. *Front. Immunol.* 13, 960925. doi:10.3389/fimmu.2022.960925

Kota, D. J., Prabhakara, K. S., Toledano-Furman, N., Bhattarai, D., Chen, Q., DiCarlo, B., et al. (2017). Prostaglandin E2 indicates therapeutic efficacy of mesenchymal stem cells in experimental traumatic brain injury. *Stem Cells* 35, 1416–1430. doi:10.1002/stem.2603

Liao, N., Zheng, Y., Xie, H., Zhao, B., Zeng, Y., Liu, X., et al. (2017). Adipose tissue-derived stem cells ameliorate hyperglycemia, insulin resistance and liver fibrosis in the type 2 diabetic rats. *Stem Cell Res. Ther.* 8, 286. doi:10.1186/s13287-017-0743-7

Lin, Z., Shibuya, Y., Imai, Y., Oshima, J., Sasaki, M., Sasaki, K., et al. (2023). Therapeutic potential of adipose-derived stem cell-conditioned medium and extracellular vesicles in an *in vitro* radiation-induced skin injury model. *Int. J. Mol. Sci.* 24, 17214. doi:10.3390/ijms242417214

Lv, D., Cao, X., Zhong, L., Dong, Y., Xu, Z., Rong, Y., et al. (2023). Targeting phenylpyruvate restrains excessive NLRP3 inflammasome activation and pathological inflammation in diabetic wound healing. *Cell Rep. Med.* 4, 101129. doi:10.1016/j.xcrm.2023.101129

Ma, H., Siu, W. S., and Leung, P. C. (2023). The potential of MSC-Based cell-free therapy in wound healing-a thorough literature review. *Int. J. Mol. Sci.* 24, 9356. doi:10.3390/ijms24119356

Martin, P., and Nunan, R. (2015). Cellular and molecular mechanisms of repair in acute and chronic wound healing. *Br. J. Dermatol.* 173, 370–378. doi:10.1111/bjd.13954

Maughon, T. S., Shen, X., Huang, D., Michael, A. O. A., Shockey, W. A., Andrews, S. H., et al. (2022). Metabolomics and cytokine profiling of mesenchymal stromal cells identify markers predictive of T-cell suppression. *Cytotherapy* 24, 137–148. doi:10.1016/j.jcyt.2021.08.002

Quagliariello, V., De Laurentiis, M., Rea, D., Barbieri, A., Monti, M. G., Carbone, A., et al. (2021). The SGLT-2 inhibitor empagliflozin improves myocardial strain, reduces cardiac fibrosis and pro-inflammatory cytokines in non-diabetic mice treated with doxorubicin. *Cardiovasc. Diabetol.* 20, 150. doi:10.1186/s12933-021-01346-y

Ren, H., Su, P., Zhao, F., Zhang, Q., Huang, X., He, C., et al. (2024). Adipose mesenchymal stem cell-derived exosomes promote skin wound healing in diabetic mice by regulating epidermal autophagy. *Burns Trauma* 12, tkae001. doi:10.1093/burnst/tkae001

Roux, S., Marchès, A., Galiacy, S., Merbahi, N., and Simon, M. (2025). Biological solutions activated by cold plasma at atmospheric pressure: a new therapeutic approach for skin wound healing. *Biomed. Pharmacother.* 186, 118001. doi:10.1016/j.biopha.2025.118001

Schürmann, C., Goren, I., Linke, A., Pfeilschifter, J., and Frank, S. (2014). Deregulated unfolded protein response in chronic wounds of diabetic Ob/ob mice: a potential connection to inflammatory and angiogenic disorders in diabetes-impaired wound healing. *Biochem. Biophys. Res. Commun.* 446, 195–200. doi:10.1016/j.bbrc.2014.02.085

Wang, K., Yang, Z., Zhang, B., Gong, S., and Wu, Y. (2024). Adipose-derived stem cell exosomes facilitate diabetic wound healing: mechanisms and potential applications. *Int. J. Nanomedicine.* 19, 6015–6033. doi:10.2147/IJN.S466034

Wang, M., Zhao, J., Li, J., Meng, M., and Zhu, M. (2024). Insights into the role of adipose-derived stem cells and secretome: potential biology and clinical applications in hypertrophic scarring. *Stem Cell Res. Ther.* 15, 137. doi:10.1186/s13287-024-03749-6

Wei, J. T., He, T., Shen, K., Xu, Z. G., Han, J. T., and Yang, X. K. (2024). Adipose stem cell-derived exosomes in the treatment of wound healing in preclinical animal models: a meta-analysis. *Burns Trauma* 12, tkae025. doi:10.1093/burnst/tkae025

Yan, D., Song, Y., Zhang, B., Cao, G., Zhou, H., Li, H., et al. (2024). Progress and application of adipose-derived stem cells in the treatment of diabetes and its complications. *Stem Cell Res. Ther.* 15, 3. doi:10.1186/s13287-023-03620-0

Yin, D., and Shen, G. (2024). Exosomes from adipose-derived stem cells regulate macrophage polarization and accelerate diabetic wound healing *via* the circ-Rps5/miR-124-3p axis. *Immun. Inflamm. Dis.* 12, e1274. doi:10.1002/iid3.1274

Yu, S., Yu, S., Liu, H., Liao, N., and Liu, X. (2023). Enhancing mesenchymal stem cell survival and homing capability to improve cell engraftment efficacy for liver diseases. *Stem Cell Res. Ther.* 14, 235. doi:10.1186/s13287-023-03476-4

Zhang, C., Wang, T., Zhang, L., Chen, P., Tang, S., Chen, A., et al. (2021). Combination of lyophilized adipose-derived stem cell concentrated conditioned medium and polysaccharide hydrogel in the inhibition of hypertrophic scarring. *Stem Cell Res. Ther.* 12, 23. doi:10.1186/s13287-020-02061-3

Zhao, H., Li, Z., Wang, Y., Zhou, K., Li, H., Bi, S., et al. (2023). Bioengineered MSC-derived exosomes in skin wound repair and regeneration. *Front. Cell Dev. Biol.* 11, 1029671. doi:10.3389/fcell.2023.1029671

Zhu, S., Yu, Y., Ren, Y., Xu, L., Wang, H., Ling, X., et al. (2021). The emerging roles of neutrophil extracellular traps in wound healing. *Dis* 12, 984. doi:10.1038/s41419-021-04294-3

frontiers | Frontiers in Cell and Developmental Biology

TYPE Original Research
PUBLISHED 23 October 2025
DOI 10.3389/fcell.2025.1655408

OPEN ACCESS

EDITED BY
Mustapha Najimi,
Institute of Experimental and Clinical Research- UCLouvain, Belgium

REVIEWED BY
Ahmet Emin Topal,
Bahçeşehir University, Türkiye
Najib Al Idrissi,
Mohammed VI University of Health Sciences, Morocco

*CORRESPONDENCE
Ming Pei,
mpei@hsc.wvu.edu
Chaoliang Lv,
lvchaolianggk@163.com
† ORCID: Ying Zhang, orcid.org/0009-0007-4884-2927

RECEIVED 27 June 2025
ACCEPTED 30 September 2025
PUBLISHED 23 October 2025

CITATION
Zhang Y, Pei M and Lv C (2025) Distinct effect of preconditioning with p38 MAPK signals on matrix-expanded human synovium-derived stem cell chondrogenesis: sb203580 favors chondrogenic differentiation while anisomycin benefits endochondral bone formation.
Front. Cell Dev. Biol. 13:1655408.
doi: 10.3389/fcell.2025.1655408

Distinct effect of preconditioning with p38 MAPK signals on matrix-expanded human synovium-derived stem cell chondrogenesis: sb203580 favors chondrogenic differentiation while anisomycin benefits endochondral bone formation

Ying Zhang [1,2,3], Ming Pei[3,4]* and Chaoliang Lv[2]*

[1]Jinfeng Laboratory, Chongqing, China, [2]Department of Spine Surgery, Jining NO.1 People's Hospital Affiliated to Shandong First Medical University & Shandong Academy of Medical Sciences, Jining, China, [3]Stem Cell and Tissue Engineering Laboratory, Department of Orthopaedics, West Virginia University, Morgantown, WV, United States, [4]WVU Cancer Institute, Robert C. Byrd Health Sciences Center, West Virginia University, Morgantown, WV, United States

Introduction: Cartilage defects are often accompanied by inflammation, presenting a major challenge in clinical treatment. Adult stem cells offer a promising approach for cartilage regeneration; however, *in vitro* expansion leads to replicative senescence, hindering their application. Our previous studies have demonstrated that decellularized extracellular matrix (dECM) can serve as an *in vitro* "microenvironment" to promote stem cell expansion and chondrogenic potential. In this study, we hypothesized that pretreatment with p38 mitogen-activated protein kinase (MAPK), a key pathway driving inflammation, would impair chondrogenesis in dECM-expanded adult stem cells.
Methods: Human synovium-derived stem cells (SDSCs) were expanded for one passage on either dECM or plastic culture flasks and pretreated with p38 MAPK, followed by chondrogenic or osteogenic induction.
Results: We found that pretreatment with sb203580, a p38 MAPK inhibitor, enhanced chondrogenic differentiation of dECM-expanded SDSCs, whereas pretreatment with anisomycin, a p38 MAPK activator, favored both chondrogenic hypertrophy and osteogenic differentiation of dECM-expanded SDSCs. In SDSC pretreatment, p38 MAPK significantly upregulated the non-canonical Wnt signaling pathway during dECM expansion and chondrogenic induction. The significant upregulation of Wnt5a induced by anisomycin combined with dECM expansion may indicate the highest osteogenic potential; SDSC pretreatment with sb203580 combined with dECM expansion exhibited the strongest chondrogenic differentiation and the highest levels of Wnt11.

Discussion: This study suggests that p38 MAPK pretreatment may play a key role in dECM-expanded tissue-specific stem cell-mediated cartilage regeneration. Further verification of Wnt-related regenerative mechanisms remains to be determined.

KEYWORDS

extracellular matrix, p38 MAPK signal, mesenchymal stem cell, chondrogenic potential, non-canonical wnt signal

Introduction

Cartilage defects do not readily heal spontaneously due to a lack of blood supply. Although adult stem cells are a promising cell source for cartilage regeneration (Toh et al., 2014), *in vitro* expansion, a necessary step prior to *in vivo* application, remains a major challenge for adult stem cells to survive replicative senescence (Li and Pei, 2012). Accumulating evidence suggests that expansion on decellularized extracellular matrix (dECM), a microenvironment resembling an *in vivo* "niche", is an effective method for rejuvenating adult stem cells in terms of proliferation and chondrogenic potential (Pei, 2017). The effects of dECM preconditioning on tissue-specific stem cell cartilage regeneration have also been demonstrated *in vivo* (Pei et al., 2013a; Pei et al., 2022).

Because post-traumatic joint inflammation is often accompanied by cartilage defects, inflammation may contribute to the reduced efficacy of dECM for adult SDSCs, hindering dECM-mediated cell rejuvenation (Pei et al., 2013a; Yan et al., 2020; Zhang et al., 2015). Fortunately, p38 mitogen-activated protein kinase (MAPK) has been shown to play an important role in stress and inflammatory signals, although it was originally considered a mediator of growth and development (Joos et al., 2009; Long and Loeser, 2010). p38 MAPK has been identified as a major signaling pathway activated by degradative cytokines such as interleukin 1beta (IL-1β) and tumor necrosis factor alpha (TNFα) (Martel-Pelletier et al., 1999; Sondergaard et al., 2010). Furthermore, it has been reported that basal levels of p38 phosphorylation were reduced in osteoarthritic chondrocytes compared with normal chondrocytes, while p38 MAPK inhibitors upregulated the expression of chondrogenic and hypertrophic genes in normal rat chondrocytes (Prasadam et al., 2012).

p38 MAPK inhibitors are used to treat cartilage defects to suppress inflammation; however, the p38 MAPK inhibitor also blocks chondrogenesis (Oh et al., 2000). To exploit their anti-inflammatory effect and limit their inhibitory effects on cartilage regeneration, this study evaluated the potential effects of p38 MAPK inhibitors or activators on chondrogenesis during SDSC pretreatment and cell expansion. Given the interplay between MAPK and Wnt signaling during cartilage regeneration (Zhang et al., 2014), we investigated whether Wnt signaling is also actively involved in the enhanced chondrogenic differentiation of SDSCs following pretreatment with p38 MAPK inhibitors or activators combined with dECM expansion.

Materials and methods

SDSC culture

Adult human SDSCs were purchased from Asterand (North America Laboratories, Detroit, MI) (Pei et al., 2013b) and isolated from four donors: two men and two women with a mean age of 43 years and no known joint diseases. These SDSCs were cultured in growth medium consisting of αMEM (alpha minimum essential medium) supplemented with 10% FBS (fetal bovine serum), 100 U/mL penicillin, 100 μg/mL streptomycin, and 0.25 μg/mL fungizone (Invitrogen, Carlsbad, CA). Cultures were maintained in a humidified incubator at 37 °C with 5% CO_2, and the growth medium was changed every 3 days.

dECM preparation

The preparation of dECM has been described previously (Li and Pei, 2018). Briefly, Plastic (tissue culture plastic) was pre-coated with 0.2% gelatin (MilliporeSigma, Burlington, MA) and incubated at 37 °C for 1 h, followed by fixation with 1% glutaraldehyde and treatment with 1M ethanolamine. P3 (passage 3) SDSCs were seeded at a density of 6,000 cells/cm^2 and cultured to 90% confluence. Growth medium was supplemented with 250 μM L-ascorbic acid phosphate (Wako Chemicals United States, Inc., Richmond, VA) and cultured for 8 days. The deposited matrix was treated with 0.5% Triton X-100 containing 20 mM ammonium hydroxide at 37 °C for 5 min to remove cells and then stored in PBS (phosphate-buffered saline) containing 100 U/mL penicillin, 100 μg/mL streptomycin, and 0.25 μg/mL fungizone at 4 °C.

Morphological characterization of dECM with or without SDSCs

After post-fixation in 2.5% glutaraldehyde (MilliporeSigma) for 2 hrs, representative samples (n = 2) were re-post-fixed in 2% osmium tetroxide (MilliporeSigma) for 2 hrs. Samples were dehydrated using a graded ethanol series and then treated twice with HMDS (hexamethyldisilazane) (MilliporeSigma) mixed with ethanol at a 1:1 ratio for 1 hour each, followed by overnight treatment with HMDS at a 1:2 ratio with ethanol, and finally three times with HMDS for 4 hrs each. After air-drying for 24-h, samples were gold-sputtered. Images were captured using a scanning electron microscope (SEM) (Hitachi, Model S 2400).

Global gene expression by microarrays and data analyses

P3 SDSCs were expanded for one passage on dECM or Plastic and then induced into chondrogenic tissue for 21 days in a pellet culture system (designated as Ep and Pp, respectively). Total RNA was purified from the expanded cells and 21-day pellets using TRIzol (Invitrogen) and further purified using the RNeasy Mini Kit (Qiagen, Valencia, CA) according to the manufacturer's instructions. The specified amount of cDNA (5.5 μg) was then fragmented and biotinylated using the GeneChip® WT Terminal Labeling Kit (Affymetrix, Santa Clara, CA). This entire reaction mixture, containing 50 μL of fragmented biotinylated cDNA and hybridization controls, was hybridized to a Human GeneChip® 1.0 ST Exon Arrays (Affymetrix) in a GeneChip® 640 Hybridization Chamber (Affymetrix) at 45 °C for 17 h. Parameters such as the scale factor, background noise, and percent presence were calculated according to the manufacturer's instructions (Affymetrix). The resulting raw data were then uploaded to GeneSpring (Agilent, Santa Clara, CA) and Partek (St. Louis, MO) software for preliminary analysis. Pathway and functional analysis was performed using Ingenuity Pathway Analysis (IPA, Redwood City, CA). Briefly, raw intensity values were adjusted by background subtraction, then normalized by robust multiarray analysis (RMA), log-transformed, and fold-changes assessed. All batch effects related to scan date were eliminated before fold-change calculation.

SDSC expansion and p38 MAPK pretreatment

P3 SDSCs were seeded at a density of 3,000 cells/cm^2 on two substrates (dECM and Plastic) for one passage. To investigate the effects of p38 MAPK on the expanded cells, 10 μM sb203580 (a p38 MAPK inhibitor, LC Laboratories, Woburn, MA) or 1 μM anisomycin (a p38 MAPK activator, also from LC Laboratories) was added 48 h after seeding and maintained throughout the culture period. Groups not treated with p38 MAPK served as controls. The experimental design included six groups: dECM expansion group (denoted as Econ), dECM expansion combined with sb203580 group (denoted as Esb), dECM expansion combined with anisomycin group (denoted as Ean), Plastic expansion alone (Pcon), Plastic expansion combined with sb203580 group (denoted as Psb), and Plastic expansion combined with anisomycin group (denoted as Pan). Cell counts were performed using a hemocytometer to determine the cell number in each group.

Chondrogenic induction of expanded SDSCs

0.3 × 10^6 SDSCs from each group were placed in a 15-mL polypropylene tube and centrifuged at 500 *g* for 5 min to form a pellet. The pellet was incubated overnight in growth medium and then cultured in serum-free chondrogenic medium for 35 days. This medium consisted of high-glucose DMEM (Dulbecco's Modified Eagle's Medium) supplemented with 40 μg/mL proline, 100 nM dexamethasone, 100 U/mL penicillin, 100 μg/mL streptomycin, 0.1 mM ascorbic acid-2-phosphate, and 1×ITS™ Premix (BD Biosciences, San Jose, CA). In addition, 10 ng/mL TGF-β3 (transforming growth factor beta 3) (PeproTech Inc., Rocky Hill, NJ) was added. Chondrogenic differentiation was assessed at 14 and 35 days by histology, immunostaining, biochemical analysis, and real-time qPCR (quantitative polymerase chain reaction).

For histological analysis, representative pellets (n = 3) were fixed with 4% paraformaldehyde overnight at 4 °C and then dehydrated using a graded ethanol series. Samples were cleared with xylene and embedded in paraffin blocks. Histochemical staining of 5-μm-thick sections was performed using Alcian blue (MilliporeSigma) and counterstained with Fast Red to visualize sulfated glycosaminoglycan (sGAG). For immunohistochemistry (IHC) analysis, sections were labeled with primary antibodies against type II collagen (II-II6B3; Developmental Studies Hybridoma Bank, Iowa City, IA), type I collagen (GeneTex Inc., Irvine, CA), type X collagen (MilliporeSigma), and matrix metalloproteinase 13 (MMP13) (VIIIA2, Abcam, Cambridge, MA). A biotinylated horse anti-mouse IgG secondary antibody (Vector, Burlingame, CA) was then applied, and immunoactivity was visualized using Vectastain ABC reagent (Vector) with 3,3′-diaminobenzidine as a substrate.

For biochemical quantification, another representative set of pellets (n = 4) was digested in PBE buffer (100 mM phosphate and 10 mM ethylenediaminetetraacetic acid, pH 6.5) containing 125 μg/mL papain and 10 mM cysteine for 4 hours at 60 °C, using 200 μL of enzyme per sample. DNA concentration in the papain digests was quantified using the Quant-iT™ PicoGreen™ dsDNA Assay kit (Invitrogen) using a CytoFluor® 4000 Series (Applied Biosystems, Foster City, CA). GAG levels were measured using a Spectronic BioMate 3 Spectrophotometer (ThermoFisher Scientific, Milford, MA) using dimethylmethylene blue dye and bovine chondroitin sulfate as a standard.

For qPCR analysis, total RNA from another set of pellets (n = 4) was extracted in TRIzol® (Invitrogen) using an RNase-free pestle. Approximately 1 μg of RNA was reverse transcribed using the High Capacity cDNA Archive Kit (Applied Biosystems) at 37 °C for 120 min. Custom genes included chondrogenic marker genes such as *COL2A1* (type II collagen; assay ID: Hs00156568_m1), *ACAN* (aggrecan; assay ID: Hs00153935_m1), and *SOX9* [SRY (sex determining region Y)-box 9; assay ID: Hs00165814_m1), as well as hypertrophic marker genes *COL10A1* (type X collagen; assay ID: H200166657_m1) and *MMP13* (assay ID: Hs00233992_m1). The endogenous control gene was eukaryotic *18S RNA* (assay ID: Hs99999901_s1). Real-time qPCR was performed using the iCycler iQ™ Multicolor Real-Time PCR Detection System (Perkin-Elmer, Waltham, MA). Relative transcript levels were calculated using the formula $\chi = 2^{-\Delta\Delta Ct}$, where $\Delta\Delta Ct = \Delta E - \Delta C$, $\Delta E = Ct_{exp} - Ct_{18s}$, and $\Delta C = Ct_{ct1} - Ct_{18s}$.

Western blot

To investigate the potential effects of dECM expansion combined with p38 MAPK on cell proliferation and chondrogenic differentiation through Wnt signaling, we homogenized expanded cells and chondrogenically differentiated pellets from each group. These samples were dissolved in lysis buffer supplemented with

protease inhibitors (Cell Signaling, Danvers, MA). Total protein concentration was then measured using a BCA™ Protein Assay Kit (ThermoFisher Scientific).

For subsequent analysis, 30 μg of protein from each sample was denatured, separated by gel electrophoresis, and transferred to a nitrocellulose membrane (Invitrogen). The membrane was incubated with primary monoclonal antibodies diluted in 5% bovine serum albumin, 1× TBS (10 mM Tris-HCl, 150 mM NaCl, pH 7.5), and 0.05% Tween-20 for 1 h at room temperature. A horseradish peroxidase-conjugated goat anti-mouse secondary antibody (ThermoFisher Scientific) was then added and incubated for 1 h. Blots were exposed using SuperSignal West Femto Maximum Sensitivity Substrate and CL-X exposure film (ThermoFisher Scientific). Primary antibodies used in immunoblotting included Wnt3a, Wnt5a, and Wnt11 (ThermoFisher Scientific) and β-actin (Cell Signaling).

Osteogenic induction of expanded SDSCs

Expanded SDSCs (n = 3) were reseeded at a density of 8,000 cells per cm^2. When the cultures reached 90% confluence, the medium was changed to an osteogenic induction medium, consisting of growth medium supplemented with 0.01 μM dexamethasone, 10 mM β-glycerophosphate, 50 μM ascorbate-2-phosphate, and 0.01 μM 1,25-dihydroxyvitamin D3. Induction culture continued for 21 days.

To assess osteogenic differentiation, ALP (alkaline phosphatase) activity was measured using a kit (MilliporeSigma). To assess calcium deposition, induced cells (n = 3) were fixed with 70% ice-cold ethanol for 1 h and then incubated in 40 mM Alizarin Red S (ARS), pH 4.2, for 20 min with agitation. After rinsing twice with deionized water, matrix mineral-binding staining was documented using a Nikon TE300 phase-contrast microscope (Nikon, Japan). Total ALP and calcium accumulation was analyzed using NIH ImageJ software (U.S. National Institutes of Health, Bethesda, MD).

Statistics

Numerical data are presented as the mean and standard error. Pairwise comparisons in biochemical and real-time qPCR data analysis were performed using the Mann-Whitney U test. All statistical analyses were performed using SPSS 13.0 statistical software (SPSS Inc., Chicago, IL). A *p*-value of less than 0.05 was considered statistically significant.

Results

dECM-expanded SDSCs and chondrogenic potential

SEM data (Figure 1A) showed that SDSCs expanded on dECM had a small, fibroblast-like shape, while those grown on Plastic had a flat, broad shape. To determine whether SDSCs expanded on dECM possessed enhanced chondrogenic potential, we induced chondrogenesis in a pellet culture system. Histology data (Figure 1B) revealed that pellets of SDSCs expanded on dECM were not only larger in size but also stained more intensely for sGAG and type II collagen, two typical cartilage markers. Microarray data (Figure 1C) showed that compared to Plastic-expanded cells, dECM-expanded SDSCs showed upregulation of chondrogenic markers [*HAPLN1* (hyaluronan and proteoglycan link protein 1), *ACAN*, *COL2A1*, *COL9A1* (type IX collagen), and *COL11A1* (type XI collagen)]. Notably, dECM-expanded chondrogenically induced SDSCs exhibited upregulation of these chondrogenic markers, consistent with histology data (Figure 1B). Interestingly, the chondrogenic transcription factor SOX9 remained upregulated during both the dECM expansion period and the subsequent chondrogenic induction period (Figure 1C). These microarray data were also confirmed by real-time qPCR analysis of *SOX9*, *ACAN*, and *COL2A1* expression in chondrogenically induced SDSCs (Figure 1D).

Effect of dECM pretreatment on wnt signaling during sdsc expansion and subsequent chondrogenic induction

To determine the involvement of Wnt signaling in dECM expansion, we used microarray to analyze canonical and non-canonical Wnt signaling in SDSCs expanded on dECM and Plastic, and during subsequent chondrogenic induction. In Figure 2A, SDSCs expanded on dECM showed slight downregulation of the canonical Wnt signaling antagonist *DKK1* [dickkopf 1 homolog (*Xenopus laevis*)] and slight upregulation of the Wnt signaling pathway activator *CTNNB1* (cadherin-associated protein beta 1), suggesting that canonical Wnt signaling may be enhanced during dECM-mediated cell expansion. However, microarray data did not detect a fold change in *WNT3A* (a typical canonical Wnt signaling ligand) after SDSC expansion on dECM (but not on Plastic), despite a dramatic decrease in dECM-expanded chondrogenically induced SDSCs, as confirmed by Western blotting data (Figure 2B). Notably, dECM expansion upregulated *WNT5A* and *WNT11*, as well as *NFATC2* (nuclear factor of activated T-cells, cytoplasmic, calcineurin-dependent 2) and *CAMK2A* (calcium/calmodulin-dependent protein kinase type II alpha chain) in expanded and chondrogenically induced SDSCs (Figure 2C). This finding indicates that non-canonical Wnt signaling may be involved in dECM-mediated SDSC rejuvenation in terms of cell proliferation and chondrogenic potential, as confirmed by Western blotting data (Figure 2D).

Pretreatment with p38 MAPK inhibitor enhanced the chondrogenic potential of SDSCs, while p38 MAPK activator promoted chondrogenic hypertrophy, particularly in SDSCs expanded on dECM

To determine whether pretreatment with p38 MAPK inhibitor plays a role in SDSC expansion and chondrogenic potential, 10 μM sb203580 was added to the culture medium of SDSCs expanded on Plastic or dECM; 1 μM anisomycin (an activator of p38 MAPK) was also added as a control. Although dECM

10.3389/fcell.2025.1655408

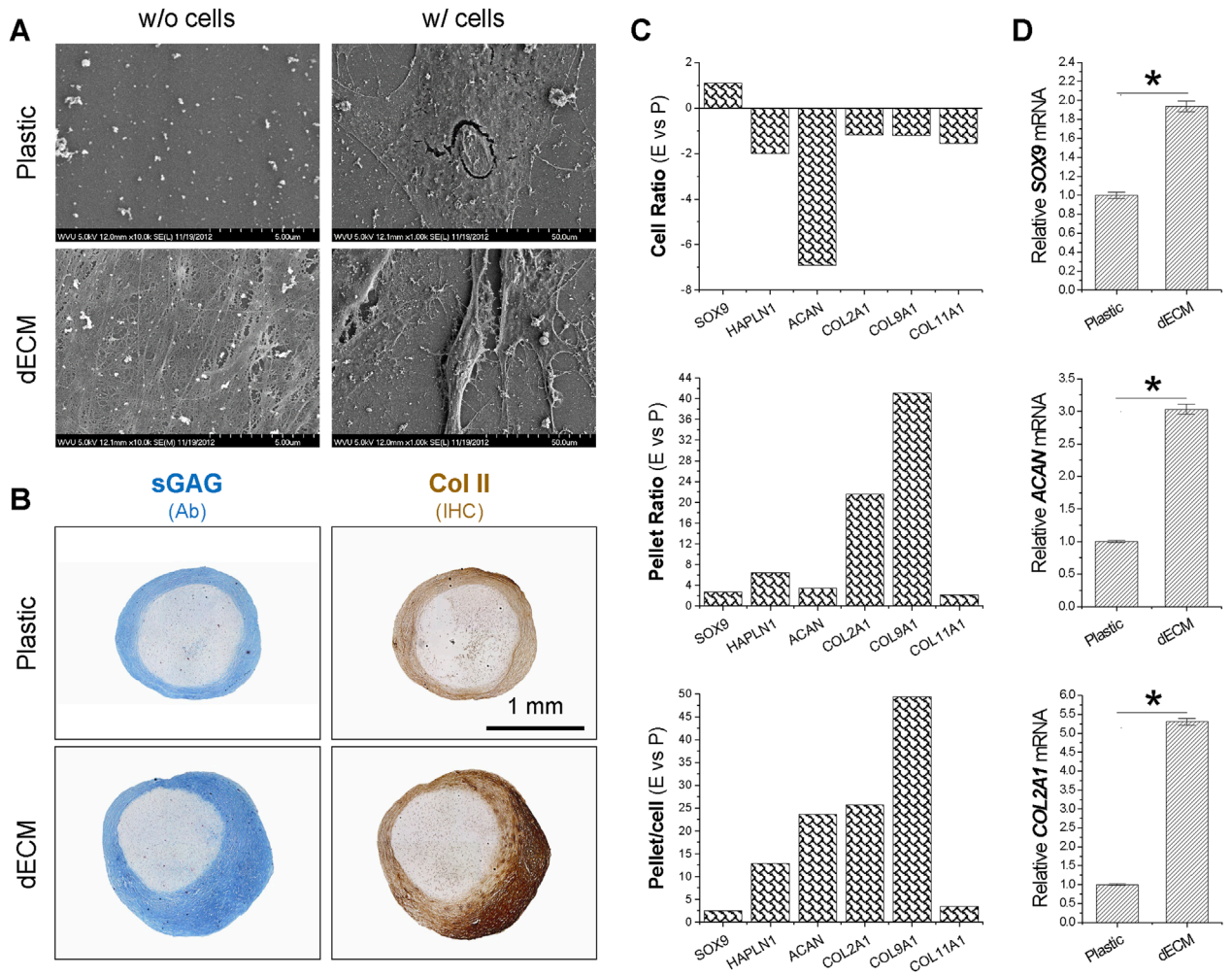

FIGURE 1
Effects of dECM pretreatment on the chondrogenic potential of SDSCs. Human SDSCs were expanded for one passage on dECM or Plastic and then induced to form chondrocytes. **(A)** SEM was used to evaluate culture substrates (dECM versus Plastic) (w/o cells) and SDSCs expanded on culture substrates (w/cells). **(B)** Alcian blue (Ab) was used to stain sulfated GAG (sGAG) and immunohistochemistry (IHC) was for staining of type II collagen (Col II). Scale bar = 1 mm. **(C)** Microarray was used to measure fold changes in cartilage marker genes during cell expansion (cell ratio) and chondrogenic differentiation (pellet ratio) in SDSCs expanded on dECM versus Plastic (E vs. P). **(D)** Real-time qPCR was used to confirm changes in representative cartilage marker genes in SDSCs induced by chondrogenic medium after expansion on dECM. Data are shown as mean ± SD (standard deviation) for n = 4. *$p < 0.05$ indicates statistical significance.

expansion increased cell number by 1.19-fold compared to Plastic expansion, supplementation with sb203580 increased cell number both when expanded on dECM (1.21-fold versus 0.20-fold) and Plastic (1.85-fold versus 0.44-fold), whereas anisomycin reduced this increase. Surprisingly, sb203580 pretreatment also increased the size of chondrogenically SDSC pellets on day 14, with comparable staining intensity for sGAGs and type II collagen; the benefits of sb203580 pretreatment on the chondrogenic potential of dECM-expanded SDSCs were amplified (Figure 3A). These histological data were supported by real-time qPCR data (Figure 3B).

The 35-day pellets further confirmed the data from the 14-day pellets described above, with dECM-expanded SDSCs producing larger pellets (Figure 4A) and higher cell viability and GAG content compared to the corresponding Plastic group (Figure 4B). Pretreatment with dECM and sb203580 produced the largest SDSC pellets (Figure 4A) with the highest cell viability and GAG content, followed by the dECM group, while the anisomycin-combination group had the least viability (Figure 4B). In contrast, pretreatment with anisomycin slightly reduced the pellet size of chondrogenically differentiated SDSCs, despite comparable staining intensity for sGAG and type II collagen (Figure 4A); cell viability and GAG content did not decrease significantly (Figure 4B).

Intriguingly, sb203580 pretreatment reduced the intensity of type X collagen immunostaining in SDSC pellets in the Plastic group, whereas no significant difference was observed in the dECM group (Figure 5A), consistent with the real-time qPCR data (Figure 5C). Anisomycin pretreatment enhanced immunostaining of MMP13, another hypertrophic marker, in SDSC pellets in both the Plastic and dECM groups, while sb203580 pretreatment resulted in the weakest MMP13 immunostaining in SDSCs in the dECM group (Figure 5B), which was supported by real-time qPCR data (Figure 5D).

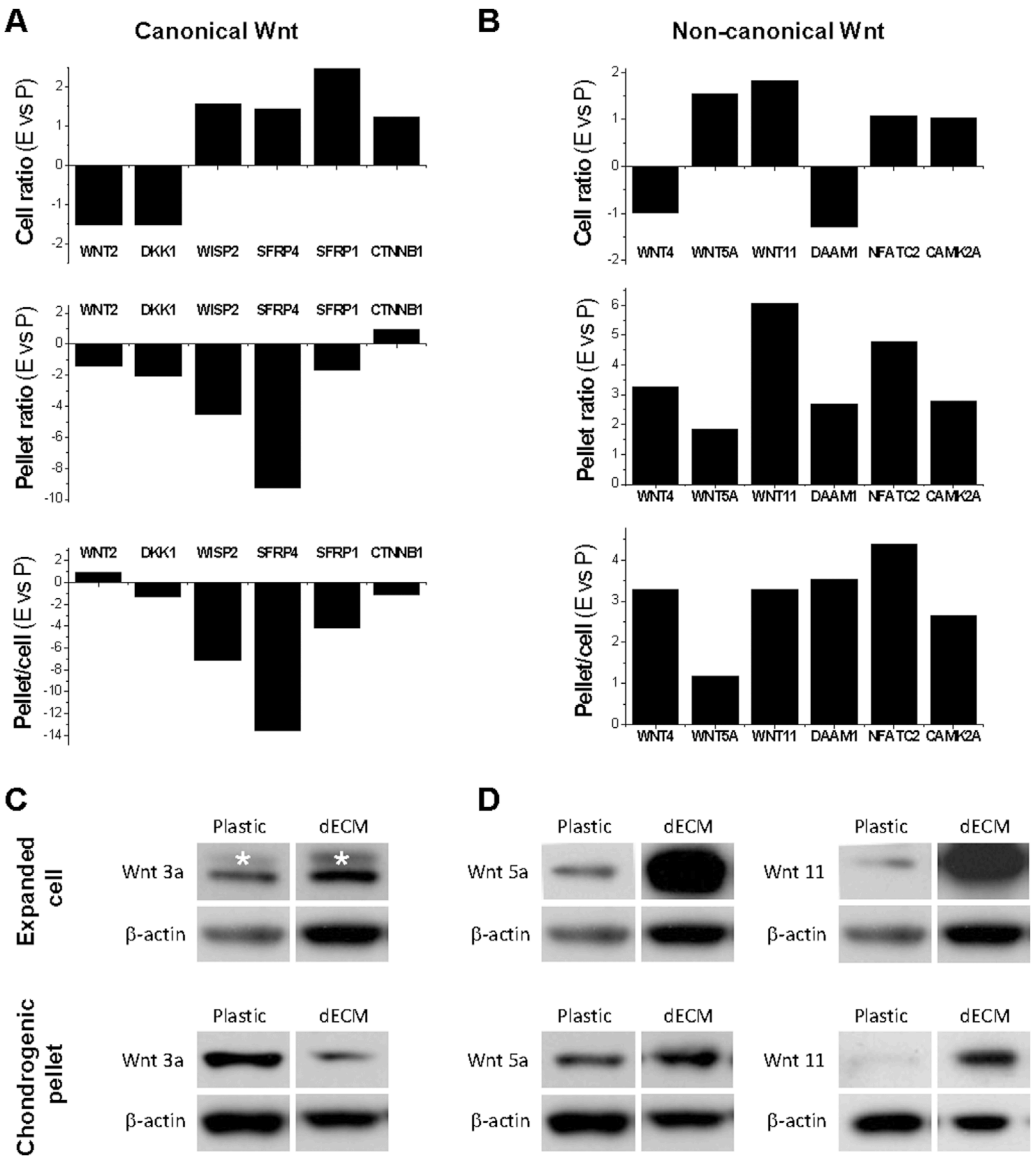

FIGURE 2
Effects of dECM pretreatment on Wnt signaling changes after SDSC expansion and subsequent chondrogenic induction. Human SDSCs were expanded on dECM or Plastic for one passage and then subjected to chondrogenic induction. Microarray was used to measure the fold changes in canonical **(A)** and non-canonical **(B)** Wnt signaling-related genes during cell expansion (cell ratio) and chondrogenic differentiation (pellet ratio) in SDSCs expanded on dECM versus Plastic (E vs. P). Western blot was used to confirm the above changes in canonical **(C)** and non-canonical **(D)** Wnt signaling in chondrogenically induced SDSCs after expansion on dECM. β-actin was used as a loading control.

WNT5A was upregulated in chondrogenically differentiated SDSCs pretreated with p38 MAPK activator, while WNT11 was upregulated in chondrogenically differentiated SDSCs pretreated with p38 MAPK inhibitor

To determine whether the Wnt pathway is involved in the chondrogenic potential of SDSCs expanded on dECM pretreated with p38 MAPK, we assessed canonical and non-canonical Wnt signaling in chondrogenically differentiated SDSCs using Western blotting. We found that Wnt3a expression was upregulated in chondrogenically differentiated SDSCs expanded on dECM compared to Plastic (Figure 6A). We also found that both Wnt5a (Figure 6B) and Wnt11 (Figure 6C) expression was upregulated in chondrogenically differentiated SDSCs expanded on dECM compared to Plastic. Notably, Wnt5a expression levels were highest in SDSC pellets generated when dECM expansion was combined with anisomycin (Figure 6B), while Wnt11 expression levels were highest in SDSC pellets generated when dECM expansion was combined with sb203580 (Figure 6C).

10.3389/fcell.2025.1655408

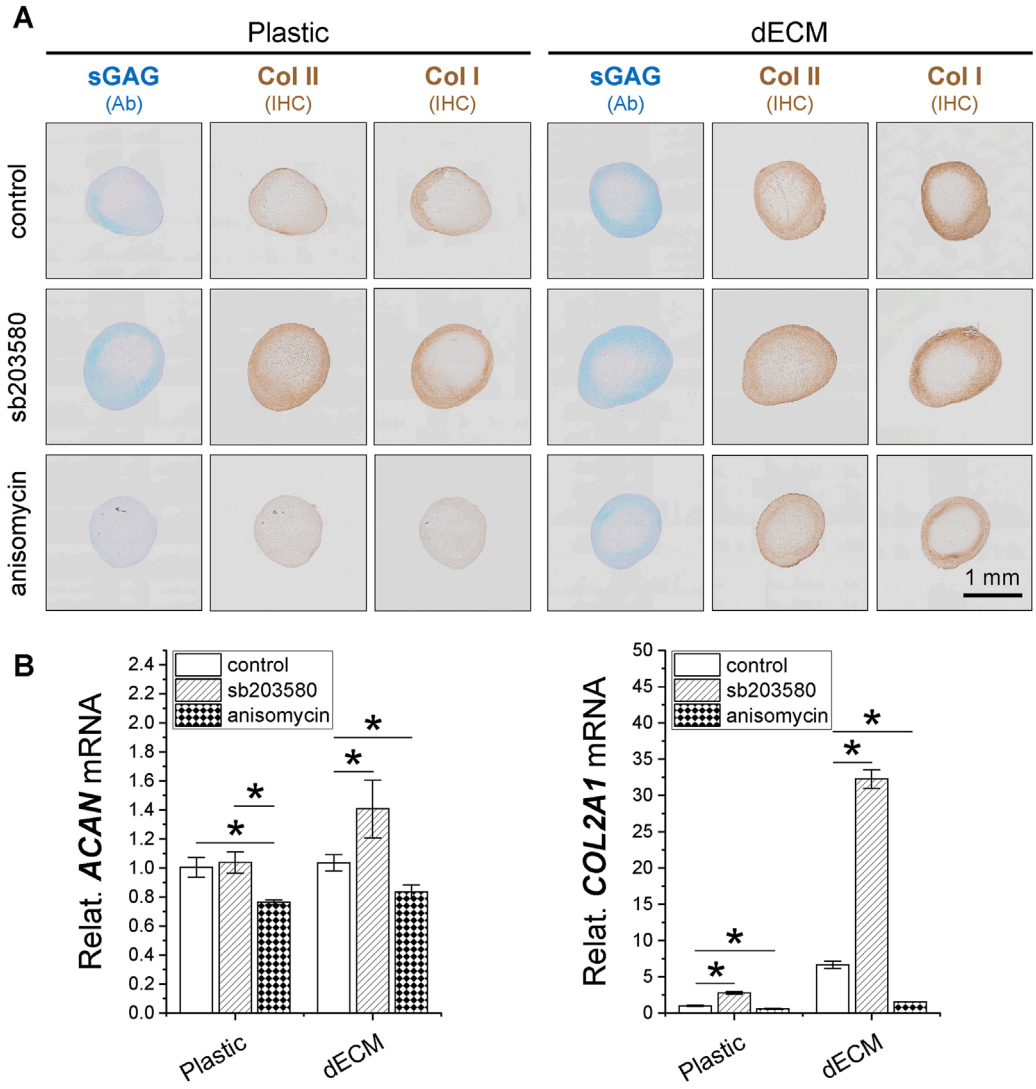

FIGURE 3
Effects of SDSC pretreatment [p38 MAPK inhibitor (sb203580) or activator (anisomycin)] combined with dECM expansion on their chondrogenic potential. Human SDSCs were expanded for one passage on dECM or Plastic in the presence of sb203580 or anisomycin, followed by chondrogenic induction for 14 and 35 days. **(A)** Alcian blue (Ab) was used to stain sGAG, and immunohistochemistry (IHC) was for staining of type I collagen (Col I) and type II collagen (Col II). Scale bar = 1 mm. **(B)** Real-time qPCR was used for *ACAN* and *COL2A1*. Data are shown as mean ± SD for n = 4. $^{*}p < 0.05$ indicates statistical significance.

Pretreatment with a p38 MAPK activator enhanced the osteogenic potential of dECM-Expanded SDSCs

To further determine whether pretreatment with a p38 MAPK activator plays a role in the osteogenic potential of SDSCs, dECM- or Plastic-expanded cells (with or without pretreatment of sb203580 and anisomycin) were incubated in osteogenic induction medium for 21 days. Our ARS staining revealed that supplementation with either sb203580 or anisomycin enhanced calcium deposition in expanded cells, although no significant differences were observed between dECM and Plastic expansion. Interestingly, combined dECM expansion and anisomycin pretreatment resulted in the highest staining intensity (Figure 7A), which was confirmed by ARS quantification data (Figure 7B). ALP staining (Figure 7C) and activity analysis (Figure 7D) also demonstrated that combined dECM expansion and anisomycin pretreatment resulted in expanded SDSCs with the highest ALP activity, another marker of osteogenic differentiation.

Discussion

Despite the increasing application of dECM in cell-based cartilage regeneration (Pei et al., 2013b; Pei et al., 2022), little is known about the involvement of the MAPK and Wnt signaling pathways in the proliferation of dECM-expanded cells and their subsequent chondrogenic differentiation. Our previous reports

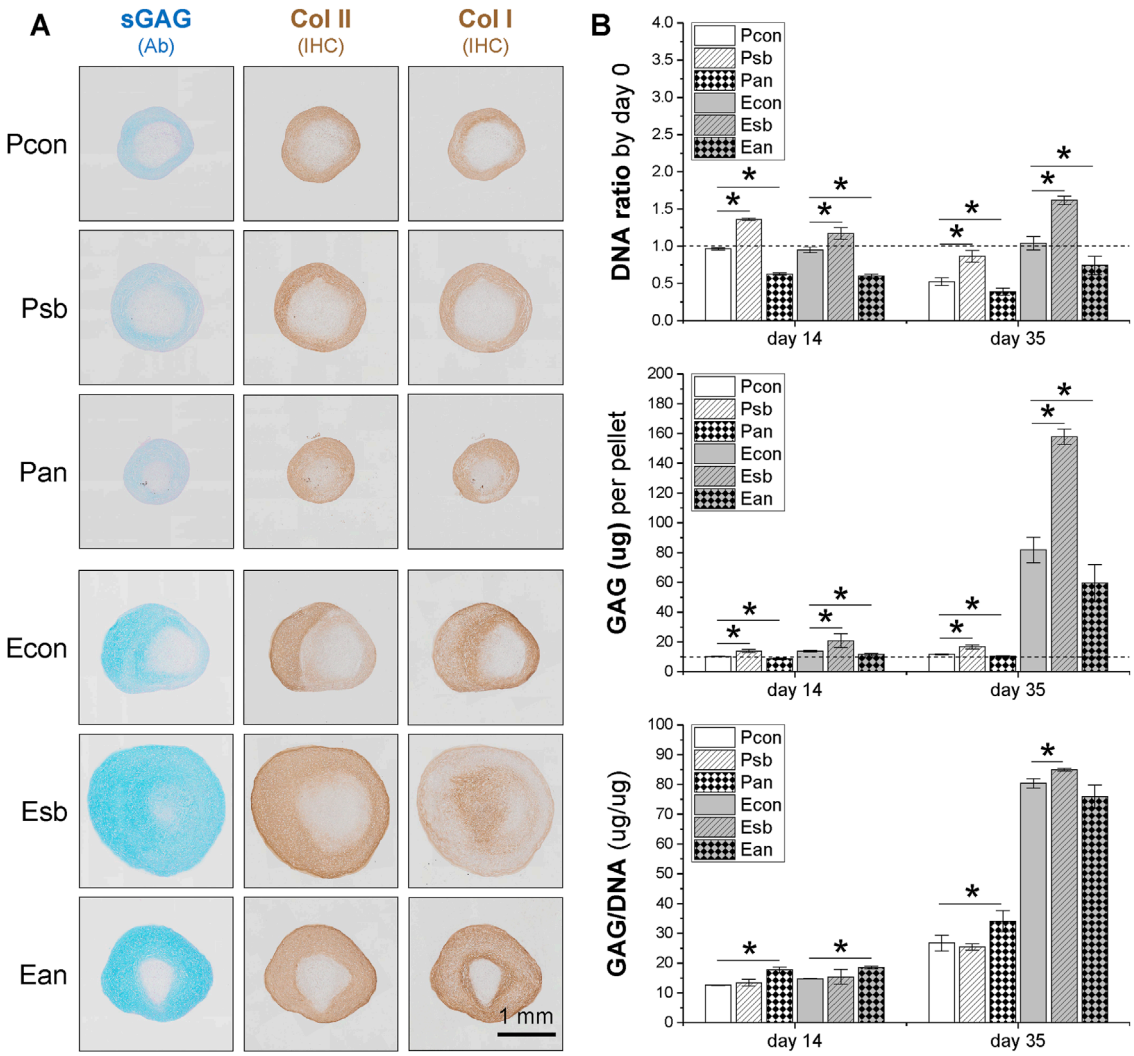

FIGURE 4
Effects of SDSC pretreatment [p38 MAPK inhibitor (sb203580) or activator (anisomycin)] combined with dECM expansion on SDSC chondrogenic potential. Human SDSCs were expanded for one passage on dECM or Plastic in the presence of sb203580 or anisomycin, followed by 35 days of chondrogenic induction. **(A)** Alcian blue (Ab) was used to stain sGAG, and immunohistochemistry (IHC) was for staining of type I collagen (Col I) and type II collagen (Col II). Scale bar = 1 mm. **(B)** Biochemical analysis was used to analyze the DNA and GAG contents in the chondrogenic pellets. Cell proliferation and viability were assessed using the DNA ratio (DNA content on days 35 and 14 were adjusted to the DNA content on day 0). The chondrogenic index was assessed using the GAG to DNA ratio. Data are shown as mean ± SD for n = 4. *$p < 0.05$ indicates statistical significance.

have shown that non-canonical Wnt signaling is upregulated in dECM-mediated expansion and chondrogenic induction of SDSCs (Li et al., 2014; Li et al., 2020). To further investigate whether pretreatment with p38 MAPK affects the chondrogenic differentiation capacity of expanded cells and the associated changes in Wnt signaling, in this study, we expanded SDSCs for one passage on dECM or Plastic in the presence of sb203580 or anisomycin. We found that sb203580 pretreatment favored chondrogenic differentiation of dECM-expanded SDSCs, whereas anisomycin pretreatment favored chondrogenic hypertrophy of dECM-expanded SDSCs. Osteogenic induction studies also demonstrated the contribution of anisomycin to endochondral bone formation of dECM-expanded SDSCs. During dECM expansion and chondrogenic differentiation, the non-canonical Wnt signaling pathway was greatly upregulated in SDSCs pretreated with p38 MAPK. In SDSCs pretreated with anisomycin combined with dECM expansion, significant upregulation of Wnt5a was associated with the highest osteogenic potential whereas, in SDSCs pretreated with both sb203580 and dECM expansion, the highest chondrogenic differentiation was associated with the highest levels of Wnt11.

Dedifferentiation refers to a cellular process in which differentiated cells revert to an earlier developmental stage and may be involved in regeneration (Casimir et al., 1988). Alternatively, cells cultured in a monolayer may lose their original properties, such as protein expression, or change shape. For instance, proliferation and differentiation are unique features of human chondrocytes; *in vitro* expansion often results in a loss of differentiation (Schnabel et al., 2002). Similar to the former definition, dECM expansion can lead to "dedifferentiation", resulting in expanded SDSCs possessing enhanced chondrogenic potential.

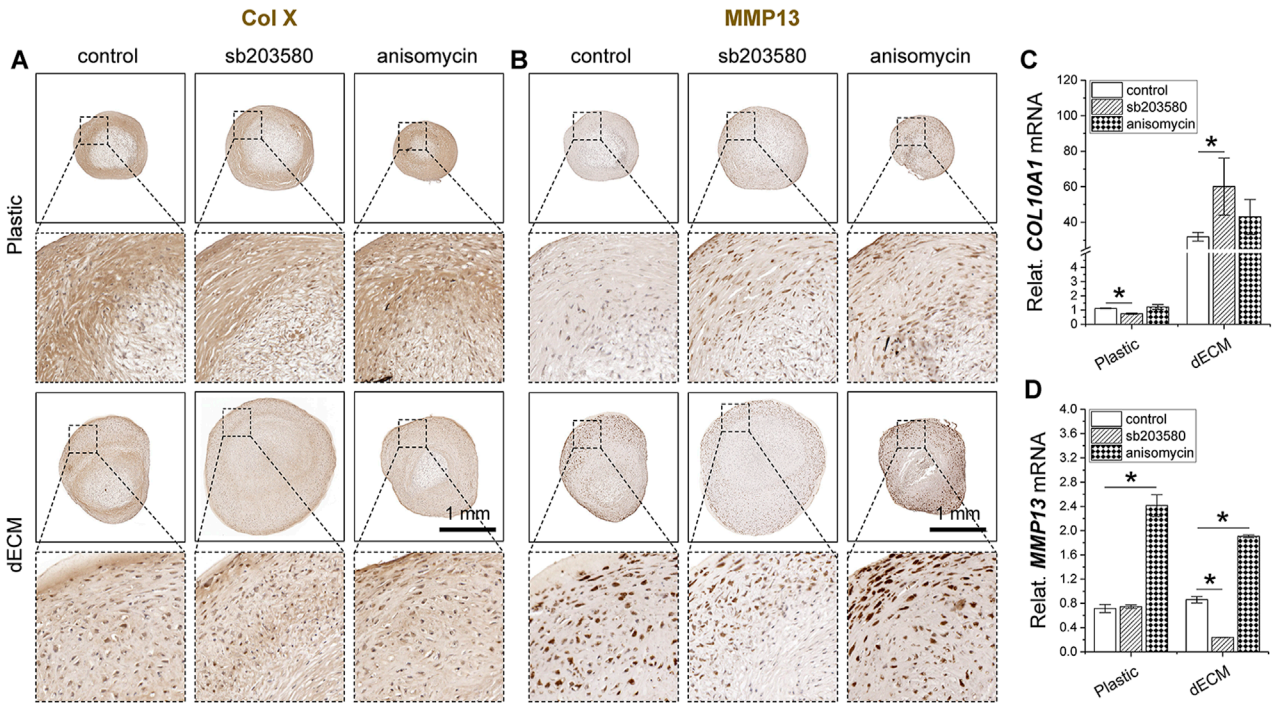

FIGURE 5
Effects of SDSC pretreatment [p38 MAPK inhibitor (sb203580) or activator (anisomycin)] combined with dECM expansion on SDSC chondrogenic hypertrophy. Human SDSCs were expanded for one passage on dECM or Plastic in the presence of sb203580 or anisomycin, followed by 35 days of chondrogenic induction. Immunohistochemistry (IHC) staining of type X collagen (Col X) **(A)** and MMP13 **(B)** in pellets was performed. Scale bar = 1 mm. Real-time qPCR for *COL10A1* mRNA **(C)** and *MMP13* mRNA **(D)** was performed to validate the histological staining. Data are shown as mean ± SD for n = 4. *$p < 0.05$ indicates a statistically significant difference.

This process is distinct from the "dedifferentiation" induced by monolayer culture, in which dedifferentiated chondrocytes typically irreversibly lose their chondrogenic potential (Li and Pei, 2012). Downregulation of chondrogenic differentiation genes (such as *ACAN*) and upregulation of chondrogenic transcriptional genes (such as *SOX9*) during dECM expansion may be one of the mechanisms by which mesenchymal stem cells (MSCs) maintain stemness and chondrogenic potential (Wang et al., 2021).

Research into the mechanisms underlying dECM expansion and its rejuvenation ability on stem cells is in its infancy and warrants further investigation. Wnt signaling plays a particularly important role in regulating MSC proliferation and differentiation. Our microarray data suggest that the Wnt pathway is involved in SDSC dECM expansion and subsequent chondrogenic differentiation. Canonical Wnt signaling, mediated by Wnt3a, has been reported to maintain stem cells in an undifferentiated and highly proliferative state (Kawakami et al., 2001; Reya et al., 2003). However, we found that, regardless of whether SDSCs were expanded on dECM or Plastic, dECM expansion resulted in a higher proliferation rate, but upregulation of Wnt3a mRNA (from microarray) or protein levels (from Western blot) was not significant. Intriguingly, after chondrogenic induction, dECM-expanded SDSCs exhibited a rapid upregulation of Wnt3a, which may be due in part to the inhibition of chondrogenesis by Wnt3a, leading to accelerated chondrogenic differentiation (Reinhold et al., 2006). While all Wnt inhibitors were upregulated during chondrogenesis, we also found that *WISP2* (WNT1-inducible-signaling pathway protein 2), *SFRP1* (Secreted frizzled-related protein 1), and *SFRP4* were also upregulated during the proliferation phase, when *DKK1* was upregulated, suggesting a delicate balance between canonical Wnt signaling in dECM-expanded SDSCs. Compared to the relatively stable canonical Wnt signaling, non-canonical Wnt signaling (such as *WNT5A* and *WNT11* and their downstream effectors *NFATC2* and *CAMK2A*) was significantly upregulated in dECM-expanded SDSCs during both the proliferation and chondrogenesis phases, as confirmed by our Western blot data at the protein level. It is well known that non-canonical signaling can antagonize canonical Wnt activity (Maye et al., 2004; Topol et al., 2003). Our results indicate that non-canonical Wnt signaling increases with dECM expansion until a balance is reached between canonical and non-canonical Wnt signaling. However, during chondrogenic induction, this balance was disrupted, with canonical Wnt signaling downregulated and non-canonical Wnt signaling upregulated in dECM-expanded SDSCs.

dECM expansion promoted cell proliferation, and concurrently upregulated Wnt5a levels, suggesting a possible parallel between cell proliferation and Wnt5a levels. Wnt5a-mediated non-canonical Wnt signaling has been reported to regulate endothelial cell proliferation (Cheng et al., 2008), promote fibroblast proliferation, and enhance relative resistance to hydrogen peroxide induced apoptosis (Vuga et al., 2009). Our data corroborated these findings, with dECM expansion leading to significant upregulation of Wnt5a and Wnt11, but not Wnt3a. The primary function of Wnt5a during early chondrogenesis is to cooperate with other Wnt antagonists

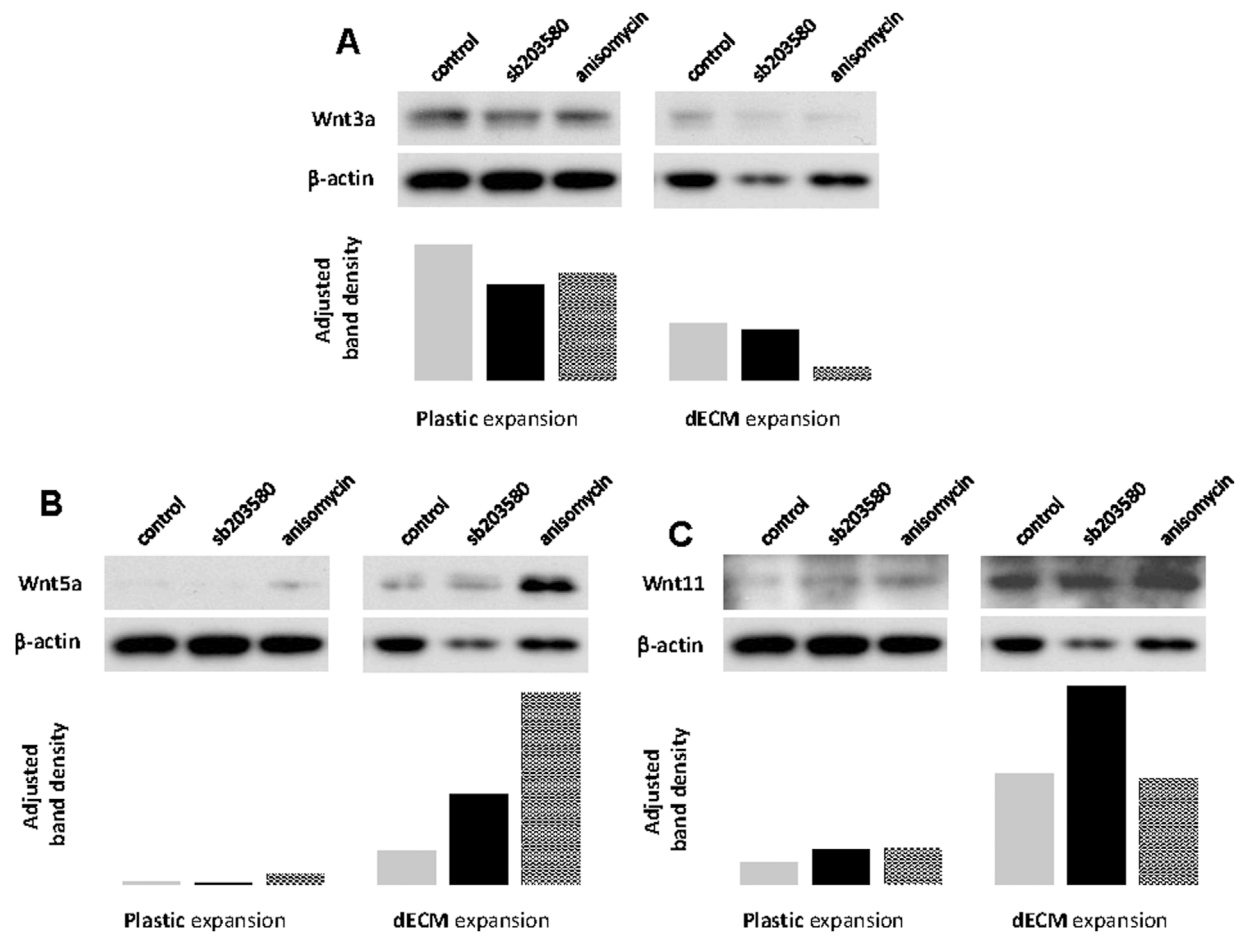

FIGURE 6
Involvement of non-canonical Wnt signaling during pretreatment with dECM and p38 MAPK signaling. Human SDSCs expanded on dECM or Plastic in the presence of sb203580 or anisomycin were evaluated for canonical **(A)** Wnt3a) and non-canonical **(B)** Wnt5a and **(C)** Wnt11) signaling. β-actin served as a loading control. Immunoblotting bands were semi-quantitatively analyzed using ImageJ software.

to maintain low levels of canonical signaling, thereby enabling cartilage differentiation (Hosseini-Farahabadi et al., 2013). Studies have shown that supplementation of Wnt5a during chondrogenesis promotes chondrogenic differentiation but inhibits hypertrophic chondrocyte differentiation (Bradley and Drissi, 2010). Wnt5a also reduces cell-cell adhesion (Torres et al., 1996), consistent with the fact that cell-matrix interactions govern dECM expansion and are responsible for active migration (Lin et al., 2012). Our results also suggest the possibility of a canonical WNT-to-WNT11 signaling loop, in which canonical WNT signaling induces *WNT11* upregulation, which then activates a non-canonical WNT signaling cascade to induce cellular motility, as recently described (Katoh and Katoh, 2009). *WNT11* can also activate the Ca^{2+}-MAP3K7-NLK signaling cascade, thereby attenuating canonical WNT signaling (Katoh and Katoh, 2009). Although Wnt11 was upregulated in dECM-expanded SDSCs, current evidence is insufficient to support a self-renewal function for Wnt11 (Singla et al., 2006) which needs to be further elucidated in future studies.

The p38 MAPK signaling cascade is not only involved in cell proliferation and differentiation (Onom and Han, 2000) but is also activated by various pro-inflammatory and stressful stimuli (Schindler et al., 2007). Evidence suggests that *in vivo* administration of p38 MAPK inhibitor can alleviate inflammation and associated damage; however, these inhibitors can also have side effects, such as the suppression of tissue regeneration (Yong et al., 2009). Interestingly, in this study, we found that preconditioning stem cells with p38 MAPK inhibitor during expansion significantly enhanced dECM-mediated chondrogenesis in SDSCs, likely by preventing inflammation. We also found that pretreatment with sb203580 promoted chondrogenic differentiation of dECM-expanded SDSCs, concomitantly with upregulation of Wnt11 expression, suggesting that p38 MAPK inhibitors may enhance Wnt11-mediated chondrogenesis in dECM-expanded SDSCs. Although Wnt11 plays multiple roles in regulating cell properties (Ouko et al., 2004; Lako et al., 1998; Sekiya et al., 2002), its precise functions and mechanisms of action remain unclear. Unlike the canonical Wnts, Wnt11 is classified as one of the few recognized pro-differentiation Wnts, acting through a β-catenin-independent pathway involving PKC (protein kinase C) and Jnk (c-Jun N-terminal kinase) (Eisenberg et al., 1997; Pandur et al., 2002).

We also found that pretreatment with anisomycin promoted osteogenic differentiation of dECM-expanded SDSCs and upregulated Wnt5a expression, suggesting that anisomycin may enhance Wnt5a-mediated osteogenesis in dECM-expanded SDSCs.

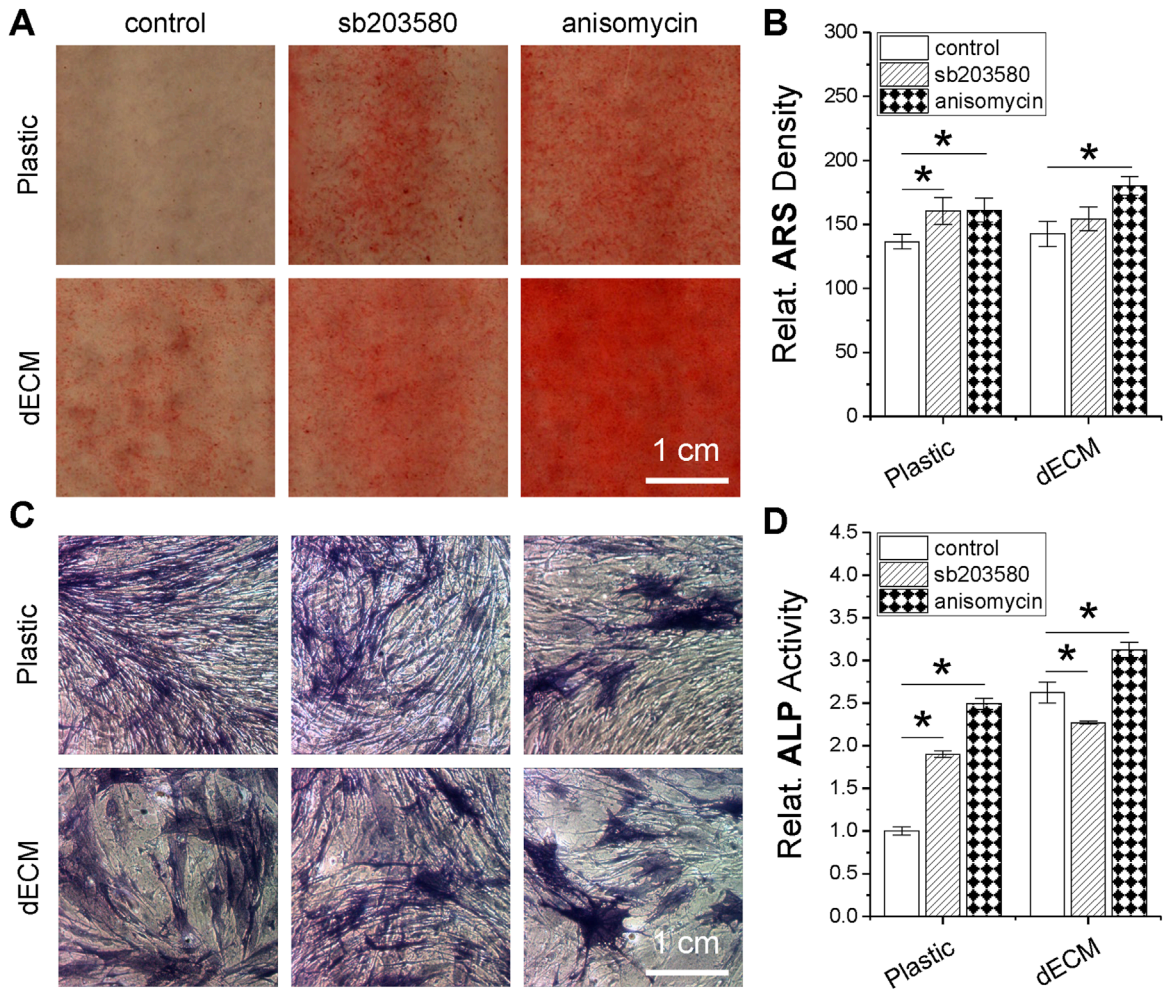

FIGURE 7
Effects of SDSC pretreatment [p38 MAPK inhibitor (sb203580) or activator (anisomycin)] combined with dECM expansion on SDSC osteogenic potential. Human SDSCs were expanded for one passage on dECM or Plastic in the presence of sb203580 or anisomycin, followed by 21 days of osteogenic induction. Alizarin Red S (ARS) was used for calcium deposition staining **(A)** and staining density was quantified **(B)**. Alkaline phosphatase (ALP) staining was also performed **(C)**, and activity was quantified **(D)**. Data are shown as mean ± SD for n = 4. $^{*}p < 0.05$ indicates statistical significance.

This finding is consistent with numerous reports. For example, Lee et al. found that osteogenic transcription factor Runx2 (Runt-related transcription factor-2) was effectively inhibited by sb203580, while anisomycin significantly induced its expression (Lee et al., 2002); Wnt5a plays a key role in the osteogenic differentiation of human MSCs both *in vitro* and *in vivo* (Guo et al., 2008; Baksh and Tuan, 2007). Given that Wnt5a signaling leads to intracellular Ca^{2+} release and activation of PKC and CaMKII (calcium/calmodulin-dependent protein kinase II) (Kühl et al., 2000), upregulation of Wnt5a through pretreatment with anisomycin may predispose SDSCs to osteogenic development. Our assessment of SDSC chondrogenic hypertrophy supports this conclusion. In this study, pretreatment with sb203580 reduced early hypertrophic markers (such as *COL10A1*), whereas anisomycin increased them in expanded SDSCs. Our hypertrophy analysis was performed on 35-day chondrogenically induced SDSC pellets, which exceeds the chondrogenic hypertrophy phase of human MSCs (typically occurring between 14 and 28 days after incubation in a TGF-β-chondrogenic medium) (Mueller et al., 2010). This stage of endochondral ossification is regulated by MMPs (Ortega et al., 2004). Our data showed that pretreatment with anisomycin significantly upregulated *MMP13* in chondrogenically differentiated SDSCs, whereas pretreatment with sb203580 upregulated *MMP13* in dECM-expanded SDSCs, suggesting that pretreatment with p38 MAPK activator favors endochondral ossification, while pretreatment with p38 MAPK inhibitor favors chondrogenic differentiation. Furthermore, secreted MMP13 can degrade type II collagen (Inada et al., 2004) and aggrecan (Fosang et al., 1996), which may explain why pretreatment with p38 MAPK inhibitor resulted in more functional cartilage matrix, whereas pretreatment with p38 MAPK activator produced less functional cartilage matrix.

Conclusion

Our results suggest that pretreatment with p38 MAPK signaling plays distinct roles in matrix-expanded SDSC chondrogenesis:

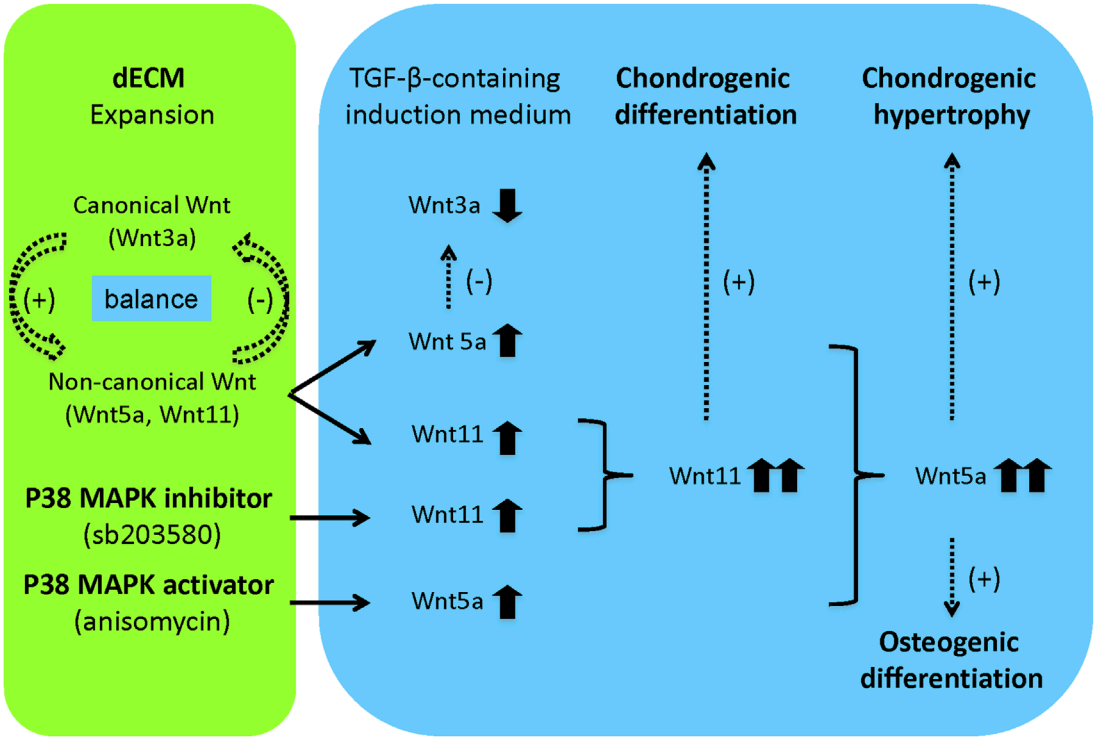

FIGURE 8
Flowchart of future research hypotheses. In this study, the dECM model provided a cell expansion matrix to maintain a balance of canonical and non-canonical Wnt signaling, thereby promoting expanded cell proliferation, migration, and chondrogenic potential. When expanded cells were released from the dECM and induced to chondrogenesis in a defined medium containing TGF-β, a shift from canonical to non-canonical Wnt signaling occurred, favoring chondrogenic differentiation. Pretreatment with a p38 MAPK inhibitor confirmed the effect of dECM on the chondrogenic potential of expanded SDSCs, possibly through interaction with Wnt11-mediated signaling. Pretreatment with a p38 MAPK activator accelerated the effect of dECM on the osteogenic potential of expanded SDSCs, perhaps through interaction with Wnt5a-mediated signaling. Dotted arrows indicated hypotheses that require verification in future studies.

sb203580 favors chondrogenic differentiation, while anisomycin favors endochondral bone formation. Our Wnt signaling data also suggest a novel hypothesis (Figure 8): pretreatment with a p38 MAPK inhibitor may underlie the effects of dECM on the chondrogenic potential of expanded SDSCs through interaction with Wnt11-mediated signaling, whereas pretreatment with a p38 MAPK activator may accelerate the effects of dECM on the osteogenic potential of expanded SDSCs through interaction with Wnt5a-mediated signaling. This hypothesis warrants further investigation.

Data availability statement

The datasets presented in this study can be found in online repositories. The names of the repository/repositories and accession number(s) can be found in the article/supplementary material.

Ethics statement

Ethical approval was not required for the studies on humans in accordance with the local legislation and institutional requirements because only commercially available established cell lines were used.

Author contributions

YZ: Methodology, Writing – original draft, Investigation, Visualization, Validation, Resources, Formal Analysis. MP: Formal Analysis, Project administration, Conceptualization, Supervision, Writing – review and editing, Investigation. CL: Writing – review and editing, Investigation, Methodology, Validation, Supervision.

Funding

The author(s) declare that financial support was received for the research and/or publication of this article. This work was supported by the Natural Science Foundation of Chongqing (Grant No. CSTB2023NSCQ-MSX0578).

Acknowledgments

We thank Suzanne Danley for editing the manuscript.

Conflict of interest

The authors declare that the research was conducted in the absence of any commercial or financial relationships that could be construed as a potential conflict of interest.

The author(s) declared that they were an editorial board member of Frontiers, at the time of submission. This had no impact on the peer review process and the final decision.

Generative AI statement

The author(s) declare that no Generative AI was used in the creation of this manuscript.

Any alternative text (alt text) provided alongside figures in this article has been generated by Frontiers with the support of artificial intelligence and reasonable efforts have been made to ensure accuracy, including review by the authors wherever possible. If you identify any issues, please contact us.

Publisher's note

All claims expressed in this article are solely those of the authors and do not necessarily represent those of their affiliated organizations, or those of the publisher, the editors and the reviewers. Any product that may be evaluated in this article, or claim that may be made by its manufacturer, is not guaranteed or endorsed by the publisher.

References

Baksh, D., and Tuan, R. S. (2007). Canonical and non-canonical wnts differentially affect the development potential of primary isolate of human bone marrow mesenchymal stem cells. *J. Cell Physiol.* 212, 817–826. doi:10.1002/jcp.21080

Bradley, E. W., and Drissi, M. H. (2010). WNT5A regulates chondrocyte differentiation through differential use of the CaN/NFAT and IKK/NF-kappaB pathways. *Mol. Endocrinol.* 24, 1581–1593. doi:10.1210/me.2010-0037

Casimir, C. M., Gates, P. B., Patient, R. K., and Brockes, J. P. (1988). Evidence for dedifferentiation and metaplasia in amphibian limb regeneration from inheritance of DNA methylation. *Development* 104, 657–668. doi:10.1242/dev.104.4.657

Cheng, C. W., Yeh, J. C., Fan, T. P., Smith, S. K., and Charnock-Jones, D. S. (2008). Wnt5a-mediated non-canonical wnt signalling regulates human endothelial cell proliferation and migration. *Biochem. Biophys. Res. Commun.* 365, 285–290. doi:10.1016/j.bbrc.2007.10.166

Eisenberg, C. A., Gourdie, R. G., and Eisenberg, L. M. (1997). Wnt-11 is expressed in early avian mesoderm and required for the differentiation of the quail mesoderm cell line QCE-6. *Development* 124, 525–536. doi:10.1242/dev.124.2.525

Fosang, A. J., Last, K., Knäuper, V., Murphy, G., and Neame, P. J. (1996). Degradation of cartilage aggrecan by collagenase-3 (MMP-13). *FEBS Lett.* 380, 17–20. doi:10.1016/0014-5793(95)01539-6

Guo, J., Jin, J., and Cooper, L. F. (2008). Dissection of sets of genes that control the character of wnt5a-deficient mouse calvarial cells. *Bone* 43, 961–971. doi:10.1016/j.bone.2008.06.011

Hosseini-Farahabadi, S., Geetha-Loganathan, P., Fu, K., Nimmagadda, S., Yang, H. J., and Richman, J. M. (2013). Dual functions for WNT5A during cartilage development and in disease. *Matrix Biol.* 32, 252–264. doi:10.1016/j.matbio.2013.02.005

Inada, M., Wang, Y., Byrne, M. H., Rahman, M. U., Miyaura, C., López-Otín, C., et al. (2004). Critical roles for collagenase-3 (Mmp13) in development of growth plate cartilage and in endochondral ossification. *Proc. Natl. Acad. Sci. U. S. A.* 101, 17192–17197. doi:10.1073/pnas.0407788101

Joos, H., Albrecht, W., Laufer, S., and Brenner, R. E. (2009). Influence of p38MAPK inhibition on IL-1beta-stimulated human chondrocytes: a microarray approach. *Int. J. Mol. Med.* 23, 685–693. doi:10.3892/ijmm_00000181

Katoh, M., and Katoh, M. (2009). Integrative genomic analyses of WNT11: transcriptional mechanisms based on canonical WNT signals and GATA transcription factors signaling. *Int. J. Mol. Med.* 24, 247–251. doi:10.3892/ijmm_00000227

Kawakami, Y., Capdevila, J., Büscher, D., Itoh, T., Rodríguez Esteban, C., and Izpisúa Belmonte, J. C. (2001). WNT signals control FGF-dependent limb initiation and AER induction in the chick embryo. *Cell* 104, 891–900. doi:10.1016/s0092-8674(01)00285-9

Kühl, M., Sheldahl, L. C., Park, M., Miller, J. R., and Moon, R. T. (2000). *The Wnt/Ca^{2+} pathway: a new vertebrate wnt signaling pathway takes shape*. *Trends Genet.* 16, 279–283. doi:10.1016/s0168-9525(00)02028-x

Lako, M., Strachan, T., Bullen, P., Wilson, D. I., Robson, S. C., and Lindsay, S. (1998). Isolation, characterisation, and embryonic expression of WNT11, a gene which maps to 11q13.5 and has possible roles in the development of skeleton, kidney, and lung. *Gene* 219, 101–110. doi:10.1016/s0378-1119(98)00393-x

Lee, K. S., Hong, S. H., and Bae, S. C. (2002). Both the smad and p38 MAPK pathways play a crucial role in Runx2 expression following induction by transforming growth factor-beta and bone morphogenetic protein. *Oncogene* 21, 7156–7163. doi:10.1038/sj.onc.1205937

Li, J. T., and Pei, M. (2012). Cell senescence: a challenge in cartilage engineering and regeneration. *Tissue Eng. Part B* 18, 270–287. doi:10.1089/ten.TEB.2011.0583

Li, J., and Pei, M. (2018). A protocol to prepare decellularized stem cell matrix for rejuvenation of cell expansion and cartilage regeneration. *Methods Mol. Biol.* 1577, 147–154. doi:10.1007/7651_2017_27

Li, J., Hansen, K., Zhang, Y., Dong, C., Dinu, C., Dzieciatkowska, M., et al. (2014). Rejuvenation of chondrogenic potential in a young stem cell microenvironment. *Biomaterials* 35, 642–653. doi:10.1016/j.biomaterials.2013.09.099

Li, J., Narayanan, K., Zhang, Y., Hill, R. C., He, F., Hansen, K. C., et al. (2020). Role of lineage-specific matrix in stem cell chondrogenesis. *Biomaterials* 231, 119681. doi:10.1016/j.biomaterials.2019.119681

Lin, H., Yang, G., Tan, J., and Tuan, R. S. (2012). Influence of decellularized matrix derived from human mesenchymal stem cells on their proliferation, migration and multi-lineage differentiation potential. *Biomaterials* 33, 4480–4489. doi:10.1016/j.biomaterials.2012.03.012

Long, D. L., and Loeser, R. F. (2010). p38gamma mitogen-activated protein kinase suppresses chondrocyte production of MMP-13 in response to catabolic stimulation. *Osteoarthr. Cartil.* 18, 1203–1210. doi:10.1016/j.joca.2010.05.016

Martel-Pelletier, J., Mineau, F., Jovanovic, D., Di Battista, J. A., and Pelletier, J. P. (1999). Mitogen-activated protein kinase and nuclear factor kappaB together regulate interleukin-17-induced nitric oxide production in human osteoarthritic chondrocytes: possible role of transactivating factor mitogen-activated protein kinase-activated proten kinase (MAPKAPK). *Arthritis Rheum.* 42, 2399–2409. doi:10.1002/1529-0131(199911)42:11<2399::AID-ANR19>3.0.CO;2-Y

Maye, P., Zheng, J., Li, L., and Wu, D. (2004). Multiple mechanisms for Wnt11-mediated repression of the canonical wnt signaling pathway. *J. Biol. Chem.* 279, 24659–24665. doi:10.1074/jbc.M311724200

Mueller, M. B., Fischer, M., Zellner, J., Berner, A., Dienstknecht, T., Prantl, L., et al. (2010). Hypertrophy in mesenchymal stem cell chondrogenesis: effect of TGF-beta isoforms and chondrogenic conditioning. *Cells Tissues Organs* 192, 158–166. doi:10.1159/000313399

Oh, C. D., Chang, S. H., Yoon, Y. M., Lee, S. J., Lee, Y. S., Kang, S. S., et al. (2000). Opposing role of mitogen-activated protein kinase subtypes, erk-1/2 and p38, in the regulation of chondrogenesis of mesenchymes. *J. Biol. Chem.* 275, 5613–5619. doi:10.1074/jbc.275.8.5613

Onom, K., and Han, J. (2000). The p38 signal transduction pathway: activation and function. *Cell Signal* 12, 1–13. doi:10.1016/s0898-6568(99)00071-6

Ortega, N., Behonick, D. J., and Werb, Z. (2004). Matrix remodeling during endochondral ossification. *Trends Cell Biol.* 14, 86–93. doi:10.1016/j.tcb.2003.12.003

Ouko, L., Ziegler, T. R., Gu, L. H., Eisenberg, L. M., and Yang, V. W. (2004). Wnt11 signaling promotes proliferation, transformation, and migration of IEC6 intestinal epithelial cells. *J. Biol. Chem.* 279, 26707–26715. doi:10.1074/jbc.M402877200

Pandur, P., Läsche, M., Eisenberg, L. M., and Kühl, M. (2002). Wnt-11 activation of a non-canonical wnt signalling pathway is required for cardiogenesis. *Nature* 418, 636–641. doi:10.1038/nature00921

Pei, M. (2017). Environmental preconditioning rejuvenates adult stem cells' proliferation and chondrogenic potential. *Biomaterials* 117, 10–23. doi:10.1016/j.biomaterials.2016.11.049

Pei, M., He, F., Li, J., Tidwell, J. E., Jones, A. C., and McDonough, E. B. (2013a). Repair of large animal partial-thickness cartilage defects through intraarticular injection of

matrix-rejuvenated synovium-derived stem cells. *Tissue Eng. Part A* 19, 1144–1154. doi:10.1089/ten.TEA.2012.0351

Pei, M., Zhang, Y., Li, J. T., and Chen, D. Q. (2013b). Antioxidation of decellularized stem cell matrix promotes human synovium-derived stem cell-based chondrogenesis. *Stem Cells Dev.* 22, 889–900. doi:10.1089/scd.2012.0495

Pei, M., Pei, Y. A., Zhou, S., Mikaeiliagah, E., Erickson, C., Giertych, B., et al. (2022). Matrix from urine stem cells boosts tissue-specific stem cell mediated functional cartilage reconstruction. *Bioact. Mater* 23, 353–367. doi:10.1016/j.bioactmat.2022.11.012

Prasadam, I., Mao, X., Wang, Y., Shi, W., Crawford, R., and Xiao, Y. (2012). Inhibition of p38 pathway leads to OA-like changes in a rat animal model. *Rheumatology* 51, 813–823. doi:10.1093/rheumatology/ker360

Reinhold, M. I., Kapadia, R. M., Liao, Z., and Naski, M. C. (2006). The Wnt-inducible transcription factor Twist1 inhibits chondrogenesis. *J. Biol. Chem.* 281, 1381–1388. doi:10.1074/jbc.M504875200

Reya, T., Duncan, A. W., Ailles, L., Domen, J., Scherer, D. C., Willert, K., et al. (2003). A role for wnt signalling in self-renewal of haematopoietic stem cells. *Nature* 423, 409–414. doi:10.1038/nature01593

Schindler, J. F., Monahan, J. B., and Smith, W. G. (2007). p38 pathway kinases as anti-inflammatory drug targets. *J. Dent. Res.* 86, 800–811. doi:10.1177/154405910708600902

Schnabel, M., Marlovits, S., Eckhoff, G., Fichtel, I., Gotzen, L., Vécsei, V., et al. (2002). Dedifferentiation-associated changes in morphology and gene expression in primary human articular chondrocytes in cell culture. *Osteoarthr. Cartil.* 10, 62–70. doi:10.1053/joca.2001.0482

Sekiya, I., Vuoristo, J. T., Larson, B. L., and Prockop, D. J. (2002). *In vitro* cartilage formation by human adult stem cells from bone marrow stroma defines the sequence of cellular and molecular events during chondrogenesis. *Proc. Natl. Acad. Sci. U. S. A.* 99, 4397–4402. doi:10.1073/pnas.052716199

Singla, D. K., Schneider, D. J., LeWinter, M. M., and Sobel, B. E. (2006). wnt3a but not wnt11 supports self-renewal of embryonic stem cells. *Biochem. Biophys. Res. Commun.* 345, 789–795. doi:10.1016/j.bbrc.2006.04.125

Sondergaard, B. C., Schultz, N., Madsen, S. H., Bay-Jensen, A. C., Kassem, M., and Karsdal, M. A. (2010). MAPKs are essential upstream signaling pathways in proteolytic cartilage degradation–divergence in pathways leading to aggrecanase and MMP-mediated articular cartilage degradation. *Osteoarthr. Cartil.* 18, 279–288. doi:10.1016/j.joca.2009.11.005

Toh, W. S., Foldager, C. B., Pei, M., and Hui, J. H. (2014). Advances in mesenchymal stem cell-based strategies for cartilage repair and regeneration. *Stem Cell Rev. Rep.* 10, 686–696. doi:10.1007/s12015-014-9526-z

Topol, L., Jiang, X., Choi, H., Garrett-Beal, L., Carolan, P. J., and Yang, Y. (2003). Wnt-5a inhibits the canonical wnt pathway by promoting GSK-3-independent beta-catenin degradation. *J. Cell Biol.* 162, 899–908. doi:10.1083/jcb.200303158

Torres, M. A., Yang-Snyder, J. A., Purcell, S. M., DeMarais, A. A., McGrew, L. L., and Moon, R. T. (1996). Activities of the Wnt-1 class of secreted signaling factors are antagonized by the Wnt-5A class and by a dominant negative cadherin in early xenopus development. *J. Cell Biol.* 133, 1123–1137. doi:10.1083/jcb.133.5.1123

Vuga, L. J., Ben-Yehudah, A., Kovkarova-Naumovski, E., Oriss, T., Gibson, K. F., Feghali-Bostwick, C., et al. (2009). WNT5A is a regulator of fibroblast proliferation and resistance to apoptosis. *Am. J. Respir. Cell Mol. Biol.* 41, 583–589. doi:10.1165/rcmb.2008-0201OC

Wang, Y., Hu, G., Hill, R. C., Dzieciatkowska, M., Hansen, K. C., Zhang, X. B., et al. (2021). Matrix reverses immortalization-mediated stem cell fate determination. *Biomaterials* 265, 120387. doi:10.1016/j.biomaterials.2020.120387

Yan, J., Chen, X., Pu, C., Zhao, Y., Liu, X., Liu, T., et al. (2020). Synovium stem cell-derived matrix enhances anti-inflammatory properties of rabbit articular chondrocytes via the SIRT1 pathway. *Mater Sci. Eng. C Mater Biol. Appl.* 106, 110286. doi:10.1016/j.msec.2019.110286

Yong, H. Y., Koh, M. S., and Moon, A. (2009). The p38 MAPK inhibitors for the treatment of inflammatory diseases and cancer. *Expert Opin. Investig. Drugs* 18, 1893–1905. doi:10.1517/13543780903321490

Zhang, Y., Pizzute, T., and Pei, M. (2014). A review of crosstalk between MAPK and wnt signals and its impact on cartilage regeneration. *Cell Tissue Res.* 358, 633–649. doi:10.1007/s00441-014-2010-x

Zhang, Y., Pizzute, T., Li, J., He, F., and Pei, M. (2015). sb203580 preconditioning recharges matrix-expanded human adult stem cells for chondrogenesis in an inflammatory environment - a feasible approach for autologous stem cell based osteoarthritic cartilage repair. *Biomaterials* 64, 88–97. doi:10.1016/j.biomaterials.2015.06.038

Frontiers in
Cell and Developmental Biology

Explores the fundamental biological processes of life, covering intracellular and extracellular dynamics.

The world's most cited developmental biology journal, advancing our understanding of the fundamental processes of life. It explores a wide spectrum of cell and developmental biology, covering intracellular and extracellular dynamics.

Discover the latest Research Topics

See more →

Frontiers

Avenue du Tribunal-Fédéral 34
1005 Lausanne, Switzerland
frontiersin.org

Contact us

+41 (0)21 510 17 00
frontiersin.org/about/contact